21

Developmental Programming of Blood Pressure and Renal Function Through the Life Course

Valérie A. Luyckx | Karen M. Moritz | John F. Bertram

CHAPTER OUTLINE

The large variation in individual susceptibility to kidney disease and other chronic diseases is not easily explained.[1] Genetic factors are important determinants of development and function of major organ systems as well as of susceptibility to disease. Rare genetic and congenital abnormalities leading to abnormal kidney development are associated with the occurrence of subsequent renal dysfunction, often manifest very early in life.[2,3] Most renal disease in the general population, however, is not ascribable to genetic mutations, with the most common etiologic associations with end-stage kidney disease (ESKD) worldwide being the polygenic disorders of diabetes and hypertension. Of note here is the association between mutations in the apolipoprotein-1 (*APOL1*) gene in people of African descent with increased predisposition to the development of HIV-associated nephropathy and focal and segmental glomerulosclerosis (FSGS). However, searches for other specific gene polymorphisms or mutations have not implicated specific genes but instead point to a likely complex interplay between polygenic predisposition and environmental factors in the development of hypertension, diabetes, and renal disease.[4–9] Hypertension and renal disease prevalence vary between populations from different ethnic backgrounds, with very high rates observed among Aboriginal Australians, Native Americans, and people of African descent.[10–12] It is well established that lifestyle and socioeconomic factors pose significant risk for the development and persistence of hypertension and diabetes in the general population, with obesity becoming an increasing concern, especially in the developing world.[7,13] However, more and more evidence is pointing also to the far-reaching effects of the intrauterine environment and early postnatal growth on organ development, organ function, and subsequent susceptibility to adult disease.[14–16] Stresses experienced during fetal life (for which low birth weight, being small for gestational age, preterm birth, or high birth weight may be surrogate markers), such as maternal malnutrition, ill health, preeclampsia, or gestational diabetes, or those experienced in early childhood, such as poor early nutrition, infections, and environmental exposures, may "program" long-term organ function and may be the first in a succession of challenges or "hits" that ultimately manifest in overt disease. This chapter outlines the effects of fetal and early-life programming on renal development (particularly nephrogenesis), nephron endowment, and the risks of hypertension and kidney disease throughout the life course. Major congenital renal anomalies are discussed elsewhere in this book (see Chapter 72). In addition, it must be borne in mind that low birth weight and preterm birth also predict later-life diabetes, cardiovascular disease, metabolic syndrome, and preeclampsia; therefore, renal function may be additionally impacted through developmental programming

of these disorders and in turn may impact outcomes of these diseases, the discussion of which is beyond the scope of the current chapter.[16–20]

DEVELOPMENTAL PROGRAMMING

The process through which an environmental insult experienced early in life can predispose to adult disease is known as "developmental programming," which refers to the observation that an environmental stimulus experienced during a critical period of development in utero or early postbirth can induce long-term structural and functional effects in the organism.[15,21] This phenomenon, often termed "developmental origins of health and disease," can have far-reaching implications in that the effects can be perpetuated across generations.[22,23] The association between adverse intrauterine events and subsequent cardiovascular disease has long been recognized.[15,21,24,25] In early studies, adults of low birth weight were found to have higher cardiovascular morbidity and mortality than those of normal birth weight.[26] Subsequently, evidence from diverse populations has confirmed these findings and expanded them to include other conditions, such as hypertension, impaired glucose tolerance, type 2 diabetes, obesity, preeclampsia, and chronic kidney disease (CKD).[21,27–33] Of these, the associations between low birth weight and preterm birth and subsequent hypertension have been the most studied.[34–37] Until recently, attention has largely focused on preterm birth and low birth weight as markers for developmental programming of hypertension and renal disease, but being small for gestational age or having a high birth weight, often as a result of a diabetic pregnancy or maternal obesity, are also emerging as risk factors.[38–41] Currently, birth weight and preterm birth are the best available surrogates for an adverse intrauterine environment, but some intrauterine stresses may not manifest as such and therefore may not be recognized. Ongoing work is required to develop more sensitive measures of developmental stress. Table 21.1 outlines the definitions of birth weight and gestational age categories, which are referred to throughout this chapter. Globally, the respective incidences of low birth weight and preterm birth are around 15%–20% and 11%.[42,43] Importantly, as shown in Fig. 21.1, a large proportion of babies born small for gestational age have a birth weight above 2.5 kg, highlighting the need to identify all small-for-gestational-age infants who are also at risk of programming effects.[44] The global incidence of high birth weight is rising, ranging from 5%–20% in high-income and 0.5%–15% in lower-income countries.[40] A significant number of infants born yearly therefore likely undergo developmental programming and are at risk for chronic disease later in life.

Table 21.1 Definitions of Birth Weight and Prematurity Categories

Category	Definition
Birth Weight Categories	
Normal birth weight	>2500 g and <4000 g (usually)
Large for gestational age	>2 standard deviations above the mean birth weight for gestational age
Low birth weight	<2500 g
Very low birth weight	<1500 g
Appropriate for gestational age	Within ±2 standard deviations of the mean birth weight for gestational age
Small for gestational age	>2 standard deviations below the mean birth weight for gestational age
Intrauterine growth restriction	Evidence of fetal malnutrition and growth restriction at any time during gestation
Gestational Categories	
Extremely preterm	<28 weeks of gestation
Very preterm	<32 and >28 weeks of gestation
Moderately preterm	<34 and >32 weeks of gestation
Late preterm	<37 and >34 weeks of gestation
Full term	>37 weeks of gestation

Taken from Abitbol CL, Rodriguez MM. The long-term renal and cardiovascular consequences of prematurity. *Nat Rev Nephrol.* 2012;8:265–274.

DEVELOPMENTAL PROGRAMMING IN THE KIDNEY

The kidney is the organ central to the development of hypertension. The relationship between renal sodium handling, intravascular volume homeostasis, and hypertension is well accepted.[45,46] That factors intrinsic to the kidney itself affect blood pressure has been demonstrated clinically in kidney transplantation in which the blood pressure in the recipient after transplantation has been shown to be related to the blood pressure or hypertension risk factors of the donor: that is, hypertension "follows" the kidney.[47] In 1988, Brenner and colleagues[48] proposed that congenital (programmed) low nephron number may explain why some individuals are susceptible to hypertension and renal injury, whereas others may seem relatively resistant under similar circumstances (e.g., sodium excess or diabetes mellitus). Low nephron number and low whole-kidney glomerular surface area would result in reduced sodium excretory capacity, enhancing susceptibility to hypertension, and a relatively reduced renal reserve capacity, limiting compensation for renal injury. This hypothesis was attractive in that an association between low nephron number and low birth weight, for example, could explain differences in hypertension and renal disease prevalence observed in populations of different ethnicity, among whom those who tend to have lower birth weights often have a greater prevalence of hypertension and renal disease.[49–52]

PLAUSIBILITY OF THE NEPHRON NUMBER HYPOTHESIS

An obstacle to investigation of the nephron number hypothesis has been the difficulty of accurately counting or estimating the total number of nephrons in a kidney.[53] Review of early studies shows that humans were believed to have an average of approximately 1 million nephrons per kidney.[54] This was the nephron number published in textbooks for decades, and implied that there is little variability in human nephron number and therefore likely little relationship with adult disease risk. Such studies, however, were performed using

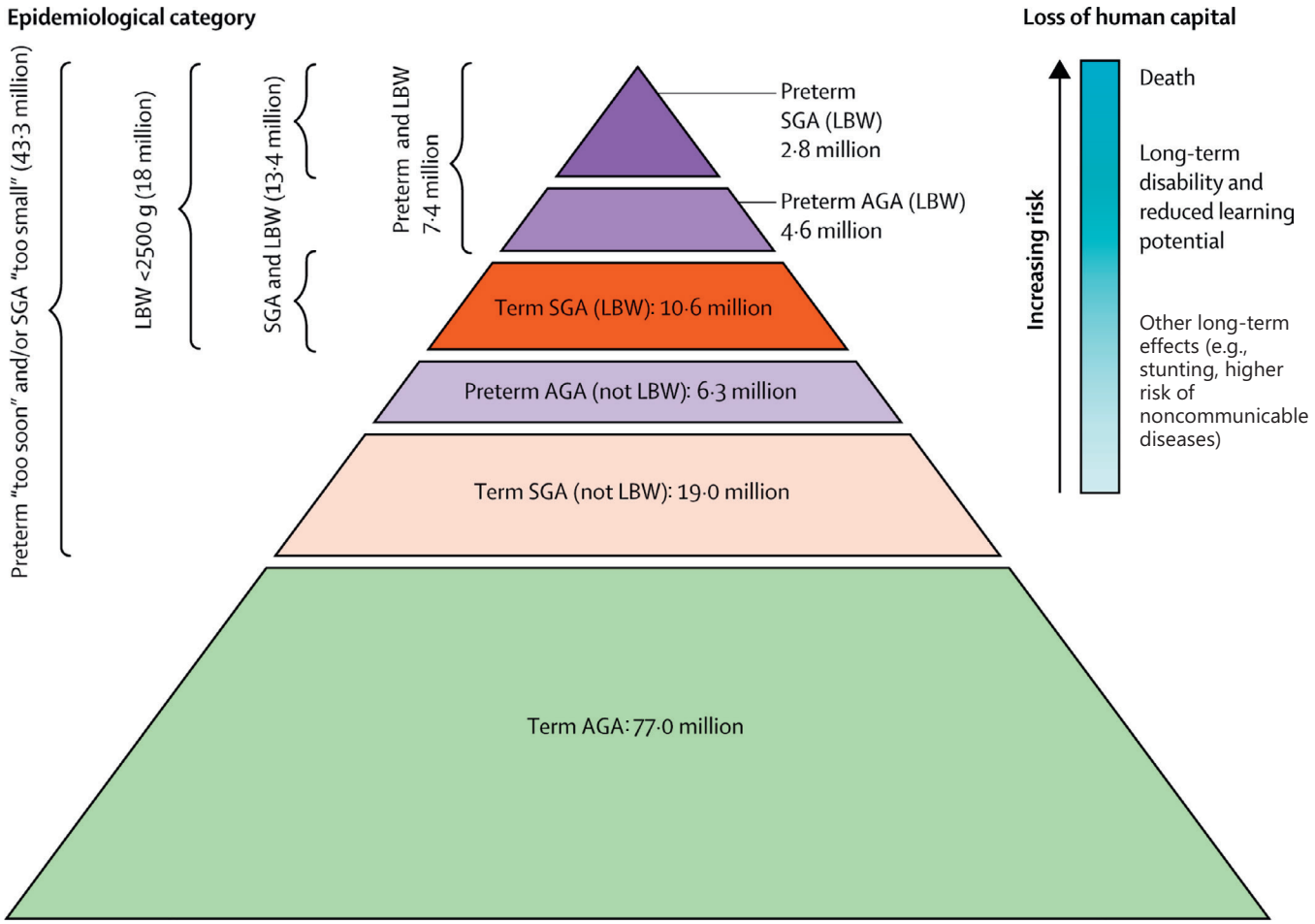

Fig. 21.1 Public health implications of the burden of preterm and SGA births for 120 million births in countries of low and middle income in 2010. *AGA*, Appropriate for gestational age; *LBW*, low birth weight; *SGA*, small for gestational age. (From Lee AC, Katz J, Blencowe H, et al. National and regional estimates of term and preterm babies born small for gestational age in 138 low-income and middle-income countries in 2010. *Lancet Glob Health*.)

techniques such as acid maceration or traditional model-based stereologic approaches, which are prone to bias because of required assumptions, extrapolations, and operator sensitivity.[53–55] Moreover, many of the early studies analyzed only a handful of kidneys, and therefore, population variability in nephron number was not observed.

Over the past 25 years, the design-based (often termed "unbiased") dissector/fractionator method has emerged as the gold standard method for estimating total glomerular, and thereby nephron, number because it generates accurate (no bias) and precise (low-variance) estimates.[53–55] With this approach, the dissector principle[56] is used to sample glomeruli in representative histologic samples of the three-dimensional renal cortex with equal probability (regardless of their size, shape, and location), and then these sampled glomeruli are counted. Glomeruli are counted in a "known" fraction of kidney tissue, allowing simple algebraic estimation of the total number of glomeruli in the whole kidney.

As the dissector/fractionator method requires sampling from a whole kidney, all studies to date with this technique have been performed on autopsy samples. For 37 normal Danish adults, the average glomerular (nephron) number was reported to be 617,000 per kidney (range: 331,000–1,424,000).[54] A positive correlation was noted between glomerular number and kidney weight, but this has not been the case in all studies.[57] The large variation in nephron number in Danes has subsequently been reported in several other populations (Table 21.2), with the largest range to date being a 13-fold variation in the largest sample yet investigated (African Americans; 159 subjects; 210,332 to 2,702,079 per kidney).[58] This previously unappreciated variability in total nephron number in subjects without kidney disease, apart from age-associated changes, may influence susceptibility to hypertension and kidney disease.[54,58,59]

In general, numbers of viable glomeruli are reduced in kidneys from older subjects, owing to age-related glomerulosclerosis and obsolescence.[54,60] Recently, Denic et al.[61] estimated glomerular number in 1638 living donor kidneys using a method combining computed tomographic (CT) estimation of renal cortical volume (prior to donation) with stereologic estimation of glomerular numerical density (number per unit volume of cortex) obtained on biopsies at the time of donation. Multiplication of these two estimates provided an estimate of total glomerular number. Separate estimates of nonsclerotic and sclerotic glomeruli were obtained. A striking decrease in numbers of nonsclerotic glomeruli was observed between 18–29-year-olds and donors aged 70–75 years. Moreover, the total number of sclerotic and nonsclerotic

Table 21.2 Variability of Nephron Number Per Kidney in Humans

Population	Sample Size	Mean	Range	Fold[a]	Reference
Danish	37	617,000	331,000–1,424,000	4.3	54
French	28	1,107,000	655,000–1,554,000	2.4	534
German (all)	20	1,074,414	531,140–1,959,914	3.7	59
German hypertensive	10	702,379	531,140–954,893	1.8	
German normotensive	10	1,429,200	884,458–1,959,914	2.2	
African-American	105	884,938	210,332–2,026,541	9.6	292
White American	84	843,106	227,327–1,660,232	7.3	
Australian non-Aborigines	24	861,541	380,517–1,493,665	3.9	220
Australian Aborigines	19	713,209	364,161–1,129,223	3.1	
Senegalese	47	992,353	536,171–1,764,421	3.3	291, 535
African and white Americans, Australian Aborigines and non-Aborigines and Senegalese	420	901,902	210,332–2,702,079	12.8	536
Japanese males (all)	18	544,819	306,092–960,756	3.1	221
Japanese Hypertensive (males)	9	423,498	306,092–550,222	1.8	
Japanese Normotensive (males)	9	666,140	419,282–960,756	2.3	
Kidney donors	1638	873,696			61

[a]Fold change from lowest to highest nephron number.

Adapted from Puelles VG, Hoy WE, Hughson MD, et al. Glomerular number and size variability and risk for kidney disease. *Curr Opin Nephrol Hypertens.* 2011;20:7–15.

glomeruli was much lower in the older donors, suggesting that many glomeruli had disappeared without trace following global glomerulosclerosis, and/or older donors were born with fewer nephrons.

In support of the nephron number hypothesis, it is known that persons born with severe nephron deficits, for example, unilateral renal agenesis, bilateral renal hypoplasia, and oligomeganephronia, develop progressive proteinuria, glomerulosclerosis, and renal dysfunction with time.[3,62] Analogously, therefore, people born with nephron numbers at or below the median level may be more susceptible to superimposed postnatal factors that act as subsequent "hits"; thus, a significant proportion of the population may be at risk for the development of hypertension and renal disease, given that some 30% of the world's adult population is hypertensive.[7,14]

The counterargument to the nephron number hypothesis is that in experimental animals and in humans, removal of one kidney (presumed reduction in nephron number by 50%) under varying circumstances may be associated with higher blood pressures or low-grade proteinuria but does not always lead to hypertension and renal disease.[55,63,64] Of interest, however, uninephrectomy on postnatal day 1 in rats or fetal uninephrectomy in sheep, that is, loss of nephrons at a time when nephrogenesis is not yet completed, does lead to adult hypertension prior to any evidence of renal injury.[65–67] These data support the hypothesis that congenitally acquired low nephron number may be associated with different compensatory mechanisms in the developing and growing kidney, or with a reduced compensatory capacity compared with later nephron loss, resulting in increased risk of hypertension. Consistent with this, kidneys from rats that underwent unilateral nephrectomy at 3 days of age showed a similar total glomerular number but a significantly reduced number of mature glomeruli in the remaining kidney compared with those that underwent nephrectomy at 120 days of age.[68] Furthermore, the mean glomerular volume in the remaining kidney of rats following unilateral nephrectomy in the neonatal period increased by 59% as compared with 20% in adult rats, likely indicating a greater burden of compensatory hypertrophy and hyperfiltration in response to neonatal nephrectomy. Similarly, rats spontaneously born with a solitary kidney are highly susceptible to the induction of hypertension (via deoxycorticosterone acetate (DOCA) salt), as well as proteinuria and reduced glomerular filtration rate (GFR) compared with rats that underwent a uninephrectomy 8 weeks after birth.[69] Nephrons in mice born with low nephron endowment were found to be less capable of coping with a stress such as unilateral ureteral obstruction than mice with the normal nephron complement.[70]

In potential contrast, however, a study of 97 subjects with a radiologically normal single kidney, aged 2.5–25 years, found that renal function declined faster over time in those with acquired single kidneys (surgical removal of the other kidney) versus congenital single kidneys, although blood pressures and proteinuria were not different.[71] These findings may be confounded by indication for nephrectomy, however, as approximately 25% of the nephrectomies were performed for obstruction, which may impact nephron development in the contralateral kidney as will be discussed later.[72,73] In addition, unilateral in utero nephrectomy in sheep was associated with significant renal hypertrophy and a 45% increase in nephron number in the remaining kidney, indicating that a congenital solitary kidney may have a higher than normal nephron endowment and therefore be relatively protected compared with an acquired single kidney.[74,75] Thus, timing of nephron loss is likely a crucial factor in determining the compensatory capacity of remaining nephrons.

ESTIMATING NEPHRON NUMBER

Until recently, most estimates of glomerular number were obtained using acid maceration of kidneys obtained at autopsy or model-based or design-based stereological analysis of histological samples obtained at autopsy. While useful, reliance on autopsy samples precludes studies in living animals and

Table 21.3 Glomerular Characteristics by Birth Weight in Humans

Birth Weight Mean (Range), kg	*N*	Number of Glomeruli[a]	Mean Glomerular Tuft Volume ($\mu m^3 \times 10^6$)	Total Glomerular Tuft Volume (cm^3)
2.65 (1.81–3.12)	29	770,860 (658,757–882,963)	9.2	6.7
3.27 (3.18–3.38)	28	965,729 (885,714–1,075,744)	7.2	6.8
3.93 (3.41–4.94)	30	1,005,356 (900,094–1,110,599)	6.9	6.6

[a]Adjusted for age, gender, race, body surface area.

From Hoy WE, Hughson MD, Bertram JF, et al. Nephron number, hypertension, renal disease, and renal failure. *J Am Soc Nephrol.* 2005;16:2557–2264.

patients, as well as longitudinal studies. In recent years, we have seen the development of several new approaches for imaging, counting, and sizing glomeruli, some of which do not require autopsy tissue. For example, the methods of Denic et al.[61,76] and of Fulladosa et al.,[77] which use CT or magnetic resonance imaging (MRI) estimation of cortical volume and estimation of glomerular numerical density in biopsies, do not require autopsy tissue. The number of functional (nonsclerotic) glomeruli has also been estimated by dividing the whole kidney ultrafiltration coefficient (K_f; calculated from renal plasma flow from para-amino-hippurate clearance) by single-nephron K_f estimated from electron microscopic measurements of the glomerular filtration barrier using kidney biopsies.[78,79]

An MRI technique using cationic ferritin to label glomeruli shows promise,[80,81] but to date, studies have been ex vivo. Cationic ferritin is injected intravenously into animals or into ex vivo human kidneys via the renal artery and binds to anionic charges on the glomerular basement membrane. With this approach, all glomeruli in whole rat,[82,83] mouse,[84] and human[80] kidneys are imaged, counted, and sized, providing, for the first time, the glomerular volume distribution for whole kidneys. New tissue-clearing approaches also facilitate imaging (using light sheet microscopy), counting, and sizing of all glomeruli in ex vivo rodent kidneys,[85] but whether modifications to this approach can be safely used in vivo appears unlikely at this time. With these recent advances in glomerular imaging and counting, we can hope that in vivo glomerular imaging and quantitation will be possible in the not-too-distant future.

NEPHRON NUMBER AND GLOMERULAR VOLUME

Human glomeruli have been reported to increase in size up to sevenfold from infancy to adulthood.[86–88] This can be considered normal physiological growth. Glomerular size also increases in adulthood in people without overt renal disease and is associated with increasing age, increasing body size, and lower birth weight.[89] Mean glomerular volume has also been consistently noted to vary inversely with total glomerular number, although the correlation appears stronger among Caucasians and Australian Aboriginals than in people of African origin.[59,90–92] This relationship suggests that larger glomeruli may reflect compensatory hyperfiltration and hypertrophy in subjects with fewer nephrons and may therefore be a surrogate marker for a reduced nephron number.[60,91] In fact, Hoy and coworkers[90] found that, although mean glomerular volume was increased in subjects with reduced nephron number, total renal glomerular tuft volume (a surrogate for total renal filtration surface area) was not different among groups with different nephron numbers (Table 21.3). This suggests that total renal filtration surface area may initially be maintained in the setting of a low or reduced nephron number but at the expense of glomerular hypertension and hypertrophy, which are maladaptive and predictors of poor outcomes.[93–95] Consistent with this possibility, glomerulomegaly is common in renal biopsies from Australian Aborigines, a population with high rates of low birth weight and renal disease, and has also been associated with faster rate of decline of GFR in Pima Indians.[96–98] Furthermore, in a study of donor kidneys, maximal planar area of glomeruli was found to be higher in kidneys from African Americans compared with whites and a predictor of poorer transplant function.[94] Among 111 adult males from four ethnic groups, mean glomerular volume and variability were highest among African Americans and Aboriginal Australians, likely associated with susceptibility to hypertension and renal disease.[99] In populations at high risk of kidney failure, therefore, large glomeruli are a common finding at early stages of renal disease and may reflect programmed reductions in nephron number in these populations in which access to prenatal and subsequent health care is often suboptimal.[100–102] An increase in glomerular volume, however, is not always associated with lower glomerular number, and individual glomerular volume varies considerably within kidneys.[92] Overall, however, glomerulomegaly and greater intrasubject variability in glomerular volume were associated with older age, fewer nephrons, lower birth weight, hypertension, obesity, and severity of cardiovascular disease.[99]

EVIDENCE FOR PROGRAMMING IN THE KIDNEY

DEVELOPMENTAL PROGRAMMING OF NEPHRON ENDOWMENT

EXPERIMENTAL EVIDENCE FOR PROGRAMMING OF NEPHRON ENDOWMENT

Developmental programming of nephron number has been the most rigorously studied link to later-life hypertension and kidney disease so far. Numerous animal models have demonstrated the association between low birth weight (induced by gestational exposure to low-protein or low-calorie diets, uterine ischemia, dexamethasone, vitamin A deprivation, alcohol) with subsequent hypertension.[103–110] The link between

Table 21.4 Associations of Nephron Number and Renal Size With Blood Pressure and Renal Function

Experimental Evidence

Reduction in Nephron Number

Experimental Model	*Animal*	*Glomerular Number (% change)*	*Birth Weight*	*Blood Pressure*	*Renal Function*
Maternal calorie restriction[174,537,538]	Rat	↓ 20–40	↓	↑	↓ GFR proteinuria
Uterine artery ligation[112,302,402]	Rat	↓ 20–30	↓	↑	Impaired proteinuria
Low-protein diet during gestation[108,115,539–541]	Rat	↓ 25 ↓ 17 ↓ 16	↓/↔	↑	↓ GFR proteinuria ↓Longevity
Postnatal nutrient restriction[406]	Rat	↓ 27	Normal	↑	NA
Iron deficiency[322]	Rat	↓ 22	↓	↑	NA
Vitamin A deficiency[115,326]	Rat	↓ 20	↔	NA	NA
Zinc deficiency[324]	Rat	↓ 25	NA	↑	↓ GFR proteinuria
Ethanol[379,381]	Sheep Rat	↓ 11	↔ ↓	NA ↑	NA ↓ GFR (females) ↑ GFR (males)
Hypoxia[542]	Rats	↓ 26–52	↓	NA	NA
Cigarette smoke[543]	Mouse	NA	↓	NA	↓ Kidney mass
Ureteral obstruction, neonatal[73]	Rat	↓ 50	NA	↑	↓ GFR ↓ Renal growth postrelief of obstruction
Prematurity[113]	Mouse	↓ 17–24	↓	↑	↓ GFR ↑ Albuminuria
Glucocorticoids[103,107,356,544]	Rat Sheep	↓ 20 ↓ 38	↓/↔ ↔	↑ ↑	Glomerulosclerosis ↑ Collagen deposition
Maternal diabetes[148,341]	Rat	↓ 10–35	↔	↑	Salt sensitivity
Gentamicin[370,372]	Rat	↓ 10–20	↓	NA	NA
β-Lactams[374]	Rat	↓ 5–10	↔	NA	Tubular dilatation Interstitial inflammation
Cyclosporine[176,545]	Rabbits	↓ 25–33	↓/↔	↑	↓ GFR ↑ RVR proteinuria
Dahl salt sensitive[48]	Rat	↓ 15		↑ with Na intake	Accelerated FSGS
Munich-Wistar-Frömter[48,546]	Rat	↓ 40		↑ with age	↑ SNGFR FSGS
Milan hypertensive[48]	Rat	↓ 17		↑	NA
PVG/c[48]	Rat	↑ 122		Resistant	Resistant to FSGS
PAX2 mutations[306,396,400]	Mouse Human	↓ 22		NA	Renal coloboma syndrome in humans, small kidneys
GDNF heterozygote[392,547]	Mouse	↓ 30	↔	↑	Normal GFR Enlarged glomeruli
c-ret null mutant[297]	Mouse	↓	NA	NA	Severe renal dysplasia
hIGFBP-1 overexpression[339]	Mouse	↓ 18–25	↓	NA	Glomerulosclerosis
Bcl-2 deficiency[397]	Mouse	↓	NA	NA	↑BUN and creatinine
p53 transgenic[401]	Mouse	↓ 50	NA	NA	Glomerular hypertrophy Renal failure
COX2 null mutant[548]	Mouse	NA	↔	↔	↓GFR
Fibroblast growth factor (FGF) 7 null mutant[115]	Mouse	↓ 30	NA	NA	Reduced ureteric branching

Augmentation of Nephron Number

Vitamin A supplementation (with low-protein diet)[419]	Rat	Normalized	NA	NA	NA
Amino acid (glycine, urea, or alanine) supplementation to maternal low protein diet[549]	Rat	Normalized	NA	Normalized with glycine only	NA
Restoration of postnatal nutrition postintrauterine growth restriction[112]	Rat	Normalized	↓	Normalized	NA

Table 21.4 Associations of Nephron Number and Renal Size With Blood Pressure and Renal Function (Cont'd)

Experimental Model	*Animal*	*Glomerular Number (% change)*	*Birth Weight*	*Blood Pressure*	*Renal Function*
Iron supplementation to iron-deficient mothers[323]	Rat	Partial rescue	NA	NA	NA
Ouabain administration (with low-protein diet)[415]	Mouse	Prevented ↓	NA	NA	NA
Maternal uninephrectomy prior to gestation[420]	Rat	↑	NA	NA	NA
Postnatal overfeeding, normal birth weight[137]	Rat	↑ 20	↔	↑	Glomerulosclerosis
Maternal high-fat diet prior to and during pregnancy and lactation[350]	Mouse	↑ 20–25	↔	NA	NA
Human Evidence					
Clinical Circumstance	*Population/ Age*	*Glomerular Number/ Kidney Volume[a] (% change)*	*Birth Weight*	*Blood Pressure*	*Renal Function*
Low birth weight[91,124]	Human 0–1 year	↓ 13–35	↓	NA	NA
Preterm birth[122]	Human	↓ Correlated with gestational age	↓	NA	NA
Females vs. males[285]	Human	↓ 12	NA	Variable	Variable
Hypertensive vs. normotensive Caucasian[59,120]	Human 35–59 years	↓ 19–50	NA	↑	No ↑ Glomerulosclerosis
Hypertensive vs. normotensive African American[120]	Human 35–59 years	NS ↓	NA	↑	No ↑ Glomerulosclerosis
Aboriginal Australians vs. Caucasian Australians[55]	Human 0–85 years	↓ 23	↓	NA	
Senegalese Africans[535,550]	Human 5–70 years	NA	NA	NA	↑ Variability of glomerular size with ↓ glomerular numbers
Maternal vitamin A deficiency[460]	Indian vs. Canadian newborns	↓ Newborn renal volume	NA	NA	NA
Genetic polymorphisms:					
RET(1476A) polymorphism[121]	Newborns	↓ 10[a]	NA	NA	NA
PAX2 AAA haplotype[306]	Newborns	↓ 10[a]	NA	NA	NA
Combined *RET(1476A)* polymorphism and *PAX2 AAA* haplotype[121]	Newborns	↓ 23[a]	NA	NA	NA
I/D ACE polymorphism[551]	Newborns	↓ 8[a]	NA	NA	NA
BMPR1A^{rs7922846} polymorphism[307]	Newborns	↓ 13[a]	NA	NA	NA
OSR1$^{rs12329305(T)}$ polymorphism[310]	Newborns	↓ 12[a]	NA	NA	NA
Combined *OSR1* and *RET* polymorphisms[310]	Newborns	↓ 22[a]	NA	NA	NA
Combined *OSR1* and *PAX2* polymorphisms[310]	Newborns	↓ 27[a]	NA	NA	NA
ALDH1A2$^{rs7169289(G)}$ polymorphism[308]	Newborns	↑ 22[a]	NA	NA	NA

[a]Numbers relate to kidney volume and not to glomerular number.

BUN, Blood urea nitrogen; *FSGS*, focal segmental glomerulosclerosis; *GDNF*, glial cell line-derived neurotrophic factor; *GFR*, glomerular filtration rate; *NA*, not assessed; *NS*, nonsignificant; *RVR*, renal vascular resistance; *SNGFR*, single-nephron GFR.

Adapted from Luyckx VA, Bertram JF, Brenner BM, et al. Effect of fetal and child health on kidney development and long-term risk of hypertension and kidney disease. *Lancet.* 2013;382:273–283; Brenner BM, Garcia DL, Anderson S. Glomeruli and blood pressure. Less of one, more the other? *Am J Hypertens.* 1988;1:335–347; Kett MM, Bertram JF. Nephron endowment and blood pressure: what do we really know? *Curr Hypertens Rep.* 2004;6:133–139; Clark AT, Bertram JF. Molecular regulation of nephron endowment. *Am J Physiol.* 1999;276:F485–F497; Moritz KM, Wintour EM, Black MJ, et al. Factors influencing mammalian kidney development: implications for health in adult life. *Adv Anat Embryol Cell Biol.* 2008;196:1–78.

adult hypertension and low birth weight in these animal models appears to be mediated, at least in part, by an associated congenital nephron deficit.[103,107,108] Corresponding blood pressures and nephron numbers associated with various programming models are outlined in Table 21.4. As shown, the association between birth weight, nephron numbers, and blood pressures varies between models, as discussed in detail later, underscoring the complexity of developmental programming and the need for better markers than birth weight.

Vehaskari and colleagues[108] demonstrated an almost 30% lower glomerular number in offspring of pregnant rats fed a low-protein diet compared with a normal-protein diet during pregnancy (see Fig. 21.2A). As shown in Fig. 21.2B, the low-protein offspring had tail-cuff systolic blood pressures that were around 40 mm Hg higher by 8 weeks of age.[108] Similarly, prenatal administration of dexamethasone was associated with low birth weight and fewer glomeruli than controls.[103] In these nephron-deficient rats, GFR was reduced, albuminuria was increased, and urinary sodium excretion was lower than those with a normal nephron complement.[103] Uteroplacental insufficiency, induced by maternal uterine artery ligation late in gestation, also results in low nephron number and was associated with increased profibrotic renal gene expression with age, although hypertension developed only in males.[111,112] Conversely, adequate postnatal nutrition, by cross-fostering onto normal lactating females at birth, restored nephron number and prevented subsequent hypertension in growth-restricted male rats.[112] In a study of the impact of preterm birth, mice delivered 1–2 days early (normal mouse gestation, 21 days) had lower nephron numbers, lower GFR, and higher blood pressures and albuminuria than mice born at term.[113] Interestingly, nephron numbers were lower in mice delivered 2 days compared with 1 day early, suggesting the degree of preterm birth is important in determining final nephron endowment, even though nephrogenesis continues for about 5 days after birth in the normal mouse. Not surprisingly, in animal studies, timing of the gestational insult has been found to be crucial in renal programming, with the greatest impact on nephron number occurring during periods of most active nephrogenesis.[114]

The complexity of the effects of perturbations to the feto-maternal environment and genetic variants on kidney development was recently highlighted in two studies. Sampogna et al.[115] compared the effects of vitamin A deficiency,

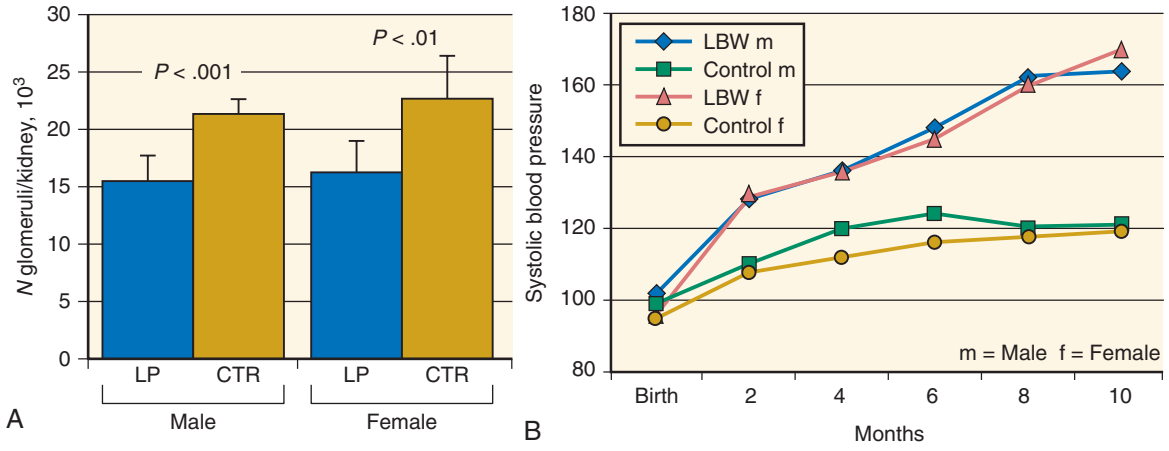

Fig. 21.2 Fetal programming of hypertension in low-birth-weight rats (induced by maternal low-protein diet). (A) Total number of glomeruli per kidney at 8 weeks of age, and (B) systolic blood pressure throughout life, in male (n = 7) and female (n = 6) offspring from low-protein pregnancies and in male (n = 7) and female (n = 7) control rats *(Control)*. *LBW*, Low birth weight. (Adapted from Vehaskari VM, Aviles DH, Manning J. Prenatal programming of adult hypertension in the rat. *Kidney Int.* 2001;59:238–245.)

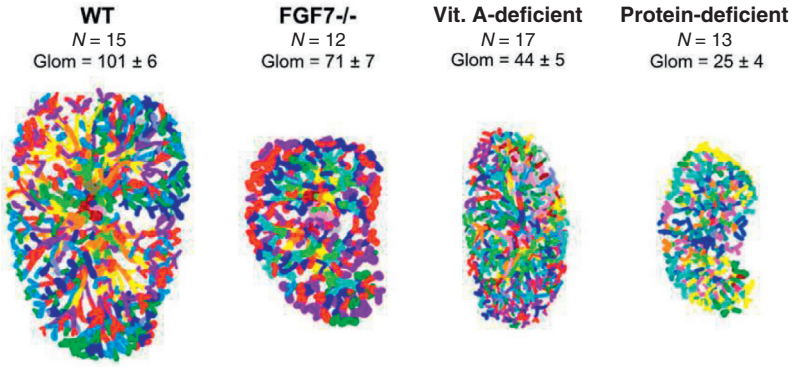

Fig. 21.3 Architecture of wild type (*WT*), FGF7 null mutant, vitamin A–deficient, and protein-deficient mouse kidneys. Embryonic day 15.5 ureteric tree tracings for each condition (to scale). *N* is the maximum branching generation number, and *Glom* represents the mean glomerular count (minimum of three kidneys studied per condition). In each case, glomerular count is reduced compared with the wild type. The number of branching generations is specific to each condition. (From Sampogna RV, Schneider L, Al-Awqati Q. Developmental program- ming of branching morphogenesis in the kidney. *J Am Soc Nephrol*. 2015;26(10):2414–2422.)

protein deficiency, and FGF7 deletion on kidney development and nephron endowment in mice (Fig. 21.3). Perturbations to kidney development included developmental delay, defects in nephron induction, changes in the growth axis, and alterations in ureteric branching morphogenesis. These produced up to a threefold decrease in glomerular number and a twofold decrease in total branching events. Boubred et al.[116] carefully compared the effects of two perturbations to the feto-maternal environment on nephron number and adult renal physiology in rats. Maternal gestational low-protein diet and betamethasone both led to a similar level of growth restriction, but nephron numbers were lower in betamethasone than the low-protein-diet offspring. Betamethasone offspring had impaired GFR, increased blood pressure, and glomerulosclerosis, whereas renal function and structure were unaltered in low-protein-diet offspring at 22 months of age. These findings suggest that the degree of reduction in nephron number is a risk factor for cardiovascular and renal disease. In summary, the available evidence suggests that the effect of a suboptimal feto-maternal environment on offspring nephron endowment and adult health may be influenced by species, the nature, timing, duration and severity of the perturbation, gender, and the postnatal nutritional environment (including lactation, infant nutrition, and subsequent growth).

PROGRAMMING OF NEPHRON NUMBER IN HUMANS

As noted earlier, total nephron number varies widely in the normal human population (see Table 21.2).[58,117] A significant proportion of the interindividual variability in nephron number appears to be already present perinatally, demonstrating a strong developmental effect.[118,119] Overall, the data support a direct relationship between nephron number and birth weight and an inverse relationship between nephron number and glomerular volume.[87,91,120,121] Hughson and colleagues[87] reported a linear relationship between glomerular number and birth weight, and calculated a regression coefficient predicting an increase of 257,426 glomeruli per increase in birth weight, although the generalizability of the regression coefficient to populations in which the distribution of nephron number appears bimodal, such as among African Americans, may not be valid.

In recent years, glomerular loss associated with aging in healthy human kidneys has come to be better appreciated. Rates of loss of glomeruli per year have been variously reported as approximately 6750 glomeruli per year after the age of 18 years,[60] 4500 glomeruli per year,[90] and 6200 glomeruli per year.[61] Specifically, the number of nonsclerotic functional glomeruli per kidney was found to decrease by almost 50% from young adulthood (aged 18–29 years: 990,661 glomeruli) to old age (aged 70–75 years: 520,410 glomeruli).[61] Glomerular number tends to be lower in women than in men.[60,61] A kidney starting with a lower nephron number, therefore, would conceivably reach a critical reduction of nephron mass, either with age or in response to a renal insult, earlier than a kidney with a greater nephron complement, predisposing to hypertension and/or renal dysfunction.

Nephrogenesis in humans begins during the 9th week of gestation and continues until the 34th to 36th week.[90] Nephron number at birth is therefore largely dependent on the intrauterine environment and gestational age. It is generally believed that no new nephrons are formed in humans after term birth. To investigate whether glomerulogenesis does continue postnatally in preterm infants, Rodriguez and colleagues[122] studied kidneys at autopsy from 56 extremely preterm infants compared with 10 full-term infants as controls. The radial glomerular counts (an estimate of glomerular number based on the number of layers of glomeruli in the cortex) were lower in preterm versus full-term infants and correlated with gestational age. Furthermore, evidence of active glomerulogenesis, indicated by the presence of S-shaped bodies immediately under the renal capsule, was seen in preterm infants who died before 40 days, but was absent in those who died after 40 days of life, suggesting that nephrogenesis may continue for up to 40 days after preterm birth. These authors also stratified their cases by presence or absence of renal failure.[122] Among infants surviving longer than 40 days, those with renal failure (serum creatinine >2.0 mg/dL) had significantly fewer glomeruli than those without renal failure. This cross-sectional observation may suggest that renal failure inhibited glomerulogenesis or, conversely, that fewer glomeruli lowered the threshold to develop renal failure in these infants. Those preterm infants surviving longer than 40 days without renal failure exhibited glomerulomegaly, which may reflect, at least in the short term, a compensatory renoprotective response. Faa and colleagues[118] also reported evidence of active glomerulogenesis in kidneys of preterm infants and two term infants who died at birth, but not in a child who died at age 3 months, suggesting that glomerular maturation may continue even after term birth for a short period.

In contrast, Hinchliffe and associates[123,124] studied nephron number in preterm or full-term stillbirths or infants who died at 1 year of age and who were born with either appropriate weight for gestational age or small-for-gestational age. At both time points, growth-restricted infants had fewer nephrons than controls. In addition, the number of nephrons in growth-restricted infants dying at 1 year of age had not increased compared with the growth-restricted stillbirths, demonstrating a lack of postnatal nephrogenesis (Fig. 21.4A). Manalich and coworkers[91] examined the kidneys of neonates dying within 2 weeks of birth in relation to their birth weights (see Fig. 21.4B). A significant direct correlation was found between glomerular number and birth weight, and a strong inverse correlation between glomerular volume and glomerular number, independent of sex and race. These studies all support the hypothesis that an adverse intrauterine environment, which may manifest as low birth weight, small-for-gestational age, or preterm birth, is associated with a congenital reduction in nephron endowment and an early, compensatory increase in glomerular volume.

In a population of 140 adults aged 18 to 65 years who died of various causes, a significant correlation was also observed between birth weight and glomerular number.[120] Glomerular volume was inversely correlated with glomerular number. Total glomerular number did not differ statistically between African-American and white subjects, although the distribution among African Americans appeared bimodal. The range of nephron number was greatest in African Americans. Significantly, however, none of the subjects in this study had been of low birth weight; therefore, no conclusion can be drawn as to whether an association with low birth weight and nephron number existed in either population group.[120] It may be argued that as low birth weight is more

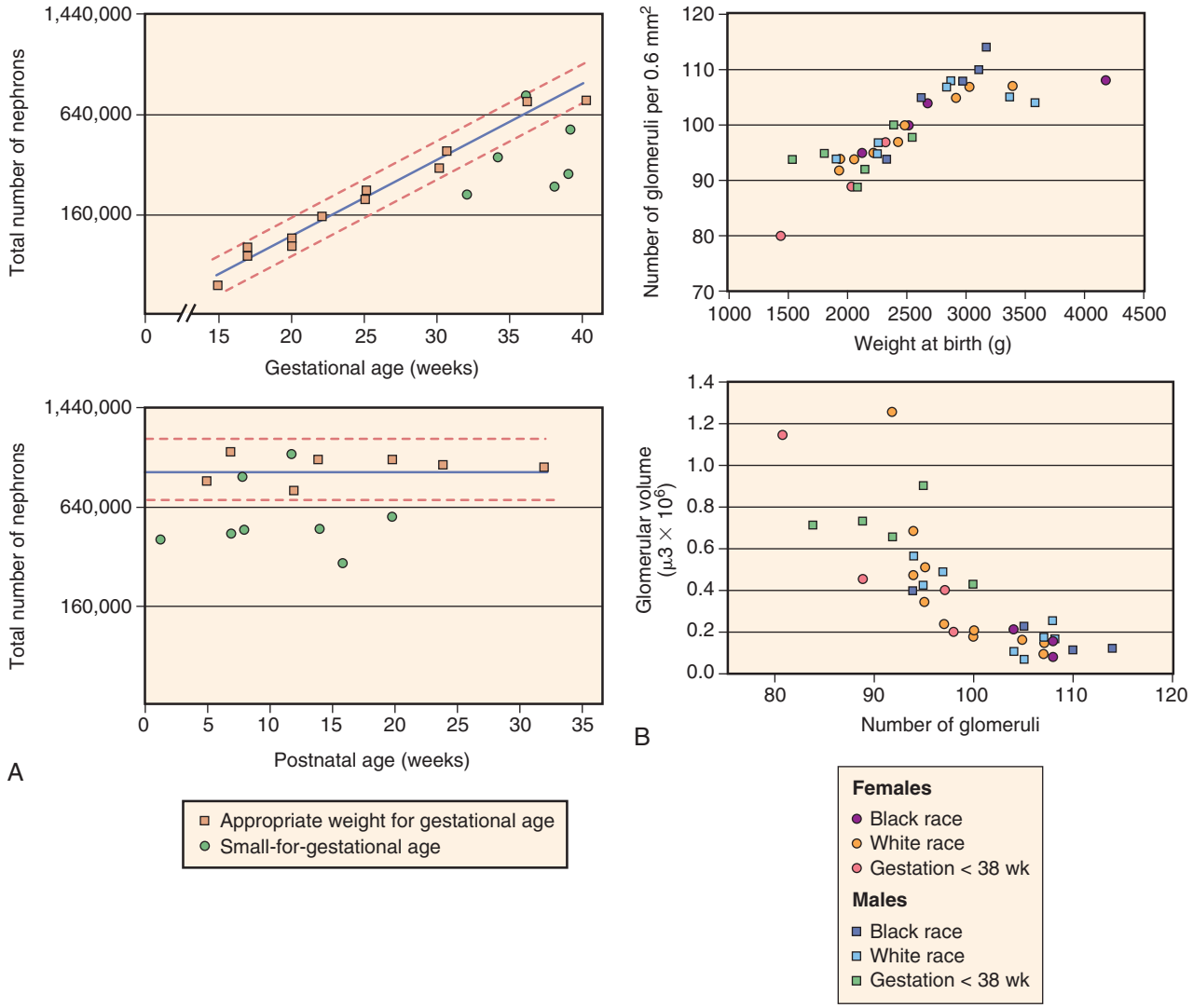

Fig. 21.4 Effect of intrauterine grown restriction (IUGR) on nephron number in humans. (A) Nephron number at birth in relation to gestational age (*upper panel*), and lack of postnatal catch-up in nephron number (*lower panel*). (From Hinchliffe SA, Lynch MR, Sargent PH, et al. The effect of intrauterine growth retardation on the development of renal nephrons. *Br J Obstet Gynaecol.* 1992;99:296–301.) (B) Relationship between birth weight and glomerular number (*upper panel*), and between glomerular number and glomerular volume (*lower panel*) in neonates. (From Manalich R, Reyes L, Herrera M, et al. Relationship between weight at birth and the number and size of renal glomeruli in humans: a histomorphometric study. *Kidney Int.* 2000;58:770–773.)

prevalent among African Americans, this cohort was more representative of the general white population than the general black population, having included only subjects of normal birth weight.[125] In a European study, among 26 subjects with non–insulin-dependent diabetes compared with 19 age-matched nondiabetic controls, no difference in glomerular number was found, but again, all subjects had birth weights above 3 kg; therefore, the impact of low birth weight on nephron number could not be assessed.[126]

Kidney Size as a Correlate for Nephron Number

Analysis of the relationship between kidney weight and nephron endowment in infants younger than 3 months of age (a time at which compensatory hypertrophy has likely not yet occurred) revealed a direct relationship (Fig. 21.5).[121] Regression analysis predicted an increase of 23,459 nephrons per gram of kidney weight.[121] Renal mass is therefore proportional to nephron number in the early postnatal period, and renal volume is proportional to renal mass; therefore, renal volume has been used as a surrogate for nephron endowment in infants in vivo.[54] Ultrasound evaluation of fetal renal function in utero revealed a reduction in hourly urine volume, higher prevalence of oligohydramnios, reduced renal perfusion, and reduced renal volume in growth-restricted fetuses.[127–129] These findings may represent reduced fetal perfusion in situations of uterine compromise, however, and do not necessarily reflect altered renal development. Similarly, among preterm infants, kidney volume at a corrected age of 38 weeks was significantly lower than in term infants and was associated with a significantly lower GFR estimated from serum cystatin C.[130] Analysis of kidney size and postnatal growth measured by ultrasound in 178 children born preterm or small for gestational age compared with 717 mature children with appropriate weight for gestational age at 0, 3, and 18 months found that weight for gestational age was positively associated with kidney volume at all three time points.[131] Slight

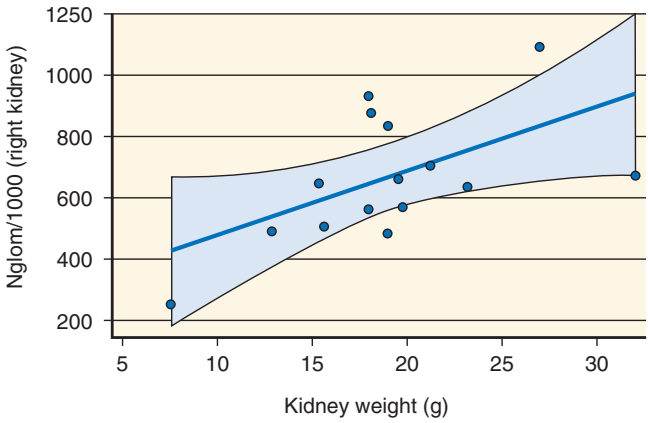

Fig. 21.5 Relationship between nephron number and mass of the right kidney in Caucasian infants aged ≤3 months who died within the first 3 months of life. *Nglom/1000,* Number of glomeruli per kidney in 1000s. (From Zhang Z, Quinlan J, Hoy WE, et al. A common RET variant is associated with reduced newborn kidney size and function. *J Am Soc Nephrol.* 2008;19:2027–2034.)

catch-up in kidney growth was observed in growth-restricted infants but not in preterm infants. Similarly, in a South Indian population, kidney volumes were lower in low-birth-weight and small-for-gestational-age neonates compared with those of normal and appropriate-for-gestational-age birth weights.[132] Kidneys in the low-birth-weight and small-for-gestational-age infants remained small and grew more slowly than kidneys of normal-birth-weight or appropriate birth-weight-for-gestational-age infants during the first 2 years of life. In a study of multiethnic children in the Netherlands, lower fetal weight gain and lower early infant weight gain led to smaller kidneys at 6 years of age.[133] However, only lower fetal weight gain, not postnatal weight gain, was associated with lower estimated GFR (eGFR). These findings suggest that suboptimal early growth affects kidney function in later life.

Among term neonates, renal parenchymal thickness, proposed as a more accurate screening tool than renal volume estimation, was significantly reduced in those with low compared with normal birth weights.[134] In Australian Aboriginal children, low birth weight was also found to be associated with lower renal volumes on ultrasound.[135] Comparison of renal volume between children aged 9–12 years born preterm, at either small or appropriate weight for gestational age, and controls, found that kidneys were smallest in those who had been preterm and small for gestational age, but when adjusted for body surface area (BSA), there were no significant differences between the groups.[136] A smaller kidney size, therefore, may be a surrogate marker for a reduced nephron endowment, but importantly, growth in kidney size on ultrasound cannot distinguish between normal growth with age and renal hypertrophy. In contrast to the situation in infants and children, in adults, kidney size is not a reliable marker of nephron number tautology. Findings from six studies in adults in which kidney size was reported and nephron number had been estimated using the dissector/fractionator combination were analyzed.[57] Only data from subjects aged 18–60 years without renal disease were included. Although an association between renal size and nephron number was found, only about 5% of the variation in nephron numbers was explained by differences in renal size.

Table 21.5 Developmentally Programmed Changes Observed in the Kidney

- Nephron number
- Glomerular volume
- Accelerated maturation of glomeruli
- Tubular sodium transporter expression and/or activity
- Altered renal vascular reactivity
- Alterations in renin-angiotensin system
- Alterations in sympathetic nervous system activity
- Accelerated senescence, especially after catch-up growth
- Predisposition to inflammation and fibrosis
- Kidney size

EVIDENCE OF ADDITIONAL PROGRAMMING EFFECTS IN THE KIDNEY

Taken together, there is no doubt that nephron endowment varies widely in human kidneys and that a range of perturbations to the feto-maternal environment in animal models can dramatically influence nephron endowment. Once nephrogenesis ends, no new nephrons can form, and therefore, any deficit in nephron number is permanent. Nephron endowment is likely an independent factor determining susceptibility to essential hypertension and subsequent renal injury. However, low nephron number alone does not account for all observed programmed hypertension (see Table 21.4). Supplementation of a low-protein diet during gestation with glycine, urea, or alanine resulted in a normalization of nephron number in rat offspring, but blood pressure only normalized in those supplemented with glycine.[34] Likewise, augmentation of nephron number by postnatal hypernutrition resulted in a 20% increase in nephron number but also obesity, hypertension, and glomerulosclerosis with age.[137] These findings suggest that additional factors also contribute to developmental programming of hypertension. Recent evidence has shown alterations in renal tubular sodium handling and vascular function in developmentally programmed kidneys that likely also contribute to later-life blood pressure and renal functional changes, as outlined in Table 21.5.[114,138]

Altered Sodium Handling by the Kidney

The pressure–natriuresis curve is shifted to the right in most forms of hypertension. A low total renal filtration surface area associated with a low nephron number is one plausible hypothesis to explain the associated higher blood pressures. Consistent with this, salt sensitivity has been reported in several animal models associated with low birth weight and low nephron number.[35,139–143] Some authors have reported the presence of salt-sensitive hypertension in rats in which low birth weight was induced by maternal uterine artery ligation, whereas others report no salt sensitivity in rats in which low birth weight was induced by maternal protein restriction, although timing of dietary intervention and age at study appear to play a role.[140,144,145] Elevations in blood pressure in response to a high-salt diet have been more consistently observed in aging rather than young rats, suggesting an early adaptive mechanism that may decline with age or worsening salt sensitivity as nephron number declines with age.[146] In

young rats, however, despite no change in blood pressure, an increase in plasma volume was observed, consistent with sodium retention.[147] Similar salt sensitivity was observed in adult rat offspring exposed to maternal gestational diabetes, a model also associated with low nephron number.[148]

The effect of nephron "dose" and total renal filtration surface area on salt sensitivity was examined in glial cell line–derived neurotrophic factor (GDNF) heterozygous mice that have either 1 kidney (HET1K) and 65% few nephrons than wild type littermates, or two kidneys (HET2K) and 25% fewer nephrons than GDNF wild type mice.[149] Given the accompanying glomerular hypertrophy, total glomerular surface area was normal in HET2K but remained reduced in HET1K mice at 48–52 weeks of age. At baseline, the mice did not have elevated blood pressures; however, both heterozygous groups became hypertensive in response to high-sodium feeding. A gradient of increasing blood pressure was observed from GDNF wild type to HET2K to HET1K, suggesting dependence on nephron number and filtration surface area, given that no change in expression of tubular sodium transporters was observed.[149] In contrast, transforming growth factor-β2 (TGF-β2) heterozygous mice, which have 30% more nephrons than TGF-β2 wild type mice, were relatively protected against developing high blood pressures on a chronic high-salt diet compared with wild type mice.[150] Surprisingly, however, these mice did develop increased blood pressures in response to an acute sodium load, suggesting that the benefit conferred by the higher nephron number requires time for adaptation to occur. Early change in sodium diet in itself has been found to have a long-term impact on programming of hypertension in low-birth-weight rats. Short-term feeding of a low-salt diet from weaning to 6 weeks of age abrogated, whereas high-salt feeding exacerbated hypertension at 10 and 51 weeks despite reinstitution of normal salt diet at 6 weeks.[139,151] The role of sodium intake on long-term renal programming requires further study.

Salt sensitivity, therefore, does appear to be developmentally programmed. From the GDNF mouse data, total renal filtration surface area may be crucial in determining salt sensitivity, but as discussed earlier, it is often not reduced in the setting of low nephron number due to concomitant glomerular hypertrophy. Expression and activity of renal tubule sodium transporters have therefore been investigated. Expression of the Na-K-2Cl (NKCC2) and Na-Cl (NCC) transporters were significantly increased in prehypertensive offspring of rats fed a protein-restricted diet during gestation compared with controls, although expression of the sodium–hydrogen exchanger type III (NHE3) and epithelial sodium channel (ENaC) were not changed (Fig. 21.6A).[152] Increased activity of NKCC2 was shown by increases in chloride transport and lumen positive transepithelial potential difference in the medullary thick ascending limb in offspring of protein-restricted or dexamethasone-treated mothers (Fig. 21.6B).[153] Furthermore, after development of hypertension, furosemide administration reduced blood pressure, supporting increased NKCC2 activity as a mediator of hypertension in the protein restriction model.[153] Expression of the glucocorticoid receptor and the glucocorticoid responsive α1- and β1-subunits of Na-K-ATPase were increased in offspring of pregnant rats fed a low-protein diet.[154] In rats suckled by low protein–fed mothers during lactation, expression of Na-K-ATPase was increased by 40%, but Na-K-ATPase activity was increased by 300%, demonstrating that expression levels may not fully reflect activity levels.[155] Prenatal dexamethasone administration was associated with increased expression of proximal tubular NHE3, as well as the more distal NKCC2 and NCC, but no change in ENaC expression.[156] Interestingly, renal denervation reduced systolic blood pressure and sodium transporter expression in this model, suggesting indirect regulation of these genes via sympathetic nerve activity.[156] In rats subjected to maternal diabetes, baseline expression of β and γ ENaC, but not α ENaC, as well as Na-K-ATPase, were significantly increased compared with controls.[148] Despite several studies showing no change in ENaC expression in programmed animals, an enhanced natriuretic response to the ENaC inhibitor benzamil demonstrated increased ENaC activity in offspring of mothers fed a low-protein diet (Fig. 21.6C).[157] Taken together, despite differences among models, the data suggest increased sodium transport in all segments of the renal tubule. Whether a reduced nephron number contributes indirectly to increased sodium transport through increased single-nephron GFR (SNGFR), necessitating glomerulotubular balance, or sodium transporter activity is independently programmed, has not yet been elucidated.

Renin–Angiotensin System

All components of the renin–angiotensin–aldosterone system (RAAS) are expressed in the developing kidney.[158] Alterations in the renal RAAS have been studied in various programming models, and a common, though not universal, finding has been inhibition of the system during the period of active nephrogenesis with an upregulation in adulthood, often associated with changes in blood pressure.[159] For example, expression of angiotensinogen and renin mRNA was decreased in neonatal kidneys of rats subjected to uterine ischemia but increased in mouse offspring of diabetic mothers.[160,161] Outcomes likely reflect species differences, differences in timing of intervention, timing of study, and so on, as summarized in Table 21.6.[75] The importance of angiotensin II in nephrogenesis was demonstrated by the administration of the angiotensin II subtype 1 receptor (AT1R) blocker, losartan, to normal rats during the first 12 days of life (while nephrogenesis is proceeding), which resulted in a low final nephron number and subsequent development of hypertension.[162,163] Angiotensin II can stimulate the expression of Pax-2 (an antiapoptotic factor) through AT2R.[164] AT2R expression, therefore, is likely to affect nephrogenesis and kidney development, but its role in programming is still unclear. Administration of an angiotensin-converting enzyme inhibitor (ACEI), captopril, or losartan to low-birth-weight rats from 2 to 4 weeks of age abrogated the development of adult hypertension.[21,112,160,165] Similarly, administration of angiotensin II or ACEI to adult rats subjected to a low-protein diet in utero resulted in a more exaggerated hypertensive or hypotensive response, respectively, than in control rats.[21,166–168] However, a recent study in aged offspring born growth restricted demonstrated that AT1 receptor blockade could not prevent hypertension, suggesting lesser dependence on the RAAS with age.[169] Differential regulation of the RAAS by sex hormones during development is thought to contribute to the observation that the effects of developmental programming are often less severe in young females.[159,170] Overall, programmed suppression of the intrarenal RAAS during nephrogenesis is likely to contribute to low nephron number

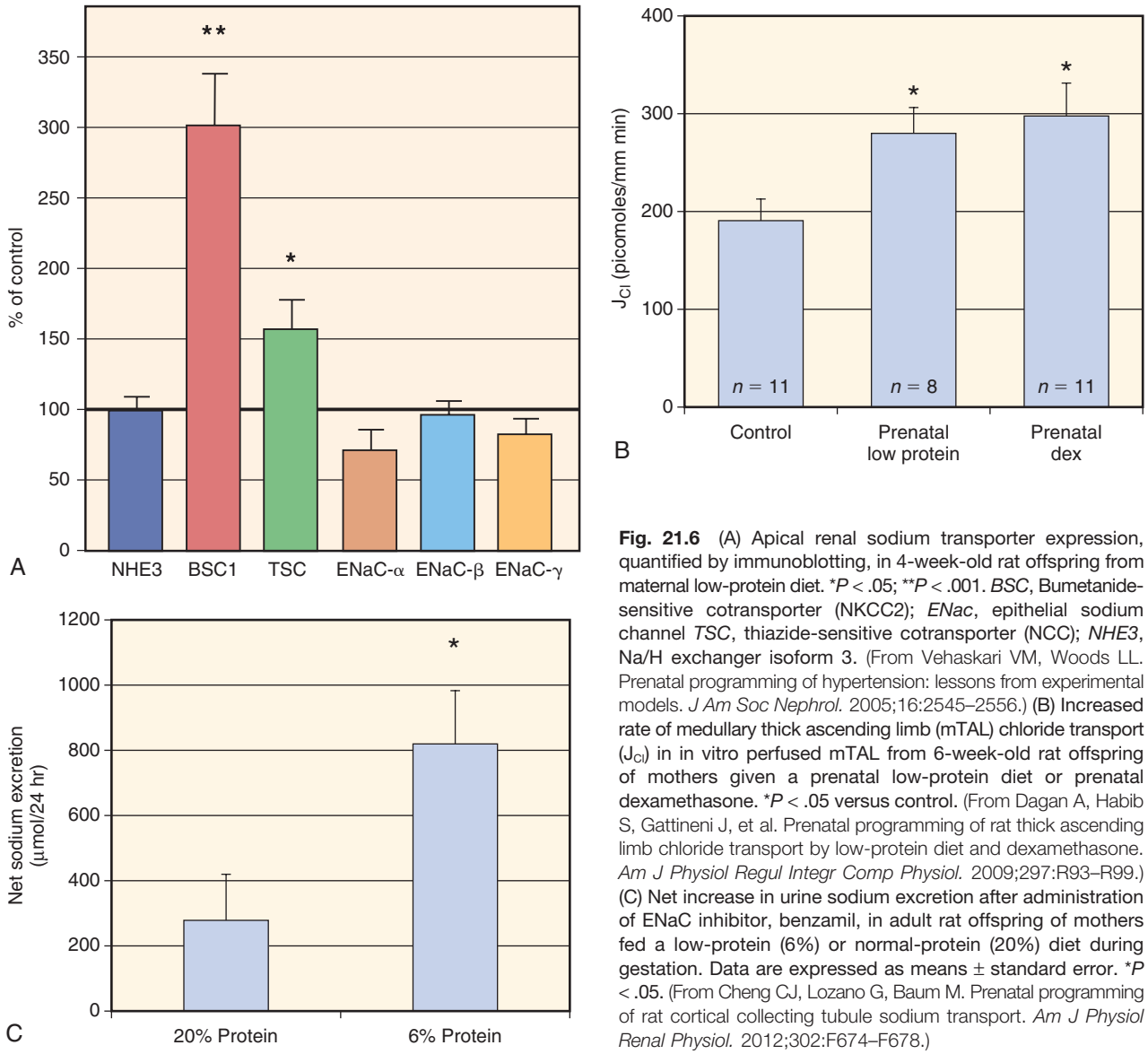

Fig. 21.6 (A) Apical renal sodium transporter expression, quantified by immunoblotting, in 4-week-old rat offspring from maternal low-protein diet. *$P < .05$; **$P < .001$. *BSC*, Bumetanide-sensitive cotransporter (NKCC2); *ENac*, epithelial sodium channel *TSC*, thiazide-sensitive cotransporter (NCC); *NHE3*, Na/H exchanger isoform 3. (From Vehaskari VM, Woods LL. Prenatal programming of hypertension: lessons from experimental models. *J Am Soc Nephrol.* 2005;16:2545–2556.) (B) Increased rate of medullary thick ascending limb (mTAL) chloride transport (J_{Cl}) in in vitro perfused mTAL from 6-week-old rat offspring of mothers given a prenatal low-protein diet or prenatal dexamethasone. *$P < .05$ versus control. (From Dagan A, Habib S, Gattineni J, et al. Prenatal programming of rat thick ascending limb chloride transport by low-protein diet and dexamethasone. *Am J Physiol Regul Integr Comp Physiol.* 2009;297:R93–R99.) (C) Net increase in urine sodium excretion after administration of ENaC inhibitor, benzamil, in adult rat offspring of mothers fed a low-protein (6%) or normal-protein (20%) diet during gestation. Data are expressed as means ± standard error. *$P < .05$. (From Cheng CJ, Lozano G, Baum M. Prenatal programming of rat cortical collecting tubule sodium transport. *Am J Physiol Renal Physiol.* 2012;302:F674–F678.)

under adverse circumstances, and postnatal upregulation of the AT1R, possibly mediated by an increase in glucocorticoid activity or sensitivity, may contribute to the subsequent development of hypertension and glomerular hyperfiltration as reviewed in detail elsewhere.[75,159]

Underscoring the relevance of the RAAS in developmental programming of blood pressure, angiotensin-converting enzyme (ACE) activity was significantly elevated in children of low birth weight compared with normal birth weight, and there was a greater frequency of the ACE gene DD genotype among low-birth-weight children with highest blood pressures, suggesting that the programming effect of blood pressure may be in part modulated by ACE gene polymorphisms.[171]

The Sympathetic Nervous System and Renal Vascular Reactivity

Within the kidney, the sympathetic nervous system modulates activity of the RAAS, sodium transport, and vascular function and thereby contributes to blood pressure through regulation of vascular tone and volume status.[75] Development of the renal sympathetic nervous system and how this may be programmed during nephrogenesis, and modulated by the RAAS, is expertly reviewed by Kett and Denton.[75] Renal denervation has been shown to abrogate development of adult hypertension and alter sodium transporter expression in the prenatal dexamethasone and uterine ischemia programming models, as well as the age-associated hypertension that develops in growth-restricted female rats.[156,172,173] Consistent with the whole animal findings, within the kidney, an increase in baseline renal vascular resistance has been described in several programming models.[174–176] For example, renal arterial responses to β-adrenergic stimulation and sensitivity to adenylyl cyclase were increased in 21-day-old growth-restricted offspring subjected to placental insufficiency.[177] Although the renal expression of β2-adrenoreceptor mRNA was increased in these pups, there was also evidence of adaptations

Table 21.6 Programming Effects on the Renin–Angiotensin System

Model	Species	Timing of Insult	Age and Sex of Offspring at Study	mRNA or Protein Expression	Physiologic Response	Reference(s)
Glucocorticoids	Sheep	Early gestation	40 mo ♀	↔ Plasma renin, ANG II, or Aogen	↑ Basal MAP, females only	116
	Rat		6–7 mo ♂♀	↔ Renal Aogen ↑ PRA, plasma Aogen in females only	↑ Basal TBP, females only	108
	Rat	Mid- to late gestation	6 mo	↑ Renal ACE and renin in males and females	ND	159
	Rat	Mid- to late gestation	4 and 8 wk ♂	↔ PRA, plasma ANG II, and renal ANG II levels ↑ Urine ANG II at 4 and 8 wk	↑ Basal TBP at 8 but not 4 wk of age	27
Maternal nutrient restriction or low-protein diet	Sheep	Early- to midgestation	9 mo old	↑ Renal cortical ACE protein ↔ AT1R in the renal cortex and medulla ↔ Renal cortical but ↑ renal medulla AT2R	↑ Basal MAP	47
	Rat	Mid- to late gestation	4–12 wk ♂♀	↑ PRA	↑ Basal TBP from 8 wk of age	11
	Rat	Throughout gestation	1–5 days and 22 wk ♂	↓ Renal renin mRNA and ANG II levels at 1 to 5 days of age	↑ Basal MAP at 22 wk of age ↔ No change GFR or RBF	154, 155
	Rat	Throughout gestation	16 wk ♂	↓ Renal AT1R and AT2R protein	↑ Basal TBP, ↓ sodium excretion, ↔ GFR	99
	Rat	Throughout gestation	4 wk ♂	↑ Renal AT1R protein ↓ Renal AT2R protein ↑ Ang II receptor binding ↔ Renal renin and Ang II tissue levels	↑ Basal MAP (anesthetized) ↑ Basal renal vascular resistance ↔ No change GFR or RBF	125, 126
	Rat	Mid- to late gestation	1 to 11 mo ♂♀:		↑ Basal TBP at 8 wk of age	94, 95, 146, 147
			1–2 mo	↓ PRA ↓ Renal AT1R protein and mRNA ↓ Renal AT2R protein, ↑ AT2R mRNA	Salt-sensitive TBP TBP normalized by ACE inhibition and low-salt diet Urinary protein/creatinine ratio increased in males only	
			6 to 11 mo	↑ PRA ↔ Plasma or renal ANG I and ANG II ↑ AT1R protein and mRNA ↑ AT2R protein, ↔ AT2R mRNA		
Placental insufficiency	Rat	Late gestation	0 to 16 wk ♂ Newborn:	↓ renal renin and aogen	↑ Basal MAP that was abolished by ACEi treatment	53, 110
			16 wk:	↑ Renal renin and aogen mRNA, ↑ ACE activity ↔ Renal AT_1R and ANG II, ↔ PRA and plasma ACE	↑ Pressor response to ANG II in presence of ACEi ↓ GFR	
Maternal renal hypertension	Rabbit	Throughout gestation	10–45 wk, ♂ ♀	↓ PRA–5 and 10 wk ↔ PRA 30 and 45 wk	↑ Basal MAP at 30 and 45 wk	31, 32, 92

ACE, Angiotensin-converting enzyme; *ACEi*, angiotensin-converting enzyme inhibition; *Aogen*, angiotensinogen; *AT1R*, angiotensin receptor type 1; *GFR*, glomerular filtration rate; *MAP*, mean arterial pressure; *ND*, not done; *PRA*, plasma renin activity; *RBF*, renal blood flow; *TBP*, tail artery pressure.

Taken from Kett MM, Denton KM. Renal programming: cause for concern? *Am J Physiol Regul Integr Comp Physiol.* 2011;300:R791–R803.

to the signal transduction pathway contributing to the β-adrenergic hyperresponsiveness.[177] Intriguingly, these findings were much more marked in the right compared with the left kidney, an observation that remains unexplained but that is not without precedent: asymmetry of renal blood flow was found in 51% of a cohort of hypertensives without renovascular disease.[177,178] In this study, the growth-restricted rats had low glomerular number, glomerular hyperfiltration, and hyperperfusion, and had significantly increased proteinuria compared with controls, suggesting alteration in glomerular pressures likely mediated by renal vasoreactivity. Interestingly, in a cohort of white and black U.S. subjects, the effect of birth weight on subsequent blood pressures was significantly modified by β-adrenergic receptor genotype, further underscoring a relationship between birth weight, sympathetic activity, and blood pressure.[179]

PROGRAMMING OF RENAL FUNCTION AND DISEASE

In contrast to preterm infants or those of low birth weight in whom nephron numbers have been shown to be reduced, in adults, there are no data on nephron number, specifically in those born with low birth weight. The association between nephron number and birth weight and preterm birth, however, is a consistent finding in infants, so it seems reasonable to extrapolate that nephron numbers would remain reduced in adults of low birth weight.[87] The determination of nephron number in vivo is not yet possible; therefore, the most used in vivo surrogate markers at present are birth weight and preterm birth. Importantly, however, in some animal models, low nephron numbers have also been observed in the setting of normal birth weight (see Table 21.4). Therefore, in humans, if birth weight is the only surrogate marker used, the impact of renal programming on any outcome is likely to be underestimated.[180] Other clinical surrogates for an adverse intrauterine environment and low nephron numbers are outlined in Table 21.7.

EXPERIMENTAL EVIDENCE

Glomerulomegaly is consistently observed in the setting of low nephron number (see Fig. 21.4B). In rats in which low birth weight was induced by maternal protein restriction, GFR was reduced by 10%, although nephron number was reduced by 25%, implying some degree of compensatory hyperfunction per nephron.[35] Although this may be a compensatory mechanism to restore filtration surface area, it is conceivable that renal reserve in these kidneys is reduced.[90] If this is the case, these kidneys may be expected to be less able to compensate further in the setting of additional renal insults and to begin to manifest signs of renal dysfunction (i.e., proteinuria, elevations in serum creatinine, and hypertension). To investigate this hypothesis, diabetes was induced by streptozotocin injection in subgroups of low-birth-weight (induced by maternal protein restriction) and normal-birth-weight rats.[181] Low-birth-weight rats had reduced nephron numbers and higher blood pressures compared with those of normal birth weight. Among those rendered diabetic, there was a greater proportional increase in renal size and glomerular hypertrophy in the low-birth-weight rats compared with normal-birth-weight controls after 1 week (Fig. 21.7).[181] This study demonstrates that the renal response to injury in the setting of a reduced nephron number may be exaggerated and could lead to accelerated loss of renal function.

Subsequently, the same authors published outcomes in low-birth-weight versus normal-birth-weight diabetic rats at 40 weeks.[182] Histologically, the podocyte density was reduced and the average area covered by each podocyte was greater in the low-birth-weight diabetic rats than in the normal-birth-weight controls. These findings correlated with urine albumin excretion rate, which was higher in low-birth-weight diabetic rats, although this did not reach statistical significance. In support of the role of altered podocyte physiology in renal disease progression, similar findings were observed in the Munich Wistar-Frömter rat, a strain that has congenitally reduced nephron numbers and develops spontaneous renal disease.[183] Whether these podocyte changes are secondary to an increase in glomerular pressure in the setting of reduced nephron numbers or a primary programmed structural change leading to glomerular injury is not yet known. The podocyte depletion hypothesis has emerged as a potentially unifying concept in glomerular pathology in recent years, with podocyte depletion defined as either loss of podocytes, decreased podocyte density due to glomerular hypertrophy, or a change in podocyte phenotype.[184] Given that podocytes have little or no capacity to increase their numbers in adulthood, it will be important to determine if those feto-maternal environmental factors that result in low nephron endowment also produce low podocyte endowment. Humans and animals born with both a low nephron endowment and low podocyte endowment could be expected to be at further risk of developing CKD.

Of interest, in contrast, in low-birth-weight rats exposed to prenatal dexamethasone and subsequently fed a high-protein diet, GFR was similar to that in normal-birth-weight controls.[185] Nephron numbers were reduced by 13% in only the male low-birth-weight rats. This finding suggests that there is a threshold reduction in nephron number, above which compensation is adequate or that the high-protein diet–induced supranormal GFRs in both groups, masking subtle differences in baseline GFR. Another study that measured GFR in low-birth-weight rats, induced by placental insufficiency, also failed to demonstrate lower GFRs in low-birth-weight rats, but the low-birth-weight offspring were hypertensive compared with normal-birth-weight controls.[110] Conceivably, in this study, the higher intraglomerular pressure due to elevated blood pressure and reduced nephron mass in low-birth-weight rats

Table 21.7 Clinical Surrogates for Programmed Low Nephron Number in Humans

- Low birth weight[91,122,124]
- Preterm birth[122,124]
- Low kidney mass[54,121]
- Reduced kidney volume[131,135]
- Glomerulomegaly[87,91,124]
- Female sex[285]
- Ethnicity: Australian Aboriginal[285]
- Older age[61]

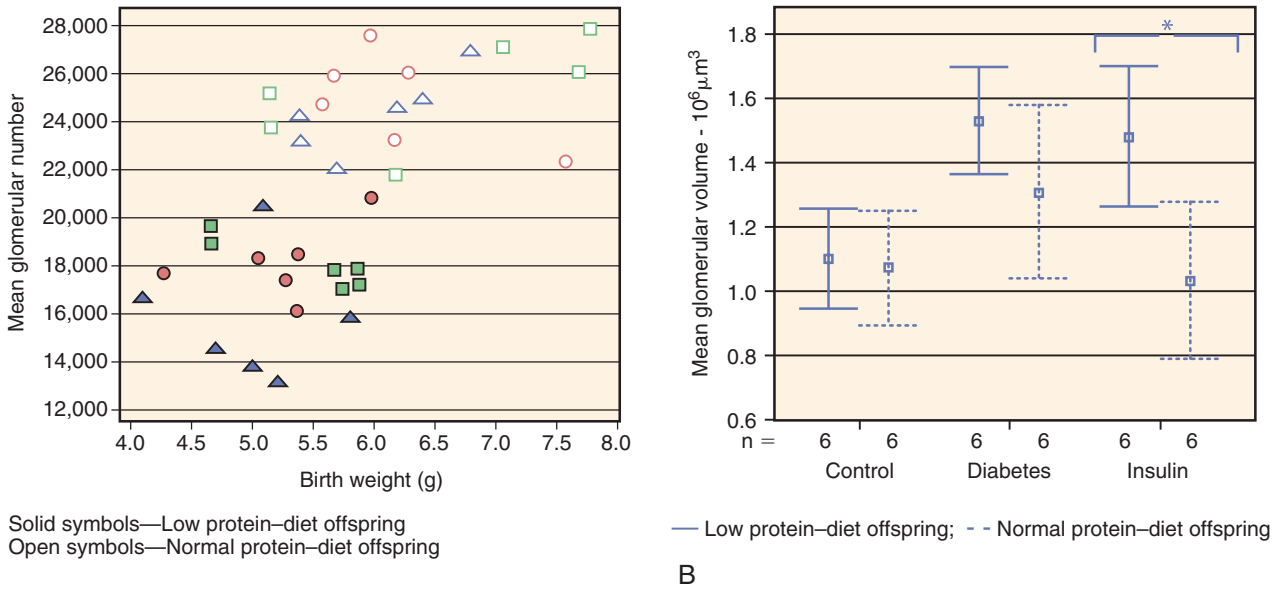

Fig. 21.7 Influence of glomerular number on adaptation to diabetes in rats. (A) Scatterplot of mean glomerular number and birth weight in rats on low-protein diet *(solid symbols)* and normal protein diet *(open symbols)*; control groups *(triangles)*; diabetes *(circles)*; diabetes treated with insulin *(squares)*. (B) Plot of glomerular volume in rats on low-protein diet *(solid lines)* and normal-protein diet *(dotted lines)*. Error bars represent 95% confidence intervals. **P* = .015. (From Jones SE, Bilous RW, Flyvbjerg A, et al. Intra-uterine environment influences glomerular number and the acute renal adaptation to experimental diabetes. *Diabetologia* 2001;44:721–728.)

may have led to a compensatory increase in SNGFR and, thus, normalization of whole-kidney GFR.

The definitive pathophysiologic impact of a reduction in nephron number in the development of renal dysfunction is difficult to elucidate from the existing literature comprising very varied experimental conditions. Overall, however, it is possible that, although whole-kidney GFR may not change, SNGFR is likely to be increased in the setting of a reduced nephron number and exacerbated in the face of renal injury. Interestingly, SNGFR was found to be significantly elevated in the Munich-Wistar-Frömter rat, which has reduced nephron numbers and is known to develop spontaneous progressive glomerular injury, compared with the control Wistar rat strain.[183] Renal dysfunction may also result from a programmed predisposition to inflammation and scarring, which may be independent of glomerular pressures. In a glomerulonephritis model, anti–Thy-1 antibody injection in low-birth-weight rats resulted in significant upregulation of inflammatory markers and development of sclerotic lesions by day 14, but with no difference in blood pressure or proteinuria compared with normal-birth-weight controls.[186]

HUMAN EVIDENCE

Most human data rely on the surrogates of birth weight and preterm birth and kidney size to reflect likelihood of renal programming. Although there is no direct proven relationship between renal risk and nephron number in humans, the consistency of the data is strongly suggestive of a programming effect.

BIRTH WEIGHT, PRETERM BIRTH, AND BLOOD PRESSURE

Two meta-analyses and systematic reviews have shown consistent associations with lower birth weight and preterm birth and higher blood pressures in later life.[36,37] Meta-analysis of 27 studies investigating the relationship between birth weight and blood pressure found that systolic blood pressures were 2.28 mm Hg (95% confidence interval 1.24–3.33 mm Hg) higher in subjects with birth weights below, compared with higher 2.5 kg (Fig. 21.8A).[37] Many studies do not discriminate between low birth weight occurring as a result of growth restriction (a marker of intrauterine stress) at any gestational age or as a result of preterm birth with an appropriate (low) weight for gestational age. Therefore the relative impact of growth restriction and preterm birth on subsequent blood pressures is not always easy to dissect.[187] To investigate this question, a study of 50-year-old subjects all born at term, but with or without growth restriction, reported an odds ratio (OR) of 1.9 (95% confidence interval [CI]: 1.1 to 3.3) for hypertension among those who had experienced growth restriction compared with those who had normal birth weights.[188] Growth restriction before birth per se, therefore, is associated with subsequent higher blood pressure.

A systematic review of 10 studies comparing preterm or very low–birth-weight subjects versus those born at term found that the preterm subjects, having a mean gestational age of 30.2 weeks and a mean birth weight of 1280 g, had 2.5 mm Hg higher (95% CI: 1.7 to 3.3 mm Hg) systolic blood pressures in later life compared with those born at term (see Fig. 21.8B).[36] Preterm birth, therefore, is also independently associated with higher blood pressure, which, in some studies, meets the definition of hypertension by 1–2 years of age.[189–191] Whether the risk of higher blood pressure is greater among preterm subjects who were born small for gestational age (growth restricted) versus appropriate for gestational age, however, is not yet clear, with some studies suggesting an additional effect of growth restriction, whereas others do not.[192–195] Ultimately, the importance of dissecting the risk from low birth weight "versus" preterm birth may lie in the

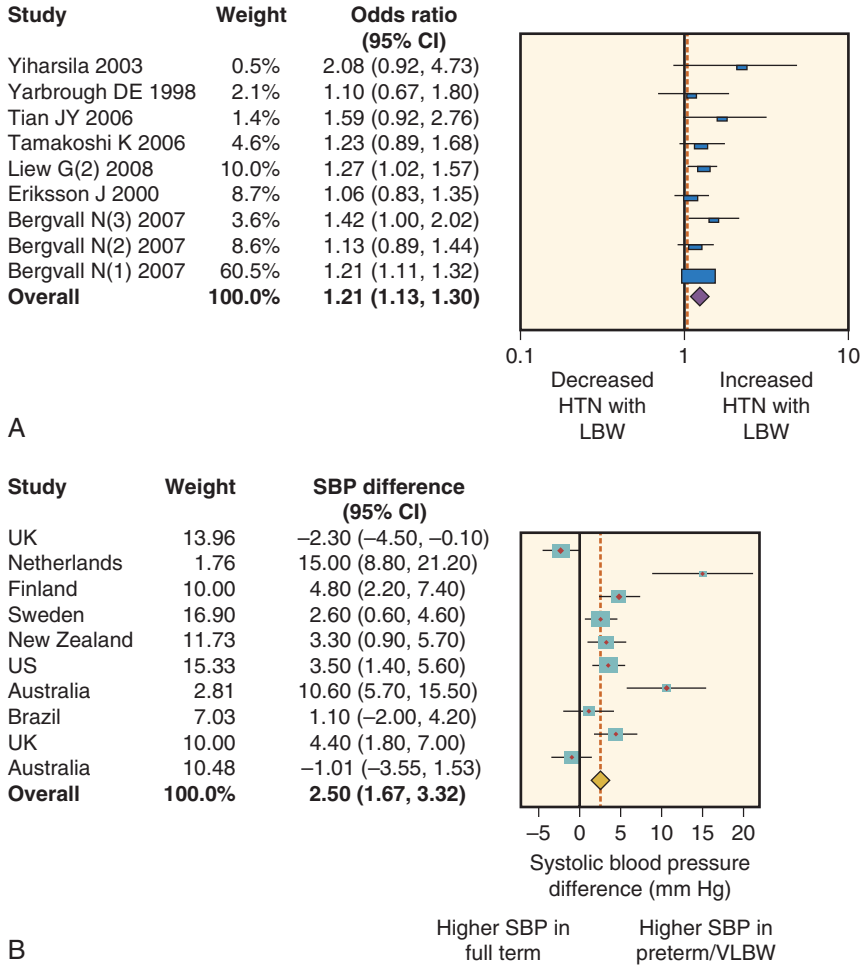

Fig. 21.8 Relationship between birth weight, preterm birth, and blood pressure. (A) Meta-analysis of odds for hypertension *(HTN)* in individuals with birth weights below 2500 g (low birth weight *[LBW]*) compared with birth weights above 2500 g. The pooled odds ratio is shown as a *diamond*. (From Mu M, Wang SF, Sheng J, et al. Birth weight and subsequent blood pressure: a meta-analysis. *Arch Cardiovasc Dis.* 2012;105:99–113; see original paper for full references). (B) Meta-analysis of difference in systolic blood pressure *(SBP)* between individuals born preterm or very low birth weight *(VLBW)* compared with full term. Pooled SBP difference is indicated by the *diamond* and *dashed vertical line*. (From de Jong F, Monuteaux MC, van Elburg RM, et al. Systematic review and metaanalysis of preterm birth and later systolic blood pressure. *Hypertension.* 2012;59:226–234; see original paper for full references).

future potential for prevention, but, given that effect estimates for risk of higher blood pressures were similar in the meta-analyses and systematic reviews cited earlier, at present, both events must be deemed important risk factors for subsequent high blood pressure.

Importantly, blood pressures of low- and normal-birth-weight subjects, although different, may still be within the normal range in childhood, but differences become amplified with age, such that adults who had been of low birth weight often develop overt hypertension, which increases with age.[196] Although the majority of studies have been conducted in Caucasian populations, generally consistent data are accumulating in other populations.[197] An association of higher blood pressure with lower birth weight in African-American children has been reported in some studies, but not all, suggesting additional factors may contribute to the greater severity of blood pressure in those of African origin.[197–202] An important effect modifier of the association with low birth weight or preterm birth and blood pressure, noted in diverse populations, is current body mass index, which may override an effect of birth weight, especially in children at different stages of growth.[197,203] Furthermore, in most populations, blood pressures are highest in those born preterm or of low birth weight who "catch up" fastest in postnatal weight (i.e., rapid upward crossing of weight centiles), highlighting the importance of early postnatal nutrition in developmental programming.[204–208]

Elevated blood pressure associated with low birth weight was recently reported in a multiethnic cohort of adolescents.[209] From the National Health and Nutrition Examination Survey (NHANES) study, 5352 participants aged 12–15 years were classified as low birth weight, very low birth weight, or normal birth weight by parental/proxy recall. Low/very low-birth-weight adolescents had a greater odds of having a blood pressure ≥95th percentile for age, height, and sex [Low birth weight: OR: 2.90; 95% CI: 1.48 to 5.71; very low birth weight: OR 5.23; 95% CI: 1.11 to 24.74]. Whether preterm birth and/or small for gestational age contributed to the low birth weight in the population was not known.

Associations between blood pressure and other markers of potential developmental stresses have also been reported.

A meta-analysis of 31 studies found that blood pressures were also higher in children who had high birth weights; however, blood pressures tended to be lower in high-birth-weight adults, suggesting that age may modify this risk differently compared with that in low-birth-weight subjects in whom it increases with age (Table 21.8).[39,210] Additionally, a systematic review and meta-analysis investigating the impact of a diabetic pregnancy on blood pressure found an overall association with higher blood pressure in offspring aged 2–20 years, but this effect was only seen in males (Table 21.8).[211] The authors did not discuss the potential impact of birth weight in this study, however, and whether these effects may have been modified by offspring of high birth weight was not reported. Another potential risk factor for higher offspring blood pressure is maternal gestational hypertension or preeclampsia.[212,213] Indeed, in a systematic review of 18 studies among children and young adults, systolic blood pressures were 2.39 mm Hg (95% CI: 1.74 to 3.05) higher in young adults who had been exposed to preeclampsia compared with those not exposed (Table 21.8).[214] Whether the effect is mediated by the often accompanying fetal growth restriction or preterm birth or may be associated with circulating antiangiogenic factors or other humoral changes in preeclampsia requires further investigation. In a recent study of young adults (males and females) born preterm, soluble endoglin and soluble fms-like tyrosine kinase-1 (sflt-1) levels were significantly elevated ($P < .001$ for both) compared with controls born at term, and proportional to current systolic blood pressures, suggesting a programming effect of preterm birth on angiogenesis and blood pressure.[215] Interestingly, sflt-1 levels in this study were even further elevated in those who had been preterm and exposed to a hypertensive pregnancy ($P < .002$), suggesting an additional impact of preeclampsia. Having been born small for gestational age or preterm, in turn, are risk factors for a woman subsequently developing preeclampsia in her own pregnancies, emphasizing the intergenerational effects of developmental programming.[33,190] Whether the programmed risk for preeclampsia is mediated by elevated circulating antiangiogenic factors and/or the programmed risk of higher blood pressures and renal dysfunction resulting from a mother's own low birth weight or preterm birth status is not known.

Gender differences in programming effects on blood pressure have been inconsistently reported. In some studies, programming effects appear more pronounced in males, and in others, the differential effects of gender are modified by age, ethnicity, and body mass index.[197] In a meta-regression of 20 Nordic cohorts, including 183,026 males and 14,928 women, a linear inverse association between birth weight and systolic blood pressure was present across all birth weights in males, which strengthened with age, whereas the relationship was U-shaped in women, with increasing risk also observed with birth weights above 4 kg.[216] Potential mechanisms whereby developmental programming may be expressed differently in males and females will be discussed later and are reviewed in detail elsewhere.[159,170]

The relative importance of genetics and environmental factors in programming of blood pressure has been studied in twins.[217-219] In a large Swedish cohort of 16,265 twins, the overall adjusted OR for hypertension was 1.42 (95% CI: 1.25 to 1.62) for each 500-g decrease in birth weight. Within like-sexed twin pairs, the ORs were 1.43 (95% CI: 1.07 to 1.69) and 1.74 (95% CI: 1.13 to 2.70) for dizygotic and monozygotic pairs, respectively, suggesting that environmental factors that contributed to differences in birth weight had a greater impact than genetics in this cohort, consistent with a developmental programming effect.[217]

Nephron Number and Blood Pressure

In support of the potential association between nephron number and hypertension, a study of Caucasians aged 35 to 59 years who died in accidents found that in 10 subjects with a history of essential hypertension, the number of glomeruli per kidney was significantly lower and glomerular volume significantly higher than in 10 normotensive-matched controls (Fig. 21.9).[59] Birth weights were not reported in this study, but the authors concluded that a reduced nephron number is associated with susceptibility to essential hypertension. Similarly, kidneys of Australian Aborigines with a history of hypertension contained approximately 30% fewer nephrons than Aborigines with no history of hypertension.[220] Although the sample size was small and birth weights were not available, this is a population with high rates of socioeconomic disadvantage and low birth weight. Kanzaki et al.[221] also recently reported that kidneys from Japanese men with a history of hypertension contained approximately 40% fewer nephrons than age-matched normotensive men. The data therefore seem consistent across several populations that higher blood

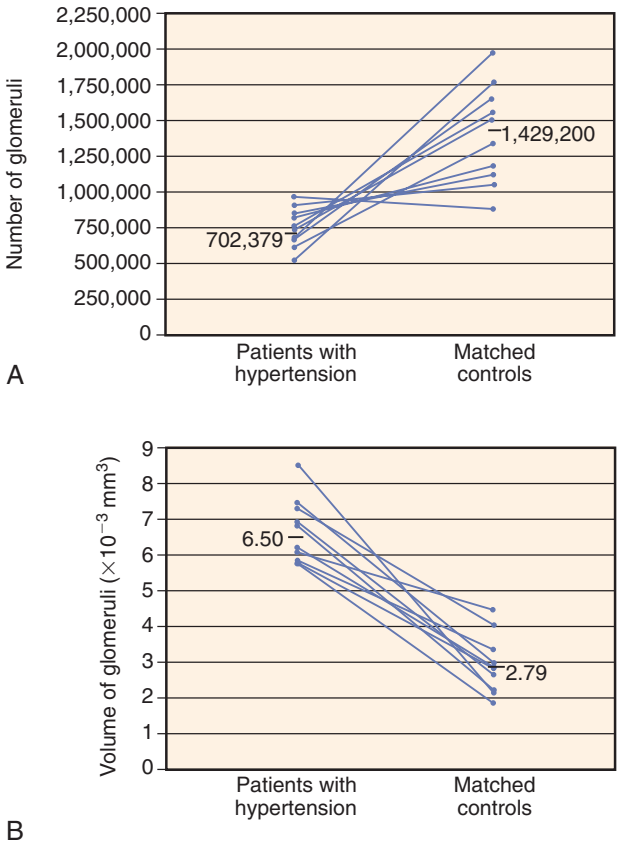

Fig. 21.9 (A) Nephron number, and (B) glomerular volume in Caucasian subjects with primary hypertension compared with controls. (From Keller G, Zimmer G, Mall G, et al. Nephron number in patients with primary hypertension. *N Engl J Med.* 2003;348:101–108.)

Table 21.8 Systematic Reviews, Metaanalyses, and Population-Based Studies of Developmentally Programmed Associations With Blood Pressure and Kidney Disease

Reference	Condition	Age	Number Included in the Analysis	Study Type	Outcome	Risk (95% CI)
Programmed Associations With Blood Pressure						
36	Preterm birth[a]	17.8 years	3080 subjects	Systematic review and meta-analysis	SBP	Increase by 2.5 mm Hg (1.7–3.3 mm Hg) vs. term birth
37	Low birth weight	4–84 years	20 studies	Meta-analysis	Hypertension	OR 1.21 (1.13–1.3)
					SBP	Increase by 2.28 mm Hg (1.24–3.33 mm Hg) for BW <2500 g vs. BW >2500 g
	High birth weight				SBP	Decrease by 2.08 mm Hg (–2.98 to –1.17 mm Hg) for BW >4000 g vs. BW <4000 g
39	High birth weight	4–83 years	31 studies	Meta-analysis	Hypertension, children	RR 1.18 (95% CI 1.05–1.32)
					Hypertension, adult	RR 0.97 (95% CI 0.86–0.97)
					Overall	RR 1.0 (95% CI 0.93–1.06)
552	Birth weight	0–84 years	444,000 subjects	Systematic review	SBP	Decrease by 2 mm Hg per kg increase in BW
	Catch-up growth				SBP	Increase with catch-up growth
						Highest blood pressure values in LBW after catch-up
214	Offspring of pregnancy complicated by preeclampsia	Children, young adult	45,249 subjects	Systematic review	SBP	Increase by 2.39 mm Hg (1.74–3.05 mm Hg)
					DBP	Increase by 1.35 mm Hg (0.9–1.8 mm Hg)
					BMI	Increase by 0.62 kg/m^2
					SBP	
211	Pregnancy complicated by diabetes	2–17 years	61,852 individuals	Systematic review and meta-analysis	SBP	Increase (0.47–3.28 mm Hg) in ODM (only statistically significant in males when stratified by sex)
217	Genes vs. environment	Birth years 1926–1958	16,265 subjects	Same-sex twin study, all	Hypertension	OR 1.42 (1.25–1.69) per 500-g decrease
			595 subjects	Dizygotic pairs[b]	Hypertension	OR 1.34 (1.07–1.69) per 500-g decrease
			250 subjects	Monozygotic pairs[b]	Hypertension	OR 1.74 (1.13–2.70) per 500-g decrease
293	Fetal and/or infant exposure to famine	37– 43 years	1,339 subjects	Cohort, Biafra famine, Nigeria (1967–1970)	SBP	Increase in exposure
					Hypertension	OR 2.87 (1.9–4.34) in exposure
295		59 years	971 subjects	Cohort, Dutch famine (1944–1945)	SBP	Increase (0.25–5.30 mm Hg) after ≥10 weeks' exposure
					DBP	Not significant
					Hypertension	OR 1.44 (1.04–2.00) after ≥10 weeks' exposure
238		48–53 years	724 subjects	Cohort, Dutch famine (1944–1945)	Albuminuria	OR 3.2 (1.4–7.7) for exposure to famine in midgestation
					SBP, DBP	Not significant
553		52–53 years	549 subjects	Cohort, siege of Leningrad (1941–1944)	SBP	Not significant
					Albuminuria	Not significant

Continued on following page

Table 21.8 Systematic Reviews, Metaanalyses, and Population-Based Studies of Developmentally Programmed Associations With Blood Pressure and Kidney Disease (Cont'd)

Reference	Condition	Age	Number Included in the Analysis	Study Type	Outcome	Risk (95% CI)
Programmed Associations With Kidney Disease						
32	Low birth weight	12–75 years	46,249 subjects	Systematic review	Chronic kidney disease	OR 1.73 (1.44–2.08)
					End-stage renal disease	OR 1.58 (1.33–1.88)
					Albuminuria	OR 1.81 (1.19–2.77)
					Reduced glomerular filtration rate	OR 1.79 (1.31–2.45)
274	Low birth weight	<21 years	1994 cases	Case–control study	Childhood chronic kidney disease[c]	OR 2.88 (2.28–3.63)
	Maternal GDM		20,032 controls			OR 1.54 (1.13–2.09)
	Maternal overweight					OR 1.24 (1.05–1.48)
	Maternal obesity					OR 1.26 (1.05–1.52)
	High birth weight					Not significant

[a]Mean gestational age 30.2 weeks, mean birth weight 1280 g.
[b]Twin pairs discordant for hypertension.
[c]Chronic kidney disease definition included reduced renal function, renal dysplasia and/or aplasia, and obstructive uropathy.
BMI, Body mass index; *CI*, confidence interval; *DBP*, diastolic blood pressure; *GDM*, gestational diabetes mellitus; *ODM*, offspring of diabetic mother; *OR*, odds ratio; *RR*, relative risk; *SBP*, systolic blood pressure.
From Luyckx VA, Brenner BM. Birth weight, malnutrition and kidney-associated outcomes—a global concern. *Nat Rev Nephrol.* 2015;11:135–149.

pressures are associated with lower nephron numbers. These studies attempted to exclude loss of nephrons due to hypertension as a potential confounder of the association in the absence of birth weight data.

Interestingly, among a subset of 63 subjects in whom mean arterial pressures and birth weights were available, Hughson and coworkers[120] reported a significant correlation between birth weight and glomerular number, mean arterial pressure, and glomerular number as well as mean arterial pressure and birth weight among Caucasian but not African American subjects. Among African Americans having nephron numbers below the mean, however, twice as many were hypertensive as normotensive, suggesting a possible contribution of lower nephron number in this group as well.[120] The relationship of low birth weight and nephron number was similar in a cohort of black and white Cuban neonates; therefore, it is expected that a similar relationship between low birth weight and low nephron number exists in the black population.[91] Glomerular volumes were found to be higher among the hypertensive African American subjects than the hypertensive whites.[120] The consistent finding of larger glomeruli among African Americans may suggest a greater prevalence of low nephron number in this population as a result of the known higher prevalence of low birth weight, or may reflect independent or additional programming of glomerular size. This topic warrants further research.

Consistent with an association between nephron number and blood pressure in humans, salt sensitivity has been found to correlate inversely with birth weight and inversely with kidney size in adults and children (Fig. 21.10).[142,143] In both studies, salt-induced changes were independent of GFR, excluding confounding by renal function. Among 1512 subjects aged 62 years, investigators found an inverse association between birth weight and blood pressure among those with birth weights below 3050 g, with a progressive 2.48-mm Hg (95% CI: 0.4 to 4.52 mm Hg) increase in blood pressure for every 1-g rise in daily salt intake until 10 g/d.[222] Interestingly, above this threshold birth weight, there was no association between blood pressure and salt intake, potentially suggesting protection against salt sensitivity with higher birth weights.

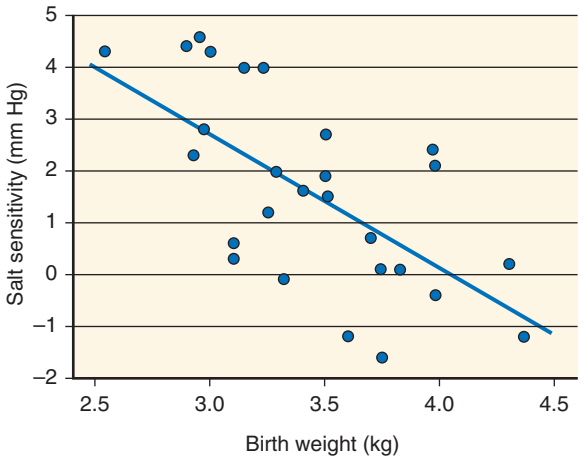

Fig. 21.10 Correlation between birth weight and salt sensitivity in 27 normotensive adults. Salt sensitivity of blood pressure was defined as the difference of mean arterial pressure on high-salt diet (200 mmol/d) compared with low-salt diet (60 mmol/d). $R = -0.06$; $P = .002$. (From de Boer MP, Ijzerman RP, de Jongh RT, et al. Birth weight relates to salt sensitivity of blood pressure in healthy adults. *Hypertension* 51:928–932, 2008.)

BIRTH WEIGHT, PRETERM BIRTH, AND KIDNEY FUNCTION

As with blood pressure, programmed changes in renal function that occur, at least in the early stages, may not be outside of normal limits. With time or exposure to additional insults, however, these changes may manifest as kidney disease.

Glomerular Filtration Rate

The GFR, in the absence of compensatory hyperfiltration, should reflect the filtration surface area and, therefore, nephron number. Compensatory hyperfiltration is thought not to occur in the immediate neonatal period, and therefore, measurement of neonatal GFR may be a good proxy for nephron endowment. Consistent with this, amikacin clearance on day 1 of life, measured as a correlate for neonatal GFR, was found to be significantly lower in low-birth-weight and preterm neonates than in term controls.[223] Similarly, in a cohort of very preterm children aged 7.6 years, although still within the normal range, GFR measured by inulin clearance was significantly lower among those who had been growth restricted compared with non–growth restricted perinatally.[224] Importantly, the GFR was lower among children who had been growth restricted before (in utero) or in the first weeks after birth (in intensive care), pointing also to the role of postnatal nutrition in renal programming. Several studies in children found similar associations of decreased GFR in low-birth-weight or preterm children; however, studies using creatinine-based formulas may underestimate the impact of birth weight on GFR, suggesting a need to validate measures of renal function in low-birth-weight and preterm subjects, whose body composition may remain different over time.[223,225–231] The relationship between birth weight and eGFR appears to track with time, suggesting consistency of the associations. Among 5352 adolescents from the NHANES study, eGFRs were lower in low-birth-weight (OR: 1.49; 95% CI: 1.06 to 2.10) and very low–birth-weight (OR: 2.49; 95% CI: 1.20 to 5.18) subjects compared with those with normal birth weight.[209] As discussed earlier, this study is the first population-based assessment among adolescents of multiple ethnicities permitting an estimation of the population-attributable fraction of birth weight to blood pressures and eGFR: 1 in 13 low-birth-weight or 1 in 5 very low–birth-weight adolescents had systolic blood pressures ≥95th percentile and/or eGFR < 90 mL/min/1.73 m^2.[209]

Overall, a recent metaanalysis found an OR of 1.79 (95% CI: 1.31 to 2.45) for a reduced GFR with low birth weight (see Table 21.8).[32] Linear regression analysis in a cohort of 2192 British adults aged 60–64 years revealed that for each 1-kg decrease in birth weight, adult GFR estimated using cystatin C was reduced by 2.25 mL/min per 1.73 m^2 (95% CI: 0.69 to 3.58 mL/min per 1.73 m^2).[232] Taken together, these findings are consistent with low birth weight and preterm birth being risk factors for a reduced GFR. The relative contributions of genetics and the fetal environment on programming of renal function were investigated in 653 twins.[233] Creatinine clearance was significantly lower in low-birth-weight compared with normal-birth-weight twins. Furthermore, intrapair birth weight differences were positively correlated with GFR in both monozygotic and dizygotic twin pairs, suggesting that feto-placental factors have a greater impact than genetic factors on adult renal function.

To approach an understanding of the mechanism of the reduced GFR in low-birth-weight and preterm individuals, renal functional reserve, determined by measuring GFR and effective renal plasma flow (ERPF) before and after low-dose dopamine infusion or an oral amino acid load, was studied in 20-year-old subjects who had been preterm and either small or appropriate for gestational age, versus controls, born full term and normal birth weight.[192] After renal stimulation, the relative increase in GFR tended to be lower in small-for-gestational-age compared with appropriate-for-gestational-age and control subjects, and ERPF was lower in both groups of preterm subjects, although statistical significance was not reached, likely because of small numbers. Reduced renal functional reserve was also observed among young adults with type 1 diabetic mothers, who had been exposed to diabetes during gestation, but not those with diabetic fathers, again suggesting a programming rather than genetic effect.[72] A reduced renal reserve capacity in these subjects may be consistent with a programmed reduction in nephron number.

Proteinuria

One of the earliest signs of hyperfiltration, which would be expected in the setting of a reduced nephron number and filtration surface area, is microalbuminuria, which may progress to overt proteinuria with ongoing renal injury and worsening hyperfiltration. Consistent with this hypothesis, Aboriginal Australians who had low birth weights evidenced an OR for macroalbuminuria of 2.8 (95% CI: 1.26 to 6.31) compared with those who had normal birth weights, and this increased with age.[234] Importantly, proteinuria was also associated with a higher rate of cardiovascular and renal deaths, underscoring its clinical relevance.[97] A meta-analysis including eight additional studies reported an OR of 1.81 (95% CI: 1.19 to 2.77) for albuminuria with low birth weight (see Table 21.8).[32] More recently, the Australian group reported that low birth weight, childhood poststreptococcal glomerulonephritis, and current body mass were all independent predictors of albumin to creatinine levels in young Aboriginal adults.[235,236] These findings are compatible with the "multihit" model of CKD, of which nephron endowment at birth may be the first "hit" increasing susceptibility to kidney disease throughout the life course.

As with blood pressure, whether preterm birth modifies the association of birth weight with proteinuria is not always easy to dissect, although studies of preterm children and adolescents show consistent findings. Among children aged 4 years who had been preterm, albuminuria was higher in both boys and girls who had reached normal height (presumably caught up in growth), and among 19-year-olds who had been very preterm, albuminuria was higher among those who had been growth restricted, again highlighting the interplay between preterm birth, growth restriction, and catch-up growth on later risk of disease.[230,237] In contrast, however, among 12- to 15-year-old NHANES participants, despite there being significant differences in blood pressure and eGFRs, there was no difference in the albumin/creatinine ratio between adolescents born with low birth weight, very low birth weight, or normal birth weight.[209] This unexpected finding might be due to the fact that albuminuria was determined on a single random, nonsupine sample, which may lack the specificity needed to distinguish patients with true kidney disease.

Analysis of 724 subjects aged 48 to 53 years who had been subjected to malnutrition in midgestation during the Dutch famine revealed an increased prevalence of microalbuminuria (12%) when compared with those subjected to malnutrition during early gestation (9%), late gestation (7%), or not exposed to famine (4%–8%) (see Table 21.8).[238] Size at birth was not associated with the observed increase in microalbuminuria, however, suggesting that renal development may have been irreversibly affected in midgestation, although in later gestation, whole-body growth was able to catch up with restoration of more normal nutrition. This observation again emphasizes the need for surrogate markers in addition to birth weight in order to identify individuals at risk for renal programming.

A U-shaped association between birth weight and proteinuria was described among Pima Indians, showing that the risk increased for birth weights below 2.5 kg and above 4.5 kg.[12] The strongest predictor of proteinuria among high-birth-weight subjects in this study was exposure to gestational diabetes, raising the question of whether gestational diabetes exposure, rather than birth weight per se, was the predominant programming risk factor.[12] In a Canadian study, urine albumin/creatinine ratios were lower in infants of diabetic mothers compared with nondiabetic mothers at 1 year of age, but were higher at 3 years, although independent of birth weight.[239] The authors interpret these findings to reflect abnormal renal programming in offspring of diabetic mothers; however, the effects of gestational diabetes and high birth weight on renal programming require much more study.

Neonatal Acute Kidney Injury

Preterm birth is an important risk factor for acute kidney injury (AKI) in neonates, estimated to occur in between 12.5% and 71%, depending on the population studied.[240,241] In turn, AKI in very low–birth-weight infants is an independent predictor of longer hospital stays, mortality, and subsequent CKD.[187,242] A retrospective analysis of preoperative renal volume in neonates undergoing congenital heart surgery found higher peak postoperative creatinine values and, therefore, potentially increased risk of AKI in infants with a renal volume ≤ 17 cm^3.[243] High creatinine values were associated with lower gestational age and lower birth weight *z*-score. Neonates in intensive care are particularly susceptible to renal dysfunction, not only because of potentially programmed risk and low nephron number but also because of critical illness and frequent nephrotoxin exposure such as aminoglycosides and nonsteroidal antiinflammatory drugs.[122,241,244–248] Medications administered during pregnancy or prior to delivery, such as tocolytics and antibiotics, may also impact fetal nephrogenesis and increase the risk of neonatal AKI.[249–251] These factors all likely adversely impact any postnatal nephrogenesis, which may occur under optimal circumstances for several weeks following preterm birth.[122]

The actual risk of AKI with exposure to nephrotoxins among preterm infants is not well described. Among 269 infants perinatally exposed to potential nephrotoxic medication (i.e., in late pregnancy or within the first 7 days postbirth), ibuprofen exposure was associated with an OR of 2.6 (95% CI: 1.2 to 5.3) for a reduced GFR on day 7 of life, which persisted over the first month.[250] Other authors found that exposure to aminoglycosides was associated with higher serum creatinine in preterm infants born small for gestational age at 2 months.[252] Neonatologists are working to raise awareness of the renal risk; however, the definition of renal failure in this population remains a challenge. Creatinine cutoff values have been proposed according to gestational age.[227] Serum creatinine in the neonate reflects maternal creatinine early on, however; therefore, urinary biomarkers and cystatin C have been proposed as superior markers to detect AKI early.[244,253] More recently, the Neonatal Kidney Disease: Improving Global Outcomes Classification has been proposed for more consistency in the definition.[244] The risk and significant adverse consequences of AKI associated with preterm birth therefore highlight the need for long-term follow-up of preterm infants.[240] Studies are emerging linking perinatal AKI to the long-term risk of CKD, which is significantly increased among those who subsequently become obese.[187,254–257] Prevention of perinatal AKI may therefore be important to reduce the risk of later-life CKD, and long-term follow-up of infants who develop AKI is required to appropriately modify this risk.[242,258]

Chronic Kidney Disease and End-Stage Kidney Disease

A case series of six patients, aged 15–52 years, who had been born preterm with very low birth weight, described findings consistent with secondary FSGS, associated with glomerulomegaly in all biopsies.[259] The authors suggest a susceptibility to hyperfiltration and glomerulosclerosis associated with preterm birth and low birth weight. Similar histologic findings have been reported in several Japanese individuals who had very low birth weights and developed early renal dysfunction or proteinuria.[260,261] These individuals responded well to ACEI therapy, supporting the pathophysiologic role of hyperfiltration in developmental programming of renal disease. Consistent with these findings, a variety of generally small studies have reported a greater severity of renal disease and more rapid progression of diverse renal diseases, including immunoglobulin A (IgA) nephropathy, membranous nephropathy, minimal change disease, chronic pyelonephritis, Alport syndrome, and polycystic kidney disease among children and adults who had been of low birth weight.[41,262–270] A handful of studies have examined the relationship between birth weight and diabetic nephropathy and found an increased susceptibility among subjects who had been growth restricted, although not invariably.[12,265,271,272]

Strong associations have recently been reported between both low birth weight (defined as <2.5 kg) and gestational age with the development of CKD in Japanese and North American children attending pediatric CKD clinics.[273,274] In the U.S. population, low birth weight, maternal gestational diabetes, and maternal overweight and obesity were all significantly associated with an increased risk of childhood CKD (see Table 21.8).[274] In addition, a significant association was found between low birth weight and maternal pregestational diabetes and real dysplasia/aplasia, and between low birth weight, maternal gestational diabetes, and maternal overweight or obesity and congenital obstruction. In the Japanese population, the association remained highly significant, even after exclusion of children with congenital anomalies of the kidney and urinary tract (CAKUT), with an estimated population attributable fraction of pediatric CKD being 21.1% (95% CI: 16.0% to 26.1%) for low birth weight and 18.2% (95% CI: 16.5 to 25.6%) for preterm birth.[273]

Table 21.9 Risk of End-Stage Renal Disease According to Birth Weight and Gestational Age Category[a]

	LBW (BW <10th percentile)	LBW (<2.5 kg)	SGA (<37 weeks)	Preterm (<37 weeks)	Term LBW	Preterm LBW	Term SGA	Preterm AGA	Preterm SGA
All ages	1.63 (1.29–2.06)	2.25 (1.59–3.19)	1.67 (1.3–2.07)	1.36 (0.94–1.99)	1.56 (1.18–2.07)	1.89 (1.25–2.86)	1.54 (1.2–1.96)	1.09 (0.69–1.73)	4.03 (2.08–7.80)
1–18 y	2.72 (1.88–3.92)		1.93 (1.28–2.91)						
18–42 y	1.23 (0.9–1.68)		1.53 (1.15–2.03)			1.42 (0.82–2.48)	1.41 (1.05–1.90)		4.02 (1.79–9.03)

[a]All comparisons for term birth, LBW term, AGA term as relevant. Data expressed as hazard ratios (95% confidence intervals).
AGA, Appropriate for gestational age; *BW*, birth weight; *LBW*, low birth weight; *SGA*, small for gestational age.
Reproduced from Low Birth Weight and Nephron Number Working Group. The impact of kidney development on the life course: a consensus document for action. *Nephron.* 2017;136:3–49.
Derived from Ruggajo P, Skrunes R, Svarstad E, et al. Familial factors, Low birth weight, and development of ESRD: a nationwide registry study. *Am J Kidney Dis*. 2016;67(4):601–608.

Taken together, most observations suggest that low birth weight and preterm birth are risk factors for renal disease. Consistent with this notion, a meta-analysis of 18 studies reported an OR for CKD of 1.73 (95% CI: 1.44 to 2.08) with low birth weight (see Table 21.8).[32] Similarly, in retrospective analysis of a cohort of over 2 million white children, the relative risk of developing ESKD was 1.7 (95% CI: 1.4 to 2.2) in those with birth weights <10th percentile.[31] In a follow-up study, these investigators showed a stronger relationship between low birth weight and ESKD in individuals under 18 years (OR: 2.72; 95% CI: 1.88 to 3.92) compared with 18–42 years of age (OR: 1.23; 95% CI: 1.15 to 2.03), again demonstrating the likely impact of CAKUT in the younger population (Table 21.9).[41] Overall in this study, both low birth weight and being small for gestational age were associated with a progressively increasing risk of ESKD (Fig. 21.11). There was no evidence for modulation of these associations by familial factors, again emphasizing the strong impact of environmental exposures in renal programming.[41] In a dialysis-based study, low birth weight was also associated with increased risk of ESKD, but the OR for diabetic ESKD was also increased among those having birth weights greater than 4000 g (OR 2.4; 95% CI: 1.3 to 4.2).[50] The relevance of high birth weight was also highlighted by a U-shaped association of renal disease with birth weight found in two large population-based studies, although effects differed between males and females in both studies, again reflecting potential effect modification by gender under conditions as yet not fully elucidated.[30,31] Whether high birth weight in these studies was associated with intrauterine exposure to diabetes is not known.

Among 1850 Pima Indians younger than 45 years with diabetes, the incidence rate ratio of developing ESKD was 4.12 (95% CI: 1.54 to 11.02) among those who had been exposed to diabetes in utero compared with those without exposure.[275] Interestingly, this effect disappeared after controlling for duration of diabetes in this relatively young cohort, suggesting the ESKD risk may be mediated predominantly by a programmed risk for earlier-onset diabetes among those exposed to diabetes in utero. This study emphasizes that programming of renal risk may be indirect as a consequence of programming of other disorders such as diabetes, underscoring the need for a holistic and life-course approach to understand and tackle programming of renal disease.

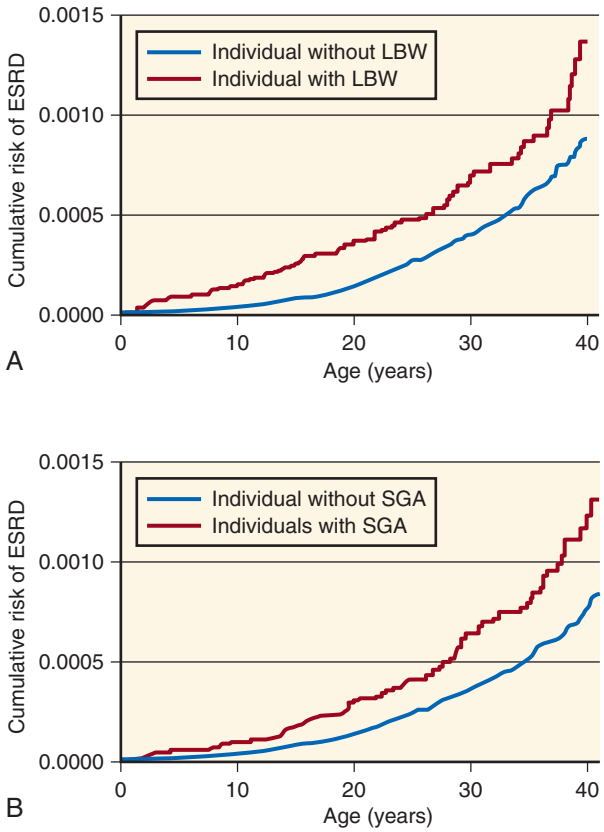

Fig. 21.11 Cumulative risk for end-stage renal disease *(ESRD)* in individuals with age, according to whether the individual was (A) low birth weight *(LBW)* or (B) small for gestational age *(SGA)*. From Ruggajo P, Skrunes R, Svarstad E, et al. Low birth weight, and development of ESRD: a nationwide registry study. *Am J Kidney Dis.* 2016;67:601–608.

It is likely too simplistic to assume that altered kidney development associated with low birth weight, preterm birth, or other developmental stresses itself is enough to cause renal disease, but exposure to additional "hits" (e.g., nephrotoxin exposure, AKI, glomerulonephritis), or superimposed

developmental programming of conditions that are themselves risk factors for kidney disease (i.e., diabetes, cardiovascular disease, metabolic syndrome, obesity), all likely exacerbate renal risk.[16,19,187,235,275,276] Overall, combined meta-analysis of 31 studies, including over 2 million subjects, concluded that individuals of low birth weight have a 70% increased risk of developing CKD, including albuminuria, reduced GFR, and renal failure in later life.[32] Clinical associations of developmental programming in the kidney are outlined in Table 21.10.

RELATIVE IMPACT OF BEING BORN SMALL OR PRETERM ON RENAL PROGRAMMING

As illustrated in Fig. 21.1, a low birth weight may be the result of preterm birth and/or growth restriction. Most studies have not differentiated between these two occurrences, so the relative impact of each has remained unclear. A recent Norwegian population study including data from >1.8 million subjects under age 40 years has examined these effects, using the following definitions: low birth weight <10th percentile for Norway (<2800 g), small for gestational age <10th percentile for gestational age (determined by ultrasonography in gestational weeks 17–20), and preterm birth <37 weeks' gestation (see Table 21.9).[41] Overall, the hazard ratio (HR) for ESKD was 1.56 (95% CI: 1.18 to 2.07) for low-birth-weight term births, 1.89 (95% CI: 1.25 to 2.86) for low-birth-weight preterm births, 1.54 (95% CI: 1.20 to 1.96) for term small-for-gestational-age births, and 4.03 (95% CI: 2.08 to 7.80) for preterm small-for-gestational-age births (Fig. 21.11).[41] Preterm birth with appropriate weight for gestational age was not associated with an increased risk of ESKD in this study. Being born small for gestational age was therefore the strongest predictor of ESKD risk. Subsequently, the same authors reported that being small for gestational age and low birth weight were associated with an increased risk of ESKD among a cohort of young adults with IgA nephropathy.[277] The IgA subgroup was chosen because it is a common disease and unlikely to be directly impacted by programming (in contrast to CAKUT or diabetic nephropathy). Low birth weight and small for gestational age were associated with increased risk of progression to ESKD in IgA nephropathy.[41] This study again points to developmental programming being a first "hit" leading to accelerated progression of a primary renal disease. Again, in this study, the highest risk for ESKD was conferred by a small birth weight for gestational age (HR: 2.2; 95% CI: 1.1 to 4.2); however, this effect was only significant in males. Patients who were both low birth weight and small for gestational age had the highest risk (HR: 3.2; 95%: CI 1.5 to 6.8), suggesting a greater impact at lower birth weights, likely reflecting more adverse intrauterine exposures.

POTENTIAL IMPACT OF ETHNICITY ON RENAL PROGRAMMING

The nephron number hypothesis was initially put forward as a potential explanation for the disproportionately higher risks of hypertension and kidney disease among disadvantaged populations.[48] Hypertension, CKD, and ESKD prevalences tend to be highest among Aboriginal Australians, Native Americans, people of African origin, and ethnic minorities in developed countries.[10,12,50,278] The incidence of birth circumstances and maternal risk factors for renal programming are high across low- and middle-income countries, as highlighted in Table 21.11, suggesting a potentially significant population impact. Most studies regarding programming of blood pressure and kidney disease have thus far been conducted in western Caucasian populations and may not be generalizable to all populations. In the Norwegian population, for example, only 3.3% of subjects had birth weights below 2.5 kg, whereas around 13%–15% of babies in sub-Saharan Africa have low birth weights.[41,279] Furthermore, the causes of low birth weight or preterm birth differ across regions, with maternal nutrition, poverty, and infections being important in lower-income regions and advanced maternal age, multiple gestations, and use of assisted reproduction technology predominating in high-income regions.[280–282] How such differences may modulate programming risk across populations is not known.[283–286]

Kidney size, as measured by ultrasound at birth, among 715 South Asians (Pakistani, Indian, and Bangladeshi origin) from the Born in Bradford (United Kingdom) cohort study was smaller than that among 872 white babies, and the difference persisted after adjustment for potential confounders, including birth weight.[287] Total kidney volume was also found to be lower in low-birth-weight and preterm Australian Aborigines at 32 and 38 weeks of gestation and at term compared within nonindigenous Australians, suggesting a lower nephron number in the indigenous children.[288] However, in this study, calculated GFR (serum cystatin C) was similar in Aboriginal and nonindigenous neonates, suggesting SNGFR was increased in the Aborigines. In a study comparing eGFR in 152 African and white American children at a mean age of 1.5 years, the eGFR was found to be significantly lower among African American children (82 vs. 95 mL/min/1.73 m^2).[289] Birth weight was significantly and positively associated with eGFR in African American but not white children, suggesting that some of the racial disparities in adult CKD may have origins in the prenatal period.

Nephron numbers have thus far been counted only in small cohorts of Caucasians, African Americans, Australian Aboriginals, Senegalese Africans, and Japanese males, in many of whom birth weights were not available. Therefore, the relationship between birth weight and nephron number remains unknown in most populations. A recent study on nephron number and hypertension among older Japanese males found the nephron count in the normotensive subjects was one of the lowest reported to date (~640,000 nephrons), suggesting that Japanese people may be especially vulnerable to adult hypertension and CKD, particularly if a "second hit" occurs.[221] This hypothesis would be consistent with the fact that Japan has the second-highest incidence of ESKD in the world.[290] Low birth weight is strongly associated with reduced nephron numbers and susceptibility to kidney disease among Australian Aboriginals, a population that is also significantly disadvantaged compared with their white counterparts.[96,97] The association between nephron number and birth weight does appear to be consistent among subjects of African origin as in Caucasian subjects.[87,91,291,292] The relationship between low nephron numbers and higher blood pressures seen in Aboriginal Australians and Caucasians, however, was not as consistent among African Americans.[285] Similarly, the association of low birth weight with blood pressure is also less consistently reported among African-American compared with Caucasian children; therefore, additional factors likely augment blood pressure risk in the African-origin population.[198,289]

Evidence for developmental programming of blood pressure in an African population has, however, been shown among

Table 21.10 Clinical Associations of Renal Programming

	Low Birth Weight	Small for Gestational Age	Preterm Birth	High Birth Weight	Gestational Diabetes Exposure	Exposure to Preeclampsia/ Eclampsia	Maternal Overweight/ Obesity	Maternal Vitamin A Deficiency	Rapid Catch-Up Growth/ Overweight	Low Nephron Number	Smaller Kidney Size/ Weight	Increased Glomerular Volume
Increased blood pressure	✓		✓	✓	✓	✓	✓		✓	✓	✓	✓
Salt sensitivity	✓				a					a	✓	
Reduced GFR	✓	✓	✓		a				✓	a	✓	
Reduced renal functional reserve		✓	✓		✓							
Proteinuria	✓		✓	✓	✓				✓	a	✓	
Acute kidney injury (neonates)			✓							✓	✓	
Chronic kidney disease	✓	✓	✓		✓	✓	✓		✓	a	✓	✓
End-stage renal disease	✓			✓	✓							
Transplant outcomes	✓										✓	✓
Death	✓											
Increased glomerular volume	✓		✓		a				✓	✓		
Smaller kidney size/weight	✓	✓	✓					✓		✓		
Congenital obstruction	✓			NS	✓		✓			a		
Renal dysplasia/ aplasia	✓			NS	✓		NS			✓		✓

✓, Evidence from human studies; *a*, evidence from animal studies only; *NS*, not significant.
Modified from prior Table 23.8, readapted from Luyckx, 2015, 2002.

Table 21.11 Prevalence of LBW, Preterm Birth, Maternal Diabetes, and Obesity in Low- and Middle-Income Countries[a]

	LBW (2010)	Preterm Birth (2010)	HBW (2004-2008)	Gestational Diabetes[a] (2013)	Maternal Overweight (2003–2009)	Maternal Obesity (2003–2009)	Chronic Hypertension/ Preeclampsia/ Eclampsia
Proportions in LMICs (country *n*)	15% (138)	11.3% (138)	0.5%–14.9% (23)	0.4%–24.3% (15)	13.7% (27 Sub-Saharan countries)	5.3% (27 sub-Saharan countries)	2.3% (17)

[a]Variable rates in part related to differences in cut-off values for diagnosis.
HBW, High birth weight; *LBW*, low birth weight; *LMIC*, low- and middle-income countries.
Adapted from Low Birth Weight and Nephron Number Working Group. The impact of kidney development on the life course: a consensus document for action. *Nephron.* 2017;136:3–49. Compiled from Koyanagi A, Zhang J, Dagvadorj A, et al. Macrosomia in 23 developing countries: an analysis of a multicountry, facility-based, cross-sectional survey. *Lancet.* 2013;381:476–483; Lee AC, Katz J, Blencowe H, et al. National and regional estimates of term and preterm babies born small for gestational age in 138 low-income and middle-income countries in 2010. *Lancet Glob Health.* 2013;1:e26–e36; Cresswell JA, Campbell OM, De Silva MJ, et al. Effect of maternal obesity on neonatal death in sub-Saharan Africa: multivariable analysis of 27 national datasets. *Lancet.* 2012;380:1325–1330; (Kanguru L, Bezawada N, Hussein J, et al. The burden of diabetes mellitus during pregnancy in low- and middle-income countries: a systematic review. *Glob Health Action*. 2014;1;7:23987; and Abalos E, Cuesta C, Carroli G, et al. Pre-eclampsia, eclampsia and adverse maternal and perinatal outcomes: a secondary analysis of the world health organization multicountry survey on maternal and newborn health. *BJOG*. 2014;121(suppl 1):14–24.).

Nigerian adults exposed to the Biafran famine (1967–1970) during fetal life and early childhood.[293] Consistent with observations among Caucasians exposed to the Dutch famine (1944–1945), blood pressures were elevated in adult Nigerians exposed to the famine.[293–295] Interestingly, however, blood pressures in Biafran subjects were elevated 15 to 20 years earlier than among the Dutch subjects (see Table 21.8), potentially again suggesting aggravating factors present in African-origin subjects.[293,295] In addition, in both populations, exposure to famine was also associated with increased risks of glucose intolerance and obesity, again underscoring the multisystem consequences of developmental programming.[293,294]

Variants in the *APOL1* gene have been strongly linked to risk of CKD in African Americans and in West Africans.[4,9] The relationship between *APOL1* genotype and nephron number was recently investigated.[296] Glomerular number was not reduced, and glomerular size was not increased among African Americans with one or two *APOL1* variant alleles, but there was evidence of more accelerated loss of nephrons after the age of 38 years, which was exacerbated by obesity.[296] A programming interaction with *APOL1* genotype, therefore, has not yet been established; however, age-related loss of glomeruli appears accelerated.

PROPOSED MECHANISMS OF DEVELOPMENTAL PROGRAMMING IN THE KIDNEY

Kidney development is a complex process involving tightly controlled expression of many genes and constant remodeling.[111,297–301] The molecular regulation of kidney development is exhaustively reviewed elsewhere (see Chapter 1).[298–301] Many experimental models, as discussed earlier and outlined in Table 21.4, have been shown to result in a reduced nephron number, and these have been used to gain insight into potential mechanisms contributing to programmed disease outcomes. In many of the experimental models of programming, reduced nephron number has been shown to be associated with low birth weight and subsequent hypertension and renal injury. Interestingly, in normal rat litters, those pups with naturally occurring low birth weight (i.e., birth weights < –2 standard deviations [SDs] from the mean) were found to have a 13% reduction in nephron number, which was associated with glomerulomegaly and proteinuria.[302] Low birth weight in rodents, therefore, may be associated with a low nephron number, even under nonexperimental conditions. Maternal factors that affect birth weight and preterm birth in humans may also directly affect nephrogenesis, as illustrated in Table 21.12, and some of these factors may compound the effect of low birth weight or preterm birth.[90,303] In humans, nephrogenesis begins in week 9 of gestation and continues until about 36 weeks. Approximately two-thirds of the nephrons develop during the last trimester, making this the window of greatest susceptibility to adverse effects, although earlier insults can also impact nephrogenesis.[123,304] In rodents, nephrogenesis continues for up to 10 days after birth but is most active mid- to late gestation when studies show the most impact from manipulation of environmental factors.[304]

Our current understanding highlights three processes that are considered to play critical roles in determining nephron endowment at the conclusion of nephrogenesis: branching of the ureteric tree, condensation of metanephric mesenchymal cells at the ureteric branch tips, and conversion of these mesenchymal condensates into nephron epithelium.[298–301] It has been estimated that a 2% decrease in ureteric tree branching efficiency would result in a 50% reduction in final nephron complement after 20 generations of branching.[305] The specific molecular mechanisms whereby nephron numbers may be affected and/or function altered, however, are not yet completely understood. Perturbations to the feto-maternal environment that result in reduced nephron endowment are summarized in Table 21.13 and discussed later.

Table 21.12 Potential Renal Programming Effects of Risk Factors for Preterm Delivery

	Animal		Human		
Maternal Risk Factor for Preterm Birth	**BP**	**Nephron Number/ Kidney Size**	**BP**	**Nephron Number/ Kidney Size[a]**	**Kidney Function**
Vitamin D deficiency	↑	↑ Immature glomeruli	ND	ND	ND
Anemia/iron deficiency	↑	↓	ND	ND	ND
Smoking	ND	↓	↑	↓	↓
Alcohol intake	ND	↓	ND	ND	ND
Antibiotic use (UTI)	ND	↓	ND	ND	ND
Chorioamnionitis	ND	↓	ND	ND	ND
Steroids	↑	↓	Normal	Not different	Unknown
Cyclosporine/tacrolimus (maternal transplant)	↑	↓	ND	ND	Possibly normal
Maternal dialysis	ND	ND	ND	ND	Some ↓
Maternal diabetes	↑	↓	↑	ND	↓
Preeclampsia	ND	ND	↑	ND	ND

[a]Kidney size generally determined by ultrasound.
BP, Blood pressure; *ND*, not determined; *UTI,* urinary tract infection; ↑, increased; ↓, decreased.
Compiled from references 176, 246, 322, 330, 356, 362, 363, 374, 379, 465, 466, 543, and 555–559.
Reprinted with permission from Luyckx VA. Preterm birth and its impact on renal health. *Semin Nephrol.* 2017;37:311–319.

GENETIC VARIANTS ASSOCIATED WITH KIDNEY SIZE AND NEPHRON NUMBER IN HUMANS

Rare genetic and CAKUT contribute to about 40% of all childhood ESKD (NAPRTCS Report 2014). The common pathology linking these malformations involves a disturbance of the normal interaction between the ureteric bud and the pool of renal progenitor cells.[383] Of the >25 mutant genes associated with monogenic forms of CAKUT, most encode transcription factors (e.g., *PAX2, GATA3*) and growth factor receptors (e.g., *RET*) expressed in ureteric bud/tree cells during branching morphogenesis or in intermediate mesoderm (e.g., *SIX2, EYA1, ROBO*), where they set the fate of renal progenitor cells and regulate interactions with the ureteric bud.

Completely dysfunctional alleles for crucial developmental genes are rare, because they produce malformations with a major disadvantage. However, there is some evidence that mild mutations of these same genes exert subtler effects on renal mesenchyme/ureteric bud interactions and may be fairly common in the normal population (see Table 21.4). For example, heterozygous null alleles of the *PAX2* gene cause the rare autosomal dominant renal coloboma syndrome, characterized by decreased ureteric branching during fetal life, sharply reduced nephron number at birth, and progressive renal failure in childhood. *PAX2* is highly expressed in the ureteric bud, where it suppresses apoptosis and optimizes the extent of branching. Interestingly, an intronic *PAX2* polymorphism, which reduces *PAX* transcript levels from the mutant allele by only 50%, is found in 18.5% of Canadians and is associated with a subtle (10%) reduction in newborn kidney size.[306] Ureteric branching morphogenesis is also highly dependent on *GDNF* signaling from the metanephric mesenchyme to the ureteric bud via the *RET* tyrosine kinase receptor on ureteric tip cells. Although no common hypomorphic variants of the human *GDNF* gene have been shown to affect kidney size, a polymorphic variant of the *GDNF* receptor, *RET(1476A),* was associated with a 10% reduction in kidney volume at birth compared with the wild type (*RET 1476G*) allele.[121] In this study, newborn kidney volume was shown to be proportional to nephron number, suggesting that the modest renal hypoplasia seen with somewhat dysfunctional *PAX2* and *RET* polymorphisms represents a reduction in congenital nephron number.[121] Newborn kidney size was reduced by 13% among Polish babies with a common variant of the *BMPR1A* gene, encoding a bone morphogenetic protein receptor on ureteric epithelial cells.[307] Conversely, 22% of Canadian newborns inherit a variant of the *ALHD1A2* gene *(rs7169289)* associated with increased production of all-*trans* retinoic acid metabolism in fetal tissues; this retinoid is known to enhance RET expression in the ureteric epithelium, and newborns with the G allele were shown to have a 22% increase in newborn kidney size compared with the wild type allele.[308]

Although final nephron number is clearly affected by genes regulating the extent of ureteric branching, animal studies also indicate that the size of the renal progenitor cell pool may also be rate limiting. One of the earliest transcription factors marking the nephron progenitor cells of intermediate mesoderm is *OSR1*; Osr1 knockout mice lack nephrogenic mesenchyme and are anephric at birth.[309] A variant of the human *OSR1* gene that interferes with mRNA splicing was identified in about 6% of normal Caucasians.[310] This *OSR1rs12329305(T)* variant was associated with a 12% reduction in newborn kidney size. Taken together, these observations suggest that final nephron endowment may represent a complex polygenic trait determined by the additive effects of multiple genes regulating either the extent of ureteric branching or the renal progenitor cell pool during fetal life. As reviewed by Walker and Bertram,[301] full or partial deletion of more than 25 genes has been shown to result in kidney hypoplasia, and deletion of several of these genes results in low nephron endowment. Not all have been studied in humans; therefore, the impact of genetic variation on nephron endowment alone and in the context of developmental stresses and the risk of later-life hypertension and renal disease requires further study.

Table 21.13 Proposed Mechanisms of Developmental Programming in the Kidney

Experimental Model	Possible Mechanism of Nephron Number Reduction	References
Maternal low-protein diet	↑ Apoptosis in metanephros and postnatal kidney	313, 315, 320, 488
	Altered gene expression in developing kidney	
	Altered gene methylation	
	↓ Placental 11-β HSD2 expression → increased fetal exposure to glucocorticoids	
Maternal vitamin A restriction	↓ Branching of ureteric bud	326
	? Maintenance of spatial orientation of vascular development	
	↓ c-ret expression	
Maternal iron restriction	? Reduced oxygen delivery	322, 323
	? Altered glucocorticoid responsiveness	
	? Altered micronutrient availability	
	↑ Inflammation	
	? Tissue hypoxia	
Maternal zinc deficiency	↑ Apoptosis	324
	↓ Antioxidant activity	
Gestational glucocorticoid exposure	↑ Fetal glucocorticoid exposure	154, 356, 361, 560
	? Enhanced tissue maturation	
	↑ Glucocorticoid receptor expression	
	↑ Na-K-ATPase, α_1 and β_2 subunit expression	
	↓ Renal and adrenal 11-β HSD2 expression	
Uterine artery ligation/ embolization	↑ Proapoptotic gene expression in developing kidney: caspase-3, Bax, p53	160, 402
	↓ Antiapoptotic gene expression: PAX2, bcl-2	
	Altered gene methylation	
	Altered renin–angiotensin gene expression	
Maternal diabetes/ hyperglycemia	↓ IGF-2/mannose-6-phosphate receptor expression	161, 338, 342, 345
	Altered IGF-2 activity/bioavailability	
	Activation of NF-κB	
	Altered ureteric branching morphogenesis	
Gestational drug exposure		176, 372, 374, 376
• Gentamicin	↓ Branching morphogenesis	
• β-lactams	↑ Mesenchymal apoptosis	
• Cyclosporine	Arrest of nephron formation	
• Ethanol	? Via reduced vitamin A levels	
• COX2 inhibitors	Affects prostaglandins	
Maternal hypoxia	? Affects expression of retinoid receptors	542
	? Increased expression of glucocorticoid receptors	
	? Increased expression of angiopoietin-2	
	Accelerated aging	
Ureteral obstruction: postnatal	↓ Cell proliferation	73
	↑ Apoptosis of tubular cells	
	Delayed maturation of interstitial fibroblasts → interstitial fibrosis	
	? Alteration of postinductive processes	
Preterm birth	Abnormal maturation of glomeruli	113, 561
	? Factors associated with shift from intrauterine to extrauterine environment	
	? Loss of progenitor cell populations	

MATERNAL NUTRITION

UNDERNUTRITION

Suboptimal maternal nutrition during pregnancy has long been thought to be the basis of programmed deficits in offspring.[311] In humans, maternal malnutrition, as measured by hemoglobin, triceps skinfold thickness, or lower weight gain during later pregnancy, were all associated with higher offspring blood pressures, suggesting a programming effect.[312] Longitudinal study of people conceived or born during the Dutch Hunger Winter of 1944–1945 has demonstrated that periods of severe undernourishment can result in hypertension[295] and albuminuria,[238] even in the absence of overt fetal growth restriction. Experimental alterations in maternal dietary composition at different stages of gestation have been shown to program kidney gene expression early in the course of gestation, which later affects nephron number (Table 21.13).[313] Maternal "protein and calorie restriction" during all or the later stages of pregnancy have been the most widely studied models of low birth weight and reduced nephron number since as early as 1968.[314] Not all low-protein diets have the same programming effects, however. It has been proposed that the source of carbohydrate and the relative deficiencies of specific amino acids—methionine or glycine, for example—may have a greater impact on organ development than total protein restriction per se, potentially through epigenetic modulation of gene expression.[34,315] Effects are also dependent on the degree of protein restriction and the sex of the fetus, with a more severe restriction required to impair kidney development and program hypertension in

female rats than males.[141,316] Fetal nutrient supply is also affected by alterations in placental development that affect uteroplacental blood flow and transfer of nutrients to the fetus. Placental insufficiency is the most common cause of fetal growth restriction in the Western world, and as recently reviewed,[317] the placental phenotype most likely underpins the developmental programming of chronic disease in the offspring. Similarly, in the rat, uterine ischemia in late pregnancy resulted in a nephron deficit and hypertension in male offspring, but interestingly, restoration of good fetal nutrition postnatally, during ongoing nephrogenesis, resulted in restoration of nephron number.[112]

Increased fetal exposure to glucocorticoids and alterations to the RAAS have been proposed as mechanisms whereby low-protein diet reduces nephron number, both of which are discussed later.[318] Other potential mechanisms include reduced renal angiogenesis, associated with reduced VEGF expression, observed in offspring of mothers exposed to 50% calorie restriction during gestation[319]; global downregulation of gene expression, as seen in fetal kidneys of microswine exposed to low-protein diet in late gestation/early lactation[320]; and altered epigenetic DNA methylation, which may affect gene expression, described in livers of offspring of protein-restricted mothers.[321]

In terms of micronutrients, maternal "iron restriction" during pregnancy also leads to a reduction in birth weight and nephron number and the development of hypertension in rat offspring.[322] In another study, offspring of iron-deficient dams had reduced radial glomerular counts and increased tubulointerstitial fibrosis, which were rescued with iron supplementation during gestation.[323] Conceivably, fetal anemia may result in reduced tissue oxygen delivery, altered fetal kidney glucocorticoid sensitivity, or altered availability of other micronutrients that may affect nephrogenesis.[322] Similarly, pre- or postweaning "zinc deficiency" was also associated with decreased nephron number, reduced GFR, and higher blood pressures in rats, potentially mediated by reduction in the antioxidant antiapoptotic effects of zinc.[324] As yet, there is no evidence for programmed renal outcomes in children of iron- or zinc-deficient mothers, although in a population with a high prevalence of anemia, iron supplementation resulted in an increase in birth weight.[325]

Maternal "vitamin A restriction" has also been associated with a reduction in nephron number in rat offspring.[106,326] Severe vitamin A deficiency during pregnancy is associated with congenital malformations and renal defects in the offspring. Vitamin A and all-*trans* retinoic acid have been shown to stimulate nephrogenesis through modulation of branching capacity in ureteric epithelial cell culture and in maintenance of spatial organization of blood vessel development in cultured renal cortical explants.[326] Analysis of 21-day-old fetal rats (just before birth) revealed a direct correlation between plasma retinol concentration and nephron number, as shown in Fig. 21.12.[326] The reduction in nephron number in the setting of vitamin A deficiency is likely mediated, at least in part, by modulation of genes regulating branching morphogenesis.[326] In vivo, a vitamin A–deficient diet sufficient to reduce circulating vitamin A levels by 50% in pregnant rats resulted in a 25% reduction in nephron endowment in the offspring, whereas supplementation of vitamin A increased nephron endowment.[326] In contrast, supplemental retinoic acid was studied as a means

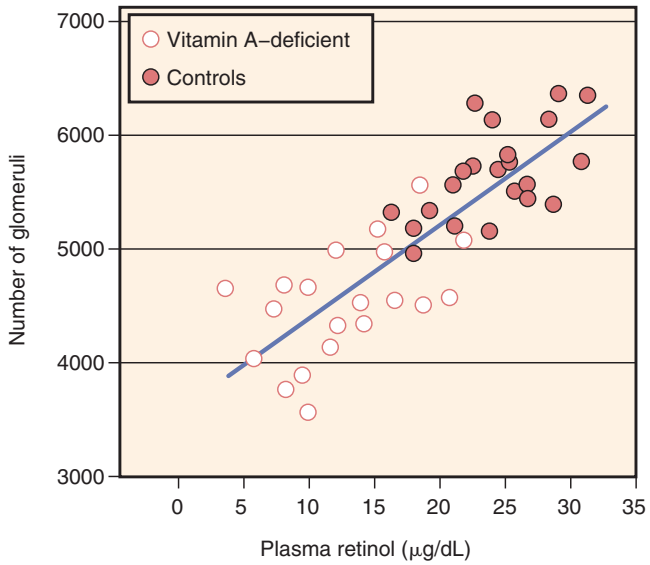

Fig. 21.12 Relationship between nephron number (number of glomeruli) and plasma retinol concentration in term rat fetuses. $P < .001$; $R = 0.829$. (From Merlet-Benichou C. Influence of fetal environment on kidney development. *Int J Dev Biol.* 1999;43:453–456.)

to stimulate nephrogenesis in postnatal preterm baboons, but no effect was observed, suggesting a more proximal window where vitamin A may be most critical.[327]

It is interesting to note that smoking and alcohol intake may be associated with reduced levels of circulating vitamin A, and both, as discussed later, are associated with low birth weight and programming of disease outcomes. Subtle differences in vitamin A level during pregnancy, therefore, may be a significant factor contributing to the wide distribution of nephron number in the general population.[90]

Emerging evidence also suggests "vitamin D deficiency" during pregnancy can alter kidney development; in animal models, offspring from vitamin D–deficient dams had delayed glomerular development and altered renal function.[328–330] In humans, severe 25-hydroxy Vitamin D (25OHD) deficiency is associated with low birth weight and gestational age at delivery, both of which are known to influence kidney development.[329]

Recognizing the importance of nutrition during pregnancy and after birth, maternal and neonatal replacement of micronutrients has been implemented as a public health policy in several countries (Table 21.14).[331] From a global review, the incidence of low birth weight was reduced by 19% with iron and folate supplementation and by 11%–13% with multimicronutrient supplements, and balanced energy supplementation increased birth weights by a mean of 73 g and reduced the risk of being small for gestational age by 34%.[331,332] Vitamin A supplementation alone did not affect birth weight but did improve child mortality.[331,333,334] Interestingly, children of mothers who received folate or a preparation containing folate + iron + zinc during pregnancy in addition to vitamin A supplementation in early postpartum in Nepal had a lower risk of low birth weight but no change in later blood pressure.[334,335] Microalbuminuria was less frequent, however, suggesting a potential programming effect of these micronutrients.[335] Very high doses of vitamin A have been

Table 21.14 Impact of Nutritional Interventions on Birth Weight and Preterm Birth and Programming of Blood Pressure and Kidney Disease

	LBW/SGA	Preterm Birth	Preeclampsia/ Eclampsia	HBW/LGA	Child Blood Pressure	Child GFR	Child Microalbuminuria
Iron and folate supplementation	↓	↓			↓	↑	
Micronutrient supplementation	↓				↑ or ↓ (No effect vs. iron/folate)		
Calcium supplementation		↓	↓		↓		
Protein supplementation	↓				No effect		
Vitamin A supplementation	No effect/↓				Possible ↓		
Folate supplementation							↓
Zinc supplementation		↓			No effect		
Iodine supplementation	↓						
Malaria prevention and Rx	↓						
Rx of genital infections	↓	↓					
Rx asymptomatic bacteriuria	↓						
Magnesium sulphate			↓				
Antiplatelet agents	↓	↓	↓				
Diabetes education				↓			
Smoking cessation	↓	↓					

GFR, Glomerular filtration rate; *HBW*, high birth weight; *LBW*, low birth weight, *LGA*, large for gestational age; *SGA*, small for gestational age.
Compiled from references 461, 457, 334, 335, 562, and 577–583.
Reproduced from Low Birth Weight and Nephron Number Working Group. The impact of kidney development on the life course: a consensus document for action. *Nephron.* 2017;136:3–49.

shown to be teratogenic and reduce nephrogenesis; therefore, vitamin A supplementation as a strategy to rescue nephron number should target normalization of vitamin A levels and avoid excess.[336] Folate is not known to impact renal development; however, it does affect gene methylation, and deficiencies may program epigenetic effects.[321] Diastolic blood pressures appeared marginally lower (0.78 mm Hg; 95% CI: 0.16 to 1.28) in 4.5-year-old children whose mothers had received early prenatal food supplements in Bangladesh, but were marginally higher (0.87 mm Hg: 95% CI: 0.18 to 1.56) among those whose mothers received a multimicronutrient supplement.[337] GFRs were 4.98 mL/min per 1.73 m^2 higher in children whose mothers had received higher-dose iron supplementation, however.[337] Potential confounders or effect modifiers in these cohorts include baseline vitamin A supplementation, which may have an overriding renal programming effect in all subjects, as well as frequent persistent malnutrition and stunting. Long-term follow-up of children of mothers who received supplements during pregnancy is sparse and thus far does not consistently suggest a positive impact on renal programming. The effects should become clearer as cohorts of children age and more data emerges.[331,337]

OVERNUTRITION: EXPOSURE TO MATERNAL DIABETES AND OBESITY

Focus on long-term programming effects of maternal diet has more recently moved to consider the effects of overnutrition, including the consequences for offspring born to diabetic women and obese women. As discussed earlier, in some populations high birth weight is associated with an increased susceptibility to proteinuria and renal disease.[12,38,50] High birth weight is a complication of gestational hyperglycemia and diabetes and may therefore also be a surrogate marker of abnormal intrauterine programming. Human offspring of diabetic pregnancies have a higher incidence of congenital malformations, resulting from defects in early organogenesis and have an increased risk of CKD (see Table 21.8).[274,338] It is known that expression and bioavailability of the insulin-like growth factors (IGFs) are altered in diabetic pregnancies and that IGFs and their binding proteins are important regulators of fetal development.[338] The impact of maternal diabetes on metanephric expression of IGFs and their receptors was studied in rats in which diabetes was induced by streptozotocin compared with gestational age–matched normal controls.[338] There was no significant difference in IGF-1 or IGF-2 or insulin receptor expression at any stage, but in offspring of diabetic mothers, there was a significantly increased expression of the IGF-2/mannose-6-phosphate receptor. This receptor tightly regulates the action of IGF-2, and an increase in expression would lead to reduced IGF-2 bioavailability.[338] IGF-2 is a critical player in renal development. The same investigators examined the role of IGF binding protein-1 (IGFBP-1) on nephrogenesis in genetically modified mice.[339] Offspring of females overexpressing human IGFBP-1 were growth restricted and had an 18% to 25% reduction in nephron number, depending on whether human IGFBP-1 was overexpressed in the mother only, fetus only, or both. When metanephroi from these mice were cultured in the presence of IGF-I or IGF-II, only IGF-2 increased nephron numbers by 25% to 40% in a concentration-dependent manner.[339] Interestingly, in a cohort of preterm infants, diastolic blood pressure at age 4 years was found to correlate positively with IGFBP-1 levels measured at postnatal weeks 32.6–34.6, potentially suggesting a programming effect of this pathway in humans.[340]

In offspring of rats rendered hyperglycemic during pregnancy either by inducing diabetes mellitus with streptozotocin

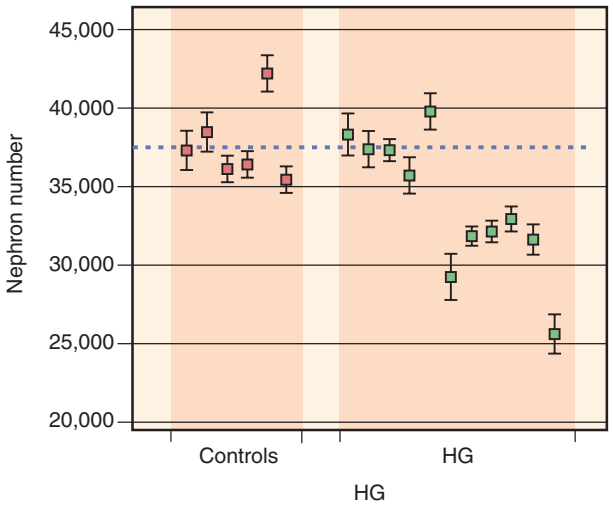

Fig. 21.13 Effects of maternal hyperglycemia on nephron number in rat offspring. *Dotted line* represents mean value in control group. *HG,* Hyperglycemia. (From Amri K, Freund N, Vilar J, et al. Adverse effects of hyperglycemia on kidney development in rats: in vivo and in vitro studies. *Diabetes* 1999;48:2240–2245.)

or by infusing glucose from gestational days 12 to 16, nephron numbers were reduced by 10% to 35%, correlating with the degree of maternal hyperglycemia (Fig. 21.13).[341] Furthermore, culture of metanephroi in varying glucose concentrations demonstrated that tight glucose control is necessary for optimal metanephric growth and differentiation. In mice, offspring of diabetic mothers had fewer nephrons, associated with increased evidence of apoptosis in tubules and podocytes, potentially mediated via increased renal angiotensinogen and renin mRNA expression and NF-κB activation.[161] Other authors suggest altered branching morphogenesis, increased asymmetric dimethylarginine, and reduced nitric oxide levels as potential mediators of reduced nephron numbers in offspring of diabetic mothers.[342,343] These offspring developed higher blood pressures and renal hypertrophy and had greater tubulointerstitial injury compared with controls, and these changes were abrogated by normalization of asymmetric dimethyl arginine (ADMA) levels achieved by maternal supplementation with L-citrulline.[343] Multiple pathways are therefore likely implicated in hyperglycemia-induced renal programming. Functionally, study of adult rat offspring of diabetic mothers revealed glomerular hypertrophy, reduced GFR and renal plasma flow, hypertension, and decreased endothelium-mediated vasodilation.[344,345]

Maternal obesity and associated pregnancy complications, including gestational diabetes, maternal hypertension, and sleep apnea, are now thought to present the greatest risk for in utero programming of adult disease. Pregnancies in overweight and obese mothers can result in both low- and high-weight infants, suggesting that programming of offspring by maternal obesity may be multifactorial.[346] Feeding animals a high-fat (+/– high carbohydrate) diet prior to and throughout pregnancy can result in programmed outcomes. Exposure to a high-fat diet for 10 days prior to pregnancy until weaning resulted in rat female offspring with hypertension but no change in nephron endowment, although renal renin and Na/K-ATPase activity were altered.[347] Rat dams fed an obesogenic diet for a more sustained period (a high-fat/high-fructose diet from 6 weeks prior to mating) resulted in offspring with albuminuria, which was further exacerbated by a postnatal high-fat diet.[348] A similar model also caused increased renal norepinephrine and renin expression in offspring.[349] Conversely, in mice, a maternal high-fat diet caused an increase in offspring nephron number, with no consequences for renal function.[350] Dams in that study were glucose intolerant prior to mating but had normal glucose tolerance during pregnancy, suggesting complex interactions between maternal obesity and diabetes. These data suggest that it may not be the high-fat diet per se causing changes in renal development but rather the resultant maternal hyperglycemia. Of note, many calorie-dense foods are also deficient in essential micronutrients.[279]

MATERNAL AND FETAL EXPOSURE TO GLUCOCORTICOIDS

Elevated maternal glucocorticoids due to stress or glucocorticoid therapy may impact fetal growth and renal development. Under normal circumstances, the fetus is protected, at least in part, from exposure to excess endogenous maternal corticosteroids by the placental enzyme 11β-hydroxysteroid dehydrogenase type 2 (11β-HSD2), which metabolizes corticosterone to the inert 11-dehydrocorticosterone.[21] However, this barrier is not complete, and administration of high physiologic concentrations of cortisol (in sheep) or corticosterone (in rats and mice) all resulted in offspring with low nephron number.[351–353] Offspring of these models developed hypertension and impairment of renal function, including albuminuria, that was, in all cases, associated with changes in the renal renin–angiotensin system (discussed later).[351,354,355] These outcomes occurred even following very short-term exposure (48–60 hours) that did not affect birth weight in sheep and mice.[353,356] Prenatal administration of dexamethasone, a steroid not metabolized by 11β-HSD2, lead to fetal growth restriction, 20% to 60% lower nephron number, glomerulomegaly, and subsequent hypertension in rats and sheep.[103,107,185,356] Metanephric organ culture experiments have demonstrated that dexamethasone can cause a dose-dependent inhibition of branching morphogenesis in part through regulation of *GDNF* gene expression.[357] Rats and humans with mutations in the *11β-HSD2* gene have low levels of placental *11β-HSD2* and give birth to low birth weight offspring in whom hypertension develops prematurely.[358,359] Maternal low-protein diet during gestation has been shown to result in decreased placental expression of *11β-HSD2*, therefore likely increasing exposure of the fetus to maternal corticosteroids.[34,154] Treatment of pregnant rats fed a low-protein diet with an inhibitor of steroid synthesis ameliorates the programming of hypertension and increases nephron numbers in the offspring.[21,34,360] Although this rescue was not complete, these data strongly implicate glucocorticoids as modulators of nephrogenesis in the setting of maternal low-protein diet.[360] Excessive fetal steroid exposure may drive inappropriate gene expression and affect growth and nephrogenesis, potentially through more rapid maturation of tissues.[34] Furthermore, expression of steroid-responsive receptors, including the corticosteroid responsive renal Na/K-ATPase α_1- and β_1-subunits, was found to be significantly increased in offspring of rats fed a low-protein diet during gestation.[154] In another

study, prenatal dexamethasone was associated with increased proximal tubule sodium transport, in part related to increased activity of the tubular NHE3.[361] These changes may contribute to hypertension.

In humans, there has been concern about perinatal exposure to corticosteroids; however, follow-up of subjects whose mothers participated in a randomized placebo-controlled study of antenatal betamethasone did not find any difference in blood pressure or other cardiovascular risk factors at age 30 years in exposed compared with unexposed individuals.[362] Although no effect on blood pressure or renal function was noted among preterm infants who had received antenatal steroids within the first 2 years of life compared with those who did not, recent evidence, however, highlights glucocorticoid therapy may have lasting effects on the brain and result in increased mental disorders at age 8 years.[191,363,364] Longitudinal examination of the consequences of sustained glucocorticoid therapy (e.g., throughout pregnancy) has not been performed.

MATERNAL AND FETAL HYPOXIA

In addition to maternal iron deficiency (resulting in anemia) and placental insufficiency discussed earlier, a range of conditions, including high altitude, maternal smoking, and sleep apnea, can result in fetal hypoxia. These conditions have all been shown to result in low birth weight in humans, but as yet, there is little evidence to suggest long-term effects on kidney function. In mice, a short-term severe, hypoxic insult (5.5%–7.5% maternal oxygen) from E9.5–10.5 caused a CAKUT phenotype, whereas mild hypoxia in midpregnancy (12% from E12.5–14.5) resulted in low nephron endowment mediated in part through suppression of β-catenin signaling.[365] A similar mild hypoxia in late gestation resulted in fetal growth restriction, low nephron number in male but not female offspring, and hypertension in both sexes.[366] In a mouse model of cigarette smoke exposure, male offspring had fewer nephrons and increased albumin/creatinine ratio.[367] Short-term cord occlusion in fetal sheep did not cause overt long-term renal damage, highlighting that the timing and duration of hypoxia are important in mediating renal outcomes.[368]

FETAL DRUG AND ALCOHOL EXPOSURE

Several medications commonly used during pregnancy or in the early postnatal period have been studied for their effects on birth weight and nephrogenesis. Among 397 pregnant women, antibiotic use was associated with a 138-g lower offspring birth weight compared with nonantibiotic use.[369] Furthermore, analysis of methylation levels of imprinted genes showed antibiotic use to be associated with methylation at five differentially mediated regions, although methylation at only one region was associated with birth weight.[369] The aminoglycoside antibiotic gentamicin administered to pregnant rats results in a permanent nephron deficit in offspring.[370] Significantly lower numbers of ureteric branch points and nephrons were observed in metanephric explants cultured in the presence of gentamicin.[371,372] In contrast, however, other investigators did not find a reduction in nephron number in rat pups administered gentamicin intraperitoneally from birth to 14 days of age.[373] The β-lactams have also been shown to result in impaired nephrogenesis.[374] Administration of ampicillin to pregnant rats leads to an 11% average reduction in nephron endowment in offspring, as well as evidence of focal cystic tubule dilatation and interstitial inflammation. Administration of ceftriaxone in vivo did not result in a nephron deficit, but histologically, there was evidence of renal interstitial inflammation. The penicillins were also found to inhibit nephrogenesis in cultured metanephroi in a dose-dependent fashion, an effect that was less evident with ceftriaxone. Importantly, nephrogenesis was affected even at therapeutic doses of penicillins in the rat. The mechanism whereby the β-lactams reduce nephron endowment is likely through an increase in apoptosis in the induced mesenchyme.[106] Overall, antibiotic use during pregnancy may reduce nephron endowment. Further research on those antibiotics that are frequently used in human pregnancy and preterm infants in warranted.

The immunosuppressive medication cyclosporine is a known nephrotoxin in humans that crosses the placenta. Women treated with cyclosporine may have successful pregnancies, although infants tend to have birth weights in the low range, and its effect on the fetal kidney is not well described.[375] Cyclosporine administration in varying doses and at different stages of gestation was evaluated in pregnant rabbits compared with rabbits receiving either vehicle or no drug.[375] Cyclosporine administration in the later, but not the earlier, period of gestation resulted in smaller litters and growth-restricted pups. All pups exposed to cyclosporine in utero had a 25% to 33% lower nephron number than controls. The reduction in nephron number was accompanied by glomerulomegaly and was independent of birth weight. At 1 month of age, these kidneys also demonstrated foci of glomerulosclerosis. Subsequent functional evaluation of the kidneys of rabbits exposed to cyclosporine in utero demonstrated lower GFR at 18 and 35 weeks of age and an increase in proteinuria at 11, 18, and 35 weeks of age.[176] Rabbits exposed to cyclosporine in utero developed spontaneous hypertension by 11 weeks of age, which worsened progressively with time.[176] In the presence of cyclosporine, nephron formation was found to be arrested, potentially due to inhibition of conversion of metanephric mesenchyme to epithelium.[106]

Nonsteroidal antiinflammatory drugs are sometimes used in preterm children postnatally. Administration of a cyclooxygenase 2 inhibitor, but not a cyclooxygenase 1 inhibitor, postnatally in rats and mice resulted in reduced cortical volume, impairment of nephrogenesis, and reduced glomerular diameter.[376] Administration of indomethacin or ibuprofen postnatally did not affect nephron number in rats.[373] In the preterm baboon kidney, early postnatal administration of five doses of ibuprofen (consistent with recommended dosing in preterm infants with patent ductus arteriosus) was associated with a reduction in width of the nephrogenic zone, suggesting premature termination of nephrogenesis.[377] The impact of these medications on human nephrogenesis is not known.

Maternal alcohol consumption: Renal malformations have been reported in children with fetal alcohol syndrome.[378] In sheep, repeated ethanol exposure during the second half of pregnancy resulted in an 11% reduction in nephron number and impaired vascular function in late pregnancy, although offspring outcomes were not examined.[379,380] In rats, exposure to 2 days of a high dose of alcohol in mid–late

pregnancy resulted in a low nephron number and offspring with hypertension and sex-dependent impairments in GFR.[381] Using metanephric organ culture, alcohol was found to cause dose-dependent decreases in branching morphogenesis, which were prevented by retinoic acid supplementation.[382] An abstract has reported an impact of maternal alcohol ingestion on kidney development in children, but it is not known whether the effects were mediated by associated vitamin A deficiency or other mechanisms.[90]

OBSTRUCTION OF THE DEVELOPING KIDNEY

Around one-half of all pediatric kidney transplants are required as a result of CAKUT, predominantly obstructive nephropathy, and hypoplasia/dysplasia.[383] Being small for gestational age was associated with a higher risk of ESKD (OR: 2.5; 95% CI: 1.6 to 3.7) compared with normal birth weight, suggesting that nephron number acquired at birth may be an important modulator of this risk.[31] Most cases of CAKUT result from multiple genetic, epigenetic, and fetal developmental factors such as exposure to maternal diabetes, as discussed earlier (see Table 21.8).[274] As recently reviewed, many developmental abnormalities of the urinary tract are associated with impaired nephrogenesis, which, in turn, is compounded by obstructive injury.[384,385] From animal studies, it has become clear that perinatal urinary obstruction may lead to reduced nephron numbers, which may exacerbate the impact of other programming factors.[70,386] In rats, unilateral ureteral obstruction (UUO) on postnatal day 1 and relieved on day 5, or on postnatal day 14 and relieved on day 19, reduced nephron number by 50% in both groups.[73] Similar intervention in adult rats did not affect nephron number or tubular development. A follow-up study using this model of early-life UUO demonstrated that renin was decreased and glomerulotubular maturation was delayed.[387] These studies demonstrate that urinary obstruction in a normal developing kidney can impact not only nephrogenesis but also tubular development, which may have long-term impacts on renal solute handling. Importantly, temporary neonatal urinary obstruction was also associated with histologic scarring and loss of function of the contralateral kidney in 1-year-old rats, suggesting consequent programming in the contralateral kidney as well.[388] Developing and neonatal kidneys therefore appear to be highly susceptible to obstructive injury, suggesting that early relief of urinary tract obstruction may be important to preserve nephron number.

MOLECULAR PATHWAYS AFFECTED IN FETAL PROGRAMMING OF THE KIDNEY

The molecular regulation of kidney development, particularly in the mouse, has been comprehensively described elsewhere.[298] In a number of animal models of developmental programming, changes in expression levels of genes regulating branching morphogenesis, apoptosis, and renal growth have been described (for a review, see Wang and Garrett[389]), and studies have applied microarray or deep-sequencing techniques to determine the effects of a maternal perturbation on the whole genome.[299,313,390] Epigenetic changes are now thought to play a role in programming of disease across generations, but as yet, the evidence for epigenetic changes within the kidney is limited.[391]

URETERIC BRANCHING MORPHOGENESIS

GDNF signaling through its receptor-tyrosine kinase Ret is a key ligand–receptor interaction driving ureteric budding and branching. The *c-ret* receptor is expressed on the tips of the ureteric bud branches, and knockout of this receptor in mice leads to severe renal dysplasia and reduction in nephron number.[297] Homozygous *GDNF*-null mutant mice have complete renal agenesis and die shortly after birth.[392] Heterozygous *GDNF* mice, as described earlier, have reduced nephron numbers, develop glomerulomegaly, and are susceptible to hypertension.[149] Polymorphisms in *RET*, but not *GDNF*, are associated with newborn renal size in humans.[121,393] As described earlier, maternal dietary vitamin A has a significant impact on nephrogenesis (Fig. 12.12). In cultured metanephroi, the expression of *c-ret* was found to be regulated by retinoic acid supplementation in a dose-dependent manner.[326] *GDNF* expression was not affected by vitamin A fluctuations. Modulation of *c-ret* expression is therefore likely to be a significant pathway through which vitamin A availability regulates nephrogenesis and nephron endowment. Expression of *GDNF* has also been shown to be decreased following maternal glucocorticoid exposure[357] and maternal alcohol consumption,[381] which may contribute to a reduction in branching morphogenesis and lower nephron endowment.

Further evidence for impairments in ureteric branching comes from a mouse model of maternal diabetes during pregnancy, where optical projection tomography was used to demonstrate a reduction in branch number and length within the developing kidney.[342] In another mouse model of diabetes, changes in TGF-β1 signaling were disrupted due to increased expression of a hedgehog interacting protein.[394] This protein was localized to differentiated metanephric mesenchyme and the ureteric epithelium during early kidney development and then was found in maturing glomerular endothelial and tubulointerstitial cells. Increased expression of this protein due to high glucose-impaired branching morphogenesis resulted in neonates with small kidneys.

APOPTOSIS

To evaluate at which stage of development a low-protein diet impacts nephrogenesis, embryonic rat metanephroi were studied at different time points.[313] At embryonic day 13, the metanephros has just formed, the ureteric bud has branched once, branch tips are surrounded by condensed mesenchyme that later transforms into tubule epithelium, and the ureteric stalk is surrounded by loose stromal mesenchyme.[313] By day 15, multiple branching cycles have occurred, and primitive nephrons begin to be formed.[313] At embryonic day 13, there was no difference in the number of cells in metanephroi from embryos whose mothers received low- or normal-protein diets, but by day 15, there were significantly fewer cells per metanephros in the low-protein group. In contrast, a significant increase in the number of apoptotic cells was observed in the low-protein group at day 13 but not at day 15, suggesting that increased apoptosis on day 13 likely contributed to the reduced cell numbers on day 15.[313] On postnatal day 1 in kidneys from offspring of mothers exposed to 50% calorie restriction, apoptosis was most evident in the nephrogenic zone, colocalizing to the mesenchyme and peritubular aggregates, suggesting a role in modulation of

nephrogenesis.[395] In 8-week-old hypertensive low-birth-weight rat offspring of mothers subjected to a low-protein diet, the kidneys were histologically normal but also showed evidence of increased apoptosis, without an increase in proliferation, compared with normal-birth-weight controls.[108] The increase in apoptotic activity observed in the kidney in these studies suggests possible successive waves of apoptosis at different stages of nephrogenesis in programmed rats that may impact nephron endowment.

Several studies have suggested that altered regulation of apoptosis in the developing kidney may be due to downregulation of antiapoptotic factors (e.g., Pax-2 or Bcl-2) and/or upregulation of proapoptotic factors in response to environmental or other stimuli (e.g., Bax, p53, Fas receptor, caspase 3 and 9).[395–399] Humans with haploinsufficiency of *PAX2* have renal coloboma syndrome, and those with certain *PAX2* polymorphisms have smaller neonatal kidney size as discussed earlier.[306,396,400] *PAX2* is an antiapoptotic transcriptional regulator that is highly expressed in the branching ureteric tree as well as in foci of induced nephrogenic mesenchyme during kidney development.[396] Heterozygous mice with *Pax2* mutations were very small at birth and had significant reductions in nephron number. In addition, there was a significant increase in apoptotic cell death in the developing kidneys. Subsequently, the same group[400] demonstrated that loss of *Pax2* antiapoptotic activity reduced ureteric branching and increased ureteric apoptosis. Similarly, loss of the antiapoptotic factor *Bcl-2* or gain of function of the proapoptotic factor p53 are both associated with a significant reduction in nephron number, associated with increased apoptosis in metanephric blastemas, in *Bcl-2* knockout mice and *p53* transgenic mice.[397,401]

Mutant mouse models, although providing evidence that an increase in apoptosis results in reduced nephron numbers, do not, however, address the impact of environmental factors on renal development. Pham and associates[402] examined gene expression in the kidneys of offspring of rats subjected to uterine artery ligation during gestation. These authors found a 25% reduction in glomerular number was associated with increased evidence of apoptosis and increased proapoptotic caspase-3 activity in the kidney at birth. Furthermore, they found evidence of increased mRNA expression of the proapoptotic genes *Bax* and *p53* and decreased expression of the antiapoptotic gene *Bcl-2*. These authors also found evidence of hypomethylation of the *p53* gene, which, in addition to a decrease in *Bcl-2* expression, would lead to an increase in *p53* activity, suggesting epigenetic programming of a proapoptotic milieu as a potential modulator of nephron endowment. Increased apoptosis was also observed in a similar rat model during late gestation (E20) and 1 week after birth (PN7), suggesting inappropriate apoptosis even after birth.[403] Of great interest in that study, the growth-restricted offspring, but not control offspring, had evidence of ongoing nephrogenesis at PN7, suggesting a delay in kidney development in the growth-restricted group. Gene microarray studies in rodent models of maternal iron deficiency[390] and diabetes[404] have also identified apoptotic signaling pathways in fetal kidneys.

IMPACT OF SEX

In some experimental models and human studies, although not all, programming effects on blood pressure and kidney function appear to be different between males and females, especially at young ages. In female rats with similar programmed reductions in nephron numbers, blood pressures are often not as high or increase much later than in males.[108,405] Often a secondary challenge such as pregnancy, however, will "unmask" a disease phenotype in females. For example, males but not females born small as a result of bilateral uterine vessel ligation develop hypertension and insulin resistance.[111,406,407] However, growth-restricted females develop glucose intolerance during pregnancy.[408] Sex hormones may, in part, explain these differences. Growth-restricted males (induced by uterine artery ligation) have elevated testosterone levels compared with controls, and hypertension can be abrogated by castration.[405] Such changes are not observed in male offspring of protein-restricted mothers, however, pointing to the intricacies of the programming models. In female rats growth restricted by placental insufficiency, hypertension only develops late, but onset can be accelerated by ovariectomy.[405] These data suggest that in the uterine ischemia programming model, testosterone exacerbates and estrogen protects against hypertension. Sex differences in relative expression of components of the RAAS appear to participate in programming of hypertension, potentially differentially altering the balance between vasoconstriction and vasodilation and sodium handling.[159,405] Furthermore, growth-restricted male rats exhibit increased markers of renal oxidative stress compared with controls, which are absent in similarly programmed females, and antioxidant treatment normalized blood pressure in the male rats.[170,409] Multiple other suggested mechanisms underlying these gender differences have been reviewed by Ojeda et al., as outlined in Fig. 21.14.[170,405]

Sex differences may also originate in utero due to differences in growth of male and female fetuses and sex-specific placental responses to maternal perturbations (reviewed in Kalisch-Smith et al.[410]). In particular, the placenta has an important role in preventing excess maternal glucocorticoids from reaching the fetus via the activity of placental 11β-HSD2. This enzyme has the ability to convert the active glucocorticoid into an inactive form, as discussed earlier. The placenta of female fetuses is known to have higher levels of this enzyme compared with males,[411] and as such, the male fetus is likely to be exposed to more glucocorticoids. Furthermore, in women treated with synthetic glucocorticoids when threatening to deliver preterm, placental 11β-HSD2 was elevated more in placentas of females than males.[412] The sex of the fetus has not always been taken into account when performing studies on renal development; however, a recent metaanalysis demonstrated the adult human kidney showed sex-specific expression of more than 200 genes.[413]

POTENTIAL FOR RESCUE OF NEPHRON NUMBER

Given the evidence for developmental programming of hypertension and kidney disease and the associations with birth weight, preterm birth, other intrauterine exposures, and the impact of nutrition in early childhood, it is possible that interventions could be designed to modulate developmentally programmed changes in the kidney and reduce long-term disease risk. Optimization of maternal health and nutrition prior to and during pregnancy to attenuate any risk factors for low birth weight and preterm birth is the most obvious

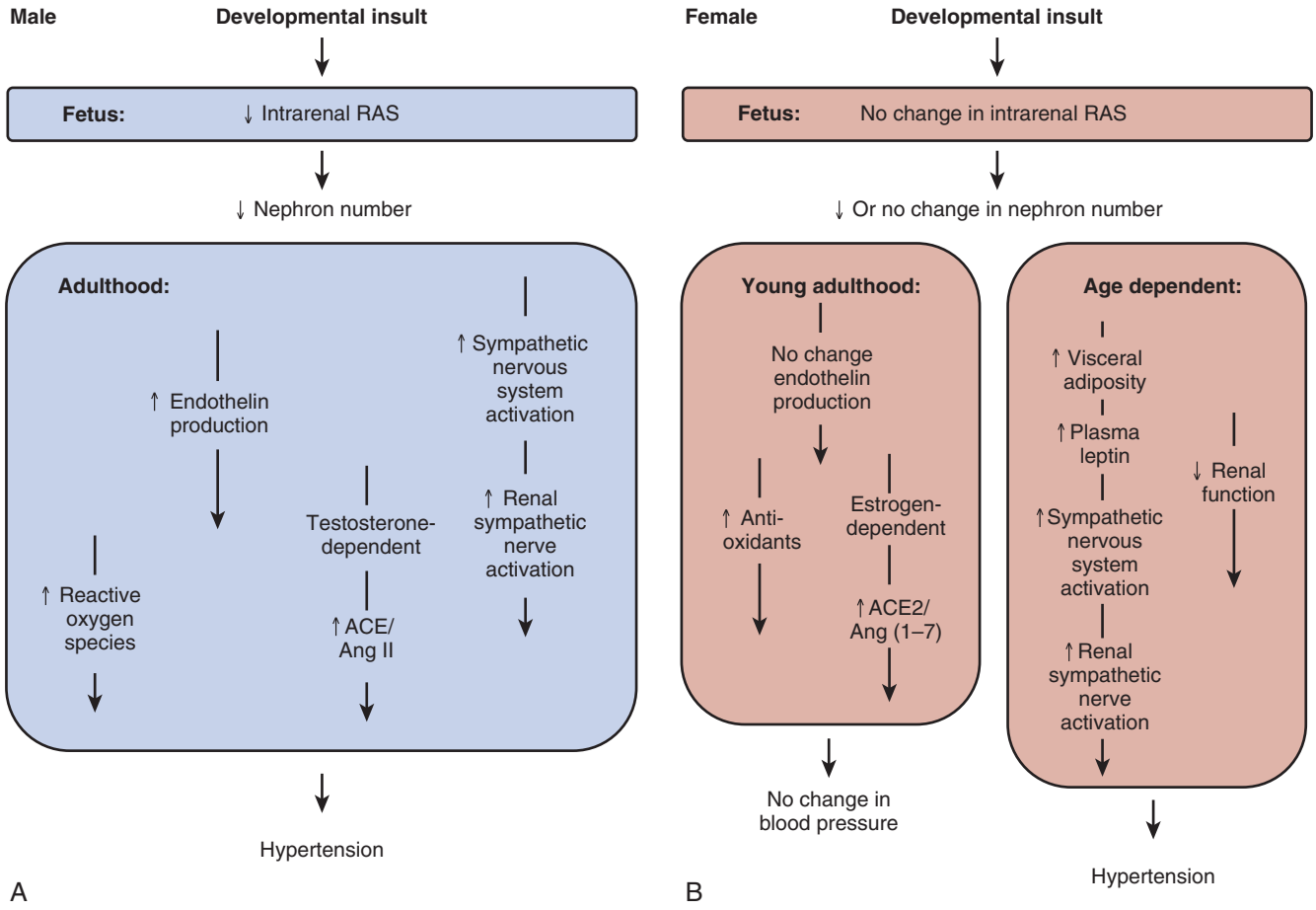

Fig. 21.14 Potential differing mechanisms impacting developmental programming of blood pressure in (A) males, and (B) females. These mechanisms may be due to the influence of the hormonal milieu on the renin–angiotensin system *(RAS)* due to innate sex differences in production of reactive oxygen species or endothelin, or impacted by increased susceptibility that occurs with age and the development of age-dependent increases in adiposity leading to activation of the sympathetic renal nerves (females). The fetus also exhibits innate sex differences in expression of the intrarenal RAS, which may or may not (as in females) reduce nephron number. *ACE*, Angiotensin-converting enzyme; *Ang*, angiotensin. (From Ojeda NB, Intapad S, Alexander BT. Sex differences in the developmental programming of hypertension. *Acta Physiol (Oxf)*. 2014;210:307–316.)

intervention, as it has been estimated that intrauterine factors determine around 60% of the variation in birth weight.[414] In addition, minimization of nephrotoxin exposure and attention to neonatal nutrition in preterm infants are important to permit optimal nephrogenesis after birth. Specific interventions that may augment nephron number per se have been investigated, some of which are clinically feasible, while others are still in research stages (see Table 21.4). Interventions to modulate other aspects of developmental programming in the kidney have not yet been reported, but the assumption would be that the impact may be similar to those affecting nephrogenesis.

Prevention is likely more realistic than rescue of low nephron number. Ouabain is a highly specific ligand for Na/K-ATPase, the activity of which is known to be reduced in erythrocytes of low-birth-weight young men.[415,416] Na/K-ATPase is a ubiquitously expressed plasma membrane protein that regulates the release of calcium waves and thereby is an important regulator of early development.[415] In vitro addition of ouabain to the medium of metanephroi in culture was found to abrogate the effect of serum starvation on ureteric branching.[415] Similarly, in vivo, ouabain administration throughout pregnancy prevented the reduction in nephron number in rats subjected to maternal low-protein diet.[415] Whether ouabain can rescue nephron number if given late in pregnancy was not addressed in this study. Supplementation of glycine, urea, or alanine to a maternal low-protein diet prevented development of low nephron numbers in rat offspring, but only glycine supplementation prevented subsequent hypertension.[34] Intriguingly, water restriction of rat mothers during gestation resulted in augmentation of normal nephron number but also induced hypertension in the offspring. The authors implicate vasopressin as a mediator of this programming effect.[417]

Vitamin A deficiency is common among women in poorer nations and in animals is associated with reduced nephron number as discussed earlier.[326,418] In rats exposed to maternal low-protein diet, nephron number was restored to normal by one dose of retinoic acid given to the pregnant dams during early nephrogenesis.[419] In preterm baboons, however, administration of retinoic acid postnatally did not rescue nephron number, suggesting that vitamin A is likely necessary earlier in gestation.[327] These baboons also received postnatal antibiotics, which may have confounded the effect of the vitamin A.

Postnatal nutrition is an important modulator of kidney development, especially in preterm infants. Restoration of normal protein intake by cross-fostering growth-restricted pups onto normal mothers after birth reduced nephron number and prevented hypertension compared with those fed by protein-deficient mothers.[112]

A maternal single kidney may impact fetal kidney development. In offspring of rats that had undergone nephrectomy prior to pregnancy, nephron numbers were increased at birth, although not at 6 weeks.[420,421] A circulating renotrophic factor in the mother may therefore accelerate nephrogenesis but does not appear to affect final nephron endowment. How these observations would apply in humans is difficult to extrapolate, as outcomes may be different depending on maternal age, whether she has a congenital or acquired single kidney, or a kidney transplant with the attendant required medications, which, in turn, may affect nephrogenesis.

Modulation of regression of nephron number, although still hypothetical, has been suggested as a potential pathway to augment final nephron number.[422] Glomerular number was evaluated from postnatal days 7 to 28 in normal mice. Maximal nephron number was seen at day 7, with a subsequent regression and plateau at day 18. Such a time course would need to be studied in growth-restricted animals before any potential intervention to inhibit this regression could be tested.

CATCH-UP GROWTH

Postnatal nutrition is important for infant growth, especially in the setting of preterm birth or growth restriction, and can impact nephron number and long-term renal function, as discussed earlier.[187,224] Cross-fostering of growth-restricted newborn rats (induced by placental insufficiency) onto normal mothers permitted restoration of normal nephron number and prevented subsequent hypertension, demonstrating the potential "rescue" effect of adequate postnatal nutrition.[112] Postnatal overfeeding of low-birth-weight rats, induced by reduction of litter size to three pups, however, did not augment low nephron numbers, and with aging, rats became obese and hypertensive and developed renal injury.[423] In this model, despite the mother being switched to a normal-protein diet at time of delivery, the pups may remain somewhat protein deficient despite consuming larger quantities of milk, as opposed to cross-fostering, which provides normal milk immediately, which may explain why nephron number remained low and underscores the importance of diet composition. In contrast, overfeeding of normal-birth-weight rats led to higher than normal nephron numbers, despite which high blood pressure and renal injury developed over time.[137] These animal data suggest that restoration of normal dietary components after growth restriction may permit some reversal of programmed changes, but overfeeding appears harmful.

In diverse populations worldwide, rapid "catch-up" growth (defined as upward crossing of weight centiles), or an increase in body mass index, even in children of normal birth weight, is associated with higher blood pressures and increased cardiovascular risk.[424–426] On the other hand, catch-up growth has been advocated in poorer countries to improve child survival from infectious diseases and reduce stunting and malnutrition.[427] Among 7-year-old children who had been preterm, GFRs were reduced in those who had experienced either intrauterine or extrauterine growth restriction (i.e., inadequate growth early postbirth), highlighting the importance of adequate early postnatal nutrition for kidney development.[224] Nutrition in preterm infants is challenging, and balancing benefits and risks of rapid growth must be considered, including optimizing neurodevelopment and metabolic outcomes.[428]

The timing of catch-up growth in early infancy and childhood, which tends to occur rapidly in low-birth-weight children when adequate nutrition is available, appears a crucial factor in determining this long-term risk.[426,427,429,430] The importance of birth weight and catch-up growth was examined in a cohort of British 22-year-olds, in whom systolic blood pressure was observed to increase by 1.3 mm Hg (95% CI: 0.3 to 2.3 mm Hg) for each SD decrease in birth weight and to increase by 1.6 mm Hg (95% CI: 0.6 to 2.7 mm Hg) for each SD increase in weight gain between the ages of 1 and 10 years.[431] Such observations have been reproduced in several populations, together with evidence of increased arterial stiffness and greater prevalence of cardiovascular risk factors in early childhood after rapid growth, with children who had been of low birth weight but became overweight being at highest risk.[208,424,429] The consequences of catch-up growth may, however, differ if growth is linear (i.e., growth in height) or in weight, and may differ between developed and developing countries where health priorities differ.[432] Thus far, it appears that among those born with low birth weight or preterm, the development of overweight or obesity is the predominant risk factor.[208,426,429,430,433] Low birth weight independently predicted both proteinuria and obesity in a rural Canadian cohort, demonstrating likely simultaneous programming of multiple risk factors for kidney disease.[434] Risk factors for childhood overweight and obesity also include high birth weight and exposure to gestational diabetes.[435] Obesity, in turn, is a risk factor for renal disease.[436,437] Finding the balance where postnatal nutrition is optimized to improve short-term survival and reduce long-term risk of chronic disease requires further study. In general, avoidance of overweight through diet and exercise are safe principles.[438,439]

IMPACT OF EARLY GROWTH ON KIDNEY FUNCTION

Grijalva-Eternod[440] and colleagues developed a model to test whether "mismatch" between a small kidney and a (relatively) larger body, as would occur with catch-up growth and overweight after being born small, is associated with hypertension. Birth weight was presumed to reflect the homeostatic metabolic capacity of the kidney and childhood body composition to reflect the metabolic load. When applied to a birth cohort of children, the model found that a high metabolic load, relative to innate metabolic capacity, was associated with higher blood pressures (Fig. 21.15). Consistent with this hypothesis, proteinuric renal disease progressed faster in children who had been born prematurely and became obese compared with those who were not obese.[441] In this study, all obese children, whether born at term or preterm, were found to have glomerulomegaly, although kidney size remained small in all those born preterm, even among the obese. Similarly, excessive weight gain was a predictor of worse renal function at age 7.5 years in a cohort of very low–birth-weight preterm infants who had experienced AKI.[442]

Accelerated senescence has been proposed as a potential mechanism whereby catch-up growth may increase the risk of

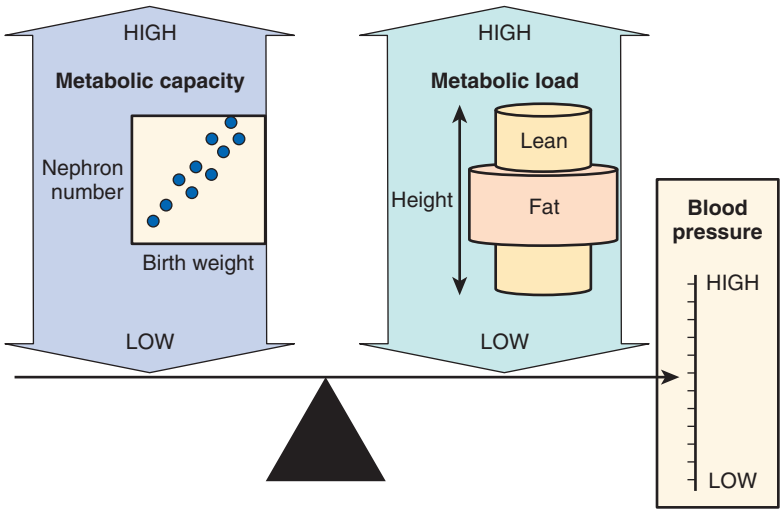

Fig. 21.15 Diagram illustrating the concepts of metabolic capacity and metabolic load in relation to blood pressure. Metabolic capacity, meaning the capacity to maintain normal metabolic homeostasis, is dependent on nephron number, which scales positively with birth weight. Metabolic load, meaning the demand placed on homeostatic systems, is dependent on body size and adiposity, and hence on height, lean mass, and fat mass. Here they are portrayed using a cylinder model in which cylinder lengths are proportional to height, and the volumes are proportional to the masses of lean and fat mass. A high load and low capacity are each predicted to increase blood pressure. (From Grijalva-Eternod CS, Lawlor DA, Wells JC. Testing a capacity-load model for hypertension: disentangling early and late growth effects on childhood blood pressure in a prospective birth cohort. *PLoS One.* 2013;8:e56078.)

cardiovascular and renal disease.[443] Senescence is a state of cellular growth arrest that naturally occurs with age but may be accelerated in the face of stress, mediated by upregulation of cell cycle inhibitors (p53, p21, and p16INK4a) and progressive shortening of telomeres.[444] Increased expression of senescence markers has been observed in diseased human kidneys.[445] In animals, rapid weight gain in growth-restricted animals was associated with evidence of accelerated senescence in the kidney and cardiovascular system and premature death, consistent with accelerated aging.[443,446,447] Senescence markers are not more highly expressed at birth in growth-restricted versus normal birth weight animals but increase more rapidly as the animals age.[446] Hyperfiltration in a small kidney, exacerbated by high metabolic demand from increasing body size, likely contributes to ongoing injury and progressive senescence.[445,446] Senescence markers have not been studied in low-birth-weight human kidneys, but leukocyte telomere length was found to be significantly shorter among 5-year-old Bangladeshi children who had been of low birth weight compared with those of normal birth weight, lending support to this hypothesis.[448,449] Oxidative stress is a driver of senescence, and in small-for-gestational-age children, markers of oxidative stress were higher in those who experienced catch-up growth compared with controls, suggesting oxidative stress as a possible initiator of accelerated senescence.[450] A programmed link between low nephron number, catch-up growth, and accelerated senescence as a potential mediator of hypertension and renal disease in humans has yet to be proven.

Given the normal age-related loss of nephrons and potential for accelerated senescence in the kidney, it could be expected that the impact of prenatal programming would be compounded by age.[41] This has not yet been extensively studied; however, a single Japanese study found that among elderly subjects with ESKD, diabetic nephropathy was more common among those who had had a low birth weight.[451] This observation may suggest a programming effect of diabetes, kidney disease, or both and requires further study.[275]

MATERNAL HEALTH AND INTERGENERATIONAL EFFECTS OF PROGRAMMING

Maternal health and nutrition are crucial determinants of a healthy pregnancy, offspring birth weight, and fetal kidney development.[279] Socioeconomic and structural factors are important determinants of maternal health and thereby the health of future generations.[1] Maternal prepregnancy underweight is associated with a higher odds of having a small-for-gestational-age (OR: 1.81; 95% CI: 1.76 to 1.87) or low-birth-weight infant (OR: 1.47; 95% CI: 1.27 to 1.71), as well as a higher risk of preterm birth.[452,453] In contrast, being overweight before pregnancy increases the risk of high birth weight compared with nonobese women (OR: 1.67; 95% CI: 1.42 to 1.97).[453] The risks of gestational diabetes and preeclampsia double with prepregnancy maternal overweight.[452] Preconception care and weight loss may positively impact these adverse outcomes, although around two-thirds of preterm births remain unexplained.[452,454–456]

Maternal risk factors for low birth weight or preterm birth are highlighted in Table 21.15, and global prevalences of some of these factors are outlined in Table 21.16.[1] Short maternal stature, maternal underweight, or iron deficiency are risk factors for offspring low birth weight.[284,457–459] Maternal vitamin A levels are associated with newborn kidney size and nephron number.[460] Supplementation of various nutrients in pregnant women has been shown to reduce the risks of low birth weight or preterm birth, but the long-term impact on childhood or later blood pressure and kidney function are not yet clear (see Table 21.14).[1,457,461] Maternal smoking, alcohol, and caffeine consumption during pregnancy may also increase

Table 21.15 Maternal Factors Associated With Birth Weight and Preterm Delivery

Maternal Factor	
Developmental	Maternal birth weight <2.5 kg or >4.0 kg
	Short stature, stunting (height <145 cm)
Behavioral	Cigarette smoking
	Alcohol consumption
	Substance and/or drug abuse
Demographic	Age <18 years or >40 years
	Ethnicity
Health-related	Undernutrition, low maternal BMI
	Iron deficiency
	Malaria
	Diabetes or gestational diabetes mellitus
	Hypertension
	Preeclampsia, eclampsia
	Chronic kidney disease, transplant, dialysis
	Birth before term
	Multiple gestations
	Multiparous (≥3)
	Assisted reproduction
	Infections
	Obesity
Social	Highly active antiretroviral therapy for HIV
	Prenatal care
	Unplanned pregnancy, birth spacing
	Teenage pregnancy
	Marriage during childhood
	Conflict, war, stress
	Environmental conditions
	Education level
	Poverty
Environmental	Seasonal variations in nutrient availability
	Toxin or pollutant exposure

BMI, Body mass index.

From Luyckx VA, Brenner BM. Birth weight, malnutrition and kidney-associated outcomes—a global concern. *Nat Rev Nephrol.* 2015;11:135–149, Box 2.

the risk of low birth weight and preterm birth and have been associated with changes in childhood blood pressures and kidney size and function.[462–467] Infections during pregnancy or chronic maternal illness all increase the risks of adverse pregnancy outcomes (Table 21.15).[303,468,469] Acute infections such as malaria are highly prevalent in lower-income regions and may contribute to a large number of low-birth-weight or preterm births annually.[470] In high-income countries, delays in pregnancy, use of assisted reproduction, or chronic maternal illness are increasingly common, ranging from 3%–20% in different studies.[471,472] Maternal chronic disease increases the risk of having a preterm birth or small-for-gestational-age infant; therefore, planning of pregnancies in such women is important to minimize these risks.[456,473] Specifically, pregnant women with CKD have a higher risk of low birth weight, small for gestational age, and preterm birth.[474,475] CKD is also a major risk factor for preeclampsia, in addition to maternal preexisting hypertension, diabetes, anemia, heart disease, and urinary tract infections/pyelonephritis.[476] Teenage pregnancies are at higher risk of preeclampsia, low birth weight, and preterm birth.[454,477,478] These factors therefore may all impact fetal programming.

In a population-based cohort of women, the odds of pregnancy-associated gestational diabetes or gestational hypertension (including preeclampsia or eclampsia) among those who had been born preterm were significantly increased and were higher with lower gestational age, suggesting a "dose–response" relationship with degree of maternal prematurity (OR: 1.95; 95% CI: 1.54 to 2.47 if mother born at <32 weeks; OR: 1.14; 95% CI: 1.03 to 1.25 if mother born at 32–36 weeks).[190] Gestational hypertension and preeclampsia, in turn, are risk factors for low birth weight and preterm birth, and gestational diabetes is a risk factor for high birth weight; therefore, the offspring of these pregnancies are likely at risk for programmed hypertension and renal dysfunction, including gestational hypertension.[476] The programming cycle could therefore continue across generations. Maternal low birth weight or preterm birth are also risk factors for having low-birth-weight or preterm infants.[1,479,480] A direct intergenerational programming effect of maternal preterm birth on subsequent offspring preterm birth is supported by the observed increasing risk of preterm birth with lower maternal gestational age and the absence of risk if the father was born preterm.[481] Maternal obesity and gestational diabetes are increasing worldwide and are established risk factors for both low and high birth weight.[482–484] Obesity in pregnant women who had themselves been born with low birth weight was associated with a 3.65-fold increased risk of preterm delivery compared with those who were not obese.[480] Maternal low or high birth weight is also associated with a higher risk of developing gestational diabetes.[485] Maternal birth circumstances and subsequent obesity therefore affect risk of adverse pregnancy outcomes and may program the health of their offspring. The mechanisms, however, remain unclear.[391,408,486,487]

In rats, maternal protein restriction results in transgenerational programming persisting into the F2 generation.[488] These effects have been proposed to be mediated largely by changes in DNA methylation, determined by amino acid availability, resulting in epigenetic changes in gene expression.[21] Whether these epigenetic changes can be transmitted through the germline and persist in the offspring, or whether a mother who had been subjected to adverse intrauterine events may experience changes in renal function and blood pressure during pregnancy that may, in turn, de novo impact the development of her offspring is still a point of debate.[391,408,486] The latter hypothesis seems more likely.

IMPACT OF NEPHRON ENDOWMENT IN TRANSPLANTATION

Nephron endowment in transplantation is relevant for both the donor and the recipient. Removal of a kidney in a healthy donor implies loss of 50% of original nephron endowment, and gain of a kidney in a recipient may provide more or less than half of the recipient's original nephron endowment, depending on relative sizes of donor and recipient, periprocedural nephron loss, and other factors. Consideration of nephron endowment prior to transplantation could impact long-term renal health in both donors and recipients.

Table 21.16 Global Incidence/Prevalence of Programming Risk Factors

Maternal Risk Factors	Global Incidence/Prevalence (%)	Reference
Undernutrition women 20–49 years (BMI <18)	12	280, 457
Short stature women of reproductive age (<155 cm)	19.7–68.5	457, 459
Malaria during pregnancy	41.2 (LMIC)	470
Hepatitis B infection (sAg) in women of childbearing age	1.5–8.5 (2005)	563
Anemia in pregnant women (Hb <110 g/L)	38.2 (95 CI: 34.3–42.0)	331, 457
Iron deficiency in pregnant women	19.2 (95 CI: 17.1–21.5)	
Vitamin A deficiency in pregnant women (night blindness)	7.8 (95 CI: 6.5–9.1)	
Zinc deficiency (general population)	17.3 (95 CI: 15.9–18.8)	
Preeclampsia	4.6 (95 CI: 2.7–8.2)	564
Eclampsia	1.4 (95 CI: 1.0–2.0)	
Hyperglycemia in pregnancy women 20–49 years (diabetes/gestational diabetes)	16.9	565
Maternal chronic illness	15.8 (Denmark, 2013)	471
Maternal overweight (BMI 25–29.9 kg/m^2)	30	457, 566, 567
Maternal obesity (BMI ≥30 kg/m^2)	11	457, 482
Maternal smoking	9–16 HIC 2.6 (LMIC)	568, 569
Assisted reproduction technology	2–3 annual births HIC	570, 571
Teenage pregnancy (<19 years)	15 million per year	478, 572, 573
Infant/Child Risk Factors		
Low birth weight	15	44
Preterm birth	11.1	44, 574
Small for gestational age (<10th percentile)	12.1	44
High birth weight (>4 kg)	0.5–14.9 (LMIC)	40
Not weighed at birth	48	43
Child <5 years of age Overweight/obesity, 2016	6.0 (95 CI: 5.1, 7.1)	575
Childhood stunting (2016)	22.9 (95 CI: 21.1, 24.7)	

BMI, Body mass index; *HIC*, high-income country; *LMIC*, low- and middle-income country; *sAg*, surface antigen–positive hepatitis B.

IMPLICATIONS OF NEPHRON ENDOWMENT FOR THE DONOR

Living donation, after appropriate donor screening, has generally been presumed to be safe, although recent studies have described some risk of ESKD after kidney donation, highlighting the urgent need to better understand predictors of renal function postdonation in living donors.[489–492] In predominantly Caucasian cohorts, hypertension and proteinuria do increase over time in living donors, but renal function remains generally well preserved over the first decades.[64,493,494] In a cross-sectional retrospective study of donors followed for up to 40 years, however, donor GFRs were found to decline after 15–17 years postdonation; therefore, duration of follow-up is important to fully understand potential associations with risk.[495] Obesity significantly increases this risk over time.[496] There are donor groups, including the young and obese, the older donor, and some ethnic groups, that may be at increased risk of long-term renal dysfunction but have not been well represented in the current literature.[489,497] A recent analysis of the U.S. donor population estimated the risk of ESKD among average donors to be 34 cases per 10,000 donors; however, this risk increased to 256 cases per 10,000 in higher-risk donors and was associated with black race, elevated body mass index, donation to a first-degree relative, and with age among nonblack donors.[497] Black race was associated with the greatest risk of ESKD (HR: 2.96; 95% CI: 2.25 to 3.89).[497] Whether developmental programming of nephron number in a prospective donor may impact these risks has not been studied. Among African Americans, we now know that many donors may carry *APOL1* risk genotypes; therefore, this risk may be multifactorial. In support of a programmed risk of accelerated loss of renal function postdonation, Aboriginal Australian donors were found to have a significantly increased risk of hypertension, renal dysfunction, and ESKD at a median of 16 years postdonation compared with Caucasians (Table 21.17).[498] Similarly, hypertension and proteinuria were much more prevalent among Aboriginal compared with Caucasian Canadian donors at 20 years of follow-up, and African Americans as well as Hispanics had more hypertension and CKD after donation than white Americans (Table 21.17).[499–501] These data are troubling because the donors were screened prior to donation; therefore, donor nephrectomy can be implicated in the disease process. Importantly, African Americans and Aboriginal Australian populations have lower birth weights than their Caucasian counterparts, and Canadian Aboriginals have higher birth weights; therefore, developmental programming of the kidney may be a risk factor contributing to poorer outcomes postdonation.[502] Given the increasing need for donors worldwide, better understanding of renal risk in these populations is urgently needed.

Table 21.17 Hypertension and Renal Function in Living Kidney Donors at Risk of Adverse Renal Programming

	United States		Australia		Canada		Germany	
Population	Black Donor	White Donor	Indigenous Donors	Nonindigenous Donors	Aboriginal Donors	White Donors	BW ≤2.5 kg	BW >2.5 kg
Donor number	12,387	71,769	22	28	38	76	18	73
Programmed risk	LBW prematurity	ref	LBW	ref	HBW (offspring of DM pregnancies)	ref	LBW	ref
HT	–	–	50%	6%	42%	19%	39%	15%
Proteinuria	–	–	81%	6%	21%	4%	81%	35%
↓ GFR	–	–	81%	38%	Not different		Not different	
ESKD	74.4 per 10,000 vs. 23.9 per 10,000 in nondonors	22.7 per 10,000 vs. 0.0 per 10,000 in nondonors	19%	0%	1	0	0	0
Follow-up (years)	7.6 (IQR 3.9–11.5)		16.1 (1.27–20.2)	6.37 (2.54–21.2)	14.6 ± 9.3	13.4 ± 9.5	≥5	≥1–3
Reference	490		498		501		503	

BW, Body weight; *DM*, diabetes mellitus; *ESKD*, end-stage kidney disease; *GFR*, glomerular filtration rate; *HBW*, high birth rate; *IQR*, interquartile range; *LBW*, low birth weight.

Reproduced from Low Birth Weight and Nephron Number Working Group. The impact of kidney development on the life course: a consensus document for action. *Nephron.* 2017;136:3–49.

A study from Germany found that GFRs were lower and proteinuria and hypertension were more frequent at 5 years postdonation among donors with birth weights <2.5 kg (see Table 21.17).[503] A group of potential donors that has not been studied is women who have had preeclampsia, who are known to be at an increased, albeit small, risk of ESKD.[504] As discussed earlier, the risk of preeclampsia is increased in women who had been of low birth weight or preterm; therefore, a proportion of women with preeclampsia were likely at risk of renal programming.[190] The risk of gestational hypertension and preeclampsia is also increased among female donors, suggesting that a reduced nephron mass may be a risk factor.[505] Caution should therefore be advised in considering women with a history of preeclampsia, low birth weight, or having been born preterm as kidney donors, as each of these factors may be a marker for programmed renal risk.[1]

IMPLICATIONS OF NEPHRON ENDOWMENT FOR THE RECIPIENT

Prescription of donor kidneys is largely based on immunologic matching. In animal experiments of renal transplantation, however, the impact of transplanted nephron mass, independent of immunologic factors, on the subsequent development of chronic allograft nephropathy has been demonstrated.[506–510] Despite such evidence, prescription of kidneys on the basis of the physiologic capacity of the donor organ to meet the metabolic needs of the recipient has not generally been considered.[511] More and more data are accumulating, however, suggesting a significant impact of transplanted renal mass on long-term posttransplantation outcomes.

Demographic and anthropomorphic factors associated with late renal allograft loss include donor age, sex, and race, as well as recipient BSA.[512–514] In general, kidneys from older, female, and African American donors fare worse.[54,77,95,515] Indirectly, these observations suggest that the intrinsic nephron endowment of the transplanted kidney is likely to play a role in the development of chronic allograft nephropathy. As nephron numbers are not yet measurable in vivo, several investigators have compared recipient and donor BSA as surrogates for metabolic demand and kidney size; others have used kidney weights or renal volumetric measurements by ultrasound as surrogates for nephron mass.[516–520] Importantly, although kidney mass and kidney volume have been thought to be proportional to nephron number, and measures of body size tend to be proportional to kidney size, these relationships do vary in strength of association[57]; therefore, these data should be interpreted cautiously. In general, however, the preponderance of evidence does support the hypothesis that small kidneys perform less well when transplanted into larger recipients.[516–520]

A retrospective analysis of 32,083 patients who received a first cadaver kidney found that large recipients of kidneys from small donors had a 43% increased risk of late allograft failure compared with medium-sized recipients receiving kidneys from medium-sized donors.[519] Outcomes were best in small recipients receiving kidneys from large donors. Subsequently, among 69,737 deceased donor kidney transplants, a severe recipient/donor size mismatch (BSA ratio >1.38) was associated with higher 10-year graft loss compared with closer matches, and the risk was doubled in the case of extended criteria donors with severe mismatches (22% vs. 10%, respectively).[521] Similar findings were seen among recipients of older (>60 years) versus younger kidneys.[522] These data suggest that donor and recipient size should be considered in organ allocation decisions, especially if the donor kidney is known to be "suboptimal." Smaller studies have not consistently found similar results, however, potentially reflecting lack of statistical power.[518,519]

Kidney size, however, may not always be directly proportional to BSA; therefore, ratios of donor to recipient BSA may not be an ideal method of estimating nephron mass to recipient mismatch. Kidney weight may be a better surrogate for nephron mass.[54,523] Using this parameter, Kim and associates[524] analyzed the ratio of donor kidney weight to recipient body weight (DKW/RBW) in 259 live-donor transplants. These authors found that a higher DKW/RBW of greater than 4.5 g/kg was significantly associated with improved allograft function at 3 years compared with a ratio of less than 3.0 g/kg. A similar study including 964 recipients of cadaveric kidneys, in whom proteinuria and Cockroft-Gault creatinine clearances were also calculated, found that 10% of the subjects were "strongly" mismatched, having a DKW/RBW ratio of less than 2 g/kg.[515] The DKW/RBW ratio was lowest when male recipients received kidneys from female donors. The risk of having proteinuria higher than 0.5 g/24 h was significantly greater, and developed earlier, in those with DKW/RBW below 2 g/kg as compared with those with higher ratios. Proteinuria was present in 50% of those with DKW/RBW less than 2 g/kg, 33% of those with DKW/RBW of 2 to 4 g/kg, and 23% in those with DKW/RBW of 4 g/kg or greater. At 5 years follow-up, however, there was no difference in graft survival among the three DKW/RBW groups, but the authors conceded that longer follow-up was needed.[515] Subsequent analysis of the same cohort 5 years later showed that GFR declined more rapidly after 7 years in the low versus the high DKW/RBW group, suggesting that the smaller kidneys were likely hyperfiltering early on, which initiated the cycle of progressive nephron loss (see Fig. 21.16).[525]

In an attempt to more accurately reflect transplanted nephron mass, other investigators have used renal ultrasonography to measure cadaveric transplant kidney (Tx) cross-sectional area in relation to recipient body weight (W) to calculate a "nephron dose index," Tx/W.[526] These authors found that during the first 5 years after transplantation, serum creatinine was significantly lower in patients with a high Tx/W compared with those with lower values, with a trend toward better graft survival. A similar analysis using renal volume determined by CT angiographic volumetry (done pretransplant in living donors) to recipient BSA found that posttransplant GFRs during the first year correlated with recipient GFR, more significantly among those with a donor/recipient BSA ratio of 1 or less.[527] A small kidney transplanted into a large recipient may not have an adequate capacity to meet the metabolic needs of the recipient without imposing glomerular hyperfiltration, which ultimately leads to nephron loss and eventual allograft failure.[528,529]

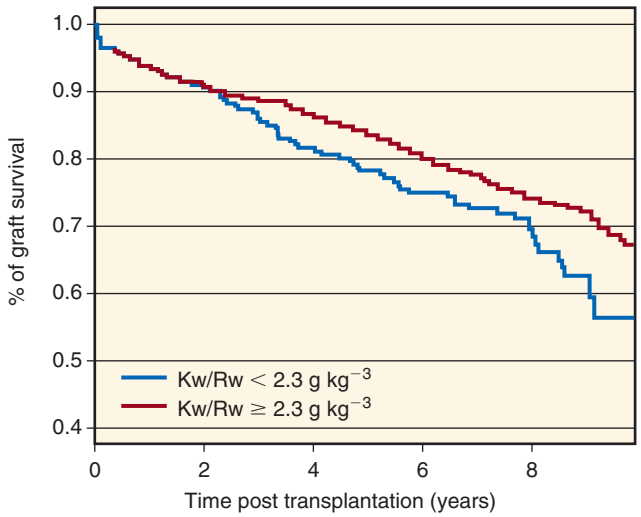

Fig. 21.16 Correlation between kidney weight *(Kw)*–to–recipient weight *(Rw)* ratio and long-term graft survival in renal transplantation. Graft survival declines faster with a Kw/Rw <2.3 g/kg ($P = .016$). (From Giral M, Foucher Y, Karam G, et al. Kidney and recipient weight incompatibility reduces long-term graft survival. *J Am Soc Nephrol.* 2010;21:1022–1029.)

Transplanted nephron mass may be a function of congenital endowment and attrition of nephrons with age but is also impacted by peritransplant renal injury (i.e., donor hypotension, prolonged cold and warm ischemia, nephrotoxic immunosuppressive drugs). All of these factors must be closely considered, in addition to immunologic matching, in selection of appropriate recipients in whom the allograft is likely to function for the longest time and therefore provide best possible improvement in quality of life.

GLOBAL HEALTH RELEVANCE OF RENAL PROGRAMMING

The known risk factors—low birth weight, small for gestational age, preterm birth, high birth weight—are prevalent worldwide, in both low- and high-income settings, although underlying causes may differ (see Table 21.16). Millions of infants born each year are at risk, therefore, of future hypertension and kidney disease as well as other programmed conditions. How much developmental programming contributes to the growing burden of chronic noncommunicable diseases worldwide is unknown but may be significant, especially in regions where access to preventive health care is limited. In the current era of sustainable development goals, it may be possible to reduce the impact of developmental programming on future generations through a multisectoral approach encompassing not only the health system but education, infrastructure, and reducing social inequities. Strategies to reduce the impact of developmental programming in individual infants should be simple to implement and, as reviewed in depth elsewhere,[1] include documentation of birth weight and gestational age in each child to identify those at risk; heightened awareness of the risk of neonatal AKI in preterm infants and implementation of strategies to reduce these risks; and education of parents about healthy lifestyle choices to prevent obesity and stunting, low birth weight, small for gestational age, and preterm. Children born to mothers with preeclampsia, diabetes, or obesity should be screened for hypertension and proteinuria, especially if they become overweight; as adults these individuals require long-term screening, early intervention with renoprotective strategies, and strong emphasis on healthy lifestyles.

CONCLUSION

The association between an adverse fetal environment and subsequent hypertension as well as kidney disease in later life is now quite compelling and appears to be mediated, at least in part, by impaired nephrogenesis and suboptimal

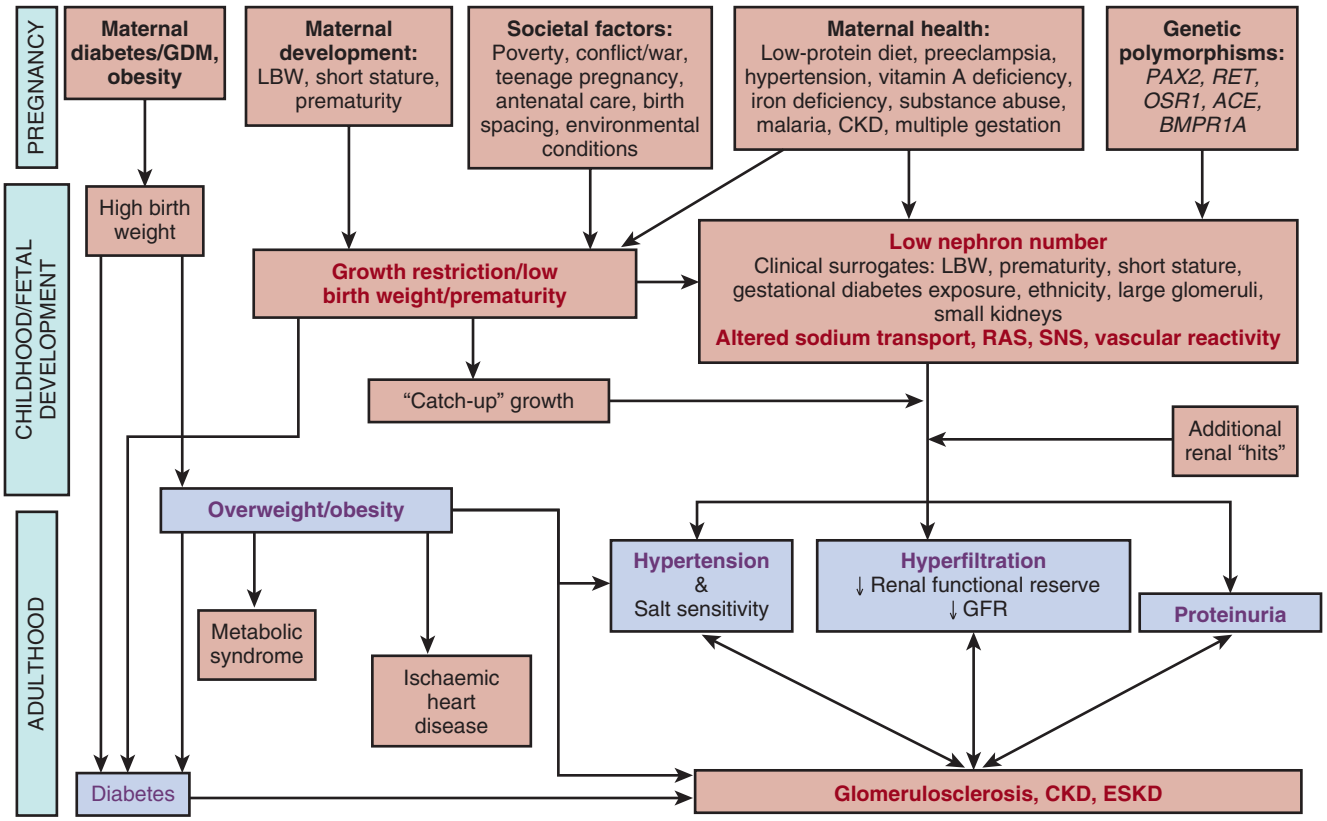

Fig. 21.17 Proposed mechanisms of fetal programming of hypertension and renal disease. *CKD*, Chronic kidney disease; *ESKD*, end-stage kidney disease; *GDM*, gestational diabetes mellitus; *GFR*, glomerulat filtration rate; *LBW*, low birth weight; *RAS*, renin–angiotensin system; *SNS*, sympathetic nervous system. (Adapted from Luyckx VA, Bertram JF, Brenner BM, et al. Effect of fetal and child health on kidney development and long-term risk of hypertension and kidney disease. *Lancet* 2013;382:273–283.)

nephron endowment (Fig. 21.17). Concomitant glomerular hypertrophy and altered expression of sodium transporters in the programmed kidney also contribute to the vicious circle of glomerular hypertension, glomerular injury, and sclerosis, leading to worsening hypertension and ongoing renal injury. In addition, numerous other factors, such as increased oxidative stress, renal inflammation, accelerated senescence, and catch-up body growth, are all likely contributors to ongoing nephron loss and eventual renal disease.[284,530–533] The number of nephrons in humans without kidney disease varies widely, suggesting that a significant proportion of the general population, especially in areas where high or low birth weights are prevalent, may be at increased risk of developing later-life hypertension and renal dysfunction. Measurement of nephron number in vivo remains an obstacle, with the best surrogate markers thus far being a low birth weight, high birth weight, preterm birth, being small for gestational age, and, in the absence of other known renal diseases, a reduced kidney volume on ultrasound, especially in children, and glomerular enlargement on kidney biopsy. A kidney with a reduced complement of nephrons would have less renal reserve to adapt to dietary excesses or to compensate for renal injury. The molecular mechanisms through which fetal programming exerts its effects on nephrogenesis are varied and likely complementary and intertwined. Although in some animal studies, nephron number and blood pressure can be "rescued" by good postnatal nutrition or vitamin A supplementation, applicability of these findings to humans requires further study. The fact that even seemingly minor influences, such as composition of maternal diet during fetal life, can have major consequences on renal development in the offspring underscores the critical importance of optimization of perinatal care and early nutrition, which could have a major impact on population health in the future.

Complete reference list available at ExpertConsult.com.

KEY REFERENCES

1. Low Birth W, Nephron Number Working G. The impact of kidney development on the life course: a consensus document for action. *Nephron.* 2017;136(1):3–49.
15. Barker DJ. Developmental origins of adult health and disease. *J Epidemiol Community Health.* 2004;58(2):114–115.
26. Barker DJ, Hales CN, Fall CH, et al. Type 2 (non-insulin-dependent) diabetes mellitus, hypertension and hyperlipidaemia (syndrome X): relation to reduced fetal growth. *Diabetologia.* 1993;36(1):62–67.
32. White SL, Perkovic V, Cass A, et al. Is low birth weight an antecedent of CKD in later life? A systematic review of observational studies. *Am J Kidney Dis.* 2009;54(2):248–261.
34. Langley-Evans S, Langley-Evans A, Marchand M. Nutritional programming of blood pressure and renal morphology. *Arch Physiol Biochem.* 2003;111(1):8–16.
36. de Jong F, Monuteaux MC, van Elburg RM, et al. Systematic review and meta-analysis of preterm birth and later systolic blood pressure. *Hypertension.* 2012;59(2):226–234.
37. Mu M, Wang SF, Sheng J, et al. Birth weight and subsequent blood pressure: a meta-analysis. *Arch Cardiovasc Dis.* 2012;105(2):99–113.

38. Nelson RG, Morgenstern H, Bennett PH. Intrauterine diabetes exposure and the risk of renal disease in diabetic pima Indians. *Diabetes*. 1998;47(9):1489–1493.
48. Brenner BM, Garcia DL, Anderson S. Glomeruli and blood pressure. Less of one, more the other? *Am J Hypertens*. 1988;1(4 Pt 1):335–347.
58. Puelles VG, Hoy WE, Hughson MD, et al. Glomerular number and size variability and risk for kidney disease. *Curr Opin Nephrol Hypertens*. 2011;20(1):7–15.
75. Kett MM, Denton KM. Renal programming: cause for concern? *Am J Physiol Regul Integr Comp Physiol*. 2011;300(4):R791–R803.
87. Hughson M, Farris AB, Douglas-Denton R, et al. Glomerular number and size in autopsy kidneys: the relationship to birth weight. *Kidney Int*. 2003;63(6):2113–2122.
99. Hoy WE, Hughson MD, Diouf B, et al. Distribution of volumes of individual glomeruli in kidneys at autopsy: association with physical and clinical characteristics and with ethnic group. *Am J Nephrol*. 2011;33(suppl 1):15–20.
108. Vehaskari VM, Aviles DH, Manning J. Prenatal programming of adult hypertension in the rat. *Kidney Int*. 2001;59(1):238–245.
112. Wlodek ME, Mibus A, Tan A, et al. Normal lactational environment restores nephron endowment and prevents hypertension after placental restriction in the rat. *J Am Soc Nephrol*. 2007;18(6):1688–1696.
114. Baum M. Role of the kidney in the prenatal and early postnatal programming of hypertension. *Am J Physiol Renal Physiol*. 2010;298(2):F235–F247.
121. Zhang Z, Quinlan J, Hoy W, et al. A common RET variant is associated with reduced newborn kidney size and function. *J Am Soc Nephrol*. 2008;19(10):2027–2034.
122. Rodriguez MM, Gomez AH, Abitbol CL, et al. Histomorphometric analysis of postnatal glomerulogenesis in extremely preterm infants. *Pediatr Dev Pathol*. 2004;7(1):17–25.
159. Moritz KM, Cuffe JS, Wilson LB, et al. Review: sex specific programming: a critical role for the renal renin-angiotensin system. *Placenta*. 2010;31(suppl):S40–S46.
170. Ojeda NB, Intapad S, Alexander BT. Sex differences in the developmental programming of hypertension. *Acta physiologica*. 2014;210(2):307–316.
181. Jones SE, Bilous RW, Flyvbjerg A, et al. Intra-uterine environment influences glomerular number and the acute renal adaptation to experimental diabetes. *Diabetologia*. 2001;44(6):721–728.
187. Abitbol CL, Rodriguez MM. The long-term renal and cardiovascular consequences of prematurity. *Nat Rev Nephrol*. 2012;8(5):265–274.
190. Boivin A, Luo ZC, Audibert F, et al. Pregnancy complications among women born preterm. *CMAJ*. 2012;184(16):1777–1784.
209. Khalsa DD, Beydoun HA, Carmody JB. Prevalence of chronic kidney disease risk factors among low birth weight adolescents. *Pediatr Nephrol*. 2016;31(9):1509–1516.
217. Bergvall N, Iliadou A, Johansson S, et al. Genetic and shared environmental factors do not confound the association between birth weight and hypertension: a study among Swedish twins. *Circulation*. 2007;115(23):2931–2938.
223. Schreuder MF, Wilhelm AJ, Bokenkamp A, et al. Impact of gestational age and birth weight on amikacin clearance on day 1 of life. *Clin J Am Soc Nephrol*. 2009;4(11):1774–1778.
224. Bacchetta J, Harambat J, Dubourg L, et al. Both extrauterine and intrauterine growth restriction impair renal function in children born very preterm. *Kidney Int*. 2009;76(4):445–452.
230. Keijzer-Veen MG, Schrevel M, Finken MJ, et al. Microalbuminuria and lower glomerular filtration rate at young adult age in subjects born very premature and after intrauterine growth retardation. *J Am Soc Nephrol*. 2005;16(9):2762–2768.
235. Hoy WE, White AV, Tipiloura B, et al. The multideterminant model of renal disease in a remote Australian aboriginal population in the context of early life risk factors: lower birth weight, childhood post-streptococcal glomerulonephritis, and current body mass index influence levels of albuminuria in young aboriginal adults. *Clin Nephrol*. 2015;83(7 suppl 1):75–81.
244. Selewski DT, Charlton JR, Jetton JG, et al. Neonatal acute kidney injury. *Pediatrics*. 2015;136(2):e463–e473.
246. Sutherland M, Ryan D, Black MJ, et al. Long-term renal consequences of preterm birth. *Clin Perinatol*. 2014;41(3):561–573.
274. Hsu CW, Yamamoto KT, Henry RK, et al. Prenatal risk factors for childhood CKD. *J Am Soc Nephrol*. 2014;25(9):2105–2111.
276. Hanson M, Gluckman P. Developmental origins of noncommunicable disease: population and public health implications. *Am J Clin Nutr*. 2011;94(6 suppl):1754S–1758S.
284. Luyckx VA, Brenner BM. Birth weight, malnutrition and kidney-associated outcomes—a global concern. *Nat Rev Nephrol*. 2015;11(3):135–149.
299. Little MH, McMahon AP. Mammalian kidney development: principles, progress, and projections. *Cold Spring Harb Perspect Biol*. 2012;4(5).
300. Moritz KM, Wintour EM, Black MJ, et al. Factors influencing mammalian kidney development: implications for health in adult life. *Adv Anat Embryol Cell Biol*. 2008;196:1–78.
303. Luyckx VA. Preterm birth and its impact on renal health. *Semin Nephrol*. 2017;37(4):311–319.
315. Langley-Evans SC. Nutritional programming of disease: unravelling the mechanism. *J Anat*. 2009;215(1):36–51.
341. Amri K, Freund N, Vilar J, et al. Adverse effects of hyperglycemia on kidney development in rats: in vivo and in vitro studies. *Diabetes*. 1999;48(11):2240–2245.
348. Jackson CM, Alexander BT, Roach L, et al. Exposure to maternal overnutrition and a high-fat diet during early postnatal development increases susceptibility to renal and metabolic injury later in life. *Am J Physiol Renal Physiol*. 2012;302(6):F774–F783.
385. Chevalier RL. Congenital urinary tract obstruction: the long view. *Adv Chronic Kidney Dis*. 2015;22(4):312–319.
391. O'Sullivan L, Combes AN, Little MH, et al. Epigenetics and developmental programming of adult onset diseases. *Pediatr Nephrol*. 2012;27(12):2175–2182.
405. Ojeda NB. Prenatal programming of hypertension: role of sympathetic response to physical stress. *Hypertension*. 2013;61(1):16–17.
427. Jain V, Singhal A. Catch up growth in low birth weight infants: striking a healthy balance. *Rev Endocr Metab Disord*. 2012;13(2):141–147.
440. Grijalva-Eternod CS, Lawlor DA, Wells JC. Testing a capacity-load model for hypertension: disentangling early and late growth effects on childhood blood pressure in a prospective birth cohort. *PLoS ONE*. 2013;8(2):e56078.
441. Abitbol CL, Chandar J, Rodriguez MM, et al. Obesity and preterm birth: additive risks in the progression of kidney disease in children. *Pediatr Nephrol*. 2009;24(7):1363–1370.
442. Abitbol CL, Bauer CR, Montane B, et al. Long-term follow-up of extremely low birth weight infants with neonatal renal failure. *Pediatr Nephrol*. 2003;18(9):887–893.
479. Boivin A, Luo ZC, Audibert F, et al. Risk for preterm and very preterm delivery in women who were born preterm. *Obstet Gynecol*. 2015;125(5):1177–1184.
486. Aiken CE, Ozanne SE. Transgenerational developmental programming. *Hum Reprod Update*. 2014;20(1):63–75.
489. Mueller TF, Luyckx VA. The natural history of residual renal function in transplant donors. *J Am Soc Nephrol*. 2012;23(9):1462–1466.
525. Giral M, Foucher Y, Karam G, et al. Kidney and recipient weight incompatibility reduces long-term graft survival. *J Am Soc Nephrol*. 2010;21(6):1022–1029.

REFERENCES

1. Low Birth W, Nephron Number Working G. The impact of kidney development on the life course: a consensus document for action. *Nephron.* 2017;136(1):3–49.
2. Kemper MJ, Muller-Wiefel DE. Renal function in congenital anomalies of the kidney and urinary tract. *Curr Opin Urol.* 2001;11(6):571–575.
3. Schreuder MF, Langemeijer ME, Bokenkamp A, et al. Hypertension and microalbuminuria in children with congenital solitary kidneys. *J Paediatr Child Health.* 2008;44(6):363–368.
4. Genovese G, Friedman DJ, Ross MD, et al. Association of trypanolytic apol1 variants with kidney disease in African Americans. *Science.* 2010;329(5993):841–845.
5. Bianchi G. Genetic variations of tubular sodium reabsorption leading to "primary" hypertension: from gene polymorphism to clinical symptoms. *Am J Physiol Regul Integr Comp Physiol.* 2005;289(6):R1536–R1549.
6. Hubner N, Yagil C, Yagil Y. Novel integrative approaches to the identification of candidate genes in hypertension. *Hypertension.* 2006;47(1):1–5.
7. Kaplan NM, Opie LH. Controversies in hypertension. *Lancet.* 2006;367(9505):168–176.
8. Lifton RP, Wilson FH, Choate KA, et al. Salt and blood pressure: new insight from human genetic studies. *Cold Spring Harb Symp Quant Biol.* 2002;67:445–450.
9. Tzur S, Rosset S, Shemer R, et al. Missense mutations in the APOL1 gene are highly associated with end stage kidney disease risk previously attributed to the MYH9 gene. *Hum Genet.* 2010;128(3):345–350.
10. Hoy WE, Rees M, Kile E, et al. Low birthweight and renal disease in Australian aborigines. *Lancet.* 1998;352(9143):1826–1827.
11. Lackland DT. Mechanisms and fetal origins of kidney disease. *J Am Soc Nephrol.* 2005;16(9):2531–2532.
12. Nelson RG, Morgenstern H, Bennett PH. Birth weight and renal disease in Pima Indians with type 2 diabetes mellitus. *Am J Epidemiol.* 1998;148(7):650–656.
13. Norton JM, Moxey-Mims MM, Eggers PW, et al. Social determinants of racial disparities in CKD. *J Am Soc Nephrol.* 2016;27(9):2576–2595.
14. Luyckx VA, Bertram JF, Brenner BM, et al. Effect of fetal and child health on kidney development and long-term risk of hypertension and kidney disease. *Lancet.* 2013;382(9888):273–283.
15. Barker DJ. Developmental origins of adult health and disease. *J Epidemiol Community Health.* 2004;58(2):114–115.
16. Whincup PH, Kaye SJ, Owen CG, et al. Birth weight and risk of type 2 diabetes: a systematic review. *JAMA.* 2008;300(24):2886–2897.
17. Hales CN, Barker DJ. Type 2 (non-insulin-dependent) diabetes mellitus: the thrifty phenotype hypothesis. *Diabetologia.* 1992;35(7):595–601.
18. Demicheva E, Crispi F. Long-term follow-up of intrauterine growth restriction: cardiovascular disorders. *Fetal Diagn Ther.* 2014;36(2):143–153.
19. Parkinson JR, Hyde MJ, Gale C, et al. Preterm birth and the metabolic syndrome in adult life: a systematic review and meta-analysis. *Pediatrics.* 2013;131(4):e1240–e1263.
20. Rothermund L, Lorenz M, Schnieber A, et al. Impact of nephron number dosing on cardiorenal damage and effects of ACE inhibition. *Am J Hypertens.* 2011;24(4):474–481.
21. McMillen IC, Robinson JS. Developmental origins of the metabolic syndrome: prediction, plasticity, and programming. *Physiol Rev.* 2005;85(2):571–633.
22. Drake AJ, Walker BR. The intergenerational effects of fetal programming: non-genomic mechanisms for the inheritance of low birth weight and cardiovascular risk. *J Endocrinol.* 2004;180(1):1–16.
23. Nathanielsz PW, Poston L, Taylor PD. In utero exposure to maternal obesity and diabetes: animal models that identify and characterize implications for future health. *Clin Perinatol.* 2007;34(4):515–526, v.
24. Forsdahl A. Are poor living conditions in childhood and adolescence an important risk factor for arteriosclerotic heart disease? *Br J Prev Soc Med.* 1977;31(2):91–95.
25. Kermack WO, McKendrick AG, McKinlay PL. Death-rates in Great Britain and Sweden. Some general regularities and their significance. *Lancet.* 1934;i:698–703.
26. Barker DJ, Hales CN, Fall CH, et al. Type 2 (non-insulin-dependent) diabetes mellitus, hypertension and hyperlipidaemia (syndrome X): relation to reduced fetal growth. *Diabetologia.* 1993;36(1):62–67.
27. Bellinger L, Langley-Evans SC. Fetal programming of appetite by exposure to a maternal low protein diet in the rat. *Clin Sci.* 2005;109(4):413–420.
28. Gardner DS, Tingey K, Van Bon BW, et al. Programming of glucose-insulin metabolism in adult sheep after maternal undernutrition. *Am J Physiol Regul Integr Comp Physiol.* 2005;289(4):R947–R954.
29. Wust S, Entringer S, Federenko IS, et al. Birth weight is associated with salivary cortisol responses to psychosocial stress in adult life. *Psychoneuroendocrinology.* 2005;30(6):591–598.
30. Li S, Chen SC, Shlipak M, et al. Low birth weight is associated with chronic kidney disease only in men. *Kidney Int.* 2008;73(5):637–642.
31. Vikse BE, Irgens LM, Leivestad T, et al. Low birth weight increases risk for end-stage renal disease. *J Am Soc Nephrol.* 2008;19(1):151–157.
32. White SL, Perkovic V, Cass A, et al. Is low birth weight an antecedent of CKD in later life? A systematic review of observational studies. *Am J Kidney Dis.* 2009;54(2):248–261.
33. Zetterstrom K, Lindeberg S, Haglund B, et al. Being born small for gestational age increases the risk of severe pre-eclampsia. *BJOG.* 2007;114(3):319–324.
34. Langley-Evans S, Langley-Evans A, Marchand M. Nutritional programming of blood pressure and renal morphology. *Arch Physiol Biochem.* 2003;111(1):8–16.
35. Vehaskari VM, Woods LL. Prenatal programming of hypertension: lessons from experimental models. *J Am Soc Nephrol.* 2005;16(9):2545–2556.
36. de Jong F, Monuteaux MC, van Elburg RM, et al. Systematic review and meta-analysis of preterm birth and later systolic blood pressure. *Hypertension.* 2012;59(2):226–234.
37. Mu M, Wang SF, Sheng J, et al. Birth weight and subsequent blood pressure: a meta-analysis. *Arch Cardiovasc Dis.* 2012;105(2):99–113.
38. Nelson RG, Morgenstern H, Bennett PH. Intrauterine diabetes exposure and the risk of renal disease in diabetic Pima Indians. *Diabetes.* 1998;47(9):1489–1493.
39. Zhang Y, Li H, Liu SJ, et al. The associations of high birth weight with blood pressure and hypertension in later life: a systematic review and meta-analysis. *Hypertens Res.* 2013;36(8):725–735.
40. Koyanagi A, Zhang J, Dagvadorj A, et al. Macrosomia in 23 developing countries: an analysis of a multicountry, facility-based, cross-sectional survey. *Lancet.* 2013;381(9865):476–483.
41. Ruggajo P, Skrunes R, Svarstad E, et al. Familial factors, low birth weight, and development of ESRD: a nationwide registry study. *Am J Kidney Dis.* 2016;67(4):601–608.
42. Blencowe H, Cousens S, Chou D, et al. Born too soon: the global epidemiology of 15 million preterm births. *Reprod Health.* 2013;10(suppl 1):S2.
43. World Health Organisation. *Global nutrition targets 2025: low birth weight policy brief (WHO/NMH/NHD/14.5).* 2014. http://www.who.int/nutrition/publications/globaltargets2025_policybrief_lbw/en/.
44. Lee AC, Katz J, Blencowe H, et al. National and regional estimates of term and preterm babies born small for gestational age in 138 low-income and middle-income countries in 2010. *Lancet Glob Health.* 2013;1(1):e26–e36.
45. Guyton AC, Coleman TG, Young DB, et al. Salt balance and long-term blood pressure control. *Annu Rev Med.* 1980;31:15–27.
46. Guyton AC, Young DB, DeClue JW, et al. Fluid balance, renal function, and blood pressure. *Clin Nephrol.* 1975;4(4):122–126.
47. Guidi E, Menghetti D, Milani S, et al. Hypertension may be transplanted with the kidney in humans: a long-term historical prospective follow-up of recipients grafted with kidneys coming from donors with or without hypertension in their families. *J Am Soc Nephrol.* 1996;7(8):1131–1138.
48. Brenner BM, Garcia DL, Anderson S. Glomeruli and blood pressure. Less of one, more the other? *Am J Hypertens.* 1988;1(4 Pt 1):335–347.
49. Hsu CY, Lin F, Vittinghoff E, et al. Racial differences in the progression from chronic renal insufficiency to end-stage renal disease in the United States. *J Am Soc Nephrol.* 2003;14(11):2902–2907.
50. Lackland DT, Bendall HE, Osmond C, et al. Low birth weights contribute to high rates of early-onset chronic renal failure in the southeastern United States. *Arch Intern Med.* 2000;160(10):1472–1476.
51. Lackland DT, Egan BM, Ferguson PL. Low birth weight as a risk factor for hypertension. *J Clin Hypertens (Greenwich).* 2003;5(2):133–136.
52. Lackland DT, Egan BM, Syddall HE, et al. Associations between birth weight and antihypertensive medication in black and white medicaid recipients. *Hypertension.* 2002;39(1):179–183.
53. Bertram JF. Counting in the kidney. *Kidney Int.* 2001;59(2):792–796.

54. Nyengaard JR, Bendtsen TF. Glomerular number and size in relation to age, kidney weight, and body surface in normal man. *Anat Rec.* 1992;232(2):194–201.
55. Kett MM, Bertram JF. Nephron endowment and blood pressure: what do we really know? *Curr Hypertens Rep.* 2004;6(2):133–139.
56. Sterio DC. The unbiased estimation of number and sizes of arbitrary particles using the disector. *J Microsc.* 1984;134(Pt 2):127–136.
57. Bueters RR, van de Kar NC, Schreuder MF. Adult renal size is not a suitable marker for nephron numbers: an individual patient data meta-analysis. *Kidney Blood Press Res.* 2013;37(6):540–546.
58. Puelles VG, Hoy WE, Hughson MD, et al. Glomerular number and size variability and risk for kidney disease. *Curr Opin Nephrol Hypertens.* 2011;20(1):7–15.
59. Keller G, Zimmer G, Mall G, et al. Nephron number in patients with primary hypertension. *N Engl J Med.* 2003;348(2):101–108.
60. Hoy WE, Douglas-Denton RN, Hughson MD, et al. A stereological study of glomerular number and volume: preliminary findings in a multiracial study of kidneys at autopsy. *Kidney Int Suppl.* 2003;83: S31–S37.
61. Denic A, Lieske JC, Chakkera HA, et al. The substantial loss of nephrons in healthy human kidneys with aging. *J Am Soc Nephrol.* 2017;28(1):313–320.
62. Bhathena DB, Julian BA, McMorrow RG, et al. Focal sclerosis of hypertrophied glomeruli in solitary functioning kidneys of humans. *Am J Kidney Dis.* 1985;5(5):226–232.
63. Kasiske BL, Ma JZ, Louis TA, et al. Long-term effects of reduced renal mass in humans. *Kidney Int.* 1995;48(3):814–819.
64. Ibrahim HN, Foley R, Tan L, et al. Long-term consequences of kidney donation. *N Engl J Med.* 2009;360(5):459–469.
65. Moritz KM, Wintour EM, Dodic M. Fetal uninephrectomy leads to postnatal hypertension and compromised renal function. *Hypertension.* 2002;39(6):1071–1076.
66. Woods LL, Weeks DA, Rasch R. Hypertension after neonatal uninephrectomy in rats precedes glomerular damage. *Hypertension.* 2001;38(3):337–342.
67. Singh RR, Denton KM, Bertram JF, et al. Development of cardiovascular disease due to renal insufficiency in male sheep following fetal unilateral nephrectomy. *J Hypertens.* 2009;27(2): 386–396.
68. Nyengaard JR. Number and dimensions of rat glomerular capillaries in normal development and after nephrectomy. *Kidney Int.* 1993;43(5):1049–1057.
69. Wang X, Johnson AC, Sasser JM, et al. Spontaneous one-kidney rats are more susceptible to develop hypertension by DOCA-NaCl and subsequent kidney injury compared with uninephrectomized rats. *Am J Physiol Renal Physiol.* 2016;310(10):F1054–F1064.
70. Sergio M, Galarreta CI, Thornhill BA, et al. The fate of nephrons in congenital obstructive nephropathy: adult recovery is limited by nephron number despite early release of obstruction. *J Urol.* 2015;194(5):1463–1472.
71. Abou Jaoude P, Dubourg L, Bacchetta J, et al. Congenital versus acquired solitary kidney: is the difference relevant? *Nephrol Dial Transplant.* 2011;26(7):2188–2194.
72. Abi Khalil C, Travert F, Fetita S, et al. Fetal exposure to maternal type 1 diabetes is associated with renal dysfunction at adult age. *Diabetes.* 2010;59(10):2631–2636.
73. Chevalier RL, Thornhill BA, Chang AY, et al. Recovery from release of ureteral obstruction in the rat: relationship to nephrogenesis. *Kidney Int.* 2002;61(6):2033–2043.
74. Douglas-Denton R, Moritz KM, Bertram JF, et al. Compensatory renal growth after unilateral nephrectomy in the ovine fetus. *J Am Soc Nephrol.* 2002;13(2):406–410.
75. Kett MM, Denton KM. Renal programming: cause for concern? *Am J Physiol Regul Integr Comp Physiol.* 2011;300(4):R791–R803.
76. Lenihan CR, Busque S, Derby G, et al. Longitudinal study of living kidney donor glomerular dynamics after nephrectomy. *J Clin Invest.* 2015;125(3):1311–1318.
77. Fulladosa X, Moreso F, Narvaez JA, et al. Estimation of total glomerular number in stable renal transplants. *J Am Soc Nephrol.* 2003;14(10):2662–2668.
78. Tan JC, Busque S, Workeneh B, et al. Effects of aging on glomerular function and number in living kidney donors. *Kidney Int.* 2010;78(7):686–692.
79. Lenihan CR, Busque S, Derby G, et al. The association of predonation hypertension with glomerular function and number in older living kidney donors. *J Am Soc Nephrol.* 2015;26(6):1261–1267.
80. Beeman SC, Cullen-McEwen LA, Puelles VG, et al. MRI-based glomerular morphology and pathology in whole human kidneys. *Am J Physiol Renal Physiol.* 2014;306(11):F1381–F1390.
81. Beeman SC, Mandarino LJ, Georges JF, et al. Cationized ferritin as a magnetic resonance imaging probe to detect microstructural changes in a rat model of non-alcoholic steatohepatitis. *Magn Reson Med.* 2013;70(6):1728–1738.
82. Beeman SC, Zhang M, Gubhaju L, et al. Measuring glomerular number and size in perfused kidneys using MRI. *Am J Physiol Renal Physiol.* 2011;300(6):F1454–F1457.
83. Heilmann M, Neudecker S, Wolf I, et al. Quantification of glomerular number and size distribution in normal rat kidneys using magnetic resonance imaging. *Nephrol Dial Transplant.* 2012;27(1):100–107.
84. Baldelomar EJ, Charlton JR, Beeman SC, et al. Phenotyping by magnetic resonance imaging nondestructively measures glomerular number and volume distribution in mice with and without nephron reduction. *Kidney Int.* 2016;89(2):498–505.
85. Klingberg A, Hasenberg A, Ludwig-Portugall I, et al. Fully automated evaluation of total glomerular number and capillary tuft size in nephritic kidneys using lightsheet microscopy. *J Am Soc Nephrol.* 2017;28(2):452–459.
86. Cortes P, Zhao X, Dumler F, et al. Age-related changes in glomerular volume and hydroxyproline content in rat and human. *J Am Soc Nephrol.* 1992;2(12):1716–1725.
87. Hughson M, Farris AB, Douglas-Denton R, et al. Glomerular number and size in autopsy kidneys: the relationship to birth weight. *Kidney Int.* 2003;63(6):2113–2122.
88. Puelles VG, Douglas-Denton RN, Cullen-McEwen LA, et al. Podocyte number in children and adults: associations with glomerular size and numbers of other glomerular resident cells. *J Am Soc Nephrol.* 2015;26(9):2277–2288.
89. Hoy WE, Hughson MD, Zimanyi M, et al. Distribution of volumes of individual glomeruli in kidneys at autopsy: association with age, nephron number, birth weight and body mass index. *Clin Nephrol.* 2010;74(S1):105–112.
90. Hoy WE, Hughson MD, Bertram JF, et al. Nephron number, hypertension, renal disease, and renal failure. *J Am Soc Nephrol.* 2005;16(9):2557–2564.
91. Manalich R, Reyes L, Herrera M, et al. Relationship between weight at birth and the number and size of renal glomeruli in humans: a histomorphometric study. *Kidney Int.* 2000;58(2):770–773.
92. Zimanyi MA, Hoy WE, Douglas-Denton RN, et al. Nephron number and individual glomerular volumes in male Caucasian and African American subjects. *Nephrol Dial Transplant.* 2009;24(8):2428–2433.
93. Abdi R, Dong VM, Rubel JR, et al. Correlation between glomerular size and long-term renal function in patients with substantial loss of renal mass. *J Urol.* 2003;170(1):42–44.
94. Abdi R, Slakey D, Kittur D, et al. Baseline glomerular size as a predictor of function in human renal transplantation. *Transplantation.* 1998;66(3):329–333.
95. Abdi R, Slakey D, Kittur D, et al. Heterogeneity of glomerular size in normal donor kidneys: impact of race. *Am J Kidney Dis.* 1998;32(1):43–46.
96. Hoy WE, Wang Z, VanBuynder P, et al. The natural history of renal disease in Australian Aborigines. Part 1. Changes in albuminuria and glomerular filtration rate over time. *Kidney Int.* 2001;60(1):243–248.
97. Hoy WE, Wang Z, VanBuynder P, et al. The natural history of renal disease in Australian aborigines. Part 2. Albuminuria predicts natural death and renal failure. *Kidney Int.* 2001;60(1):249–256.
98. Lemley KV. A basis for accelerated progression of diabetic nephropathy in Pima Indians. *Kidney Int Suppl.* 2003;83:S38–S42.
99. Hoy WE, Hughson MD, Diouf B, et al. Distribution of volumes of individual glomeruli in kidneys at autopsy: association with physical and clinical characteristics and with ethnic group. *Am J Nephrol.* 2011;33(suppl 1):15–20.
100. Lu MC, Halfon N. Racial and ethnic disparities in birth outcomes: a life-course perspective. *Matern Child Health J.* 2003;7(1):13–30.
101. Schmidt K, Pesce C, Liu Q, et al. Large glomerular size in Pima Indians: lack of change with diabetic nephropathy. *J Am Soc Nephrol.* 1992;3(2):229–235.
102. Young RJ, Hoy WE, Kincaid-Smith P, et al. Glomerular size and glomerulosclerosis in Australian aborigines. *Am J Kidney Dis.* 2000; 36(3):481–489.
103. Celsi G, Kistner A, Aizman R, et al. Prenatal dexamethasone causes oligonephronia, sodium retention, and higher blood pressure in the offspring. *Pediatr Res.* 1998;44(3):317–322.

104. Gilbert T, Lelievre-Pegorier M, Merlet-Benichou C. Long-term effects of mild oligonephronia induced in utero by gentamicin in the rat. *Pediatr Res.* 1991;30(5):450–456.
105. Langley-Evans SC. Intrauterine programming of hypertension in the rat: nutrient interactions. *Comp Biochem Physiol A Physiol.* 1996;114(4):327–333.
106. Merlet-Benichou C. Influence of fetal environment on kidney development. *Int J Dev Biol.* 1999;43(5 Spec No):453–456.
107. Ortiz LA, Quan A, Weinberg A, et al. Effect of prenatal dexamethasone on rat renal development. *Kidney Int.* 2001;59(5):1663–1669.
108. Vehaskari VM, Aviles DH, Manning J. Prenatal programming of adult hypertension in the rat. *Kidney Int.* 2001;59(1):238–245.
109. Woods LL, Ingelfinger JR, Nyengaard JR, et al. Maternal protein restriction suppresses the newborn renin-angiotensin system and programs adult hypertension in rats. *Pediatr Res.* 2001;49(4):460–467.
110. Alexander BT. Placental insufficiency leads to development of hypertension in growth-restricted offspring. *Hypertension.* 2003;41(3):457–462.
111. Moritz KM, Mazzuca MQ, Siebel AL, et al. Uteroplacental insufficiency causes a nephron deficit, modest renal insufficiency but no hypertension with ageing in female rats. *J Physiol.* 2009;587(Pt 11):2635–2646.
112. Wlodek ME, Mibus A, Tan A, et al. Normal lactational environment restores nephron endowment and prevents hypertension after placental restriction in the rat. *J Am Soc Nephrol.* 2007;18(6):1688–1696.
113. Stelloh C, Allen KP, Mattson DL, et al. Prematurity in mice leads to reduction in nephron number, hypertension, and proteinuria. *Transl Res.* 2012;159(2):80–89.
114. Baum M. Role of the kidney in the prenatal and early postnatal programming of hypertension. *Am J Physiol Renal Physiol.* 2010;298(2):F235–F247.
115. Sampogna RV, Schneider L, Al-Awqati Q. Developmental programming of branching morphogenesis in the kidney. *J Am Soc Nephrol.* 2015;26(10):2414–2422.
116. Boubred F, Daniel L, Buffat C, et al. The magnitude of nephron number reduction mediates intrauterine growth-restriction-induced long term chronic renal disease in the rat. A comparative study in two experimental models. *J Transl Med.* 2016;14(1):331.
117. Bertram JF, Douglas-Denton RN, Diouf B, et al. Human nephron number: implications for health and disease. *Pediatr Nephrol.* 2011;26(9):1529–1533.
118. Faa G, Gerosa C, Fanni D, et al. Marked interindividual variability in renal maturation of preterm infants: lessons from autopsy. *J Matern Fetal Neonatal Med.* 2010;23(suppl 3):129–133.
119. Sutherland MR, Gubhaju L, Moore L, et al. Accelerated maturation and abnormal morphology in the preterm neonatal kidney. *J Am Soc Nephrol.* 2011;22(7):1365–1374.
120. Hughson MD, Douglas-Denton R, Bertram JF, et al. Hypertension, glomerular number, and birth weight in African Americans and white subjects in the southeastern United States. *Kidney Int.* 2006;69(4):671–678.
121. Zhang Z, Quinlan J, Hoy W, et al. A common RET variant is associated with reduced newborn kidney size and function. *J Am Soc Nephrol.* 2008;19(10):2027–2034.
122. Rodriguez MM, Gomez AH, Abitbol CL, et al. Histomorphometric analysis of postnatal glomerulogenesis in extremely preterm infants. *Pediatr Dev Pathol.* 2004;7(1):17–25.
123. Hinchliffe SA, Howard CV, Lynch MR, et al. Renal developmental arrest in sudden infant death syndrome. *Pediatr Pathol.* 1993;13(3):333–343.
124. Hinchliffe SA, Lynch MR, Sargent PH, et al. The effect of intrauterine growth retardation on the development of renal nephrons. *Br J Obstet Gynaecol.* 1992;99(4):296–301.
125. Lackland DT, Barker DJ. Birth weight: a predictive medicine consideration for the disparities in CKD. *Am J Kidney Dis.* 2009;54(2):191–193.
126. Nyengaard JR, Bendtsen TF, Mogensen CE. Low birth weight—is it associated with few and small glomeruli in normal subjects and NIDDM patients? *Diabetologia.* 1996;39(12):1634–1637.
127. Deutinger J, Bartl W, Pfersmann C, et al. Fetal kidney volume and urine production in cases of fetal growth retardation. *J Perinat Med.* 1987;15(3):307–315.
128. Kurjak A, Kirkinen P, Latin V, et al. Ultrasonic assessment of fetal kidney function in normal and complicated pregnancies. *Am J Obstet Gynecol.* 1981;141(3):266–270.
129. Silver LE, Decamps PJ, Korst LM, et al. Intrauterine growth restriction is accompanied by decreased renal volume in the human fetus. *Am J Obstet Gynecol.* 2003;188(5):1320–1325.
130. Kandasamy Y, Smith R, Wright IM, et al. Extra-uterine renal growth in preterm infants: oligonephropathy and prematurity. *Pediatr Nephrol.* 2013;28(9):1791–1796.
131. Schmidt IM, Damgaard IN, Boisen KA, et al. Increased kidney growth in formula-fed versus breast-fed healthy infants. *Pediatr Nephrol.* 2004;19(10):1137–1144.
132. Iyengar A, Nesargi S, George A, et al. Are low birth weight neonates at risk for suboptimal renal growth and function during infancy? *BMC Nephrol.* 2016;17(1):100.
133. Bakker H, Gaillard R, Franco OH, et al. Fetal and infant growth patterns and kidney function at school age. *J Am Soc Nephrol.* 2014;25(11):2607–2615.
134. Brennan S, Kandasamy Y. Renal parenchymal thickness as a measure of renal growth in low-birth-weight infants versus normal-birth-weight infants. *Ultrasound Med Biol.* 2013;39(12):2315–2320.
135. Spencer J, Wang Z, Hoy W. Low birth weight and reduced renal volume in aboriginal children. *Am J Kidney Dis.* 2001;37(5):915–920.
136. Rakow A, Johansson S, Legnevall L, et al. Renal volume and function in school-age children born preterm or small for gestational age. *Pediatr Nephrol.* 2008;23(8):1309–1315.
137. Boubred F, Buffat C, Feuerstein JM, et al. Effects of early postnatal hypernutrition on nephron number and long-term renal function and structure in rats. *Am J Physiol Renal Physiol.* 2007;293(6):F1944–F1949.
138. Morton JS, Cooke CL, Davidge ST. In utero origins of hypertension: mechanisms and targets for therapy. *Physiol Rev.* 2016;96(2):549–603.
139. Manning J, Vehaskari VM. Postnatal modulation of prenatally programmed hypertension by dietary Na and ACE inhibition. *Am J Physiol Regul Integr Comp Physiol.* 2005;288(1):R80–R84.
140. Sanders MW, Fazzi GE, Janssen GM, et al. High sodium intake increases blood pressure and alters renal function in intrauterine growth-retarded rats. *Hypertension.* 2005;46(1):71–75.
141. Woods LL, Weeks DA, Rasch R. Programming of adult blood pressure by maternal protein restriction: role of nephrogenesis. *Kidney Int.* 2004;65(4):1339–1348.
142. de Boer MP, Ijzerman RG, de Jongh RT, et al. Birth weight relates to salt sensitivity of blood pressure in healthy adults. *Hypertension.* 2008;51(4):928–932.
143. Simonetti GD, Raio L, Surbek D, et al. Salt sensitivity of children with low birth weight. *Hypertension.* 2008;52(4):625–630.
144. Zimanyi MA, Bertram JF, Black MJ. Does a nephron deficit in rats predispose to salt-sensitive hypertension? *Kidney Blood Press Res.* 2004;27(4):239–247.
145. Gilbert JS. Sex, salt, and senescence: sorting out mechanisms of the developmental origins of hypertension. *Hypertension.* 2008;51(4):997–999.
146. Salazar F, Reverte V, Saez F, et al. Age- and sodium-sensitive hypertension and sex-dependent renal changes in rats with a reduced nephron number. *Hypertension.* 2008;51(4):1184–1189.
147. Magalhaes JC, da Silveira AB, Mota DL, et al. Renal function in juvenile rats subjected to prenatal malnutrition and chronic salt overload. *Exp Physiol.* 2006;91(3):611–619.
148. Nehiri T, Duong Van Huyen JP, Viltard M, et al. Exposure to maternal diabetes induces salt-sensitive hypertension and impairs renal function in adult rat offspring. *Diabetes.* 2008;57(8):2167–2175.
149. Ruta LA, Dickinson H, Thomas MC, et al. High-salt diet reveals the hypertensive and renal effects of reduced nephron endowment. *Am J Physiol Renal Physiol.* 2010;298(6):F1384–F1392.
150. Walker KA, Cai X, Caruana G, et al. High nephron endowment protects against salt-induced hypertension. *Am J Physiol Renal Physiol.* 2012;303(2):F253–F258.
151. Stewart T, Ascani J, Craver RD, et al. Role of postnatal dietary sodium in prenatally programmed hypertension. *Pediatr Nephrol.* 2009;24(9):1727–1733.
152. Manning J, Beutler K, Knepper MA, et al. Upregulation of renal BSC1 and TSC in prenatally programmed hypertension. *Am J Physiol Renal Physiol.* 2002;283(1):F202–F206.
153. Dagan A, Habib S, Gattineni J, et al. Prenatal programming of rat thick ascending limb chloride transport by low-protein diet and dexamethasone. *Am J Physiol Regul Integr Comp Physiol.* 2009;297(1):R93–R99.
154. Bertram C, Trowern AR, Copin N, et al. The maternal diet during pregnancy programs altered expression of the glucocorticoid

receptor and type 2 11beta-hydroxysteroid dehydrogenase: potential molecular mechanisms underlying the programming of hypertension in utero. *Endocrinology.* 2001;142(7):2841–2853.
155. Luzardo R, Silva PA, Einicker-Lamas M, et al. Metabolic programming during lactation stimulates renal Na+ transport in the adult offspring due to an early impact on local angiotensin II pathways. *PLoS ONE.* 2011;6(7):e21232.
156. Dagan A, Kwon HM, Dwarakanath V, et al. Effect of renal denervation on prenatal programming of hypertension and renal tubular transporter abundance. *Am J Physiol Renal Physiol.* 2008;295(1): F29–F34.
157. Cheng CJ, Lozano G, Baum M. Prenatal programming of rat cortical collecting tubule sodium transport. *Am J Physiol Renal Physiol.* 2012;302(6):F674–F678.
158. Guron G, Friberg P. An intact renin-angiotensin system is a prerequisite for normal renal development. *J Hypertens.* 2000;18(2):123–137.
159. Moritz KM, Cuffe JS, Wilson LB, et al. Review: sex specific programming: a critical role for the renal renin-angiotensin system. *Placenta.* 2010;31(suppl):S40–S46.
160. Grigore D, Ojeda NB, Robertson EB, et al. Placental insufficiency results in temporal alterations in the renin angiotensin system in male hypertensive growth restricted offspring. *Am J Physiol Regul Integr Comp Physiol.* 2007;293(2):R804–R811.
161. Tran S, Chen YW, Chenier I, et al. Maternal diabetes modulates renal morphogenesis in offspring. *J Am Soc Nephrol.* 2008;19(5):943–952.
162. Woods LL, Rasch R. Perinatal ANG II programs adult blood pressure, glomerular number, and renal function in rats. *Am J Physiol.* 1998;275(5 Pt 2):R1593–R1599.
163. McCausland JE, Bertram JF, Ryan GB, et al. Glomerular number and size following chronic angiotensin II blockade in the postnatal rat. *Exp Nephrol.* 1997;5(3):201–209.
164. Zhang SL, Moini B, Ingelfinger JR. Angiotensin II increases Pax-2 expression in fetal kidney cells via the AT2 receptor. *J Am Soc Nephrol.* 2004;15(6):1452–1465.
165. Langley-Evans SC, Jackson AA. Captopril normalises systolic blood pressure in rats with hypertension induced by fetal exposure to maternal low protein diets. *Comp Biochem Physiol A Physiol.* 1995;110(3): 223–228.
166. McMullen S, Gardner DS, Langley-Evans SC. Prenatal programming of angiotensin II type 2 receptor expression in the rat. *Br J Nutr.* 2004;91(1):133–140.
167. Sahajpal V, Ashton N. Increased glomerular angiotensin II binding in rats exposed to a maternal low protein diet in utero. *J Physiol.* 2005;563(Pt 1):193–201.
168. Vehaskari VM, Stewart T, Lafont D, et al. Kidney angiotensin and angiotensin receptor expression in prenatally programmed hypertension. *Am J Physiol Renal Physiol.* 2004;287(2):F262–F267.
169. Dasinger JH, Intapad S, Backstrom MA, et al. Intrauterine growth restriction programs an accelerated age-related increase in cardiovascular risk in male offspring. *Am J Physiol Renal Physiol.* 2016;311(2):F312–F319.
170. Ojeda NB, Intapad S, Alexander BT. Sex differences in the developmental programming of hypertension. *Acta physiologica.* 2014;210(2):307–316.
171. Ajala AR, Almeida SS, Rangel M, et al. Association of ACE gene insertion/deletion polymorphism with birth weight, blood pressure levels, and ACE activity in healthy children. *Am J Hypertens.* 2012;25(7):827–832.
172. Alexander BT, Hendon AE, Ferril G, et al. Renal denervation abolishes hypertension in low-birth-weight offspring from pregnant rats with reduced uterine perfusion. *Hypertension.* 2005;45(4):754–758.
173. Intapad S, Tull FL, Brown AD, et al. Renal denervation abolishes the age-dependent increase in blood pressure in female intrauterine growth-restricted rats at 12 months of age. *Hypertension.* 2013;61(4):828–834.
174. Franco Mdo C, Arruda RM, Fortes ZB, et al. Severe nutritional restriction in pregnant rats aggravates hypertension, altered vascular reactivity, and renal development in spontaneously hypertensive rats offspring. *J Cardiovasc Pharmacol.* 2002;39(3):369–377.
175. Paixao AD, Maciel CR, Teles MB, et al. Regional Brazilian diet-induced low birth weight is correlated with changes in renal hemodynamics and glomerular morphometry in adult age. *Biol Neonate.* 2001;80(3):239–246.
176. Tendron-Franzin A, Gouyon JB, Guignard JP, et al. Long-term effects of in utero exposure to cyclosporin A on renal function in the rabbit. *J Am Soc Nephrol.* 2004;15(10):2687–2693.
177. Sanders MW, Fazzi GE, Janssen GM, et al. Reduced uteroplacental blood flow alters renal arterial reactivity and glomerular properties in the rat offspring. *Hypertension.* 2004;43(6):1283–1289.
178. van Onna M, Houben AJ, Kroon AA, et al. Asymmetry of renal blood flow in patients with moderate to severe hypertension. *Hypertension.* 2003;41(1):108–113.
179. Chen W, Srinivasan SR, Hallman DM, et al. The relationship between birthweight and longitudinal changes of blood pressure is modulated by beta-adrenergic receptor genes: the Bogalusa Heart Study. *J Biomed Biotechnol.* 2010;2010:543514.
180. Gilbert JS, Lang AL, Grant AR, et al. Maternal nutrient restriction in sheep: hypertension and decreased nephron number in offspring at 9 months of age. *J Physiol.* 2005;565(Pt 1):137–147.
181. Jones SE, Bilous RW, Flyvbjerg A, et al. Intra-uterine environment influences glomerular number and the acute renal adaptation to experimental diabetes. *Diabetologia.* 2001;44(6):721–728.
182. Jones SE, White KE, Flyvbjerg A, et al. The effect of intrauterine environment and low glomerular number on the histological changes in diabetic glomerulosclerosis. *Diabetologia.* 2006;49(1):191–199.
183. Macconi D, Bonomelli M, Benigni A, et al. Pathophysiologic implications of reduced podocyte number in a rat model of progressive glomerular injury. *Am J Pathol.* 2006;168(1):42–54.
184. Wiggins RC. The spectrum of podocytopathies: a unifying view of glomerular diseases. *Kidney Int.* 2007;71(12):1205–1214.
185. Martins JP, Monteiro JC, Paixao AD. Renal function in adult rats subjected to prenatal dexamethasone. *Clin Exp Pharmacol Physiol.* 2003;30(1–2):32–37.
186. Plank C, Ostreicher I, Hartner A, et al. Intrauterine growth retardation aggravates the course of acute mesangioproliferative glomerulonephritis in the rat. *Kidney Int.* 2006;70(11):1974–1982.
187. Abitbol CL, Rodriguez MM. The long-term renal and cardiovascular consequences of prematurity. *Nat Rev Nephrol.* 2012;8(5):265–274.
188. Spence D, Stewart MC, Alderdice FA, et al. Intra-uterine growth restriction and increased risk of hypertension in adult life: a follow-up study of 50-year-olds. *Public Health.* 2012;126(7):561–565.
189. Duncan AF, Heyne RJ, Morgan JS, et al. Elevated systolic blood pressure in preterm very-low-birth-weight infants ≤3 years of life. *Pediatr Nephrol.* 2011;26(7):1115–1121.
190. Boivin A, Luo ZC, Audibert F, et al. Pregnancy complications among women born preterm. *CMAJ.* 2012;184(16):1777–1784.
191. Crowther CA, Doyle LW, Haslam RR, et al. Outcomes at 2 years of age after repeat doses of antenatal corticosteroids. *N Engl J Med.* 2007;357(12):1179–1189.
192. Keijzer-Veen MG, Kleinveld HA, Lequin MH, et al. Renal function and size at young adult age after intrauterine growth restriction and very premature birth. *Am J Kidney Dis.* 2007;50(4):542–551.
193. Rossi P, Tauzin L, Marchand E, et al. Respective roles of preterm birth and fetal growth restriction in blood pressure and arterial stiffness in adolescence. *J Adolesc Health.* 2011;48(5):520–522.
194. Smal JC, Uiterwaal CS, Bruinse HW, et al. Inverse relationship between birth weight and blood pressure in growth-retarded but not in appropriate for gestational age infants during the first week of life. *Neonatology.* 2009;96(2):86–92.
195. Dalziel SR, Parag V, Rodgers A, et al. Cardiovascular risk factors at age 30 following pre-term birth. *Int J Epidemiol.* 2007;36(4):907–915.
196. Law CM, de Swiet M, Osmond C, et al. Initiation of hypertension in utero and its amplification throughout life. *Br Med J.* 1993;306(6869):24–27.
197. Richardson LJ, Hussey JM, Strutz KL. Origins of disparities in cardiovascular disease: birth weight, body mass index, and young adult systolic blood pressure in the national longitudinal study of adolescent health. *Ann Epidemiol.* 2011;21(8):598–607.
198. Hemachandra AH, Klebanoff MA, Furth SL. Racial disparities in the association between birth weight in the term infant and blood pressure at age 7 years: results from the collaborative perinatal project. *J Am Soc Nephrol.* 2006;17(9):2576–2581.
199. Rostand SG, Cliver SP, Goldenberg RL. Racial disparities in the association of foetal growth retardation to childhood blood pressure. *Nephrol Dial Transplant.* 2005;20(8):1592–1597.
200. Vancheri F, Alletto M, Burgio A, et al. Inverse relationship between fetal growth and arterial pressure in children and adults. *G Ital Cardiol.* 1995;25(7):833–841.
201. Zhao M, Shu XO, Jin F, et al. Birthweight, childhood growth and hypertension in adulthood. *Int J Epidemiol.* 2002;31(5):1043–1051.
202. Cruickshank JK, Mzayek F, Liu L, et al. Origins of the "black/white" difference in blood pressure: roles of birth weight, postnatal growth,

early blood pressure, and adolescent body size: the Bogalusa Heart Study. *Circulation*. 2005;111(15):1932–1937.
203. Stewart CP, Christian P, Schulze KJ, et al. Size at birth is associated with blood pressure but not insulin resistance in 6-8 year old children in rural Nepal. *J Dev Origins Health Dis*. 2010;1(2):114–122.
204. Ben-Shlomo Y, McCarthy A, Hughes R, et al. Immediate postnatal growth is associated with blood pressure in young adulthood: the Barry Caerphilly Growth Study. *Hypertension*. 2008;52(4):638–644.
205. Hemachandra AH, Howards PP, Furth SL, et al. Birth weight, postnatal growth, and risk for high blood pressure at 7 years of age: results from the Collaborative Perinatal Project. *Pediatrics*. 2007;119(6):e1264–e1270.
206. Bowers K, Liu G, Wang P, et al. Birth weight, postnatal weight change, and risk for high blood pressure among Chinese children. *Pediatrics*. 2011;127(5):e1272–e1279.
207. Rotteveel J, van Weissenbruch MM, Twisk JW, et al. Infant and childhood growth patterns, insulin sensitivity, and blood pressure in prematurely born young adults. *Pediatrics*. 2008;122(2):313–321.
208. Vohr BR, Allan W, Katz KH, et al. Early predictors of hypertension in prematurely born adolescents. *Acta Paediatr*. 2010;99(12):1812–1818.
209. Khalsa DD, Beydoun HA, Carmody JB. Prevalence of chronic kidney disease risk factors among low birth weight adolescents. *Pediatr Nephrol*. 2016;31(9):1509–1516.
210. Zhao Y, Wang SF, Mu M, et al. Birth weight and overweight/obesity in adults: a meta-analysis. *Eur J Pediatr*. 2012;171(12):1737–1746.
211. Aceti A, Santhakumaran S, Logan KM, et al. The diabetic pregnancy and offspring blood pressure in childhood: a systematic review and meta-analysis. *Diabetologia*. 2012;55(11):3114–3127.
212. Fraser A, Nelson SM, Macdonald-Wallis C, et al. Hypertensive disorders of pregnancy and cardiometabolic health in adolescent offspring. *Hypertension*. 2013;62(3):614–620.
213. Miettola S, Hartikainen AL, Vaarasmaki M, et al. Offspring's blood pressure and metabolic phenotype after exposure to gestational hypertension in utero. *Eur J Epidemiol*. 2013;28(1):87–98.
214. Davis EF, Lazdam M, Lewandowski AJ, et al. Cardiovascular risk factors in children and young adults born to preeclamptic pregnancies: a systematic review. *Pediatrics*. 2012;129(6):e1552–e1561.
215. Lewandowski AJ, Davis EF, Yu G, et al. Elevated blood pressure in preterm-born offspring associates with a distinct antiangiogenic state and microvascular abnormalities in adult life. *Hypertension*. 2015;65:607–614.
216. Gamborg M, Byberg L, Rasmussen F, et al. Birth weight and systolic blood pressure in adolescence and adulthood: meta-regression analysis of sex- and age-specific results from 20 nordic studies. *Am J Epidemiol*. 2007;166(6):634–645.
217. Bergvall N, Iliadou A, Johansson S, et al. Genetic and shared environmental factors do not confound the association between birth weight and hypertension: a study among Swedish twins. *Circulation*. 2007;115(23):2931–2938.
218. Levine RS, Hennekens CH, Jesse MJ. Blood pressure in prospective population based cohort of newborn and infant twins. *Br Med J*. 1994;308(6924):298–302.
219. Poulter NR, Chang CL, MacGregor AJ, et al. Association between birth weight and adult blood pressure in twins: historical cohort study. *BMJ*. 1999;319(7221):1330–1333.
220. Hoy WE, Hughson MD, Singh GR, et al. Reduced nephron number and glomerulomegaly in Australian Aborigines: a group at high risk for renal disease and hypertension. *Kidney Int*. 2006;70(1):104–110.
221. Kanzaki G, Puelles VG, Cullen-McEwen LA, et al. New insights on glomerular hyperfiltration: a Japanese autopsy study. *JCI Insight*. 2017;2(19).
222. Perala MM, Moltchanova E, Kaartinen NE, et al. The association between salt intake and adult systolic blood pressure is modified by birth weight. *Am J Clin Nutr*. 2011;93(2):422–426.
223. Schreuder MF, Wilhelm AJ, Bokenkamp A, et al. Impact of gestational age and birth weight on amikacin clearance on day 1 of life. *Clin J Am Soc Nephrol*. 2009;4(11):1774–1778.
224. Bacchetta J, Harambat J, Dubourg L, et al. Both extrauterine and intrauterine growth restriction impair renal function in children born very preterm. *Kidney Int*. 2009;76(4):445–452.
225. Ingelfinger JR. Weight for gestational age as a baseline predictor of kidney function in adulthood. *Am J Kidney Dis*. 2008;51(1):1–4.
226. Kandasamy Y, Smith R, Wright IM, et al. Relationships between glomerular filtration rate and kidney volume in low-birth-weight neonates. *J Nephrol*. 2013;26(5):894–898.
227. Bruel A, Roze JC, Flamant C, et al. Critical serum creatinine values in very preterm newborns. *PLoS ONE*. 2013;8(12):e84892.
228. Rodriguez-Soriano J, Aguirre M, Oliveros R, et al. Long-term renal follow-up of extremely low birth weight infants. *Pediatr Nephrol*. 2005;20(5):579–584.
229. Franco MC, Nishida SK, Sesso R. GFR estimated from cystatin C versus creatinine in children born small for gestational age. *Am J Kidney Dis*. 2008;51(6):925–932.
230. Keijzer-Veen MG, Schrevel M, Finken MJ, et al. Microalbuminuria and lower glomerular filtration rate at young adult age in subjects born very premature and after intrauterine growth retardation. *J Am Soc Nephrol*. 2005;16(9):2762–2768.
231. Johnson MJ, Wootton SA, Leaf AA, et al. Preterm birth and body composition at term equivalent age: a systematic review and meta-analysis. *Pediatrics*. 2012;130(3):e640–e649.
232. Silverwood RJ, Pierce M, Hardy R, et al. Low birth weight, later renal function, and the roles of adulthood blood pressure, diabetes, and obesity in a British birth cohort. *Kidney Int*. 2013;84(6):1262–1270.
233. Gielen M, Pinto-Sietsma SJ, Zeegers MP, et al. Birth weight and creatinine clearance in young adult twins: influence of genetic, prenatal, and maternal factors. *J Am Soc Nephrol*. 2005;16(8):2471–2476.
234. Hoy WE, Rees M, Kile E, et al. A new dimension to the Barker hypothesis: low birthweight and susceptibility to renal disease. *Kidney Int*. 1999;56(3):1072–1077.
235. Hoy WE, White AV, Tipiloura B, et al. The multideterminant model of renal disease in a remote Australian Aboriginal population in the context of early life risk factors: lower birth weight, childhood post-streptococcal glomerulonephritis, and current body mass index influence levels of albuminuria in young aboriginal adults. *Clin Nephrol*. 2015;83(7 suppl 1):75–81.
236. Hoy WE, White AV, Tipiloura B, et al. The influence of birthweight, past poststreptococcal glomerulonephritis and current body mass index on levels of albuminuria in young adults: the multideterminant model of renal disease in a remote Australian aboriginal population with high rates of renal disease and renal failure. *Nephrol Dial Transplant*. 2016;31(6):971–977.
237. Vieux R, Hascoet JM, Franck P, et al. Increased albuminuria in 4-year-old preterm-born children with normal height. *J Pediatr*. 2012;160(6):923–928.e1.
238. Painter RC, Roseboom TJ, van Montfrans GA, et al. Microalbuminuria in adults after prenatal exposure to the Dutch famine. *J Am Soc Nephrol*. 2005;16(1):189–194.
239. Dyck RF, Bingham WT, Lim H, et al. Decreased urine albumin:creatinien ratios in infants fo diabetic mothers: does exposure to diabetic pregnancies alter fetal renal development? *J Dev Origins Health Dis*. 2011;2(5):265–271.
240. Carmody JB, Charlton JR. Short-term gestation, long-term risk: prematurity and chronic kidney disease. *Pediatrics*. 2013;131(6):1168–1179.
241. Jetton JG, Askenazi DJ. Acute kidney injury in the neonate. *Clin Perinatol*. 2014;41(3):487–502.
242. Carmody JB, Swanson JR, Rhone ET, et al. Recognition and reporting of AKI in very low birth weight infants. *Clin J Am Soc Nephrol*. 2014;9(12):2036–2043.
243. Carmody JB, Seckeler MD, Ballengee CR, et al. Pre-operative renal volume predicts peak creatinine after congenital heart surgery in neonates. *Cardiol Young*. 2014;24(5):831–839.
244. Selewski DT, Charlton JR, Jetton JG, et al. Neonatal acute kidney injury. *Pediatrics*. 2015;136(2):e463–e473.
245. Rhone ET, Carmody JB, Swanson JR, et al. Nephrotoxic medication exposure in very low birth weight infants. *J Matern Fetal Neonatal Med*. 2014;27(14):1485–1490.
246. Sutherland M, Ryan D, Black MJ, et al. Long-term renal consequences of preterm birth. *Clin Perinatol*. 2014;41(3):561–573.
247. Hanna MH, Askenazi DJ, Selewski DT. Drug-induced acute kidney injury in neonates. *Curr Opin Pediatr*. 2016;28(2):180–187.
248. Girardi A, Raschi E, Galletti S, et al. Drug-induced renal damage in preterm neonates: state of the art and methods for early detection. *Drug Saf*. 2015;38(6):535–551.
249. Cuzzolin L, Fanos V, Pinna B, et al. Postnatal renal function in preterm newborns: a role of diseases, drugs and therapeutic interventions. *Pediatr Nephrol*. 2006;21(7):931–938.
250. Vieux R, Fresson J, Guillemin F, et al. Perinatal drug exposure and renal function in very preterm infants. *Arch Dis Child Fetal Neonatal Ed*. 2011;96(4):F290–F295.

251. Magnani C, Moretti S, Ammenti A. Neonatal chronic renal failure associated with maternal ingestion of nimesulide as analgesic. *Eur J Obstet Gynecol Reprod Biol.* 2004;116(2):244–245.
252. Giapros V, Papadimitriou P, Challa A, et al. The effect of intrauterine growth retardation on renal function in the first two months of life. *Nephrol Dial Transplant.* 2007;22(1):96–103.
253. Askenazi DJ, Koralkar R, Patil N, et al. Acute kidney injury urine biomarkers in very low-birth-weight infants. *Clin J Am Soc Nephrol.* 2016;11(9):1527–1535.
254. Bruel A, Roze JC, Quere MP, et al. Renal outcome in children born preterm with neonatal acute renal failure: IRENEO—a prospective controlled study. *Pediatr Nephrol.* 2016;31(12):2365–2373.
255. Kwinta P, Klimek M, Drozdz D, et al. Assessment of long-term renal complications in extremely low birth weight children. *Pediatr Nephrol.* 2011;26(7):1095–1103.
256. Mammen C, Al Abbas A, Skippen P, et al. Long-term risk of CKD in children surviving episodes of acute kidney injury in the intensive care unit: a prospective cohort study. *Am J Kidney Dis.* 2012;59(4):523–530.
257. Nishizaki N, Hirano D, Nishizaki Y, et al. Increased urinary angiotensinogen is an effective marker of chronic renal impairment in very low birth weight children. *Clin Exp Nephrol.* 2014;18(4):642–648.
258. Chaturvedi S, Ng KH, Mammen C. The path to chronic kidney disease following acute kidney injury: a neonatal perspective. *Pediatr Nephrol.* 2017;32(2):227–241.
259. Hodgin JB, Rasoulpour M, Markowitz GS, et al. Very low birth weight is a risk factor for secondary focal segmental glomerulosclerosis. *Clin J Am Soc Nephrol.* 2009;4(1):71–76.
260. Hibino S, Abe Y, Watanabe S, et al. Proteinuria caused by glomerular hypertension during adolescence associated with extremely premature birth: a report of two cases. *Pediatr Nephrol.* 2015;30(10):1889–1892.
261. Hayashi A, Santo Y, Satomura K. Proteinuria and glomerular hypertrophy in extremely low-birthweight children. *Pediatr Int.* 2014;56(6):860–864.
262. Duncan RC, Bass PS, Garrett PJ, et al. Weight at birth and other factors influencing progression of idiopathic membranous nephropathy. *Nephrol Dial Transplant.* 1994;875.
263. Garrett P, Sandeman D, Reza M, et al. Weight at birth and renal disease in adulthood. *Nephrol Dial Transplant.* 1993;8:920.
264. Na YW, Yang HJ, Choi JH, et al. Effect of intrauterine growth retardation on the progression of nephrotic syndrome. *Am J Nephrol.* 2002;22(5–6):463–467.
265. Sandeman D, Reza M, Phillips DI, et al. Why do some type 1 diabetic patients develop nephropathy? A possible role of birth weight. *Diabet Med.* 1992;9(suppl 1):36A.
266. Zidar N, Cavic MA, Kenda RB, et al. Effect of intrauterine growth retardation on the clinical course and prognosis of IgA glomerulonephritis in children. *Nephron.* 1998;79(1):28–32.
267. Zidar N, Cor A, Premru Srsen T, et al. Is there an association between glomerular density and birth weight in healthy humans? *Nephron.* 1998;80(1):97–98.
268. Teeninga N, Schreuder MF, Bokenkamp A, et al. Influence of low birth weight on minimal change nephrotic syndrome in children, including a meta-analysis. *Nephrol Dial Transplant.* 2008;23(5):1615–1620.
269. Orskov B, Christensen KB, Feldt-Rasmussen B, et al. Low birth weight is associated with earlier onset of end-stage renal disease in Danish patients with autosomal dominant polycystic kidney disease. *Kidney Int.* 2012;81(9):919–924.
270. Rajan T, Barbour SJ, White CT, et al. Low birth weight and nephron mass and their role in the progression of chronic kidney disease: a case report on identical twins with alport disease. *Nephrol Dial Transplant.* 2011;26(12):4136–4139.
271. Rossing P, Tarnow L, Nielsen FS, et al. Short stature and diabetic nephropathy. *BMJ.* 1995;310(6975):296–297.
272. Jacobsen P, Rossing P, Tarnow L, et al. Birth weight—a risk factor for progression in diabetic nephropathy? *J Intern Med.* 2003;253(3):343–350.
273. Hirano D, Ishikura K, Uemura O, et al. Association between low birth weight and childhood-onset chronic kidney disease in Japan: a combined analysis of a nationwide survey for paediatric chronic kidney disease and the National Vital Statistics Report. *Nephrol Dial Transplant.* 2016;31(11):1895–1900.
274. Hsu CW, Yamamoto KT, Henry RK, et al. Prenatal risk factors for childhood CKD. *J Am Soc Nephrol.* 2014;25(9):2105–2111.
275. Pavkov ME, Hanson RL, Knowler WC, et al. Effect of intrauterine diabetes exposure on the incidence of end-stage renal disease in young adults with type 2 diabetes. *Diabetes Care.* 2010;33(11):2396–2398.
276. Hanson M, Gluckman P. Developmental origins of noncommunicable disease: population and public health implications. *Am J Clin Nutr.* 2011;94(6 suppl):1754S–1758S.
277. Ruggajo P, Svarstad E, Leh S, et al. Low birth weight and risk of progression to end stage renal disease in IgA nephropathy—a retrospective registry-based cohort study. *PLoS ONE.* 2016;11(4):e0153819.
278. Couser WG, Remuzzi G, Mendis S, et al. The contribution of chronic kidney disease to the global burden of major noncommunicable diseases. *Kidney Int.* 2011;80(12):1258–1270.
279. World Health Organisation Regional Office for Europe. *Good Maternal Nutrition. The Best Start in Life.* 2016. http://www.euro.who.int/__data/assets/pdf_file/0008/313667/Good-maternal-nutrition-The-best-start-in-life.pdf?ua=1. Accessed November 3, 2016.
280. Ahmed T, Hossain M, Sanin KI. Global burden of maternal and child undernutrition and micronutrient deficiencies. *Ann Nutr Metab.* 2012;61(suppl 1):8–17.
281. Chang HH, Larson J, Blencowe H, et al. Preventing preterm births: analysis of trends and potential reductions with interventions in 39 countries with very high human development index. *Lancet.* 2013;381(9862):223–234.
282. Sharma D, Shastri S, Sharma P. Intrauterine growth restriction: antenatal and postnatal aspects. *Clin Med Insights Pediatr.* 2016;10:67–83.
283. Christian P. Micronutrients, birth weight, and survival. *Annu Rev Nutr.* 2010;30:83–104.
284. Luyckx VA, Brenner BM. Birth weight, malnutrition and kidney-associated outcomes—a global concern. *Nat Rev Nephrol.* 2015;11(3):135–149.
285. Hoy WE, Bertram JF, Denton RD, et al. Nephron number, glomerular volume, renal disease and hypertension. *Curr Opin Nephrol Hypertens.* 2008;17(3):258–265.
286. Uauy R, Kain J, Corvalan C. How can the Developmental Origins of Health and Disease (DOHaD) hypothesis contribute to improving health in developing countries? *Am J Clin Nutr.* 2011;94(6 suppl):1759S–1764S.
287. Roderick PJ, Jeffrey RF, Yuen HM, et al. Smaller kidney size at birth in South Asians: findings from the Born in Bradford Birth Cohort study. *Nephrol Dial Transplant.* 2016;31(3):455–465.
288. Kandasamy Y, Smith R, Wright IM, et al. Reduced nephron endowment in the neonates of indigenous Australian peoples. *J Dev Orig Health Dis.* 2014;5(1):31–35.
289. Cassidy-Bushrow AE, Wegienka G, Barone CJ 2nd, et al. Race-specific relationship of birth weight and renal function among healthy young children. *Pediatr Nephrol.* 2012;27(8):1317–1323.
290. Liyanage T, Ninomiya T, Jha V, et al. Worldwide access to treatment for end-stage kidney disease: a systematic review. *Lancet.* 2015;385(9981):1975–1982.
291. McNamara BJ, Diouf B, Douglas-Denton RN, et al. A comparison of nephron number, glomerular volume and kidney weight in Senegalese Africans and African Americans. *Nephrol Dial Transplant.* 2010;25(5):1514–1520.
292. Douglas-Denton RN, McNamara BJ, Hoy WE, et al. Does nephron number matter in the development of kidney disease? *Ethn Dis.* 2006;16(2 suppl 2):S2-40-5.
293. Hult M, Tornhammar P, Ueda P, et al. Hypertension, diabetes and overweight: looming legacies of the biafran famine. *PLoS ONE.* 2010;5(10):e13582.
294. Painter RC, Roseboom TJ, Bleker OP. Prenatal exposure to the Dutch famine and disease in later life: an overview. *Reprod Toxicol.* 2005;20(3):345–352.
295. Stein AD, Zybert PA, van der Pal-de Bruin K, et al. Exposure to famine during gestation, size at birth, and blood pressure at age 59 y: evidence from the Dutch famine. *Eur J Epidemiol.* 2006;21(10):759–765.
296. Hoy WE, Hughson MD, Kopp JB, et al. APOL1 risk alleles are associated with exaggerated age-related changes in glomerular number and volume in African-American adults: an autopsy study. *J Am Soc Nephrol.* 2015;26(12):3179–3189.
297. Clark AT, Bertram JF. Molecular regulation of nephron endowment. *Am J Physiol.* 1999;276(4 Pt 2):F485–F497.
298. Costantini F, Kopan R. Patterning a complex organ: branching morphogenesis and nephron segmentation in kidney development. *Dev Cell.* 2010;18(5):698–712.

299. Little MH, McMahon AP. Mammalian kidney development: principles, progress, and projections. *Cold Spring Harb Perspect Biol.* 2012;4(5).
300. Moritz KM, Wintour EM, Black MJ, et al. Factors influencing mammalian kidney development: implications for health in adult life. *Adv Anat Embryol Cell Biol.* 2008;196:1–78.
301. Walker KA, Bertram JF. Kidney development: core curriculum 2011. *Am J Kidney Dis.* 2011;57(6):948–958.
302. Schreuder MF, Nyengaard JR, Fodor M, et al. Glomerular number and function are influenced by spontaneous and induced low birth weight in rats. *J Am Soc Nephrol.* 2005;16(10):2913–2919.
303. Luyckx VA. Preterm birth and its impact on renal health. *Semin Nephrol.* 2017;37(4):311–319.
304. Simeoni U, Zetterstrom R. Long-term circulatory and renal consequences of intrauterine growth restriction. *Acta Paediatr.* 2005;94(7):819–824.
305. Sakurai H, Nigam SK. In vitro branching tubulogenesis: implications for developmental and cystic disorders, nephron number, renal repair, and nephron engineering. *Kidney Int.* 1998;54(1):14–26.
306. Quinlan J, Lemire M, Hudson T, et al. A common variant of the PAX2 gene is associated with reduced newborn kidney size. *J Am Soc Nephrol.* 2007;18(6):1915–1921.
307. Kaczmarczyk M, Goracy I, Loniewska B, et al. Association of BMPR1A polymorphism, but not BMP4, with kidney size in full-term newborns. *Pediatr Nephrol.* 2012.
308. El Kares R, Manolescu DC, Lakhal-Chaieb L, et al. A human ALDH1a2 gene variant is associated with increased newborn kidney size and serum retinoic acid. *Kidney Int.* 2010;78(1):96–102.
309. Mugford JW, Sipila P, McMahon JA, et al. Osr1 expression demarcates a multi-potent population of intermediate mesoderm that undergoes progressive restriction to an Osr1-dependent nephron progenitor compartment within the mammalian kidney. *Dev Biol.* 2008;324(1):88–98.
310. Zhang Z, Iglesias D, Eliopoulos N, et al. A variant OSR1 allele which disturbs OSR1 mRNA expression in renal progenitor cells is associated with reduction of newborn kidney size and function. *Hum Mol Genet.* 2011;20(21):4167–4174.
311. Barker DJ, Gluckman PD, Godfrey KM, et al. Fetal nutrition and cardiovascular disease in adult life. *Lancet.* 1993;341(8850):938–941.
312. Godfrey KM, Forrester T, Barker DJ, et al. Maternal nutritional status in pregnancy and blood pressure in childhood. *Br J Obstet Gynaecol.* 1994;101(5):398–403.
313. Welham SJ, Riley PR, Wade A, et al. Maternal diet programs embryonic kidney gene expression. *Physiol Genomics.* 2005;22(1):48–56.
314. Zeman FJ. Effects of maternal protein restriction on the kidney of the newborn young of rats. *J Nutr.* 1968;94(2):111–116.
315. Langley-Evans SC. Nutritional programming of disease: unravelling the mechanism. *J Anat.* 2009;215(1):36–51.
316. Woods LL, Ingelfinger JR, Rasch R. Modest maternal protein restriction fails to program adult hypertension in female rats. *Am J Physiol Regul Integr Comp Physiol.* 2005;289(4):R1131–R1136.
317. Burton GJ, Fowden AL, Thornburg KL. Placental origins of chronic disease. *Physiol Rev.* 2016;96(4):1509–1565.
318. Langley-Evans SC, Phillips GJ, Benediktsson R, et al. Protein intake in pregnancy, placental glucocorticoid metabolism and the programming of hypertension in the rat. *Placenta.* 1996;17(2–3):169–172.
319. Khorram O, Khorram N, Momeni M, et al. Maternal undernutrition inhibits angiogenesis in the offspring: a potential mechanism of programmed hypertension. *Am J Physiol Regul Integr Comp Physiol.* 2007;293(2):R745–R753.
320. Denisenko O, Lin B, Louey S, et al. Maternal malnutrition and placental insufficiency induce global downregulation of gene expression in fetal kidneys. *J Dev Origins Health Dis.* 2011;2(2):124–133.
321. Altobelli G, Bogdarina IG, Stupka E, et al. Genome-wide methylation and gene expression changes in newborn rats following maternal protein restriction and reversal by folic acid. *PLoS ONE.* 2013;8(12):e82989.
322. Lisle SJ, Lewis RM, Petry CJ, et al. Effect of maternal iron restriction during pregnancy on renal morphology in the adult rat offspring. *Br J Nutr.* 2003;90(1):33–39.
323. Drake KA, Sauerbry MJ, Blohowiak SE, et al. Iron deficiency and renal development in the newborn rat. *Pediatr Res.* 2009;66(6):619–624.
324. Tomat AL, Inserra F, Veiras L, et al. Moderate zinc restriction during fetal and postnatal growth of rats: effects on adult arterial blood pressure and kidney. *Am J Physiol Regul Integr Comp Physiol.* 2008;295(2):R543–R549.
325. Mishra V, Thapa S, Retherford RD, et al. Effect of iron supplementation during pregnancy on birthweight: evidence from Zimbabwe. *Food Nutr Bull.* 2005;26(4):338–347.
326. Merlet-Benichou C, Vilar J, Lelievre-Pegorier M, et al. Role of retinoids in renal development: pathophysiological implication. *Curr Opin Nephrol Hypertens.* 1999;8(1):39–43.
327. Sutherland MR, Gubhaju L, Yoder BA, et al. The effects of postnatal retinoic acid administration on nephron endowment in the preterm baboon kidney. *Pediatr Res.* 2009;65(4):397–402.
328. Boyce AC, Palmer-Aronsten BJ, Kim MY, et al. Maternal vitamin D deficiency programmes adult renal renin gene expression and renal function. *J Dev Orig Health Dis.* 2013;4(5):368–376.
329. Reichetzeder C, Chen H, Foller M, et al. Maternal vitamin D deficiency and fetal programming—lessons learned from humans and mice. *Kidney Blood Press Res.* 2014;39(4):315–329.
330. Nascimento FA, Ceciliano TC, Aguila MB, et al. Maternal vitamin D deficiency delays glomerular maturity in F1 and F2 offspring. *PLoS ONE.* 2012;7(8):e41740.
331. Bhutta ZA, Das JK, Rizvi A, et al. Evidence-based interventions for improvement of maternal and child nutrition: what can be done and at what cost? *Lancet.* 2013;382(9890):452–477.
332. Vaidya A, Saville N, Shrestha BP, et al. Effects of antenatal multiple micronutrient supplementation on children's weight and size at 2 years of age in Nepal: follow-up of a double-blind randomised controlled trial. *Lancet.* 2008;371(9611):492–499.
333. Sommer A, Tarwotjo I, Djunaedi E, et al. Impact of vitamin A supplementation on childhood mortality. A randomised controlled community trial. *Lancet.* 1986;1(8491):1169–1173.
334. da Silva Lopes K, Ota E, Shakya P, et al. Effects of nutrition interventions during pregnancy on low birth weight: an overview of systematic reviews. *BMJ Glob Health.* 2017;2(3):e000389.
335. Stewart CP, Christian P, Schulze KJ, et al. Antenatal micronutrient supplementation reduces metabolic syndrome in 6- to 8-year-old children in rural Nepal. *J Nutr.* 2009;139(8):1575–1581.
336. Lee LM, Leung CY, Tang WW, et al. A paradoxical teratogenic mechanism for retinoic acid. *Proc Natl Acad Sci U S A.* 2012;109(34):13668–13673.
337. Hawkesworth S, Wagatsuma Y, Kahn AI, et al. Combined food and micronutrient supplements during pregnancy have limited impact on child blood pressure and kidney function in rural Bangladesh. *J Nutr.* 2013;143(5):728–734.
338. Amri K, Freund N, Van Huyen JP, et al. Altered nephrogenesis due to maternal diabetes is associated with increased expression of IGF-II/mannose-6-phosphate receptor in the fetal kidney. *Diabetes.* 2001;50(5):1069–1075.
339. Doublier S, Amri K, Seurin D, et al. Overexpression of human insulin-like growth factor binding protein-1 in the mouse leads to nephron deficit. *Pediatr Res.* 2001;49(5):660–666.
340. Kistner A, Sigurdsson J, Niklasson A, et al. Neonatal IGF-1/IGFBP-1 axis and retinopathy of prematurity are associated with increased blood pressure in preterm children. *Acta Paediatr.* 2014;103(2):149–156.
341. Amri K, Freund N, Vilar J, et al. Adverse effects of hyperglycemia on kidney development in rats: in vivo and in vitro studies. *Diabetes.* 1999;48(11):2240–2245.
342. Hokke SN, Armitage JA, Puelles VG, et al. Altered ureteric branching morphogenesis and nephron endowment in offspring of diabetic and insulin-treated pregnancy. *PLoS ONE.* 2013;8(3):e58243.
343. Tain YL, Lee WC, Hsu CN, et al. Asymmetric dimethylarginine is associated with developmental programming of adult kidney disease and hypertension in offspring of streptozotocin-treated mothers. *PLoS ONE.* 2013;8(2):e55420.
344. Rocha SO, Gomes GN, Forti AL, et al. Long-term effects of maternal diabetes on vascular reactivity and renal function in rat male offspring. *Pediatr Res.* 2005;58(6):1274–1279.
345. Magaton A, Gil FZ, Casarini DE, et al. Maternal diabetes mellitus—early consequences for the offspring. *Pediatr Nephrol.* 2007;22(1):37–43.
346. Blackmore HL, Ozanne SE. Maternal diet-induced obesity and offspring cardiovascular health. *J Dev Orig Health Dis.* 2013;4(5):338–347.
347. Armitage JA, Lakasing L, Taylor PD, et al. Developmental programming of aortic and renal structure in offspring of rats fed fat-rich diets in pregnancy. *J Physiol.* 2005;565(Pt 1):171–184.
348. Jackson CM, Alexander BT, Roach L, et al. Exposure to maternal overnutrition and a high-fat diet during early postnatal development increases susceptibility to renal and metabolic injury later in life. *Am J Physiol Renal Physiol.* 2012;302(6):F774–F783.

349. Samuelsson AM, Morris A, Igosheva N, et al. Evidence for sympathetic origins of hypertension in juvenile offspring of obese rats. *Hypertension.* 2010;55(1):76–82.
350. Hokke S, Puelles VG, Armitage JA, et al. Maternal fat feeding augments offspring nephron endowment in mice. *PLoS ONE.* 2016;11(8):e0161578.
351. Moritz KM, De Matteo R, Dodic M, et al. Prenatal glucocorticoid exposure in the sheep alters renal development in utero: implications for adult renal function and blood pressure control. *Am J Physiol Regul Integr Comp Physiol.* 2011;301(2):R500–R509.
352. Singh RR, Cuffe JS, Moritz KM. Short- and long-term effects of exposure to natural and synthetic glucocorticoids during development. *Clin Exp Pharmacol Physiol.* 2012;39(11):979–989.
353. O'Sullivan L, Cuffe JS, Koning A, et al. Excess prenatal corticosterone exposure results in albuminuria, sex-specific hypotension, and altered heart rate responses to restraint stress in aged adult mice. *Am J Physiol Renal Physiol.* 2015;308(10):F1065–F1073.
354. O'Sullivan L, Cuffe JS, Paravicini TM, et al. Prenatal exposure to dexamethasone in the mouse alters cardiac growth patterns and increases pulse pressure in aged male offspring. *PLoS ONE.* 2013;8(7):e69149.
355. Singh RR, Cullen-McEwen LA, Kett MM, et al. Prenatal corticosterone exposure results in altered AT1/AT2, nephron deficit and hypertension in the rat offspring. *J Physiol.* 2007;579(Pt 2):503–513.
356. Wintour EM, Moritz KM, Johnson K, et al. Reduced nephron number in adult sheep, hypertensive as a result of prenatal glucocorticoid treatment. *J Physiol.* 2003;549(Pt 3):929–935.
357. Singh RR, Moritz KM, Bertram JF, et al. Effects of dexamethasone exposure on rat metanephric development: in vitro and in vivo studies. *Am J Physiol Renal Physiol.* 2007;293(2):F548–F554.
358. Dave-Sharma S, Wilson RC, Harbison MD, et al. Examination of genotype and phenotype relationships in 14 patients with apparent mineralocorticoid excess. *J Clin Endocrinol Metab.* 1998;83(7):2244–2254.
359. Seckl JR, Meaney MJ. Glucocorticoid programming. *Ann N Y Acad Sci.* 2004;1032:63–84.
360. Habib S, Gattineni J, Twombley K, et al. Evidence that prenatal programming of hypertension by dietary protein deprivation is mediated by fetal glucocorticoid exposure. *Am J Hypertens.* 2010.
361. Dagan A, Gattineni J, Cook V, et al. Prenatal programming of rat proximal tubule Na+/H+ exchanger by dexamethasone. *Am J Physiol Regul Integr Comp Physiol.* 2007;292(3):R1230–R1235.
362. Dalziel SR, Walker NK, Parag V, et al. Cardiovascular risk factors after antenatal exposure to betamethasone: 30-year follow-up of a randomised controlled trial. *Lancet.* 2005;365(9474):1856–1862.
363. Carballo-Magdaleno D, Guizar-Mendoza JM, Amador-Licona N, et al. Renal function, renal volume, and blood pressure in infants with antecedent of antenatal steroids. *Pediatr Nephrol.* 2011;26(10):1851–1856.
364. Khalife N, Glover V, Taanila A, et al. Prenatal glucocorticoid treatment and later mental health in children and adolescents. *PLoS ONE.* 2013;8(11):e81394.
365. Wilkinson LJ, Neal CS, Singh RR, et al. Renal developmental defects resulting from in utero hypoxia are associated with suppression of ureteric beta-catenin signaling. *Kidney Int.* 2015;87(5):975–983.
366. Walton SL, Bielefeldt-Ohmann H, Singh RR, et al. Prenatal hypoxia leads to hypertension, renal renin-angiotensin system activation and exacerbates salt-induced pathology in a sex-specific manner. *Sci Rep.* 2017;7(1):8241.
367. Al-Odat I, Chen H, Chan YL, et al. The impact of maternal cigarette smoke exposure in a rodent model on renal development in the offspring. *PLoS ONE.* 2014;9(7):e103443.
368. O'Connell AE, Boyce AC, Lumbers ER, et al. The effects of asphyxia on renal function in fetal sheep at midgestation. *J Physiol.* 2003;552(Pt 3):933–943.
369. Vidal AC, Murphy SK, Murtha AP, et al. Associations between antibiotic exposure during pregnancy, birth weight and aberrant methylation at imprinted genes among offspring. *Int J Obes (Lond).* 2013;37(7):907–913.
370. Gilbert T, Lelievre-Pegorier M, Merlet-Benichou C. Immediate and long-term renal effects of fetal exposure to gentamicin. *Pediatr Nephrol.* 1990;4(4):445–450.
371. Gilbert T, Gaonach S, Moreau E, et al. Defect of nephrogenesis induced by gentamicin in rat metanephric organ culture. *Lab Invest.* 1994;70(5):656–666.
372. Gilbert T, Cibert C, Moreau E, et al. Early defect in branching morphogenesis of the ureteric bud in induced nephron deficit. *Kidney Int.* 1996;50(3):783–795.
373. Kent AL, Douglas-Denton R, Shadbolt B, et al. Indomethacin, ibuprofen and gentamicin administered during late stages of glomerulogenesis do not reduce glomerular number at 14 days of age in the neonatal rat. *Pediatr Nephrol.* 2009;24(6):1143–1149.
374. Nathanson S, Moreau E, Merlet-Benichou C, et al. In utero and in vitro exposure to beta-lactams impair kidney development in the rat. *J Am Soc Nephrol.* 2000;11(5):874–884.
375. McKay DB, Josephson MA. Pregnancy in recipients of solid organs—effects on mother and child. *N Engl J Med.* 2006;354(12):1281–1293.
376. Komhoff M, Wang JL, Cheng HF, et al. Cyclooxygenase-2-selective inhibitors impair glomerulogenesis and renal cortical development. *Kidney Int.* 2000;57(2):414–422.
377. Sutherland MR, Yoder BA, McCurnin D, et al. Effects of ibuprofen treatment on the developing preterm baboon kidney. *Am J Physiol Renal Physiol.* 2012;302(10):F1286–F1292.
378. Qazi Q, Masakawa A, Milman D, et al. Renal anomalies in fetal alcohol syndrome. *Pediatrics.* 1979;63(6):886–889.
379. Gray SP, Kenna K, Bertram JF, et al. Repeated ethanol exposure during late gestation decreases nephron endowment in fetal sheep. *Am J Physiol Regul Integr Comp Physiol.* 2008;295(2):R568–R574.
380. Parkington HC, Kenna KR, Sozo F, et al. Maternal alcohol consumption in pregnancy enhances arterial stiffness and alters vasodilator function that varies between vascular beds in fetal sheep. *J Physiol.* 2014;592(12):2591–2603.
381. Gray SP, Denton KM, Cullen-McEwen L, et al. Prenatal exposure to alcohol reduces nephron number and raises blood pressure in progeny. *J Am Soc Nephrol.* 2010;21(11):1891–1902.
382. Gray SP, Cullen-McEwen LA, Bertram JF, et al. Mechanism of alcohol-induced impairment in renal development: could it be reduced by retinoic acid? *Clin Exp Pharmacol Physiol.* 2012;39(9):807–813.
383. North American Pediatric Renal Trials and Collaborative Studies (NAPRTCS). *Annual Transplant Report.* 2014. https://web.emmes.com/study/ped/annlrept/annualrept2014.pdf.
384. Chevalier RL. Prognostic factors and biomarkers of congenital obstructive nephropathy. *Pediatr Nephrol.* 2016;31(9):1411–1420.
385. Chevalier RL. Congenital urinary tract obstruction: the long view. *Adv Chronic Kidney Dis.* 2015;22(4):312–319.
386. Puddu M, Fanos V, Podda F, et al. The kidney from prenatal to adult life: perinatal programming and reduction of number of nephrons during development. *Am J Nephrol.* 2009;30(2):162–170.
387. Forbes MS, Thornhill BA, Galarreta CI, et al. Chronic unilateral ureteral obstruction in the neonatal mouse delays maturation of both kidneys and leads to late formation of atubular glomeruli. *Am J Physiol Renal Physiol.* 2013;305(12):F1736–F1746.
388. Chevalier RL, Thornhill BA, Chang AY. Unilateral ureteral obstruction in neonatal rats leads to renal insufficiency in adulthood. *Kidney Int.* 2000;58(5):1987–1995.
389. Wang X, Garrett MR. Nephron number, hypertension, and CKD: physiological and genetic insight from humans and animal models. *Physiol Genomics.* 2017;49(3):180–192.
390. Swali A, McMullen S, Hayes H, et al. Processes underlying the nutritional programming of embryonic development by iron deficiency in the rat. *PLoS ONE.* 2012;7(10):e48133.
391. O'Sullivan L, Combes AN, Little MH, et al. Epigenetics and developmental programming of adult onset diseases. *Pediatr Nephrol.* 2012;27(12):2175–2182.
392. Cullen-McEwen LA, Drago J, Bertram JF. Nephron endowment in glial cell line-derived neurotrophic factor (GDNF) heterozygous mice. *Kidney Int.* 2001;60(1):31–36.
393. Zhang Z, Quinlan J, Grote D, et al. Common variants of the glial cell-derived neurotrophic factor gene do not influence kidney size of the healthy newborn. *Pediatr Nephrol.* 2009;24(6):1151–1157.
394. Zhao XP, Liao MC, Chang SY, et al. Maternal diabetes modulates kidney formation in murine progeny: the role of hedgehog interacting protein (HHIP). *Diabetologia.* 2014;57(9):1986–1996.
395. Tafti SA, Nast CC, Desai M, et al. Maternal undernutrition upregulates apoptosis in offspring nephrogenesis. *J Dev Origins Health Dis.* 2012;2(4):226–235.
396. Porteous S, Torban E, Cho NP, et al. Primary renal hypoplasia in humans and mice with PAX2 mutations: evidence of increased apoptosis in fetal kidneys of Pax2(1Neu) +/- mutant mice. *Hum Mol Genet.* 2000;9(1):1–11.

397. Sorenson CM, Rogers SA, Korsmeyer SJ, et al. Fulminant metanephric apoptosis and abnormal kidney development in bcl-2-deficient mice. *Am J Physiol.* 1995;268(1 Pt 2):F73–F81.
398. Torban E, Eccles MR, Favor J, et al. PAX2 suppresses apoptosis in renal collecting duct cells. *Am J Pathol.* 2000;157(3):833–842.
399. Welham SJ, Wade A, Woolf AS. Protein restriction in pregnancy is associated with increased apoptosis of mesenchymal cells at the start of rat metanephrogenesis. *Kidney Int.* 2002;61(4):1231–1242.
400. Dziarmaga A, Clark P, Stayner C, et al. Ureteric bud apoptosis and renal hypoplasia in transgenic PAX2-Bax fetal mice mimics the renal-coloboma syndrome. *J Am Soc Nephrol.* 2003;14(11): 2767–2774.
401. Godley LA, Kopp JB, Eckhaus M, et al. Wild-type p53 transgenic mice exhibit altered differentiation of the ureteric bud and possess small kidneys. *Genes Dev.* 1996;10(7):836–850.
402. Pham TD, MacLennan NK, Chiu CT, et al. Uteroplacental insufficiency increases apoptosis and alters p53 gene methylation in the full-term IUGR rat kidney. *Am J Physiol Regul Integr Comp Physiol.* 2003;285(5):R962–R970.
403. Cuffe JS, Briffa JF, Rosser S, et al. Uteroplacental insufficiency in rats induces renal apoptosis and delays nephrogenesis completion. *Acta Physiol (Oxf)* 2018;222(3). doi:10.1111/apha.12982.
404. Lin CY, Lin TY, Lee MC, et al. Hyperglycemia: GDNF-EGR1 pathway target renal epithelial cell migration and apoptosis in diabetic renal embryopathy. *PLoS ONE.* 2013;8(2):e56731.
405. Ojeda NB. Prenatal programming of hypertension: role of sympathetic response to physical stress. *Hypertension.* 2013;61(1):16–17.
406. Wlodek ME, Westcott K, Siebel AL, et al. Growth restriction before or after birth reduces nephron number and increases blood pressure in male rats. *Kidney Int.* 2008;74(2):187–195.
407. Siebel AL, Mibus A, De Blasio MJ, et al. Improved lactational nutrition and postnatal growth ameliorates impairment of glucose tolerance by uteroplacental insufficiency in male rat offspring. *Endocrinology.* 2008;149(6):3067–3076.
408. Gallo LA, Tran M, Moritz KM, et al. Developmental programming: variations in early growth and adult disease. *Clin Exp Pharmacol Physiol.* 2013;40(11):795–802.
409. Ojeda NB, Hennington BS, Williamson DT, et al. Oxidative stress contributes to sex differences in blood pressure in adult growth-restricted offspring. *Hypertension.* 2012;60(1):114–122.
410. Kalisch-Smith JI, Simmons DG, Dickinson H, et al. Review: sexual dimorphism in the formation, function and adaptation of the placenta. *Placenta.* 2017;54:10–16.
411. Clifton VL, Murphy VE. Maternal asthma as a model for examining fetal sex-specific effects on maternal physiology and placental mechanisms that regulate human fetal growth. *Placenta.* 2004;25(supplA):S45–S52.
412. Stark MJ, Wright IM, Clifton VL. Sex-specific alterations in placental 11beta-hydroxysteroid dehydrogenase 2 activity and early postnatal clinical course following antenatal betamethasone. *Am J Physiol Regul Integr Comp Physiol.* 2009;297(2):R510–R514.
413. Mayne BT, Bianco-Miotto T, Buckberry S, et al. Large scale gene expression Meta-analysis reveals tissue-specific, sex-biased gene expression in humans. *Front Genet.* 2016;7:183.
414. Guilloteau P, Zabielski R, Hammon HM, et al. Adverse effects of nutritional programming during prenatal and early postnatal life, some aspects of regulation and potential prevention and treatments. *J Physiol Pharmacol.* 2009;60(suppl 3):17–35.
415. Li J, Khodus GR, Kruusmagi M, et al. Ouabain protects against adverse developmental programming of the kidney. *Nat Commun.* 2010;1:42.
416. Vasarhelyi B, Dobos M, Reusz GS, et al. Normal kidney function and elevated natriuresis in young men born with low birth weight. *Pediatr Nephrol.* 2000;15(1–2):96–100.
417. Mansano R, Desai M, Garg A, et al. Enhanced nephrogenesis in offspring of water-restricted rat dams. *Am J Obstet Gynecol.* 2007;196(5):480.e1–480.e6.
418. World Health Organization. *Global Prevalence of Vitamin a Deficiency in Populations at Risk 1995-2005: WHO Global Database of Vitamin A Deficiency.* Geneva: World Health Organization; 2009.
419. Makrakis J, Zimanyi MA, Black MJ. Retinoic acid enhances nephron endowment in rats exposed to maternal protein restriction. *Pediatr Nephrol.* 2007;22(11):1861–1867.
420. Averbukh Z, Bogin E, Cohn M, et al. The renotrophic factor, a persistent stimulus that crosses the placenta in mice. *J Physiol.* 1988;404:31–38.
421. Okada T, Yamagishi T, Morikawa Y. Morphometry of the kidney in rat pups from uninephrectomized mothers. *Anat Rec.* 1994;240(1):120–124.
422. Zhong J, Perrien DS, Yang HC, et al. Maturational regression of glomeruli determines the nephron population in normal mice. *Pediatr Res.* 2012;72(3):241–248.
423. Boubred F, Daniel L, Buffat C, et al. Early postnatal overfeeding induces early chronic renal dysfunction in adult male rats. *Am J Physiol Renal Physiol.* 2009;297(4):F943–F951.
424. Andersen LG, Angquist L, Eriksson JG, et al. Birth weight, childhood body mass index and risk of coronary heart disease in adults: combined historical cohort studies. *PLoS ONE.* 2010;5(11):e14126.
425. Barker DJ, Osmond C, Forsen TJ, et al. Trajectories of growth among children who have coronary events as adults. *N Engl J Med.* 2005;353(17):1802–1809.
426. Fall CH, Sachdev HS, Osmond C, et al. Adult metabolic syndrome and impaired glucose tolerance are associated with different patterns of BMI gain during infancy: data from the New Delhi birth cohort. *Diabetes Care.* 2008;31(12):2349–2356.
427. Jain V, Singhal A. Catch up growth in low birth weight infants: striking a healthy balance. *Rev Endocr Metab Disord.* 2012;13(2):141–147.
428. Harding JE, Cormack BE, Alexander T, et al. Advances in nutrition of the newborn infant. *Lancet.* 2017;389(10079):1660–1668.
429. Bansal N, Ayoola OO, Gemmell I, et al. Effects of early growth on blood pressure of infants of British European and South Asian origin at one year of age: the Manchester children's growth and vascular health study. *J Hypertens.* 2008;26(3):412–418.
430. Bhargava SK, Sachdev HS, Fall CH, et al. Relation of serial changes in childhood body-mass index to impaired glucose tolerance in young adulthood. *N Engl J Med.* 2004;350(9):865–875.
431. Law CM, Shiell AW, Newsome CA, et al. Fetal, infant, and childhood growth and adult blood pressure: a longitudinal study from birth to 22 years of age. *Circulation.* 2002;105(9):1088–1092.
432. Yang Z, Huffman SL. Nutrition in pregnancy and early childhood and associations with obesity in developing countries. *Matern Child Nutr.* 2013;9(suppl 1):105–119.
433. Adair LS, Fall CH, Osmond C, et al. Associations of linear growth and relative weight gain during early life with adult health and human capital in countries of low and middle income: findings from five birth cohort studies. *Lancet.* 2013;382(9891):525–534.
434. Oster RT, Luyckx VA, Toth EL. Birth weight predicts both proteinuria and overweight/obesity in a rural population of Aboriginal and non-Aboriginal Canadians. *J Dev Origins Health Dis.* 2013;4(2):139–145.
435. Skelton JA, Irby MB, Grzywacz JG, et al. Etiologies of obesity in children: nature and nurture. *Pediatr Clin North Am.* 2011;58(6):1333–1354, ix.
436. Wang Y, Chen X, Klag MJ, et al. Epidemic of childhood obesity: implications for kidney disease. *Adv Chronic Kidney Dis.* 2006;13(4): 336–351.
437. Vivante A, Golan E, Tzur D, et al. Body mass index in 1.2 million adolescents and risk for end-stage renal disease. *Arch Intern Med.* 2012;172(21):1644–1650.
438. Laaksonen DE, Lakka HM, Lynch J, et al. Cardiorespiratory fitness and vigorous leisure-time physical activity modify the association of small size at birth with the metabolic syndrome. *Diabetes Care.* 2003;26(7):2156–2164.
439. Siebel AL, Carey AL, Kingwell BA. Can exercise training rescue the adverse cardiometabolic effects of low birth weight and prematurity? *Clin Exp Pharmacol Physiol.* 2012;39(11):944–957.
440. Grijalva-Eternod CS, Lawlor DA, Wells JC. Testing a capacity-load model for hypertension: disentangling early and late growth effects on childhood blood pressure in a prospective birth cohort. *PLoS ONE.* 2013;8(2):e56078.
441. Abitbol CL, Chandar J, Rodriguez MM, et al. Obesity and preterm birth: additive risks in the progression of kidney disease in children. *Pediatr Nephrol.* 2009;24(7):1363–1370.
442. Abitbol CL, Bauer CR, Montane B, et al. Long-term follow-up of extremely low birth weight infants with neonatal renal failure. *Pediatr Nephrol.* 2003;18(9):887–893.
443. Ozanne SE, Hales CN. Lifespan: catch-up growth and obesity in male mice. *Nature.* 2004;427(6973):411–412.
444. Tarry-Adkins JL, Ozanne SE. Mechanisms of early life programming: current knowledge and future directions. *Am J Clin Nutr.* 2011;94(suppl):1765S–1771S.
445. Melk A. Senescence of renal cells: molecular basis and clinical implications. *Nephrol Dial Transplant.* 2003;18(12):2474–2478.

446. Luyckx VA, Compston CA, Simmen T, et al. Accelerated senescence in kidneys of low-birth-weight rats after catch-up growth. *Am J Physiol Renal Physiol.* 2009;297(6):F1697–F1705.
447. Tarry-Adkins JL, Martin-Gronert MS, Chen JH, et al. Maternal diet influences DNA damage, aortic telomere length, oxidative stress, and antioxidant defense capacity in rats. *FASEB J.* 2008;22(6):2037–2044.
448. Akkad A, Hastings R, Konje JC, et al. Telomere length in small-for-gestational-age babies. *BJOG.* 2006;113(3):318–323.
449. Raqib R, Alam DS, Sarker P, et al. Low birth weight is associated with altered immune function in rural Bangladeshi children: a birth cohort study. *Am J Clin Nutr.* 2007;85(3):845–852.
450. Mohn A, Chiavaroli V, Cerruto M, et al. Increased oxidative stress in prepubertal children born small for gestational age. *J Clin Endocrinol Metab.* 2007;92(4):1372–1378.
451. Nagai K, Saito C, Yamagata K. Birth weight and end-stage diabetic nephropathy in later life: a Japanese multicenter study. *Ther Apher Dial.* 2014;18(1):111–112.
452. Dean SV, Lassi ZS, Imam AM, et al. Preconception care: closing the gap in the continuum of care to accelerate improvements in maternal, newborn and child health. *Reprod Health.* 2014;11(suppl 3):S1.
453. Yu Z, Han S, Zhu J, et al. Pre-pregnancy body mass index in relation to infant birth weight and offspring overweight/obesity: a systematic review and meta-analysis. *PLoS ONE.* 2013;8(4):e61627.
454. Dean SV, Lassi ZS, Imam AM, et al. Preconception care: promoting reproductive planning. *Reprod Health.* 2014;11(suppl 3):S2.
455. Ferrero DM, Larson J, Jacobsson B, et al. Cross-country individual participant analysis of 4.1 million singleton births in 5 countries with very high human development index confirms known associations but provides no biologic explanation for 2/3 of all preterm births. *PLoS ONE.* 2016;11(9):e0162506.
456. Lassi ZS, Imam AM, Dean SV, et al. Preconception care: screening and management of chronic disease and promoting psychological health. *Reprod Health.* 2014;11(suppl 3):S5.
457. Black RE, Victora CG, Walker SP, et al. Maternal and child undernutrition and overweight in low-income and middle-income countries. *Lancet.* 2013;382(9890):427–451.
458. Christian P, Lee SE, Donahue Angel M, et al. Risk of childhood undernutrition related to small-for-gestational age and preterm birth in low- and middle-income countries. *Int J Epidemiol.* 2013;42(5):1340–1355.
459. Kozuki N, Katz J, Lee AC, et al. Short maternal stature increases risk of small-for-gestational-age and preterm births in low- and middle-income countries: individual participant data meta-analysis and population attributable fraction. *J Nutr.* 2015;145(11):2542–2550.
460. Goodyer P, Kurpad A, Rekha S, et al. Effects of maternal vitamin a status on kidney development: a pilot study. *Pediatr Nephrol.* 2007;22(2):209–214.
461. Bhutta ZA, Das JK, Bahl R, et al. Can available interventions end preventable deaths in mothers, newborn babies, and stillbirths, and at what cost? *Lancet.* 2014;384(9940):347–370.
462. Caputo C, Wood E, Jabbour L. Impact of fetal alcohol exposure on body systems: a systematic review. *Birth Defects Res C Embryo Today.* 2016;108(2):174–180.
463. Chen LW, Wu Y, Neelakantan N, et al. Maternal caffeine intake during pregnancy is associated with risk of low birth weight: a systematic review and dose-response meta-analysis. *BMC Med.* 2014;12:174.
464. Cnattingius S, Granath F, Petersson G, et al. The influence of gestational age and smoking habits on the risk of subsequent preterm deliveries. *N Engl J Med.* 1999;341(13):943–948.
465. Hogberg L, Cnattingius S, Lundholm C, et al. Effects of maternal smoking during pregnancy on offspring blood pressure in late adolescence. *J Hypertens.* 2012;30(4):693–699.
466. Kooijman MN, Bakker H, Franco OH, et al. Fetal smoke exposure and kidney outcomes in school-aged children. *Am J Kidney Dis.* 2015;66(3):412–420.
467. Nykjaer C, Alwan NA, Greenwood DC, et al. Maternal alcohol intake prior to and during pregnancy and risk of adverse birth outcomes: evidence from a British cohort. *J Epidemiol Community Health.* 2014;68(6):542–549.
468. Sharma D, Shastri S, Farahbakhsh N, et al. Intrauterine growth restriction—part 1. *J Matern Fetal Neonatal Med.* 2016;29(24):3977–3987.
469. Liu J, Zhang S, Liu M, et al. Maternal pre-pregnancy infection with hepatitis B virus and the risk of preterm birth: a population-based cohort study. *Lancet Glob Health.* 2017;5(6):e624–e632.
470. Walker PG, Ter Kuile FO, Garske T, et al. Estimated risk of placental infection and low birthweight attributable to *plasmodium falciparum* malaria in Africa in 2010: a modelling study. *Lancet Glob Health.* 2014;2(8):e460–e467.
471. Jolving LR, Nielsen J, Kesmodel US, et al. Prevalence of maternal chronic diseases during pregnancy—a nationwide population based study from 1989 to 2013. *Acta Obstet Gynecol Scand.* 2016;95(11):1295–1304.
472. Kersten I, Lange AE, Haas JP, et al. Chronic diseases in pregnant women: prevalence and birth outcomes based on the SNiP-study. *BMC Pregnancy Childbirth.* 2014;14:75.
473. Ota E, Ganchimeg T, Morisaki N, et al. Risk factors and adverse perinatal outcomes among term and preterm infants born small-for-gestational-age: secondary analyses of the WHO Multi-Country Survey on Maternal and Newborn Health. *PLoS ONE.* 2014;9(8):e105155.
474. Hladunewich MA, Melamad N, Bramham K. Pregnancy across the spectrum of chronic kidney disease. *Kidney Int.* 2016;89(5):995–1007.
475. Piccoli GB, Minelli F, Versino E, et al. Pregnancy in dialysis patients in the new millennium: a systematic review and meta-regression analysis correlating dialysis schedules and pregnancy outcomes. *Nephrol Dial Transplant.* 2016;31(11):1915–1934.
476. Bilano VL, Ota E, Ganchimeg T, et al. Risk factors of pre-eclampsia/eclampsia and its adverse outcomes in low- and middle-income countries: a WHO secondary analysis. *PLoS ONE.* 2014;9(3):e91198.
477. Fall CH, Sachdev HS, Osmond C, et al. Association between maternal age at childbirth and child and adult outcomes in the offspring: a prospective study in five low-income and middle-income countries (COHORTS collaboration). *Lancet Glob Health.* 2015;3(7):e366–e377.
478. Ganchimeg T, Ota E, Morisaki N, et al. Pregnancy and childbirth outcomes among adolescent mothers: a World Health Organization multicountry study. *BJOG.* 2014;121(suppl 1):40–48.
479. Boivin A, Luo ZC, Audibert F, et al. Risk for preterm and very preterm delivery in women who were born preterm. *Obstet Gynecol.* 2015;125(5):1177–1184.
480. De B, Lin S, Lohsoonthorn V, et al. Risk of preterm delivery in relation to maternal low birth weight. *Acta Obstet Gynecol.* 2007;86:565–571.
481. Wilcox AJ, Skjaerven R, Terje Lie R. Familial patterns of preterm delivery: maternal and fetal contributions. *Am J Epidemiol.* 2007;167(4):474–479.
482. Poston L, Caleyachetty R, Cnattingius S, et al. Preconceptional and maternal obesity: epidemiology and health consequences. *Lancet Diabetes Endocrinol.* 2016;4(12):1025–1036.
483. Goldenberg RL, McClure EM, Harrison MS, et al. Diabetes during pregnancy in low- and middle-income countries. *Am J Perinatol.* 2016;33(13):1227–1235.
484. Luyckx VA, Perico N, Somaschini M, et al. A developmental approach to the prevention of hypertension and kidney disease: a report from the Low Birth Weight and Nephron Number Working Group. *Lancet.* 2017;390(10092):424–428.
485. Innes KE, Byers TE, Marshall JA, et al. Association of a woman's own birth weight with subsequent risk for gestational diabetes. *JAMA.* 2002;287(19):2534–2541.
486. Aiken CE, Ozanne SE. Transgenerational developmental programming. *Hum Reprod Update.* 2014;20(1):63–75.
487. Cheong JN, Wlodek ME, Moritz KM, et al. Programming of maternal and offspring disease: impact of growth restriction, fetal sex and transmission across generations. *J Physiol.* 2016;594(17):4727–4740.
488. Harrison M, Langley-Evans SC. Intergenerational programming of impaired nephrogenesis and hypertension in rats following maternal protein restriction during pregnancy. *Br J Nutr.* 2009;101(7):1020–1030.
489. Mueller TF, Luyckx VA. The natural history of residual renal function in transplant donors. *J Am Soc Nephrol.* 2012;23(9):1462–1466.
490. Muzaale AD, Massie AB, Wang MC, et al. Risk of end-stage renal disease following live kidney donation. *JAMA.* 2014;311(6):579–586.
491. Mjoen G, Hallan S, Hartmann A, et al. Long-term risks for kidney donors. *Kidney Int.* 2014;86(1):162–167.
492. Al-Sehli R, Grebe S, Jacaj Z, et al. What should the serum creatinine be after transplantation? An approach to integrate donor and recipient information to assess posttransplant kidney function. *Transplantation.* 2015;99(9):1960–1967.
493. Hakim RM, Goldszer RC, Brenner BM. Hypertension and proteinuria: long-term sequelae of uninephrectomy in humans. *Kidney Int.* 1984;25(6):930–936.

494. Ibrahim HN, Foley RN, Reule SA, et al. Renal function profile in white kidney donors: the first 4 decades. *J Am Soc Nephrol.* 2016;27(9):2885–2893.
495. Fehrman-Ekholm I, Kvarnstrom N, Softeland JM, et al. Post-nephrectomy development of renal function in living kidney donors: a cross-sectional retrospective study. *Nephrol Dial Transplant.* 2011;26(7): 2377–2381.
496. Locke JE, Reed RD, Massie A, et al. Obesity increases the risk of end-stage renal disease among living kidney donors. *Kidney Int.* 2017;91(3):699–703.
497. Massie AB, Muzaale AD, Luo X, et al. Quantifying postdonation risk of ESRD in living kidney donors. *J Am Soc Nephrol.* 2017;28(9):2749–2755.
498. Rogers NM, Lawton PD, Jose MD. Indigenous Australians and living kidney donation. *N Engl J Med.* 2009;361(15):1513–1516.
499. Gibney EM, Parikh CR, Garg AX. Age, gender, race, and associations with kidney failure following living kidney donation. *Transplant Proc.* 2008;40(5):1337–1340.
500. Lentine KL, Schnitzler MA, Xiao H, et al. Racial variation in medical outcomes among living kidney donors. *N Engl J Med.* 2010; 363(8):724–732.
501. Storsley LJ, Young A, Rush DN, et al. Long-term medical outcomes among Aboriginal living kidney donors. *Transplantation.* 2010;90(4):401–406.
502. UNICEF, WHO. *Low Birthwieght: Country, Regional and Global Estimates.* New York: United Nations Children's Fund and World Health Organization; 2004.
503. Schachtner T, Reinke P. Estimated nephron number of the remaining donor kidney: impact on living kidney donor outcomes. *Nephrol Dial Transplant.* 2016;31(9):1523–1530.
504. Vikse BE, Irgens LM, Leivestad T, et al. Preeclampsia and the risk of end-stage renal disease. *N Engl J Med.* 2008;359(8): 800–809.
505. Garg AX, Nevis IF, McArthur E, et al. Gestational hypertension and preeclampsia in living kidney donors. *N Engl J Med.* 2015;372(2):124–133.
506. Azuma H, Nadeau K, Mackenzie HS, et al. Nephron mass modulates the hemodynamic, cellular and molecular response of the rat renal allograft. *Transplantation.* 1997;63(4):519–528.
507. Heeman UW, Azuma H, Tullius SG, et al. The contribution of reduced functioning mass to chronic kidney allograft dysfunction in rats. *Transplantation.* 1994;58(12):1317–1321.
508. Mackenzie HS, Azuma H, Rennke HG, et al. Renal mass as a determinant of late allograft outcome: insights from experimental studies in rats. *Kidney Int.* 1995;48(suppl 52):S-38–S-42.
509. Mackenzie HS, Azuma H, Troy JL, et al. Augmenting kidney mass at transplantation abrogates chronic renal allograft injury in rats. *Proc Assoc Am Phys.* 1996;108(2):127–133.
510. Szabo AJ, Muller V, Chen GF, et al. Nephron number determines susceptibility to renal mass reduction-induced CKD in Lewis and Fisher 344 rats: implications for development of experimentally induced chronic allograft nephropathy. *Nephrol Dial Transplant.* 2008;23(8):2492–2495.
511. Brenner BM, Milford EL. Nephron underdosing: a programmed cause of chronic renal allograft failure. *Am J Kidney Dis.* 1993;21(5, suppl 2):66–72.
512. Chertow GM, Brenner BM, Mackenzie HS, et al. Non-immunologic predictors of chronic renal allograft failure: data from the United Network of Organ Sharing. *Kidney Int.* 1995;48(suppl 52): S48–S51.
513. Chertow GM, Brenner BM, Mori M, et al. Antigen-independent determinants of graft survival in living-related kidney transplantation. *Kidney Int.* 1997;52(suppl 63):S-84–S-86.
514. Chertow GM, Milford EL, Mackenzie HS, et al. Antigen-independent determinants of cadaveric kidney transplant failure. *JAMA.* 1996;276(21): 1732–1736.
515. Giral M, Nguyen JM, Karam G, et al. Impact of graft mass on the clinical outcome of kidney transplants. *J Am Soc Nephrol.* 2005;16(1):261–268.
516. Douverny JB, Baptista-Silva JC, Pestana JO, et al. Importance of renal mass on graft function outcome after 12 months of living donor kidney transplantation. *Nephrol Dial Transplant.* 2007;22(12): 3646–3651.
517. el Agroudy AE, Hassan NA, Bakr MA, et al. Effect of donor/recipient body weight mismatch on patient and graft outcome in living-donor kidney transplantation. *Am J Nephrol.* 2003;23(5):294–299.
518. Gaston RS, Hudson SL, Julian BA, et al. Impact of donor/recipient size matching on outcomes in renal transplantation. *Transplantation.* 1996;61(3):383–388.
519. Kasiske BL, Snyder JJ, Gilbertson D. Inadequate donor size in cadaver kidney transplantation. *J Am Soc Nephrol.* 2002;13:2152–2159.
520. Kim YS, Moon JI, Kim DK, et al. Ratio of donor kidney weight to recipient bodyweight as an index of graft function. *Lancet.* 2001;357(9263):1180–1181.
521. Goldberg RJ, Smits G, Wiseman AC. Long-term impact of donor-recipient size mismatching in deceased donor kidney transplantation and in expanded criteria donor recipients. *Transplantation.* 2010;90(8):867–874.
522. Nakatani T, Sugimura K, Kawashima H, et al. The influence of recipient body mass on the outcome of cadaver kidney transplants. *Clin Exp Nephrol.* 2002;6:158–162.
523. Taal MW, Tilney NL, Brenner BM, et al. Renal mass: an important determinant of late allograft outcome. *Transpl Rev.* 1998;12(2):74–84.
524. Kim YS, Kim MS, Han DS, et al. Evidence that the ratio of donor kidney weight to recipient body weight, donor age, and episodes of acute rejection correlate independently with live-donor graft function. *Transplantation.* 2002;72(2):280–283.
525. Giral M, Foucher Y, Karam G, et al. Kidney and recipient weight incompatibility reduces long-term graft survival. *J Am Soc Nephrol.* 2010;21(6):1022–1029.
526. Nicholson ML, Windmill DC, Horsburgh T, et al. Influence of allograft size to recipient body-weight ratio on the long-term outcome of renal transplantation. *Br J Surg.* 2000;87:314–319.
527. Choi JY, Kwon OJ. Is the graft function of living donor renal transplants associated with renal mass matching by computed tomography angiographic volumetry? *Transplant Proc.* 2013;45(8):2919–2924.
528. Luyckx VA, Brenner BM. Low birth weight, nephron number, and kidney disease. *Kidney Int Suppl.* 2005;97:S68–S77.
529. Vazquez MA, Jeyarajah DR, Kielar ML, et al. Long-term outcomes of renal transplantation: a result of the original endowment of the donor kidney and the inflammatory response to both alloantigens and injury. *Curr Opin Nephrol Hypertens.* 2000;9(6):643–648.
530. Luyckx VA, Brenner BM. The clinical importance of nephron mass. *J Am Soc Nephrol.* 2010;21(6):898–910.
531. Franco MC, Kawamoto EM, Gorjao R, et al. Biomarkers of oxidative stress and antioxidant status in children born small for gestational age: evidence of lipid peroxidation. *Pediatr Res.* 2007;62(2):204–208.
532. Jennings BJ, Ozanne SE, Dorling MW, et al. Early growth determines longevity in male rats and may be related to telomere shortening in the kidney. *FEBS Lett.* 1999;448(1):4–8.
533. Stewart T, Jung FF, Manning J, et al. Kidney immune cell infiltration and oxidative stress contribute to prenatally programmed hypertension. *Kidney Int.* 2005;68(5):2180–2188.
534. Merlet-Benichou C, Gilbert T, Vilar J, et al. Nephron number: variability is the rule. Causes and consequences. *Lab Invest.* 1999; 79(5):515–527.
535. McNamara BJ, Diouf B, Hughson MD, et al. Renal pathology, glomerular number and volume in a West African urban community. *Nephrol Dial Transplant.* 2008;23(8):2576–2585.
536. Hoy WE, Ingelfinger JR, Hallan S, et al. The early development of the kidney and implications for future health. *J Dev Origins Health Dis.* 2010;1:216–233.
537. Almeida JR, Mandarim-de-Lacerda CA. Maternal gestational protein-calorie restriction decreases the number of glomeruli and causes glomerular hypertrophy in adult hypertensive rats. *Am J Obstet Gynecol.* 2005;192(3):945–951.
538. Lucas SR, Costa Silva VL, Miraglia SM, et al. Functional and morphometric evaluation of offspring kidney after intrauterine undernutrition. *Pediatr Nephrol.* 1997;11(6):719–723.
539. Langley-Evans A, Phillips GJ, Jackson AA. In utero exposure to maternal low protein diets induces hypertension in weanling rats, independently of maternal blood pressure changes. *Clin Nutr.* 1994;13:319–324.
540. Nwagwu MO, Cook A, Langley-Evans SC. Evidence of progressive deterioration of renal function in rats exposed to a maternal low-protein diet in utero. *Br J Nutr.* 2000;83(1):79–85.
541. Hoppe CC, Evans RG, Bertram JF, et al. Effects of dietary protein restriction on nephron number in the mouse. *Am J Physiol Regul Integr Comp Physiol.* 2007;292(5):R1768–R1774.
542. Gonzalez-Rodriguez P Jr, Tong W, Xue Q, et al. Fetal hypoxia results in programming of aberrant angiotensin II receptor expression patterns and kidney development. *Int J Med Sci.* 2013;10(5):532–538.

543. Jagadapillai R, Chen J, Canales L, et al. Developmental cigarette smoke exposure: kidney proteome profile alterations in low birth weight pups. *Toxicology.* 2012;299(2–3):80–89.
544. Ortiz LA, Quan A, Zarzar F, et al. Prenatal dexamethasone programs hypertension and renal injury in the rat. *Hypertension.* 2003;41(2):328–334.
545. Tendron A, Decramer S, Justrabo E, et al. Cyclosporin A administration during pregnancy induces a permanent nephron deficit in young rabbits. *J Am Soc Nephrol.* 2003;14(12):3188–3196.
546. Fassi A, Sangalli F, Maffi R, et al. Progressive glomerular injury in the MWF rat is predicted by inborn nephron deficit. *J Am Soc Nephrol.* 1998;9(8):1399–1406.
547. Cullen-McEwen LA, Kett MM, Dowling J, et al. Nephron number, renal function, and arterial pressure in aged GDNF heterozygous mice. *Hypertension.* 2003;41(2):335–340.
548. Norwood VF, Morham SG, Smithies O. Postnatal development and progression of renal dysplasia in cyclooxygenase-2 null mice. *Kidney Int.* 2000;58(6):2291–2300.
549. Jackson AA, Dunn RL, Marchand MC, et al. Increased systolic blood pressure in rats induced by a maternal low-protein diet is reversed by dietary supplementation with glycine. *Clin Sci.* 2002;103(6):633–639.
550. McNamara BJ, Diouf B, Hughson MD, et al. Associations between age, body size and nephron number with individual glomerular volumes in urban West African males. *Nephrol Dial Transplant.* 2009;24(5):1500–1506.
551. Kaczmarczyk M, Loniewska B, Kuprjanowicz A, et al. An insertion/deletion ACE polymorphism and kidney size in Polish full-term newborns. *J Renin Angiotensin Aldosterone Syst.* 2013;14(4):369–374.
552. Huxley RR, Shiell AW, Law CM. The role of size at birth and postnatal catch-up growth in determining systolic blood pressure: a systematic review of the literature. *J Hypertens.* 2000;18(7):815–831.
553. Stanner SA, Bulmer K, Andres C, et al. Does malnutrition in utero determine diabetes and coronary heart disease in adulthood? Results from the leningrad siege study, a cross sectional study. *BMJ.* 1997;315(7119):1342–1348.
554. Abalos E, Cuesta C, Carroli G, et al. Pre-eclampsia, eclampsia and adverse maternal and perinatal outcomes: a secondary analysis of the world health organization multicountry survey on maternal and newborn health. *BJOG.* 2014;121(suppl 1):14–24.
555. Abou-Jaoude P, Dubourg L, Bessenay L, et al. What about the renal function during childhood of children born from dialysed mothers? *Nephrol Dial Transplant.* 2012;27(6):2365–2369.
556. Geelhoed JJ, Fraser A, Tilling K, et al. Preeclampsia and gestational hypertension are associated with childhood blood pressure independently of family adiposity measures: the Avon Longitudinal Study of Parents and Children. *Circulation.* 2010;122(12):1192–1199.
557. Luyckx VA, Goodyer P, Bertram JF. Nephron endowment and developmental programming of blood pressure and renal function. In: Taal MW, Chertow GM, Marsden PA, et al, eds. *Brenner and Rector's the Kidney.* 10th ed. Philadelphia: Elsevier; 2015.
558. Taal HR, Geelhoed JJ, Steegers EA, et al. Maternal smoking during pregnancy and kidney volume in the offspring: the Generation R study. *Pediatr Nephrol.* 2011;26(8):1275–1283.
559. Cochat P, Decramer S, Robert-Gnansia E, et al. Renal outcome of children exposed to cyclosporine in utero. *Transplant Proc.* 2004;36(2 suppl):208S–210S.
560. Seckl JR. Prenatal glucocorticoids and long-term programming. *Eur J Endocrinol.* 2004;151(suppl 3):U49–U62.
561. Gubhaju L, Sutherland MR, Yoder BA, et al. Is nephrogenesis affected by preterm birth? Studies in a non-human primate model. *Am J Physiol Renal Physiol.* 2009;297(6):F1668–F1677.
562. Rolnik DL, Wright D, Poon LC, et al. Aspirin versus placebo in pregnancies at high risk for preterm preeclampsia. *N Engl J Med.* 2017;377(17):613–622.
563. Ott JJ, Stevens GA, Groeger J, et al. Global epidemiology of hepatitis B virus infection: new estimates of age-specific HBsAg seroprevalence and endemicity. *Vaccine.* 2012;30(12):2212–2219.
564. Abalos E, Cuesta C, Grosso AL, et al. Global and regional estimates of preeclampsia and eclampsia: a systematic review. *Eur J Obstet Gynecol Reprod Biol.* 2013;170(1):1–7.
565. Guariguata L, Whiting DR, Hambleton I, et al. Global estimates of diabetes prevalence for 2013 and projections for 2035. *Diabetes Res Clin Pract.* 2014;103(2):137–149.
566. Cresswell JA, Campbell OM, De Silva MJ, et al. Effect of maternal obesity on neonatal death in sub-Saharan Africa: multivariable analysis of 27 national datasets. *Lancet.* 2012;380(9850):1325–1330.
567. Hanson M, Barker M, Dodd JM, et al. Interventions to prevent maternal obesity before conception, during pregnancy, and post partum. *Lancet Diabetes Endocrinol.* 2017;5(1):65–76.
568. Levy D, Mohlman MK, Zhang Y. Estimating the potential impact of tobacco control policies on adverse maternal and child health outcomes in the United States using the SimSmoke tobacco control policy simulation model. *Nicotine Tob Res.* 2016;18(5):1240–1249.
569. Caleyachetty R, Tait CA, Kengne AP, et al. Tobacco use in pregnant women: analysis of data from demographic and health surveys from 54 low-income and middle-income countries. *Lancet Glob Health.* 2014;2(9):e513–e520.
570. Qin JB, Sheng XQ, Wu D, et al. Worldwide prevalence of adverse pregnancy outcomes among singleton pregnancies after in vitro fertilization/intracytoplasmic sperm injection: a systematic review and meta-analysis. *Arch Gynecol Obstet.* 2016.
571. von Ehr J, von Versen-Hoynck F. Implications of maternal conditions and pregnancy course on offspring's medical problems in adult life. *Arch Gynecol Obstet.* 2016;294(4):673–679.
572. Althabe F, Moore JL, Gibbons L, et al. Adverse maternal and perinatal outcomes in adolescent pregnancies: the Global Network's Maternal Newborn Health Registry Study. *Reprod Health.* 2015;12(suppl 2):S8.
573. Ganchimeg T, Mori R, Ota E, et al. Maternal and perinatal outcomes among nulliparous adolescents in low- and middle-income countries: a multi-country study. *BJOG.* 2013;120(13):1622–1630, discussion 30.
574. Blencowe H, Cousens S, Oestergaard MZ, et al. National, regional, and worldwide estimates of preterm birth rates in the year 2010 with time trends since 1990 for selected countries: a systematic analysis and implications. *Lancet.* 2012;379(9832):2162–2172.
575. World Health Organization. *Joint Child Malnutrition Estimates—Levels and Trends 2017.* http://apps.who.int/gho/data/node.wrapper.nutrition-2016&showonly=nutrition. 2017. Accessed July 14, 2017.
576. Jamshidi F, Kelishadi R. A systematic review on the effects of maternal calcium supplementation on offspring's blood pressure. *J Res Med Sci.* 2015;20(10):994–999.
577. Haider BA, Bhutta ZA. Multiple-micronutrient supplementation for women during pregnancy. *Cochrane Database Syst Rev.* 2015;(11):CD004905.
578. Kinra S, Rameshwar Sarma KV, Ghafoorunissa, et al. Effect of integration of supplemental nutrition with public health programmes in pregnancy and early childhood on cardiovascular risk in rural Indian adolescents: long term follow-up of hyderabad nutrition trial. *BMJ.* 2008;337:a605.
579. Hawkesworth S, Prentice AM, Fulford AJ, et al. Maternal protein-energy supplementation does not affect adolescent blood pressure in the Gambia. *Int J Epidemiol.* 2009;38(1):119–127.
580. Hawkesworth S, Sawo Y, Fulford AJ, et al. Effect of maternal calcium supplementation on offspring blood pressure in 5- to 10-y-old rural Gambian children. *Am J Clin Nutr.* 2010;92(4):741–747.
581. Bergel E, Barros AJD. Effect of maternal calcium intake during pregnancy on children's blood pressure: a systematic review of the literature. *BMC Pediatr.* 2007;7:15.
582. Devakumar D, Fall CH, Sachdev HS, et al. Maternal antenatal multiple micronutrient supplementation for long-term health benefits in children: a systematic review and meta-analysis. *BMC Med.* 2016;14:90.
583. Mispireta ML, Caulfield LE, Zavaleta N, et al. Effect of maternal zinc supplementation on the cardiometabolic profile of Peruvian children: results from a randomized clinical trial. *J Dev Orig Health Dis.* 2017;8(1):56–64.

BOARD REVIEW QUESTIONS

1. A mother brings her 6-month-old daughter for a routine health check. The pregnancy was complicated by preeclampsia. The child was born at 32 weeks of gestation and weighed 1.5 kg (appropriate weight for gestation) but now looks happy and healthy. The mother is worried about long-term consequences for her child. Which of the following is incorrect?
   a. The child herself is at risk of preeclampsia.
   b. The child is at increased risk of hypertension and cardiovascular disease.
   c. The child likely has small kidneys, but her glomerular filtration rate (GFR) is normal.
   d. The child had an appropriate weight for gestational age and therefore is not at increased risk of kidney disease.
   e. Perinatal steroid use to accelerate lung maturation is not associated with increased risk of hypertension.

   Answer: d

   Rationale: Preterm birth is associated with a mother's own risk for preeclampsia and gestational hypertension as well as delivering a preterm infant. Exposure to preeclampsia in utero is also associated with higher blood pressures in children. Such findings illustrate the intergenerational impact of developmental programming. Babies born preterm are at increased risk of high blood pressure, cardiovascular, and kidney disease, the risk of which appear exacerbated if the child becomes overweight or obese. In preterm infants, kidney size is smaller, but GFR is generally well preserved, which may reflect some degree of hyperfiltration in the small kidney, which may predispose to subsequent risk. There is no evidence of hypertension after having received short-term steroids prenatally.

2. Which statements about developmental programming in the kidney are true?
   a. Environmental stress experienced during development may result in permanent structural changes in major organ systems.
   b. Programming effects can be transmitted across generations.
   c. Males and females are always equally affected.
   d. Attempts to reverse effects of developmental programming (e.g., accelerating catch-up growth) can contribute to additional risk of long-term consequences.
   e. Only low birth weight and preterm infants should be considered at risk and require follow-up.

   Answer: a, b, d

   Rationale: Programming occurs as a result of a variety of factors that may occur during gestation and impact fetal development. Offspring of a woman who has experienced the effects of developmental programming are at higher risk of being exposed to hypertension, diabetes, and preeclampsia during gestation and thereby themselves experience developmental programming. The impact on males and females is different in both experimental animals and humans, but both should be considered at risk. Rapid crossing of weight centiles (catch-up growth) is associated with increased risk of higher blood pressure and kidney dysfunction, especially if the child becomes obese. Not all infants who are at risk of developmental programming are low birth weight (birth weight <2.5 kg) or preterm. Being born small for gestational age, of high birth weight, or being exposed to a diabetic, hypertensive, or preeclamptic pregnancy are also known factors impacting offspring risk of hypertension and kidney disease.

3. It is important to identify individuals at risk of developmental programming of hypertension and kidney disease. Which of the following maternal factors may increase the risk of a preterm birth or a low-birth-weight infant?
   a. Short maternal stature
   b. Maternal anemia
   c. Refugee status
   d. Maternal obesity
   e. In vitro fertilization

   Answer: All of the above

   Rationale: All of the factors listed are recognized risk factors for low birth weight or preterm birth, and therefore, such women need be counseled to optimize nutrition before and during pregnancy, plan pregnancies, and attend antenatal clinics to permit monitoring of fetal growth.

4. A 30-year-old Caucasian male wishes to donate a kidney to his mother. The mother has end-stage kidney disease because of hypertension and kidney damage that was first diagnosed during a preeclamptic pregnancy with the son. The son was born at a birth weight of 2.4 kg at 37 weeks of gestation. The son has a blood pressure around 135/80 measured on three occasions by his family doctor, normal renal function, and no microalbuminuria. He is a nonsmoker and has a body mass index (BMI) of 29.8.
   Which of the following could impact your decision on whether he should donate a kidney?
   a. Low birth weight
   b. Birth in a preeclamptic pregnancy
   c. Ethnicity
   d. Current BMI
   e. The mother's 56-year-old brother with mild hypertension is willing to donate, although HLA match is less good.

   Answer: a, b, d, e

   Rationale: Low birth weight and being born in a preeclamptic pregnancy are known risk factors for later-life hypertension and kidney disease. The man is relatively young, and therefore, his risk of future hypertension and kidney dysfunction is real, especially given his borderline high BMI. His ethnicity is not a risk factor for worse outcomes after living donation. In this case, given the possibility that this young donor may have a reduced nephron endowment, one may be more hesitant to accept the son. In this case, a likely potential donor does exist; however, ideally this fact per se should not impact on whether to decline the young man as a donor or not. He should be counseled to lose weight, and given his borderline blood pressure, this requires follow-up and early treatment should his pressures remain in this range.

22 The Physiology and Pathophysiology of the Kidneys in Aging

Richard J. Glassock | Aleksandar Denic | Andrew D. Rule

CHAPTER OUTLINE

GENERAL OVERVIEW OF THE BIOLOGY OF AGING

All, or nearly all, biologic organisms exhibit the phenomenon of aging. The few exceptions are scientific curiosities.[1] Many speculations and hypotheses concerning the biologic basis of aging have been advanced, but as yet none have provided a universal explanation for the aging process.[2] The life span of humans is regarded as limited at some maximum term that few approach.[1–3] Aging is an inevitable consequence of life. The rate of aging varies considerably, even among identical members of the same species,[1] an indication of the relatively minor role of heredity per se in determination of the life span of species. It has been estimated, from studies of monozygotic twins, that only 20% to 35% of the life span can be attributed to heredity (chromosomal or mitochondrial).[4] Thus, most theories of aging consider heredity, the environment, and chance to play variable roles in determination of the observed life span.[1] Metabolic rates and the balance of energy demand and supply appear to have a strong influence on life span.[5]

The fundamental biologic pathways accounting for the diverse manifestations of aging have been the subject of intense investigation for many decades. Much progress has been made; however, many gaps in our knowledge of this process still remain,[6–31] including the process of renal aging. It is generally regarded that aging is a composite effect of disordered gene function, environmental influences, and chance.[1] At the cellular level, degeneration and faulty gene repair are core mechanisms of aging.[1] The net result is cellular and organ senescence. The rate of aging appears to be partially controlled by genetic pathways and biochemical processes. The explanation for the conservation of these processes that occur after maximal reproductive success is largely lacking.[1,3,4] As such, it is possible that many aspects of the aging process have not been evolutionarily conserved. Because of these factors, it seems likely that the biologic events responsible for aging may differ among species, complicating the study of aging enormously—studies of aging in experimental animals may therefore have limited relevance to human aging.

The major hallmarks of aging are genomic instability, epigenetic alterations, mitochondrial dysfunction, dysregulated nutrient sensing, telomere attrition, loss of protein homeostasis, stem cell exhaustion, accumulation of senescent cells, oxidation and glycation of tissue proteins, and altered intercellular communication (reviewed by Sturmlechner and coworkers[27] and López-Otín and associates[32]).

A detailed description of these processes underlying aging is beyond the scope of this brief introductory review. Age-dependent accumulation of stochastic damage to critical molecular pathways seems to be a dominant driver of aging.[1] The generation of ATP to provide energy to sustain cellular function is key for life, and this process is systematically altered in aging.[33]

Energy production, via mitochondrial dysfunction, regularly declines with age,[1,33] possibly due to stochastic damage to mitochondrial DNA and inefficient repair. Oxidative damage

to DNA has been postulated to be one of the root causes of aging.[5,34] Mitochondrial inefficiency can lead to impaired cellular autophagy and cellular senescence.[35–38] Alternate hypotheses of defects in oxidative metabolism leading to a shift from aerobic to anaerobic metabolism are also possible.[5] A mismatch occurs in aging between lowered energy demand and excess supply. Caloric restriction has been found to be one of the most powerful experimental means of retarding the aging process.[32,39] Sirtuins, nicotinamide adenine dinucleotide (NAD^+)-dependent proteins, which deacetylate crucial enzymes in the oxidative metabolic pathway, may be responsible for this effect.[10,11,32,40,41] Sirtuin production diminishes with age and promotion of sirtuin production, as by the administration of mammalian target of rapamycin (mTOR) inhibitors, which mimic caloric restriction, can prolong life span.[32] This is known as the "bioenergetic theory of aging."[2] Whether a genetic program (the aging clock) defines the decline in bioenergetics with aging is unclear.[42] However, as stated above, it is well known that the rate of aging varies considerably, even among genetically identical humans and other species.[1] Epigenetic alterations and DNA methylation may account for some of these variations.[43]

Aging is also associated with shortening of the telomeres in nuclear DNA due to changes in the activity of telomerase, an enzyme essential for maintaining telomere length in dividing cells.[2,44,45] Gradual loss of telomeres leads to cessation of cell division after a maximum number of cell divisions, known as the *Hayflick limit*, and induces senescence, ultimately leading to cell death.[46] Attrition of telomeres with aging may explain in part the association of a higher risk for cancer in older people. Diseases of premature aging, such as progeria or Cockayne syndrome, can be caused by specific mutations (laminin in progeria), and are associated with marked telomere shortening or defects in DNA repair.[47,48] Indeed, telomere length and urinary 8-oxo-7,8-dihydroguanosine excretion are good biomarkers of aging.[49]

The individual organ systems of the human body exhibit phenomena connected to the overall aging process, also at variable rates. These organ-based manifestations of aging include loss of skin elasticity, decreases in hair pigmentation, slowing of nerve impulses, decreased mineral density of bone, decreased compliance of major vessels, decreased forced expiratory lung volume, decreased muscle mass, reduced metabolic rate, and many others. The kidneys share in these inevitable biologic consequences of aging, as will be detailed in this chapter. Numerous reviews and treatises covering the general topic of renal aging have been published over the past 4 decades. They represent a rich source of collateral reading on this fascinating subject.[6–31] It seems likely that the complex processes operating in aging at the organism level also play important roles in the manifestations of organ-based senescence, such as that displayed the kidneys.

The genetic component of renal aging has been analyzed by genome-wide association studies and transcriptomics,[50–52] and several candidate loci and factors have been identified. Increased oxidative or glycative stress,[53,54] reduced Klotho generation,[15,55–58] enhanced fibrosis,[59,60] increased capillary rarefaction,[9] and increased activation of the angiotensin II type 1 receptor[61–63] may all play important roles in renal aging. Klotho deficiency promotes inflammation.[55,56] Toxins such as D-serine[64] might be involved in the development of fibrosis in aging. Experimental evidence (in mice) has suggested that the level of fructokinase activity may be essential for renal aging.[65] In addition, endostatin and transglutaminase activity might also be involved in the renal fibrosis of aging according to studies in mice, but both these effects might be species specific.[66] The factors postulated to be involved in renal aging are summarized in Box 22.1.

Box 22.1 Some Factors Postulated to be Involved in Renal Aging

↓Sirtuin 1/6 (a histone deacetylase enzyme)
↓Klotho expression (and Wnt signaling)
↓Antioxidant production,↑oxidant activity
↓ Energy demand: ↑energy supply (mitochondrial dysfunction)
↑Telomere shortening
↑ DNA damage repair
↑ DNA methylation
↑Angiotensin II receptor signaling (via Wnt)
↑Cell cycle arrest (GI, via P16ink)
↓Autophagy
↑Fibrosis (transforming growth factor beta [TGF-β]–mediated)
↓Elimination of senescent cells
↓Insulin-like growth factor 1 (IGF-1) signaling
↓Proliferator-activated receptor-γ (PPARγ) activity
↑Capillary rarefaction
↑Podocyte apoptosis or detachment (podocytopenia—absolute and/or relative to capillary surface area)
↑Vascular sclerosis and glomerular ischemia
↑Advanced glycation end products
↑D-Serine toxicity
↑ Endostatin, transglutaminase activation

GI, Gastrointestinal.

HEALTHY AGING AND AGE-RELATED COMORBIDITY

The aging process not only leads to subtle and cumulative alterations in cellular and organ function, but it also predisposes an individual to certain age-related diseases, such as atherosclerosis, hypertension, diabetes, cancer, osteoporosis, and dementia. Disentanglement of these disease states from phenomena that might be called "healthy" aging can be very challenging. Healthy aging might be defined as the state that is universal, or nearly so, in all aging subjects, whereas age-related comorbidities affect only some of the aging population and involve processes that are disease-specific. For example, a decline in bone density or forced expiratory lung volume is characteristic of aging; defining a threshold for a disease-associated decline in these functions requires comparison with the expected changes with healthy aging. Type 2 diabetes prevalence increases with aging, and the aging process leads to beta cell exhaustion in the pancreatic islet cells. Therefore, aging per se predisposes some older subjects to develop overt diabetes.[67] The best examples of healthy aging are individuals selected for the donation of one kidney for renal transplantation, but even this healthiest of the healthy may not be entirely normal because they also may be mildly obese, have treated mild hypertension, or have covert diseases not easily identifiable, even in an exhaustive clinical, laboratory, and imaging-based pretransplantation

evaluation. Studies of older apparently healthy adults in the community are inevitably an admixture of healthy aging and aging with comorbidity, sometimes clinically unrecognized.[68] In this context, proteomic analyses of low-molecular-weight proteins in urine obtained from supposedly healthy subjects have suggested resemblances between healthy aging and chronic kidney disease (CKD), but these findings might be the consequence of overlapping comorbidities (covert and overt) with aging per se.[69] In this chapter, we will use the healthy adult living kidney donor as the prototype for normal aging, recognizing some of the pitfalls in this assumption. A detailed discussion on the approach to management of the kidney disease in older adults can be found in Chapter 84.

DIFFERENCES BETWEEN HUMANS AND OTHER ANIMALS

Although many of the fundamental cellular processes of biologic aging are evolutionarily conserved, disparities at the organ system level may exist between species concerning the anatomic and functional consequences of aging. For example, many animal species (e.g., murine species) continue to grow throughout their life span, whereas humans cease growing after attaining maturity. The growth regulatory genetic program might be evolutionarily conserved among mammals, but the pace of growth is modulated in larger animals, including humans.[70] Metabolic demand may therefore differ among aging humans and aging experimental animals. Such differences can have profound effects on the organ-based manifestations of aging, including the kidneys. Thus, one needs to be cautious about inferring mechanisms of organ aging in humans from studies of experimental animals or lower organisms. The circumstances of birth, unique to humans, and in utero organogenesis can also have effects later in life, as will be discussed later.[71]

ANATOMIC CHANGES OF THE KIDNEYS WITH AGING

MACROSCOPIC CHANGES

As presently understood, aging is a universal and inevitable biologic process that is associated with macroscopic and microscopic structural changes in the kidneys, likely to be a causal association. Advances in the understanding of macroscopic structural changes have been made, first using ultrasound and more recently using computed tomography (CT) and magnetic resonance imaging (MRI).

KIDNEY SIZE AND VOLUME

Older studies that investigated kidney size with one- or two-dimensional measurements of kidney length or area have noted some degree of decrease with age.[72,73] Emamian and colleagues obtained ultrasound measurements of the kidney in 665 adult volunteers between 30 and 70 years of age and found that smaller kidney volumes correlated with older age.[74] Gourtsoyiannis and colleagues analyzed CT scans from 360 patients with no kidney disease to estimate kidney parenchymal thickness.[75] They found that for each decade of older age, kidney parenchymal thickness decreased about 10%. Another CT study in 1040 asymptomatic adults found that the factors associated with larger kidney size were male gender, taller height, and larger body mass index (BMI); whereas age and renal artery stenosis were associated with smaller kidney size.[76] Another study of 1056 patients showed similar findings and provided evidence that atherosclerosis accelerated the kidney size decline with older age.[77] However, a study of 225 adult healthy potential kidney donors did not find a statistically significant decrease in kidney size with older age, although the findings may have been limited by the age range and sample size of the study.[78]

A large MRI study assessed total kidney volume in 1852 subjects from the Framingham Heart Study.[79] The authors reported that the average decline in the total kidney volume in both genders was 16.3 cm^3/decade, with a stronger decline beyond 60 years of age, and a stronger decline in men than in women. In addition, using a subset of 196 healthy women and 112 apparently healthy men, this study determined the gender-specific upper and lower 10th percentile thresholds for the total kidney volume. In the multivariable models, the kidney volume above the 90th percentile was associated with younger age (odds ratio [OR], 0.67), whereas kidney volume below the 10th percentile was associated with older age (OR, 1.67).

KIDNEY CORTEX AND MEDULLA

Wang and colleagues have studied the CT scans of 1344 potential living kidney donors up to 75 years of age. They found a stable kidney parenchymal volume in those up to 50 years of age and a decline thereafter.[80] This study also obtained the volumes of the kidney cortex (average, 73% of parenchymal volume) and medulla (average, 27% of parenchymal volume) separately. An increasing medullary volume with age seems to attenuate some of the loss of total kidney parenchymal volume with age due to decreasing cortical volume (Fig. 22.1). Besides increased medullary volume, with age masking some of the kidney volume decline with age,

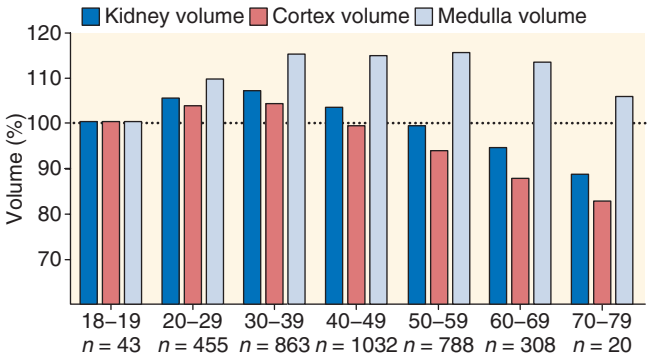

Fig. 22.1 Total kidney, cortical, and medullary volumes among 3509 potential kidney donors in the Aging Kidney Anatomy study (expansion of previously reported findings). Among all donors, older than 40 years, cortical volume decreases and medullary volume increases, making total kidney volume relatively constant until 50 years of age. Beyond that, medullary volume no longer increases, leading to a decrease in total kidney volume from the decreasing cortical volume. Findings were compared proportional to the respective volumes in the youngest age group (18–19 years). (From Wang X, Vrtiska TJ, Avula RT, et al. Age, kidney function, and risk factors associate differently with cortical and medullary volumes of the kidney. *Kidney Int.* 2014;85:677–685.)

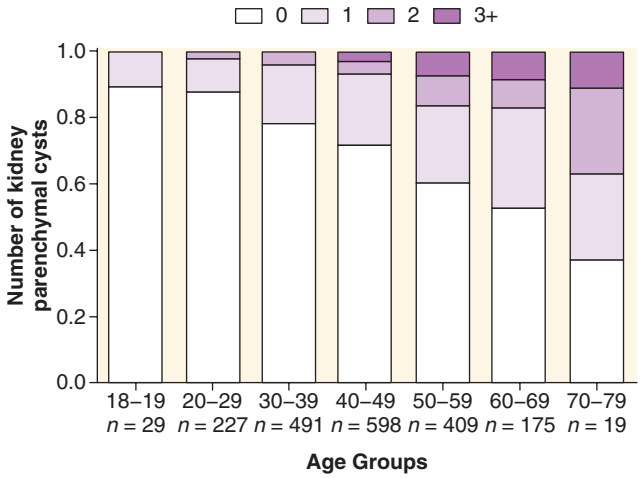

Fig. 22.2 Number of cortical and medullary simple cysts 5 mm or more by age among 1948 potential living kidney donors. In the figure fraction, *white* represents no cysts, whereas *dark purple* represents the fraction of three or more cysts. Intermediate fractions on a *light purple* scale represent the presence of one or two cysts.

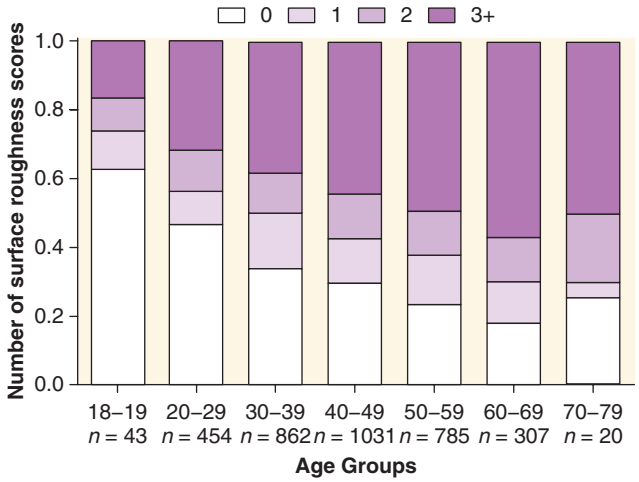

Fig. 22.3 Kidney surface roughness increasing with age among 3502 potential kidney donors in the Aging Kidney Anatomy study (expansion of previously reported findings). Based on the involved proportion of kidney surface with roughness (lumpy irregular rather than smooth surface), scores were given from 0 to 3 for each kidney and then averaged between kidneys. A score of 0 indicates no roughness; 1, roughness up to 25%; 2, roughness of 26% to 50%; and 3, roughness >50% of the kidney surface. (From Denic A, Alexander MP, Kaushik V, et al. Detection and clinical patterns of nephron hypertrophy and nephrosclerosis among apparently healthy adults. *Am J Kidney Dis.* 2016; 68:58–67.)

other studies have also suggested that an increase in renal sinus fat with age also masks some of the observed total kidney volume decline with older age.[74,75]

KIDNEY CYSTS

Kidney cysts are relatively common, of tubular diverticuli origin,[81] and their frequency and size increase with older age (Fig. 22.2).[82,83] There has been increased detection of cysts due to technologic advancements with imaging modalities, so it is important to consider cyst size thresholds when counting cysts.[82] A study of 1948 potential kidney donors demonstrated that even in this predominantly healthy population, cortical and medullary cysts larger than or equal to 5 mm were more frequent in older men and were associated with larger body surface area, albuminuria, and hypertension.[82] Moreover, this study generated upper reference limits (97.5th percentile) for the number of cysts in both genders by age. The upper reference limit for the number of cysts in both kidneys of 18 to 29-year-olds is one for both men and women, but increases to ten in men and four in women older than 60 years. Besides simple kidney cysts, parapelvic cysts, hyperdense cysts, angiomyolipomas, and cysts or tumors suspicious for cancer are also more frequent with older age.[82] Parapelvic cysts are thought to have a lymphatic origin[84] and increase with age, but are not associated with hypertension or albuminuria.

OTHER STRUCTURAL CHANGES

Other kidney parenchymal changes that become more prevalent with older age in ostensibly healthy adults include calcifications, focal cortical scars, fibromuscular dysplasia, and renal artery atherosclerosis without stenosis.[85] Of these, the two findings most strongly associated with age are atherosclerosis of renal arteries and focal cortical scarring. In donors younger than 30 years, the prevalence of atherosclerosis and focal scarring were 0.4% and 1.5%, respectively. However, in donors older than 60 years, the prevalence of atherosclerosis was nearly 25%, and the prevalence of focal scarring was 8%. Focal scarring also contributes to an increase in a kidney surface roughness with age (Fig. 22.3).[86]

MICROSCOPIC CHANGES

GLOMERULI

Number of Glomeruli

Several different approaches have been used to count the total number of glomeruli per kidney, with similar findings. On average, humans have 900,000 glomeruli/kidney, but with significant variability, ranging from as low as 200,000 up to 2.7 million glomeruli/kidney.[87,88] Lower glomerular number counts are likely the result of both the reduction in nephrogenesis stemming from intrauterine events and the progressive loss of glomeruli with age. Counts of the glomerular number have been obtained from autopsy studies, where complete sectioning of the kidney can be performed.[89] However, many autopsy studies have not distinguished normal nonsclerotic glomeruli from globally sclerotic glomeruli in their counts. Furthermore, the comorbid state in autopsy studies (often unknown, with sudden unexpected deaths) may increase global glomerulosclerosis beyond that expected from aging alone.

Living kidney donors provide a unique opportunity to determine how the glomerular number relates to aging. A study in 1638 living kidney donors who were carefully screened to confirm health estimated numbers of nonsclerotic and globally sclerotic glomeruli using the predonation CT scan and the implantation biopsy.[88] The youngest kidney donors (18–29 years of age) had a mean number of nonsclerotic glomeruli of about 990,000 and 17,000 globally sclerotic glomeruli/kidney. The oldest kidney donors (70–75 years) had about 520,000 nonsclerotic glomeruli and 142,000 globally

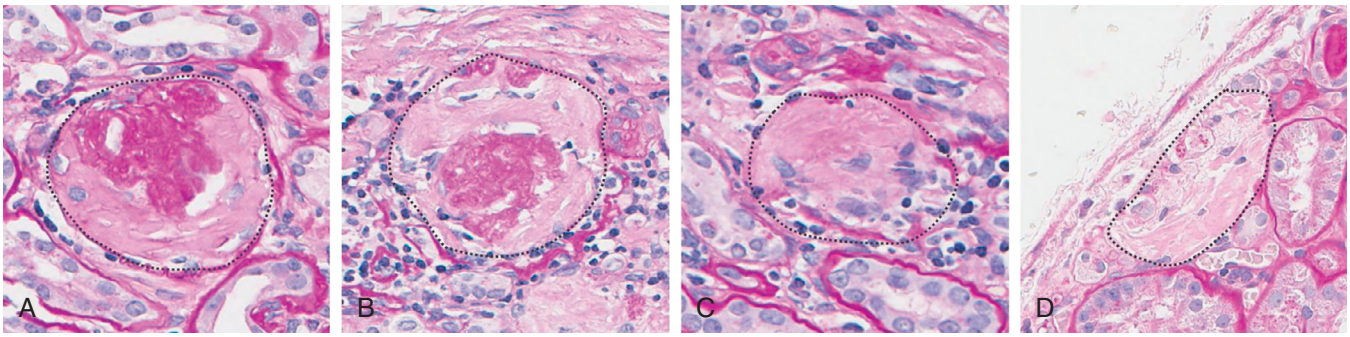

Fig. 22.4 Examples of globally sclerosed glomeruli (GSG) in different stages of their involution. (A, B) GSG are easily discernible in the biopsy sample. (C, D) GSG that may be overlooked because they progressively atrophy and lose a discernible capsule. All GSG are traced with a *black dashed line.*

sclerotic glomeruli per kidney. The 48% loss in nonsclerotic glomeruli, with only a 15% increase in globally sclerotic glomeruli numbers, supports the hypothesis that globally sclerotic glomeruli are eventually completely reabsorbed or significantly atrophied so that they can no longer be clearly detected on tissue sections examined by light microscopy (Fig. 22.4). This is in agreement with an older study by Hayman and associates, who postulated that "scars of destroyed glomeruli disappear without leaving recognizable traces."[90] The concept of missing or reabsorbed glomeruli is very important because a regular pathology report of the percentage of glomerulosclerosis on a renal biopsy may substantially underappreciate the true age-related loss of glomeruli.

Clinical Relevance 1
The reabsorption of globally sclerosed glomeruli with age may lead to an underappreciation of the older kidneys according to renal biopsy assessment.

Despite significant methodologic differences, studies have reported strikingly similar rates of glomerular loss per kidney per year—6200 in living kidney donors[88] and 6800 in autopsy studies.[89]

Table 22.1 Expected Number of Globally Sclerotic Glomeruli per Biopsy Section[a]

Age Group (years)	Total Number of Glomeruli Found per Biopsy Section							
	1	2	3–4	5–8	9–16	17–32	33–48	49–64
18–29	0.5	0.5	0.5	0.5	1	1	1	1
30–34	0.5	0.5	0.5	0.5	1	1	1	1.5
35–39	0.5	0.5	0.5	0.5	1	1.5	2	2
40–44	0.5	0.5	0.5	1	1	2	2.5	3
45–49	0.5	0.5	1	1	1.5	2	3	4
50–54	1	1	1	1.5	2	3	5	5
55–59	1	1	1.5	1.5	2	3.5	4.5	6
60–64	1	1.5	1.5	2	2.5	4	5.5	7
65–69	1	2	2	2.5	3	4.5	6.5	8
70–74	1	2	2.5	3	4	5.5	7.5	9
75–77	1	2	2.5	3	4	6	8	9.5

[a]As predicted by the total number of glomeruli and age from the Aging Kidney Anatomy study.
Adapted from Kremers WK, Denic A, Lieske JC, et al. Distinguishing age-related from disease-related glomerulosclerosis on kidney biopsy: the Aging Kidney Anatomy study. *Nephrol Dial Transplant.* 2015;30:2034–2039.

Glomerulosclerosis

An increasing percentage of global glomerulosclerosis is a feature of an aging kidney that has been demonstrated in autopsy and living kidney donor studies.[89,91,92] An autopsy study of 58 kidneys (48 from adults) from a mixed population of Australian Aborigines and non-Aborigines, US Caucasians, and African-Americans has shown a range of 0% to 23% with global glomerulosclerosis and a strong association with older age.[89] A study of 1203 living kidney donors has confirmed these findings and showed an increasing prevalence of focal and global glomerulosclerosis (FGGS), but not focal and segmental glomerulosclerosis (FSGS) with older age.[91] Whereas the prevalence of any global glomerulosclerosis was only 19% in the youngest kidney donors (age 18–29 years), the prevalence was 82% among the 11 oldest donors (70–77 years of age). In a study of 1847 of 2052 living kidney donors who were normotensive across three centers, the upper 95th percentile reference limit of glomerulosclerosis expected for age was determined (Table 22.1).[93] For example, for a 25-year-old who has a biopsy with 24 glomeruli, up to one globally sclerotic glomeruli on biopsy would be reasonable before suspecting glomerulosclerosis from disease. However, for a 76-year-old who has a biopsy with 24 glomeruli, up to six globally sclerotic glomeruli on biopsy would be reasonable before suspecting glomerulosclerosis from disease. In this study, among the 5% of donors in whom the number of globally sclerotic glomeruli was higher than the 95th percentile expected for age, a greater prevalence of hypertension and interstitial fibrosis and a higher percentage of ischemic-appearing glomeruli (pericapsular fibrosis, capsular thickening, and capillary loop wrinkling) on a biopsy were observed.[93] The association between the abnormal number of globally

sclerotic glomeruli for age and ischemic glomeruli remained, even after hypertensive donors were excluded. Interestingly, use of these age-specific reference limits for globally sclerotic glomeruli helps identify which patients with nephrotic syndrome will develop progressive CKD.[94]

Certain morphologic findings of globally sclerotic glomeruli should also be taken into consideration; for example, solidification forms of glomerulosclerosis are always pathologic and are never simply an age-related finding.[95–97]

Clinical Relevance 2
Glomerulosclerosis associated with aging is focal and global, in contrast to focal, segmental, and solidification forms of glomerulosclerosis occurring with disease.

The obsolescent type of morphology of global glomerulosclerosis is characterized by the filling of Bowman's space with collagenous material, accompanied by retraction of the capillary tuft. This is the type of global glomerulosclerosis obsereved in normal aging kidneys. Alternatively, the solidified type of glomeruloscleroisis is assocated with and commonly seen in hypertensive nephrosclerosis found in black people, with or without high-risk alleles on the APOL1 locus.[98] The obsolescent-type global glomerulosclerosis is presumed to reflect an ischemic process. FSGS is not associated with healthy aging in humans, unlike murine species. The lesion of FSGS in growing rats is likely to be mediated by podocyte injury and detachment. FSGS lesions in humans, therefore almost always indicates an underlying pathologic disease process and not simple renal senescence.[95–97]The possession of two risk alleles for APOL1 appears to enhance age-related global glomerulosclerosis in individuals of (West) African ancestry.[99,100] This phenomenon might help explain in part the higher risk of black people for the development of hypertension and GFR decline at an earlier age among black people compared with white people.[101]

Glomerular Hypertrophy

Entire nephrons hypertrophy in diabetes and obesity,[102–105] conditions that often become more prevalent with older age. Nephron hypertrophy is also seen in subjects with low nephron endowment at birth.[106] Although hypertrophy occurs in the glomerular and tubular segments of a nephron unit,[107] glomerulomegaly is much easier to appreciate on visual inspection of a kidney biopsy than tubular enlargement. The relationship between glomerular size and older age needs to account for the underlying study population (e.g., age-related comorbidites such as diabetes and obesity or nephron endowement at birth) and whether glomerular size was estimated from only nonsclerotic glomeruli or both nonsclerosed and the smaller globally sclerosed glomeruli that become more common with age.

Many studies have reported conflicting results, likely related to these issues, with some showing an increase in glomerular size with age[108–110] and others showing a decrease in glomerular size with age.[111,112] Studies that were limited to carefully screened healthy living kidney donors and only studied nonsclerosed glomeruli have found no change in glomerular size with aging.[86,88,113] Nonsclerosed glomerular volume in patients with renal tumors who underwent radical nephrectomy was stable until 75 years of age, similar to findings in living kidney donors.[114] However, beyond 75 years of age, nonsclerosed glomerular volume decreased due to a higher proportion of smaller, ischemic-appearing glomeruli. Given this lack of increase in glomerular volume, albuminuria would not be expected with aging alone in humans because albuminuria occurs with glomerular hypertrophy via a disorganized glomerular structure that is unable to prevent protein leaking efficiently.[110] Glomerular enlargement is also observed in blacks with two risk alleles at the APOL1 locus, which rather suggests low nephron endowment (see later) and/or accelerated loss of nephrons with aging.[99–101] Increased glomerular volume (glomerular hypertrophy) and glomerulosclerosis in aging subjects is predicted by comorbidity, such as obesity, diabetes, hypertension, and proteinuria. Such hypertrophy is also associated with male gender, taller height, and a family history of end-stage kidney disease (ESKD).[105,113]

TUBULES

Tubular Hypertrophy

Notably, glomeruli only comprise about 4% of the total cortical volume.[88] The remaining parenchymal volume is largely comprised of renal tubules and tubular enlargement.[107–115] Although glomerulomegaly most likely does not occur with healthy aging (or in the absence of APOL1 risk alleles in individuals of African origin), in humans tubular enlargement with older age is evident with increased area of tubular profiles.[86] Increase in tubular size as well as atrophy and disappearance of globally sclerotic glomeruli disperses the remaining glomeruli further apart from each other, thereby decreasing glomerular density with aging.[116] However, the relationship between glomerular (nonsclerosed and globally sclerosed) density varies, depending on how much global glomerulosclerosis is present in the section biopsied. In biopsy sections with less than 10% global glomerulosclerosis, the glomerular density is decreased with age, whereas in biopsy sections with more than 10% global glomerulosclerosis, the glomerular density is increased with age.[116] In regions of the renal cortex without significant glomerulosclerosis, age-related tubular enlargement disperses glomeruli further apart, decreasing their density. However, in regions with significant glomerulosclerosis, the overall atrophy of tubules and glomeruli brings the glomeruli closer together, thereby increasing their density (Fig. 22.5).

Tubular Diverticuli

Darmady and colleagues found in an autopsy study that tubular diverticuli increase with older age.[110] This finding parallels two other age-related findings in healthy adults. First, simple parenchymal cysts, which likely originate from these diverticuli,[81] become more frequent with older age. Second, the mean profile tubular area increases with older age.[86] Enlargement of tubules, with upregulation of growth factors, may contribute to the development of diverticuli, with the eventual formation of cysts.[117,118]

ARTERIES AND ARTERIOLES

Arteriosclerosis and arteriolar hyalinosis are two common findings in the kidney biopsy of normal adults that become

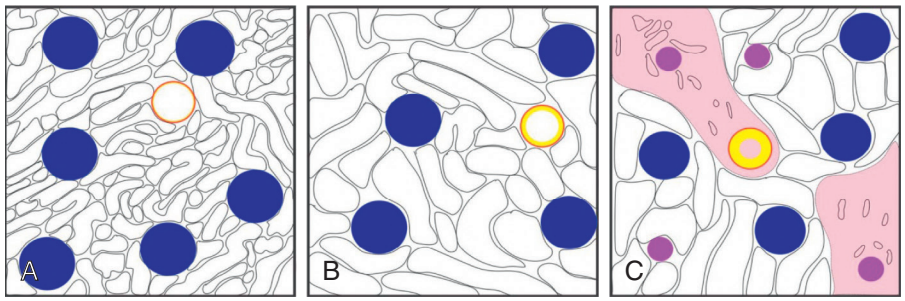

Fig. 22.5 Schematic illustration of how the percentage of glomerulosclerosis influences glomerular density. (A) Example of a young individual with a certain glomerular density *(blue solid circle)*, normal tubules and normal artery *(orange circle),* with minimal to no intimal thickening *(yellow circle).* (B) In an older person in whom the biopsy shows less than 10% glomerulosclerosis, tubules become larger and disperse the glomeruli apart, and their density decreases. (C) In older persons in whom there is more than 10% glomerulosclerosis *(pink solid circles)*, the associated interstitial fibrosis and tubular atrophy *(light pink areas)* bring the glomeruli closer together, thus increasing their density. Arteriosclerosis with intimal thickening *(thicker yellow line)* is also pronounced in these regions in older adults.

more prevalent with age.[86] Arteriosclerosis (luminal stenosis by intimal thickening) with aging may cause ischemic injury, leading to a lower cortical to medullary volume ratio, even in healthy adults.[86] Arteriolar hyalinosis increases with age and is associated with renal artery atherosclerosis in healthy adults, consistent with studies that associate arterolar hyalinosis with renal atherosclerosis in hypertensive patients.[119–121] Older age and hypertension may lead to global glomerulosclerosis and nephrosclerosis via reduced blood flow due to ischemic injury from the narrowing of small arteries and arterioles.[122] Notably, lower total nephron number/kidney is associated with arteriosclerosis, even after adjusting for age and gender.[88]

NEPHROSCLEROSIS AND INTERSTITIAL FIBROSIS

The term *nephrosclerosis* describes a microstructural biopsy pattern of global glomerulosclerosis, arteriosclerosis, and interstitial fibrosis with tubular atrophy. Nephrosclerosis is notably seen with hypertension,[123] but is also described in healthy older kidney donors without hypertension or only mild hypertension.[91] The nephrosclerosis appearance is thought to be due to increased intimal thickening of small arteries in the kidneys (arteriosclerosis, arteriolosclerosis), leading to glomerular ischemia, with the wrinkling of capillary tufts, thickening of the basement membrane, and progressive pericapsular fibrosis.[123,124] Simultaneously, proteinaceous material accumulates in Bowman's space, likely due to a combination of a disturbed balance between formation and breakdown of the glomerular extracellular matrix[125] and podocyte depletion,[91,109,125] probably due to perturbations in local mechanical forces.[126] Eventually, ischemic glomerular tufts fully collapse, forming globally sclerosed glomeruli. As a consequence of glomerulosclerosis, accompanying tubules atrophy, with an accumulation of surrounding interstitial fibrosis.

All four features of nephrosclerosis—global glomerulosclerosis, arteriosclerosis, interstitial fibrosis, and tubular atrophy—increase with older age and, when combined together (at equal weighting) they represent a so-called nephrosclerosis score (Fig. 22.6).[91] If we define the nephrosclerosis as presence of at least two of the previously mentioned abnormalities, then from Fig. 22.6 we can see that the youngest donors (18–19 years of age) do not have detectable nephrosclerosis. The prevalence of nephrosclerosis

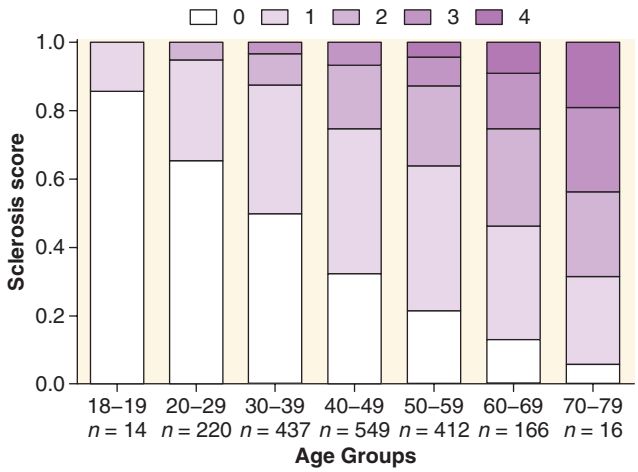

Fig. 22.6 The nephrosclerosis score increases with age among 1814 living kidney donors from the Aging Kidney Anatomy study (expansion of previously reported findings). The total nephrosclerosis score is obtained by adding the individual scores of histologic abnormalities: any global glomerulosclerosis, any arteriosclerosis, interstitial fibrosis greater than 5%, and any tubular atrophy. *White bars* in all age groups represent a score of 0 (no abnormalities present), and a *dark purple bar* represents a score of 4 (presence of all four pathologic abnormalities). Three intermediate scores are presented with different shades of *purple color*. (From Rule AD, Amer H, Cornell LD, et al. The association between age and nephrosclerosis on renal biopsy among healthy adults. *Ann Intern Med.* 2010;152:561–567.)

in 20- to 29-year-old donors is 5% and rises to 69% among the oldest donors.

Thus, the number and size of the nephrons are the primary determinants of the kidney cortical volume. A combination of age-related glomerulosclerosis with corresponding interstitial fibrosis and tubular atrophy is responsible for the observed loss of cortical volume with healthy aging seen in living kidney donors. This nephrosclerosis typically starts in glomeruli in the superficial cortical zones. Because the corresponding tubules of these superficial glomeruli contribute more to the cortical volume, their atrophy with age-related nephrosclerosis leads to a decrease in cortical volume with aging. At the same time, there is tubular hypertrophy of the remaining nephrons,

particularly those in the medulla. This observation explains why, despite a 48% decrease in nephron number from ages 18 to 76 years, there is only a 17% decrease in cortical volume and only a 12% decrease in kidney volume.[74,75]

One might expect that with age-related nephrosclerosis, there would be compensatory hypertrophy of the remaining, still functional glomeruli. However, studies in living kidney donors have not confimed this hypothesis.[116] A possible explanation may be that with healthy human aging, there is a decreased metabolic demand for glomerular function, so that the loss of glomeruli does not cause the enlargement of the remaining glomeruli. Notably, comorbidities that can become more prevalent in old age, such as obesity and diabetes, with albuminuria, do associate with glomerular hypertrophy.[116] Also, low nephron endowment at birth, or disorders that accelarate nephron loss with advancing age, can contibute to the glomerulomegaly observed in adulthood.

FUNCTIONAL CHANGES OF THE KIDNEYS WITH AGING

These include changes in the GFR and other functional changes.

GLOMERULAR FILTRATION RATE

WHOLE-KIDNEY GLOMERULAR FILTRATION RATE

In a series of pioneering studies begun over 60 years ago, Davies and Shock examined 70 healthy adults between the ages of 24 and 89 years and, in a cross-sectional analysis, showed (by urinary inulin clearance) a linear GFR decline in subjects older than 30 years.[127] The GFR in the oldest group was found to be 46% less as compared with the GFR in the youngest group. Several decades later, Lindeman and colleagues carried out a longitudinal study (the first of its kind) by following 254 mostly healthy adult individuals, although some had diabetes, for up to 14 years.[128] They found that the mean annual decline in GFR, estimated by 24-hour urinary creatinine clearance, was 7.5 mL/min per decade; however, one-third of the subjects had no decrease in kidney function, and a small subset actually had an increase. In addition to measurement error explaining this finding, a rise in GFR with age might also be explained by hyperfiltration due to the comorbidities (e.g., obesity, diabetes) that become more common with aging.[129] This longitudinal rate of GFR decline is similar to the cross-sectional decline of 6.3 mL/min per decade obtained from a study of potential kidney donors (GFR measured by iothalamate clearance).[91] Among 4500 potential kidney donors in the expanded analysis from the Aging Kidney Anatomy study (Fig. 22.7), the average decline per decade for estimated GFR was 7.4 mL/min, whereas for measured GFR (iothalamate clearance) it was 6.1 mL/min/1.73 m^2. The estimated GFR by the Chronic Kidney Disease Epidemiology Collaboration (CKD-EPI) equation underestimates the GFR in healthy populations, such as potential kidney donors, because it was developed using mostly CKD patients.[130,131]

Although Fig. 22.7 shows mean estimated GFR (eGFR) and measured GFR, there is variability within each age group (Table 22.2).[132] It can be appreciated that both upper and lower reference limits also decline with aging. Similar findings in healthy donors have been reported by Pottel and colleagues.[133] Other longitudinal studies of the decline in renal function (GFR or creatinine clearance) with aging have shown generally similar findings to those of Lindeman and associates,[128] including the relative stability of renal function for extended periods in some otherwise healthy aging subjects.[134–136] In addition, in these studies, the rate of decline of renal function appeared to increase with each passing decade in those older than about 30 to 40 years.

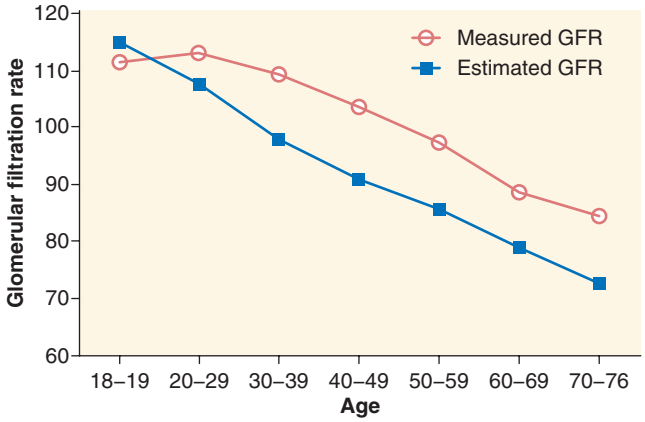

Fig. 22.7 Age-related glomerular filtration rate (*GFR*; mean values) decline among 4500 potential kidney donors in the Aging Kidney Anatomy study (expansion of previously reported findings). Decline in the estimated GFR (CKD-EPI study equation; see text) is calculated to be 7.4 mL/min/decade and 6.1 mL/min/decade for the measured GFR. (From Rule AD, Amer H, Cornell LD, et al. The association between age and nephrosclerosis on renal biopsy among healthy adults. *Ann Intern Med.* 2010;152:561–567.)

Table 22.2 Reference Values for Estimated and Measured Glomerular Filtration Rate in Potential Kidney Donors[a]

Age Group (years)	No.	Estimated Glomerular Filtration Rate (GFR) (Measured GFR)			
		Fifth Percentile	Median	Mean	95th Percentile
18–19	46	88 (87)	114 (107)	115 (111)	145 (144)
20–29	584	81 (84)	108 (111)	108 (113)	130 (149)
30–39	1090	75 (82)	98 (106)	98 (109)	118 (147)
40–49	1364	69 (77)	91 (102)	91 (104)	110 (135)
50–59	1001	65 (72)	85 (94)	85 (97)	103 (133)
60–69	379	61 (64)	78 (87)	79 (88)	97 (118)
70–76	36	55 (57)	71 (85)	73 (84)	91 (113)

[a]Expansion of previously reported findings.

From Murata K, Baumann NA, Saenger AK, et al. Relative performance of the MDRD and CKD-EPI equations for estimating glomerular filtration rate among patients with varied clinical presentations. *Clin J Am Soc Nephrol.* 2011;6:1963–1972.

SINGLE-NEPHRON GLOMERULAR FILTRATION RATE

Several studies have found that a higher whole-kidney GFR correlates with larger kidneys or kidney cortical volume.[79,80,86] A study of 1520 healthy living kidney donors also investigated

how the whole-kidney GFR correlated with the microstructural components of cortical volume. After age and gender adjustments, a higher whole-kidney GFR was associated with larger nephrons (larger glomeruli and tubules), whereas a lower whole-kidney GFR did not associate with any measure of nephrosclerosis, including global glomerulosclerosis, interstitial fibrosis with tubular atrophy, and arteriosclerosis.[86] The age-related nephron loss due to increased nephrosclerosis is followed by a parallel whole-kidney GFR decline.[88] To disentangle whole-kidney GFR from the nephron number, further single-nephron GFR (snGFR) studies are required.

Although in vivo measurements of snGFR through micropuncture are possible and have been done in animal studies,[137,138] a direct measure of snGFR (by micropuncture) is not feasible or safe in humans. However, dividing the whole-kidney GFR by the number of functional (nonsclerosed) glomeruli in both kidneys allows for an estimation of the mean snGFR.[139] The snGFR remains stable with age because the loss of nephrons parallels the loss in the total GFR.[88] Thus, the effect of age on snGFR is minimal, consistent with other physiologic characteristics, including height and gender, whereas obesity, family history of ESKD, and nephrosclerosis exceeding that expected for age are associated with an increased snGFR.[139,140] There may be higher snGFR among the oldest donors (70–75 years of age), but this finding may be confounded by donor selection factors (e.g., the requirement of whole-kidney GFR >80 mL/min/1.73 m^2) in this age group, which may only allow those with some degree of hyperfiltration to donate and be available to study with a kidney biopsy.[139,140]

Although other studies of snGFR in living human subjects are lacking, there have been studies assessing the single-nephron ultrafiltration coefficient (snK_f) in individuals similar to living kidney donors.[141–143] The snK_f represents the filtering capacity of the glomerulus, as determined by the surface area and permeability of the glomerular filtration barrier. In these studies, snK_f was estimated from electron microscopy measures of the glomeruli on kidney biopsy.[141] The snGFR could be calculated by multiplying snK_f by the perfusion pressure across the glomerular filtration barrier.[144] Thus, it is possible that the relationship of clinical characteristics to snGFR may be similar to that of snK_f. Consistent with the findings of a relatively stable snGFR across the age spectrum described above, snK_f did not show significant differences between younger and older living kidney donors.[141,145] Adaptive hyperfiltration does occur in the aging kidney following unilateral nephrectomy[146]; however, either due to an increase in Kf, glomerular capillary filtration pressure, or increased glomerular plasma flow or some combination of the three, the extent of the increase in snGFR (and whole-kidney GFR [wkGFR]) is reduced compared with younger persons. The definition of hyperfiltration based on measurements of the whole-kidney GFR is best determined by an age-adapted measured GFR (not eGFR), uncorrected for body surface area. However, such definitions do not distinguish between a higher snGFR and higher nephron number.[147]

OTHER FUNCTIONAL CHANGES

RENAL PLASMA FLOW

Renal plasma flow (RPF) represents the volume of plasma delivered to both kidneys per unit of time. The RPF can be calculated from the amount of plasma that is cleared of para-aminohippurate (PAH) per unit of time. PAH is a compound with a nearly 100% extraction through the kidneys. A Swedish study of 122 potential kidney donors, ages 21 to 67, has shown that similar to the GFR, the RPF declines with older age.[140] Older age influences the degree of renal blood flow change as a response to exercise,[148,149] attenuates the renal hemodynamic response to atrial natriuretic peptide[150] and the degree of vasodilation.[151] One study has postulated that higher levels of the endogenous nitric oxide (NO) inhibitor asymmetric dimethylarginine (ADMA) lead to a reduced RPF and hypertension with older age.[152] Animal studies have provided some evidence that ADMA is associated with tubulointerstitial ischemia and fibrosis,[153] glomerular capillary loss, and glomerulosclerosis.[154] In a study of 19 healthy individuals, divided into three age groups—young, middle-aged, and older—an infusion of dopamine and amino acids was used to test the effects of maximal vasodilation on RPF and NO levels. Whereas both RPF and NO levels increased in young and middle-aged individuals, they did not change in the older group.[155] This suggests that due to advanced age-related vascular changes in older adults, renal blood vessels are less responsive to maximal vasodilation.

FILTRATION FRACTION

The filtration fraction (FF) represents the proportion of fluid entering the kidneys that reaches into the renal tubules—that is, it is a ratio between the GFR and RPF. Normally, the value for FF is about 20%. However, in older age, atherosclerosis and arteriosclerosis of the arteries and arterioles reduces blood flow to kidneys. Thus, the FF may increase, particularly in those of very advanced age.[140]

RENAL RESERVE IN AGING

The phenomenon of renal reserve refers to an acute increase in GFR (usually by 20% or more from basal values) when subjects are fed oral protein loads (typically cooked red meat) or infused intravenously with certain amino acids.[155–159] The mechanisms underlying such physiologic changes is not fully understood, but appears to be a consequence of vasodilatation, an increase in glomerular plasma flow, and an increase in the snGFR.[160] See Chapter 3. Growth hormone may be involved, but this is controversial[155–157] The efficiency of renal reserve is blunted to some degree by aging per se, most often in the very older.[155] Renal functional reserve is well maintained up to about age 80 years in otherwise healthy men and women.[161] Diminished levels of sex hormones may play a role in the diminished renal reserve seen with aging (see later). The diurnal variation in GFR is also blunted with aging.[162]

Aging in indigenous Kuna Indians (Panama), who subsist on a low-protein, high–dark chocolate diet and remain largely free of hypertension and cardiovascular disease (CVD), even at an advanced age, is associated with a steady decline in GFR and RFP with aging, similar to that observed in westernized countries.[163] These findings are not consistent with a hypothesis that rising blood pressures (hypertension) are causally related to the decline in GFR with aging.

SEXUAL DIMORPHISM IN AGING

In a series of studies, mainly focused in murine species, Baylis and coworkers developed the concept of sexual dimorphism

in renal aging[164–168] (also see review by Gava and associates[169]). Females develop less age-related decline in renal function, perhaps due to a renoprotective action of estrogens. In contrast, males have a greater loss of renal function with age, perhaps due to the adverse effects of androgens. The mechanisms involved are complex, but seem to implicate disturbances of the NO synthesis pathways, and a lower rate of NO production might be influenced by sex steroids.[165,166] A role for the renin-angiotensin-aldosterone system (RAAS) has also been described.[168] Interestingly, in aging experimental animals, there was no observed rise in glomerular capillary pressure or glomerulomegaly in males or females, castrated or not. This suggests that the age-dependent sexually dimorphic loss of renal function does not appear to be dependent on hemodynamic changes or glomerular hypertrophy, similar to that observed in humans.[168] Age-dependent sexual dimorphic effects on renal function might be related to increased body size in males and therefore may be conditional to a disparity between energy demand and supply.

Pathophysiologic Explanations for Aging-Associated Nephrosclerosis

Podocentric Versus Ischemic Hypotheses (Animal and Human Studies). As stated earlier, it has been shown that renal blood flow declines with older age.[170] Studies in rats have shown that in addition to the reduction in blood flow, renal arterioles in older rats have altered sensitivity to NO[171] and angiotensin II.[172] However, the main limitation of animal studies is the virtual absence of arteriosclerosis, thus limiting studies of age-related ischemic changes. Studies in human kidneys have demonstrated that age-related arteriolosclerosis and intimal and medial hypertrophy in intrarenal arteries resemble those observed in extrarenal arteries.[173,174] These pathologic changes are especially common in interlobular arteries and are frequently observed in renal biopsies from normal individuals without cardiovascular disease. Although it is unclear what causes the vascular changes in intrarenal arteries, Martin and Sheaff have postulated that they are directly linked to global glomerulosclerosis, which occurs first in the superficial cortical layers and is followed by local interstitial fibrosis and tubular atrophy.[124] Subsequently, as a compensatory mechanism, the deeper glomeruli hypertrophy and, over time, undergo hyperfiltration injury, ultimately developing glomerulosclerosis. More recently, studies in healthy living kidney donors have corroborated the hypothesis of Martin and Sheaff that age-related glomerulosclerosis is primarily of vascular origin due to observed ischemic changes in the glomeruli, intracapsular fibrosis,[175] and increased prevalence of arteriosclerosis.[91] Moreover, implantation renal biopsies of healthy kidney donors can also be ischemic appearing, presumably still functional glomeruli, with a wrinkling of capillary loops, thickened basement membrane, and mild intracapsular fibrosis. All these described findings may be associated with ischemia and gradually lead to progressive shrinkage of the glomerular tufts and collagen deposition in Bowman's space, finally ending with complete global glomerulosclerosis.

Alternatively, podocyte depletion can also give rise to the glomerulosclerosis of aging. The podocytes are highly differentiated and specialized epithelial cells in a glomerulus, with limited capacity for cell division and turnover.[176,177] The two main reasons that lead to podocyte depletion, in absolute or relative terms, are actual loss of podocytes (cell death or detachment from the tuft) and glomerulomegaly—each podocyte subsequently has to cover the increased filtration surface area. The notion that podocyte dysbiosis may be the culprit for glomerulosclerosis is not new. Three decades ago, Kriz and colleagues[178] postulated that podocyte depletion and a subsequent bare glomerular basement membrane is the first step that leads to focal and segmental glomerulosclerosis. Studies in rats have provided evidence that reduced numbers of podocytes lead to glomerulosclerosis.[179,180] Using puromycin aminonucleoside (PAN) treatment as a model for podocyte oxidative injury, one study has linked glomerulosclerosis and podocyte number depletion.[179] Others have shown increased glomerulosclerosis (usually of the focal and segmental variety) when podocytes fail to follow glomerular growth as a result of molecular growth signalling[180] or may be due to podocyte hypertrophic stress associated with glomerulomegaly in rats without calorie restriction.[181] Interestingly, calorie restriction abolished glomerulomegaly, podocyte hypertrophy/stress and pydocyte loss with resulting glomerulosclerosis.[181] Using a transgenic approach in rats, the same group has also developed evidence that the reduced number of podocytes alone is sufficient to cause glomerulosclerosis.[182]

Taken together, all these animal (murine) studies favor the concept that acquired or congenital podocytopenia (absolute or relative) is a critical driving force for the development of glomerulosclerosis, particularly of the focal and segmental variety (see review by Kriz and associates[178]). However, the biology of aging in experimental animals differs from that of humans (see above), and these differences must be taken into account when translating pathophysiologic concepts from animals to humans.

More recently, human kidney biopsies have been used to study podocytes; these have found that the pattern of global glomerulosclerosis with aging is somewhat different in studies not limited to living kidney donors.[108] A study of 89 kidney biopsies from living kidney donors, deceased kidney donors, and normal poles of radical nephrectomy specimens performed for tumor, found that podocyte depletion is identified as a potential culprit for age-related glomerulosclerosis.[108] The authors counted podocytes, measured their size and density, and demonstrated a decline in podocyte density with older age due to a reduced count of podocytes per glomerulus and larger glomerular volume. In particular, younger individuals had more than a threefold higher podocyte density compared with individuals older than 70 years (>300 podocytes/10^6 μm^3 vs. <100 podocytes/10^6 μm^3). In the older individuals, not only was the podocyte density lower, but their detachment rate was much higher, and podocytes showed molecular evidence of cell stress. Moreover, in some glomeruli with significant podocyte detachment, the authors observed binucleated podocytes as evidence of failed mitotic attempts and glomerular capillary wrinkling, tuft collapse, and pericapsular fibrosis. All these findings led the authors to propose a hypothesis (the podocentric hypothesis) for the glomerular natural history with aging, extending from glomerular hypertrophy to tuft collapse to glomerulosclerosis.[108] However, studies limited to living donors did not show glomerular hypertrophy with aging,[86] suggesting that age-related comorbidities rather than aging alone may explain these findings. In addition, it is noteworthy that increasing albuminuria is not a feature of normal healthy aging.[91] Thus, the podocentric hypothesis may not be relevant to human renal aging.

CONTRIBUTION OF COMORBIDITIES TO RENAL AGING

Aging is commonly accompanied by comorbidities that can have an independent impact on renal structure and function. These include obesity, diabetes, and nephron endowment at birth. For example, obesity and/or diabetes (type 2) can lead to glomerulomegaly, glomerular hyperfiltration, and albuminuria (see Chapter 51). In part, these comorbidities contribute to the rising prevalence of increased albuminuria with aging seen in cross-sectional epidemiologic studies.[68] Hypertension, commonly seen in older adults, can also modify the underlying normal pattern of renal senescence seen with aging, as discussed earlier.

It also seems likely that nephron endowment at birth will have a modifying effect on the pace of normal physiologic renal aging. Nephron underendowment at birth, due to fetal dysmaturity, will be accompanied by early single-nephron hyperfiltration and glomerular enlargement, which can lead to maladaptive glomerular injury, podocytopenia, glomerulosclerosis and perhaps an acceleration of the normal rate of nephron loss.[183] The combination of glomerulopenia (low nephron endowment at birth) and physiologic renal senescence could, at least theoretically, lead to features of CKD (reduced GFR and/or albuminuria) observed in later life. This postulated phenomenon has not been well studied, so these effects are largely speculative. Reduced glomerular density and glomerular hypertrophy are signs of nephron underendowment and have been shown to have an adverse effect on the progression of many renal diseases, including some that may affect older adults.[184,185] Low birth weight, fetal dysmaturity, and impaired nephrogenesis can contribute to the burden of kidney disease globally, especially in older adults and in subjects with primary or secondary glomerular diseases (see Chapter 21).[185]

FLUID, ELECTROLYTE, AND ACID-BASE HOMEOSTASIS IN AGING

SODIUM HOMEOSTASIS

A study in 89 healthy subjects has demonstrated that older age significantly affects the kidney's capacity to reabsorb filtered sodium. Following the initiation of sodium restriction, subjects older than 60 years needed nearly twice as much time to reduce sodium excretion than subjects younger than 30 years (31 vs. 17.6 hours, respectively).[186] The observed difference may be due to the significantly reduced sodium reabsorption in the distal tubules, which was found to be nearly 30% less in older people versus younger controls.[187] Sodium homeostasis can also be influenced by age-related changes in levels and responses to renin and aldosterone, hormones that regulate sodium conservation (discussed further in Chapter 14). Although plasma renin activity and aldosterone levels are lower in older adults, they are not associated with changes in fluid or electrolyte metabolism.[188] These changes increase older adults' susceptibility to sodium retention in disease states or with the use of medications that alter renin release. More recently, the slower response to sodium restriction observed in older adults was reproduced by using angiotensin-converting enzyme (ACE) inhibitors and blocking the RAAS.[189]

One group studied the natriuretic response in normal individuals of different ages after volume expansion and volume contraction. In the 24-hour period following a 2-L infusion of normal saline, the natriuresis was slower in older individuals.[190] It has been hypothesized that the higher prevalence of hypertension in older subjects may be due in part to this attenuated natriuretic response with aging. There is also a reduction in the natriuretic response to saline loading in older versus younger kidney donors after donation.[189]

Atrial natriuretic peptide (ANP) is a hormone secreted by atrial myocytes, and one of its many functions is to control sodium excretion at the tubular level. With older age, the tubular response to ANP is reduced. ANP inhibits sodium reabsorption from the luminal side and induces hyperfiltration and suppression of renin release, all of which together lead to natriuresis, diuresis, and lowering of blood pressure. Normally, ANP is cleared rapidly from plasma; however, if degradation enzymes or clearance receptors are blocked, the half-life can be prolonged.[191] Studies have shown that the plasma ANP levels are several times higher in older individuals, and this may be a compensatory effect of the reduced response at the receptor level. This hypothesis is in agreement with two studies in which sodium excretion plateaued after an ANP infusion in older subjects,[192,193] whereas in younger subjects sodium excretion continued to increase with increasing ANP dose.[192] Of importance, it appears that ANP production does not change with older age; therefore the observed increase of ANP levels in older adults results from reduced metabolic clearance.[194,195] Moreover, others have shown that in response to a saline load, plasma levels of ANP increase more robustly in older compared with younger individuals.[196,197]

The role of altered renal sodium handling in the pathogenesis of age-related elevation of systemic arterial pressure is a topic of great contemporary interest (see also Chapter 46; reviewed by Frame and Wainford[198]). Clearly vascular factors, such as reduced compliance of major arterial vessels, and neurohumoral alterations, such as increased sympathetic nervous system activity, play important roles in the elevation of systolic blood pressure with aging. The sensitivity of blood pressure changes consequent to salt administration increases with age.[199] Animal studies have also suggested increased intrarenal angiotensin II signaling in age-related blood pressure increases.[200] Experimental studies in rodents has also shown decreased expression of the sodium potassium chloride cotransporter (NKCC2) in the loop of Henle with aging[201]; the activity of the thiazide-sensitive sodium chloride cotransporter (NCC) in the distal tubule may be altered in aging, but this is controversial.[198]

The expression of the epithelial sodium channel (ENaC) can be reduced in aging rodents.[202] These studies collectively indicate that dysregulation of sodium handling by the aging nephron can be involved in age-related blood pressure elevation. Integration of this knowledge into the complex array of biologic factors in systems affecting blood pressure (e.g., aortic compliance, sympathetic nervous system activity, RAAS) will be challenging.[198] The role of reduced nephron mass (glomerulopenia) that accompanies physiologic aging cannot be ignored as a participant in blood pressure changes with aging.

POTASSIUM HOMEOSTASIS

Potassium homeostasis is regulated by several different mechanisms; specifically, in the kidney, the potassium excretion rate is altered depending on the intake. The role of the kidney in potassium homeostasis is very important because normally around 90% of the dietary potassium intake is excreted in the urine and only around 10% in the gastrointestinal tract. The normal internal potassium distribution is also regulated by hormones, such as insulin, catecholamines, and aldosterone. In general, after filtering through the glomerulus, potassium is primarily reabsorbed via the proximal tubule and thick ascending limb of Henle such that only a small amount should normally reach the distal tubules (discussed further in Chapter 17).[203]

Total body potassium (TBK) declines with older age with a reduction in intracellular stores that accompany the decline in muscle mass (sarcopenia) seen with normal aging. A study of 188 healthy volunteers has shown that the annual rate of TBK decline is 7.2 mg/kg in women and 9.2 mg/kg in men,[204] which increases in both genders after 60 years of age.[205] The observed decline in TBK may also be explained by the lower renin and aldosterone levels,[206] as well as the blunted response to aldosterone in older adults (see later).[207] A study of 43 healthy older individuals demonstrated a relative decrease in fractional potassium excretion in relation to creatinine clearance.[208] This finding is consistent with animal studies in which potassium excretion was less efficient in old rats fed a high-potassium diet.[209] The same group subsequently showed that the transtubular potassium gradient is reduced in older compared with young subjects, implying reduced efficiency in potassium excretion in older adults.[210] Insulin-mediated potassium homeostasis in human subjects is not influenced by the age of the subject.[211]

Older age is usually accompanied by comorbidities, and older adults often take medications that interfere with potassium excretion. Examples are potassium-sparing diuretics, renin inhibitors, ACE inhibitors, angiotensin receptor blockers, heparin, calcineurin inhibitors, sodium channel blockers, and nonsteroidal antiinflammatory drugs (NSAIDs). Care is needed when starting these medications for older patients, given their increased propensity to develop hyperkalemia.

Clinical Relevance 3
Older adults are at increased risk of hyperkalemia, even given their reduced total body potassium stores and altered tubular potassium transport.

MAGNESIUM HOMEOSTASIS

It is estimated that about 99% of magnesium is stored in cells, predominantly in bones and muscles, and only about 1% is in extracellular fluid, including plasma. Normally, the kidneys reabsorb 96% of filtered magnesium[212] and regulate magnesium homeostasis (see Chapter 18).

Because plasma and intracellular magnesium homeostasis are very finely regulated,[213] total plasma magnesium is maintained remarkably stable with increasing age in healthy individuals.[214,215] However, a study of 36 healthy older individuals has demonstrated a significant subclinical deficit of magnesium that was not detected by serum magnesium levels.[216] Another more recent study has confirmed this finding, and older subjects (>65 years) had significantly reduced serum levels of both ionized and total magnesium.[214]

The published literature is scarce with regard to normal age-related changes in magnesium homeostasis in the kidneys. Changes in magnesium homeostasis are likely due to diseases that frequently occur in older age, use of therapeutic agents that alter its metabolism, and previously discussed age-related kidney functional decline.[214] The microstructural changes that lead to functional decline in older kidneys may also result in reduced tubular reabsorption of magnesium, thus causing hypomagnesemia. In addition to the age-related changes in the kidney, other comorbidities and drugs (e.g., loop diuretics, digitalis) in older adults can further worsen the magnesium deficiency.[214] On the other hand, hypermagnesemia occurs very rarely, even in the disease setting, including in those with severe acute kidney injury (AKI), CKD, or ESKD.[217] Interestingly, low dietary magnesium intake in older adults may also contribute to a faster rate of decline in the GFR, potentially exacerbating a proinflammatory milieu, endothelial dysfunction, and promotion of vascular calcification.[218]

CALCIUM HOMEOSTASIS

In normal adults, every day approximately 10 g of calcium is filtered through the glomeruli, and 98% to 99% is reabsorbed, so that net calcium excretion during a 24-hour period ranges from 100 to 200 mg. Most filtered calcium reabsorption (≈60%–70%) occurs in the proximal tubules, around 20% in the loop of Henle (thick ascending limb), around 5% to 10% in the distal convoluted tubule, and only around 5% in the collecting ducts (see also Chapter 18).

There have been several studies of calcium homeostasis with aging. A study of rats in three different age groups has shown that calcium excretion and reabsorption are equally maintained in all three groups, which may be linked to observed age-related renal hypertrophy in older rats.[219] However, other animal studies and studies in humans have shown that there are age-related changes in renal calcium homeostasis, such as decreased tubular reabsorption and/or the renal response to parathyroid hormone (PTH).[220–223] Renal and intestinal calbindins are proteins with a critical role in active transcellular calcium transport, and their expression decreases with age.[224–226] There is also an age-related decrease in the capacity of 1,25-dihydroxyvitamin D_3 (1,25-$(OH)_2D_3$) to stimulate calcium reabsorption, increasing PTH levels in both rats and humans.[227,228] A study in mice has found that an age-related reduction in TRPV5 and TRPV6 (renal and duodenal calcium intracellular transporters, respectively) lead to impaired renal and duodenal calcium reabsorption, consistent with the increased calciuria observed in older mice.[229] Alpha-Klotho (α-Klotho) is a gene associated with accelerated aging when mutated.[230] It encodes a protein that is predominantly expressed in tissues involved with calcium homeostasis. A study in mice has demonstrated that alpha-klotho binds to a subunit of sodium-potassium adenosine triphosphatase (Na^+-K^+-ATPase),[231] suggesting that the age-related decline in klotho protein could contribute to reduced

sodium potassium ATPase sensing of low calcium levels. Serum-soluble α-Klotho (sKlotho) levels decline with advancing age in humans, independent of the GFR.[55]

There is also an age-related decrease in intestinal calcium reabsorption, which is linked with reduced 1α-hydroxylase activity, 1,25-$(OH)_2D_3$ levels, and increased basal PTH levels. A study of 22 healthy men has found that older individuals have a twofold higher serum PTH level, with no difference in blood ionized calcium. Moreover, older men also had a higher threshold for PTH release; however, this was not associated with a decrease in blood ionized calcium or 1,25-$(OH)_2D_3$.[232] This finding suggests that the relationship between PTH and calcium in older age is changed so that regardless of calcium concentrations, PTH levels are higher. An interesting study has compared healthy older individuals (≥75 years of age) to patients with CKD and a similar GFR and found that CKD patients have higher serum levels and fractional excretion of calcium, suggesting greater calcium wasting in these patients.[233] Concentrations of vitamin D–dependent calcium-binding proteins also decrease with older age, which is associated with the change in intestinal calcium absorption.[209,224] Another study of healthy young and older men sought to determine whether older age affects renal responsiveness to PTH infusion. The authors found that the renal response to PTH infusion and renal vitamin D levels were equivalent in both groups, with the only difference being that the production of vitamin D is somewhat delayed in older adults.[234]

PHOSPHORUS HOMEOSTASIS

More than 99% of body phosphorus is stored in the bones and less than 1% is in the serum in the form of inorganic phosphate (Pi). The maintenance of a narrow range of serum Pi levels is critical for numerous cellular functions, including energy metabolism and bone formation, or as a constituent of phospholipids and nucleic acids. Decline in the GFR with older age leads to reduced levels of non–protein-bound (free) serum calcium, but increased levels of serum phosphate.[235] In response to this, PTH synthesis increases, which in turn decreases the number of sodium phosphate cotransporters in the proximal tubules, thus leading to increased phosphaturia. High serum phosphate levels also stimulate the production of fibroblast growth factor 23 (FGF23), which has been suggested to be involved in regulating normal serum phosphate levels during kidney functional decline and suppressing 1,25 $(OH)_2D_3$ formation. FGF23 levels have been found to increase with declining GFR but not with age per se.[55]

In addition to the hormonal regulation of phosphate levels in aging, animal studies have demonstrated a PTH-independent reduction in the intrinsic tubular capacity to reabsorb phosphate.[236] In this study, kidneys of older thyroparathyroidectomized animals responded to pharmacologic dose of PTH to a lesser extent than younger animals.[236] Others have demonstrated that kidneys in aged animals show impaired phosphate transport in renal tubules in response to a low-phosphate diet.[237,238] It has been proposed that the reason for this impaired phosphate transport is decreased fluidity of a luminal brush border membrane due to the age-related increase in cholesterol and sphingomyelin,[238] which then negatively affects sodium phosphate cotransporter activity directly.[239] The same group later showed that acute and chronic changes in cholesterol differentially affected sodium phosphate cotransporter activity.[240] Whereas acute changes in cholesterol modulate the apical membrane expression of sodium phosphate cotransporter (posttranslational regulation), chronic changes modulate the abundance of this cotransporter (translational regulation).[240] Consistent with in vivo studies, an in vitro study of cultured renal tubular cells harvested from young and adult rats has shown reduced phosphate uptake and adaptation to a phosphate-free medium only in the adult renal cells.[241] Another study has revealed that the reason for the age-related decline in tubular phosphate reabsorption and tubular adaptation to a low dietary phosphate is the lower expression of the renal sodium phosphate cotransporters on the apical brush border membrane.[242]

VITAMIN D HOMEOSTASIS

Older persons commonly exhibit vitamin D insufficiency or deficiency, often in association with a subtle state of chronic inflammation. Serum levels of 25-hydroxyvitamin D (25- [OH]D) are inversely associated with biomarkers of inflammation in older adults, such as C-reactive protein and interleukin 6 (IL-6).[243] It is not known whether these changes are due to primary changes in vitamin D metabolism or to a secondary effect of inflammation. Vitamin D absorption from dietary sources may not be impaired with aging, but reduced dietary intake can contribute to low serum 25-(OH) D levels in aging individuals.[244] The reduced production of 7-deoxyhydrocholestrol in the aging epidermis with ultraviolet exposure is likely involved in the decreased production of pre–vitamin D_3 (cholecalciferol) in older adults.[245] Serum 1,25-$(OH)_2D$ (calcitriol) levels decline in aging, at least in part due to the decline in the GFR and impaired hydroxylation of 25-(OH)D mentioned above.[244] Changes in vitamin D sufficiency or insufficiency in older subjects can modulate left ventricular geometry and participate in the risk of left ventricular hypertrophy in hypertensive older subjects.[246]

It is important to keep in mind the age-related changes of 1,25-$(OH)_2D$ metabolism on intestinal phosphate absorption (described earlier), because several studies have shown that dietary vitamin D supplementation improves renal and intestinal phosphate absorption in vitamin D–deficient animals.[247–249] Regarding the previously mentioned role of cholesterol in the fluidity of the apical brush membrane, it appears that deprivation or administration of vitamin D alters the levels of several fatty acids in this membrane.[250] Therefore, age-related changes in 1,25-$(OH)_2D$ production may potentially have an effect on phosphate reabsorption by modulating lipid content in the apical brush membrane.

Thus, aging has diverse effects on calcium, phosphorus, and vitamin D metabolism. These include a decrease in intestinal absorption of calcium, impaired vitamin D production in the skin, dietary vitamin D deficiency, impaired production of 1,25-$(OH)_2D_3$, increased PTH secretion, lower serum Klotho levels, higher FGF23 levels, and alterations in renal tubular handling of calcium and phosphorus.

ACID-BASE HOMEOSTASIS

The kidneys also play a major role in the regulation of acid-base homeostasis. Normally, during the 24-hour period,

kidneys reabsorb around 4500 mmol of filtered bicarbonate. Kidneys have a large capacity to excrete the endogenously generated proton (H^+) by generating ammonia (NH_3) and its excretion (NH_4^+; see Chapter 16). Older adults are more prone to develop acid-base dysregulation for several reasons. First, age-related structural and functional changes in the kidney lead to reduced adaptive responsiveness to dietary and/or environmental changes. Second, the age-related decline in the GFR reduces the capacity of the kidney to buffer metabolic changes and excrete the excess H^+ load.[251] Along with age-related kidney functional decline, there is also a reduced capacity for bicarbonate conservation and generation, which, combined with the stable endogenous H^+ production, may lead to metabolic acidosis. This process is enhanced and worrisome in patients with concomitant CKD.[252] A community-based observational study of healthy subjects aged 6 to 75 years has found that the capacity for H^+ excretion is similar from childhood to young adulthood, but is significantly reduced in older age.[253]

Ammonium excretion decreases with age. Administration of an acute acid load in 26 healthy men of various ages has demonstrated that despite a prompt increase in acid excretion in all of them, the older subjects excreted a much lower percentage of ingested acid.[254] Interestingly, because reduced acid excretion was equivalent to reduced inulin clearance, acid excretion normalized per the GFR was similar in both young and old subjects. Additional studies in four young and four older subjects who, in addition to acid load, received glutamine, showed equivalent responses of young and old kidneys to glutamine.[254] Taken together, it has been suggested that the age-related decrease in H^+ excretion is due to reduced renal tubular mass, rather than tubular dysfunction.[254] A study of young and old rats who received an acid load was consistent with the human study.[255] After rats received the acid load, total H^+ excretion was reduced in older rats—50% the first day and 25% the second day. Additional insights from this study were the increased activity of the sodium-hydrogen exchanger and decreased phosphate transport in isolated proximal tubules in both age groups.[255]

Overall, these studies suggest that older age appears not to alter the physiologic regulation of acid-base homeostasis but does lead to reduced and diminished responses. The age-related perturbations of acid-base homeostasis seem to influence electrolyte balance. A Swedish study of 85 healthy older individuals has shown an association between net acid excretion and potassium-adjusted magnesuria, irrespective of magnesium intake.[256] Another study of 384 older individuals, followed over 3 years, found that a potassium-rich, alkaline residue (vegetable-rich) diet, which results in increased potassium excretion, was associated with a higher percentage of lean body mass.[257] The protective effect of an alkaline residue diet on muscle mass in older adults is consistent with the opposing effect of an acid residue (red meat-rich) diet. A study of nearly 10,000 participants in the general population has found that a higher dietary acid load is associated with lower serum bicarbonate concentrations; the association is much stronger in middle-aged and older than younger individuals.[258] Consistent with this, a study of older patients with CKD has found that oral sodium bicarbonate supplementation corrects metabolic acidosis, improves serum albumin levels, and decreases whole-body protein degradation.[259] Potassium bicarbonate supplementation in postmenopausal women neutralized the endogenous acid, improved calcium and phosphate balance, and reduced bone reabsorption.[260] This was confirmed in a more recent double-blind study of older men and women—in which particularly bicarbonate and not potassium—had a protective effect on bone reabsorption and calcium excretion.[261] Another recent randomized, double-blind, placebo-controlled study of 52 healthy older men and women has found that oral potassium citrate neutralizes the dietary acid load and has a long-lasting effect to reduce calciuria, without affecting gastrointestinal calcium absorption.[262] Taken together, the results of several studies are consistent with the hypothesis that a higher alkaline residue (vegetarian) diet prevents bone loss in older individuals.

WATER HOMEOSTASIS

Water homeostasis is regulated by a high-gain feedback mechanism that involves the hypothalamus, neurohypophysis, and kidneys.[263,264] In kidneys, the water and sodium from the glomerular filtrate are reabsorbed in tubules through water channel aquaporins (AQPs) and sodium cotransporters.[265–267] The tubular reabsorption of water primarily depends on the driving force (high interstitial osmolality in the deeper medullary zones) and osmotic equilibrium of water across the tubular epithelia (high osmotic water permeability of the membrane). The large majority of glomerular filtrate is reabsorbed in the proximal tubules and descending thin limbs of the loop of Henle.[266,268] The next tubular segments (thin and thick ascending limbs and distal convoluted tubules) are relatively water-impermeable.[269,270] Finally, the main parts of the nephron where vasopressin-based regulation of body water homeostasis occurs are the connecting tubule and collecting duct[271–273] (see also Chapter 15). Both maximum urinary concentration and diluting capacity are decreased by aging,[274] leading to a higher risk for hypernatremia and hyponatremia, respectively.

Findley has proposed an age-related dysfunction of the hypothalamic-renal axis based on clinical observations of increased vasopressin secretion in older age.[275] With older age, maximal urine concentrating ability is particularly reduced.[274] Compared with younger individuals, older adults have about a 50% reduced capacity to conserve water and solutes. Due to the combined effect of age-related changes in body composition, progressive microstructural changes in the kidney, and changes in plasma osmolality and fluid volume, some older adults are more prone to developing disturbances in water homeostasis. One of the major changes in body composition is an increase in total fraction of body fat by 5% to 10% and an equivalent decrease in total body water, so that an older man on average has 7 to 8 fewer liters of total body water than a young man with the same body weight.[276] The obvious consequence is that in the event of acute loss, or overload of body water, a more severe change in osmolality will occur in older men. A study comparing plasma osmolality in older and younger individuals before and after a similar extent of water deprivation has confirmed this presumption.[277] Alterations in water and sodium balance frequently lead to hypo- or hypernatremia associated with hypo- or hypervolemia in older adults.[278,279] In addition, dysfunction in water homeostasis may also occur due to abnormal expression and trafficking of AQPs and solute transporters. For example, an animal

study has shown that the AQP2 transporter involved in urine-concentrating ability is downregulated in the medulla of older rats.[280] This molecular mechanism is consistent with a reduced urine-concentrating ability in older adults. Water homeostasis is also influenced by the previously described microstructural changes that occur with the aging kidney. These changes occurring with healthy aging do not pose an acute threat or have an impact while an individual is healthy. However, in the event of stress, acute disease, volume load, or dehydration, the combined effects of age-related loss of renal mass (i.e., functional reserve) and the change in body composition may cause a significant disruption in water and solute homeostasis.[281,282]

One of the consequences of the age-related GFR decline is an increase in filtrate reabsorption in the proximal tubules and decreased fluid delivery to the distal diluting tubules, resulting in a reduced diluting capacity of the kidney.[283] This is evidenced by a reduced ability to excrete a free water load[277] or reduced maximal free water clearance in older adults.[283] In addition to the reduced diluting capacity, older kidneys also lose the capacity to conserve water during states of dehydration.[284] Interestingly, another study has demonstrated that the reduced capacity of water conservation occurs regardless of high plasma vasopressin levels; thus, this is most likely due to intrinsic renal factors.[285] Taken together, therefore, these age-related changes may have significant clinical implications, such as worsening of dehydration in older adults in the setting of vomiting, diarrhea, or reduced water and food intake.

Vasopressin secretion, the renal response to vasopressin, and thirst control are also affected by aging. Vasopressin secretion in the hypothalamus is under the delicate control of osmoreceptors in and around the organum vasculosum of the lamina terminalis and the anterior wall of the third ventricle in the brain. Most studies have found that basal vasopressin concentrations in the healthy older are usually higher than in younger controls.[276] One study has reported no age-related differences in basal vasopressin levels,[286] whereas another study has found that basal vasopressin may actually be lower in older individuals.[287] Nevertheless, most studies about water homeostasis in aging have shown that compared with younger individuals, older adults have a greater increase of vasopressin secretion per unit change in plasma osmolality, and this is consistent with the higher osmoreceptor sensitivity in older adults.[288]

Vasopressin regulates renal water excretion by controlling the abundance of the water channel AQP2 and its insertion into the apical membrane of epithelial cells in the distal nephron and collecting tubules.[289] In the membrane, AQP2 proteins form channels that allow reabsorption of water molecules from the lumen of the collecting ducts into the medullary interstitium driven by the medullary osmotic gradient. Given that vasopressin levels are mostly found to be higher in older adults, a potential secretory defect in the pituitary gland is improbable and cannot explain the age-related reduced renal response to vasopressin. Animal studies have offered potential explanations for the reduced renal response to vasopressin, which include reduced expression of vasopressin receptors in the collecting ducts and impaired second messenger response to vasopressin receptor signaling. One study has demonstrated that despite a normal vasopressin secretory response, there is an age-related reduction in renal concentrating ability after moderate water restriction.[290] This occurred due to the lower expression of AQP2 water channels in older rats and an impaired ability to upregulate AQP2 production. Other animal studies have proposed that reduced vasopressin receptor signaling significantly hinders the medullary concentrating gradient required for urine concentration.[289,290]

Normally, stimulation of thirst osmoreceptors in the hypothalamus signals the higher cerebral cortex to develop a conscious perception of thirst and water-seeking behavior. Aging also affects thirst control.[291] One study has demonstrated that water-deprived older men do not show a subjective thirst increase or mouth dryness.[287] Moreover, when access to water was allowed, compared with younger participants, older adults consumed less water and were unable to restore serum and plasma osmolality to predeprivation levels.[287] This finding suggests that older adults have a reduced thirst response to osmotic changes. It has been proposed that they may have a higher osmolal set point for thirst—that is, for a given plasma osmolality, older adults have a reduced degree of perceived thirst, thus leading to less water intake.[292] Maximum diluting capacity is mildly impaired in older adults, largely a reflection of the reduced GFR.[293] The minimum urinary osmolality (Uosm) after a water load averages about 90 mOsm/kg H_2O in subjects older than 70 years, whereas in younger subjects the value is about 50 mOsm/kg H_2O. If solute excretion is reduced (e.g., with protein or salt restriction), the mild impairment of diluting capacity can expose older patients to water excess syndromes (hyponatremia), with only modest intakes of free water. For example, at a Uosm of 90 mOsm/kg H_2O (maximum dilution in older adults) and a daily osmolal excretion of 360 mOsm/day (about half of normal levels), the maximal electrolyte free water intake would be about 4 L/day. Any free water intake in excess of this value would lead to dilutional hyponatremia.

Thus, aging undoubtedly influences water homeostasis in many different ways. Water conservation (urinary concentrating ability) is primarily affected, although a mild form of impaired diluting capacity may also be present. This is important to keep in mind, not only during the diagnostic process, but also while taking care of older adults and planning for different clinical, surgical, or pharmacologic interventions. Alterations in solute intake (e.g., protein or sodium) in older adults can also have profound effects on water homeostasis.

RENAL ENDOCRINE CHANGES WITH AGING

RENIN-ANGIOTENSIN-ALDOSTERONE SYSTEM

Aging is associated with a decline in plasma renin activity (PRA), serum aldosterone levels, and urinary aldosterone excretion rates, accompanied by reduced responses to actions that stimulate the RAAS, such as upright posture or salt depletion.[62,63] This state is known as *aging-associated hyporeninemic hypoaldosteronism*. Both renal renin formation and release are reduced in aging.[294] In addition, activity of the RAAS has been linked to aging phenomena in a pathogenic fashion.[295] Defects in renal NO generation can be linked to reduced activity of the RAAS in aging.[10] The activity of the RAAS can also be linked to canonical Wnt signaling,[10] and both can be dysregulated in the aging process.[8] Although a decline in activity of the RAAS regularly occurs with aging (independently of gender), neither a change in renal perfusion

pressure or delivery of solute to the macula densa appears to be involved.[10] Increased ANP levels, reduced sympathetic nervous system activity, or both can be seen with aging and might be involved in the perturbations of the RAAS seen with aging.[10] Reduced renal renin generation with aging appears to be a posttranslational phenomenon due to impaired release of stored renin.[10] Trivial changes in ACE activity and angiotensinogen conversion occur in aging.[10] The sensitivity of the glomerular afferent and efferent vessels to angiotensin II appear to increase with aging.[10] Treatment of animals (rats) with an age-dependent decline in renal function and proteinuria can reduce proteinuria and glomerulosclerosis, but this does not have any effect on glomerulomegaly or the snGFR.[8,10] Distinguishing the effects of aging per se and superimposed disease states (e.g., low nephron endowment) on the RAAS can be very difficult.

Aldosterone production and serum and urinary aldosterone levels are lower in older adults compared with younger persons,[296] and there may also be reduced aldosterone responsivity to elevations in serum potassium levels.[297] In addition, there are age-related changes in adrenal aldosterone synthetase–producing cells, causing islands or clusters of aldosterone-producing cells in the adrenal cortex of aging humans. These may be precursors of aldosterone-secreting adenomas in some cases.[296]

ERYTHROPOIETIN

Serum levels of erythropoietin (EPO) levels tend to increase with age, even in nonanemic subjects.[297,298] This might be in compensation for increased (subclinical) blood loss, accelerated red blood cell turnover (decreased erythrocyte half-life), or increased resistance of red cell precursors to the effect of EPO.[298] Testosterone deficiency might be involved in the latter phenomenon.[299] A mild anemia (hemoglobin <12 g/dL) is fairly common in aging, but this varies by geography.[300] In about one-third of these subjects, a nutritional deficiency (e.g., iron, folate, vitamin B_{12}) is responsible, in one-third, a concomitant chronic disease is the culprit (e.g., CKD, cancer, infection), but in one-third no precise cause can be determined.[300] Independent of anemia, high spontaneous EPO levels in older adults are associated with an increased risk of congestive heart failure, but not myocardial infarction or progressive CKD.[301] The mechanisms responsible for this association are not well understood, but could be due to tissue hypoxia in low-perfusion states associated with heart failure.

IMPLICATIONS OF NORMAL PHYSIOLOGY ON RENAL FUNCTION

This has effects on the diagnosis and prognosis of chronic kidney disease in aging adults.

DIAGNOSIS

The diagnosis of CKD has been codified by the Kidney Disease Outcomes Quality Initiative (KDOQI) and Kidney Disease: Improving Global Outcomes (KDIGO) clinical practice guideline initiatives,[302,303] published in 2002 and 2013, respectively, as well as others from more regional formulations, such as NICE in the United Kingdom and CARI in Australia.[304,305] These classification and categorization recommendations rely principally on the GFR (estimated or measured, in mL/min/1.73 m^2) and albuminuria (usually the urinary albumin-to-creatinine ratio [uACR], in mg/g or mg/mmol] in spot urine samples; see also Chapters 23 and 30). However, other signs of renal injury, such as abnormal urinalyses (e.g., hematuria), imaging, or renal biopsy findings could lead to a diagnosis of CKD, even with a normal GFR (even adjusted for age) or uACR. Abnormalities in these biomarkers must persist for at least 3 months to qualify as a valid indicator of CKD, a requirement that is frequently not met in many epidemiologic studies that are carried out only once. When these classification schemes were developed, it was arbitrarily decided that any adult subject, 20 years of age or older, with a persisting GFR of less than 60 mL/min/1.73 m^2, could be classified as having CKD (category 3A, 3B, 4, or 5), irrespective of any other signs of renal injury, including abnormal urinalysis, albuminuria, imaging, or renal pathology. Thus, a persisting GFR of 45 to 59 mL/min/1.73^2 could lead to a diagnosis of CKD (category 3A) in an adult. This guideline created a conundrum because values of the GFR in this range can also be observed in healthy older adults. The lower limit of normal for the measured GFR (mGFR) in a healthy adult 60 to 69 years of age is about 55 mL/min/1.73 m^2 and, for an adult 70 to 79 years of age, it is about 49 mL/min/1.73 m^2.[133] Significant overlap is present between the threshold for classifying CKD (independent of age) and the normal values for GFR in older adults. The lower value for the GFR in older adults is a manifestation of a physiologic process of nephron loss unaccompanied by compensatory hyperfiltration in the residual nephrons (see above), so it is difficult to conflate these findings as a disease. Not surprisingly, a substantial and continuing debate has arisen concerning the utility of an absolute threshold for defining CKD, based on the GFR alone, without any modification for age.[306–310] Because abnormal albuminuria is not consistent with normal, healthy human aging, this controversy largely focuses on possible overdiagnosis in older adults of the G3A/a1 category of CKD (GFR, 45 to 59 mL/min/1.73 m^2 and uACR of <30 mg/g [3 mg/mmol]) according to KDIGO.[311] The GFR may fall below 45 mL/min/1.73 m^2 in subjects older than 80 years, but it can be very difficult to determine if such subjects are entirely healthy because they frequently have concomitant disorders, such as cancer, heart failure, dietary protein deficiency, and sarcopenia. This can complicate evaluation of the GFR (mGFR or eGFR). In addition, significant comorbidity and biochemical abnormalities are commonly observed in individuals older than 60 years of age, compounding the difficulty of ascertaining kidney health based on the GFR alone.[312,313]

Typically, the GFR values used in categorizing CKD are estimates rather than measured values. This use of estimating formulas for the GFR (eGFR) results in another conundrum in the diagnosis of CKD in aging—namely, the imprecision and variability in eGFR formulas for evaluating the true GFR in older adults[312] (discussed further in Chapters 59 and 84). In a population-wide study of community-living adults, Ebert and coworkers[312] found the prevalence of CKD categories 3, 4, and 5 (eGFR <60 mL/min/1.73 m^2) in subjects 70 to 79 years of age to range between 16% and 52%, depending on the formula used to estimate the GFR. The corresponding value for subjects 80 to 89 years of age were 42% to 84%.

The lowest values for CKD prevalence were found using the CKD-EPI creatinine equation; the highest values were found using the Berlin Initiative Study (BIS)-1 creatinine equation.[312] In subjects older than 70 years of age, the BIS-1 creatine equation is a more precise estimate of mGFR compared with the CKD-EPI equation, at least in a European, largely white population.[314] Estimating formulas for GFR when applied at the population level generally give high values for CKD prevalence (≈11%– 14%),[315] especially when the formulas were derived from a largely CKD cohort. Much lower values for CKD are observed when eGFR formulas are derived from a normal healthy cohort[316]

The use of cystatin C–based GFR estimating equations (alone or in combination with creatinine-based equations) has been advanced as a tool to aid in the diagnosis of CKD. In 2012, KDIGO suggested measuring eGFR-creatinine-cystatin C and eGFR-cystatin C in adults (including older adults) when the eGFR-creatinine is 45 to 59 mL/min/1.73 m^2 (and no other markers of CKD are present). If eGFR-cystatin C or eGFR-creatinine-cystatin C are less than 60 mL/min/1.73 m^2, the diagnosis of CKD is confirmed.[303] The degree to which these suggestions specifically apply to older adults has not been rigorously tested and may depend on the form of the eGFR-cystatin C or eGFR-creatinine-cystatin C equation. For example, in older adults, the BIS-2 cystatin C equation is a more accurate estimate of mGFR than the CKD-EPI-cystatin C equation.[314] Other eGFR equations, such as the FAS-creatinine, FAS-cystatin C equation, or Lund-Malmo creatinine equation need further evaluation for improving the precision and accuracy of the diagnosis of CKD in older adults using the eGFR alone, but early studies have shown great promise for the utility of these equations in an older population.[317]

It must also be recalled that cystatin C is a mid-molecular-weight (13.3 kD) serine proteinase inhibitor involved in the inflammatory response.[318] It is normally filtered and then completely destroyed by tubular reabsorption and degradation. Very little cystatin C is present in normal urine. Thus, production rates of cystatin C are difficult to assess and can vary in many states (e.g., obesity, diabetes, thyroid disease, inflammation) commonly found in older adults. Like creatinine, there are many non-GFR determinants of its serum concentration, the variable used in calculation of the eGFR.[319,320] In older adults, loss of muscle mass (sarcopenia) may lower serum creatinine values relative to the measured GFR and give rise to an overestimate of mGFR by eGFR creatinine equations. However, serum cystatin C levels tend not be affected greatly by muscle mass or gender, and not at all by ancestry. In contrast, in older adults with chronic inflammation (of any cause), obesity, diabetes, and the metabolic syndrome may alter cystatin C production, leading to underestimation of the mGFR. The combination of eGFR-creatinine-cystatin C may give a slightly more accurate assessment of the true GFR in population-based studies,[321] but there will still be much individual variation.[322–324] Tracking eGFR-cystatin C with metabolic factors that can contribute to CVD complicates its suitability as a biomarker for CVD risk related to the GFR in older adults.[325] In addition, endothelial injury consequent to inflammation or capillary hypertension might further impair the transglomerular permeability coefficient for cystatin C (the shrunken pore theory),[326] giving rise to reduced cystatin C eGFR values relative to the inulin or iohexol mGFR.[326] Furthermore, a low serum albumin level (perhaps reflecting subtle degrees of chronic inflammation) is associated with reduced eGFR-creatinine in older frail subjects.[327]

Direct comparisons of a gold standard method of measuring the GFR and estimating formulas for the GFR in aging subjects are relatively uncommon, but both the BIS[314] and Reykjavik older cohort studies[322] have provided much valuable information. In the latter study, the Lund-Malmo and full age spectrum (FAS) creatinine equation have somewhat higher accuracy than the CKD-EPI-creatinine formula. The CKD-EPI, Lund-Malmo, and FAS creatinine-based equations were roughly equivalent for the detection of a mGFR less than 60 mL/min/1.73 m^2. All formulas incorporating a cystatin C measurement exhibited consistent improvements in accuracy compared with the corresponding creatinine-based equations. The relevance of these findings to the diagnosis of CKD in individual older subjects needs further study, but they clearly demonstrate some of the pitfalls in using creatinine-based eGFR formulas for the older adult population.

Thus, the effects of physiologic renal aging on the GFR confound its use as the defining characteristic of CKD in older adults because CKD is a diagnosis made most frequently in older adults with category 3A CKD (GFR, 45–59 mL/min/1.73 m^2), usually with normal albuminuria (category A1; uACR <30 mg/g [3 mg/mmol]). This conundrum raises an issue of possible overdiagnosis and mislabeling of CKD, both at the individual and population-wide level, that distorts evaluation of the true societal burden of CKD. When added to the false-positive identification of CKD in single epidemiologic studies (see above), this leads to the possibility that CKD is not as common as it is alleged to be, and calls for revising the definition of CKD in older adults should be taken seriously. The vagaries of estimating equations for the GFR in older adults cannot be ignored.[328]

PROGNOSIS

In the KDIGO classification of CKD, the prognosis for adverse events (all-cause mortality, ESKD, doubling of serum creatinine level, CVD [e.g., ischemic heart disease, congestive heart failure, stroke]) is the third dimension of the scheme. This is usually displayed as a multicolored heat map of the rising risk of events—green, no added risk; red, high risk—often determined from large-scale epidemiologic studies.[302,303] The risk values are usually stated as relative risk or odds ratio compared with some arbitrary control group, often those with eGFR greater than 60 mL/min/1.73 m^2 and no signs of renal injury (e.g., normal uACR). These prognosis- based heat maps are commonly assembled from data acquired from single time point epidemiologic studies, so that the persistence of the CKD-defining abnormality (eGFR, uACR, or both) is not confirmed. When a more rigorous assessment of chronicity is pursued, it has been noted that such single time point studies commonly overestimate the prevalence of CKD by as much as 30% due to false-positives.[329]

The use of the eGFR to evaluate prognosis is also confounded by the fact that an age variable is included in all adult estimating formulas to adjust for the effects of age per se on the synthesis and production biomarker (creatinine or cystatin C). The age coefficients in these formulas are optimized for estimating the mGFR, not prognostication for all-cause mortality or ESKD risk. However, when the values

obtained by such estimates are applied to prognostication, the age variable becomes important, because age, independent of the GFR, has a marked influence on some of the risks evaluated, such as mortality. If an estimating equation using one or more biomarkers that accurately assess GFR, without a requirement for the age variable, were developed, the accuracy of the risk prediction might be improved and made comparable to that found with the true GFR. It should be stressed that although the number and size of studies using the mGFR as the dependent variable in prognostic evaluation are relatively small in comparison to the large-scale, eGFR-based epidemiologic studies, the patterns linking the GFR to outcome are similar. These studies describe a pattern of a threshold (nonlinear) relationship, in which the threshold varies according to age.[330] With albuminuria, the risks varies in a log-linear fashion with the uACR, independent of age, and without a threshold (above normal values). When one compares the relative risk of all-cause mortality using a reference value for the GFR that approximates the normal young adult mean value (≈107 mL/min/1.73 m^2), then the minimum relative risk for an all-cause mortality event is above an eGFR of 75 mL/min/1.73 m^2 for subjects 18 to 54 years of age, but above 45 mL/min/1.73 m^2 for those older than 75 years.[331] The relative risk of all-cause mortality relative to a declining eGFR is blunted by advancing age, but the absolute rates of all-cause mortality remain high with aging. This analysis strongly suggests that with a prognosis-dominated matrix for creating a GFR threshold for CKD, an age-stratified approach is desirable. It is noteworthy that the remaining life expectancy at any age older than about 35 years is not materially affected until the eGFR falls below about 45 mL/min/1.73 m^2.[332–334] Adding an age stratification to the existing scheme for identifying true CKD and its associated risks has proven to be a challenging task. Simple adjustments, such as altering the threshold of eGFR to <45 mL/min/1.73 m^2 for subjects without abnormal albuminuria who are older than 65 years, may be useful, but result in unintended consequences, like the so-called birthday paradox (when a 64-year-old reaches a 65th birthday, CKD is "cured").

Other methods of age stratification for CKD diagnosis have been advanced that may have greater practicality in large health care systems for improved triage.[335] Creation of multiple age-stratified heat maps using the eGFR and estimates of prognosis for all-cause mortality may also be helpful.[336] Whatever the solution may be to this ongoing conundrum of defining CKD and its risks in aging subjects, it is imperative also to recognize that the specific formula for identifying the eGFR as the variable introduces a complexity of its own due to the variability of bias, precision, and accuracy among the numerous estimating formulas and biomarkers used, especially when applied to older adults. For example, the eGFR-creatinine formulas do not add much to the prediction of CVD (and thereby all-cause mortality) risk in older adults, whereas eGFR-cystatin C formulas do, despite not being superior to eGFR-creatinine for estimating the mGFR.[325] Both formulas can incrementally increase the accuracy of CVD risk prediction (see later).

CARDIOVASCULAR DISEASE AND DECLINE IN THE GLOMERULAR FILTRATION RATE WITH AGING

There is little doubt that a progressive decline in the GFR is associated with an increased risk of fatal or nonfatal CVD, including atherosclerotic CVD and congestive heart failure (CHF), sudden cardiac death, nonvalvular atrial fibrillation, stroke, and peripheral vascular disease. Cross-sectional, population-based epidemiologic studies cannot easily determine whether these associations are causal or not. In fact, the existence of CVD may itself result in a decline in the GFR (e.g., severe CHF, atherosclerotic renovascular diseases, ischemic nephropathy), thus confounding the directional nature of the observed associations. Aging itself can be a mechanism for some of the associations between a decline in the GFR and CVD, but this can be adjusted for by examining the CVD prevalence in older subjects with a better-preserved GFR. However, the fact that the GFR declines regularly with aging requires that the comparator group used for such adjustments have GFR values (on average) similar to those predicted for by normal physiologic aging. Teasing out age-related GFR decline from pathologic GFR decline in an aging individual can be difficult, but the demonstration of other biomarkers of renal injury, such as the presence of abnormal albuminuria or abnormal imaging, can be very helpful (abnormal albuminuria does not occur with healthy aging).[91] The threshold for a GFR-related augmentation of CVD risk is likely to be age-dependent. In studies of older individuals, the risk of excess CVD events seem to appear at an eGFR less than 45 mL/min/1.73 m^2 (category 3B CKD),[333] but this will likely be modified by the nature and severity of comorbidities present, such as dyslipidemia, diabetes, or long-standing hypertension. A decreased GFR can influence the risk of CVD, independent of the traditional risk factors (e.g., obesity, smoking, dyslipidemia, diabetes, hypertension), but the magnitude of the additional risk for CVD events imposed by a reduced GFR in the range of 45 to 59 mL/min/1.73 m^2 is small in older adults. For this reason, a reduced GFR is not commonly included in CVD risk prediction scoring systems (e.g., Framingham Risk Score, American College of Cardiology/American Heart Association [ACC/AHA] pooled risk prediction model).[337]

As discussed in detail in other chapters (see Chapters 40 and 54), more advanced forms of CKD can augment the CVD risk by numerous mechanisms, including endothelial cell or vascular wall injury from uremic toxins, vascular ossification, myocardial hypertrophy and pathologic remodeling, chronic volume expansion, chronic inflammation, uremic dyslipidemia (proatherogenic high-density lipoprotein [HDL], hypertriglyceridemia), arterial hypertension, and thrombotic microangiopathy. The fundamental phenomenon of aging can interact with these pathologic processes in numerous ways that are very difficult to disentangle unambiguously.

END-STAGE RENAL DISEASE AND AGING

A requirement for treatment by renal replacement modalities (renal replacement therapy [RRT]; dialysis and/or transplantation) is not uncommon in older adults. According to the US Renal Data System (USRDS) Annual Report in 2017, the age-specific annual incidence rate for RRT for subjects 75 years of age or older was about 1600 per million population (pmp) and, for those 65 to 74 years of age, was about 1250 pmp in 2015 (www.usrds.org). Both these values have been slowly declining (for uncertain reasons) since about 2010 but are still well above the average (all-age) RRT incident rate of 378 pmp/year. As has been the case for

many years, males outnumber females for incident counts of RRT by about 20% to 30%. For pre-ESKD CKD, the male-to-female ratio is exactly the opposite (www.usrds.org). However, this may in part be artifactual due to the gender coefficient in eGFR creatinine equations, which give women lower eGFR values, and the lower muscle mass in women than men, which increases their ACR. The precursors of ESKD are the earlier stages (categories) of CKD, some of which progress, at varying rates, to ESKD. An important consideration of the development of RRT requiring ESKD is the competing risk of death, usually from a CVD or neoplasia event. This risk is magnified in older adults so that at an advanced age, any patient with CKD category 3 (eGFR, 30–59 mL/min/1.73 m^2) is more likely to die before reaching ESKD.[338]

In a landmark study, Eriksen and Ingebretsen conducted a 10-year, population- based study in Tromso, Norway, including subjects (median age, 75 years; interquartile range [IQR], 67.7–80.4 years) with confirmed CKD category 3.[340] About 70% of the subjects experienced some decline in the eGFR over time, somewhat slower in females than in males. The 10-year cumulative risk of reaching treated ESKD was 4% (greater in men than in women), whereas the cumulative risk of death was 51% (greater in men than in women). The prognosis of CKD and the eventual likelihood of requiring RRT was highly gender-dependent and greatly influenced by the competing risk of death. In another key study, O'Hare and coworkers[338] studied 209,622 US veterans (97% male; mean age, 73 ± 9 years) with category 3 to 5 CKD followed for a mean of 3.2 years. Although the rates of death and ESKD were inversely related to the eGFR value at baseline irrespective of age, at comparable levels of eGFR, older age was associated with higher death rates and a lower rate of ESKD treatment. The threshold of eGFR below which the rate of ESKD exceeded the risk of death was about 15 mL/min/1.73 m^2 for subjects 65 to 84 years of age. As with the Eriksen and Ingebretsen study,[340] the rate of decline of the eGFR was slower in the older subjects. The effect of gender could not be examined in this study. Nevertheless, both these studies clearly indicated that both age and gender are important modifying factors for the transition from CKD (category 3–5) to treated ESKD.

The impact of age on the association of eGFR and albuminuria on outcomes of mortality and treated ESKD were also studied in an exhaustive analysis of 2,051,244 participants from 33 general population or high-risk CVD cohorts and 13 CKD cohorts by Hallan and colleagues in the CKD Prognosis Consortium.[330] In most of these cohorts, the eGFR values were determined only once, and CKD was not confirmed by the duration criteria, leading to the possibility of a high false-positive rate for the identification of CKD. In addition, the analysis used a single reference value of 80 mL/min/1.73 m^2 for the eGFR. The study showed a roughly comparable hazard ratio for the risk of ESKD with declining eGFR at all ages, but the average absolute rate of ESKD declined substantially with age as a function of the declining eGFR, consistent with the observations discussed above. The relative and absolute risks for ESKD both increased as the uACR rose above 10 mg/g, but the magnitude of these risks were somewhat blunted in much older adults (>75 years). Although a threshold of about 60 mL/min/1.73 m^2 was noted for defining an increased relative risk of ESKD at all ages, the choice of a single reference comparator of 80 mL/min/1.73 m^2 (rather than the lowest risk group for age as the reference comparator) might have influenced the findings, as discussed above in relationship to the impact of the eGFR on all-cause mortality at varying ages). It is noteworthy that the absolute rate of ESKD in the very old (>75 years) did not increase above baseline values until the eGFR was well below 45 mL/min/1.73 m^2.

In a longitudinal study conducted by Shardlow and colleagues[341,342] in the United Kingdom, older subjects (mean age, 73 years) with category 3 CKD (mean eGFR, 53 mL/min/1.73 m^2) had a low prevalence of abnormal albuminuria (16%). After 5 years of additional follow-up, they had a low prevalence of ESKD (0.2%), progression to a higher stage of CKD occurred in 17.7%, remissions of CKD developed in 19.3%, and stable renal function was observed in 34.1%. Albuminuria at diagnosis was a key risk factor for progression. In this study, 14.2% died before the 5-year follow-up and 14.8% were lost to follow-up.

ACUTE KIDNEY INJURY AND DISEASES OF THE KIDNEY AND URINARY TRACT IN AGING

A strong relationship exists between the incidence and prevalence of AKI and age.[343] The pathophysiologic mechanisms underlying this association are complex and multifactorial (discussed further in Chapter 28). The physiologic reduction of nephron number and GFR with advancing age, discussed above, alters the pharmacokinetics of many water-soluble drugs. This can lead to an accumulation of nephrotoxic levels of agents in body fluids, leading to AKI.[344] Dosage modifications, primarily in the interval between dosing, rather than in loading dosage, are required to minimize such risks.[198] Agents that affect glomerular hemodynamics, such as NSAIDs or RAAS inhibitors, can cause a reduction in the GFR in aging subjects that is more profound than in younger subjects, particularly when combined with some degree of extracellular volume depletion. Older subjects also may have a comorbidity that exposes them to an episode of AKI, such as CHF, diabetes, urosepsis, and cancer, and require more interventions that may predispose to AKI, such as surgery and angiography. As discussed later, aging is also associated with an increased prevalence of diseases of the kidney and urinary tract that may directly cause AKI.

DISEASES OF THE KIDNEY AND URINARY TRACT IN AGING

The occurrence of specific diseases of the kidneys and urinary tract can be influenced markedly by the age of a subject. These diseases are discussed in detail in Chapters 36, 37, and 41 and will not be elaborated further here. Certain glomerular and vascular diseases have a predilection to affect older adults (Box 22.2).[31,345–347] Benign prostatic hypertrophy is common in older men and can result in lower urinary tract obstruction and CKD, sometimes irreversible. Obstructive uropathy can also be the consequence of ureteric involvement in gynecologic cancer in older women and bladder dysfunction associated with neurologic diseases and diabetes.

Box 22.2 Kidney and Urinary Tract Diseases That Occur More Commonly in Older Adults

Glomerular and Vascular Diseases

Crescentic glomerulonephritis due to systemic or renal-limited antineutrophil cytoplasmic autoantibody (ANCA)–associated vasculitis
Membranous nephropathy (primary and cancer-related)
Monoclonal immunoglobulin deposition diseases (AL amyloidosis and nonamyloid types)
Diabetic nephropathy
Fibrillary glomerulonephritis
Anti–glomerular basement membrane (GBM) disease (mainly females)
Atheroembolic disease
Atheromatous renovascular stenosis

Tubulointerstitial Diseases

Acute kidney injury (toxic or ischemic cause)
Lymphomatous infiltration
Renal cell cancer

Urinary Tract Disorders

Lower urinary tract obstruction due to prostate disease
Ureteric obstruction from cancer (cervical cancer in females)
Transitional cell carcinoma of the bladder
Prostate cancer

CAN RENAL AGING BE MODIFIED?

As the molecular mechanisms of organ senescence are gradually revealed, it is natural to ask about their potential for modification.[348–351] This is a difficult question because the biologic processes are so complex and are active over an extended time period. In addition, it is necessary to make a clear distinction between the effects of interventions directed at diseases associated with aging (e.g., better glycemic control in diabetes, avoidance of obesity, control of hypertension) and the modification of the fundamental aging process itself. So far, no elixir of life or "fountain of youth" has been discovered, but several promising avenues have been identified. Caloric restriction, mTOR inhibition, and RAAS blockade all retard aging across many animal species,[352] but their effects in humans are less well understood for obvious reasons. It is possible that all three of these approaches converge on mitochondrial energy production to slow aging. The angiotensin II type I receptor may play a pivotal role in renal senility,[352] independent of angiotensin II, perhaps via a sirtuin-linked mechanism.[352,353] However, because normal healthy aging, with the steady attrition of glomeruli, is not usually accompanied by albuminuria or a rise in the snGFR (see above), the prospects of RAAS inhibition as a means of retarding the rate of renal aging are not promising. Caloric restriction seems to cause a reduction in renal fibrosis (via mTOR inhibition and 5'-adenosine monophosphate-activated protein kinase [AMPK] activation).[35,353] Calorie restriction and mTOR inhibition activates sirtuin 1, which has antiaging properties. Other agents, such as the biguanide metformin, may also have antiaging effects via an action on the AMPK/mTOR pathway.[354] Telomere shortening can be modulated by telomerase activity, but whether the manipulation of telomere length will be safe and effective in delaying organ senescence is unknown. Modulating Klotho expression pharmacologically might have beneficial effects, via reduced oxidative stress. Elimination of senescent cells (senolytic therapy) by targeting apoptosis of senescent cells (TASCs) via disruption of the FOX04 peptide-p53 interaction, shows great promise in improving renal function in aging mice.[355,356] Resveratrol, a polyphenol present in many pigmented vegetables and fruits, can ameliorate aging as a calorie restriction mimetic, possibly by improving the metabolic profile and inhibiting cyclic adenosine monophosphate (cAMP) phosphodiesterases and the AMPK pathway.[357] Because an imbalance of energy demand and energy supply may underlie aging, a reprogramming of metabolism from anaerobic glycolysis to aerobic glycolysis might be an effective strategy.[5] Antifibrosis regimens, such as with the transforming growth factor beta (TGF-β)/smad pathway inhibition, BMP-7 administration, or the use of other agents, represents a promising avenue of research,[339,358] especially in the domain of renal aging. Translating studies carried out in lower animals (e.g., *Caenorhabditis elegans*, mice, rats) to the human organism will be tedious, time-consuming, and fraught with obstacles. Armed with new tools, however, such as nephron number quantification, it may be possible to test some of the most promising strategies directly in humans. Hopefully, in the not too distant future, renal aging will not be inevitable, even though immortality will of course continue to be an elusive goal.

Complete reference list available at ExpertConsult.com.

KEY REFERENCES

2. Robert L, Fulop T. Aging: facts and theories. *Interdiscip Top Gerontol.* 2014;39:1–215.
7. Epstein M. Aging and the kidney. *J Am Soc Nephrol.* 1996;7(8):1106–1122. Review.
23. Bitzer M, Wiggins J. Aging biology in the kidney. *Adv Chronic Kidney Dis.* 2016;23(1):12–18. doi:10.1053/j.ackd.2015.11.005. Review.
30. Choudhury D, Levi M. Aging and kidney Disease. In: *Brenner and Rector, the Kidney.* 10th ed. New York: Elsevier; 2015:727–751.
60. Yang HC, Fogo AB. Fibrosis and renal aging. *Kidney Int Suppl (2011).* 2014;4(1):75–78. Review.
63. Conti S, Cassis P, Benigni A. Aging and the renin-angiotensin system. *Hypertension.* 2012;60(4):878–883. [Epub 2012 Aug 27]; Review.
68. Inker LA, Okparavero A, Tighiouart H, et al. Midlife blood pressure and late-life GFR and albuminuria: an elderly general population cohort. *Am J Kidney Dis.* 2015;66(2):240–248. doi:10.1053/j.ajkd.2015.03.030. [Epub 2015 May 16].
71. Luyckx VA, Brenner BM. Birth weight, malnutrition and kidney-associated outcomes–a global concern. *Nat Rev Nephrol.* 2015;11(3):135–149. doi:10.1038/nrneph.2014.251. [Epub 2015 Jan 20]; Review.
86. Denic A, Alexander MP, Kaushik V, et al. Detection and clinical patterns of nephron hypertrophy and nephrosclerosis among apparently healthy adults. *Am J Kidney Dis.* 2016;68:58–67.
88. Denic A, Lieske JC, Chakkera HA, et al. The substantial loss of nephrons in healthy human kidneys with aging. *J Am Soc Nephrol.* 2017;28:313–320.
91. Rule AD, Amer H, Cornell LD, et al. The association between age and nephrosclerosis on renal biopsy among healthy adults. *Ann Intern Med.* 2010;152:561–567.
106. Thomson SC, Vallon V, Blantz RC. Kidney function in early diabetes: the tubular hypothesis of glomerular filtration. *Am J Physiol Renal Physiol.* 2004;286:F8–F15.
109. Hodgin JB, Bitzer M, Wickman L, et al. Glomerular aging and focal global glomerulosclerosis: a podometric perspective. *J Am Soc Nephrol.* 2015;26:3162–3178.

114. Denic A, Mathew J, Nagineni VV, et al. Clinical and pathology findings associate consistently with larger glomerular volume. *J Am Soc Nephrol.* 2018;29(7):1960–1969. [Epub 2018 May 22]; Erratum in: *J Am Soc Nephrol.* 2018;29(9):2445.
116. Rule AD, Semret MH, Amer H, et al. Association of kidney function and metabolic risk factors with density of glomeruli on renal biopsy samples from living donors. *Mayo Clin Proc.* 2011;86:282–290.
124. Martin JE, Sheaff MT. Renal ageing. *J Pathol.* 2007;211:198–205.
128. Lindeman RD, Tobin J, Shock NW. Longitudinal studies on the rate of decline in renal function with age. *J Am Geriatr Soc.* 1985;33:278–285.
133. Pottel H, Delanaye P, Weekers L, et al. Age-dependent reference intervals for estimated and measured glomerular filtration rate. *Clin Kidney J.* 2017;10(4):545–551. doi:10.1093/ckj/sfx026. [Epub 2017 Apr 28].
135. Cohen E, Nardi Y, Krause I, et al. A longitudinal assessment of the natural rate of decline in renal function with age. *J Nephrol.* 2014;27(6):635–641.
139. Denic A, Mathew J, Lerman LO, et al. Single-nephron glomerular filtration rate in healthy adults. *N Engl J Med.* 2017;376:2349–2357.
145. Hoang K, Tan JC, Derby G, et al. Determinants of glomerular hypofiltration in aging humans. *Kidney Int.* 2003;64(4):1417–1424.
147. Chakkera HA, Denic A, Kremers WK, et al. Comparison of high glomerular filtration rate thresholds for identifying hyperfiltration. *Nephrol Dial Transplant.* 2018;doi:10.1093/ndt/gfy332. [Epub ahead of print].
160. De Moor B, Vanwalleghem JF, Swennen Q, et al. Haemodynamic or metabolic stimulation tests to reveal the renal functional response: requiem or revival? *Clin Kidney J.* 2018;11(5):623–654.
164. Reckelhoff JF, Samsell L, Dey R, et al. The effect of aging on glomerular hemodynamics in the rat. *Am J Kidney Dis.* 1992;20(1):70–75.
175. Glassock RJ, Rule AD. The implications of anatomical and functional changes of the aging kidney: with an emphasis on the glomeruli. *Kidney Int.* 2012;82:270–277.
198. Frame AA, Wainford RD. Mechanisms of altered renal sodium handling in age-related hypertension. *Am J Physiol Renal Physiol.* 2018;315(1):F1–F6.
205. Kyle UG, Genton L, Hans D, et al. Age-related differences in fat-free mass, skeletal muscle, body cell mass and fat mass between 18 and 94 years. *Eur J Clin Nutr.* 2001;55:663–672.
230. Kuro-o M, Matsumura Y, Aizawa H, et al. Mutation of the mouse klotho gene leads to a syndrome resembling ageing. *Nature.* 1997; 390:45–51.
233. Musso CG, Juarez R, Vilas M, et al. Renal calcium, phosphorus, magnesium and uric acid handling: comparison between stage III chronic kidney disease patients and healthy oldest old. *Int Urol Nephrol.* 2012;44:1559–1562.
246. Ameri P, Canepa M, Milaneschi Y, et al. Relationship between vitamin D status and left ventricular geometry in a healthy population: results from the Baltimore Longitudinal Study of Aging. *J Intern Med.* 2013;273(3):253–262.
258. Amodu A, Abramowitz MK. Dietary acid, age, and serum bicarbonate levels among adults in the United States. *Clin J Am Soc Nephrol.* 2013;8:2034–2042.
274. Sands JM. Urine concentrating and diluting ability during aging. *J Gerontol A Biol Sci Med Sci.* 2012;67:1352–1357.
281. Beck LH. The aging kidney. Defending a delicate balance of fluid and electrolytes. *Geriatrics.* 2000;55:26–28, 31–32.
297. Mulkerrin E, Epstein FH, Clark BA. Aldosterone responses to hyperkalemia in healthy older humans. *J Am Soc Nephrol.* 1995;6(5): 1459–1462.
298. Ershler WB, Sheng S, McKelvey J, et al. Serum erythropoietin and aging: a longitudinal analysis. *J Am Geriatr Soc.* 2005;53(8):1360–1365.
307. Glassock R, Delanaye P, El Nahas M. An age-calibrated classification of chronic kidney disease. *JAMA.* 2015;314(6):559–560.
308. Levey AS, Inker LA, Coresh J. Chronic kidney disease in older people. *JAMA.* 2015;314(6):557–558.
312. Ebert N, Jakob O, Gaedeke J, et al. Prevalence of reduced kidney function and albuminuria in older adults: the Berlin Initiative Study. *Nephrol Dial Transplant.* 2017;32(6):997–1005.
315. Glassock RJ, Warnock DG, Delanaye P. The global burden of chronic kidney disease: estimates, variability and pitfalls. *Nat Rev Nephrol.* 2017;13(2):104–114.
317. Pottel H, Delanaye P, Schaeffner E, et al. Estimating glomerular filtration rate for the full age spectrum from serum creatinine and cystatin C. *Nephrol Dial Transplant.* 2017;32(3):497–507.
323. Meeusen JW, Rule AD, Voskoboev N, et al. Performance of cystatin C- and creatinine-based estimated glomerular filtration rate equations depends on patient characteristics. *Clin Chem.* 2015;61(10):1265–1272.
324. Fan L, Levey AS, Gudnason V, et al. Comparing GFR estimating equations using cystatin C and creatinine in older individuals. *J Am Soc Nephrol.* 2015;26(8):1982–1989.
325. Nerpin E, Ingelsson E, Risérus U, et al. The combined contribution of albuminuria and glomerular filtration rate to the prediction of cardiovascular mortality in older men. *Nephrol Dial Transplant.* 2011;26(9):2820–2827.
326. Grubb A, Lindström V, Jonsson M, et al. Reduction in glomerular pore size is not restricted to pregnant women. Evidence for a new syndrome: 'Shrunken pore syndrome'. *Scand J Clin Lab Invest.* 2015;75(4):333–340.
330. Hallan SI, Matsushita K, Sang Y, et al. Age and association of kidney measures with mortality and end-stage renal disease. *JAMA.* 2012;308(22):2349–2360.
331. Denic A, Glassock RJ, Rule AD. Structural and functional changes with the aging kidney. *Adv Chronic Kidney Dis.* 2016;23(1):19–28.
332. Gansevoort RT, Correa-Rotter R, Hemmelgarn BR, et al. Chronic kidney disease and cardiovascular risk: epidemiology, mechanisms, and prevention. *Lancet.* 2013;382(9889):339–352.
336. Warnock DG, Delanaye P, Glassock RJ. Risks for all-cause mortality: stratified by age, estimated glomerular filtration rate and albuminuria. *Nephron.* 2017;136(4):292–297.
338. O'Hare AM, Choi AI, Bertenthal D, et al. Age affects outcomes in chronic kidney disease. *J Am Soc Nephrol.* 2007;18(10):2758–2765.
341. Shardlow A, McIntyre NJ, Fluck RJ, et al. Chronic kidney disease in primary care: outcomes after five years in a prospective cohort study. *PLoS Med.* 2016;13(9):e1002128.
346. Jin B, Zeng C, Ge Y, et al. The spectrum of biopsy-proven kidney diseases in elderly Chinese patients. *Nephrol Dial Transplant.* 2014;29(12):2251–2259.
351. Kanasaki K, Kitada M, Koya D. Pathophysiology of the aging kidney and therapeutic interventions. *Hypertens Res.* 2012;35(12):1121–1128.

REFERENCES

1. Finch CE, Kirkwood TBL. *Chance, Development and Aging*. Oxford: Oxford University Press; 2000.
2. Robert L, Fulop T. Aging: facts and theories. *Interdiscip Top Gerontol*. 2014;39:1–215.
3. Vijg J, Le Bourg E. Aging and the Inevitable Limit to Human Life Span. *Gerontology*. 2017;63(5):432–434. doi:10.1159/000477210. [Epub 2017 May 17]; PubMed PMID: 28511176.
4. van den Berg N, Beekman M, Smith KR, et al. Historical demography and longevity genetics: back to the future. *Ageing Res Rev*. 2017;38:28–39. doi:10.1016/j.arr.2017.06.005. [Epub 2017 Jul 5]; Review. PubMed PMID: 28689042.
5. Feng Z, Hanson RW, Berger NA, et al. Reprogramming of energy metabolism as a driver of aging. *Oncotarget*. 2016;7(13):15410–15420. doi:10.18632/oncotarget.7645. Review. PubMed PMID: 26919253. PubMed Central PMCID: PMC4941250.
6. Kaysen GA, Myers BD. The aging kidney. *Clin Geriatr Med*. 1985; 1(1):207–222. Review. PubMed PMID: 3913500.
7. Epstein M. Aging and the kidney. *J Am Soc Nephrol*. 1996;7(8):1106–1122. Review. PubMed PMID: 8866401.
8. Baylis C, Schmidt R. The aging glomerulus. *Semin Nephrol*. 1996; 16(4):265–276. Review. PubMed PMID: 8829265.
9. Thomas SE, Anderson S, Gordon KL, et al. Tubulointerstitial disease in aging: evidence for underlying peritubular capillary damage, a potential role for renal ischemia. *J Am Soc Nephrol*. 1998;9(2):231–242. PubMed PMID: 9527399.
10. Baylis C, Corman B. The aging kidney: insights from experimental studies. *J Am Soc Nephrol*. 1998;9(4):699–709. Review. PubMed PMID: 9555673.
11. Schlanger L. Kidney senesceence. Geriatric nephrology curriculum. *Am Soc Nephrol*. 2009;1–7.
12. Weinstein JR, Anderson S. The aging kidney: physiological changes. *Adv Chronic Kidney Dis*. 2010;17(4):302–307. doi:10.1053/j.ackd.2010.05.002. Review. PubMed PMID: 20610357. PubMed Central PMCID: PMC2901622.
13. Rodríguez-Castro EM, Córdova HR. Aging and the kidney. *Bol Asoc Med P R*. 2011;103(3):57–62. Review. PubMed PMID: 23210336.
14. Perico N, Remuzzi G, Benigni A. Aging and the kidney. *Curr Opin Nephrol Hypertens*. 2011;20(3):312–317. doi:10.1097/MNH.0b013e328344c327. Review. PubMed PMID: 21358327.
15. John GB, Cheng CY, Kuro-o M. Role of Klotho in aging, phosphate metabolism, and CKD. *Am J Kidney Dis*. 2011;58(1):127–134. doi:10.1053/j.ajkd.2010.12.027. [Epub 2011 Apr 15]; Review. PubMed PMID: 21496980. PubMed Central PMCID: PMC3191324.
16. Sataranatarajan K, Feliers D, Mariappan MM, et al. Molecular events in matrix protein metabolism in the aging kidney. *Aging Cell*. 2012;11(6):1065–1073. doi:10.1111/acel.12008. [Epub 2012 Oct 19]; PubMed PMID: 23020145. PubMed Central PMCID: PMC5812369.
17. Wiggins JE. Aging in the glomerulus. *J Gerontol A Biol Sci Med Sci*. 2012;67(12):1358–1364. doi:10.1093/gerona/gls157. [Epub 2012 Jul 25]; Review. PubMed PMID: 22843670. PubMed Central PMCID: PMC3636672.
18. Karam Z, Tuazon J. Anatomic and physiologic changes of the aging kidney. *Clin Geriatr Med*. 2013;29(3):555–564. doi:10.1016/j.cger.2013.05.006. Review. PubMed PMID: 23849007.
19. Bolignano D, Mattace-Raso F, Sijbrands EJ, et al. The aging kidney revisited: a systematic review. *Ageing Res Rev*. 2014;14:65–80. doi:10.1016/j.arr.2014.02.003. [Epub 2014 Feb 15]; Review. PubMed PMID: 24548926.
20. Wang X, Bonventre JV, Parrish AR. The aging kidney: increased susceptibility to nephrotoxicity. *Int J Mol Sci*. 2014;15(9):15358–15376. doi:10.3390/ijms150915358. Review. PubMed PMID: 25257519. PubMed Central PMCID: PMC4200815.
21. Schmitt R, Susnik N, Melk A. Molecular aspects of renal senescence. *Curr Opin Organ Transplant*. 2015;20(4):412–416. doi:10.1097/MOT.0000000000000214. Review. PubMed PMID: 26126196.
22. O'Sullivan ED, Hughes J, Ferenbach DA. Renal aging: causes and consequences. *J Am Soc Nephrol*. 2017;28(2):407–420. doi:10.1681/ASN.2015121308. [Epub 2016 Nov 15]; Review. PubMed PMID: 28143966. PubMed Central PMCID: PMC5280008.
23. Bitzer M, Wiggins J. Aging biology in the kidney. *Adv Chronic Kidney Dis*. 2016;23(1):12–18. doi:10.1053/j.ackd.2015.11.005. Review. PubMed PMID: 26709058.
24. Schmitt R, Melk A. Molecular mechanisms of renal aging. *Kidney Int*. 2017;92(3):569–579. doi:10.1016/j.kint.2017.02.036. [Epub 2017 Jul 18]; Review. PubMed PMID: 28729036.
25. Gekle M. Kidney and aging - A narrative review. *Exp Gerontol*. 2017;87(Pt B):153–155. doi:10.1016/j.exger.2016.03.013. [Epub 2016 Mar 24]; Review. PubMed PMID: 27032877.
26. Sobamowo H, Prabhakar SS. The kidney in aging: physiological changes and pathological implications. *Prog Mol Biol Transl Sci*. 2017;146:303–340. doi:10.1016/bs.pmbts.2016.12.018. [Epub 2017 Feb 13]; Review. PubMed PMID: 28253989.
27. Sturmlechner I, Durik M, Sieben CJ, et al. Cellular senescence in renal ageing and disease. *Nat Rev Nephrol*. 2017;13(2):77–89. doi:10.1038/nrneph.2016.183. [Epub 2016 Dec 28]; Review. PubMed PMID: 28029153.
28. Shiels PG, McGuinness D, Eriksson M, et al. The role of epigenetics in renal ageing. *Nat Rev Nephrol*. 2017;13(8):471–482. doi:10.1038/nrneph.2017.78. [Epub 2017 Jun 19]; Review. PubMed PMID: 28626222.
29. Hommos MS, Glassock RJ, Rule AD. Structural and functional changes in human kidneys with healthy aging. *J Am Soc Nephrol*. 2017;28(10):2838–2844. doi:10.1681/ASN.2017040421. [Epub 2017 Aug 8]; Review. PubMed PMID: 28790143. PubMed Central PMCID: PMC5619977.
30. Choudhury D, Levi M. Aging and kidney Disease. In: *Brenner and Rector, the Kidney*. 10th ed. New York: Elsevier; 2015:727–751.
31. Nunez JFM, Cameron JS, Oreopoulos DG, eds. *The Aging Kidney in Health and Disease*. New York: Springer; 2008.
32. López-Otín C, Blasco MA, Partridge L, et al. The hallmarks of aging. *Cell*. 2013;153(6):1194–1217. doi:10.1016/j.cell.2013.05.039. Review. PubMed PMID: 23746838. PubMed Central PMCID: PMC3836174.
33. Chistiakov DA, Sobenin IA, Revin VV, et al. Mitochondrial aging and age-related dysfunction of mitochondria. *Biomed Res Int*. 2014;2014:238463. doi:10.1155/2014/238463. [Epub 2014 Apr 10]; Review. PubMed PMID: 24818134. PubMed Central PMCID: PMC4003832.
34. Davies JMS, Cillard J, Friguet B, et al. The Oxygen Paradox, the French Paradox, and age-related diseases. *Geroscience*. 2017;39(5–6):499–550. doi:10.1007/s11357-017-0002-y. [Epub 2017 Dec 21]; Review. PubMed PMID: 29270905. PubMed Central PMCID: PMC5745211.
35. Dong D, Cai GY, Ning YC, et al. Alleviation of senescence and epithelial-mesenchymal transition in aging kidney by short-term caloric restriction and caloric restriction mimetics via modulation of AMPK/mTOR signaling. *Oncotarget*. 2017;8(10):16109–16121. doi:10.18632/oncotarget.14884. PubMed PMID: 28147330. PubMed Central PMCID: PMC5369951.
36. Takabatake Y, Kimura T, Takahashi A, et al. Autophagy and the kidney: health and disease. *Nephrol Dial Transplant*. 2014;29(9):1639–1647. doi:10.1093/ndt/gft535. [Epub 2014 Feb 10]; Review. PubMed PMID: 24520117.
37. Lenoir O, Tharaux PL, Huber TB. Autophagy in kidney disease and aging: lessons from rodent models. *Kidney Int*. 2016;90(5):950–964. doi:10.1016/j.kint.2016.04.014. [Epub 2016 Jun 18]; Review. PubMed PMID: 27325184.
38. Han X, Tai H, Wang X, et al. AMPK activation protects cells from oxidative stress-induced senescence via autophagic flux restoration and intracellular NAD(+) elevation. *Aging Cell*. 2016;15(3):416–427. doi:10.1111/acel.12446. [Epub 2016 Feb 18]; PubMed PMID: 26890602. PubMed Central PMCID: PMC4854918.
39. Jankauskas SS, Pevzner IB, Andrianova NV, et al. The age-associated loss of ischemic preconditioning in the kidney is accompanied by mitochondrial dysfunction, increased protein acetylation and decreased autophagy. *Sci Rep*. 2017;7:44430. doi:10.1038/srep44430. PubMed PMID: 28294175. PubMed Central PMCID: PMC5353572.
40. Chuang PY, Cai W, Li X, et al. Reduction in podocyte SIRT1 accelerates kidney injury in aging mice. *Am J Physiol Renal Physiol*. 2017;313(3):F621–F628. doi:10.1152/ajprenal.00255.2017. [Epub 2017 Jun 14]; PubMed PMID: 28615249. PubMed Central PMCID: PMC5625108.
41. Huang W, Liu H, Zhu S, et al. Sirt6 deficiency results in progression of glomerular injury in the kidney. *Aging (Albany NY)*. 2017;9(3):1069–1083. doi:10.18632/aging.101214. PubMed PMID: 28351995. PubMed Central PMCID: PMC5391219.
42. Lowe D, Horvath S, Raj K. Epigenetic clock analyses of cellular senescence and ageing. *Oncotarget*. 2016;7(8):8524–8531. doi:10.18632/

oncotarget.7383. PubMed PMID: 26885756. PubMed Central PMCID: PMC4890984.
43. Marioni RE, Shah S, McRae AF, et al. DNA methylation age of blood predicts all-cause mortality in later life. *Genome Biol.* 2015;16:25. doi:10.1186/s13059-015-0584-6. PubMed PMID: 25633388. PubMed Central PMCID: PMC4350614.
44. Rizvi S, Raza ST, Mahdi F. Telomere length variations in aging and age-related diseases. *Curr Aging Sci.* 2014;7(3):161–167. Review. PubMed PMID: 25612739.
45. De Vusser K, Pieters N, Janssen B, et al. Telomere length, cardiovascular risk and arteriosclerosis in human kidneys: an observational cohort study. *Aging (Albany NY).* 2015;7(10):766–775.
46. Shay JW, Wright WE. Hayflick, his limit, and cellular ageing. *Nat Rev Mol Cell Biol.* 2000;1(1):72–76. doi:10.1038/35036093. PubMed PMID: 11413492.
47. Ullrich NJ, Gordon LB. Hutchinson-Gilford progeria syndrome. *Handb Clin Neurol.* 2015;132:249–264. doi:10.1016/B978-0-444-62702-5.00018-4. Review. PubMed PMID: 26564085.
48. Ben Chehida A, Ghali N, Ben Abdelaziz R, et al. Renal involvement in 2 siblings with Cockayne syndrome. *Iran J Kidney Dis.* 2017;11(3):253–255. PubMed PMID: 28575888.
49. Gan W, Liu XL, Yu T, et al. Urinary 8-oxo-7,8-dihydroguanosine as a Potential Biomarker of Aging. *Front Aging Neurosci.* 2018;10:34. doi:10.3389/fnagi.2018.00034. eCollection 2018. PubMed PMID: 29535624. PubMed Central PMCID: PMC5835306.
50. Noordmans GA, Hillebrands JL, van Goor H, et al. A roadmap for the genetic analysis of renal aging. *Aging Cell.* 2015;14(5):725–733. doi:10.1111/acel.12378. [Epub 2015 Jul 29]; Review. PubMed PMID: 26219736. PubMed Central PMCID: PMC4568960.
51. Rodwell GE, Sonu R, Zahn JM, et al. A transcriptional profile of aging in the human kidney. *PLoS Biol.* 2004;2(12):e427. [Epub 2004 Nov 30]; PubMed PMID: 15562319. PubMed Central PMCID: PMC532391.
52. Noordmans GA, Huang Y, Savage H, et al. Genetic analysis of intracapillary glomerular lipoprotein deposits in aging mice. *PLoS ONE.* 2014;9(10):e111308. doi:10.1371/journal.pone.0111308. eCollection 2014. PubMed PMID: 25353171. PubMed Central PMCID: PMC4213026.
53. Lim JH, Kim EN, Kim MY, et al. Age-associated molecular changes in the kidney in aged mice. *Oxid Med Cell Longev.* 2012;2012:171383. doi:10.1155/2012/171383. [Epub 2012 Dec 30]; PubMed PMID: 23326623. PubMed Central PMCID: PMC3544311.
54. Inagi R. Glycative stress and glyoxalase in kidney disease and aging. *Biochem Soc Trans.* 2014;42(2):457–460. doi:10.1042/BST20140007. Review. PubMed PMID: 24646260.
55. Koyama D, Sato Y, Aizawa M, et al. Soluble αKlotho as a candidate for the biomarker of aging. *Biochem Biophys Res Commun.* 2015;467(4):1019–1025. doi:10.1016/j.bbrc.2015.10.018. [Epub 2015 Oct 14]; PubMed PMID: 26462468.
56. Zeng Y, Wang PH, Zhang M, et al. Aging-related renal injury and inflammation are associated with downregulation of Klotho and induction of RIG-I/NF-κB signaling pathway in senescence-accelerated mice. *Aging Clin Exp Res.* 2016;28(1):69–76. doi:10.1007/s40520-015-0371-y. [Epub 2015 May 19]; PubMed PMID: 25986237.
57. Kalaitzidis RG, Duni A, Siamopoulos KC. Klotho, the Holy Grail of the kidney: from salt sensitivity to chronic kidney disease. *Int Urol Nephrol.* 2016;48(10):1657–1666. doi:10.1007/s11255-016-1325-9. [Epub 2016 May 23]; Review. PubMed PMID: 27215557.
58. Drew DA, Katz R, Kritchevsky S, et al. Association between soluble Klotho and change in kidney function: the health aging and body composition study. *J Am Soc Nephrol.* 2017;28(6):1859–1866. doi:10.1681/ASN.2016080828. [Epub 2017 Jan 19]; PubMed PMID: 28104822. PubMed Central PMCID: PMC5461794.
59. Humphreys BD. Mechanisms of renal fibrosis. *Annu Rev Physiol.* 2018;80:309–326. doi:10.1146/annurev-physiol-022516-034227. [Epub 2017 Oct 25]; PubMed PMID: 29068765.
60. Yang HC, Fogo AB. Fibrosis and renal aging. *Kidney Int Suppl (2011).* 2014;4(1):75–78. Review. PubMed PMID: 26312154. PubMed Central PMCID: PMC4536965.
61. Uneda K, Wakui H, Maeda A, et al. Angiotensin II type 1 receptor-associated protein regulates kidney aging and lifespan independent of angiotensin. *J Am Heart Assoc.* 2017;6(8):pii: e006120. doi:10.1161/JAHA.117.006120. PubMed PMID: 28751545. PubMed Central PMCID: PMC5586453.
62. Yoon HE, Choi BS. The renin-angiotensin system and aging in the kidney. *Korean J Intern Med.* 2014;29(3):291–295. doi:10.3904/kjim.2014.29.3.291. [Epub 2014 Apr 29]; Review. PubMed PMID: 24851061. PubMed Central PMCID: PMC4028516.
63. Conti S, Cassis P, Benigni A. Aging and the renin-angiotensin system. *Hypertension.* 2012;60(4):878–883. doi:10.1161/HYPERTENSIONAHA.110.155895. [Epub 2012 Aug 27]; Review. PubMed PMID: 22926952.
64. Okada A, Nangaku M, Jao TM, et al. D-serine, a novel uremic toxin, induces senescence in human renal tubular cells via GCN2 activation. *Sci Rep.* 2017;7(1):11168. doi:10.1038/s41598-017-11049-8. PubMed PMID: 28894140. PubMed Central PMCID: PMC5593843.
65. Roncal-Jimenez CA, Ishimoto T, Lanaspa MA, et al. Aging-associated renal disease in mice is fructokinase dependent. *Am J Physiol Renal Physiol.* 2016;311(4):F722–F730. doi:10.1152/ajprenal.00306.2016. [Epub 2016 Jul 27]; PubMed PMID: 27465991. PubMed Central PMCID: PMC5142232.
66. Lin CH, Chen J, Zhang Z, et al. Endostatin and transglutaminase 2 are involved in fibrosis of the aging kidney. *Kidney Int.* 2016;89(6):1281–1292. doi:10.1016/j.kint.2016.01.030. [Epub 2016 Apr 14]; PubMed PMID: 27165830. PubMed Central PMCID: PMC4868664.
67. Bucala R. Diabetes, aging, and their tissue complications. *J Clin Invest.* 2014;124(5):1887–1888. doi:10.1172/JCI75224. [Epub 2014 May 1]; Review. PubMed PMID: 24789881. PubMed Central PMCID: PMC4001559.
68. Inker LA, Okparavero A, Tighiouart H, et al. Midlife blood pressure and late-life GFR and albuminuria: an older general population cohort. *Am J Kidney Dis.* 2015;66(2):240–248. doi:10.1053/j.ajkd.2015.03.030. [Epub 2015 May 16]; PubMed PMID: 25987258. PubMed Central PMCID: PMC4516633.
69. Zürbig P, Decramer S, Dakna M, et al. The human urinary proteome reveals high similarity between kidney aging and chronic kidney disease. *Proteomics.* 2009;9(8):2108–2117. doi:10.1002/pmic.200800560. PubMed PMID: 19296547. PubMed Central PMCID: PMC2768386.
70. Delaney A, Padmanabhan V, Rezvani G, et al. Evolutionary conservation and modulation of a juvenile growth-regulating genetic program. *J Mol Endocrinol.* 2014;52(3):269–277. doi:10.1530/JME-13-0263. Print 2014 Jun. PubMed PMID: 24776848. PubMed Central PMCID: PMC4051439.
71. Luyckx VA, Brenner BM. Birth weight, malnutrition and kidney-associated outcomes–a global concern. *Nat Rev Nephrol.* 2015;11(3):135–149. doi:10.1038/nrneph.2014.251. [Epub 2015 Jan 20]; Review. PubMed PMID: 25599618.
72. Friedenberg MJ, Walz BJ, McAlister WH, et al. Roentgen size of normal kidneys: computers analysis of 1,286 cases. *Radiology.* 1965;84:1022–1030.
73. McLachlan M, Wasserman P. Changes in sizes and distensibility of the aging kidney. *Br J Radiol.* 1981;54:488–491.
74. Emamian SA, Nielsen MB, Pedersen JF, et al. Kidney dimensions at sonography: correlation with age, sex, and habitus in 665 adult volunteers. *AJR Am J Roentgenol.* 1993;160:83–86.
75. Gourtsoyiannis N, Prassopoulos P, Cavouras D, et al. The thickness of the renal parenchyma decreases with age: a CT study of 360 patients. *AJR Am J Roentgenol.* 1990;155:541–544.
76. Glodny B, Unterholzner V, Taferner B, et al. Normal kidney size and its influencing factors - a 64-slice MDCT study of 1.040 asymptomatic patients. *BMC Urol.* 2009;9:19.
77. Bax L, van der Graaf Y, Rabelink AJ, et al. Influence of atherosclerosis on age-related changes in renal size and function. *Eur J Clin Invest.* 2003;33:34–40.
78. Johnson S, Rishi R, Andone A, et al. Determinants and functional significance of renal parenchymal volume in adults. *Clin J Am Soc Nephrol.* 2011;6:70–76.
79. Roseman DA, Hwang SJ, Oyama-Manabe N, et al. Clinical associations of total kidney volume: the Framingham Heart Study. *Nephrol Dial Transplant.* 2016.
80. Wang X, Vrtiska TJ, Avula RT, et al. Age, kidney function, and risk factors associate differently with cortical and medullary volumes of the kidney. *Kidney Int.* 2014;85:677–685.
81. Baert L, Steg A. Is the diverticulum of the distal and collecting tubules a preliminary stage of the simple cyst in the adult? *J Urol.* 1977;118:707–710.
82. Rule AD, Sasiwimonphan K, Lieske JC, et al. Characteristics of renal cystic and solid lesions based on contrast-enhanced computed tomography of potential kidney donors. *Am J Kidney Dis.* 2012;59:611–618.

83. Eknoyan G. A clinical view of simple and complex renal cysts. *J Am Soc Nephrol.* 2009;20:1874–1876.
84. Schwarz A, Lenz T, Klaen R, et al. Hygroma renale: pararenal lymphatic cysts associated with renin-dependent hypertension (Page kidney). Case report on bilateral cysts and successful therapy by marsupialization. *J Urol.* 1993;150:953–957.
85. Lorenz EC, Vrtiska TJ, Lieske JC, et al. Prevalence of renal artery and kidney abnormalities by computed tomography among healthy adults. *Clin J Am Soc Nephrol.* 2010;5:431–438.
86. Denic A, Alexander MP, Kaushik V, et al. Detection and clinical patterns of nephron hypertrophy and nephrosclerosis among apparently healthy adults. *Am J Kidney Dis.* 2016;68:58–67.
87. Hoy WE, Ingelfinger JR, Hallan S, et al. The early development of the kidney and implications for future health. *J Dev Orig Health Dis.* 2010;1:216–233.
88. Denic A, Lieske JC, Chakkera HA, et al. The substantial loss of nephrons in healthy human kidneys with aging. *J Am Soc Nephrol.* 2017;28:313–320.
89. Hoy WE, Douglas-Denton RN, Hughson MD, et al. A stereological study of glomerular number and volume: preliminary findings in a multiracial study of kidneys at autopsy. *Kidney Int Suppl.* 2003; S31–S37.
90. Hayman JM, Martin JW, Miller M. Renal function and the number of glomeruli in the human kidney. *Arch Intern Med.* 1939;64:69–83.
91. Rule AD, Amer H, Cornell LD, et al. The association between age and nephrosclerosis on renal biopsy among healthy adults. *Ann Intern Med.* 2010;152:561–567.
92. Vazquez Martul E, Veiga Barreiro A. Importance of kidney biopsy in graft selection. *Transplant Proc.* 2003;35:1658–1660.
93. Kremers WK, Denic A, Lieske JC, et al. Distinguishing age-related from disease-related glomerulosclerosis on kidney biopsy: the Aging Kidney Anatomy study. *Nephrol Dial Transplant.* 2015;30: 2034–2039.
94. Hommos MS, Zeng C, Liu Z, et al. Global glomerulosclerosis with nephrotic syndrome; the clinical importance of age adjustment. *Kidney Int.* 2018;93(5):1175–1182. doi:10.1016/j.kint.2017.09.028. [Epub 2017 Dec 19]; PubMed PMID: 29273332. PubMed Central PMCID: PMC5911429.
95. Fogo AB. Causes and pathogenesis of focal segmental glomerulosclerosis. *Nat Rev Nephrol.* 2015;11:76–87.
96. Jennette JC, Charles L, Grubb W. Glomerulomegaly and focal segmental glomerulosclerosis associated with obesity and sleep-apnea syndrome. *Am J Kidney Dis.* 1987;10:470–472.
97. Bailey RR, Lynn KL, Burry AF, et al. Proteinuria, glomerulomegaly and focal glomerulosclerosis in a grossly obese man with obstructive sleep apnea syndrome. *Aust N Z J Med.* 1989;19:473–474.
98. Marcantoni C, Ma LJ, Federspiel C, et al. Hypertensive nephrosclerosis in African Americans versus Caucasians. *Kidney Int.* 2002;62(1):172–180.
99. Hoy WE, Hughson MD, Kopp JB, et al. APOL1 risk alleles are associated with exaggerated age-related changes in glomerular number and volume in African-American adults: an autopsy study. *J Am Soc Nephrol.* 2015;26(12):3179–3189. doi:10.1681/ASN.2014080768. [Epub 2015 Jun 2]; PubMed PMID: 26038529. PubMed Central PMCID: PMC4657832.
100. Meyer TW, Lenihan CR. Glomerular Effects of Age and APOL1. *J Am Soc Nephrol.* 2015;26(12):2901–2903. doi:10.1681/ASN.2015040459. [Epub 2015 Jun 2]; PubMed PMID: 26038527. PubMed Central PMCID: PMC4657849.
101. Grams ME, Rebholz CM, Chen Y, et al. Race, APOL1 risk, and eGFR decline in the general population. *J Am Soc Nephrol.* 2016;27(9):2842–2850. doi:10.1681/ASN.2015070763. [Epub 2016 Mar 10]; PubMed PMID: 26966015. PubMed Central PMCID: PMC5004654.
102. Tsuboi N, Utsunomiya Y, Kanzaki G, et al. Low glomerular density with glomerulomegaly in obesity-related glomerulopathy. *Clin J Am Soc Nephrol.* 2012;7:735–741.
103. Tsuboi N, Koike K, Hirano K, et al. Clinical features and long-term renal outcomes of Japanese patients with obesity-related glomerulopathy. *Clin Exp Nephrol.* 2013;17:379–385.
104. Tsuboi N, Utsunomiya Y, Hosoya T. Obesity-related glomerulopathy and the nephron complement. *Nephrol Dial Transplant.* 2013;28(suppl 4):iv108–iv113.
105. Chakkera HA, Chang YH, Thomas LF, et al. Obesity correlates with glomerulomegaly but is not associated with kidney dysfunction early after donation. *Transplant Direct.* 2015;1:1–6.
106. Thomson SC, Vallon V, Blantz RC. Kidney function in early diabetes: the tubular hypothesis of glomerular filtration. *Am J Physiol Renal Physiol.* 2004;286:F8–F15.
107. Abdi R, Slakey D, Kittur D, et al. Heterogeneity of glomerular size in normal donor kidneys: impact of race. *Am J Kidney Dis.* 1998;32:43–46.
108. Fulladosa X, Moreso F, Narvaez JA, et al. Estimation of total glomerular number in stable renal transplants. *J Am Soc Nephrol.* 2003;14:2662–2668.
109. Hodgin JB, Bitzer M, Wickman L, et al. Glomerular aging and focal global glomerulosclerosis: a podometric perspective. *J Am Soc Nephrol.* 2015;26:3162–3178.
110. Darmady EM, Offer J, Woodhouse MA. The parameters of the ageing kidney. *J Pathol.* 1973;109:195–207.
111. Nyengaard JR, Bendtsen TF. Glomerular number and size in relation to age, kidney weight, and body surface in normal man. *Anat Rec.* 1992;232:194–201.
112. Tan JC, Busque S, Workeneh B, et al. Effects of aging on glomerular function and number in living kidney donors. *Kidney Int.* 2010;78:686–692.
113. Hayslett JP, Kashgarian M, Epstein FH. Functional correlates of compensatory renal hypertrophy. *J Clin Invest.* 1968;47:774–799.
114. Denic A, Mathew J, Nagineni VV, et al. Clinical and pathology findings associate consistently with larger glomerular volume. *J Am Soc Nephrol.* 2018;29(7):1960–1969. doi:10.1681/ASN.2017121305. [Epub 2018 May 22]; Erratum in: *J Am Soc Nephrol.* 2018;29(9):2445. PubMed PMID: 29789431. PubMed Central PMCID: PMC6050922.
115. Elsherbiny HE, Alexander MP, Kremers WK, et al. Nephron hypertrophy and glomerulosclerosis and their association with kidney function and risk factors among living kidney donors. *Clin J Am Soc Nephrol.* 2014;9:1892–1902.
116. Rule AD, Semret MH, Amer H, et al. Association of kidney function and metabolic risk factors with density of glomeruli on renal biopsy samples from living donors. *Mayo Clin Proc.* 2011;86:282–290.
117. Liu JS, Ishikawa I, Horiguchi T. Incidence of acquired renal cysts in biopsy specimens. *Nephron.* 2000;84:142–147.
118. Konda R, Sato H, Hatafuku F, et al. Expression of hepatocyte growth factor and its receptor C-met in acquired renal cystic disease associated with renal cell carcinoma. *J Urol.* 2004;171: 2166–2170.
119. Burchfiel CM, Tracy RE, Chyou PH, et al. Cardiovascular risk factors and hyalinization of renal arterioles at autopsy. The Honolulu Heart Program. *Arterioscler Thromb Vasc Biol.* 1997;17:760–768.
120. Kubo M, Kiyohara Y, Kato I, et al. Risk factors for renal glomerular and vascular changes in an autopsy-based population survey: the Hisayama study. *Kidney Int.* 2003;63:1508–1515.
121. Ninomiya T, Kubo M, Doi Y, et al. Prehypertension increases the risk for renal arteriosclerosis in autopsies: the Hisayama Study. *J Am Soc Nephrol.* 2007;18:2135–2142.
122. Hughson MD, Puelles VG, Hoy WE, et al. Hypertension, glomerular hypertrophy and nephrosclerosis: the effect of race. *Nephrol Dial Transplant.* 2014;29:1399–1409.
123. Robbins S, Kumar V. *Robbins and Cotran Pathologic Basis of Disease.* 8th ed. Philadelphia: Saunders/Elsevier; 2010.
124. Martin JE, Sheaff MT. Renal ageing. *J Pathol.* 2007;211:198–205.
125. Mancilla E, Avila-Casado C, Uribe-Uribe N, et al. Time-zero renal biopsy in living kidney transplantation: a valuable opportunity to correlate predonation clinical data with histological abnormalities. *Transplantation.* 2008;86:1684–1688.
126. Kriz W, Lemley KV. A potential role for mechanical forces in the detachment of podocytes and the progression of CKD. *J Am Soc Nephrol.* 2015;26(2):258–269. doi:10.1681/ASN.2014030278. [Epub 2014 Jul 24]; Review. PubMed PMID: 25060060. PubMed Central PMCID: PMC4310663.
127. Davies DF, Shock NW. Age changes in glomerular filtration rate, effective renal plasma flow, and tubular excretory capacity in adult males. *J Clin Invest.* 1950;29:496–507.
128. Lindeman RD, Tobin J, Shock NW. Longitudinal studies on the rate of decline in renal function with age. *J Am Geriatr Soc.* 1985;33:278–285.
129. Eriksen BO, Lochen ML, Arntzen KA, et al. Subclinical cardiovascular disease is associated with a high glomerular filtration rate in the nondiabetic general population. *Kidney Int.* 2014;86:146–153.
130. Rule AD, Larson TS, Bergstralh EJ, et al. Using serum creatinine to estimate glomerular filtration rate: accuracy in good health and in chronic kidney disease. *Ann Intern Med.* 2004;141:929–937.

131. Murata K, Baumann NA, Saenger AK, et al. Relative performance of th e MDRD and CKD-EPI equations for estimating glomerular filtration rate among patients with varied clinical presentations. *Clin J Am Soc Nephrol.* 2011;6:1963–1972.
132. Rule AD, Gussak HM, Pond GR, et al. Measured and estimated GFR in healthy potential kidney donors. *Am J Kidney Dis.* 2004;43(1):112–119. Erratum in: *Am J Kidney Dis.* 2004;44(6):1126. *Am J Kidney Dis.* 2005;46(1):170. PubMed PMID: 14712434.
133. Pottel H, Delanaye P, Weekers L, et al. Age-dependent reference intervals for estimated and measured glomerular filtration rate. *Clin Kidney J.* 2017;10(4):545–551. doi:10.1093/ckj/sfx026. [Epub 2017 Apr 28]; PubMed PMID: 28852494. PubMed Central PMCID: PMC5570001.
134. Baba M, Shimbo T, Horio M, et al. Longitudinal Study of the Decline in Renal Function in Healthy Subjects. *PLoS ONE.* 2015;10(6):e0129036. doi:10.1371/journal.pone.0129036. eCollection 2015. Erratum in: *PLoS One.* 2015;10(8):e0135992. PubMed PMID: 26061083. PubMed Central PMCID: PMC4464887.
135. Cohen E, Nardi Y, Krause I, et al. A longitudinal assessment of the natural rate of decline in renal function with age. *J Nephrol.* 2014;27(6):635–641. doi:10.1007/s40620-014-0077-9. [Epub 2014 Mar 19]; PubMed PMID: 24643437.
136. Muntner P. Longitudinal measurements of renal function. *Semin Nephrol.* 2009;29(6):650–657. doi:10.1016/j.semnephrol.2009.07.010. PubMed PMID: 20006797.
137. Brenner BM, Troy JL, Daugharty TM, et al. Dynamics of glomerular ultrafiltration in the rat. II. Plasma-flow dependence of GFR. *Am J Physiol.* 1972;223:1184–1190.
138. Ott CE, Marchand GR, Diaz-Buxo JA, et al. Determinants of glomerular filtration rate in the dog. *Am J Physiol.* 1976;231:235–239.
139. Denic A, Mathew J, Lerman LO, et al. Single-nephron glomerular filtration rate in healthy adults. *N Engl J Med.* 2017;376:2349–2357.
140. Berg UB. Differences in decline in GFR with age between males and females. Reference data on clearances of inulin and PAH in potential kidney donors. *Nephrol Dial Transplant.* 2006;21:2577–2582.
141. Tan JC, Busque S, Workeneh B, et al. Effects of aging on glomerular function and number in living kidney donors. *Kidney Int.* 2010;78(7):686–692. doi:10.1038/ki.2010.128. [Epub 2010 May 12]; PubMed PMID: 20463656. PubMed Central PMCID: PMC3353650.
142. Lenihan CR, Busque S, Derby G, et al. Longitudinal study of living kidney donor glomerular dynamics after nephrectomy. *J Clin Invest.* 2015;125(3):1311–1318. doi:10.1172/JCI78885. [Epub 2015 Feb 17]; PubMed PMID: 25689253. PubMed Central PMCID: PMC4362245.
143. Lenihan CR, Busque S, Derby G, et al. The association of predonation hypertension with glomerular function and number in older living kidney donors. *J Am Soc Nephrol.* 2015;26(6):1261–1267. doi:10.1681/ASN.2014030304. [Epub 2014 Dec 18]; PubMed PMID: 25525178. PubMed Central PMCID: PMC4446872.
144. Chen YR, Sung K, Tharin S. Symptomatic anterior cervical osteophyte causing dysphagia: case report, imaging, and review of the literature. *Cureus.* 2016;8(2):e473. doi:10.7759/cureus.473. PubMed PMID: 27004150. PubMed Central PMCID: PMC4779080.
145. Hoang K, Tan JC, Derby G, et al. Determinants of glomerular hypofiltration in aging humans. *Kidney Int.* 2003;64(4):1417–1424. PubMed PMID: 12969161.
146. Saxena AB, Myers BD, Derby G, et al. Adaptive hyperfiltration in the aging kidney after contralateral nephrectomy. *Am J Physiol Renal Physiol.* 2006;291(3):F629–F634. [Epub 2006 Mar 8]; PubMed PMID: 16525160.
147. Chakkera HA, Denic A, Kremers WK, et al. Comparison of high glomerular filtration rate thresholds for identifying hyperfiltration. *Nephrol Dial Transplant.* 2018;doi:10.1093/ndt/gfy332. [Epub ahead of print].
148. Kenney WL, Ho CW. Age alters regional distribution of blood flow during moderate-intensity exercise. *J Appl Physiol.* 1995;79:1112–1119.
149. Ho CW, Beard JL, Farrell PA, et al. Age, fitness, and regional blood flow during exercise in the heat. *J Appl Physiol.* 1997;82:1126–1135.
150. Mulkerrin EC, Brain A, Hampton D, et al. Reduced renal hemodynamic response to atrial natriuretic peptide in older volunteers. *Am J Kidney Dis.* 1993;22:538–544.
151. Fuiano G, Sund S, Mazza G, et al. Renal hemodynamic response to maximal vasodilating stimulus in healthy older subjects. *Kidney Int.* 2001;59:1052–1058.
152. Kielstein JT, Bode-Boger SM, Frolich JC, et al. Asymmetric dimethylarginine, blood pressure, and renal perfusion in older subjects. *Circulation.* 2003;107:1891–1895.
153. Matsumoto Y, Ueda S, Yamagishi S, et al. Dimethylarginine dimethylaminohydrolase prevents progression of renal dysfunction by inhibiting loss of peritubular capillaries and tubulointerstitial fibrosis in a rat model of chronic kidney disease. *J Am Soc Nephrol.* 2007;18:1525–1533.
154. Ueda S, Yamagishi S, Matsumoto Y, et al. Involvement of asymmetric dimethylarginine (ADMA) in glomerular capillary loss and sclerosis in a rat model of chronic kidney disease (CKD). *Life Sci.* 2009;84:853–856.
155. Esposito C, Plati A, Mazzullo T, et al. Renal function and functional reserve in healthy older individuals. *J Nephrol.* 2007;20:617–625.
156. Musso CG, Reynaldi J, Martinez B, et al. Renal reserve in the oldest old. *Int Urol Nephrol.* 2011;43(1):253–256. doi:10.1007/s11255-010-9769-9. [Epub 2010 Jul 1]; PubMed PMID: 20593305.
157. Kleinman KS, Glassock RJ. Glomerular filtration rate fails to increase following protein ingestion in hypothalamo-hypophyseal-deficient adults. Preliminary observations. *Am J Nephrol.* 1986;6(3):169–174. PubMed PMID: 3740125.
158. Dullaart RP, Meijer S, Marbach P, et al. Renal reserve filtration capacity in growth hormone deficient subjects. *Eur J Clin Invest.* 1992;22(8):562–568. PubMed PMID: 1425863.
159. Nair KS, Pabico RC, Truglia JA, et al. Mechanism of glomerular hyperfiltration after a protein meal in humans. Role of hormones and amino acids. *Diabetes Care.* 1994;17(7):711–715. PubMed PMID: 7924782.
160. De Moor B, Vanwalleghem JF, Swennen Q, et al. Haemodynamic or metabolic stimulation tests to reveal the renal functional response: requiem or revival? *Clin Kidney J.* 2018;11(5):623–654.
161. Fliser D, Zeier M, Nowack R, et al. Renal functional reserve in healthy older subjects. *J Am Soc Nephrol.* 1993;3(7):1371–1377.
162. Sunaga K, Sudoh T, Fujimura A. Lack of diurnal variation in glomerular filtration rates in older adults. *J Clin Pharmacol.* 1996;36(3):203–205. PubMed PMID: 8690813.
163. Hollenberg NK, Rivera A, Meinking T, et al. Age, renal perfusion and function in island-dwelling indigenous Kuna Amerinds of Panama. *Nephron.* 1999;82(2):131–138. PubMed PMID: 10364705.
164. Reckelhoff JF, Samsell L, Dey R, et al. The effect of aging on glomerular hemodynamics in the rat. *Am J Kidney Dis.* 1992;20(1):70–75. PubMed PMID: 1621681.
165. Erdely A, Greenfeld Z, Wagner L, et al. Sexual dimorphism in the aging kidney: effects on injury and nitric oxide system. *Kidney Int.* 2003;63(3):1021–1026. PubMed PMID: 12631083. PubMed Central PMCID: PMC2793681.
166. Baylis C. Sexual dimorphism of the aging kidney: role of nitric oxide deficiency. *Physiology (Bethesda).* 2008;23:142–150. doi:10.1152/physiol.00001.2008. Review. PubMed PMID: 18556467.
167. Baylis C. Sexual dimorphism in the aging kidney: differences in the nitric oxide system. *Nat Rev Nephrol.* 2009;5(7):384–396. doi:10.1038/nrneph.2009.90. [Epub 2009 Jun 2]; Review. PubMed PMID: 19488070.
168. Baylis C. Sexual dimorphism: the aging kidney, involvement of nitric oxide deficiency, and angiotensin II overactivity. *J Gerontol A Biol Sci Med Sci.* 2012;67(12):1365–1372. doi:10.1093/gerona/gls171. [Epub 2012 Sep 7]; Review. PubMed PMID: 22960474. PubMed Central PMCID: PMC3708515.
169. Gava AL, Freitas FP, Meyrelles SS, et al. Gender-dependent effects of aging on the kidney. *Braz J Med Biol Res.* 2011;44(9):905–913. [Epub 2011 Aug 19]; Review. PubMed PMID: 21956533.
170. Hollenberg NK, Adams DF, Solomon HS, et al. Senescence and the renal vasculature in normal man. *Circ Res.* 1974;34:309–316.
171. Hill C, Lateef AM, Engels K, et al. Basal and stimulated nitric oxide in control of kidney function in the aging rat. *Am J Physiol.* 1997;272:R1747–R1753.
172. Zhang XZ, Qiu C, Baylis C. Sensitivity of the segmental renal arterioles to angiotensin II in the aging rat. *Mech Ageing Dev.* 1997;97:183–192.
173. McLachlan MS, Guthrie JC, Anderson CK, et al. Vascular and glomerular changes in the ageing kidney. *J Pathol.* 1977;121:65–78.
174. Olson JL. Hyaline arteriolosclerosis: new meaning for an old lesion. *Kidney Int.* 2003;63:1162–1163.
175. Glassock RJ, Rule AD. The implications of anatomical and functional changes of the aging kidney: with an emphasis on the glomeruli. *Kidney Int.* 2012;82:270–277.
176. Mundel P, Shankland SJ. Podocyte biology and response to injury. *J Am Soc Nephrol.* 2002;13:3005–3015.

177. Pavenstadt H, Kriz W, Kretzler M. Cell biology of the glomerular podocyte. *Physiol Rev.* 2003;83:253–307.
178. Kriz W, Gretz N, Lemley KV. Progression of glomerular diseases: is the podocyte the culprit? *Kidney Int.* 1998;54:687–697.
179. Kim YH, Goyal M, Kurnit D, et al. Podocyte depletion and glomerulosclerosis have a direct relationship in the PAN-treated rat. *Kidney Int.* 2001;60:957–968.
180. Fukuda A, Chowdhury MA, Venkatareddy MP, et al. Growth-dependent podocyte failure causes glomerulosclerosis. *J Am Soc Nephrol.* 2012;23:1351–1363.
181. Wiggins JE, Goyal M, Sanden SK, et al. Podocyte hypertrophy, "adaptation," and "decompensation" associated with glomerular enlargement and glomerulosclerosis in the aging rat: prevention by calorie restriction. *J Am Soc Nephrol.* 2005;16:2953–2966.
182. Wharram BL, Goyal M, Wiggins JE, et al. Podocyte depletion causes glomerulosclerosis: diphtheria toxin-induced podocyte depletion in rats expressing human diphtheria toxin receptor transgene. *J Am Soc Nephrol.* 2005;16:2941–2952.
183. Luyckx VA, Perico N, Somaschini M, et al. A developmental approach to the prevention of hypertension and kidney disease: a report from the Low Birth Weight and Nephron Number Working Group. *Lancet.* 2017;390(10092):424–428. doi:10.1016/S0140-6736(17)30576-7. [Epub 2017 Mar 9]; PubMed PMID: 28284520. PubMed Central PMCID: PMC5884413.
184. Ikezumi Y, Suzuki T, Karasawa T, et al. Low birthweight and premature birth are risk factors for podocytopenia and focal segmental glomerulosclerosis. *Am J Nephrol.* 2013;38(2):149–157. doi:10.1159/000353898. [Epub 2013 Aug 6]; PubMed PMID: 23920104.
185. Ruggajo P, Svarstad E, Leh S, et al. Low birth weight and risk of progression to end stage renal disease in IgA nephropathy–a retrospective registry-based cohort study. *PLoS ONE.* 2016;11(4):e0153819. doi:10.1371/journal.pone.0153819. eCollection 2016. PubMed PMID: 27092556. PubMed Central PMCID: PMC4836690.
186. Epstein M, Hollenberg NK. Age as a determinant of renal sodium conservation in normal man. *J Lab Clin Med.* 1976;87:411–417.
187. Macias Nunez JF, Garcia Iglesias C, Bondia Roman A, et al. Renal handling of sodium in old people: a functional study. *Age Ageing.* 1978;7:178–181.
188. Bauer JH. Age-related changes in the renin-aldosterone system. Physiological effects and clinical implications. *Drugs Aging.* 1993; 3:238–245.
189. Mimran A, Ribstein J, Jover B. Aging and sodium homeostasis. *Kidney Int Suppl.* 1992;37:S107–S113.
190. Luft FC, Grim CE, Fineberg N, et al. Effects of volume expansion and contraction in normotensive whites, blacks, and subjects of different ages. *Circulation.* 1979;59:643–650.
191. Brenner BM, Ballermann BJ, Gunning ME, et al. Diverse biological actions of atrial natriuretic peptide. *Physiol Rev.* 1990;70: 665–699.
192. Leosco D, Ferrara N, Landino P, et al. Effects of age on the role of atrial natriuretic factor in renal adaptation to physiologic variations of dietary salt intake. *J Am Soc Nephrol.* 1996;7:1045–1051.
193. Pollack JA, Skvorak JP, Nazian SJ, et al. Alterations in atrial natriuretic peptide (ANP) secretion and renal effects in aging. *J Gerontol A Biol Sci Med Sci.* 1997;52:B196–B202.
194. Or K, Richards AM, Espiner EA, et al. Effect of low dose infusions of ile-atrial natriuretic peptide in healthy older males: evidence for a postreceptor defect. *J Clin Endocrinol Metab.* 1993;76:1271–1274.
195. Tan AC, Jansen TL, Termond EF, et al. Kinetics of atrial natriuretic peptide in young and older subjects. *Eur J Clin Pharmacol.* 1992;42:449–452.
196. Haller BG, Zust H, Shaw S, et al. Effects of posture and ageing on circulating atrial natriuretic peptide levels in man. *J Hypertens.* 1987;5:551–556.
197. Ohashi M, Fujio N, Nawata H, et al. High plasma concentrations of human atrial natriuretic polypeptide in aged men. *J Clin Endocrinol Metab.* 1987;64:81–85.
198. Frame AA, Wainford RD. Mechanisms of altered renal sodium handling in age-related hypertension. *Am J Physiol Renal Physiol.* 2018;315(1):F1–F6. doi:10.1152/ajprenal.00594.2017. [Epub 2018 Feb 14]; PubMed PMID: 29442548. PubMed Central PMCID: PMC6087788.
199. Luft FC, Miller JZ, Grim CE, et al. Salt sensitivity and resistance of blood pressure. Age and race as factors in physiological responses. *Hypertension.* 1991;17(1 suppl):I102–I108. PubMed PMID: 1846122.
200. Tank JE, Vora JP, Houghton DC, et al. Altered renal vascular responses in the aging rat kidney. *Am J Physiol.* 1994;266(6 Pt 2): F942–F948. PubMed PMID: 8023973.
201. Tian Y, Riazi S, Khan O, et al. Renal ENaC subunit, Na-K-2Cl and Na-Cl cotransporter abundances in aged, water-restricted F344 x Brown Norway rats. *Kidney Int.* 2006;69(2):304–312. PubMed PMID: 16408120.
202. Tiwari S, Li L, Riazi S, et al. Sex and age result in differential regulation of the renal thiazide-sensitive NaCl cotransporter and the epithelial sodium channel in angiotensin II-infused mice. *Am J Nephrol.* 2009;30(6):554–562. doi:10.1159/000252776. [Epub 2009 Oct 21]; PubMed PMID: 19844087. PubMed Central PMCID: PMC2853589.
203. Palmer BF, Clegg DJ. Physiology and pathophysiology of potassium homeostasis. *Adv Physiol Educ.* 2016;40:480–490.
204. Kehayias JJ, Fiatarone MA, Zhuang H, et al. Total body potassium and body fat: relevance to aging. *Am J Clin Nutr.* 1997;66: 904–910.
205. Kyle UG, Genton L, Hans D, et al. Age-related differences in fat-free mass, skeletal muscle, body cell mass and fat mass between 18 and 94 years. *Eur J Clin Nutr.* 2001;55:663–672.
206. Noth RH, Lassman MN, Tan SY, et al. Age and the renin-aldosterone system. *Arch Intern Med.* 1977;137:1414–1417.
207. Mulkerrin E, Epstein FH, Clark BA. Aldosterone responses to hyperkalemia in healthy older humans. *J Am Soc Nephrol.* 1995;6:1459–1462.
208. Musso CG, Miguel R, Algranati L, et al. Renal potassium excretion: comparison between chronic renal disease patients and old people. *Int Urol Nephrol.* 2005;37:167–170.
209. Bengele HH, Mathias R, Perkins JH, et al. Impaired renal and extrarenal potassium adaptation in old rats. *Kidney Int.* 1983;23:684–690, 199.
210. Musso C, Liakopoulos V, De Miguel R, et al. Transtubular potassium concentration gradient: comparison between healthy old people and chronic renal failure patients. *Int Urol Nephrol.* 2006;38:387–390.
211. Minaker KL, Rowe JW. Potassium homeostasis during hyperinsulinemia: effect of insulin level, beta-blockade, and age. *Am J Physiol.* 1982;242:E373–E377.
212. Blaine J, Chonchol M, Levi M. Renal control of calcium, phosphate, and magnesium homeostasis. *Clin J Am Soc Nephrol.* 2015;10: 1257–1272.
213. Saris NE, Mervaala E, Karppanen H, et al. Magnesium. An update on physiological, clinical and analytical aspects. *Clin Chim Acta.* 2000;294:1–26.
214. Barbagallo M, Belvedere M, Dominguez LJ. Magnesium homeostasis and aging. *Magnes Res.* 2009;22:235–246.
215. Yang XY, Hosseini JM, Ruddel ME, et al. Blood magnesium parameters do not differ with age. *J Am Coll Nutr.* 1990;9:308–313.
216. Gullestad L, Nes M, Ronneberg R, et al. Magnesium status in healthy free-living older Norwegians. *J Am Coll Nutr.* 1994;13:45–50.
217. Grober U, Schmidt J, Kisters K. Magnesium in Prevention and Therapy. *Nutrients.* 2015;7:8199–8226.
218. Rebholz CM, Tin A, Liu Y, et al. Dietary magnesium and kidney function decline: the healthy aging in neighborhoods of diversity across the life span study. *Am J Nephrol.* 2016;44(5):381–387. [Epub 2016 Oct 22]; PubMed PMID: 27771720. PubMed Central PMCID: PMC5130225.
219. Corman B, Roinel N. Single-nephron filtration rate and proximal reabsorption in aging rats. *Am J Physiol.* 1991;260:F75–F80.
220. Armbrecht HJ, Zenser TV, Gross CJ, et al. Adaptation to dietary calcium and phosphorus restriction changes with age in the rat. *Am J Physiol.* 1980;239:E322–E327.
221. Hanai H, Ishida M, Liang CT, et al. Parathyroid hormone increases sodium/calcium exchange activity in renal cells and the blunting of the response in aging. *J Biol Chem.* 1986;261:5419–5425.
222. Orwoll ES, Meier DE. Alterations in calcium, vitamin D, and parathyroid hormone physiology in normal men with aging: relationship to the development of senile osteopenia. *J Clin Endocrinol Metab.* 1986;63:1262–1269.
223. Nordin BE, Horowitz M, Need A, et al. Renal leak of calcium in post-menopausal osteoporosis. *Clin Endocrinol (Oxf).* 1994;41:41–45.
224. Armbrecht HJ, Zenser TV, Bruns ME, et al. Effect of age on intestinal calcium absorption and adaptation to dietary calcium. *Am J Physiol.* 1979;236:E769–E774.
225. Armbrecht HJ, Boltz M, Strong R, et al. Expression of calbindin-D decreases with age in intestine and kidney. *Endocrinology.* 1989;125: 2950–2956.

226. Johnson JA, Beckman MJ, Pansini-Porta A, et al. Age and gender effects on 1,25-dihydroxyvitamin D3-regulated gene expression. *Exp Gerontol.* 1995;30:631–643.
227. Armbrecht HJ, Forte LR, Halloran BP. Effect of age and dietary calcium on renal 25(OH)D metabolism, serum 1,25(OH)2D, and PTH. *Am J Physiol.* 1984;246:E266–E270.
228. Chapuy MC, Durr F, Chapuy P. Age-related changes in parathyroid hormone and 25 hydroxycholecalciferol levels. *J Gerontol.* 1983;38:19–22.
229. van Abel M, Huybers S, Hoenderop JG, et al. Age-dependent alterations in Ca2+ homeostasis: role of TRPV5 and TRPV6. *Am J Physiol Renal Physiol.* 2006;291:F1177–F1183.
230. Kuro-o M, Matsumura Y, Aizawa H, et al. Mutation of the mouse klotho gene leads to a syndrome resembling ageing. *Nature.* 1997;390:45–51.
231. Imura A, Tsuji Y, Murata M, et al. Alpha-Klotho as a regulator of calcium homeostasis. *Science.* 2007;316:1615–1618.
232. Portale AA, Lonergan ET, Tanney DM, et al. Aging alters calcium regulation of serum concentration of parathyroid hormone in healthy men. *Am J Physiol.* 1997;272:E139–E146.
233. Musso CG, Juarez R, Vilas M, et al. Renal calcium, phosphorus, magnesium and uric acid handling: comparison between stage III chronic kidney disease patients and healthy oldest old. *Int Urol Nephrol.* 2012;44:1559–1562.
234. Halloran BP, Lonergan ET, Portale AA. Aging and renal responsiveness to parathyroid hormone in healthy men. *J Clin Endocrinol Metab.* 1996;81:2192–2197.
235. Marks J, Debnam ES, Unwin RJ. Phosphate homeostasis and the renal-gastrointestinal axis. *Am J Physiol Renal Physiol.* 2010;299:F285–F296.
236. Mulroney SE, Woda C, Haramati A. Changes in renal phosphate reabsorption in the aged rat. *Proc Soc Exp Biol Med.* 1998;218:62–67.
237. Levi M, Jameson DM, van der Meer BW. Role of BBM lipid composition and fluidity in impaired renal Pi transport in aged rat. *Am J Physiol.* 1989;256:F85–F94.
238. Kiebzak GM, Sacktor B. Effect of age on renal conservation of phosphate in the rat. *Am J Physiol.* 1986;251:F399–F407.
239. Levi M, Baird BM, Wilson PV. Cholesterol modulates rat renal brush border membrane phosphate transport. *J Clin Invest.* 1990;85:231–237.
240. Breusegem SY, Halaihel N, Inoue M, et al. Acute and chronic changes in cholesterol modulate Na-Pi cotransport activity in OK cells. *Am J Physiol Renal Physiol.* 2005;289:F154–F165.
241. Chen ML, King RS, Armbrecht HJ. Sodium-dependent phosphate transport in primary cultures of renal tubule cells from young and adult rats. *J Cell Physiol.* 1990;143:488–493.
242. Sorribas V, Lotscher M, Loffing J, et al. Cellular mechanisms of the age-related decrease in renal phosphate reabsorption. *Kidney Int.* 1996;50:855–863.
243. De Vita F, Lauretani F, Bauer J, et al. Relationship between vitamin D and inflammatory markers in older individuals. *Age (Dordr).* 2014;36(4):9694. doi:10.1007/s11357-014-9694-4. [Epub 2014 Aug 3]; PubMed PMID: 25086618. PubMed Central PMCID: PMC4150893.
244. Gallagher JC. Vitamin D and aging. *Endocrinol Metab Clin North Am.* 2013;42(2):319–332. doi:10.1016/j.ecl.2013.02.004. [Epub 2013 Apr 9]; Review. PubMed PMID: 23702404. PubMed Central PMCID: PMC3782116.
245. MacLaughlin J, Holick MF. Aging decreases the capacity of human skin to produce vitamin D3. *J Clin Invest.* 1985;76(4):1536–1538. PubMed PMID: 2997282. PubMed Central PMCID: PMC424123.
246. Ameri P, Canepa M, Milaneschi Y, et al. Relationship between vitamin D status and left ventricular geometry in a healthy population: results from the Baltimore Longitudinal Study of Aging. *J Intern Med.* 2013;273(3):253–262. doi:10.1111/joim.12007. [Epub 2012 Nov 12]; PubMed PMID: 23061475. PubMed Central PMCID: PMC3568460.
247. Liang CT, Barnes J, Cheng L, et al. Effects of 1,25-(OH)2D3 administered in vivo on phosphate uptake by isolated chick renal cells. *Am J Physiol.* 1982;242:C312–C318.
248. Kurnik BR, Hruska KA. Effects of 1,25-dihydroxycholecalciferol on phosphate transport in vitamin D-deprived rats. *Am J Physiol.* 1984;247:F177–F184.
249. Brandis M, Harmeyer J, Kaune R, et al. Phosphate transport in brush-border membranes from control and rachitic pig kidney and small intestine. *J Physiol.* 1987;384:479–490.
250. Brasitus TA, Dudeja PK, Eby B, et al. Correction by 1-25-dihydroxycholecalciferol of the abnormal fluidity and lipid composition of enterocyte brush border membranes in vitamin D-deprived rats. *J Biol Chem.* 1986;261:16404–16409.
251. Tareen N, Zadshir A, Martins D, et al. Alterations in acid-base homeostasis with aging. *J Natl Med Assoc.* 2004;96:921–925, quiz 5–6.
252. Vallet M, Metzger M, Haymann JP, et al. Urinary ammonia and long-term outcomes in chronic kidney disease. *Kidney Int.* 2015;88:137–145.
253. Berkemeyer S, Vormann J, Gunther AL, et al. Renal net acid excretion capacity is comparable in prepubescence, adolescence, and young adulthood but falls with aging. *J Am Geriatr Soc.* 2008;56:1442–1448.
254. Adler S, Lindeman RD, Yiengst MJ, et al. Effect of acute acid loading on urinary acid excretion by the aging human kidney. *J Lab Clin Med.* 1968;72:278–289.
255. Prasad R, Kinsella JL, Sacktor B. Renal adaptation to metabolic acidosis in senescent rats. *Am J Physiol.* 1988;255:F1183–F1190.
256. Rylander R, Remer T, Berkemeyer S, et al. Acid-base status affects renal magnesium losses in healthy, elderly persons. *J Nutr.* 2006;136:2374–2377.
257. Dawson-Hughes B, Harris SS, Ceglia L. Alkaline diets favor lean tissue mass in older adults. *Am J Clin Nutr.* 2008;87:662–665.
258. Amodu A, Abramowitz MK. Dietary acid, age, and serum bicarbonate levels among adults in the United States. *Clin J Am Soc Nephrol.* 2013;8:2034–2042.
259. Verove C, Maisonneuve N, El Azouzi A, et al. Effect of the correction of metabolic acidosis on nutritional status in elderly patients with chronic renal failure. *J Ren Nutr.* 2002;12:224–228.
260. Sebastian A, Harris ST, Ottaway JH, et al. Improved mineral balance and skeletal metabolism in postmenopausal women treated with potassium bicarbonate. *N Engl J Med.* 1994;330:1776–1781.
261. Dawson-Hughes B, Harris SS, Palermo NJ, et al. Treatment with potassium bicarbonate lowers calcium excretion and bone resorption in older men and women. *J Clin Endocrinol Metab.* 2009;94:96–102.
262. Moseley KF, Weaver CM, Appel L, et al. Potassium citrate supplementation results in sustained improvement in calcium balance in older men and women. *J Bone Miner Res.* 2013;28:497–504.
263. Knepper MA, Kwon TH, Nielsen S. Molecular physiology of water balance. *N Engl J Med.* 2015;372:1349–1358.
264. Hasler U, Leroy V, Martin PY, et al. Aquaporin-2 abundance in the renal collecting duct: new insights from cultured cell models. *Am J Physiol Renal Physiol.* 2009;297:F10–F18.
265. Kortenoeven ML, Pedersen NB, Rosenbaek LL, et al. Vasopressin regulation of sodium transport in the distal nephron and collecting duct. *Am J Physiol Renal Physiol.* 2015;309:F280–F299.
266. Moeller HB, Olesen ET, Fenton RA. Regulation of the water channel aquaporin-2 by posttranslational modification. *Am J Physiol Renal Physiol.* 2011;300:F1062–F1073.
267. Rector FC Jr. Sodium, bicarbonate, and chloride absorption by the proximal tubule. *Am J Physiol.* 1983;244:F461–F471.
268. Rocha AS, Kokko JP. Sodium chloride and water transport in the medullary thick ascending limb of Henle. Evidence for active chloride transport. *J Clin Invest.* 1973;52:612–623.
269. Burg MB, Green N. Function of the thick ascending limb of Henle's loop. *Am J Physiol.* 1973;224:659–668.
270. Fenton RA, Knepper MA. Mouse models and the urinary concentrating mechanism in the new millennium. *Physiol Rev.* 2007;87:1083–1112.
271. Knepper MA, Nielsen S, Chou CL, et al. Mechanism of vasopressin action in the renal collecting duct. *Semin Nephrol.* 1994;14:302–321.
272. Sands JM, Nonoguchi H, Knepper MA. Vasopressin effects on urea and H2O transport in inner medullary collecting duct subsegments. *Am J Physiol.* 1987;253:F823–F832.
273. Schafer JA, Andreoli TE. Cellular constraints to diffusion. The effect of antidiuretic hormone on water flows in isolated mammalian collecting tubules. *J Clin Invest.* 1972;51:1264–1278.
274. Sands JM. Urine concentrating and diluting ability during aging. *J Gerontol A Biol Sci Med Sci.* 2012;67:1352–1357.
275. Findley T. Role of the neurohypophysis in the pathogenesis of hypertension and some allied disorders associated with aging. *Am J Med.* 1949;7:70–84.
276. Cowen LE, Hodak SP, Verbalis JG. Age-associated abnormalities of water homeostasis. *Endocrinol Metab Clin North Am.* 2013;42:349–370.
277. Rolls BJ, Phillips PA. Aging and disturbances of thirst and fluid balance. *Nutr Rev.* 1990;48:137–144.
278. Carpenter CR. Geriatric emergency medicine. Preface. *Clin Geriatr Med.* 2013;29:xiii–xiv.

279. Sherman FT. Hyponatremia and SIADH in the elderly. Introducing the "water-offered test" for dehydration. *Geriatrics*. 2007;62: 8, 18.
280. Combet S, Gouraud S, Gobin R, et al. Aquaporin-2 downregulation in kidney medulla of aging rats is posttranscriptional and is abolished by water deprivation. *Am J Physiol Renal Physiol*. 2008;294:F1408–F1414.
281. Beck LH. The aging kidney. Defending a delicate balance of fluid and electrolytes. *Geriatrics*. 2000;55:26–28, 31–32.
282. Fried LF, Palevsky PM. Hyponatremia and hypernatremia. *Med Clin North Am*. 1997;81:585–609.
283. Faull CM, Holmes C, Baylis PH. Water balance in elderly people: is there a deficiency of vasopressin? *Age Ageing*. 1993;22:114–120.
284. Helderman JH, Vestal RE, Rowe JW, et al. The response of arginine vasopressin to intravenous ethanol and hypertonic saline in man: the impact of aging. *J Gerontol*. 1978;33:39–47.
285. Phillips PA, Rolls BJ, Ledingham JG, et al. Reduced thirst after water deprivation in healthy elderly men. *N Engl J Med*. 1984;311: 753–759.
286. Duggan J, Kilfeather S, Lightman SL, et al. The association of age with plasma arginine vasopressin and plasma osmolality. *Age Ageing*. 1993;22:332–336.
287. Davies I, O'Neill PA, McLean KA, et al. Age-associated alterations in thirst and arginine vasopressin in response to a water or sodium load. *Age Ageing*. 1995;24:151–159.
288. Abramow M, Beauwens R, Cogan E. Cellular events in vasopressin action. *Kidney Int Suppl*. 1987;21:S56–S66.
289. Catudioc-Vallero J, Sands JM, Klein JD, et al. Effect of age and testosterone on the vasopressin and aquaporin responses to dehydration in Fischer 344/Brown-Norway F1 rats. *J Gerontol A Biol Sci Med Sci*. 2000;55:B26–B34.
290. Combet S, Geffroy N, Berthonaud V, et al. Correction of age-related polyuria by dDAVP: molecular analysis of aquaporins and urea transporters. *Am J Physiol Renal Physiol*. 2003;284:F199–F208.
291. Phillips PA, Bretherton M, Johnston CI, et al. Reduced osmotic thirst in healthy elderly men. *Am J Physiol*. 1991;261:R166–R171.
292. Mack GW, Weseman CA, Langhans GW, et al. Body fluid balance in dehydrated healthy older men: thirst and renal osmoregulation. *J Appl Physiol*. 1994;76:1615–1623.
293. Crowe MJ, Forsling ML, Rolls BJ, et al. Altered water excretion in healthy elderly men. *Age Ageing*. 1987;16(5):285–293. PubMed PMID: 3687569.
294. Jung FF, Kennefick TM, Ingelfinger JR, et al. Down-regulation of the intrarenal renin-angiotensin system in the aging rat. *J Am Soc Nephrol*. 1995;5(8):1573–1580. PubMed PMID: 7756590.
295. Conti S, Cassis P, Benigni A. Aging and the renin-angiotensin system. *Hypertension*. 2012;60(4):878–883. doi:10.1161/HYPERTENSIONAHA.110.155895. [Epub 2012 Aug 27]; Review. No abstract available. PMID: 22926952.
296. Nanba K, Vaidya A, Rainey WE. Aging and adrenal aldosterone production. *Hypertension*. 2018;71(2):218–223. doi:10.1161/HYPERTENSIONAHA.117.10391. [Epub 2017 Dec 11]; Review. PubMed PMID: 29229745. PubMed Central PMCID: PMC5839673.
297. Mulkerrin E, Epstein FH, Clark BA. Aldosterone responses to hyperkalemia in healthy elderly humans. *J Am Soc Nephrol*. 1995;6(5):1459–1462. PubMed PMID: 8589323.
298. Ershler WB, Sheng S, McKelvey J, et al. Serum erythropoietin and aging: a longitudinal analysis. *J Am Geriatr Soc*. 2005;53(8):1360–1365. PubMed PMID: 16078962.
299. Guo W, Li M, Bhasin S. Testosterone supplementation improves anemia in aging male mice. *J Gerontol A Biol Sci Med Sci*. 2014;69(5): 505–513. doi:10.1093/gerona/glt127. [Epub 2013 Aug 23]; PubMed PMID: 23974081. PubMed Central PMCID: PMC3991143.
300. Cappellini MD, Motta I. Anemia in clinical practice-definition and classification: does hemoglobin change with aging? *Semin Hematol*. 2015;52(4):261–269. doi:10.1053/j.seminhematol.2015.07.006. [Epub 2015 Jul 17]; Review. PubMed PMID: 26404438.
301. Garimella PS, Katz R, Patel KV, et al. Association of serum erythropoietin with cardiovascular events, kidney function decline, and mortality: the health aging and body composition study. *Circ Heart Fail*. 2016;9(1):e002124. doi:10.1161/CIRCHEARTFAILURE.115.002124. PubMed PMID: 26721912. PubMed Central PMCID: PMC4698899.
302. National Kidney Foundation. K/DOQI clinical practice guidelines for chronic kidney disease: evaluation, classification and stratification. *Am J Kidney Dis*. 2002;39:S1–S266.
303. KDIGO 2012 Clinical practice guidelines for the evaluation and management of chronic kidney disease. *Kidney Int Suppl*. 2013;3:1–150.
304. Polkinghorne KR, Chadban SJ. A decade after the KDOQI CKD guidelines: a perspective from Australia. *Am J Kidney Dis*. 2012;60(5):725–726. doi:10.1053/j.ajkd.2012.08.005. PubMed PMID: 23067642.
305. National Clinical Guideline Centre (UK). *Chronic Kidney Disease (Partial Update): Early Identification and Management of Chronic Kidney Disease in Adults in Primary and Secondary Care*. London: National Institute for Health and Care Excellence (UK); 2014. PubMed PMID: 25340245.
306. Delanaye P, Glassock RJ, Pottel H, et al. An age-calibrated definition of chronic kidney disease: rationale and benefits. *Clin Biochem Rev*. 2016;37(1):17–26. PubMed PMID: 27057075. PubMed Central PMCID: PMC4810758.
307. Glassock R, Delanaye P, El Nahas M. An age-calibrated classification of chronic kidney disease. *JAMA*. 2015;314(6):559–560. doi:10.1001/jama.2015.6731. PubMed PMID: 26023760.
308. Levey AS, Inker LA, Coresh J. Chronic kidney disease in older people. *JAMA*. 2015;314(6):557–558. doi:10.1001/jama.2015.6753. PubMed PMID: 26023868.
309. Winearls CG, Glassock RJ. Classification of chronic kidney disease in the elderly: pitfalls and errors. *Nephron Clin Pract*. 2011;119(suppl 1):c2–c4. doi:10.1159/000328013. [Epub 2011 Aug 10]; Review. PubMed PMID: 21832853.
310. Winearls CG, Glassock RJ. Dissecting and refining the staging of chronic kidney disease. *Kidney Int*. 2009;75(10):1009–1014. doi:10.1038/ki.2009.49. [Epub 2009 Feb 25]; PubMed PMID: 19242501.
311. Moynihan R, Glassock R, Doust J. Chronic kidney disease controversy: how expanding definitions are unnecessarily labelling many people as diseased. *BMJ*. 2013;347:f4298. doi:10.1136/bmj.f4298. PubMed PMID: 23900313.
312. Ebert N, Jakob O, Gaedeke J, et al. Prevalence of reduced kidney function and albuminuria in older adults: the Berlin Initiative Study. *Nephrol Dial Transplant*. 2017;32(6):997–1005. doi:10.1093/ndt/gfw079. PubMed PMID: 27190381.
313. Okparavero A, Foster MC, Tighiouart H, et al. Prevalence and complications of chronic kidney disease in a representative elderly population in Iceland. *Nephrol Dial Transplant*. 2016;31(3):439–447. doi:10.1093/ndt/gfv370. [Epub 2015 Oct 31]; PubMed PMID: 26519958. PubMed Central PMCID: PMC4762399.
314. Schaeffner ES, Ebert N, Delanaye P, et al. Two novel equations to estimate kidney function in persons aged 70 years or older. *Ann Intern Med*. 2012;157(7):471–481. doi:10.7326/0003-4819-157-7-201210020-00003. PubMed PMID: 23027318.
315. Glassock RJ, Warnock DG, Delanaye P. The global burden of chronic kidney disease: estimates, variability and pitfalls. *Nat Rev Nephrol*. 2017;13(2):104–114. doi:10.1038/nrneph.2016.163. [Epub 2016 Dec 12]; Review. PubMed PMID: 27941934.
316. Rule AD, Glassock RJ. GFR estimating equations: getting closer to the truth? *Clin J Am Soc Nephrol*. 2013;8(8):1414–1420. doi:10.2215/CJN.01240213. [Epub 2013 May 23]; PubMed PMID: 23704300. PubMed Central PMCID: PMC3731897.
317. Pottel H, Delanaye P, Schaeffner E, et al. Estimating glomerular filtration rate for the full age spectrum from serum creatinine and cystatin C. *Nephrol Dial Transplant*. 2017;32(3):497–507. doi:10.1093/ndt/gfw425. PubMed PMID: 28089986. PubMed Central PMCID: PMC5837496.
318. Evangelopoulos AA, Vallianou NG, Bountziouka V, et al. Association between serum cystatin C, monocytes and other inflammatory markers. *Intern Med J*. 2012;42(5):517–522. doi:10.1111/j.1445-5994.2011.02500.x. PubMed PMID: 21470355.
319. Liu X, Foster MC, Tighiouart H, et al. Non-GFR determinants of low-molecular-weight serum protein filtration markers in CKD. *Am J Kidney Dis*. 2016;68(6):892–900. doi:10.1053/j.ajkd.2016.07.021. [Epub 2016 Sep 20]; PubMed PMID: 27663042. PubMed Central PMCID: PMC5123901.
320. Foster MC, Levey AS, Inker LA, et al. Non-GFR determinants of low-molecular-weight serum protein filtration markers in the elderly: AGES-Kidney and MESA-Kidney. *Am J Kidney Dis*. 2017;70(3):406–414. doi:10.1053/j.ajkd.2017.03.021. [Epub 2017 May 24]; PubMed PMID: 28549536. PubMed Central PMCID: PMC5572311.
321. Inker LA, Schmid CH, Tighiouart H, et al. Estimating glomerular filtration rate from serum creatinine and cystatin C. *N Engl J Med*. 2012;367(1):20–29. doi:10.1056/NEJMoa1114248. Erratum in: *N Engl J Med*. 2012;367(7):681. Erratum in: *N Engl J Med*. 2012;367(21):2060. PubMed PMID: 22762315. PubMed Central PMCID: PMC4398023.

322. Björk J, Grubb A, Gudnason V, et al. Comparison of glomerular filtration rate estimating equations derived from creatinine and cystatin C: validation in the Age, Gene/Environment Susceptibility-Reykjavik elderly cohort. *Nephrol Dial Transplant.* 2017;doi:10.1093/ndt/gfx272. [Epub ahead of print]; PubMed PMID: 29040701. PubMed Central PMCID: PMC6070032.
323. Meeusen JW, Rule AD, Voskoboev N, et al. Performance of cystatin C- and creatinine-based estimated glomerular filtration rate equations depends on patient characteristics. *Clin Chem.* 2015;61(10):1265–1272. doi:10.1373/clinchem.2015.243030. [Epub 2015 Aug 3]; PubMed PMID: 26240296. PubMed Central PMCID: PMC4726452.
324. Fan L, Levey AS, Gudnason V, et al. Comparing GFR estimating equations using cystatin C and creatinine in elderly individuals. *J Am Soc Nephrol.* 2015;26(8):1982–1989.
325. Nerpin E, Ingelsson E, Risérus U, et al. The combined contribution of albuminuria and glomerular filtration rate to the prediction of cardiovascular mortality in elderly men. *Nephrol Dial Transplant.* 2011;26(9):2820–2827. doi:10.1093/ndt/gfq848. [Epub 2011 Feb 18]; PubMed PMID: 21335440.
326. Grubb A, Lindström V, Jonsson M, et al. Reduction in glomerular pore size is not restricted to pregnant women. Evidence for a new syndrome: 'Shrunken pore syndrome'. *Scand J Clin Lab Invest.* 2015;75(4):333–340. doi:10.3109/00365513.2015.1025427. PubMed PMID: 25919022. PubMed Central PMCID: PMC4487590.
327. Lang J, Katz R, Ix JH, et al. Association of serum albumin levels with kidney function decline and incident chronic kidney disease in elders. *Nephrol Dial Transplant.* 2018;33(6):986–992. doi:10.1093/ndt/gfx229. PubMed PMID: 28992097.
328. Raman M, Middleton RJ, Kalra PA, et al. Estimating renal function in old people: an in-depth review. *Int Urol Nephrol.* 2017;49(11):1979–1988. doi:10.1007/s11255-017-1682-z. [Epub 2017 Sep 15]; Review. PubMed PMID: 28913589. PubMed Central PMCID: PMC5643354.
329. Delanaye P, Glassock RJ, De Broe ME. Epidemiology of chronic kidney disease: think (at least) twice! *Clin Kidney J.* 2017;10(3):370–374. doi:10.1093/ckj/sfw154. [Epub 2017 Feb 27]; PubMed PMID: 28617483. PubMed Central PMCID: PMC5466090.
330. Hallan SI, Matsushita K, Sang Y, et al. Age and association of kidney measures with mortality and end-stage renal disease. *JAMA.* 2012;308(22):2349–2360. PubMed PMID: 23111824. PubMed Central PMCID: PMC3936348.
331. Denic A, Glassock RJ, Rule AD. Structural and functional changes with the aging kidney. *Adv Chronic Kidney Dis.* 2016;23(1):19–28. doi:10.1053/j.ackd.2015.08.004. Review. PubMed PMID: 26709059. PubMed Central PMCID: PMC4693148.
332. Gansevoort RT, Correa-Rotter R, Hemmelgarn BR, et al. Chronic kidney disease and cardiovascular risk: epidemiology, mechanisms, and prevention. *Lancet.* 2013;382(9889):339–352. doi:10.1016/S0140-6736(13)60595-4. [Epub 2013 May 31]; Review. PubMed PMID: 23727170.
333. Malmgren L, McGuigan FE, Berglundh S, et al. Declining estimated glomerular filtration rate and its association with mortality and comorbidity over 10 years in elderly women. *Nephron.* 2015;130(4):245–255. doi:10.1159/000435790. [Epub 2015 Jul 15]; PubMed PMID: 26184510.
334. Delanaye P, Glassock RJ. Glomerular filtration rate and aging: another longitudinal Study–A long time coming! *Nephron.* 2015;131(1):1–4. doi:10.1159/000439147. [Epub 2015 Aug 21]; PubMed PMID: 26303019.
335. Rutkowski M, Mann W, Derose S, et al. Implementing KDOQI CKD definition and staging guidelines in Southern California Kaiser Permanente. *Am J Kidney Dis.* 2009;53(3 suppl 3):S86–S99. doi:10.1053/j.ajkd.2008.07.052. PubMed PMID: 19231766.
336. Warnock DG, Delanaye P, Glassock RJ. Risks for all-cause mortality: stratified by age, estimated glomerular filtration rate and albuminuria. *Nephron.* 2017;136(4):292–297. doi:10.1159/000455197. [Epub 2017 Jan 27]; Review. PubMed PMID: 28125814.
337. Goff DC Jr, Lloyd-Jones DM, Bennett G, et al. 2013 ACC/AHA guideline on the assessment of cardiovascular risk: a report of the American College of Cardiology/American Heart Association Task Force on Practice Guidelines. *J Am Coll Cardiol.* 2014;63(25 Pt B):2935–2959. doi:10.1016/j.jacc.2013.11.005. [Epub 2013 Nov 12]; Erratum in: *J Am Coll Cardiol.* 2014;63(25 Pt B):3026. PubMed PMID: 24239921. PubMed Central PMCID: PMC4700825.
338. O'Hare AM, Choi AI, Bertenthal D, et al. Age affects outcomes in chronic kidney disease. *J Am Soc Nephrol.* 2007;18(10):2758–2765. [Epub 2007 Sep 12]; PubMed PMID: 17855638.
339. Nichols LA, Slusarz A, Grunz-Borgmann EA, et al. α(E)-catenin regulates BMP-7 expression and migration in renal epithelial cells. *Am J Nephrol.* 2014;39(5):409–417. doi:10.1159/000362250. [Epub 2014 May 6]; PubMed PMID: 24818804. PubMed Central PMCID: PMC4086150.
340. Eriksen BO, Ingebretsen OC. The progression of chronic kidney disease: a 10-year population-based study of the effects of gender and age. *Kidney Int.* 2006;69(2):375–382. PubMed PMID: 16408129.
341. Shardlow A, McIntyre NJ, Fluck RJ, et al. Chronic kidney disease in primary care: outcomes after five years in a prospective cohort study. *PLoS Med.* 2016;13(9):e1002128. doi:10.1371/journal.pmed.1002128. eCollection 2016 Sep. PubMed PMID: 27648564. PubMed Central PMCID: PMC5029805.
342. Remuzzi G, Glassock R. Interplay between diagnostic criteria and prognostic accuracy in chronic kidney disease. *PLoS Med.* 2016;13(9):e1002129. doi:10.1371/journal.pmed.1002129. eCollection 2016 Sep. PubMed PMID: 27648826. PubMed Central PMCID: PMC5029803.
343. Rosner MH. Acute kidney injury in the elderly. *Clin Geriatr Med.* 2013;29(3):565–578. doi:10.1016/j.cger.2013.05.001. Review. PubMed PMID: 23849008.
344. Ponticelli C, Sala G, Glassock RJ. Drug management in the elderly adult with chronic kidney disease: a review for the primary care physician. *Mayo Clin Proc.* 2015;90(5):633–645. doi:10.1016/j.mayocp.2015.01.016. [Epub 2015 Mar 12]; Review. PubMed PMID: 25771152.
345. Glassock RJ. Glomerular disease in the elderly. *Clin Geriatr Med.* 2009;25(3):413–422. doi:10.1016/j.cger.2009.06.006. Review. PubMed PMID: 19765489.
346. Jin B, Zeng C, Ge Y, et al. The spectrum of biopsy-proven kidney diseases in elderly Chinese patients. *Nephrol Dial Transplant.* 2014;29(12):2251–2259. doi:10.1093/ndt/gfu239. [Epub 2014 Jul 17]; PubMed PMID: 25034755.
347. Perkowska-Ptasinska A, Deborska-Materkowska D, Bartczak A, et al. Kidney disease in the elderly: biopsy-based data from 14 renal centers in Poland. *BMC Nephrol.* 2016;17(1):194. PubMed PMID: 27884116. PubMed Central PMCID: PMC5123353.
348. Kirkland JL. The biology of senescence: potential for prevention of disease. *Clin Geriatr Med.* 2002;18(3):383–405. Review. PubMed PMID: 12424865.
349. Westendorp RG. What is healthy aging in the 21st century? *Am J Clin Nutr.* 2006;83(2):404S–409S. Review. PubMed PMID: 16470003.
350. Mungenast AE. Diacylglycerol signaling underlies astrocytic ATP release. *Neural Plast.* 2011;2011:537659. doi:10.1155/2011/537659. [Epub 2011 Jun 13]; PubMed PMID: 21826278. PubMed Central PMCID: PMC3151491.
351. Kanasaki K, Kitada M, Koya D. Pathophysiology of the aging kidney and therapeutic interventions. *Hypertens Res.* 2012;35(12):1121–1128. doi:10.1038/hr.2012.159. [Epub 2012 Oct 18]; Review. PubMed PMID: 23076406.
352. de Cavanagh EM, Inserra F, Ferder L. Angiotensin II blockade: how its molecular targets may signal to mitochondria and slow aging. Coincidences with calorie restriction and mTOR inhibition. *Am J Physiol Heart Circ Physiol.* 2015;309(1):H15–H44. doi:10.1152/ajpheart.00459.2014. [Epub 2015 May 1]; Review. PubMed PMID: 25934099.
353. Mazucanti CH, Cabral-Costa JV, Vasconcelos AR, et al. Longevity pathways (mTOR, SIRT, Insulin/IGF-1) as key modulatory targets on aging and neurodegeneration. *Curr Top Med Chem.* 2015;15(21):2116–2138. Review. PubMed PMID: 26059361.
354. Miles JM, Rule AD, Borlaug BA. Use of metformin in diseases of aging. *Curr Diab Rep.* 2014;14(6):490. doi:10.1007/s11892-014-0490-4. Review. PubMed PMID: 24752835. PubMed Central PMCID: PMC4209240.
355. Baar MP, Brandt RMC, Putavet DA, et al. Targeted Apoptosis of Senescent Cells Restores Tissue Homeostasis in Response to Chemotoxicity and Aging. *Cell.* 2017;169(1):132–147.e16. doi:10.1016/j.cell.2017.02.031. PubMed PMID: 28340339. PubMed Central PMCID: PMC5556182.

356. Krimpenfort P, Berns A. Rejuvenation by therapeutic elimination of senescent cells. *Cell*. 2017;169(1):3–5. doi:10.1016/j.cell.2017.03.014. PubMed PMID: 28340347.
357. Park SJ, Ahmad F, Philp A, et al. Resveratrol ameliorates aging-related metabolic phenotypes by inhibiting cAMP phosphodiesterases. *Cell*. 2012;148(3):421–433. doi:10.1016/j.cell.2012.01.017. PubMed PMID: 22304913. PubMed Central PMCID: PMC3431801.
358. Cufí S, Vazquez-Martin A, Oliveras-Ferraros C, et al. Metformin against TGFβ-induced epithelial-to-mesenchymal transition (EMT): from cancer stem cells to aging-associated fibrosis. *Cell Cycle*. 2010;9(22):4461–4468. [Epub 2010 Nov 15]; PubMed PMID: 21088486.

BOARD REVIEW QUESTIONS

1. You have been asked to see a man 78 years of age who has an estimated glomerular filtration rate (eGFR) of 45 mL/min/1.73 m^2 with a question about the need to start an angiotensin-converting enzyme (ACE) inhibitor. He has essentially been healthy apart from having two inguinal hernia repairs, and he has mild symptoms of prostatism with nocturia twice a night. Otherwise he feels well. Electrolyte levels are within normal limits, with a potassium level of 5.0 mmol/L. His urinary albumin-to-creatinine ratio is 12 mg/g of creatinine. Which outcomes are most likely in this patient?
   a. He will progress to end-stage kidney disease (ESKD) within the next 5 years.
   b. He will progress to ESKD within the next 10 years.
   c. He will die before the development of ESKD.
   d. Kidney function will remain stable.
   e. Kidney function will improve.

   Answer: c and d

   Rationale: In the absence of albuminuria, it is unlikely this patient has significant kidney disease. The GFR is low, most likely as a result of the loss of glomeruli with age. An ACE inhibitor in this patient is not indicated for his kidney function.

2. A 72-year-old woman is admitted after a fall. She was found 24 hours later at home. It is noted that her serum sodium level is 156 mmol/L. Her estimated GFR is 48 mL/min/1.73 m^2. She is on no medication and lives alone. Which age-related factors may have contributed to the hypernatremia?
   a. Reduced thirst
   b. Reduced urinary concentrating capacity
   c. Reduced total body water
   d. Increased vasopressin secretion
   e. High salt intake

   Answer: a, b, c

   Rationale: All these factors predispose to hypernatremia in older adults. Older kidneys have a reduced capacity to conserve water and solutes. Total body water is reduced (replaced with greater fat mass), and therefore older adults are more prone to volume depletion. Older adults have a reduced thirst response to increased osmolality and therefore are less likely to be able to correct hypernatremia spontaneously.

3. A 76-year-old woman wishes to donate a kidney to her 46-year-old son and is coming to you for a second opinion, given that she was declined as a donor elsewhere because her GFR is below 60 mL/min/1.73 m^2. Her body mass index (BMI) is 21. Her eGFR, calculated by the CKD-EPI formula, is 57 mL/min/1.73 m^2. She has no hypertension or diabetes, is a nonsmoker, and is a vegetarian. She exercises regularly, taking long walks three times a week with a seniors group. She is adamant that she wants to donate a kidney to her son—she sees him suffering on dialysis and wants to do everything possible to help him. Which of the following may assist in assessment of this woman as a potential donor?
   a. Determination of a cystatin C GFR
   b. Measurement of her GFR before and after a protein load (renal functional reserve)
   c. Determination of 24-hour urinary albumin excretion
   d. A renal biopsy showing the presence of 10% focal and segmental glomerulosclerosis
   e. Determination of kidney size by ultrasound

   Answer: All of the above

   Rationale: Given her relatively low BMI, use of a cystatin C GFR may assist in determining the accuracy of the creatinine-based eGFR value. Given that she is a vegetarian, the GFR may be lower than expected. Although not routinely used, detection of the capacity of her kidneys to respond to a protein load may indicate preservation of renal reserve. Any evidence of albuminuria or the presence of focal segmental glomerulosclerosis (FSGS) on the biopsy would indicate a primary renal pathology and likely exclude the woman from donation. Similarly significant renal asymmetry or small kidneys would indicate potential renal ischemia or renal disease and would be exclusion factors for donation.

23

Laboratory Assessment of Kidney Disease: Glomerular Filtration Rate, Urinalysis, and Proteinuria

Anoushka Krishnan | Adeera Levin

CHAPTER OUTLINE

KEY POINTS

- The glomerular filtration rate (GFR) is the amount of fluid filtered into the Bowman space per unit of time and is dependent on the porosity and the surface area of the glomerular membrane as well as the hydraulic pressure and oncotic pressure on the capillary side and in the Bowman space. Normal GFR is > 90 mL/min/1.73 m^2. There is a gradual decline in GFR with age, but the effect of age is variable.
- GFR measurement is cumbersome, as it needs the measurement of clearance of an exogenous filtration marker such as inulin. Hence, estimated GFRs (eGFRs) are calculated using the values of plasma creatinine. The most commonly used methods include the Cockcroft–Gault (CG) equation, the Modification of Diet in Renal Disease (MDRD) study equation, and more recently the Chronic Kidney Disease Epidemiology Collaboration (CKD-EPI) equation. The CKD-EPI equation is more accurate than the MDRD equation and both are more accurate than the CG equation.
- Special formulae may need to be used for children and the elderly, but the full age spectrum method of eGFR calculation may help circumnavigate this problem. Other unique groups include pregnant women, renal transplant recipients, and those with unusual body habitus or muscle mass.
- The main use of eGFR equations is in the detection, monitoring, and prognostication of CKD, which is largely asymptomatic. These equations have been derived from populations with stable CKD and are therefore not useful in the acute setting.
- Creatinine is a widely used marker of renal function. Many factors affect creatinine levels, such as muscle mass/injury, diet, age, gender, physical activity, and race. Creatinine is insensitive to even significant declines in GFR at the upper limit of normal due to the nonlinear relationship between creatinine and GFR. This is due to compensatory hyperfiltration of remaining functioning nephrons.
- Creatinine clearance (CrCl) is measured by collecting the patient's urine for 24 hours and measuring the total amount of excreted creatinine and the volume of urine. CrCl usually tends to overestimate eGFR.
- Proteinuria is one of the earliest markers of renal disease, occurring before a reduction in eGFR is noticed. It imparts diagnostic and prognostic information and is now a part of the Kidney Disease Improving Global Outcomes criteria for stratification of CKD.
- Casts are cylindrical bodies of renal origin that form from the aggregation of fibrils of Tamm–Horsfall glycoprotein (uromodulin). Red cell casts are always pathologic and indicate significant glomerular pathology.

An appreciation of the components of laboratory assessment of kidney disease is essential to the practicing clinician. This chapter describes three key aspects of laboratory assessment: the glomerular filtration rate (GFR), urinalysis, and proteinuria. Issues related to measurement tools, precision, bias, and interpretation are addressed for each of these variables, so that the reader may better appreciate the role of the laboratory in the diagnosis, follow-up, and management of kidney disease. Understanding the physiology of kidney function is essential to the interpretation of laboratory measurements and is highlighted within each section.

GFR is the single best measure of kidney function. Large studies consistently demonstrate the relationship of GFR to outcomes in general and renal populations, and the Kidney Disease Improving Global Outcomes (KDIGO) classification system uses GFR as one of the key dimensions in the diagnosis of chronic kidney disease (CKD). Urinary abnormalities may indicate acute or chronic conditions and isolated kidney or systemic diseases, and can be used to monitor both kidney and systemic diseases. Proteinuria is similarly an important marker of kidney disease and can also be seen in acute or chronic kidney conditions. In patients with CKD, the magnitude of albuminuria is proposed as a second dimension for the classification of severity in the KDIGO classification system because it affects prognosis.

The laboratory assessment of kidney disease can be used to diagnose, prognosticate, and measure progression of disease or response to therapy. CKD is increasingly recognized as an important public health problem, so accurate and appropriate use of laboratory testing is important. This chapter facilitates understanding and interpretation of key tests used in the assessment of kidney disease, both acute and chronic.

GLOMERULAR FILTRATION RATE

"Glomerular filtration rate" describes one of the key roles of the kidney: to filter plasma so as to excrete waste products and produce urine (an ultrafiltrate of plasma). In clinical practice, estimates of GFR are obtained using equations, and direct measurement is reserved for specific circumstances. This section reviews normal physiology, use of various filtration markers, the development and use of equations, and special circumstances in which GFR interpretation needs to be contextualized.

NORMAL PHYSIOLOGY

Separation of an ultrafiltrate of plasma across the barrier composed of the capillary wall, glomerular basement membrane, and podocyte is the first step in the production of urine and multiple functions of the kidney. The amount of fluid filtered into the Bowman space per unit of time is the GFR. Fluid movement is governed by Starling forces and so the glomerular filtrate that is produced is dependent on the following determinants:

- Porosity of the membrane (p)
- Surface area of the membrane (K)
- Hydraulic pressure and oncotic pressure on the capillary side (P_{GC} and π_{GC})
- Hydraulic pressure and oncotic pressure in the Bowman space (P_{BS} and π_{BS})

Table 23.1 Factors That May Alter Determinants of Glomerular Filtration Rate

p	Generally less important than other factors
K	↑ by relaxation of mesangial cells ↓ in glomerulonephritis and glomerulosclerosis
P_{GC}	↑ by afferent arteriole dilatation and efferent arteriole constriction
P_{BS}	↑ by raised intratubular pressure due to obstruction
π_{GC}	↑ by raised systemic oncotic pressure or decreased renal plasma flow
π_{BS}	Minimal impact

K, Surface area of the membrane; *p*, porosity of the glomerular membrane; P_{BS}, hydraulic pressure in the Bowman space; P_{GC}, glomerular capillary hydraulic pressure; π_{BS}, oncotic pressure in the Bowman space; π_{GC}, glomerular capillary oncotic pressure.

GFR can be calculated using the following equation:

$$GFR = p \times [(P_{GC} - P_{BS}) - K(\pi_{GC} - \pi_{BS})]$$

Factors that may alter these determinants of GFR are shown in Table 23.1. For further discussion of the physiology of glomerular ultrafiltration, please see Chapter 3.

The kidney filters approximately 180 L of plasma per day, which is equivalent to 125 mL/min. Kidney function is proportional to kidney size, which in turn is proportional to body surface area (BSA). Normal GFR is > 90 mL/min/1.73 m^2. In young adults GFR is approximately 120 to 130 mL/min/1.73 m^2. There is a gradual decline in GFR with age, but the effect of age is variable, in that some elderly patients have no change in renal function (see Chapter 22).

Protein intake and hyperglycemia can raise GFR by increasing renal plasma flow; the mechanism by which this occurs is unclear but may be activation of the intrarenal renin–angiotensin system.

MEASUREMENT OF GFR

GFR can be measured provided that the concentration of a substance that is freely filtered at the glomerulus and neither reabsorbed nor secreted in the renal tubule is measured in the plasma and in a timed urine collection. GFR is equivalent to the "clearance rate" of this substance or filtration marker, which can be calculated as follows:

$$GFR = \frac{\text{Urine concentration of marker} \times \text{urine volume}}{\text{Plasma concentration of marker} \times \text{duration of urine collection}}$$

Filtration markers may be endogenous (e.g., creatinine, cystatin C) or exogenous (e.g., inulin, iohexol). GFR can be expressed as normalized to BSA to reflect physiologic matching of GFR to kidney size and in turn to BSA (mL/min/1.73 m^2), or as an absolute value (mL/min). An absolute value of GFR is useful in the setting of drug dosing, which

is discussed further later. As an alternative to direct measurement of the clearance of a filtration marker, GFR can be estimated using an equation based on the plasma concentration of a filtration marker in steady state.

The most appropriate method for measurement of GFR depends on the purpose for which kidney function is being monitored. Direct measurement of GFR is time-consuming and may require medical supervision or the patient's presence at the hospital, so it is not usually performed as part of everyday practice. An exact value of the GFR is not required for most clinical settings. Understanding the trend within an individual patient's renal function is often what is needed. As a result, plasma urea and creatinine and estimated GFR (eGFR) calculations based on plasma creatinine are most often used. Alternatively, accuracy in the measurement of GFR is important for drug dosing of medications with narrow therapeutic windows (e.g., chemotherapy drugs) and is vital for appropriate selection and approval of live donors for kidney transplantation.

GLOMERULAR FILTRATION MARKERS

The ideal glomerular filtration marker probably does not exist. Such a marker would have the following characteristics:

- Distributed freely and instantaneously throughout the extracellular space
- Not bound to plasma proteins
- Freely filtered at the glomerulus
- Not secreted or reabsorbed at the tubules
- Eliminated wholly by the kidney
- Resistant to degradation
- Easy and inexpensive to measure

An understanding of the limitations of each filtration marker is important to be able to interpret results. Given that kidney disease is often asymptomatic and dependent on the accuracy of laboratory tests, it is imperative that the clinician knows the advantages and disadvantages of each specific test before making clinical decisions.

ENDOGENOUS GLOMERULAR FILTRATION MARKERS

Urea

Urea is not an accurate filtration marker because it is subject to a number of influences in addition to glomerular filtration. The liver produces urea in the urea cycle as a waste product of the digestion of protein. Therefore increased plasma levels may be due to factors independent of renal function, such as increased production in high protein intake, gastrointestinal bleeding due to absorption of amino acids from blood in the gastrointestinal tract, and high catabolic states such as those associated with glucocorticoid therapy.

Low urea levels are seen in decreased protein intake and chronic liver disease due to reduced synthesis of urea.

Urea is readily reabsorbed in the proximal tubule, particularly at low urinary flow rates. As a filtration marker, urea therefore has limited use because, although it is freely filtered, significant reabsorption means that the amount that is excreted is not what was filtered. High levels of urea may not necessarily indicate poor renal function but could instead reflect hypovolemia and renal hypoperfusion.

Serum Creatinine

Creatinine is a product of normal muscle metabolism. Phosphocreatine is a source for replenishment of phosphate when adenosine triphosphate is used by muscle cells. Creatine and phosphocreatine are nonenzymatically converted at an almost steady rate (approximately 2% of total creatine per day) to creatinine. Creatinine is not bound to plasma proteins, being freely filtered by the kidney, but it is unfortunately secreted by the tubules, making it an imperfect filtration marker. Despite its many limitations, however, its measurement is still the test most widely used by physicians to gauge renal function.

Serum creatinine level does not measure GFR but varies inversely with GFR and so is an indirect marker of GFR. The serum creatinine level can be used in estimation equations for GFR, and urinary creatinine clearance (CrCl) can be used to approximate GFR.

Factors affecting creatinine levels unrelated to renal function include muscle mass and/or injury and consumption of meat or creatine. Factors affecting muscle mass, such as age, sex, race, and physical activity, can in turn affect creatinine levels. Women, for example, have lower creatinine levels than men at the same level of GFR. Rhabdomyolysis has also been suggested to cause a greater rise in serum creatinine than other causes of acute kidney injury (AKI), because of the release of preformed creatine and phosphocreatine that is converted into creatinine.

Secretion of creatinine by the renal tubule is affected by

Drugs (decrease secretion): For example, trimethoprim, cimetidine, pyrimethamine, dapsone.

Decreased renal function: Each tubule excretes a higher proportion of creatinine as renal function declines. This secretory process is saturated when the serum creatinine level exceeds 1.5 to 2 mg/dL (132–176 μmol/L).

Extrarenal degradation of creatinine in the gut also rises as renal function declines due to bacterial overgrowth in the intestines leading to increased bacterial creatininase activity.[1] This extrarenal clearance may be as much as two-thirds of total daily creatinine excretion.

Sources of Error in Measurement of Creatinine. Clinicians may be unaware of the intricacies and complexities of creatinine measurement and how they may be relevant to day-to-day practice.

Laboratory methods to measure serum creatinine include

- Alkaline picrate (Jaffe method)
- Enzymatic methods
- Isotope dilution mass spectrometry (IDMS)
- High-performance liquid chromatography (HPLC)

There is wide variation in measured creatinine concentration, depending on the laboratory method and the instruments used. In 2003, the College of American Pathologists conducted a survey of 5624 participating laboratories that showed a bias from the reference value of between –0.06 and 0.31 mg/dL or –7% and 34%.[2] This bias was thought to be predominantly due to differences in instrument calibration among manufacturers. As a result, a creatinine standard reference material was prepared by the National Institute of Standards and

Technology, which is currently being used by almost all major manufacturers for calibration. The method of analysis (Jaffe or enzymatic) should also have minimal bias in comparison with the IDMS reference methodology.

Measurement of creatinine obviously affects measured CrCl and calculation of estimated CrCl or GFR, and therefore it has been recommended as part of the KDIGO initiative guidelines that all creatinine results be traceable to reference materials and methods listed on the Joint Committee for Traceability in Laboratory Medicine database.

The Jaffe method measures creatinine by complexing creatinine with alkaline picrate, followed by measurement with a colorimetric technique. This colorimetric assay may falsely measure normal plasma constituents such as glucose and plasma proteins as creatinine. As a result, the measured creatinine result may be falsely high. The Jaffe method may also report falsely low creatinine levels if there are very high serum bilirubin levels. Modified Jaffe methods attempt to take this into account by removing these interfering chromogens before analysis. This inference is sometimes corrected for by some manufacturers by deducting an estimated value based on average bias from measured results. Currently, the techniques used in most laboratories are modified alkaline picrate and enzymatic methods, but it is recommended that the enzymatic method be adopted because this is more specific.

Although serum creatinine concentration is widely used as a marker of renal function, it is insensitive to even significant declines in GFR at the upper limit of normal due to the nonlinear relationship between creatinine and GFR (Fig. 23.1). This is due to compensatory hyperfiltration of remaining functioning nephrons, secretion of creatinine, and extrarenal elimination of creatinine as the GFR declines. It is consequently a poor screening tool for early kidney disease.

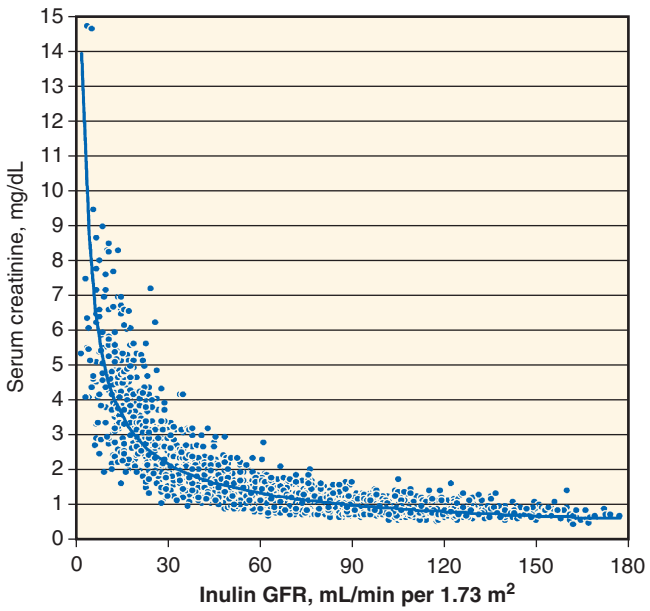

Fig. 23.1 Relationship between plasma creatinine and glomerular filtration rate (GFR). (From Botev R, Mallie JP, Couchoud C, et al. Estimating glomerular filtration rate: Cockcroft-Gault and Modification of Diet in Renal Disease formulas compared to renal inulin clearance. *Clin J Am Soc.* 2009;4:899–906.)

Within-person variability of creatinine is also significant, at 8%; therefore significant change in serum creatinine is generally defined as at least 10%, which at early stages of kidney disease may represent a significant decline in GFR.

Serum creatinine results should be interpreted in the clinical context. The same serum creatinine concentration may correspond to a vastly different GFR in patients of different body composition. Volume status should also be taken into account because dilution of creatinine leads to an apparently low result.

Creatinine Clearance. CrCl is measured by collecting the patient's urine for 24 hours and measuring the total amount of excreted creatinine and the volume of urine. With the equation discussed earlier to calculate clearance of a filtration marker, CrCl is calculated as follows:

For example, for a patient with a serum creatinine value of 100 µmol/L, a urine creatinine value of 10,000 µmol/L, and a urine volume of 1.44 L, CrCl would be calculated as follows:

$$\text{CrCl} = \frac{\text{urine creatinine concentration} \times \text{urine volume}}{\text{plasma creatinine concentration} \times \text{duration of urine collection}}$$
$$= 144\ \text{L}/24\ \text{h} = 100\ \text{mL/min}$$

If this result is adjusted for BSA in a small person (height = 160 cm, weight = 50 kg, BSA 1.5 m), then the CrCl would be

$$\frac{\text{CrCl} \times 1.73}{\text{BSA}} = \frac{100 \times 1.73}{1.5} = 115\ \text{mL/min}/1.73\ \text{m}^2$$

For a larger person with a BSA of 2.0 m (height = 180 cm, weight = 80 kg), the adjusted CrCl would be 86.5 mL/min/1.73 m^2.

Although the clearance of an ideal substance would be equivalent to GFR, CrCl tends to exceed true GFR by approximately 10% to 20% because of the secretion of creatinine by the tubules. This error was previously compensated for by errors in the Jaffe assay that would overestimate serum creatinine value. Now that creatinine measurement has been standardized CrCl will consistently overestimate true GFR.

The main problem with CrCl is its reliance on timed urine collection, which is often inaccurate. Furthermore, tubular secretion of creatinine increases with decreased renal function, thus masking a true drop in GFR. In addition, the practical difficulties of conducting a 24-h urine collection for patients and the challenges of handling large volumes of urine for laboratories have resulted in this method being used only infrequently.

Cystatin C

Cystatin C is a low-molecular-weight (LMW; 13-kD) basic protein that is produced at a constant rate by all nucleated cells. It is freely filtered by the glomerulus and is not secreted; proximal tubule cells reabsorb and catabolize the filtered cystatin C so that little is normally excreted in the urine. Therefore although plasma cystatin C levels are used in estimating GFR, cystatin C measurement cannot be used as a conventional urinary excretory marker for GFR. Rather, cystatin C has been regarded as one of several available novel markers of kidney injury.

Plasma cystatin C levels are highest in the first days of life and stabilize after 1 year of age, with levels approximating those of adults. Polymorphic variants in the *CST3* gene encoding cystatin C appear to affect production, and interindividual variations in cystatin C values account for 25% of its biologic variability, in comparison with 93% for creatinine. Within-person variation of cystatin C values is 6.8%.[3]

Cystatin C levels were reported to be independent of sex, muscle mass, and age after 12 months, but there is a growing body of evidence that this may not be the case. Cystatin C levels may be affected by factors independent of renal function, such as corticosteroids, thyroid dysfunction, obesity, diabetes, smoking, and high C-reactive protein value. This is problematic as, for example, cystatin C may not be useful in renal transplant patients because they have subclinical inflammation and commonly use long-term corticosteroids.

A meta-analysis published in 2002 showed that serum cystatin C measured with an immunonephelometric assay is more accurate than serum creatinine as a marker of GFR.[4,5] However, as noted previously, the cystatin C value, like the creatinine value, may be affected by a number of factors other than the GFR.

Laboratory techniques to measure cystatin C include latex immunoassays, such as automated particle-enhanced turbidimetric immunoassay and nephelometric immunoassay. Other techniques are radioimmunoassay, fluorescent techniques, and enzymatic immunoassays. Most of these assays are more expensive than the measurement of serum creatinine and although the International Federation of Clinical Chemists has developed a reference material for standardization of cystatin C, international standardization remains in process.[6–8]

A number of equations utilizing cystatin C have been developed to estimate GFR. The 2008 Chronic Kidney Disease Epidemiology Collaboration (CKD-EPI) cystatin C and CKD-EPI creatinine–cystatin C equations were developed in a preliminary study to assess the impact of cystatin C level on eGFR in individuals with CKD prior to the standardization of the cystatin C assay.[9] The 2012 CKD-EPI cystatin C and the CKD-EPI cystatin C–creatinine equations were developed from a diverse group of 5352 individuals from 13 studies. These equations were then validated in 1119 participants from 5 different studies in which GFR had been measured. The creatinine–cystatin C equation was found to perform better than equations that used creatinine or cystatin C alone—it produced an eGFR that was within 20% of the measured GFR (mGFR) in a significantly higher proportion of participants. Bias with the new, combined creatinine–cystatin C equation and with the average of the new cystatin C equation and the creatinine equation was similar to that with the individual creatinine and cystatin C equations, but they had greater precision and accuracy and resulted in more accurate classification of GFR as < 60 mL/min/1.73 m^2, the threshold for the diagnosis of CKD.[10] This was found to hold true even in individuals with low body mass index (a subgroup in which creatinine-based GFR estimates are known to be less accurate) and was less subject to the effects of age, sex, and race.

Other equations have been reported since the development of the CKD-EPI cystatin C and creatinine–cystatin C equations, which perform as well or better than the CKD-EPI cystatin C equation in some subgroups but do not perform better than the CKD-EPI equation in a diverse population.[11–14]

It has been proposed that cystatin C–based equations may be more accurate in populations with lower creatinine production, such as in children, the elderly, or cirrhotic patients,[15–17] although whether cystatin C correlates better with GFR than serum creatinine in patients with diabetic nephropathy is unclear.[18] In addition, steroids may affect cystatin C levels, thus making its utility in transplant recipients unclear.[15]

The 2012 KDIGO guidelines recommend using serum creatinine and a GFR estimating equation for initial assessment and to use additional testing such as cystatin C or a clearance measurement for confirmatory testing if eGFR based on serum creatinine is less accurate. For reporting $eGFR_{cys}$ and $eGFR_{cr–cys}$ in adults, the guideline recommended using the 2012 CKD-EPI cystatin C equations or another cystatin C–based GFR estimating equation if it has demonstrated improved accuracy of GFR estimates compared with these CKD-EPI cystatin C equations. The guideline recommends measuring cystatin C in adults with $eGFR_{cr}$ of 45–59 mL/min/1.73 m^2 without markers of kidney damage if CKD confirmation is required. If $eGFR_{cys}$/$eGFR_{cr–cys}$ is also < 60 mL/min/1.73 m^2, the CKD diagnosis is confirmed. If $eGFR_{cys}$/$eGFR_{cr–cys}$ is ≥ 60 mL/min/1.73 m^2, the CKD diagnosis is not confirmed.[19] While this might help in risk stratification, the guidelines do leave a number of questions unanswered, such as how to incorporate cystatin-based GFR estimates into routine clinical practice and use this equation for longitudinal follow-up of patients. The NKF-KDOQI commentary on the KDIGO guideline concurred with their recommendations for GFR evaluation but recommended against widespread use of cystatin C because of concerns regarding incomplete understanding of its non-GFR determinants, higher costs, and incomplete standardization of assays.[20]

Novel Endogenous Filtration Markers

Several alternative novel endogenous substances are under investigation as potential markers that could be used aside from urea, creatinine, and cystatin C. They are beta-trace protein (BTP), β_2-microglobulin (B2M), and symmetrical dimethylarginine.

BTP is a 23–29-kDa protein, larger isoforms of which are found in the serum and urine. In late 2000s, the White and Pöge equations were developed, using BTP alone or in combination with urea or creatinine to determine eGFR. However, they were not felt to offer any significant benefit over the Modification of Diet in Renal Disease (MDRD) equation.[21,22]

B2M is a 11.8-kDa protein commonly used as a prognostic marker for multiple myeloma. It is freely filtered by the glomerulus and is extensively reabsorbed and metabolized in the proximal tubule.[23] The CKD-EPI investigators attempted to develop eGFR equations using both BTP and B2M.[24] They found that although the combined equation was similar to the CKD-EPI creatinine and cystatin C–based equations, it did not offer an improvement over either, nor was it as accurate as the combined CKD-EPI equation.

Interestingly, both BTP and B2M were subsequently found to be strong predictors for CKD progression, cardiovascular disease, and mortality.[25,26]

Used alone, these markers have a number of shortcomings, such as lack of standardization of assays, lack of certified reference materials, and a number of non-GFR determinants (such as male gender, markers of inflammation, and body

mass index). They do, however, hold promise as potential endogenous filtration markers that could not only improve GFR estimation in combination with other measurements (by reducing bias and improving accuracy), but also potentially predict the risk of ESKD and mortality. The future of GFR measurement will likely involve the use of kidney metabolomics, looking to use several plasma-based markers to give a better estimate of GFR, predict risk, and reduce the impact of individual non-GFR determinants.[27]

Equations for Estimating GFR

Because direct measurement of GFR is not practical in clinical practice, estimation equations have been developed to aid clinicians in interpretation of serum creatinine, given the limitations previously cited.

A multitude of equations (Table 23.2) derived for the estimation of GFR are available. They all attempt to transform the serum concentration of a filtration marker into a value approximating the GFR, usually with the addition of other factors, such as age, sex, weight, and height, in part because the main filtration marker that is used is creatinine, which is known to be affected by these factors.

The main use of eGFR equations is in the detection, monitoring, and prognostication of CKD, which is largely asymptomatic. These equations have been derived from populations with stable CKD and are therefore not useful in the acute setting. Translating creatinine values, especially at the upper limit of normal (which as previously discussed do not reflect significant declines in GFR), into an eGFR has heightened the awareness of CKD. Estimation equations

Table 23.2 Most Commonly Used Equations for Estimating Glomerular Filtration Rate

Equation Name	Equation	Derivation Population
Cockcroft–Gault (1976)	(140 – age) × wt (kg)/creatinine (μmol/L) × 0.81 Female: × 0.85 (140 – age) × lean body weight (kg)/Cr (mg/dL) × 72	249 male veterans Median GFR 34
MDRD equation (1999)	$175 \times SCr^{-1.154} \times age^{-0.26} \times 0.742$ (if female) × 1.212 (if black)	1628 patients enrolled in the MDRD Study (mean age, 50.6 years)
MDRD equation without ethnicity factor[a]	$175 \times SCr^{2190} \times age^{-0.26} \times 0.742$ (if female)	Mean GFR 39.8 mL/min/1.73 m^2
CKD-EPI equation (2009)	$141 \times \min(SCr/\kappa, 1)^{\alpha} \times \max(SCr/\kappa, 1)^{-1.209} \times 0.993^{Age} \times 1.018$ (if female) × 1.159 (if black), where κ is 0.7 for females and 0.9 for males α is –0.329 for females and –0.411 for males min indicates the minimum of SCr/κ or 1 max indicates the maximum of SCr/κ or 1	8254 participants from 6 research studies and 4 clinical populations (mean age, 47 years) Mean GFR 68 mL/min/1.73 m^2
CKD-EPI cystatin C (2012)	$133 \times \min(SCysC/0.8, 1)^{-0.499} \times \max(SCysC/0.8, 1)^{-1.328} \times 0.996^{Age} \times 0.932$ (if female), where min indicates the minimum of SCysC/0.8 or 1 max indicates the maximum of SCysC/0.8 or 1	5352 participants from 13 studies (mean age, 47 years) Mean GFR 68 mL/min/1.73 m^2
CKD-EPI creatinine–cystatin C (2012)	$135 \times \min(SCr/\kappa, 1)^{\alpha} \times \max(SCr/\kappa, 1)^{-0.601} \times \min(SCysC/0.8, 1)^{-0.375} \times \max(SCysC/0.8, 1)^{-0.711} \times 0.995^{Age} \times 0.969$ (if female) × 1.08 (if black), where α is –0.248 for females and –0.207 for males κ is 0.7 for females and 0.9 for males min(SCr/κ,1) indicates the minimum of SCr/k or 1 and max(SCr/κ,1) indicates the maximum of SCr/k or 1 min(SCysC/0.8,1) indicates the minimum of SCysC/0.8 or 1 and max(SCysC/0.8,1) indicates the maximum of SCysC/0.8 or 1	34 mL/min
BIS equation BIS1: creatinine BIS2: creatinine and cystatin C (2012)	$BIS1 = 3736 \times creatinine^{-0.123} \times age^{-0.131} \times 0.82$ (if female) $BIS2 = 767 \times cystatin\ C^{-0.98} \times creatinine^{-0.77} \times age^{-0.94} \times 0.87$ (if female)	610 individuals over 70 years of age Mean age: 78.5 years
FAS equation: normalized serum creatinine (SCr/Q) (2016)	eGFR = 107.3 × / [Scr/Q] for 2 years < age ≤ 40 years eGFR = 107.3 × 0.988(age – 40)/[Scr/Q] for age >40 years	6870 individuals spanning all age groups (<18 to >70 years)

[a]African-American coefficient of the MDRD study equation.

BIS, Berlin Initiative Study; *CKD-EPI,* Chronic Kidney Disease Epidemiology Collaboration; *Cr,* creatinine; *eGFR,* estimated glomerular filtration rate; FAS, full age spectrum; *GFR,* glomerular filtration rate; *MDRD,* Modification of Diet in Renal Disease; *SCr,* serum creatinine; *SCr/Q,* normalized serum creatinine, where Q is the median serum creatinine from healthy populations to account for age and gender; *SCysC,* serum cystatin C; *wt,* weight.

Adapted from Tables 12 and 16 in Kidney Disease: Improving Global Outcomes (KDIGO) CKD Work Group. KDIGO 2012 clinical practice guideline for the evaluation and management of chronic kidney disease. *Kidney Int Suppl.* 2013;3:1–150.

also appear to be reasonably accurate for following changes in GFR over time.[28,29]

Bias, Precision, and Accuracy. The performance of estimation equations is assessed by measurements of bias, precision, and accuracy.

- "Bias" results from the systematic underestimation or overestimation of the GFR in a population due to an error within the equation itself. It is calculated as the mean or median difference between the mGFR and eGFR values.
- "Precision" refers to the reliability and reproducibility of repeated measurements with one another. In the case of eGFR, it is usually expressed as the standard deviation or interquartile range of differences between eGFR and mGFR values.
- "Accuracy" combines bias and precision and is the most useful assessment of an estimation equation. It is measured as the percentage of GFR estimations within a particular percentage range (usually 30%) from their respective GFR measurements.

The problem of bias with eGFR equations can potentially be overcome with derivation of the equation from larger sample sizes and use of filtration markers such as cystatin C, which are less subject to interference by other factors. Accuracy, however, is difficult to achieve in a heterogeneous population. Even the latest Chronic Kidney Disease Epidemiology Collaboration (CKD-EPI) equation using creatinine, which is being adopted widely, has accuracy such that 80.6% of eGFR values are within 30% of mGFR (Fig. 23.2). This means that one in five values of eGFR in the general population is incorrect. Again, in day-to-day clinical practice, accuracy may not be necessary, and establishing an eGFR trend within an individual patient with CKD is probably more important.

Modification of Diet in Renal Disease and Chronic Kidney Disease Epidemiology Collaboration Equations. Although a number of GFR estimation equations have been developed, two equations are most widely used in clinical practice.

MDRD. The MDRD study equation was initially derived in 1999 from a population of 1628 individuals who had participated in the MDRD study, using creatinine measured by a modified Jaffe method.[30] A new MDRD equation was expressed in 2004 for IDMS-traceable creatinine values. The MDRD equation was compared against a gold standard, urinary clearance of iothalamate. The performance of the MDRD equation was evaluated in a number of populations because it was initially derived from a primarily Caucasian American population. A number of coefficients have been derived to compensate for differences in body mass and diet in populations of different ethnicity with varying degrees of performance.

The MDRD equation was widely adopted in the United States, Europe, and Australia, where eGFR is now routinely reported with serum creatinine results. It is gradually being replaced by the CKD-EPI equation.

The limitations of the MDRD equation are mainly its tendency to underestimate the GFR and its relatively low accuracy at higher GFR values.

CKD-EPI. The CKD-EPI equation was derived in 2009 in 8254 patients (a further 3896 patients pooled from 16 studies were used for validation), with urinary clearance of iothalamate again used as the gold standard.[31] It has less bias and greater accuracy than the MDRD equation, especially at higher GFR. A meta-analysis involving 1.1 million adults showed that the CKD-EPI equation reclassified a significant number of patients (24.4%) into a higher GFR range[32]; 34.7% of patients who were classified as having stage 3A CKD (eGFR 45–59 mL/min/1.73 m^2) with the MDRD equation did not have GFRs < 60 mL/min/1.73 m^2 with the CKD-EPI equation

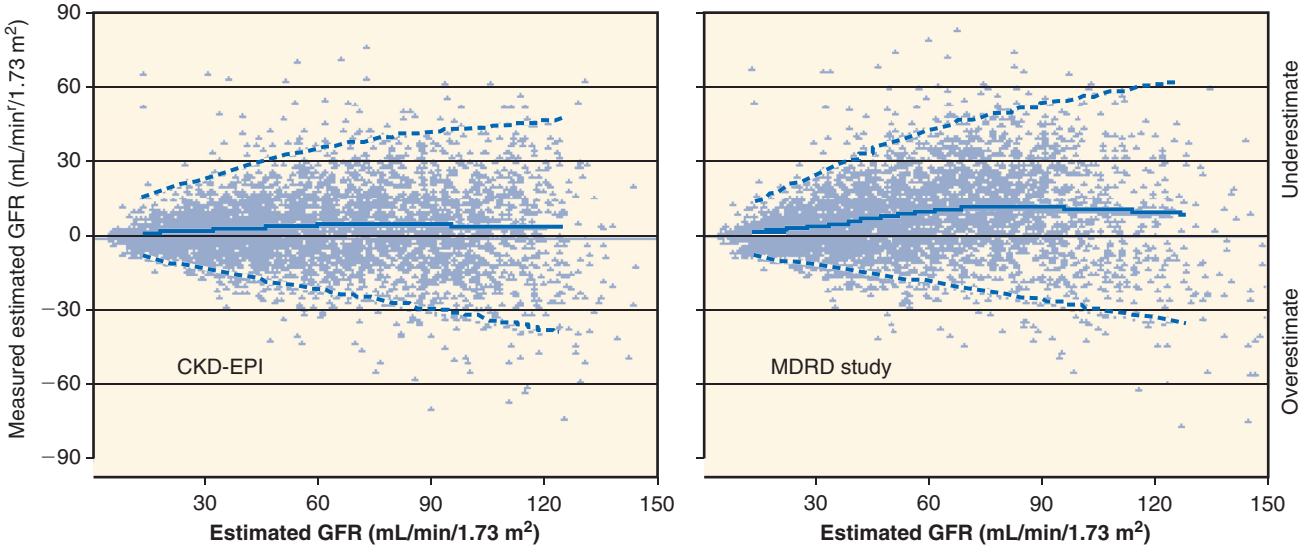

Fig. 23.2 Difference between measured and estimated glomerular filtration rate (GFR) using the Modification of Diet in Renal Disease (MDRD) and Chronic Kidney Disease Epidemiology Collaboration (CKD-EPI) estimation equations. Shown are smoothed regression lines and hashed 95% confidence interval lines. Although both the MDRD and CKD-EPI equations tend to underestimate the GFR, the CKD-EPI equation does so to a lesser degree, particularly at higher GFR. Therefore the CKD-EPI equation has less bias. (From Levey AS, Stevens LA, Schmid CH, et al. A new equation to estimate glomerular filtration rate. *Ann Intern Med.* 2009;150:604–612.)

and were therefore no longer regarded as having CKD according to the newest definition. The precision of the CKD-EPI and MDRD equations is still suboptimal, however, because eGFR and mGFR values varied by at least 16.6 and 18.3 mL/min/1.73 m^2 (the interquartile range of differences for patients across the range of GFR), respectively.

CKD-EPI equations have also been derived for cystatin C and a combination of cystatin C and creatinine. Cystatin C measurement in the derivation of these equations was traceable to the standard reference material for cystatin C, although cystatin C measurement is not uniformly standardized, as noted previously. GFR estimation using cystatin C and creatinine in combination has been shown to be more accurate than either marker alone, but eGFR using cystatin C is not superior to eGFR using creatinine.[33] The KDIGO 2012 guidelines recommend initial GFR evaluation using serum creatinine and a GFR estimating equation and confirmatory testing using tests such as serum cystatin C or a clearance measurement in certain circumstances if $eGFR_{cr}$ is less accurate. For confirmatory testing using a clearance measurement, the recommendations include using plasma or urinary clearance of an exogenous filtration marker rather than CrCl. Recommendations to clinical laboratories included using assays for creatinine and cystatin C that are traceable to reference standards, and reporting eGFR using the CKD-EPI equations, or alternative equations if they are superior.[19]

Risk Stratification of CKD with eGFR: eGFR equations transform the creatinine or cystatin C measurement into a value that approximates the mGFR. This value can also be used to classify the patient according to the stage of CKD. Decreasing values of GFR in patients with CKD have been associated with increasing risk for metabolic complications of CKD, end-stage kidney disease (ESKD), cardiovascular disease, and death.[34] The many eGFR equations have performed variably in their ability to predict certain outcomes in different populations. This difference in ability to risk stratify is due to the different degrees of importance placed on factors such as age and sex, which also affect prognosis, in these equations. The importance of accuracy in measuring GFR versus stratification of risk as a result of decreased GFR is a matter of ongoing debate and beyond the scope of this text. For further discussion of risk factors in CKD, please see Chapter 20.

Cockcroft–Gault Equation. The Cockcroft–Gault (CG) equation estimates CrCl rather than the GFR. This equation was developed in 1976 from a cohort of 249 men, and the creatinine assay method that was used to derive this equation was not standardized.[35] The equation is

$$\text{CrCl (mL/min)} = \frac{(140 - \text{age}) \times \text{lean body weight (kg)}}{\text{Cr (mg/dL)} \times 72}$$

The CG equation has not been re-expressed since the adoption of new assay methods for estimation of creatinine. For these reasons, the CG equation systematically overestimates GFR and should not be used without an understanding of its limitations, although it is currently still often used to guide drug dosing including drug research. There is especially a risk of overdosing drugs that have a narrow therapeutic index with the CG equation.

EXOGENOUS GLOMERULAR FILTRATION MARKERS

Inulin

Inulin remains the gold standard filtration marker but its use is impractical for routine clinical purposes. Inulin is a polymer of fructose found in tubers such as the Jerusalem artichoke and chicory. It distributes in extracellular fluid, does not bind to plasma proteins, is freely filtered at the glomerulus, and is neither reabsorbed nor secreted by the renal tubules.

Inulin is intravenously infused at a constant rate while blood and urine are sampled frequently over several hours, ideally following insertion of a bladder catheter. The patient takes an oral water load and must continue consuming water throughout the test to ensure a high urine output.

Clearance Methods for Other Exogenous Glomerular Filtration Markers

Owing to the difficulty and expense of using inulin, new reference standard filtration markers have been introduced as alternatives and have been widely used since the 1990s. Urinary iothalamate and iohexol have now been adopted now been adopted as the reference standard for measurement of GFR. Clearance of these filtration markers can be measured in the urine or in blood or with nuclear imaging in the case of radiolabeled markers to avoid problems with urine collection.[36]

GFR is calculated from plasma clearance after a bolus intravenous injection of an exogenous filtration marker, with clearance being calculated from the amount of the marker administered divided by the area under the curve of plasma concentration over time. The decline in serum concentration is due initially to the disappearance of the marker from the plasma into its volume of distribution (fast component) and then subsequently to renal excretion (slow component). It is best estimated using a two-compartment model that requires blood sampling early (usually two or three time points until 60 min) and late (one to three time points from 120 min onward). GFR can also be measured by counting a radioactive exogenous filtration marker over the kidneys and bladder areas; however, this technique is thought to be generally less accurate.

These methods are not perfect and are subject to imprecision, albeit at a much lower level than that of equations that estimate GFR.

Radiolabeled Markers

Radiolabeled iothalamate, ethylenediaminetetraacetic acid (EDTA), and diethylenetriaminepentaacetic acid (DTPA) are all used as glomerular filtration markers.

Iothalamate may be labeled with iodide I 125 (^{125}I) or used unlabeled. EDTA is commonly used in Europe, whereas DTPA is widely used in the United States. EDTA is usually labeled with chromium Cr 51 (^{51}Cr), but EDTA may be reabsorbed by the tubules, leading to underestimation of GFR. DTPA is labeled with technetium Tc 9m (^{99m}Tc), and the major limitation of its use is the potential for an unpredictable dissociation of ^{99m}Tc from DTPA and binding to plasma proteins, resulting in underestimation of GFR.

Unlabeled Radiocontrast Agents

Because of concerns about exposure to radiation, storage, and disposal of radionuclide markers, techniques have been

developed to measure low levels of iodine in urine and plasma. Iothalamate and iohexol concentrations have been measured using HPLC, but the main disadvantage of this approach is the complexity of the HPLC assay. X-ray fluorescence of samples may also be used to measure iodine levels but requires a higher dose of contrast agent.

Iohexol is a nonionic, low-osmolar contrast agent. It is not reabsorbed, metabolized, or secreted by the kidney and is excreted completely unmetabolized in the urine. It has low toxicity and is usually used in doses 10 to 50 times higher in radiologic procedures than those used for GFR determination.

Urinary clearances of iothalamate and iohexol closely correlate with urinary inulin clearance, and are therefore the methods most commonly used to measure GFR.

SPECIFIC CIRCUMSTANCES OR POPULATIONS

CHILDREN

Adult GFR equations such as the MDRD have been shown to be inappropriate in children aged ≤9 years (see also Chapter 72). Multiple equations (Table 23.3) have been derived for estimation of GFR in children, but the most popular is the Schwartz equation, which was devised in 1976[37]

$$\text{eGFR} = \frac{k \times L}{SCr}$$

where k depends on the age of the child, L is length or height, and SCr is serum creatinine. Like the CG equation, the Schwartz equation has now been shown to systematically overestimate GFR. The reasons are the creatinine assay technique and measurement factors specific to children. As previously mentioned, the Jaffe method can be interfered with by plasma proteins, and the correction factor that is deducted to account for this interference is estimated by taking an average bias from measured results. In children, who have lower levels of plasma proteins, this correction factor may be too high, resulting in an erroneously low creatinine value. Because of the low muscle mass of children, the influence of a measurement error is also proportionately larger than an error of the same magnitude in an adult sample.

The simple bedside Schwartz equation—eGFR = 0.413 × (height [cm]/serum creatinine [mg/dL])—was developed using standardized creatinine methods in 2009.[38] This equation provides good approximation of a more complicated Schwartz eGFR formula, using creatinine, urea, and cystatin C as well as height.[38] Cystatin C has been suggested to be more accurate than creatinine as an indirect marker of renal function in children.[39]

A limitation is that the equation was derived from a cohort of 600 children with CKD who had abnormal growth. Therefore this GFR estimation equation may not be accurate for children who have less impairment of renal function and normal skeletal growth (Table 23.3).

ELDERLY POPULATION

Elderly individuals were either not included or were poorly represented in the study populations used to develop the CG, MDRD, and CKD-EPI equations. The Berlin Initiative Study (BIS) attempted to develop an equation based on serum creatinine concentration, gender, and age using a study population that included 610 individuals aged >70 years. The equation was compared with a gold standard iohexol plasma clearance measurement, three creatinine-based equations

Table 23.3 Equations Using Serum Biomarkers for Estimating GFR in Children and Adolescents

Equation Name	Equation	Derivation Population: No. Children	Derivation Population: Age (Years)	Derivation Population: GFR Range or Median (mL/min)
Creatinine Based				
Schwartz, 1976	$0.55 \times Ht/Scr$	77	1–21	3–220
Counahan, 1976	$0.43 \times Ht/Scr$	103	0.2–14	4–200
Leger, 2002	$(0.641 \times Wt)/Scr + (0.00131 \times Ht^3)/Scr$	97	1–21	97
Schwartz, 2009	$0.413 \times Ht/Scr$ $40.7 \times (HT/Scr)^{0.640} \times (30/BUN)^{0.25}$	349	1–17	41
Cystatin C Based				
Filler, 2003	$91.62 \times (cysC)^{-1.123}$	85	1–18	103
Grubb, 2005	$84.69 \times (cysC)^{-1.680} \times 1.384$ if <14 years	85	3–17	108
Zappitelli, 2006	$75.94 \times (cysC)^{-1.17} \times 1.2$ if Tx	103	1–18	74
Creatinine and Cystatin C Based				
Bouvet, 2006	$63.2 \times (Scr/1.086)^{-0.19} \times (cysC/1.2)^{-0.93} \times (Wt/45)^{0.68} \times (years/14)^{0.77}$	100	1–23	92
Zappitelli, 2006	$43.82 \times e^{0.004} \times Ht \times (cysC)^{-0.635} \times (Scr)^{-0.547}$	103	1–18	74
Schwartz, 2009	$39.1 \times (HT/Scr)^{0.516} \times (1.8/cysC)^{0.294} \times (30/BUN)^{0.40} \times (1.099)$ if male $\times (HT/1.4)^{0.9}$	349	1–17	41

BUN, Blood urea nitrogen; *cysC,* cystatin C; *GFR,* glomerular filtration rate; *Ht/HT,* height; *Scr,* serum creatinine; *Tx,* transplant; *Wt,* weight.
Adapted from Table 3 in Schwartz GJ, Work DF. Measurement and estimation of GFR in children and adolescents. *Clin J Am Soc Nephrol.* 2009;4:1832–1843.

(CG, MDRD, and CKD-EPI), and three equations based on cystatin C and was shown to produce less bias than any of its counterparts. Four variables were taken into account—namely, age, sex, serum creatinine, and serum cystatin C—but not ethnicity as the cohort consisted of Germans of Caucasian origin. Two equations were derived—the BIS1 using serum creatinine only and BIS2 using serum creatinine and serum cystatin C (Table 23.2). These formulae showed better precision and agreement with mGFR, especially in a population with eGFR > 30 mL/min/1.73 m^2. The BIS equations appear to provide a more accurate estimation of GFR in the elderly and improve identification of individuals with CKD.[11] The BIS1 equation was subsequently shown to be useful in a Chinese group of 332 elderly subjects as well as in a different Caucasian cohort of 224 subjects.[40,41]

PREGNANCY

It is well known that there a physiologic increase in GFR, increased effective renal plasma flow, and a drop in serum creatinine occur in pregnancy. Serum creatinine decreases because of a real increase in GFR but also because of physiologic hemodilution.

Estimation equations are inappropriate for measuring GFR in pregnant women because they were not derived from this population. Most pregnant women have GFRs > 60 mL/min/1.73 m^2, which is above the range at which the MDRD or CKD-EPI equations are known to be accurate in any case. The 24-h urine collection for CrCl therefore remains the best method in pregnancy.[42]

Nevertheless, eGFR has been used to study midterm renal hyperfiltration, a hemodynamic phenomenon that occurs early in pregnancy and persists until delivery.[43] This is regarded as a marker of renal functional reserve in pregnancy. Recently, Park et al. described a retrospective study looking at 1931 singleton pregnancies with midterm serum creatinine data between 2001 and 2015 in South Korea, using the CKD-EPI equation. Midterm hyperfiltration was defined as > 120 mL/min. They demonstrated a nonlinear U-shaped relationship between midterm eGFR and adverse outcomes, with values between 120 and 150 mL/min/1.73 m^2 being associated with the lowest incidence of adverse pregnancy outcomes (defined by preterm birth, low birth weight, or preeclampsia as well as the composite of these three features). There are several limitations to this study, but the data suggest that further research is needed to understand the pathophysiology of intrarenal hemodynamic dysfunction in pregnancy and how this may contribute to adverse outcomes.[44,45]

ACUTE KIDNEY INJURY

Measurement of GFR in patients with AKI is difficult as it is constantly changing, and measurements or estimates that depend on a steady state are not readily applicable. Serum creatinine is the most commonly used marker of GFR in this setting, but creatinine is slow to rise in response to a decrease in GFR and is subject to the influence of dilution by fluid given as part of treatment for AKI.[46,47] As previously mentioned, creatinine is also insensitive to substantial decreases in GFR. Estimation equations for GFR in patients with AKI are inaccurate because these equations have been derived from stable patients, in whom the creatinine is at a steady state, and are not applicable to the diverse AKI patient population. A kinetic GFR estimation equation has been developed but has not yet been validated.[48]

Accurate measurement of GFR in this population can be achieved by calculation of the elimination kinetics after a single bolus injection of a glomerular filtration marker. Alternatively, brief-duration measurements of GFR, such as short-duration urinary CrCl, can be performed, assuming that a patient's creatinine does not increase rapidly over 2 to 8 hours.[49] These tests are not widely performed and are probably impractical in many centers. This situation has led to extensive research into a biomarker that is more sensitive in demonstrating early stages of AKI to facilitate more timely intervention.

DRUG DOSING

The CG equation, despite its limitations, is still used regularly in many jurisdictions for drug dose adjustment in patients with renal impairment. Historically this equation has been used to enroll subjects in renal impairment categories for pharmacokinetic studies. The U.S. Food and Drug Administration (FDA) in its "Guidance for Industry Pharmacokinetics in Patients with Impaired Renal Function" suggested using either the MDRD equation or the CG equation for this purpose in new drug development,[50] although one should be cautious as this does not imply that CrCl is equivalent to eGFR. The FDA guidance has not been updated since the KDIGO and KDOQI have recommended that the CKD-EPI equation replace the MDRD equation in routine clinical practice. Because the CKD-EPI and MDRD study equations perform similarly at GFR < 60 mL/min/1.73 m^2, it would be reasonable to use eGFR computed using the CKD-EPI equation or the MDRD study equation for pharmacokinetic studies and drug dosing.[51]

A large simulation study comparing drug dosages administered to patients through the use of the MDRD and CG equations showed that the concordance figures of the two equations' GFR estimates with mGFR was similar.[52] Because the majority of FDA-approved drug dosing labels use the CG equation, which expresses CrCl in mL/min, the eGFR value corrected for BSA must be converted to units of mL/min by multiplying by the individual's BSA and dividing by 1.73 m^2. The stimulation study concluded that either equation can be used for drug dosing but that caution should be exercised in patients in whom the creatinine value may be inaccurate. This caution is particularly relevant in sick or hospitalized patients, in whom low body weight or changes in body weight are present, in the elderly, and in amputees. The CG equation in these cases tends to give a lower estimate of renal function,[53] leading to a dose reduction.[54] The lower estimate results from the greater effect of age and weight on the CG equation. The use of the CG equation may lead to drug dosing errors that are due to "underdosing," thus minimizing exposure to toxicity. By contrast, in the elderly patients, the MDRD and CKD-EPI equations have been shown to overestimate the GFR in some studies but to be reliable in others.[55,56] The elderly patients are more likely to experience side effects and to be subject to the dangers of polypharmacy, so using the CG equation in these patients may be more appropriate.[53]

Ultimately the importance of drug dosage adjustment depends on the purpose of the medication as well as the therapeutic range and toxicity of the drug. In cases in which a medication has a narrow therapeutic window, such as

chemotherapy, all estimation equations may have an unacceptable degree of error, and accurate measurement of GFR using an exogenous filtration marker should be performed.

The CG equation should not be completely abandoned in favor of the MDRD equation, especially because recommendations for drug dosages of existing medications were based on the CG equation. The CKD-EPI equation has not yet been considered in this context.

FULL AGE SPECTRUM METHOD OF EGFR ESTIMATION

Owing to the methods by which various equations were developed for different populations, there can be a discontinuity when switching from pediatric equations to adult equations or from adult to older-adult equations. The full age spectrum (FAS) equation, developed in 2016, tries to correct for this disparity by deriving a single (age-knotted) eGFR equation that is applicable to all ages by normalizing serum creatinine for age (for children and adolescents) and sex (for adolescents and adults). A normalized serum creatinine (SCr/Q) is used, where Q is the median serum creatinine from healthy populations to account for age and gender (see Table 23.2).

Validation was performed in a total of 6870 healthy and kidney disease–affected white individuals including 735 children (<18 years of age), 4371 adults (aged between 18 and 70 years), and 1764 older adults (>70 years of age) with mGFR (inulin, iohexol, and iothalamate clearance) and IDMS-equivalent serum creatinine. Bias, precision, and accuracy were tested. The equation was found to be less biased and more accurate than the Schwartz equation for children and adolescents, less biased and as accurate as the CKD-EPI for young and middle-aged adults, and more accurate and less biased than CKD-EPI for older adults. The equation may not need further changes for age and gender but may need validation in other ethnicities and derivation of Q values for different populations. External validation in a large population suggested that the FAS equation might perform better than the Schwartz and CKD-EPI equations. There was better accuracy and precision for older adults with mGFR > 60 mL/min/1.73 m^2. As the FAS is based on SCr/Q values for a healthy population, it is expected that this will work better for a healthy and general population rather than in patients with CKD; however, in the validation population subgroups with mGFR < 60 mL/min/1.73 m^2 the FAS equation was not found to perform worse than the CKD-EPI equation.[57]

RENAL TRANSPLANT RECIPIENTS

Currently, renal transplant function is monitored using the endogenous marker serum creatinine along with eGFR. Serum creatinine, however, is affected by a number of drugs used in transplant medicine. For instance, corticosteroids are shown to increase eGFR in animal models as well as in humans; glomerular micropuncture studies have shown that corticosteroids vasodilate both the afferent and efferent arterioles, resulting in increased plasma flow and hence a higher eGFR. Chronic steroid administration has also been shown to increase prostaglandin synthesis in some species.[58] Paradoxically, steroids also increase serum creatinine by about 10%. This is presumably due to steroid-induced hypercatabolic state with associated protein wasting and muscle loss. In addition, muscle mass in transplant recipients may differ from the general population and those with other clinical conditions due to a chronic inflammatory state from chronic illness, infection, and episodes of rejection.[59–61] In addition, trimethoprim used for *Pneumocystis jirovecii* prophylaxis can cause elevated creatinine by blocking its tubular secretion. As discussed earlier, eGFR can decrease substantially before there is an evident increase in serum creatinine levels; thus calcineurin inhibitor toxicity and rejection may not be detected early enough.

Serum creatinine tends to be used in renal transplant recipients to detect rejection, infection, or drug toxicity and eGFR is infrequently used to guide management decisions due to concerns that the equations may be less reliable in transplant recipients than other populations. Nevertheless, in a systematic review of 3622 solid-organ transplant recipients, Shaffi et al. demonstrated that the CKD-EPI and the four-variable MDRD study equations were more accurate than alternative equations (even those developed in populations of transplant recipients only) and as accurate as observed in other clinical populations. CKD-EPI performed better at higher GFRs and MDRD performed better at lower GFRs. However, these equations were still inaccurate (different from mGFR by more than 30%) in one of five patients.[62,63]

URINALYSIS

Urinalysis may be used in the assessment of acute kidney disease or CKD, workup for kidney stones, or the evaluation of systemic conditions with potential renal involvement, such as systemic lupus erythematosus. There are three ways to obtain a urine specimen: spontaneous voiding, uretheral catheterization, and percutaneous bladder puncture. Technique is important in collecting a sample to avoid contamination. For spontaneously voided urine, a midstream sample should be collected after cleaning of the external genitalia. If a patient has an indwelling catheter, a fresh specimen should be submitted for analysis; samples that have been stagnant in the catheter tubing or bag may have undergone degradation. Suprapubic needle aspiration of the bladder is used when urine cannot easily be obtained by other means, most commonly in infants. Whatever the collection method, it is recommended that a sample be analyzed within 2 to 4 hours of the time of collection to prevent cell lysis and precipitation of solutes.[64] There are numerous techniques for examining urine; this section focuses on methods commonly used for assessment of chemical content and microscopy.

COLOR

The color of urine is determined by chemical content, concentration, and pH (Table 23.4). Urine may be almost colorless if the output is high and the osmolality is low. Abnormal color changes can be due to drugs, foods, and pathologic conditions. Cloudy urine is most commonly due to leukocytes and bacteria. The most common cause of red urine is hemoglobin. Red urine in the absence of red blood cells in the sediment usually indicates either free hemoglobin or myoglobin. In the latter case, the patient's serum is not pink. Red urine with red sediment indicates hemoglobin. By contrast, red urine with clear sediment is most often the result of myoglobin but may also be seen in some porphyrias,

Table 23.4 Main Causes of Abnormal Color Changes in Urine

	Cause	Color
Pathologic conditions	Gross hematuria, hemoglobinuria, myoglobinuria	Pink, red, brown, black
	Jaundice	Yellow to brown
	Chyluria	White milky urine
	Massive uric acid crystalluria	Pink
	Porphyrinuria, alkaptonuria	Red to black; increases after urine left to stand
Medications	Rifampin	Yellow-orange to red
	Propofol	White
	Phenytoin, phenazopyridine	Red
	Chloroquine, nitrofurantoin	Brown
	Triamterene, blue dyes of enteral feeds	Green
	Metronidazole, methyldopa, imipenem–cilastatin	Darkening after urine left to stand
Foods	Beetroot	Red
	Senna rhubarb	Yellow to brown red

From Fogazzi GB, Verdesca S, Garigali G. Urinalysis: core curriculum 2008. *Am J Kidney Dis.* 2008;51:1052–1067; and Davsion A. *Urinalysis.* 3rd ed. Oxford: Oxford University Press; 2005.

or with the use of some medications or the ingestion of beets in some individuals.[65]

ODOR

The most common cause of abnormal urine odor is infection and in this case the abnormal odor is caused by the production of ammonia by bacteria. Ketones may cause a fruity or sweet odor. Some rare pathologic conditions may confer a specific odor to the urine. Examples are maple syrup urine disease (maple syrup odor), phenylketonuria (mousy odor), isovaleric acidemia (sweaty feet odor), and hypermethioninemia (fishy odor).[64]

RELATIVE DENSITY

The concentration, or relative density, of urine can be assessed by either specific gravity or osmolality. "Specific gravity" is defined as the weight of a solution relative to that of an equal volume of water. It is determined by the number and size of particles in the urine. Specific gravity is traditionally measured by a urinometer, which is a weighted float marked with a scale from 1.000 to 1.060. This method is simple but outdated owing to the need for a larger volume of urine than with other methods and the potential for inaccuracy in reading the device. Today, specific gravity is commonly measured by refractometry or dry chemistry methods. Refractometry measures specific gravity using the refractive index of a solution, which is a function of the weight of solute per unit volume. It requires only a drop of urine.

Dry chemistry techniques are used in reagent strips. An indirect method is used to determine specific gravity, relying on the fact that there is generally a linear relationship between urine's ionic strength and its specific gravity. The reagent strip contains a polyionic polymer that has binding sites that are saturated with hydrogen ions, and an indicator substance. The release of hydrogen ions when they are competitively replaced with urinary cations causes a change in the pH-sensitive indicator dye. Specific gravity values measured by dipstick tend to be falsely high if the urine pH is <6 and falsely low if the pH is >7. The effects of nonionized molecules such as glucose and urea on osmolality are not reflected by changes in the dipstick specific gravity. Dry chemistry measurements of specific gravity therefore tend to correlate poorly with refractometry and osmolality.[64]

"Osmolality," the gold standard for relative density, is defined as the number of osmoles of solute per kilogram of solvent. It is measured directly with an osmometer. It depends on the number of particles in solution and is not influenced by their size or temperature. High-glucose solutions significantly increase osmolality (10 g/L glucose = 55.5 mOsmol/L).[64] Urine specific gravity is generally proportional to the osmolality and rises by approximately 0.001 for every 35- to 40-mOsmol/kg increase in urine osmolality.[66] A urine osmolality of 280 mOsmol/kg (which is isosmotic to normal plasma) is usually associated with a urine specific gravity of 1.008 or 1.009. Specific gravity is affected by protein, mannitol, dextrans, and radiographic contrast media. In these settings, specific gravity can be increased disproportionately to the osmolality, falsely suggesting highly concentrated urine. There are no causes of a falsely low urine specific gravity value, and thus a specific gravity ≤1.003 measured by refractometry always indicates a maximally dilute urine (≤100 mOsmol/kg).

URINE PH

Urine pH is usually measured with a reagent test strip. Most commonly, the double indicators methyl red and bromothymol blue are used in the reagent strips to give a broad range of colors at different pH values. The normal range for urine pH is 4.5 to 7.8. Significant deviations from true pH occur with values <5.5 or >7.5 with reagent strip methods.[52,56] Urine pH can be useful in diagnosing systemic acid–base disorders when used in conjunction with other investigations, although in isolation it provides little useful diagnostic information. A very alkaline urine (pH > 7.0) is suggestive of infection with a urea-splitting organism, such as *Proteus mirabilis*. Prolonged storage can lead to overgrowth of urea-splitting bacteria and the laboratory measurement of a high urine pH. Diuretic therapy, vomiting, gastric suction, and alkali

therapy can also cause a high urine pH. Acidic urine (pH < 5.0) is seen most commonly in metabolic acidosis. A urine pH > 5 in the setting of metabolic acidosis may indicate one of the forms of renal tubular acidosis, though there are forms of renal acidosis in which the urine pH is low despite a defect in the total kidney ability to excrete acid and generate bicarbonate (see also Chapters 16 and 24).[65]

BILIRUBIN AND UROBILINOGEN

Only conjugated bilirubin is passed into the urine. Thus the result of a reagent test for bilirubin is typically positive in patients with obstructive or hepatocellular jaundice, whereas it is usually negative in patients with jaundice due to hemolysis. In patients with hemolysis, the urine urobilinogen result is often positive. Reagent test strips are very sensitive to bilirubin, detecting as little as 0.05 mg/dL. However, the measurement of bilirubin in the urine is not very sensitive for detecting liver disease. Prolonged storage and exposure to light can lead to false-negative results.[65] False-positive test results for urine bilirubin can occur if the urine is contaminated with stool.

LEUKOCYTE ESTERASE AND NITRITES

The esterase method relies on the fact that esterases are released from lysed urine granulocytes (leukocytes). These esterases liberate 3-hydroxy-5-phenylpyrrole after substrate hydrolysis. The pyrrole reacts with a diazonium salt in the test strip, yielding a pink to purple color. The result is usually interpreted as negative, trace, small, moderate, or large. Factors that may increase leukocyte lysis include allowing urine to stand for long periods, low pH, and low relative density. In these settings, there may be a positive dipstick result for leukocyte esterase with no leukocytes seen on microscopy. High levels of glucose, albumin, ascorbic acid, tetracycline, cephalexin, or cephalothin or large amounts of oxalic acid may inhibit the reaction and cause false-negative results.[67]

Urinary nitrites indicate the presence of nitrate-reducing bacteria. In the reagent strip test, nitrite reacts with a *p*-arsanilic acid to form a diazonium compound; further reaction with 1,2,3,4-tetrahydrobenzo(h)quinolin-3-ol results in a pink color endpoint. Results are usually interpreted as positive or negative. High specific gravity and ascorbic acid may interfere with the test. False-negative results are common and may be due to prolonged sample storage or low dietary intake. It may take up to 4 hours to convert nitrate to nitrite, so inadequate bladder retention time can also give false-negative results.[67]

GLUCOSE

Glycosuria due to hyperglycemia may occur at blood glucose levels >10 mmol/L (180 mg/dL) in subjects with normal renal function. Less commonly, glycosuria indicates failure of proximal renal tubular reabsorption in tubular disorders such as Fanconi syndrome. Most reagent strips use an oxidase–peroxidase method to measure glucose. Glucose is first oxidized to form glucuronic acid and hydrogen peroxide. Hydrogen peroxide then reacts via a peroxidase with a reduced chromogen to form a colored product.[64] This test is sensitive to glucose concentrations between 0.5 and 20 g/L.[64] Large quantities of ketones, ascorbate, and phenazopyridine hydrochloride (Pyridium) metabolites may interfere with the color reaction, causing false-negative results. Oxidizing agents and hydrochloric acid may cause false-positive results.[67] Enzymatic methods such as a hexokinase give more precise quantification of urinary glucose levels.[64]

KETONES

Ketones (acetoacetate and acetone) are generally detected with the nitroprusside reaction.[67] Ascorbic acid and phenazopyridine can give false-positive reactions. It is important to appreciate that β-hydroxybutyrate (often 80% of total serum ketones in ketosis) is not normally detected by the nitroprusside reaction. Ketones may appear in the urine, but not in serum, with prolonged fasting or starvation. Ketones may also be detected in the urine in alcoholic or diabetic ketoacidosis.

HEMOGLOBIN AND MYOGLOBIN

Reagent strips use the peroxidase-like activity of the heme moiety of hemoglobin to catalyze the reaction between a peroxide and a chromogen, giving a colored product. This test is very sensitive for the presence of heme in the urine. False-negative results are uncommon but may be caused by ascorbic acid, a strong reducing agent. False-positive results may occur because of oxidizing contaminants, povidone-iodine, semen, or a high concentration of bacteria with pseudoperoxidase activity (such as Enterobacteriaceae, staphylococci, and *Streptococcus* spp).[64] Normally, haptoglobin binds circulating heme-containing substances, such as hemoglobin and myoglobin. When these substances are produced in large quantities, as occurs in hemolysis or rhabdomyolysis, the capacity for binding is overwhelmed and they appear in the urine. A positive dipstick test result for hemoglobin in the absence of red blood cells in the urine sediment therefore suggests either hemolysis or rhabdomyolysis.

PROTEINURIA

Proteinuria (see also Chapter 30) is an important sign of kidney disease, imparting powerful diagnostic and prognostic information. It is a cornerstone of the workup for CKD, AKI, hematuria, and preeclampsia. It is often the earliest marker of glomerular diseases, occurring before a reduction in GFR. Proteinuria is associated with hypertension, obesity, and vascular disease. It can be used to predict risks of CKD progression, cardiovascular disease, and all-cause mortality in general population[68] cohorts and patients with diabetes[69] and CKD.[70] Proteinuria-lowering therapies may be renoprotective,[71] and monitoring proteinuria is a key aspect of assessing treatment response in a variety of kidney diseases, including diabetes[72] and nondiabetic glomerulopathies.[19] In addition, filtered protein probably contributes to the pathogenesis of renal injury and disease progression rather than just being a marker of it.[73] Although measurement of urinary protein has long been recommended in clinical practice guidelines, recommendations regarding this practice vary substantially.[74] This section reviews the normal physiology of proteinuria as well

as strengths, limitations, and applications of the different measurement techniques.

NORMAL PHYSIOLOGY

In humans, on the basis of a GFR of 100 mL/min, 180 L of primary urine is produced per day from plasma that contains about 10 kg of protein. However, only about 0.01% or 1 g of protein passes through the glomerular filtration barrier into the filtrate.[75] The glomerular filtration barrier acts as a size-, shape-, and charge-dependent permselective molecular sieve, the unique properties of which are still incompletely understood. It restricts the passage of macromolecules, such as albumin and globulin, and enables the excretion of an almost protein-free ultrafiltrate containing water and small solvents.[76]

The glomerular filtration barrier acts to minimize diffusion of large molecules (with a Stokes–Einstein radius >1.5 nm)[77] that would otherwise occur down a concentration gradient from the plasma to the filtrate (see also Chapter 3). It is composed of three major layers—endothelial cells, the glomerular basement membrane, and podocytes, which cover the basement membrane on the side of the urinary space. Podocytes are highly specialized epithelial cells with long, interdigitated foot processes that wrap around the glomerular capillaries, forming 40-nm wide gaps, known as filtration slits, between adjacent processes (see also Chapter 4).[78] The slit diaphragm is a cell-to-cell contact that inserts laterally into the podocyte cell membrane, bridging the filtration slit. The podocyte plays a central role in integrating the components of the glomerular filtration barrier by interacting with the glomerular basement membrane and signaling at the slit diaphragm.[79] To date, at least 26 podocyte-specific gene defects, such as those encoding for the podocyte proteins nephrin and podocin, have been identified in hereditary causes of nephrotic syndrome.[80–82] In response to signals from the podocytes and mesangium, the endothelial cells acquire a highly fenestrated phenotype, with small pores covering about 20% of their surfaces.[78] This phenotype facilitates high-flux transport of fluid and small solutes. Normally, large quantities of high-molecular-weight (HMW) plasma proteins traverse the glomerular capillaries, mesangium, or both without entering the urinary space. Damage to any one of the three layers of the glomerular filtration barrier allows proteins through, resulting in abnormal, "glomerular" proteinuria.

Albumin, the dominant HMW protein in plasma, is a negatively charged, approximately 67-kDa protein.[76] Size selectivity restricts the passage of albumin through the glomerular filtration barrier. Charge selectivity, in which the negatively charged proteoglycans and heparan sulfates in the glomerular basement membrane repel albumin molecules, is a theory seeking to explain the low glomerular sieving coefficient of albumin in relation to other molecules of its size.[83] However, experimental data have called the role of basement membrane charge in permselectivity into question.[84–86] Some albumin filtration across the capillary wall does occur, after which it is resorbed by the proximal tubule cells.[87,88]

LMW proteins (<20,000 Da) pass readily across the glomerular capillary wall. Because the plasma concentration of these proteins is much lower than that of albumin and globulins, however, the filtered load is small. Moreover, LMW proteins are normally reabsorbed by the proximal tubule. Thus proteins such as α_2-microglobulin, apoproteins, enzymes, and peptide hormones are normally excreted in only very small amounts in the urine.[65]

A small amount of protein that normally appears in the urine is the result of normal tubular secretion. Tamm–Horsfall protein is an HMW glycoprotein (23×10^6 Da) that is formed on the epithelial surfaces of the thick ascending limb of the loop of Henle and early distal convoluted tubule. Immunoglobulin A (IgA) and urokinase are also secreted by the renal tubule and appear in the urine in small amounts.[65]

TYPES OF PROTEINURIA

The types of proteinuria are as follows:

Glomerular: Increased filtration of macromolecules across the glomerular filtration barrier may occur from a loss of charge and size selectivity. Unlike the other types listed here, glomerular proteinuria often results in urinary protein loss >1 g/day.

Tubular: Tubular damage or dysfunction may inhibit the normal resorptive capacity of the proximal tubule, resulting in higher amounts of mostly LMW proteins in the urine. A degree of tubular proteinuria often occurs with glomerular proteinuria. Classic causes of tubular proteinuria in isolation are Fanconi syndrome and Dent disease.

Overflow: Normal or abnormal plasma proteins produced in increased amounts may be filtered at the glomerulus and may overwhelm the resorptive capacity of the proximal tubule. This occurs particularly with small or positively charged proteins and is of clinical importance principally in plasma cell dyscrasias (e.g., myeloma). It may also occur with myoglobin in rhabdomyolysis and with hemoglobin in severe intravascular hemolysis.

Postrenal: Small amounts of protein, usually nonalbumin IgG or IgA, may be excreted in the urinary tract in the setting of infection or stones. Leukocytes are also commonly present in the urine sediment.

NORMAL LEVELS OF PROTEINURIA

As previously described, two main groups of proteins are present in the urine: plasma proteins, predominately albumin, that cross the filtration barrier, and nonplasma proteins, predominantly Tamm–Horsfall protein, that originate in renal tubules or the urinary tract. In normal physiologic conditions, about half of the excreted protein is Tamm–Horsfall protein, and <30 mg of albumin is excreted per day.[74] At normal levels of protein loss, albumin accounts for approximately 20% of total protein. As protein loss increases, albumin becomes the most significant single protein present.[89]

CATEGORIZATION OF PROTEINURIA

The persistent excretion of abnormal levels of urinary albumin, equivalent to between 30 and 300 mg/day, that is below the level that can be detected by a standard urine protein dipstick is now termed "moderately increased albuminuria" (historically termed "microalbuminuria") and corresponds to the KDIGO albuminuria category A2. Albumin excretion of >300 mg/day is now considered as "overt

Table 23.5 Kidney Disease: Improving Global Outcomes (KDIGO) Guideline: Categories of Proteinuria[a]

	Normal to Mildly Increased (KDIGO A1)	Moderately Increased (KDIGO A2)	Severely Increased (KDIGO A3)
AER (mg/24 h)	<30	30–300	>300
PER (mg/24 h)	<150	150–500	>500
ACR:			
mg/mmol	<3	3–30	>30
mg/g	<30	30–300	>300
PCR:			
mg/mmol	<15	15–50	>50
mg/g	<150	150–500	>500
Protein reagent strip	Negative to trace	Trace to +	+ or greater

[a]Relationships between AER and ACR and between PER and PCR are based on the assumption that average creatinine excretion rate is 1.0 g/day or 10 mmol/day (conversions are rounded for pragmatic reasons).

ACR, Albumin-to-creatinine ratio; *AER,* albumin excretion rate; *PCR,* protein-to-creatinine ratio; *PER,* protein excretion rate.

From Kidney Disease: Improving Global Outcomes (KDIGO) CKD Work Group. KDIGO 2012 clinical practice guideline for the evaluation and management of chronic kidney disease. *Kidney Int Suppl.* 2013;3:1–150.

proteinuria or severely increased albuminuria" (KDIGO albuminuria category A3, historically termed "macroalbuminuria") and can be detected by a standard urine dipstick. "Nephrotic-range proteinuria" is protein excretion of >3.5 g/24 hours and is usually indicative of glomerular pathology. The 2012 KDIGO guidelines discourage the use of the term "microalbuminuria," instead suggesting that the term "albuminuria" be used and the level subsequently quantified (Table 23.5).[19] This recommendation has been sanctioned by the Association of Laboratory Physicians and Clinical Chemists in different jurisdictions. The presence of proteinuria or albuminuria strongly predicts outcomes of CKD progression as well as of cardiovascular and all-cause mortality in the population with CKD. The risk rises continuously as albuminuria increases.[90] The 2012 KDIGO guidelines added a category for albuminuria to the classification of CKD to improve risk stratification.[19]

SOURCES OF ERROR IN MEASUREMENT

The 24-hour urine collection for protein measurement is considered the gold standard for measuring protein or albumin (Tables 23.6 and 23.7). Methods such as reagent strips, random measurement of protein or albumin concentrations, and albumin- or protein-to-creatinine ratios (ACRs or PCRs) aim to estimate a 24-hour protein measure. A positive result from a semiquantitative test, such as a urinary dipstick test, should prompt further evaluation with a quantitative test. Both preanalytical factors and factors intrinsic to the analysis itself can be sources of error in protein measurement. In the assessment of the quality of a test, both accuracy and precision need to be taken into account. Although a test may give reproducible results, it may not accurately measure all clinically significant types of proteinuria. The heterogeneous types of protein and the different molecular forms of proteins (such as albumin) that may be present in urine make for a challenge to both accuracy and precision of measurement. Using a consistent form of measurement with a consistent assay to monitor proteinuria, and using multiple measurements to confirm findings, is therefore advisable.

Table 23.6 Patient Factors That May Increase Urinary Protein or Albumin

Posture (postural proteinuria)
Urinary tract infection
Hematuria
High dietary protein intake
High-intensity exercise
Congestive cardiac failure
Menstruation or vaginal discharge
Drugs (e.g., nonsteroidal antiinflammatory drugs)

Adapted from Johnson DW, Jones GR, Mathew TH, et al. Chronic kidney disease and measurement of albuminuria or proteinuria: a position statement. *Med J Aust.* 2012;197:224–225; and Miller WG, Bruns DE, Hortin GL, et al. Current issues in measurement and reporting of urinary albumin excretion [article in French]. *Ann Biol Clin (Paris).* 2010;68:9–25.

Table 23.7 Factors Influencing Accuracy of Proteinuria Measurement

Preanalysis Phase	Analysis Phase
Collection type	Total protein or albumin measurement
Timed or random	
timing of random measurement	
Degradation of protein or albumin during storage	Assay type
adsorption to plastic	
Storage temperature	

Adapted from Miller WG, Bruns DE, Hortin GL, et al. Current issues in measurement and reporting of urinary albumin excretion [article in French]. *Ann Biol Clin (Paris).* 2010;68:9–25; and Martin H. Laboratory measurement of urine albumin and urine total protein in screening for proteinuria in chronic kidney disease. *Clin Biochem Rev.* 2011;32:97–102.

ADVANTAGES OF URINARY ALBUMIN OVER TOTAL PROTEIN MEASUREMENTS

Either albumin or total protein can be measured in urine. Many current guidelines recommend the measurement of urine albumin on the basis of a need to detect lower levels of protein than were previously thought to be clinically significant. Multiple studies have shown that the presence of small amounts of albumin in the urine—between 30 and 300 mg/day—have prognostic significance; increasing amounts of albuminuria are associated with continuous increases in risk of all-cause and cardiovascular mortality, AKI, and ESKD in the general population,[91] with decline in eGFR,[92,93] and with adverse outcomes in CKD.[94] Measures of total protein are imprecise at low levels of protein and are insensitive at detecting clinically important changes in albuminuria.[74] Relatively large increases in urinary albumin excretion can occur without causing a measurable increase in urinary total protein.[95] Urine albumin measurements are more specific and more sensitive for changes in glomerular permeability than are measures of urinary total protein.[19,74,95–97] In addition, because a single protein is being measured, standardization of albumin measurement is simpler than standardization of total protein measurements.[98]

CONSIDERATIONS REGARDING MEASURING URINARY ALBUMIN RATHER THAN TOTAL PROTEIN

EVIDENCE FOR CKD PROGRESSION RISK AND INTERVENTIONS

Much evidence on the natural history and progression of CKD has centered on measurement of 24-hour total protein.[98] In general, studies of diabetic patients have used measurements of urinary albumin, but studies of interventions and outcomes for glomerular diseases, preeclampsia, and in children have used proteinuria measurements. One difficulty with the implementation of albumin as a replacement for total protein is the lack of a constant numerical relationship between the two that would enable clinicians to translate the existing evidence base from one to the other.[74]

MISSED TUBULAR PROTEINURIA

Relying on measurement of urinary albumin risks missing "tubular" and "overflow" proteinuria, in which nonalbumin proteins predominate. However, total protein assays are generally more sensitive to albumin than to LMW proteins, and many also have poor sensitivity for detecting tubular proteinuria.[99] Although "tubular" disorders are characterized by a relative increase in the proportion of LMW protein to albumin, albumin generally still constitutes a significant portion of total protein, probably because of failure of tubular resorption of protein.[100] In the AusDiab study, random urine samples from >10,000 people in the Australian adult population were tested, using cutoff values of 3.45 mg/mmol for ACR and 22.6 mg/mmol for PCR. Of patients who screened positive for albuminuria, 68% had negative results for proteinuria. Albuminuria performed well as a screening test for proteinuria: sensitivity was 91.7%, specificity 95.3%, and negative predictive value 99.8%. However, among those with proteinuria, 8% excreted albumin within the normal range. The investigators postulated that these individuals may have had light-chain proteinuria or interstitial nephropathies.[89] In a study of 23 patients with Dent disease, a rare but classic tubular disorder, only 2 patients had no significant urinary albumin loss in addition to losses of LMW proteins. In these two patients, the levels of LMW proteinuria were low enough that they would probably also have been missed by a total protein measurement approach.[101]

Overall, the significance of this issue in both the CKD and general populations is difficult to estimate with the currently available data. If tubular proteinuria is suspected, it is best assessed with immunoassays directed at a specific tubular protein, such as α_1-microglobulin or monoclonal heavy or light chains.[19,74] One study that attempted to identify the proteins composing tubular proteinuria in elderly people with mild proteinuria was unable to consistently identify proteins using electrophoresis, and the researchers suggested that the elevated urinary protein measurements were due to artifact.[102]

DIAGNOSTIC UTILITY OF PROTEIN TYPE

Simultaneous measurement of different types of urinary protein may be a useful tool in differentiating between glomerular and tubulointerstitial diseases. Several studies using gel electrophoretic techniques to separate proteins on the basis of molecular size have shown that larger proteins such as albumin predominate in glomerular disease and that the ratio of LMW proteins is increased in tubulointerstitial disorders.[103] Higher albumin-to-total protein ratios, obtained from simultaneous measurement of ACR and PCR, have been shown to be significantly associated with glomerular rather than nonglomerular pathology on renal biopsy in patients with kidney disease.[104]

METHODS TO MEASURE URINARY TOTAL PROTEIN

Total protein in urine has been measured by chemical, turbidimetric, and dye binding (colorimetric) methods (Table 23.8). These methods are prone to interference by inorganic ions and nonprotein substances in the urine.[74] Falsely high results may occur as result of interference by aminoglycoside antibiotics,[105] plasma expanders,[106] and other substances. There is large sample-to-sample variation in the type and composition of proteins present, making accurate measurement difficult. Turbidimetric methods, which are commonly used, are imprecise, with a coefficient of variation as high as 20%.[107] Currently there is no reference measurement procedure or standardized reference material for urinary protein. Each of the different methods in use has differing sensitivity and specificity for the diverse range of proteins found in urine, potentially leading to divergent results. The range of methods and calibrants in use means that between-laboratory variation is unavoidable. Most laboratories currently use turbidimetric or colorimetric measures, which tend to react more strongly with albumin than with globulin and other nonalbumin proteins.[108]

METHODS TO MEASURE URINARY ALBUMIN

Urinary albumin can be measured in a number of ways. An antibody binding method, in particular immunoturbidimetry,

Table 23.8 Methods of Proteinuria Measurement

Method	Description	Detection Limit (mg/L)	Protein Types	Causes of Falsely Increased Results	Causes of Falsely Decreased Results
Chemical: Biuret	Copper reagent, measures peptide bonds	50	—	—	Tubular/LMW proteins
Kjeldahl	Precipitated nitrogen				
Turbidimetric (sulfosalicylic acid, trichloroacetic acid)	Addition of precipitant denatures protein; suspension's turbidity is read in a densitometer	50–100	Many, including γ-globulin light chains and albumin More sensitive to albumin than to globulins and nonalbumin proteins	Tolmetin sodium (Tolectin), tolbutamide, antibiotics (penicillin, nafcillin, oxacillin), radiocontrast agents	Tubular/LMW proteins
Dye binding (e.g., Coomassie Brilliant Blue, pyrogallol red)	Indicator changes color in presence of protein	50–100	More sensitive to albumin than to globulins and nonalbumin proteins (pyrogallol red improves this shortcoming)	Pyrogallol red: aminoglycoside, gelatin solutions such as plasma expanders	Tubular/LMW proteins

LMW, Low molecular weight.

Adapted from Cameron JS. The patient with proteinuria and or hematuria. In: Davison A, ed. *Oxford Textbook of Clinical Nephrology.* 3rd ed. Oxford: Oxford University Press; 2005:389–411.

is most commonly used.[74,108] Because a single protein is being measured, performance of albumin assays tend to be superior to total protein assays, at least at low concentrations of protein.[108] However, the urine of healthy individuals contains a range of albumin molecules. Albumin may be immunoreactive, nonimmunoreactive, fragmented, or biochemically modified[109] and the proportions of these different types of albumin molecules in normal urine are variable.

Albumin fragments may be generated during proteolysis of albumin in renal tubules or plasma and may account for a significant proportion of total urinary albumin. A study in subjects with type 1 diabetes found that 99% of albumin was excreted as fragments <10 kDa. Another study showed that albumin fragments constituted up to 30% of total urinary protein in patients with nephrotic syndrome.[110] Intact albumin has at least five antigenic sites.[111] Routine clinical methods use both polyclonal and monoclonal antibodies, which have different sensitivities for the detection of altered forms of albumin.[98] Nonimmunoreactive forms of albumin also exist; these are either fragments that do not contain the binding sites for the antibody in use in a particular assay or intact albumin in which the epitopes have undergone conformational change.[112]

HPLC detects both immunoreactive and nonimmunoreactive albumin. Higher values for urinary albumin are generally seen in HPLC than in immunologic detection methods. This observation led to a hypothesis that there are clinically significant amounts of nonimmunoreactive albumin in urine. In a study exploring this issue, differences in urinary albumin were detected by four immunoassays and HPLC. However, the higher values seen in HPLC techniques may also represent the detection of nonalbumin macromolecules.[113] Conformational change in albumin molecules may be induced by changes in urinary pH, urea, glucose, and ascorbate concentrations. Bilirubin usually occupies a small proportion of albumin molecules, but in severe hyperbilirubinemia it may bind to >50% of albumin.[98]

DIFFERENT LABORATORY METHODS TO MEASURE ALBUMIN IN THE URINE

The laboratory methods for measuring urinary albumin are as follows:

Immunoturbidimetric technique: Albumin in a sample of urine reacts with a specific antibody. The turbidity is measured with a spectrophotometer, and the absorbency is proportional to the albumin concentration.[114]

Double-antibody radioimmunoassay: Albumin in a urine sample competes with a known amount of radiolabeled albumin for fixed binding sites of antialbumin antibodies. Free albumin can be separated from bound albumin by immunoabsorption of the (albumin-bound) antibody. Albumin concentration in the resulting sample of albumin-bound antibody is inversely proportional to its radioactivity, which is measured against a standard curve.[115] This is a sensitive assay, but its use is limited by its expense and the need that it is to be performed in a laboratory that can manage radioactive substances.[109]

Nephelometry: Albumin in the urine sample reacts with a specific antialbumin antibody, forming light-scattering antigen–antibody complexes that can be measured with a laser nephelometer. The amount of albumin is directly proportional to scatter in the signal.[116]

Size-exclusion HPLC (SE-HPLC): Chromatographic techniques are used to measure both immunoreactive and nonimmunoreactive albumin. Proteins of different sizes are separated as they pass at different speeds through a column containing size-selective gel.[117] SE-HPLC is more sensitive for the detection of albumin than the immune-based methods, but its specificity is limited by an inability

to discriminate between albumin and other proteins of the same size, such as globulins.[109]

Although the correlation among results obtained using most of these quantitative assays is very good,[96] a good correlation indicates only precision, a strong linear relationship, but not accuracy in quantifying all clinically significant proteins present. Results obtained by radioimmunoassay, immunoturbidimetry, nephelometry, and HPLC may vary significantly.[109] Therefore, ideally, the same assay should be used when albuminuria results are compared over time for a given patient. The choice of assay used to measure albuminuria is largely determined by issues of accuracy, cost, and convenience. Currently, there is no standardized procedure for measuring urine albumin and reporting results in standardized units; however, considering the recommendations for using ACRs as the standard measure for urinary protein, a number of professional bodies have moved toward establishing standard laboratory collection, measuring, and reporting procedures.[98] Standardization for measurement of albumin requires a reference material and reference measurement procedure. Using purified albumin as the reference material would not reflect the various molecular forms that may be present in the urine but may be the most practical approach to standardization. Most routine methods for urinary albumin measurement are currently calibrated against dilutions of CRM 470, a higher-order serum protein reference material with an albumin concentration of 39.7 g/L.[98,108] Other issues that would need to be addressed to standardize the measurement of urinary albumin include clarification of the molecular forms of albumin in freshly voided urine, the degree of degradation that occurs during storage and freezing, and the appropriate upper limits of normal in different age and sex groups.[98]

TIMED VERSUS RANDOM COLLECTION FOR PROTEINURIA ASSESSMENT

Random "spot" specimens for urinary protein, expressed as a concentration, are often inaccurate for estimation of 24-hour levels because of the impact of patient hydration status on urine concentration. There is also variation in protein excretion, which can occur throughout the day (especially resulting from exercise and posture) and from day to day.[118] Methods to improve the accuracy of spot urine testing include corrections for urine creatinine and specific gravity.[119]

Protein or albumin measurement in 24-hour urine collection is generally considered the gold standard for measuring protein excretion. However, it can also be inaccurate, primarily through inaccurate urine collection. Urine creatinine can be measured to judge the adequacy of the 24-hour collection. If creatinine excretion is similar to that in previous 24-hour samples, the collection is likely to be reasonably accurate. If no other collections are available for comparison, the adequacy of collection can be judged from the expected normal range of creatinine excretion. For hospitalized men aged 20 to 50 years, this range was found to be 18.5 to 25.0 mg/kg of body weight per day, and for women of the same age, 16.5 to 22.4 mg/kg per day. These values declined with age, so that for men aged 50 to 70 years, creatinine excretion was 15.7 to 20.2 mg/kg per day, and for women, 11.8 to 16.1 mg/kg per day.[65] Factors influencing the daily creatinine excretion include determinants of muscle mass, such as gender, race, age, and BSA.[97]

TRANSLATING URINE PCR AND ACR VALUES INTO TOTAL DAILY PROTEIN MEASUREMENTS

Urine ACR and PCR are obtained by dividing the urine protein concentrations by the urine creatinine concentration and expressing the result as mg/mmol or mg/g. Both enzymatic and Jaffe assays are used for the measurement of creatinine in urine.[19] The ratio-based tests aim to correct for the effects of urine concentration on protein measurements. Overall, these tests have shown greater accuracy and less intraindividual variability than concentrations measured in random samples[98,119,120] and are more acceptable to patients than 24-hour protein measurements. Intraindividual variability is further reduced by using a first void rather than a daytime collection specimen to measure ACR. However, there remains substantial day-to-day variability in both PCR and ACR.[98] A positive result should be followed with a second measurement, ideally in an early morning sample, to confirm the result.[19,97]

Clinicians commonly use these tests as estimations of the 24-hour protein in milligrams by multiplying the PCR in mg/mmol or ACR in mg/mmol by 10 (given an average daily creatinine excretion of 10 mmol) or using the value as given if measured in mg/g. (Although the PCR or ACR in mg/g should be multiplied by 8.8 to get an exact value in mg/mmol, these are estimates of 24-hour levels only.) Despite the reasonable performance of the ratio-based tests to estimate 24-hour protein measurements, their ability to predict the true 24-hour protein for an individual is limited by two major factors. The first is variability in the total daily creatinine excretion, in and between individuals, which affects the ratio. The second is the fluctuations in protein excretion that occur throughout the day. An understanding of the factors that may make a urine ACR or PCR value inaccurate is important for clinicians using these tests.

CORRELATION BETWEEN RATIOS AND 24-HOUR URINE PROTEIN

Summary tables of studies comparing urine ACR and PCR with timed collections for urinary albumin and protein can be found in the 2012 KDIGO-CKD guideline. There is a relatively high degree of correlation between 24-hour urine protein excretion and PCR in random, single-voided urine samples in healthy controls[121] and in patients with a variety of kidney diseases.[122–125] The correlation has been shown in studies in patients with glomerulonephritis[126] and with type 1 diabetes mellitus (DM),[127] and in renal transplant recipients.[128,129] In some studies, the correlation between PCR and 24-hour protein measurements was less robust when proteinuria was in the nephrotic range and above.[124,127]

The urine ACR has been shown to correlate well with 24-hour urinary albumin measurements in a number of studies in people with diabetes.[130] However, a large study evaluating the correlation between ACR and 24-hour albumin excretion in 1186 subjects with type 1 DM enrolled in the Diabetes Control and Complications Trial and its follow-up study, Epidemiology of Diabetes Interventions and Complications, showed that ACR systematically underestimated albumin excretion, particularly in men.[131] Another study in the diabetic

population showed that ACR increased relative to 24-hour albumin excretion with increasing age.[132] These studies highlight the fact that variability in creatinine excretion in certain groups alters the ratio. Individuals with lower muscle mass, such as females and elderly patients, would be expected to have higher ACRs than those with higher muscle mass for the same level of urinary albumin excretion.

VARIABILITY IN CREATININE EXCRETION

Under normal circumstances, a steady rate of creatinine excretion occurs throughout the day.[133] The accuracy of the ratio-based variables depends on a constant excretion rate. This drawback limits their usefulness in the setting of rapidly changing renal function such as AKI, in which creatinine excretion is reduced, increasing the ratio for the same amount of protein excretion.

Creatinine excretion rises with increasing muscle mass, so ACR and PCR are reduced for a given level of protein excretion in groups with higher muscle mass, such as men, younger people, and certain population ancestry groups.[134,135] The fact that the average urinary creatinine excretion is 40% to 50% higher in men than in women[131,132] has led some guidelines to recommend gender-specific cutoff values for ACRs, with lower thresholds for men than women. Commonly used urine ACR thresholds for diabetic nephropathy are 25 mg/g (2.5 mg/mmol) for males and 35 mg/g (3.5 mg/mmol) for females.[97] However, the 2012 KDIGO guidelines recommend an ACR threshold of 3.0 mg/mmol for both sexes, reflecting that the ACR is an estimation with a variety of other variables, such as age and population ancestry, that are not corrected for.[19]

FLUCTUATIONS IN PROTEIN EXCRETION

Factors that may cause transient increases in urinary protein excretion include exercise, urinary tract infections, and upright posture. High-intensity exercise may cause transient proteinuria lasting for 24 to 48 hours in healthy subjects.[136,137] Patients with CKD or diabetes have been shown to have higher levels of urinary protein or albumin excretion after exercise than control subjects.[138–140] Some guidelines have recommended screening for urinary tract infection if proteinuria is detected. However, a review of available studies suggested that asymptomatic urinary tract infection was unlikely to cause proteinuria and that screening may be unnecessary.[141]

Upright posture can cause an increase in urine protein excretion in otherwise healthy young adults.[142] Postural proteinuria is usually diagnosed by detecting proteinuria in a random sample taken while that subject has been upright that is absent in a first morning void specimen. It usually does not exceed 1 g in 24 hours. Kidney histologic examination in patients with postural proteinuria generally yields normal or nonspecific findings,[142,143] and patients with postural proteinuria have been shown to have an excellent long-term prognosis.[144] An increased urine protein excretion found on a random sample in a young person should prompt a testing of an early morning specimen to exclude postural proteinuria.[98]

Diurnal variation in protein excretion occurs in healthy individuals and patients with CKD. Overnight urinary protein excretion is lower, and the amount less variable, than in the daytime.[145,146] Thus timing of urine collection is likely to influence the sensitivity and specificity of screening tests for urine protein or albumin excretion. Samples taken at first void are most likely to accurately quantify 24-hour protein or albumin excretion,[147,148] and first void specimens are therefore regarded as preferable by a number of guidelines.[19,72,97]

URINARY ACR VERSUS PCR

Because the relationship between albumin excretion and total protein excretion is nonlinear,[149] an ACR cannot be derived from a PCR, and vice versa. The ACR, rather than PCR, has been recommended by a number of guidelines because of an improved ability to standardize urinary albumin versus total protein measurement and the fact that albumin is the predominant protein lost in the urine.[19,97] These advantages have already been outlined. ACR has not been shown to be superior to PCR in determining prognosis or detecting CKD in nondiabetic subjects.[97] A retrospective cohort study comparing urine PCR, ACR, and 24-hour protein at a single center showed that the three were equal in predictive utility for doubling of serum creatinine, commencement of renal replacement therapy, and all-cause mortality.[149]

REAGENT STRIP TESTING

Multireagent dipstick urinalysis has been used widely as an initial screening tool for the evaluation of proteinuria because of its low cost, availability, and ability to provide rapid point-of-care information to clinicians. Most dipstick reagents are semiquantitative, containing a pH-sensitive colorimetric indicator that changes color when negatively charged proteins bind to it. Dipstick testing for protein has limited sensitivity for nonalbumin and positively charged proteins[64,150–152] and therefore often has false-negative results in the presence of predominantly LMW (tubular or overflow) proteinuria.[109] Albumin-specific dipsticks may also be used.

The dipstick tests protein or albumin concentration, rather than an excretion rate, so it is strongly affected by changes in urine concentration. Very dilute urine may give false-negative results, and concentrated urine may give false-positive results. Measuring specific gravity concurrently with urinary protein on a dipstick can thus help with interpretation of a urine dipstick result.[153] A very high urine pH (>7.0) can give false-positive results, as can contamination of the urine with blood. Operator-dependent differences may also occur with manual reading of dipsticks, decreasing reproducibility.[147,151] The use of automated reader devices improves interoperator variability.

ALBUMIN-SPECIFIC DIPSTICKS

In addition to dipsticks that are designed to measure total protein, albumin-specific dipsticks are in use. Many of these use dye binding methods[154–156] but antibody-based detection methods are also available.[157] Several studies have examined the sensitivity and specificity of the newer reagent strips that measure very low concentrations of urine albumin. Most of these investigations studied patients with diabetes, and most examined the Micral-Test[155,158–161] (Boehringer Mannheim, Mannheim, Germany), the Micro-Bumintest[155,162] (Ames

Division, Miles Laboratories, Elkhart, Indiana), or both. In general, these albumin reagent strip tests are more sensitive than standard dipstick tests, but they also have a relatively high rate of false-positive results.

NEW DEVICES FOR POINT-OF-CARE PROTEIN TESTING

New systems with a creatinine test pad can report ACRs in the range previously classified as "microalbuminuria" (corresponding to <300 mg/g) or total PCRs. They overcome some of the error inherent in measuring urinary protein concentrations rather than protein excretion rates. The CLINITEK system (CLINITEK microalbumin, Siemens Medical Solutions Diagnostics, Mishawaka, Indiana) uses a reagent strip with two pads, using a dye binding method for albumin measurement and a creatinine assay based on the peroxidase-like activity of a copper creatinine complex. The reagent strips are used in combination with an analyzer to give a semiquantitative assessment of ACR.[163,164]

ROLE OF POINT-OF-CARE AND REAGENT STRIP TESTING

The role of urinary reagent strip testing, using either protein or albumin-specific dipsticks, in the general and high-risk population is the subject of debate. Most guidelines do not recommend the use of the urine dipstick as an initial screening test for proteinuria.[74] However, reagent strip testing may be of particular use in settings where laboratory access is limited. Newer point-of-care devices that can measure low levels of albuminuria and provide ACRs may have a role to play in population screening, but this role has not yet been defined by large studies.[19]

General Population

Observational studies have shown that reagent strip–proven proteinuria is associated with progression to ESKD and mortality in the general population.[68,70] However, general population screening could lead to unnecessary investigations, possible harm, and excess costs.[165–168] As with all diagnostic tests, the positive and negative predictive values of the urinary reagent strips and point-of-care devices depend on the setting in which they are used as well as their sensitivity and specificity.[169,170] A study comparing urinary ACRs with protein dipsticks (Bayer Multistix) using data from the previously mentioned AusDiab study showed that positive predictive values varied greatly across low- and high-risk subgroups. The dipstick test showed a good ability to rule out proteinuria, with a reagent strip result of less than trace having a negative predictive value of 97.6% for ACR values of 30 mg/g or higher and a negative predictive value of 100% for ACR values of 300 mg/g or higher.[171] The investigators concluded that urine reagent strip testing is a reasonable "rule-out" test for proteinuria. However, an analysis by Samal and Linder argues that the rate of false-positive results, which was as high as 53% using an ACR cutoff of 30 mg/g or higher, makes urinary reagent strip testing unacceptable in the general population owing to the cost, anxiety, and workload generated by false-positive results.[168] Because of the high rate of false-positive results, a positive reagent strip test result mandates confirmation with a quantitative test. This is a factor that significantly limits the cost-effectiveness of reagent strip testing for population screening.[166,168]

Screening of schoolchildren with urinary reagent strips in Japan, Taiwan, and Korea can detect asymptomatic renal disease at an early stage.[172–174] However, there are no data to show that this policy results in improved outcomes or has benefits from a health economics perspective. Several studies have used models to assess the benefits of general population screening with urinary reagent strips, followed by angiotensin-converting enzyme inhibitor or angiotensin-receptor blocker use in the proteinuric population. One such study, assessing the utility of general practitioner–led general population screening for proteinuria in Australia in 2002, concluded that there was insufficient evidence to support this practice.[166] A study that assessed this practice in a nondiabetic, nonhypertensive U.S. population using cost per quality-adjusted life year concluded that it was cost-effective only if selectively directed toward high-risk groups (aged >60 years or with hypertension) or conducted at long intervals (10 years).[167]

High-Risk Populations

In contrast to general population screening, there are several studies showing the cost-effectiveness of high-risk population screening for proteinuria with urinary dipstick testing[167,175,176] and subsequent antiproteinuric therapy. A model based on screening of a hypertensive, diabetic U.S. population cohort with Micral-II semiquantitative reagent strips for albumin and initiating irbesartan treatment in patients who had microalbuminuria (estimated 24-hour urinary albumin excretion >20 μg/min) or higher levels of urinary albumin showed a 44% reduced incidence in the cumulative incidence of ESKD and was likely to be cost-effective.[175] Screening high-risk populations, such as patients with diabetes, hypertension, or known vascular disease, for microalbuminuria is recommended in most guidelines,[19,177,178] although the frequency at which testing should occur is either not specified or inconsistent. Guidelines generally advise the use of laboratory rather than reagent strip testing in the high-risk population.[179] Studies using newer devices such as the CLINITEK system have shown good negative predictive values, making it an effective rule-out test.[180–182] The CLINITEK system has shown good performance in diabetic, general population,[163] and CKD cohorts.[183] However, the usefulness and cost-effectiveness of these newer devices are yet to be confirmed by large studies.

PROTEINURIA MEASUREMENT IN SPECIFIC POPULATIONS

PREGNANT PATIENTS

Proteinuria is generally defined as ≥300 mg/24 hours for the diagnosis of preeclampsia. The roughly equivalent urine PCR of 300 mg/g (30 mg/mmol) showed reasonable performance in estimating 24-hour protein excretion and as a rule-out test in two systematic reviews of studies in this setting, although there were no data on PCR for predicting outcomes. Currently, there is insufficient evidence to substitute urine albumin measurement for total protein in pregnant women with hypertension or suspected preeclampsia.[184,185]

CHILDREN

Normal levels of protein excretion in children are <10 mg/m^2/day, or <4 mg/m^2/h.[186] Nephrotic-range proteinuria is defined as 1000 mg/m^2/day, or 40 mg/m^2/h, or higher.

Urine PCR has been shown to have reasonable accuracy in reflecting 24-hour levels of protein excretion in a small study of 15 children.[187] PCR has been shown to predict an increased rate of GFR decline in children.[188–190] There is currently insufficient evidence linking elevated urine ACR with adverse outcomes to recommend the use of ACR in a pediatric population.[191] A number of studies have shown contradictory data with regard to the relationship of urinary albumin excretion in healthy children and various conditions, such as obesity, hypertension, fasting glucose, and insulin resistance.[192]

KIDNEY TRANSPLANT RECIPIENTS

Proteinuria predicts allograft loss, cardiovascular risk, and death in kidney transplant recipients.[193] One study showed that 24-hour urinary albumin measurement was superior to total protein measurement in predicting graft loss[194]; another using urine ACR and PCR showed equivalent performances.[195]

URINE MICROSCOPY

Examination of the urine by microscopy has been performed systematically at least since the 19th century[196] and remains a vital investigation that is often considered a component of the physical examination of a patient in whom kidney disease is suspected.

PREPARATION AND METHOD

Formed elements in urine degrade rapidly and so urine microscopy is best performed on a fresh urine sample within 2 hours of collection. Urine preservation is not a routinely applied technique but has been performed successfully by some institutions. Traditionally, ethanol is used to preserve uroepithelial cells for cytology but this does not prevent lysis of red and white blood cells.[197] Formaldehyde-based solutions have been used to preserve urine sediment for up to 3 months, and commercial preservatives such as buffered boric acid are also available.

The first urine of the morning specimen has been recommended in the past for urine microscopy because it is acidic and concentrated, but a midstream specimen of the second urine of the morning is favored owing to the lysis of urine particles after prolonged storage of urine in the bladder overnight. Specimens should preferably not be refrigerated because this may cause precipitation of crystals. High urine pH and dilute urine lead to more degradation of formed elements.

A guideline provided by the European Confederation of Laboratory Medicine suggests standardization of preparation of the urine sediment for microscopy.[198] A sample of 5–12 mL of urine should be centrifuged at 400 g or 2000 rpm for 5 minutes, a defined volume of supernatant removed by suction rather than arbitrary decanting, and the pellet resuspended by gentle agitation. A drop of urine should be placed on a slide under a coverslip, and it should be examined ideally with phase-contrast microscopy rather than usual brightfield microscopy, at low power (×160) then at high power (×400). Staining or polarized light may also be useful to identify certain substances.

CELLS OF THE URINARY SEDIMENT

ERYTHROCYTES

"Hematuria" is defined as three or more erythrocytes per high-power field. Transient hematuria is common and may be due to strenuous exercise. Persistent hematuria on three repeated urine samples warrants investigation. Studies show great variation in the prevalence of microscopic hematuria from as low as 0.18% to as high as 16.1%.[199] A study of more than a million Israeli military recruits showed an incidence of persistent hematuria of 0.3%.[200] This finding was associated with an increased risk of subsequent ESKD (hazard ratio = 19.5) although the absolute risk of ESKD was low, at 34.0 per 100,000 person-years.

Even when the urine appears red the sediment should be examined to determine whether red blood cells are present because a red appearance may be due to other causes, such as hemoglobinuria and myoglobinuria. Macroscopic hematuria is much more likely to be due to malignancy. Isomorphic red blood cells, which look similar to the erythrocytes found in the bloodstream, are thought to be nonglomerular in origin. Dysmorphic red blood cells (Fig. 23.3) are erythrocytes from the glomerular capillary, and their irregular appearance is a consequence of damage due to pH and osmolality changes as the cells travel through the tubule. Glomerular hematuria is defined by some institutions in terms of percentage of dysmorphic red blood cells, but the threshold at which this value is believed to be significant is not standardized. Glomerular hematuria is variously defined as more than 10% to 80% dysmorphic red blood cells or more than 2% to 5% acanthocytes, which are a subtype of dysmorphic red blood cells with protruding blebs.

Automated methods of examining for glomerular or nonglomerular hematuria have been developed in an attempt to overcome the problems with reliability and reproducibility of urine microscopy. These methods function by measuring the mean corpuscular volume (MCV) of the red cells. An MCV smaller or larger than the normal range (50–80 fL) is recorded as dysmorphic. The role of urinary red blood cell MCV in diagnosis was reviewed in a meta-analysis,[201] which concluded that the diagnostic value of this test is limited and that the urinary MCV test was not reliable in cases of low-grade hematuria because of interfering debris.

Causes of hematuria are listed in Table 23.9. Although anticoagulation often unmasks another underlying etiology for hematuria, over-anticoagulation itself may cause glomerular bleeding, as in the case of the relatively newly recognized condition warfarin-induced nephropathy, in which obstruction of tubules by red blood cell casts may cause AKI.[202]

URINE CYTOLOGY

Cytology is usually performed and is recommended as part of the investigation for nonglomerular hematuria. Although it is the realm of urologists, nephrologists may frequently encounter patients with nonglomerular hematuria as part of the investigative process for asymptomatic microscopic hematuria. A number of studies have suggested that the value of routine urine cytology as part of the workup for nonglomerular hematuria is limited if other investigations such as imaging and flexible cystoscopy are performed. For example, in a study of 2778 patients[203] who presented to a

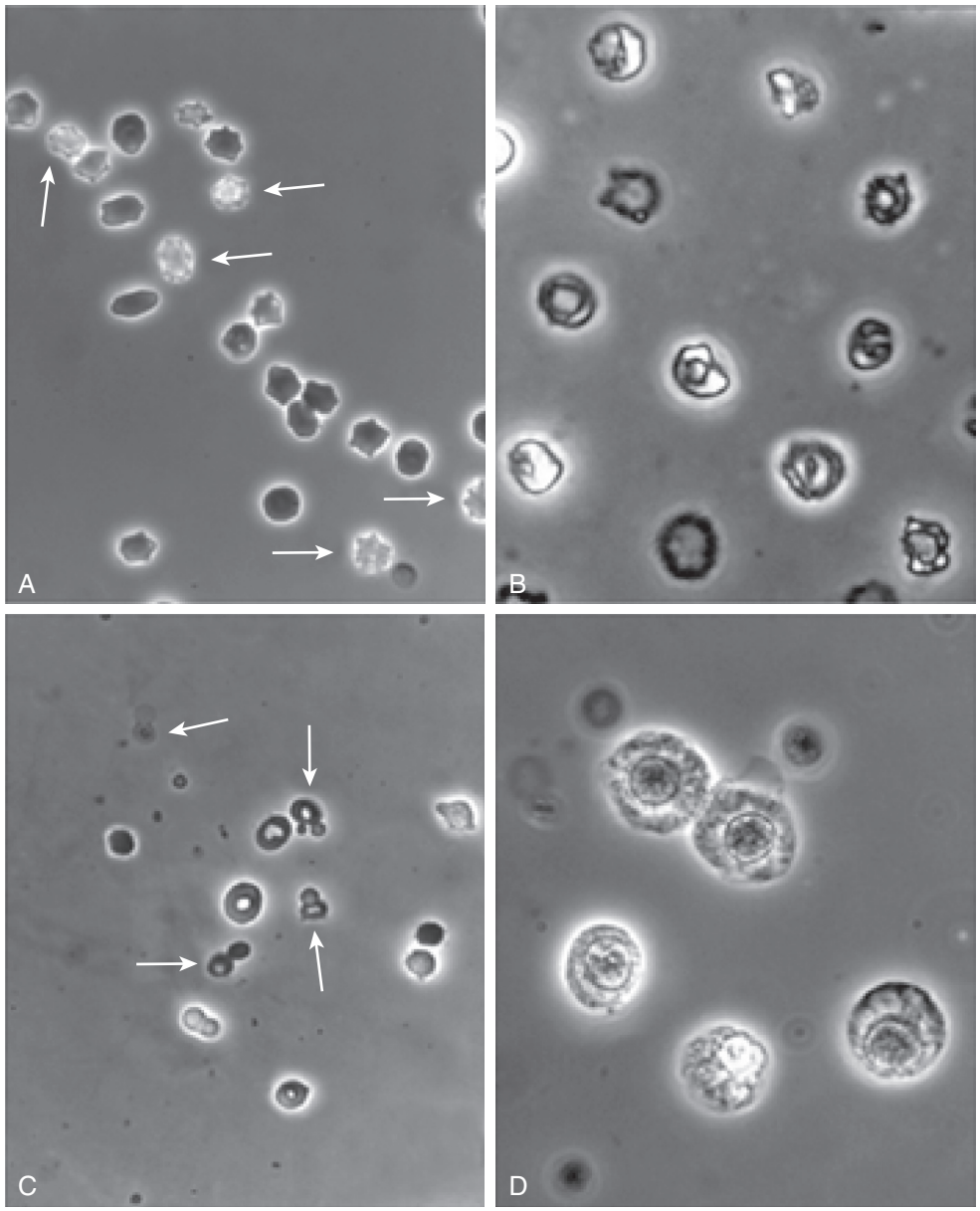

Fig. 23.3 Erythrocytes in urine. (A) Isomorphic erythrocytes, some with a "crenated" appearance *(arrows).* (B) Different types of dysmorphic erythrocytes. (C) Acanthocytes *(arrows).* (D) Proximal renal tubule cells. (From Fogazzi GB, Verdesca S, Garigali G. Urinalysis: core curriculum 2008. *Am J Kidney Dis.* 2008;51:1052–1067.)

hospital hematuria clinic in the United Kingdom, 974 patients had "nonvisible" or microscopic hematuria. Of the patients with microscopic hematuria, 4.6% had a urothelial malignancy, which in 93% was a bladder tumor. Urothelial cancer cytology demonstrated only 45.5% sensitivity and 89.5% specificity. Only two patients with abnormal urine cytology as the only positive finding had urothelial malignancy on further investigation.

LEUKOCYTES

The most common leukocytes found in the urine, neutrophils, are usually an indication of infection or contamination. Eosinophils are detectable with Wright stain or Hansel stain. Hansel stain has improved sensitivity, especially because a urine pH of <7 inhibits Wright stain. Although eosinophiluria was initially associated with drug-induced hypersensitivity, the list of diseases that may be associated with eosinophiluria is diverse and includes renal cholesterol embolism, rapidly progressive glomerulonephritis, and prostatitis.

The diagnostic value of the presence of other leukocytes, such as lymphocytes and macrophages, is currently limited, although lymphocytes have been indicative of transplant rejection, and macrophages may be found in glomerulonephritis.

OTHER CELLS

"Squamous cells," the largest cells of the urinary sediment, derive from the urethra or external genitalia. "Renal tubule

Table 23.9 Causes of Hematuria[a]

Glomerular Hematuria
Glomerular Lesions
Thin basement membrane nephropathy
Mesangial immunoglobulin A (IgA) glomerulonephritis
Focal and segmental hyalinosis and sclerosis (focal glomerulosclerosis)
Lupus glomerulonephritis
Crescentic glomerulonephritis, including Wegener granulomatosis, microscopic polyangiitis, and Goodpasture syndrome
Membranous glomerulonephritis
Mesangiocapillary glomerulonephritis
Dense deposit disease
Poststreptococcal glomerulonephritis
Nonglomerular Disease
Autosomal dominant polycystic kidney disease
Exercise hematuria
Bleeding diathesis
Drugs, including anticoagulants
Nonglomerular Hematuria
Urinary tract infection
Urinary tract calculi
Hypercalciuria and hyperuricosuria
Autosomal dominant polycystic kidney disease
Benign prostatic hypertrophy
Transitional cell carcinoma
Renal cell carcinoma
Prostatic carcinoma
Exercise hematuria
Trauma
Bleeding diathesis and anticoagulants
Drugs
Renal papillary necrosis
Sickle cell disease

[a]Unknown whether glomerular or nonglomerular hematuria after percutaneous coronary artery angioplasty.

From Kincaid Smith P, Fairley K. The investigation of haematuria. *Semin Nephrol.* 2005;25:127–135.

Table 23.10 Common Casts

Cast	Main Clinical Association(s)
Hyaline	Normal and in renal disease
Granular	Renal disease of any cause
Waxy	Renal disease of any cause
Fatty	Heavy proteinuria
Red blood cell	Proliferative glomerulonephritis, glomerular bleeding
White blood cell	Acute interstitial nephritis, acute pyelonephritis
Tubular epithelial cell	Acute tubular necrosis ("muddy brown" casts), acute interstitial nephritis, proliferative glomerulonephritis

From Fogazzi GB, Verdesca S, Garigali G. Urinalysis: core curriculum 2008. *Am J Kidney Dis.* 2008;51:1052–1067.

Table 23.11 Common Crystals and Their Appearance

Crystal	Appearance
Uric acid	Usually lozenges but varying shape, yellow-tinged
Calcium oxalate	Monohydrate: ovoid or dumbbell-shaped, biconcave disks Dihydrate: bipyramidal
Calcium phosphate	Prisms, star-like particles or needles of various sizes
Triple phosphate (struvite)	Coffin lids
Cholesterol	Transparent thin plates
Cystine	Hexagonal plates with irregular sides

From Fogazzi GB, Verdesca S, Garigali G. Urinalysis: core curriculum 2008. *Am J Kidney Dis.* 2008;51:1052–1067.

epithelial cells" may be present in tubular injury. "Urothelial cells" may be seen in urologic diseases such as malignancy.

OTHER ELEMENTS

LIPIDS

Lipids appear as spherical, translucent drops of varying size. They may also be within the cytoplasm of cells as "oval fat bodies." Under polarized light, lipid droplets look like Maltese crosses. Lipiduria is usually associated with heavy proteinuria but may also be present in Fabry disease.

CASTS

"Casts" (Fig. 23.4) are cylindrical bodies of renal origin that form from the aggregation of fibrils of Tamm–Horsfall glycoprotein (uromodulin), which is secreted by cells of the thick ascending limb of the loop of Henle. Trapping of various particles within the cast matrix, as well as degenerative processes, results in casts with different appearances and clinical significance (Table 23.10). Hyaline casts are nonspecific and may be present normally. Granular casts are nonspecific and contain protein aggregates or degenerated cellular elements. Waxy casts are also nonspecific and result from degeneration of other casts. Broad casts are wider waxy casts that are seen in chronic renal failure in which there is dilation of the tubule. Renal tubule epithelial cell casts are formed from the aggregation of desquamated cells of the tubule lining. Because the epithelial cells still appear intact, this finding is usually the result of an acute disease process such as acute tubular necrosis. Red blood cell casts are always pathologic and indicate significant glomerular bleeding, which is often due to rapidly progressive glomerulonephritis.

CRYSTALS

A large variety of crystals can be seen in the urine that may be of diagnostic value (Table 23.11). However, uric acid, calcium oxalate, and calcium phosphate crystals are common and may have little clinical significance because they may precipitate as a result of transient supersaturation of urine

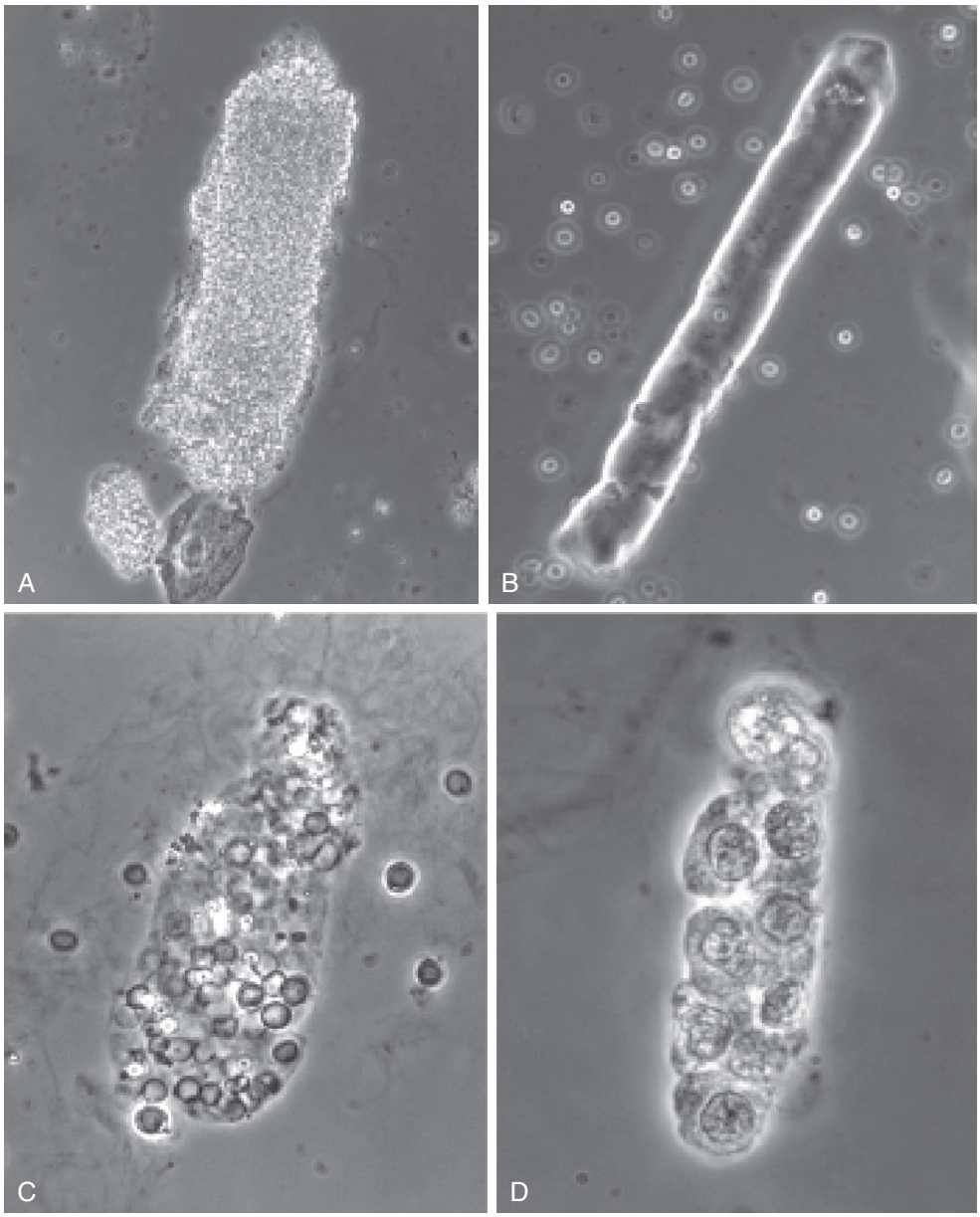

Fig. 23.4 Urinary casts. (A) A finely granular cast. (B) Waxy cast with the typical "melted wax" appearance. (C) A red blood cell cast. (D) A renal tubule epithelial cell cast. (From Stevens LA, Nolin TD, Richardson MM, et al. Comparison of drug dosing recommendations based on measured GFR and kidney function estimating equations. *Am J Kidney Dis.* 2009;54:33–42.)

due to dehydration or cooling of the sample. Of course, depending on the clinical setting, uric acid crystals may be highly significant because they are present in acute uric acid nephropathy as part of tumor lysis syndrome, and calcium oxalate crystals may indicate ethylene glycol poisoning or hyperoxaluria.

A growing list of drugs, beginning with acyclovir and indinavir, may cause crystals in the urine that commonly have unusual shapes.

MICROORGANISMS

Bacteria are commonly seen because of contamination or infection. Fungi such as *Candida,* protozoa such as *Trichomonas,* and parasites such as *Schistosoma* may also be seen.

LIMITATIONS

Urine microscopy depends on expertise and has poor interobserver reliability. In a study involving 10 nephrologists, agreement for various elements in urine microscopy ranged from 31.4% to 79.1% and interobserver agreement was not associated with seniority.[204] Despite this limitation, urinary microscopy is still a vital component of the laboratory assessment of renal disease because its findings may crucially influence management of a patient. For example, identification of dysmorphic red blood cells and red blood cell casts in a patient with AKI may prompt empirical treatment with immunosuppressive therapy in advance of results of serology or renal biopsy.

SUMMARY

Despite advances in the field of laboratory assessment of kidney disease, this domain continues to be an evolving science with future research aiming to derive tests and equations that will not only reduce bias but also improve precision and accuracy. There is an ongoing need for better understanding of the intricacies of these tests by physicians and clinical chemists to appropriately diagnose and prognosticate patients and guide their management.


Complete reference list available at ExpertConsult.com.

KEY REFERENCES

2. Miller WG, Myers GL, Ashwood ER, et al. Creatinine measurement: state of the art in accuracy and interlaboratory harmonization. *Arch Pathol Lab Med.* 2005;129(3):297–304.
5. Dharnidharka VR, Kwon C, Stevens G. Serum cystatin C is superior to serum creatinine as a marker of kidney function: a meta-analysis. *Am J Kidney Dis.* 2002;40(2):221–226.
19. Kidney Disease: Improving Global Outcomes (KDIGO) CKD Work Group. KDIGO 2012 clinical practice guideline for the evaluation and management of chronic kidney disease. *Kidney Int Suppl.* 2013;3:1–150.
30. Levey AS, Bosch JP, Lewis JB, et al. A more accurate method to estimate glomerular filtration rate from serum creatinine: a new prediction equation. Modification of Diet in Renal Disease Study Group. *Ann Intern Med.* 2009;130(6):461–470.
31. Levey AS, Stevens LA, Schmid CH, et al. A new equation to estimate glomerular filtration rate. *Ann Intern Med.* 2009;150:604–612.
32. Matsushita K, Mahmoodi BK, Woodward M, et al. Comparison of risk prediction using the CKD-EPI equation and the MDRD study equation for estimated glomerular filtration rate. *JAMA.* 2012;307(18):1941–1951.
33. Eriksen BO, Mathisen UD, Melsom T, et al. The role of cystatin C in improving GFR estimation in the general population. *Am J Kidney Dis.* 2012;59(1):32–40.
35. Cockcroft DW, Gault MH. Prediction of creatinine clearance from serum creatinine. *Nephron.* 2012;16(1):31–41.
37. Schwartz GJ, Haycock GB, Edelmann CM, et al. A simple estimate of glomerular filtration rate in children derived from body length and plasma creatinine. *Pediatrics.* 1976;58(2):259–263.
38. Schwartz GJ, Muñoz A, Schneider MF, et al. New equations to estimate GFR in children with CKD. *J Am Soc Nephrol.* 1976;20(3):629–637.
39. Schwartz GJ, Work DF. Measurement and estimation of GFR in children and adolescents. *Clin J Am Soc Nephrol.* 2009;4(11):1832–1843.
48. Chen S. Retooling the creatinine clearance equation to estimate kinetic GFR when the plasma creatinine is changing acutely. *J Am Soc Nephrol.* 2013;24(6):877–888.
49. Endre ZH, Pickering JW, Walker RJ. Clearance and beyond: the complementary roles of GFR measurement and injury biomarkers in acute kidney injury (AKI). *Am J Physiol Renal Physiol.* 2013;301(4):F697–F707.
52. Stevens LA, Nolin TD, Richardson MM, et al. Comparison of drug dosing recommendations based on measured GFR and kidney function estimating equations. *Am J Kidney Dis.* 2009;54(1):33–42.
55. Kilbride HS, Stevens PE, Eaglestone G, et al. Accuracy of the MDRD (Modification of Diet in Renal Disease) study and CKD-EPI (CKD Epidemiology Collaboration) equations for estimation of GFR in the elderly. *Am J Kidney Dis.* 2013;61(1):57–66.
64. Fogazzi GB, Verdesca S, Garigali G. Urinalysis: core curriculum 2008. *Am J Kidney Dis.* 2008;51(6):1052–1067.
65. Israni A, Kasiske B, et al. Laboratory assessment of kidney disease: glomerular filtration rate, urinalysis, and proteinuria. In: Taal M, Chertow G, Marsden P, eds. *Brenner and Rector's the Kidney.* 9th ed. Philadelphia: Saunders; 2011:868–892.
67. Jacobs D, De Mott WR, Willie GR, et al. Urinalysis and clinical microscopy. In: Jacobs D, Kasten BL, De Mott WR, eds. *Laboratory Test Handbook.* Baltimore: Williams & Wilkins; 1990:906–909.
68. Kannel WB, Stampfer MJ, Castelli WP, et al. The prognostic significance of proteinuria: the Framingham study. *Am Heart J.* 1984;108(5):1347–1352.
72. KDOQI. KDOQI clinical practice guidelines and clinical practice recommendations for diabetes and chronic kidney disease. *Am J Kidney Dis.* 2007;49(2 suppl 2):S12–S154.
74. Lamb EJ, MacKenzie F, Stevens PE. How should proteinuria be detected and measured? *Ann Clin Biochem.* 2009;46(Pt 3):205–217.
77. Cameron JS. The patient with proteinuria and or hematuria. In: Davison A, ed. *Oxford Textbook of Clinical Nephrology.* 3rd ed. Oxford: Oxford University Press; 2005:389–411.
78. Brinkkoetter PT, Ising C, Benzing T. The role of the podocyte in albumin filtration. *Nat Rev Nephrol.* 2013;9(6):328–336.
87. Russo LM, Bakris GL, Comper WD. Renal handling of albumin: a critical review of basic concepts and perspective. *Am J Kidney Dis.* 2002;39(5):899–919.
89. Atkins RC, Briganti EM, Zimmet PZ, et al. Association between albuminuria and proteinuria in the general population: the AusDiab study. *Nephrol Dial Transplant.* 2003;18(10):2170–2174.
91. Hillege HL, Fidler V, Diercks GF, et al. Urinary albumin excretion predicts cardiovascular and noncardiovascular mortality in general population. *Circulation.* 2002;106(14):1777–1782.
97. Johnson DW, Jones GR, Mathew TH, et al. Chronic kidney disease and measurement of albuminuria or proteinuria: a position statement. *Med J Aust.* 2012;197(4):224–225.
98. Miller WG, Bruns DE, Hortin GL, et al. Current issues in measurement and reporting of urinary albumin excretion. *Ann Biol Clin (Paris).* 2010;68(1):9–25.
108. Martin H. Laboratory measurement of urine albumin and urine total protein in screening for proteinuria in chronic kidney disease. *Clin Biochem Rev.* 2011;32(2):97–102.
109. Viswanathan G, Upadhyay A. Assessment of proteinuria. *Adv Chronic Kidney Dis.* 2011;18(4):243–248.
111. Sviridov D, Drake SK, Hortin GL. Reactivity of urinary albumin (microalbumin) assays with fragmented or modified albumin. *Clin Chem.* 2008;54(1):61–68.
118. Naresh CN, Hayen A, Craig JC, et al. Day-to-day variability in spot urine protein-creatinine ratio measurements. *Am J Kidney Dis.* 2012;60(4):561–566.
119. Newman DJ, Pugia MJ, Lott JA, et al. Urinary protein and albumin excretion corrected by creatinine and specific gravity. *Clin Chim Acta.* 2000;294(1–2):139–155.
124. Ruggenenti P, Gaspari F, Perna A, et al. Cross sectional longitudinal study of spot morning urine protein:creatinine ratio, 24 hour urine protein excretion rate, glomerular filtration rate, and end stage renal failure in chronic renal disease in patients without diabetes. *BMJ.* 1998;316(7130):504–509.
125. Price CP, Newall RG, Boyd JC. Use of protein:creatinine ratio measurements on random urine samples for prediction of significant proteinuria: a systematic review. *Clin Chem.* 2005;51(9):1577–1586.
142. Robinson RR. Isolated proteinuria in asymptomatic patients. *Kidney Int.* 1980;18:395–406.
148. Witte EC, Lambers Heerspink HJ, de Zeeuw D, et al. First morning voids are more reliable than spot urine samples to assess microalbuminuria. *J Am Soc Nephrol.* 2009;20(2):436–443.
149. Methven S, Macgregor MS, Traynor JP, et al. Comparison of urinary albumin and urinary total protein as predictors of patient outcomes in CKD. *Am J Kidney Dis.* 2011;57(1):21–28.
165. Iseki K, Kinjo K, Iseki C, et al. Relationship between predicted creatinine clearance and proteinuria and the risk of developing ESRD in Okinawa, Japan. *Am J Kidney Dis.* 2004;44(5):806–814.
166. Craig JC, Barratt A, Cumming R, et al. Feasibility study of the early detection and treatment of renal disease by mass screening. *Intern Med J.* 2002;32(1–2):6–14.
167. Boulware LE, Jaar BG, Tarver-Carr ME, et al. Screening for proteinuria in US adults: a cost-effectiveness analysis. *JAMA.* 2003;290(23):3101–3114.
168. Samal L, Linder JA. The primary care perspective on routine urine dipstick screening to identify patients with albuminuria. *Clin J Am Soc Nephrol.* 2013;8(1):131–135.
186. Hogg RJ, Portman RJ, Milliner D, et al. Evaluation and management of proteinuria and nephrotic syndrome in children: recommendations from a pediatric nephrology panel established at the National Kidney Foundation Conference on proteinuria, albuminuria, risk, assessment, detection, and elimination (PARADE). *Pediatrics.* 2000;105(6):1242–1249.

195. Panek R, Lawen T, Kiberd BA. Screening for proteinuria in kidney transplant recipients. *Nephrol Dial Transplant.* 2011;26(4):1385–1387.
200. Vivante A, Afek A, Frenkel-Nir Y, et al. Persistent asymptomatic isolated microscopic hematuria in Israeli adolescents and young adults and risk for end-stage renal disease. *JAMA.* 2011;306(7):729–736.
201. Offringa M, Benbassat J. The value of urinary red cell shape in the diagnosis of glomerular and post-glomerular haematuria. A meta-analysis. *Postgrad Med J.* 1992;68(802):648–654.
203. Mishriki SF, Aboumarzouk O, Vint R, et al. Routine urine cytology has no role in hematuria investigations. *J Urol.* 2013;189(4):1255–1258.
204. Wald R, Bell CM, Nisenbaum R, et al. Interobserver reliability of urine sediment interpretation. *Clin J Am Soc Nephrol.* 2009;4(3):567–571.

REFERENCES

1. Dunn SR, Gabuzda GM, Superdock KR. Induction of bacterial creatininase activity in chronic renal failure: timing of creatinine degradation and effect of antibiotics. *Am J Kidney Dis. 1997*;29(1): *72–77.*
2. Miller WG, Myers GL, Ashwood ER, et al. Creatinine measurement: state of the art in accuracy and interlaboratory harmonization. *Arch Pathol Lab Med.* 2005;129(3):297–304.
3. Selvin E, Juraschek SP, Eckfeldt J, et al. Within-person variability in kidney measures. *Am J Kidney Dis.* 2013;61(5):716–722.
4. Schwartz GJ, Schneider MF, Maier PS, et al. Improved equations estimating GFR in children with chronic kidney disease using an immunonephelometric determination of cystatin C. *Kidney Int.* 2012;82(4):445–453.
5. Dharnidharka VR, Kwon C, Stevens G. Serum cystatin C is superior to serum creatinine as a marker of kidney function: a meta-analysis. *Am J Kidney Dis.* 2002;40(2):221–226.
6. Levey AS, Fan L, Eckfeldt JH, et al. Cystatin C for glomerular filtration rate estimation: coming of age. *Clin Chem.* 2014;60:916–919.
7. Eckfeldt JH, Karger AB, Miller WG, et al. Performance in measurement of serum cystatin C by laboratories participating in the College of American pathologists 2014 CYS survey. *Arch Pathol Lab Med.* 2015;139:888–893.
8. Bargnoux AS, et al. Multicenter evaluation of cystatin C measurement after assay standardization. *Clin Chem.* 2017;63:833–841.
9. Stevens LA, Coresh J, Schmid CH, et al. Estimating GFR using serum cystatin C alone and in combination with serum creatinine: a pooled analysis of 3,418 individuals with CKD. *Am J Kidney Dis.* 2008;51:395–406.
10. Inker LA, Schmid CH, Tighiourat H, et al. Estimating glomerular filtration rate from serum creatinine and cystatin C. *N Engl J Med.* 2012;367:20–29.
11. Schaeffner ES, Ebert N, Delanaye P. Two novel equations to estimate kidney function in persons aged 70 years or older. *Ann Intern Med.* 2012;157:471–481.
12. Omuse G, et al. Comparison of equations for estimating glomerular filtration rate in screening for chronic kidney disease in asymptomatic black Africans: a cross sectional study. *BMC Nephrol.* 2017;18:369.
13. Pottel H, et al. Estimating glomerular filtration rate for the full age spectrum from serum creatinine and cystatin C. *Nephrol Dial Transplant.* 2017;32:497–507.
14. Grubb A, et al. Generation of a new cystatin C-based estimating equation for glomerular filtration rate by use of 7 assays standardized to the international calibrator. *Clin Chem.* 2014;60:974–986.
15. Rule AD, Bergstralh EJ, Slezak JM, et al. Glomerular filtration rate estimated by cystatin C among different clinical presentations. *Kidney Int.* 2006;69(2):399.
16. White C, Akbari A, Hussain A, et al. Estimating glomerular filtration rate in kidney transplantation: a comparison between serum creatinine and cystatin C based methods. *J Am Soc Nephrol.* 2005;16(12):3763–3770.
17. Poge U, Gerhardt T, Stoffel-Wagner B, et al. Calculation of glomerular filtration rate based on cystatin C in cirrhotic patients. *Nephrol Dial Transplant.* 2006;21(3):660. [Epub 2005 Dec2].
18. Stevens LA, Padala S, Levey AS. Advances in glomerular filtration rate-estimating equations. *Curr Opin Nephrol Hypertens.* 2010;19(3):298.
19. Kidney Disease: Improving Global Outcomes (KDIGO) CKD Work Group. KDIGO 2012 clinical practice guideline for the evaluation and management of chronic kidney disease. *Kidney Int Suppl.* 2013;3:1–150.
20. Inker LA, et al. KDOQI US commentary on the 2012 KDIGO clinical practice guideline for the evaluation and management of CKD. *Am J Kidney Dis.* 2014;63:713–735.
21. White CA, Akbari A, Doucette S, et al. A novel equation to estimate glomerular filtration rate using beta-trace protein. *Clin Chem.* 2007;53(11):1965–1968.
22. Pöge U, Gerhardt T, Stoffel-Wagner B, et al. Beta-trace protein-based equations for calculation of GFR in renal transplant recipients. *Am J Transplant.* 2008;8(3):608–615.
23. Argyropoulos CP, Chen SS, Ng YH, et al. Rediscovering beta-2 microglobulin as a biomarker across the spectrum of kidney diseases. *Front Med (Lausanne).* 2017;4:73.
24. Inker LA, Tighiouart H, Coresh J, et al. GFR estimation using β-trace protein and β2-microglobulin in CKD. *Am J Kidney Dis.* 2016;67(1):40–48.
25. Spanaus KS, Kollerits B, Ritz E, et al. Serum creatinine, cystatin C, and beta-trace protein in diagnostic staging and predicting progression of primary nondiabetic chronic kidney disease. *Clin Chem.* 2010;56(5):740–749.
26. Astor BC, Shafi T, Hoogeveen RC, et al. Novel markers of kidney function as predictors of ESRD, cardiovascular disease, and mortality in the general population. *Am J Kidney Dis.* 2012;59(5):653–662.
27. Karger AB, Inker LA., Coresh J, et al. Novel filtration markers for GFR estimation. *J Int Feder Clin Chem Lab Med.* 2017;28(4):277–288.
28. Wang X, Lewis J, Appel L, et al. Validation of creatinine-based estimates of GFR when evaluating risk factors in longitudinal studies of kidney disease. *J Am Soc Nephrol.* 2006;17(10):2900–2909.
29. Padala S, Tighiouart H, Inker LA, et al. Accuracy of a GFR estimating equation over time in people with a wide range of kidney function. *Am J Kidney Dis.* 2012;60(2):217–224.
30. Levey AS, Bosch JP, Lewis JB, et al. A more accurate method to estimate glomerular filtration rate from serum creatinine: a new prediction equation. Modification of Diet in Renal Disease Study Group. *Ann Intern Med.* 1999;130(6):461–470.
31. Levey AS, Stevens LA, Schmid CH, et al. A new equation to estimate glomerular filtration rate. *Ann Intern Med.* 2009;150:604–612.
32. Matsushita K, Mahmoodi BK, Woodward M, et al. Comparison of risk prediction using the CKD-EPI equation and the MDRD study equation for estimated glomerular filtration rate. *JAMA.* 2012;307(18):1941–1951.
33. Eriksen BO, Mathisen UD, Melsom T, et al. The role of cystatin C in improving GFR estimation in the general population. *Am J Kidney Dis.* 2012;59(1):32–40.
34. Go AS, Chertow GM, Fan D, et al. Chronic kidney disease and the risks of death, cardiovascular events and hospitalization. *N Engl J Med.* 2004;351:1296–1305.
35. Cockcroft DW, Gault MH. Prediction of creatinine clearance from serum creatinine. *Nephron.* 2012;16(1):31–41.
36. Stevens LA, Levey AS. Measured GFR as a confirmatory test for estimated GFR. *J Am Soc Nephrol.* 2009;20(11):2305F–2313F.
37. Schwartz GJ, Haycock GB, Edelmann CM, et al. A simple estimate of glomerular filtration rate in children derived from body length and plasma creatinine. *Pediatrics.* 1976;58(2):259–263.
38. Schwartz GJ, Muñoz A, Schneider MF, et al. New equations to estimate GFR in children with CKD. *J Am Soc Nephrol.* 1976;20(3):629–637.
39. Schwartz GJ, Work DF. Measurement and estimation of GFR in children and adolescents. *Clin J Am Soc Nephrol.* 2009;4(11):1832–1843.
40. Liu X, Chen J, Wang C. Assessment of glomerular filtration ate in elderly Chinese patients with chronic kidney disease. *Int Urol Nephrol.* 2013.
41. Koppe L, Klich A, Ecochard R, et al. Performance of creatinine based equations compared in older patients. *J Nephrol.* 2013;26(4):716–723.
42. Maynard SE, Thadhani R. Pregnancy and the kidney. *J Am Soc Nephrol.* 2009;20(1):14–22.
43. Dunlop W. Serial changes in hemodynamics during normal human pregnancy. *Br J Obstet Gynaecol.* 1981;88:1–9.
44. Park S, Lee SM, Park JS, et al. Midterm eGFR and adverse pregnancy outcomes: the clinical significance of gestational hyperfiltration. *Clin J Am Soc Nephrol.* 2017;12(7):1048–1056.
45. Bjornstad P, Cherney D. Kidney function can predict pregnancy outcomes. *CJASN. 2017.*
46. Macedo E, Bouchard J, Soroko SH, et al. Fluid accumulation, recognition and staging of acute kidney injury in critically-ill patients. *Crit Care.* 2010;14(3):R82.
47. Pickering JW, Ralib AM, Endre ZH. Combining creatinine and volume kinetics identifies missed cases of acute kidney injury following cardiac arrest. *Crit Care.* 2013;17(1):R7.
48. Chen S. Retooling the creatinine clearance equation to estimate kinetic GFR when the plasma creatinine is changing acutely. *J Am Soc Nephrol.* 2013;24(6):877–888.
49. Endre ZH, Pickering JW, Walker RJ. Clearance and beyond: the complementary roles of GFR measurement and injury biomarkers in acute kidney injury (AKI). *Am J Physiol Renal Physiol.* 2013;301(4):F697–F707.
50. U.S. Department of Health and Human Services. Food and Drug Administration. Center for Drug Evaluation and Research (CDER). *Guidance for Industry. Pharmacokinetics in patients with impaired renal function—study design, data analysis and impact on dosing and labeling.* Washington, DC: CDER, 2010.
51. Levey AS, Inker LA. Assessment of glomerular filtration rate in health and disease: a state of the art review. *Clin Pharmacol Ther.* 2017;102:405–419. doi:10.1002/cpt.729.

52. Stevens LA, Nolin TD, Richardson MM, et al. Comparison of drug dosing recommendations based on measured GFR and kidney function estimating equations. *Am J Kidney Dis.* 2009;54(1):33–42.
53. Gill J, Malyuk R, Djurdjev O, et al. Use of GFR equations to adjust drug doses in an elderly multi-ethnic group—a cautionary tale. *Nephrol Dial Transplant.* 2007;22(10):2894–2899.
54. Park EJ, Wu K, Mi Z, et al. A systematic comparison of Cockcroft-gault and Modification of Diet in Renal Disease equations for classification of kidney dysfunction and dosage adjustment. *Ann Pharmacother.* 2012;46(9):1174–1187.
55. Kilbride HS, Stevens PE, Eaglestone G, et al. Accuracy of the MDRD (Modification of Diet in Renal Disease) study and CKD-EPI (CKD Epidemiology Collaboration) equations for estimation of GFR in the elderly. *Am J Kidney Dis.* 2013;61(1):57–66.
56. Murata K, Baumann NA, Saenger AK, et al. Relative performance of the MDRD and CKD-EPI equations for estimating glomerular filtration rate among patients with varied clinical presentations. *Clin J Am Soc Nephrol.* 2011;6(8):1963–1972.
57. Pottel H, Hoste L, Dubourg L, et al. As estimated glomerular filtration rate equation for the full age spectrum. *Nephrol Dial Transplant. 2016*;31:*798–806.*
58. Baylis C, et al. Glucocorticoids and control of glomerular filtration rate. *Semin Nephrol.* 1990;10(4):320–329.
59. vanAcker B, Prummel MF, Weber JA, et al. Effect of prednisone on renal function in man. *Nephron. 1993*;Rannels SR, Jefferson LS. Effects of glucocorticoids on muscle protein turnover in perfused rat hemicorpus. Am J Physiol 1980; 238: E564±72.
60. Beaufrere FJ, Horber FF, Schenk WF, et al. Glucocorticosteroids increase leucine oxidation and impair leucine balance in humans. *Am J Physiol. 1989*;257:*E712*–E721.
61. Horber FF, Scheidegger J, Frey FJ. Overestimation of renal function in glucocorticosteroid treated patients. *Eur J Clin Pharmacol. 1985*;28:*537*–541.
62. Santos J, Martins LS. Estimating glomerular filtrations rate in kidney transplantation: still searching for the best marker. *World J Nephrol. 2015*;4(3):345–353.
63. Shaffi SK, Uhlig K, Perrone RD, et al. Performance of creatinine based GFR estimating equations in solid organ transplant recipients. *Am J Kidney Dis. 2014*;63(6):1007–1018.
64. Fogazzi GB, Verdesca S, Garigali G. Urinalysis: core curriculum 2008. *Am J Kidney Dis.* 2008;51(6):1052–1067.
65. Israni A, Kaisike B. *Laboratory Assessment of Kidney Disease: Glomerular Filtration Rate, Urinalysis, and Proteinuria.* 9th ed. Philadelphia: Saunders; 2011.
66. Rose BD, Post TW. *Clinical Physiology of Acid Base and Electrolyte Disorders.* 5th ed. New York: McGraw Hill; 2001.
67. Jacobs D, De Mott WR, Willie GR, et al. Urinalysis and clinical microscopy. In: Jacobs D, Kasten BL, De Mott WR, eds. *Laboratory Test Handbook.* Baltimore: Williams & Wilkins; 1990:906–909.
68. Kannel WB, Stampfer MJ, Castelli WP, et al. The prognostic significance of proteinuria: the Framingham study. *Am Heart J.* 1984;108(5):1347–1352.
69. Ninomiya T, Perkovic V, de Galan BE, et al. Albuminuria and kidney function independently predict cardiovascular and renal outcomes in diabetes. *J Am Soc Nephrol.* 2009;20(8):1813–1821.
70. Wen CP, Cheng TY, Tsai MK, et al. All-cause mortality attributable to chronic kidney disease: a prospective cohort study based on 462 293 adults in Taiwan. *Lancet.* 2008;371(9631):2173–2182.
71. Jafar TH, Stark PC, Schmid CH, et al. Proteinuria as a modifiable risk factor for the progression of non-diabetic renal disease. *Kidney Int.* 2001;60(3):1131–1140.
72. KDOQI. KDOQI clinical practice guidelines and clinical practice recommendations for diabetes and chronic kidney disease. *Am J Kidney Dis.* 2007;49(suppl 2):S12–S154.
73. Remuzzi G, Benigni A, Remuzzi A. Mechanisms of progression and regression of renal lesions of chronic nephropathies and diabetes. *J Clin Invest.* 2006;116(2):288–296.
74. Lamb EJ, MacKenzie F, Stevens PE. How should proteinuria be detected and measured? *Ann Clin Biochem.* 2009;46(Pt 3):205–217.
75. Hausmann R, Kuppe C, Egger H, et al. Electrical forces determine glomerular permeability. *J Am Soc Nephrol.* 2010;21(12):2053–2058.
76. Haraldsson B, Nyström J, Deen WM. Properties of the glomerular barrier and mechanisms of proteinuria. *Physiol Rev.* 2008;88(2):451–487.
77. Cameron JS. The patient with proteinuria and or hematuria. In: Davison A, ed. *Oxford Textbook of Clinical Nephrology.* 3rd ed. Oxford: Oxford University Press; 2005:389–411.
78. Brinkkoetter PT, Ising C, Benzing T. The role of the podocyte in albumin filtration. *Nat Rev Nephrol.* 2013;9(6):328–336, 46.
79. Huber TB, Benzing T. The slit diaphragm: a signaling platform to regulate podocyte function. *Curr Opin Nephrol Hypertens.* 2005;14(3):211–216.
80. Löwik MM, Groenen PJ, Levtchenko EN, et al. Molecular genetic analysis of podocyte genes in focal segmental glomerulosclerosis–a review. *Eur J Pediatr.* 2009;168(11):1291–1304.
81. Benoit G, Machuca E, Antignac C. Hereditary nephrotic syndrome: a systematic approach for genetic testing and a review of associated podocyte gene mutations. *Pediatr Nephrol.* 2010;25(9):1621–1632.
82. Tryggvason K, Patrakka J, Wartiovaara J. Hereditary proteinuria syndromes and mechanisms of proteinuria. *N Engl J Med.* 2006;354(13):1387–1401.
83. Comper WD, Glasgow EF. Charge selectivity in kidney ultrafiltration. *Kidney Int.* 1995;47(5):1242–1251.
84. Bolton GR, Deen WM, Daniels BS. Assessment of the charge selectivity of glomerular basement membrane using ficoll sulfate. *Am J Physiol.* 1998;274(5 Pt 2):F889–F896.
85. Burne MJ, Adal Y, Cohen N, et al. Anomalous decrease in dextran sulfate clearance in the diabetic rat kidney. *Am J Physiol.* 1998;274(4 Pt 2):F700–F708.
86. Asgeirsson D, Venturoli D, Rippe B, et al. Increased glomerular permeability to negatively charged ficoll relative to neutral ficoll in rats. *Am J Physiol Renal Physiol.* 2006;291(5):F1083–F1089.
87. Russo LM, Bakris GL, Comper WD. Renal handling of albumin: a critical review of basic concepts and perspective. *Am J Kidney Dis.* 2002;39(5):899–919.
88. Christov M, Alper SL. Tubular transport: core curriculum 2010. *Am J Kidney Dis.* 2010;56(6):1202–1217.
89. Atkins RC, Briganti EM, Zimmet PZ, et al. Association between albuminuria and proteinuria in the general population: the AusDiab study. *Nephrol Dial Transplant.* 2003;18(10):2170–2174.
90. Levey AS, de Jong PE, Coresh J, et al. The definition, classification, and prognosis of chronic kidney disease: a KDIGO controversies Conference report. *Kidney Int.* 2011;80(1):17–28.
91. Hillege HL, Fidler V, Diercks GF, et al. Urinary albumin excretion predicts cardiovascular and noncardiovascular mortality in general population. *Circulation.* 2002;106(14):1777–1782.
92. Obermayr RP, Temml C, Knechtelsdorfer M, et al. Predictors of new-onset decline in kidney function in a general middle-European population. *Nephrol Dial Transplant.* 2008;23(4):1265–1273.
93. Kronborg J, Solbu M, Njølstad I, et al. Predictors of change in estimated GFR: a population-based 7-year follow-up from the Tromso study. *Nephrol Dial Transplant.* 2008;23(9):2818–2826.
94. Astor BC, Matsushita K, Gansevoort RT, et al. Lower estimated glomerular filtration rate and higher albuminuria are associated with mortality and end-stage renal disease. A collaborative meta-analysis of kidney disease population cohorts. *Kidney Int.* 2011;79(12):1331–1340.
95. Newman DJ, Thakkar H, Medcalf EA, et al. Use of urine albumin measurement as a replacement for total protein. *Clin Nephrol.* 1995;43(2):104–109.
96. Ballantyne FC, Gibbons J, O'Reilly DS. Urine albumin should replace total protein for the assessment of glomerular proteinuria. *Ann Clin Biochem.* 1993;30(Pt 1):101–103.
97. Johnson DW, Jones GR, Mathew TH, et al. Chronic kidney disease and measurement of albuminuria or proteinuria: a position statement. *Med J Aust.* 2012;197(4):224–225.
98. Miller WG, Bruns DE, Hortin GL, et al. Current issues in measurement and reporting of urinary albumin excretion. *Ann Biol Clin (Paris).* 2010;68(1):9–25.
99. Goren MP, Li JT. The Coomassie Brilliant Blue method underestimates drug-induced tubular proteinuria. *Clin Chem.* 1986;32(2):386–388.
100. Gosling P. Proteinuria. In: Marshall WJ, Bangert SK, eds. *Clinical Biochemistry: Metabolic and Clinical Aspects.* 2nd ed. New York: Churchill Livingstone; 2008:156–174.
101. Wrong OM, Norden AG, Feest TG. Dent's disease; a familial proximal renal tubular syndrome with low-molecular-weight proteinuria, hypercalciuria, nephrocalcinosis, metabolic bone disease, progressive renal failure and a marked male predominance. *QJM.* 1994;87(8):473–493.
102. McTaggart MP, Stevens PE, Price CP. Investigation of apparent non-albuminuric proteinuria in a primary care population. *Clin Chem Lab Med.* 1961;51(10):2013.

103. Pesce AJ, Boreisha I, Pollak VE. Rapid differentiation of glomerular and tubular proteinuria by sodium dodecyl sulfate polyacrylamide gel electrophoresis. *Clin Chim Acta.* 1972;40(1):27–34.
104. Smith ER, Cai MM, McMahon LP, et al. The value of simultaneous measurements of urinary albumin and total protein in proteinuric patients. *Nephrol Dial Transplant.* 2012;27(4):1534–1541.
105. Marshall T, Williams KM. Extent of aminoglycoside interference in the pyrogallol red–molybdate protein assay depends on the concentration of sodium oxalate in the dye reagent. *Clin Chem.* 2004;50(5):934–935.
106. de Keijzer MH, Klasen IS, Branten AJ, et al. Infusion of plasma expanders may lead to unexpected results in urinary protein assays. *Scand J Clin Lab Invest.* 1999;59(2):133–137.
107. McIntyre NJ, Taal MW. How to measure proteinuria? *Curr Opin Nephrol Hypertens.* 2008;17(6):600–603.
108. Martin H. Laboratory measurement of urine albumin and urine total protein in screening for proteinuria in chronic kidney disease. *Clin Biochem Rev.* 2011;32(2):97–102.
109. Viswanathan G, Upadhyay A. Assessment of proteinuria. *Adv Chronic Kidney Dis.* 2011;18(4):243–248.
110. Candiano G, Musante L, Bruschi M, et al. Repetitive fragmentation products of albumin and alpha1-antitrypsin in glomerular diseases associated with nephrotic syndrome. *J Am Soc Nephrol.* 2006;17(11):3139–3148.
111. Sviridov D, Drake SK, Hortin GL. Reactivity of urinary albumin (microalbumin) assays with fragmented or modified albumin. *Clin Chem.* 2008;54(1):61–68.
112. Osicka TM, Houlihan CA, Chan JG, et al. Albuminuria in patients with type 1 diabetes is directly linked to changes in the lysosome-mediated degradation of albumin during renal passage. *Diabetes.* 2000;49(9):1579–1584.
113. Sviridov D, Meilinger B, Drake SK, et al. Coelution of other proteins with albumin during size-exclusion HPLC: implications for analysis of urinary albumin. *Clin Chem.* 2006;52(3):389–397.
114. Harmoinen A, Vuorinen P, Jokela H. Turbidimetric measurement of microalbuminuria. *Clin Chim Acta.* 1987;166(1):85–89.
115. Rowe DJ, Dawnay A, Watts GF. Microalbuminuria in diabetes mellitus: review and recommendations for the measurement of albumin in urine. *Ann Clin Biochem.* 1990;27(Pt 4):297–312.
116. Stamp RJ. Measurement of albumin in urine by end-point immunonephelometry. *Ann Clin Biochem.* 1988;25(Pt 4):442–443.
117. Comper WD, Osicka TM. Detection of urinary albumin. *Adv Chronic Kidney Dis.* 2005;12(2):170–176.
118. Naresh CN, Hayen A, Craig JC, et al. Day-to-day variability in spot urine protein-creatinine ratio measurements. *Am J Kidney Dis.* 2012;60(4):561–566.
119. Newman DJ, Pugia MJ, Lott JA, et al. Urinary protein and albumin excretion corrected by creatinine and specific gravity. *Clin Chim Acta.* 2000;294(1–2):139–155.
120. Bakker AJ. Detection of microalbuminuria. Receiver operating characteristic curve analysis favors albumin-to-creatinine ratio over albumin concentration. *Diabetes Care.* 1999;22(2):307–313.
121. Lemann J, Doumas BT. Proteinuria in health and disease assessed by measuring the urinary protein/creatinine ratio. *Clin Chem.* 1987;33(2 Pt 1):297–299.
122. Schwab SJ, Christensen RL, Dougherty K, et al. Quantitation of proteinuria by the use of protein-to-creatinine ratios in single urine samples. *Arch Intern Med.* 1987;147(5):943–944.
123. Ginsberg JM, Chang BS, Matarese RA, et al. Use of single voided urine samples to estimate quantitative proteinuria. *N Engl J Med.* 1983;309(25):1543–1546.
124. Ruggenenti P, Gaspari F, Perna A, et al. Cross sectional longitudinal study of spot morning urine protein:creatinine ratio, 24 hour urine protein excretion rate, glomerular filtration rate, and end stage renal failure in chronic renal disease in patients without diabetes. *BMJ.* 1998;316(7130):504–509.
125. Price CP, Newall RG, Boyd JC. Use of protein:creatinine ratio measurements on random urine samples for prediction of significant proteinuria: a systematic review. *Clin Chem.* 2005;51(9):1577–1586.
126. Antunes VV, Veronese FJ, Morales JV. Diagnostic accuracy of the protein/creatinine ratio in urine samples to estimate 24-h proteinuria in patients with primary glomerulopathies: a longitudinal study. *Nephrol Dial Transplant.* 2008;23(7):2242–2246.
127. Rodby RA, Rohde RD, Sharon Z, et al. The urine protein to creatinine ratio as a predictor of 24-hour urine protein excretion in type 1 diabetic patients with nephropathy. The Collaborative Study Group. *Am J Kidney Dis.* 1995;26(6):904–909.
128. Dyson EH, Will EJ, Davison AM, et al. Use of the urinary protein creatinine index to assess proteinuria in renal transplant patients. *Nephrol Dial Transplant.* 1992;7(5):450–452.
129. Steinhäuslin F, Wauters JP. Quantitation of proteinuria in kidney transplant patients: accuracy of the urinary protein/creatinine ratio. *Clin Nephrol.* 1995;43(2):110–115.
130. Zelmanovitz T, Gross JL, Oliveira JR, et al. The receiver operating characteristics curve in the evaluation of a random urine specimen as a screening test for diabetic nephropathy. *Diabetes Care.* 1997;20(4):516–519.
131. Younes N, Cleary PA, Steffes MW, et al. Comparison of urinary albumin-creatinine ratio and albumin excretion rate in the Diabetes Control and Complications Trial/Epidemiology of Diabetes Interventions and Complications Study. *Clin J Am Soc Nephrol.* 2010;5(7):1235–1242.
132. Houlihan CA, Tsalamandris C, Akdeniz A, et al. Albumin to creatinine ratio: a screening test with limitations. *Am J Kidney Dis.* 2002;39(6):1183–1189.
133. Vestergaard P, Leverett R. Constancy of urinary creatinine excretion. *J Lab Clin Med.* 1958;51(2):211–218.
134. Mattix HJ, Hsu CY, Shaykevich S, et al. Use of the albumin/creatinine ratio to detect microalbuminuria: implications of sex and race. *J Am Soc Nephrol.* 2002;13(4):1034–1039.
135. Methven S, MacGregor MS, Traynor JP, et al. Assessing proteinuria in chronic kidney disease: protein-creatinine ratio versus albumin-creatinine ratio. *Nephrol Dial Transplant.* 2010;25(9):2991–2996.
136. Heathcote KL, Wilson MP, Quest DW, et al. Prevalence and duration of exercise induced albuminuria in healthy people. *Clin Invest Med.* 2009;32(4):E261–E265.
137. Poortmans JR. Postexercise proteinuria in humans. Facts and mechanisms. *JAMA.* 1985;253(2):236–240.
138. Mogensen CE, Vittinghus E, Sølling K. Abnormal albumin excretion after two provocative renal tests in diabetes: physical exercise and lysine injection. *Kidney Int.* 1979;16(3):385–393.
139. Vittinghus E, Mogensen CE. Albumin excretion during physical exercise in diabetes. Studies on the effect of insulin treatment and of the renal haemodynamic response. *Acta Endocrinol Suppl (Copenh).* 1981;242:61–62.
140. Koh KH, Dayanath B, Doery JC, et al. Effect of exercise on albuminuria in people with diabetes. *Nephrology (Carlton).* 2011;16(8):704–709.
141. Carter JL, Tomson CR, Stevens PE, et al. Does urinary tract infection cause proteinuria or microalbuminuria? A systematic review. *Nephrol Dial Transplant.* 2006;21(11):3031–3037.
142. Robinson RR. Isolated proteinuria in asymptomatic patients. *Kidney Int.* 1980;18:395–406.
143. von Bonsdorff M, Koskenvuo K, Salmi HA, et al. Prevalence and causes of proteinuria in 20-year-old Finnish men. *Scand J Urol Nephrol.* 1981;15(3):285–290.
144. Springberg PD, Garrett LE, Thompson AL, et al. Fixed and reproducible orthostatic proteinuria: results of a 20-year follow-up study. *Ann Intern Med.* 1982;97(4):516–519.
145. Houser MT. Characterization of recumbent, ambulatory, and postexercise proteinuria in the adolescent. *Pediatr Res.* 1987;21(5):442–446.
146. Chachati A, von Frenckell R, Foidart-Willems J, et al. Variability of albumin excretion in insulin-dependent diabetics. *Diabet Med.* 1987;4(5):441–445.
147. Koopman MG, Krediet RT, Koomen GC, et al. Circadian rhythm of proteinuria: consequences of the use of urinary protein:creatinine ratios. *Nephrol Dial Transplant.* 1989;4(1):9–14.
148. Witte EC, Lambers Heerspink HJ, de Zeeuw D, et al. First morning voids are more reliable than spot urine samples to assess microalbuminuria. *J Am Soc Nephrol.* 2009;20(2):436–443.
149. Methven S, MacGregor MS, Traynor JP, et al. Comparison of urinary albumin and urinary total protein as predictors of patient outcomes in CKD. *Am J Kidney Dis.* 2011;57(1):21–28.
150. Gyure WL. Comparison of several methods for semiquantitative determination of urinary protein. *Clin Chem.* 1977;23(5):876–879.
151. Rumley A. Urine dipstick testing: comparison of results obtained by visual reading and with the Bayer CLINITEK 50. *Ann Clin Biochem.* 2000;37(Pt 2):220–221.
152. James GP, Bee DE, Fuller JB. Proteinuria: accuracy and precision of laboratory diagnosis by dip-stick analysis. *Clin Chem.* 1978;24(11):1934–1939.

153. Constantiner M, Sehgal AR, Humbert L, et al. A dipstick protein and specific gravity algorithm accurately predicts pathological proteinuria. *Am J Kidney Dis.* 2005;45(5):833–841.
154. Comper WD, Jerums G, Osicka TM. Deficiency in the detection of microalbuminuria by urinary dipstick in diabetic patients. *Diabetes Care.* 2003;26(11):3195–3196.
155. Tiu SC, Lee SS, Cheng MW. Comparison of six commercial techniques in the measurement of microalbuminuria in diabetic patients. *Diabetes Care.* 1993;16(4):616–620.
156. Pugia MJ, Lott JA, Profitt JA, et al. High-sensitivity dye binding assay for albumin in urine. *J Clin Lab Anal.* 1999;13(4):180–187.
157. Sawicki PT, Heinemann L, Berger M. Comparison of methods for determination of microalbuminuria in diabetic patients. *Diabet Med.* 1989;6(5):412–415.
158. Marshall SM. Screening for microalbuminuria: which measurement? *Diabet Med.* 1991;8(8):706–711.
159. Bangstad HJ, Try K, Dahl-Jørgensen K, et al. New semiquantitative dipstick test for microalbuminuria. *Diabetes Care.* 1991;14(11):1094–1097.
160. Minetti EE, Cozzi MG, Granata S, et al. Accuracy of the urinary albumin titrator stick 'Micral-Test' in kidney-disease patients. *Nephrol Dial Transplant.* 1997;12(1):78–80.
161. Poulsen PL, Hansen B, Amby T, et al. Evaluation of a dipstick test for microalbuminuria in three different clinical settings, including the correlation with urinary albumin excretion rate. *Diabete Metab.* 1992;18(5):395–400.
162. Tai J, Tze WJ. Evaluation of Micro-Bumintest reagent tablets for screening of microalbuminuria. *Diabetes Res Clin Pract.* 1990;9(2):137–142.
163. Graziani MS, Gambaro G, Mantovani L, et al. Diagnostic accuracy of a reagent strip for assessing urinary albumin excretion in the general population. *Nephrol Dial Transplant.* 2009;24(5):1490–1494.
164. Parsons M, Newman DJ, Pugia M, et al. Performance of a reagent strip device for quantitation of the urine albumin:creatinine ratio in a point of care setting. *Clin Nephrol.* 1999;51(4):220–227.
165. Iseki K, Kinjo K, Iseki C, et al. Relationship between predicted creatinine clearance and proteinuria and the risk of developing ESRD in Okinawa, Japan. *Am J Kidney Dis.* 2004;44(5):806–814.
166. Craig JC, Barratt A, Cumming R, et al. Feasibility study of the early detection and treatment of renal disease by mass screening. *Intern Med J.* 2002;32(1–2):6–14.
167. Boulware LE, Jaar BG, Tarver-Carr ME, et al. Screening for proteinuria in US adults: a cost-effectiveness analysis. *JAMA.* 2003;290(23):3101–3114.
168. Samal L, Linder JA. The primary care perspective on routine urine dipstick screening to identify patients with albuminuria. *Clin J Am Soc Nephrol.* 2013;8(1):131–135.
169. Lachs MS, Nachamkin I, Edelstein PH, et al. Spectrum bias in the evaluation of diagnostic tests: lessons from the rapid dipstick test for urinary tract infection. *Ann Intern Med.* 1992;117(2):135–140.
170. Mulherin SA, Miller WC. Spectrum bias or spectrum effect? Subgroup variation in diagnostic test evaluation. *Ann Intern Med.* 2002;137(7):598–602.
171. White SL, Yu R, Craig JC, et al. Diagnostic accuracy of urine dipsticks for detection of albuminuria in the general community. *Am J Kidney Dis.* 2011;58(1):19–28.
172. Cho BS, Kim SD. School urinalysis screening in Korea. *Nephrology (Carlton).* 2007;12(suppl 3):S3–S7.
173. Yap HK, Quek CM, Shen Q, et al. Role of urinary screening programmes in children in the prevention of chronic kidney disease. *Ann Acad Med Singapore.* 2005;34(1):3–7.
174. Kitagawa T. Lessons learned from the Japanese nephritis screening study. *Pediatr Nephrol.* 1988;2(2):256–263.
175. Palmer AJ, Valentine WJ, Chen R, et al. A health economic analysis of screening and optimal treatment of nephropathy in patients with type 2 diabetes and hypertension in the USA. *Nephrol Dial Transplant.* 2008;23(4):1216–1223.
176. Johnson DW. Evidence-based guide to slowing the progression of early renal insufficiency. *Intern Med J.* 2004;34(1–2):50–57.
177. Bennett PH, Haffner S, Kasiske BL, et al. Screening and management of microalbuminuria in patients with diabetes mellitus: recommendations to the Scientific Advisory Board of the National Kidney Foundation from an ad hoc committee of the Council on Diabetes Mellitus of the National Kidney Foundation. *Am J Kidney Dis.* 1995;25(1):107–112.
178. Levin A, Hemmelgarn B, Culleton B, et al. Guidelines for the management of chronic kidney disease. *CMAJ.* 2008;179(11):1154–1162.
179. Johnson DW. Global proteinuria guidelines: are we nearly there yet? *Clin Biochem Rev.* 2011;32(2):89–95.
180. Le Floch JP, Marre M, Rodier M, et al. Interest of CLINITEK microalbumin in screening for microalbuminuria: results of a multicentre study in 302 diabetic patients. *Diabetes Metab.* 2001;27(1):36–39.
181. Croal BL, Mutch WJ, Clark BM, et al. The clinical application of a urine albumin:creatinine ratio point-of-care device. *Clin Chim Acta.* 2001;307(1–2):15–21.
182. Meinhardt U, Ammann RA, Flück C, et al. Microalbuminuria in diabetes mellitus: efficacy of a new screening method in comparison with timed overnight urine collection. *J Diabetes Complications.* 2003;17(5):254–257.
183. Guy M, Newall R, Borzomato J, et al. Diagnostic accuracy of the urinary albumin:creatinine ratio determined by the CLINITEK microalbumin and DCA 2000+ for the rule-out of albuminuria in chronic kidney disease. *Clin Chim Acta.* 2009;399(1–2):54–58.
184. Côté AM, Brown MA, Lam E, et al. Diagnostic accuracy of urinary spot protein:creatinine ratio for proteinuria in hypertensive pregnant women: systematic review. *BMJ.* 2008;336(7651):1003–1006.
185. Morris RK, Riley RD, Doug M, et al. Diagnostic accuracy of spot urinary protein and albumin to creatinine ratios for detection of significant proteinuria or adverse pregnancy outcome in patients with suspected pre-eclampsia: systematic review and meta-analysis. *BMJ.* 2012;345:e4342.
186. Hogg RJ, Portman RJ, Milliner D, et al. Evaluation and management of proteinuria and nephrotic syndrome in children: recommendations from a pediatric nephrology panel established at the National Kidney Foundation Conference on proteinuria, albuminuria, risk, assessment, detection, and elimination (PARADE). *Pediatrics.* 2000;105(6):1242–1249.
187. Houser M. Assessment of proteinuria using random urine samples. *J Pediatr.* 1984;104(6):845–848.
188. Wingen AM, Fabian-Bach C, Schaefer F, et al. Randomised multicentre study of a low-protein diet on the progression of chronic renal failure in children. European Study Group of Nutritional Treatment of Chronic Renal Failure in Childhood. *Lancet.* 1997; 349(9059):1117–1123.
189. Ardissino G, Testa S, Daccò V, et al. Proteinuria as a predictor of disease progression in children with hypodysplastic nephropathy. Data from the ItalKid Project. *Pediatr Nephrol.* 2004;19(2):172–177.
190. Wong CS, Pierce CB, Cole SR, et al. Association of proteinuria with race, cause of chronic kidney disease, and glomerular filtration rate in the chronic kidney disease in children study. *Clin J Am Soc Nephrol.* 2009;4(4):812–819.
191. Tsioufis C, Mazaraki A, Dimitriadis K, et al. Microalbuminuria in the paediatric age: current knowledge and emerging questions. *Acta Paediatr.* 2011;100(9):1180–1184.
192. Flynn JT. Microalbuminuria in children with primary hypertension. *J Clin Hypertens.* 2016;18(10):962–965.
193. Knoll GA. Proteinuria in kidney transplant recipients: prevalence, prognosis, and evidence-based management. *Am J Kidney Dis.* 2009;54(6):1131–1144.
194. Nauta FL, Bakker SJ, van Oeveren W, et al. Albuminuria, proteinuria, and novel urine biomarkers as predictors of long-term allograft outcomes in kidney transplant recipients. *Am J Kidney Dis.* 2011;57(5):733–743.
195. Panek R, Lawen T, Kiberd BA. Screening for proteinuria in kidney transplant recipients. *Nephrol Dial Transplant.* 2011;26(4):1385–1387.
196. Fogazzi GB, Cameron JS, Ritz E, et al. The history of urinary microscopy to the end of the 19th century. *Am J Nephrol.* 1994;14(4–6):452–457.
197. Bottini PV, Lauand JR, Lara Cioffi SG, et al. Glomerular and nonglomerular haematuria: preservation of urine sediment. *Lab Med.* 2005;36(10):3.
198. Kouri TT, Gant VA, Fogazzi GB, et al. Towards European urinalysis guidelines. Introduction of a project under European Confederation of Laboratory Medicine. *Clin Chim Acta.* 2000;297(1–2):305–311.
199. Cohen RA, Brown RS. Clinical practice. Microscopic hematuria. *N Engl J Med.* 2003;348(23):2330–2338.
200. Vivante A, Afek A, Frenkel-Nir Y, et al. Persistent asymptomatic isolated microscopic hematuria in Israeli adolescents and young adults and risk for end-stage renal disease. *JAMA.* 2011;306(7): 729–736.
201. Offringa M, Benbassat J. The value of urinary red cell shape in the diagnosis of glomerular and post-glomerular haematuria. A meta-analysis. *Postgrad Med J.* 1992;68(802):648–654.

202. Brodsky SV, Nadasdy T, Rovin BH, et al. Warfarin-related nephropathy occurs in patients with and without chronic kidney disease and is associated with an increased mortality rate. *Kidney Int.* 2011;80(2):181–189.
203. Mishriki SF, Aboumarzouk O, Vint R, et al. Routine urine cytology has no role in hematuria investigations. *J Urol.* 2013;189(4):1255–1258.
204. Wald R, Bell CM, Nisenbaum R, et al. Interobserver reliability of urine sediment interpretation. *Clin J Am Soc Nephrol.* 2009;4(3):567–571.

BOARD REVIEW QUESTIONS

1. A 66-year-old Caucasian male presented to the renal clinic for 6-month follow-up of his known diabetic nephropathy. His baseline creatinine is 180 µmol/L with an estimated glomerular filtration rate (GFR) of 40 mL/min/1.73 m^2. The trajectory of renal function decline with regard to his estimated GFR (eGFR) has been 2–4 mL/min/1.73 m^2 over the past 4 years. He has had a slowly rising urine albumin-to-creatinine ratio (uACR) and his most recent uACR was 150 mg/mmol. Today, he reports a 2-month history of fatigue, anorexia, and unintentional weight loss of 5–6 kg. Physical examination revealed pulse rate of 80 beats/min and regular blood pressure (140/80 mm Hg), oxygen saturation 95% on room air, clear chest, 1+ pedal edema, and mild pallor.
   Laboratory investigations for this clinical visit are as follows: Hemoglobin (Hb) 103 g/dL, white cell count 8.2 ($\times 10^{32}$/L), platelets 230 ($\times 10^{32}$/L), creatinine 370 µmol/L, urea 18 mmol/L, eGFR 20 mL/min/1.73 m^2, K 5.7 mmol/L, Na 137 mmol/L, HCO_3 (bicarbonate) 20 mmol/L, glucose 7.5 mmol/L, and serum albumin 32 g/L. Urinalysis showed 2+ protein and 3+ red blood cells. Urine microscopy revealed a few red cell casts. Which of these is the most appropriate response with regard to this man's condition?
   a. This is most likely a laboratory error; repeat blood work should be organized.
   b. He has lost a significant amount of weight in the recent past, which has resulted in a rise in creatinine.
   c. He has evidence of significant acute kidney injury and needs further investigation.
   d. This is the natural progression of his underlying diabetic nephropathy.
   e. All of the above.
   Answer: c
   Rationale: This patient's history and clinical features suggest acute kidney injury. His subacute onset of symptoms with the recent rise in creatinine, active urine sediment, and presence of red cell casts on urine microscopy strongly suggest the diagnosis of a rapidly progressive glomerulonephritis and he warrants further investigation and management of this condition. Although diabetic nephropathy can rarely progress rapidly, it would be unusual to develop red cell casts in the urine. The weight loss and catabolic state should lead to a decrease in serum creatinine rather than an increase. This result is unlikely to be a laboratory error, especially in the setting of his symptoms, and further investigation and management should not be delayed.

2. A 73-year-old woman was referred to the clinic for evaluation of worsening renal function and anemia. Review of her laboratory tests showed hemoglobin (Hb) 80 g/dL (110 g/dL 1 year ago), creatinine 180 µmol/L (80 µmol/L 1 year ago), urea 15 mmol/L, K 4.6 mmol/L, Na 132 mmol/L, calcium 2.7 mmol/L. Her serum protein electrophoresis showed a monoclonal spike in the gamma region. A diagnosis of multiple myeloma is suspected. An office urine dipstick shows 1+ protein, no red cells, no leukocytes, or glucose. Which of the following statements is true with regard to the urine dipstick result?
   a. The urine dipstick reliably detects albumin but not other proteins such as monoclonal proteins which cause cast nephropathy.
   b. The urine dipstick is a sensitive marker for tubular and overflow proteinuria.
   c. A positive result from a semiquantitative test, such as a urinary dipstick test, should prompt further evaluation with a quantitative test.
   d. Both a and b.
   e. Both a and c.
   Answer: e
   Rationale: This patient has multiple myeloma as evidenced by her history and laboratory findings. Her renal function is impaired, suggesting renal involvement. The urine dipstick shows minimal proteinuria but this test only reliably detects albumin and not other proteins; hence, although it can detect glomerular proteinuria, it is a poor test to assess for tubular and overflow proteinuria. A quantitative test including an albumin-to-creatinine ratio (uACR) and a protein-to-creatinine ratio (uPCR) should be requested. In the case of cast nephropathy, one would expect a significant discrepancy in these values with a higher uPCR as compared with the uACR, suggesting that there is excretion of an alternate protein other than albumin (in this case, light chains).

3. Which of the following statements holds true with regard to estimated glomerular filtration rate (eGFR)?
   a. The Modification of Diet in Renal Disease (MDRD) study equation is the most commonly used method of determining eGFR and is more accurate than the Chronic Kidney Disease Epidemiology Collaboration (CKD-EPI) equation.
   b. The Cockcroft–Gault (CG) equation remains the most accurate method of determining drug dosing in patients with impaired kidney function.
   c. The CKD-EPI equation is more accurate than the MDRD study equation and is commonly used to determine eGFR.
   d. The Berlin Initiative Study group equation can be accurately used to determine estimated glomerular filtration rate (eGFR) for all age groups.
   Answer: c
   Rationale: The most commonly used methods include the CG equation, the MDRD study equation, and now most recently the CKD-EPI equation. The CKD-EPI equation is more accurate than the MDRD equation, especially at higher glomerular filtration rates (GFRs), and both are more accurate than the CG equation. The latter has not been validated since the adoption of new assay methods for estimation of creatinine and should ideally not be used to determine drug dosing as there is especially a risk of overdosing drugs that have a narrow therapeutic index, with the CG equation being less reliable in assessing the risk of kidney injury. The Berlin Initiative Study equation was used to determine eGFR in the elderly population, and the Full Age Spectrum equation has been used to determine eGFR across all age groups.

4. A 59-year-old man presents to the emergency room with a large-volume upper gastrointestinal (GI) bleed. His

medical history is significant for hypertension and a recent myocardial infarction for which he required percutaneous coronary intervention to the left anterior descending artery. His medications include aspirin (100 mg daily), clopidogrel (75 mg daily), atorvastatin (40 mg daily), ramipril (10 mg daily), and atenolol (25 mg daily). His blood pressure on arrival was 90/60 mm Hg and he was resuscitated with intravenous fluids and packed red blood cells. He is awaiting a gastroscopy. Laboratory investigations showed hemoglobin (Hb) 75 g/dL (baseline 110 g/dL), white cell count 9.8 ($\times 10^{32}$/L), platelets 200 ($\times 10^{32}$/L), normal international normalized ratio and partial thromboplastin time, sodium 135 mmol/L, potassium 3.8 mmol/L, urea 30 mmol/L, creatinine 120 μmol/L (baseline creatinine 100 μmol/L), and estimated glomerular filtration rate (eGFR) 50 mL/min/1.73 m^2. Which of the following holds true with regard to his renal function tests?

a. This patient has acute kidney injury as evidenced by the rise in urea.
b. This patient has acute kidney injury as evidenced by the decline in eGFR.
c. Urea is a poor marker of filtration as in this case it is influenced by upper GI bleeding.
d. Creatinine is an ideal filtration marker as it is freely filtered but not secreted from the renal tubules.
e. All of the above.

Answer: c

Rationale: Urea is not an accurate filtration marker because it is subject to a number of influences in addition to glomerular filtration. Increased plasma levels may be due to factors independent of renal function and in this case, the elevated urea is due to gastrointestinal bleeding leading to absorption of amino acids from blood in the gastrointestinal tract. Urea and eGFR are not appropriate to diagnose kidney injury in the acute setting. Creatinine is freely filtered by the kidney but is also secreted by the renal tubules and hence, it is not an ideal filtration marker.

24 Interpretation of Electrolyte and Acid-Base Parameters in Blood and Urine

Kamel S. Kamel | Mitchell L. Halperin

CHAPTER OUTLINE

An analysis of laboratory data from samples of blood and urine is essential to make accurate diagnoses and to design optimal therapy for patients with disturbances of water, sodium (Na^+), potassium (K^+), and acid-base homeostasis.[1] Our clinical approach and interpretation of these tests rely heavily on an understanding of the basic concepts of the physiology of the renal regulation of water, electrolyte, and acid-base homeostasis. Hence, each section in this chapter begins with a discussion of physiologic concepts that help focus on the important factor(s) in the regulation of the homeostasis of the substances in question.

Based on this understanding of physiology, we discuss the laboratory data used to help determine the underlying pathophysiology of the disturbance. This information is then used to construct our approach to patients with each of these disorders. At the end of each section, clinical cases are presented succinctly to illustrate how this approach is used at the bedside.

We emphasize that there are no normal values for the urinary excretion of water and electrolytes because subjects in the steady state excrete all ions that are consumed and not lost by nonrenal routes. Hence, data should be interpreted in the context of the prevailing stimulus and the expected renal response.

WATER AND SODIUM

In this section, we illustrate how we use information about the volume and composition of the urine in the clinical approach to patients with disorders causing polyuria, those causing a decreased effective arterial blood volume (EABV), and those causing hyponatremia.

POLYURIA

There are two definitions of polyuria. The conventional definition of polyuria is a urine volume that is more than 2.5 L/day. This is an arbitrary definition based on comparing the 24-hour urine volume in the patient with the usual values of 24-hour urine volumes observed in individuals who consume a typical Western diet.

We prefer a physiology-based definition. Polyuria is present if the urine flow rate is higher than what is expected in a specific setting. In the presence of vasopressin action, urine volume is determined by the rate of excretion of effective osmoles and the effective osmolality of the medullary interstitial compartment. Hence, polyuria is present if the urine volume is higher than what is expected for the rate of excretion of effective osmoles, even if the urine volume does not exceed 2.5 L/day. In contrast, if the concentration of Na^+ in plasma (P_{Na}) is less than 135 mmol/L, the release of vasopressin should be inhibited, and the urine flow rate could be as high as 10 to 15 mL/min in an adult subject (which extrapolates to around 14 to 22 L/day). A lower urine volume in this setting, although still higher than 2.5 L/day, represents oliguria and not polyuria.

There are two categories of polyuria, a water diuresis and an osmotic diuresis.

WATER DIURESIS

Concept 1

To move water across a membrane, there must be a channel that allows water to cross that membrane (an aquaporin [AQP]) and a driving force for the movement of water—a difference in the concentrations of effective osmoles or a difference in the hydrostatic pressures across that membrane.

Water Channels. There are two critically important aquaporin water channels in the luminal membranes of cells in the kidney, AQP1 and AQP2 (Fig. 24.1). AQP1 channels are nonregulated water channels that are constitutively present in the luminal membrane of proximal tubule (PT) cells. AQP1 channels are also constitutively present in the luminal membrane of the descending thin limbs of the loop of Henle

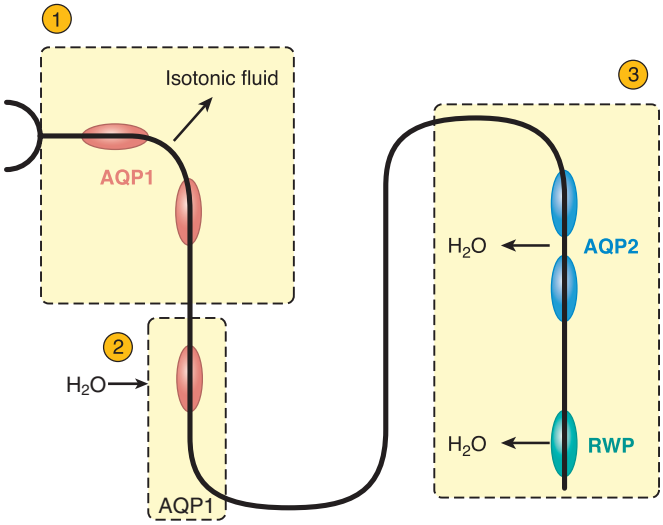

Fig. 24.1 Functional units of the nephron based on presence of aquaporins AQP1 and AQP2. The *solid line* represents a nephron; AQP1 is represented as a *small pink ovals* and AQP2 as *blue ovals*. With regard to water excretion, we divide the nephron into three functional units (delineated by rectangles with dashed lines) on the basis of the presence of AQP1 or AQP2. AQP1 is always present in the proximal tubule cells—the first functional nephron unit **(1)**. AQP1 is also present in the descending thin limb of the loop of Henle (DtL) of the juxtamedullary nephrons, which constitute about 15% of the total nephrons—the second functional nephron unit **(2)**. Vasopressin causes the insertion of AQP2 into the luminal membrane of principal cells in the cortical collecting duct (CCD) and the medullary collecting duct (MCD); together, these nephron segments constitute the final or third functional unit **(3)**. Even in the absence of vasopressin, there seems to be a small degree of water permeability in the inner MCD, which is called residual water permeability (RWP). (Modified from Halperin ML, Kamel KS, Goldstein MB. *Fluid, Electrolyte, and Acid-Base Physiology; A Problem-Based Approach.* ed 4. Philadelphia: Elsevier; 2012.)

(DtLs) of the juxtamedullary nephrons, which constitute about 15% of the total number of nephrons. Of note, AQP1 channels are not present in the luminal membrane of the DtLs of the superficial nephrons; thus, the entire loop of Henle of these nephrons (i.e., 85% of all the nephrons) is relatively impermeable to water.[2]

Vasopressin causes the insertion of AQP2 channels into the luminal membrane of principal cells in the cortical collecting duct (CCD), and the medullary collecting duct (MCD). Notwithstanding, even in the absence of vasopressin action, there seems to be a small degree of water permeability in the inner MCD, called basal or residual water permeability (RWP).

Driving Force. Water is drawn from a compartment with a lower effective osmolality to one with a higher effective osmolality. Effective osmoles are osmoles that have a difference in their concentrations between two compartments. The magnitude of this driving force could be very large, because a difference of 1 mOsmol/kg H_2O generates a pressure of 19.3 mm Hg. Vasopressin causes the insertion of AQP2 in the luminal membrane of principal cells in the CCD and MCD. Hence, as soon as water reaches a nephron segment that has AQP2 in the luminal membrane of its cells, water will be reabsorbed until the effective osmolality in the luminal fluid is nearly equal to the effective osmolality in the surrounding interstitial fluid compartment.

Because vasopressin causes the insertion of urea transporters in the luminal membrane of cells in the inner MCD, the concentration of urea in the interstitial fluid in the inner medulla becomes nearly equal to its concentration in the lumen in the inner MCD. Hence, at the usual rate of urea excretion, which does not exceed the transport capacity of the urea transporters, urea is not an effective urine osmole (i.e., the excretion of urea does not obligate the excretion of H_2O).

Concept 2

The urine volume during a water diuresis is determined by the volume of distal delivery of filtrate and the volume of filtrate that is reabsorbed in the inner MCD via its RWP.[3]

Distal Delivery of Filtrate. The volume of distal delivery of filtrate is the volume of glomerular filtration minus the volume of filtrate that is reabsorbed in the nephron segments prior to the CCD. There are data to suggest that AQP1 channels are not present in the luminal membranes of the DtLs of the superficial nephrons, which constitute 85% of the total number of nephrons.[2] If that is the case, then the entire loop of Henle of most of the nephrons is impermeable to water. Hence, the volume of distal delivery of filtrate should be approximately equal to the volume of glomerular filtration minus the volume that is reabsorbed by PT.

It was thought that about 66% of the glomerular filtration rate (GFR) is reabsorbed along the entire PT. This was based on the measured ratio of the concentration of inulin in fluid samples obtained from the lumen of the PT (TF) and its concentration in simultaneous plasma (P) samples—$(TF/P)_{inulin}$—in micropuncture studies in rats. Because inulin is freely filtered at the glomerulus and is not reabsorbed or secreted in the PT, a $(TF/P)_{inulin}$ value of around 3 has suggested that approximately 66% of the filtrate is reabsorbed in the PT. However, these micropuncture measurements underestimate the volume of fluid that is actually reabsorbed in the PT because these measurements were made at the last accessible portion of the PT at the surface of the renal cortex, and hence did not take into account that additional volume may be reabsorbed in the deeper part of the PT, including its pars recta portion.

If the entire loop of Henle of most nephrons can be assumed to lack AQP1 and thereby be largely impermeable to water, the volume of filtrate that enters the loop of Henle can be deduced from the minimum value for the $(TF/P)_{inulin}$ obtained using the micropuncture technique from the early distal convoluted tubule (DCT), which has been done in rats. Because this value is around 6, a reasonable estimate of the proportion of filtrate that is reabsorbed in the rat PTs is close to five-sixths (83%). This value is close to the estimate of fractional reabsorption in the PT obtained with measurement of lithium clearance, which is thought to be a marker for fractional reabsorption in PT in human subjects.

If these findings can be extrapolated to humans with GFR values of 180 L/day, only about 30 L of filtrate/day (180 ÷ 6) would be delivered to the early DCT if all nephrons were superficial nephrons. This value of the volume of filtrate delivered to the DCT needs to be adjusted downward because juxtamedullary nephrons have AQP1 along their DtLs and,

hence, are permeable to water. If these nephrons constitute 15% of the total number of nephrons and therefore receive 27 L of glomerular filtrate/day (15% of 180 L/day), and if five-sixths of the glomerular filtrate of these nephrons is reabsorbed along their PTs, around 4.5 L/ day reach their DtLs. Because the interstitial osmolality rises threefold (from 300 to 900 mOsmol/kg H_2O) in the outer medulla, two-thirds, or 3 L of the 4.5 L/day, are reabsorbed in the DtLs of these nephrons. Therefore, the volume of filtrate delivered to DCTs is likely to be around 27 L/day (around 30 L/day exit the PTs minus around 3 L/day that are reabsorbed in DtLs of the juxtamedullary nephrons).

Residual Water Permeability. There are two pathways for transport of water in the inner MCD, a vasopressin-responsive system via AQP2 and a vasopressin-independent system, RWP. Two factors may affect the volume of water reabsorbed via RWP. First, the driving force is the enormous difference in osmotic pressure between the luminal and interstitial fluid compartments in the inner MCD during a water diuresis. Second, the contraction of the renal pelvis, because each time the renal pelvis contracts, some of the fluid in the renal pelvis travels in a retrograde direction up toward the inner MCD, and some of that fluid may be reabsorbed via RWP after it reenters the inner MCD for a second (or maybe a third) time.

As calculated above, around 27 L/day are delivered to the distal nephron in a normal subject. The observed urine flow rate during maximum water diuresis is around 10 to 15 mL/min (around 14–22 L/day). If this maximum water diuresis could be maintained for 24 hours, then somewhat more than 5 L of water would be reabsorbed per day in the inner MCD via its RWP during water diuresis.

Concept 3

Another component of the physiology of water diuresis is the formation of electrolyte-free water. This process of desalination occurs in nephron segments that can reabsorb Na^+ but are impermeable to water because they lack AQPs (i.e., the cortical and medullary thick ascending limbs (TALs) of the loop of Henle and the DCT).

Regulation of the reabsorption of Na^+ and Cl^- in the medullary TAL (mTAL) seems to occur via dilution of the concentration of an inhibitor of this process in the medullary interstitial compartment (possibly ionized calcium) by water reabsorption from the water-permeable nephron segments in the renal medulla (i.e., the MCD and DtLs of the juxtamedullary nephrons).[4] During water diuresis, reabsorption of H_2O in inner MCD via its RWP may serve the purpose of diluting the concentration of this inhibitor of the reabsorption of Na^+ and Cl^- in the mTAL, hence allowing desalination of the luminal fluid and the formation of electrolyte-free water to occur in this nephron segment.

Tools for Assessing Water Diuresis

Urine Flow Rate. The observed urine flow rate during peak water diuresis in normal adult subjects is around 10 to 15 mL/min (extrapolated to around 14–22 L/day). Notwithstanding, this high urine flow rate will not be sustained because the volume of distal delivery of filtrate will ultimately fall.

The urine flow rate declines when desmopressin (DDAVP) is given to a patient with central diabetes insipidus (DI). The urine flow rate, however, will be higher than that observed in response to DDAVP in a normal subject who consumes a typical Western diet. The reason is that the medullary interstitial osmolality is likely to be lower owing to a prior medullary washout during the water diuresis.

Osmole Excretion Rate. The osmole excretion rate is equal to the product of the urine osmolality (U_{osm}) and the urine flow rate (see Eq. 24.1). In subjects eating a typical Western diet, the rate of excretion of osmoles is 600 to 900 mOsmol/day, with electrolytes and urea each accounting for close to half of the total urine osmoles. During a water diuresis due to the absence of vasopressin action, the rate of excretion of osmoles does not directly affect the urine volume because AQP2 are not present in the luminal membrane of principal cells in the CCD and MCD. Nevertheless, the rate of excretion of osmoles must be calculated in the patient with a water diuresis because, if high, polyuria due to an osmotic diuresis may be unmasked after there is a renal response to the administration of DDAVP.

$$\text{Osmole excretion rate} = U_{osm} \times \text{urine flow} \quad (24.1)$$

Urine Osmolality. The U_{osm} is equal to the number of excreted osmoles divided by the urine volume. Therefore during a water diuresis, a change in the U_{osm} could reflect a change in the osmole excretion rate and/or in the volume of filtrate delivered to the distal nephron, which is the major factor that determines the urine volume during a water diuresis. For example, if the rate of excretion of osmoles is 800 mOsmol/day, the U_{osm} will be 50 mOsmol/kg H_2O if the 24-hour urine volume is 16 L and 100 mOsmol/kg H_2O if the 24-hour urine volume is 8 L. This higher urine osmolality does not reflect a better urine concentrating ability, but a lower volume of distal delivery of filtrate.

Electrolyte-Free Water Balance. Tonicity is a term used to describe the effective osmolality of a solution. For plasma water, this can be approximated (in the absence of hyperglycemia) by the total concentration of cations ($Na^+ + K^+$) and their accompanying anions. The basis of the calculation of electrolyte-free water balance is the determination of how much water needs to be added to or subtracted from a solution with a given total amount of $Na^+ + K^+$ to make its tonicity equal to the normal plasma tonicity—that is, 150 mmol of cations plus an equal concentration of anions in 1 L of water. This calculation is used to determine the basis of a change in plasma Na^+ concentration (P_{Na}), and the appropriate therapy to achieve normonatremia. To calculate the electrolyte-free water balance, one must know the volume and concentrations of $Na^+ + K^+$ in the input and the output (mainly the urine).

For example, consider a patient who receives 3 L of 0.9% saline (Na^+ concentration = 150 mmol/L) and excretes 3 L of urine with a concentration of $Na^+ + K^+$ of 50 mmol/L. There is no electrolyte-free water in the input because it has the same tonicity as the plasma water (150 mmol/L cations, plus an equal concentration of anions). With regard to the output, this patient excreted the equivalent of 1 L of isotonic salt solution and 2 L of electrolyte-free water. Hence, the patient has a negative electrolyte-free water balance of 2 L, and the P_{Na} would be expected to rise. Another patient receives 3 L of 0.9% saline but excretes 3 L of urine with a concentration of $Na^+ + K^+$ of 200 mmol/L. As in the first example,

Table 24.1 Comparison of a Tonicity Balance and Electrolyte-Free Water Balance in a Patient With Hypernatremia[a]

Parameter	$Na^+ + K^+$ (mmol)	Water (L)	Electrolyte-Free Water Balance (L)
Infusion of 3 L of Isotonic Saline			
• Input	450	3	0
• Output	150	3	2
• **Balance**	**+300**	**0**	**–2**
Infusion of 4 L of Isotonic Saline			
• Input	600	4	0
• Output	150	3	2
• **Balance**	**+450**	**+1**	**–2**
No Intravenous Fluid Infusion			
• Input	0	0	0
• Output	150	3	2
• **Balance**	**–150**	**–3**	**–2**

[a]Three case examples are described, in each patient the P_{Na} rose from 140 to 150 mmol/L. In all three examples, the urine volume was 3 L with a concentration of $Na^+ + K^+$ of 50 mmol/L. The only difference is the volume of isotonic saline infused in each case example. Note that although the balances for $Na^+ + K^+$ and for water are very different in these three examples, the calculation of electrolyte-free water balance shows a negative balance of 2 L in all of them. Calculation of tonicity balance however, reveals that the patient in the first example has a positive balance of 300 mmol of $Na^+ + K^+$, while the patient in the second example has a positive balance of 450 mmol of $Na^+ + K^+$ and a positive balance of 1 L of water, and the patient in the third example has a negative balance of 150 mmol of $Na^+ + K^+$ and a negative balance of 3 L of water. The goals for therapy—to correct the hypernatremia and to return the volume and composition of the extracellular and intracellular fluid compartments to their normal values—are clear only after a tonicity balance is calculated.

there is no electrolyte-free water in the input. With regard to the output, because this patient would have needed to excrete 4 L (and not 3 L) of urine to make this total of 600 mmol of $Na^+ + K^+$ (with 600 mmol of accompanying anions) into an isotonic solution, the patient has a positive electrolyte-free water balance of 1 L; hence, the P_{Na} will fall (i.e., 1 L of body water lost 150 mmol of $Na^+ + K^+$ with 150 mmol of accompanying anions and hence, became 1 L electrolyte-free water). Calculation of the electrolyte-free water balance however, although it correctly predicts the change in P_{Na}, does not reveal whether its basis is a change in water balance or in fact a change in $Na^+ + K^+$ balance. An example of this is shown in Table 24.1. Although the balances for $Na^+ + K^+$ and for water are very different in the three examples used, calculation of the electrolyte-free water balance provided the same answer in all of them, a negative balance of 2 L of electrolyte-free water. Hence, calculation of the electrolyte-free water balance is not helpful to design the therapy needed to return the volume and composition of the extracellular fluid (ECF) and intracellular fluid (ICF) compartments to their normal values.

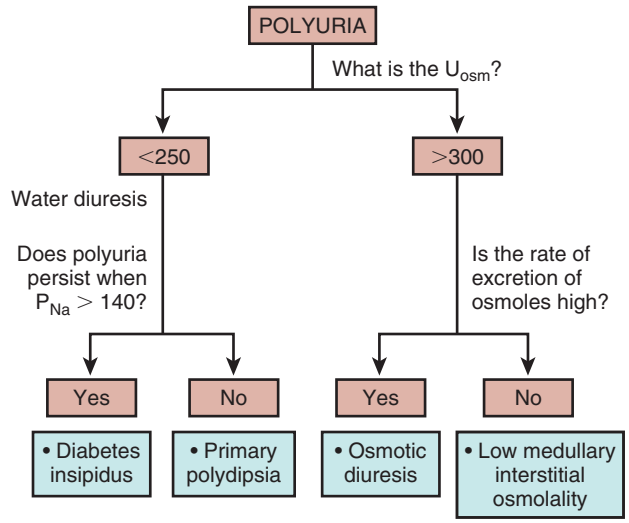

Flow Chart 24.1 (From Kamel KS, Halperin ML. *Fluid, Electrolyte, and Acid-Base Physiology; A Problem-Based Approach.* ed 5. Philadelphia: Elsevier; 2017.)

Tonicity Balance. To determine the basis for a change in the P_{Na} and to define the proper therapy to return the volume and composition of the ECF and ICF compartments to their normal values, we calculate the tonicity balance. A tonicity balance refers to the balance of water and the balance of electrolytes that determine body tonicity (i.e., $Na^+ + K^+$).[5] To calculate a tonicity balance, one must examine the input and output volumes and the quantity of Na^+ and K^+ infused and the quantity of $Na^+ + K^+$ excreted over the time period during which the P_{Na} changed (see Table 24.1). In practical terms, a tonicity balance can be calculated only in a hospital setting, where inputs and outputs are accurately recorded. In a febrile patient, balance calculations will not be as accurate because sweat losses are not measured. Nevertheless, restricting analysis of the output to the urine data would be sufficient in an acute setting if the changes in P_{Na} occurred over a relatively short period of time.

Even if measurements of the concentrations of Na^+ and K^+ in the urine are not available, if the P_{Na} at the beginning and end of a certain period, volume of the urine, and volume and amount of $Na^+ + K^+$ in the fluid infused during that period are known, the clinician can use these data together with an estimation of total body water (TBW) to calculate the quantity of $Na^+ + K^+$ excreted in the urine. Hence, the basis for the change in P_{Na} can be determined.

CLINICAL APPROACH TO THE PATIENT WITH POLYURIA

The steps to take to determine the diagnosis in a patient with polyuria are outlined in Flow Charts 24.1 and 24.2.

Step 1: What Is the Urine Osmolality?

A value of the U_{osm} that is less than 250 mOsmol/kg H_2O indicates that the polyuria is due to a water diuresis. If the P_{Na} is less than 135 mmol/L, the polyuria is due to primary polydipsia. Once the P_{Na} has returned to the normal range, the urine flow rate should decrease, and the U_{osm} should rise to a value that is at least higher than the P_{osm}. Note that the prior water diuresis may have caused a lower

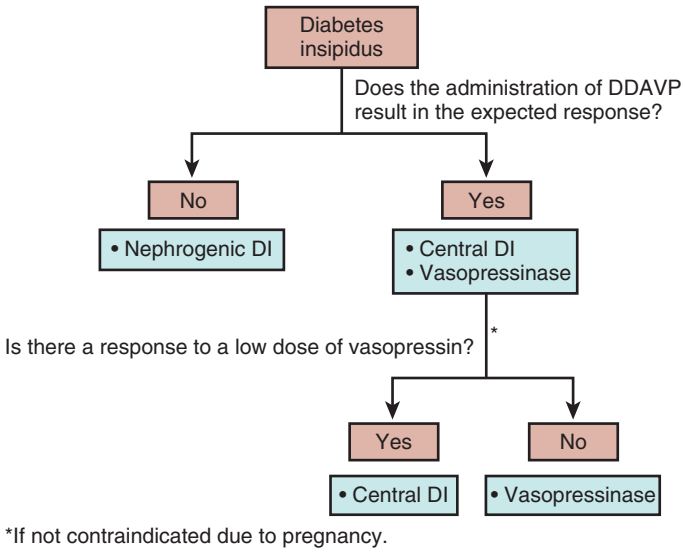

Flow Chart 24.2 *DI,* Diabetes insipidus; *DDAVP,* desmopressin. (From Kamel KS, Halperin ML. *Fluid, Electrolyte, and Acid-Base Physiology; A Problem-Based Approach.* ed 5. Philadelphia: Elsevier; 2017.)

medullary interstitial osmolality due to medullary washout, so the maximal urine-concentrating ability may not be achieved initially. In contrast, if the water diuresis persists when the P_{Na} is higher than 140 mmol/L, the cause of polyuria is DI.

If the U_{osm} is greater than 300 mOsmol/kg H_2O, calculate the osmole excretion rate (see Eq. 24.1). The usual value is close to 0.6 mOsmol/min (600–900 mOsmol/day) in subjects consuming a typical Western diet. If the osmole excretion rate is appreciably increased, then the polyuria is due to an osmotic diuresis. Conversely, if the osmole excretion rate is not increased, then the cause of the polyuria is a defect that leads to a lower medullary interstitial osmolality.

Step 2: Examine the Renal Response to Vasopressin or Desmopressin

See Flow Chart 24.2.

If the cause of the polyuria is DI, this could be due to a lesion in the hypothalamic–posterior pituitary axis, which controls the production and release of vasopressin (central DI), the presence of a circulating vasopressinase that breaks down vasopressin, or a renal lesion that prevents the binding of vasopressin to its V2 receptor (V2R) or interferes with vasopressin effect to cause the insertion of AQP2 in the luminal membrane of principal cells in the CCD and MCD (nephrogenic DI).

In the diagnostic approach to the patient with a water diuresis, DDAVP should only be administered if the patient continues to have a water diuresis, despite P_{Na} greater than 140 mmol/L. In normal subjects consuming a typical Western diet, the expected urine flow rate in response to the administration of DDAVP is around 0.5 mL/min. This is because the inner medullary interstitial effective osmolality (nonurea osmolality) is around 450 mOsmol/kg H_2O, and the rate of excretion of effective osmoles (electrolytes) is around 450 mOsmol/day; hence, the expected urine flow rate is 450/450 = 1 L/day, or 0.7 mL/min. In a patient with central DI, the urine flow rate is expected to fall in response to the administration of DDAVP but, because of medullary washout by the water diuresis, the urine flow rate is likely to be higher than 0.7 mL/min, perhaps around 1 mL/min if the effective inner medullary interstitial osmolality has fallen to say around 300 mOsmol/kg H_2O. The urine flow rate will be even higher if there is an appreciable increase in the rate of excretion of effective osmoles (e.g., because of prior expansion of the effective arterial blood volume with excessive administration of saline). In a patient with central DI, the U_{osm} should rise to a value that is at least higher than P_{osm} in response to the administration of DDAVP.

Similar responses in terms of a fall in urine flow rate and a rise in U_{osm} are also observed in patients with water diuresis caused by hydrolysis of vasopressin by circulating vasopressinase(s), because DDAVP is resistant to degradation by these enzymes. One could, in theory, examine the response to the administration of vasopressin after the effect of DDAVP has worn off, and the patient is having a water diuresis again. In contrast to the response to the administration of DDAVP, a patient in whom a vasopressinase has been released will not respond to the administration of a small dose of vasopressin. However, this should not be attempted in pregnant women because of the oxytocic effect of vasopressin.

If the urine osmolality and flow rate do not respond appropriately to DDAVP, then the diagnosis is nephrogenic diabetes insipidus.

Step 3: Establish the Basis for Central Diabetes Insipidus

Central DI results from decreased release of vasopressin because of an inborn error (hereditary central DI) or because of a variety of infiltrative, neoplastic, vascular, or traumatic lesions that may involve the osmostat, the site where vasopressin is synthesized (the hypothalamic paraventricular and supraoptic nuclei), the tracts connecting these nuclei to the posterior pituitary, and/or a lesion involving the posterior pituitary (Fig. 24.2; see also Chapter 15). In a patient with hypernatremia, the absence of thirst suggests that the lesion involves the osmostat.

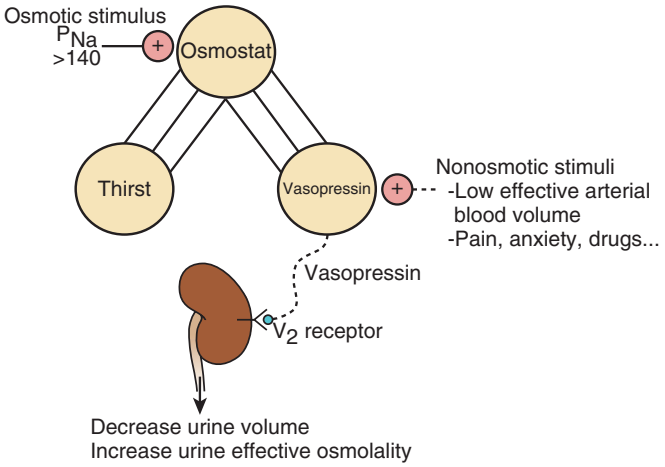

Fig. 24.2 Water control system. The sensor is the osmostat or the tonicity stat *(top circle)*, which detects a change in P_{Na} via an effect on the volume of its cells. The osmostat is linked to the thirst center *(left circle)* and to the vasopressin release center *(right circle)*. Nonosmotic stimuli (e.g., certain drugs, nausea, pain, anxiety) also influence the release of vasopressin. Vasopressin release is also stimulated when there is a large decrease in the effective arterial blood volume. (From Kamel KS, Halperin ML. *Fluid, Electrolyte, and Acid-Base Physiology; A Problem-Based Approach.* ed 5. Philadelphia: Elsevier; 2017.)

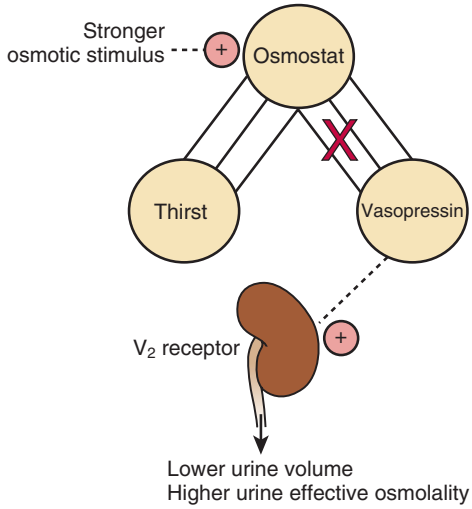

Fig. 24.3 Lesion causing partial central diabetes insipidus. The *top circle* represents the osmostat or the tonicity stat, which is the sensor, the *left circle* represents the thirst center, and the *right circle* is the vasopressin release center. The X symbol represents a hypothetic lesion that causes the severing of some but not all the fibers connecting the osmostat to the vasopressin release center. A stronger osmotic stimulus can overcome the defect and stimulate sufficient vasopressin release to concentrate the urine. (From Kamel KS, Halperin ML. *Fluid, Electrolyte, and Acid-Base Physiology; A Problem-Based Approach.* ed 5. Philadelphia: Elsevier; 2017.)

Step 4: Establish the Basis for Nephrogenic Diabetes Insipidus

If DDAVP fails to cause a rise in U_{osm} to a value that is equal to or higher than P_{osm}, the diagnosis is nephrogenic DI. Nephrogenic DI results from a lesion that prevents the binding of vasopressin to V2R or one that interferes with its effect to cause the insertion of AQP2 into the luminal membrane of principal cells in the collecting ducts. Hereditary nephrogenic DI could be due to an X-linked recessive V2R mutation (more common), or autosomal recessive or dominant AQP2 mutations. The most common cause of nonhereditary nephrogenic DI in an adult is the ingestion of lithium (see Chapter 15).

Patients with classic nephrogenic DI need to be distinguished from patients with a defect that leads to a lower medullary interstitial osmolality (e.g., due to a medullary interstitial disease). From a pathophysiologic perspective, these are two different disorders. Furthermore, in patients with classic nephrogenic DI, the urine flow rate is largely determined by the volume of distal delivery of filtrate and the volume reabsorbed via RWP in the inner MCD. In contrast, in patients with low medullary interstitial osmolality, the urine flow rate is determined by the rate of excretion of effective osmoles.

CLINICAL CASE 1: WHAT IS "PARTIAL" ABOUT PARTIAL CENTRAL DIABETES INSIPIDUS?

A 32-year-old previously healthy man had a recent basal skull fracture. Since his head injury, his urine output had been consistently about 4 L/day, and his U_{osm} around 200 mOsmol/kg H_2O in multiple 24-hour urine collections. Vasopressin was not detected in his plasma when his P_{Na} was around 140 mmol/L. During the daytime, his U_{osm} was consistently around 90 mOsmol/kg H_2O, and his P_{Na} was around 137 mmol/L. When he was given DDAVP, his urine flow rate decreased to 0.5 mL/min, and the U_{osm} rose to 900 mOsmol/kg H_2O. Interestingly, it was noted that if he stopped drinking water after supper, his sleep was not interrupted by a need to void, and his U_{osm} was around 425 mOsmol/kg H_2O in his first voided urine samples in the morning. His urine flow rate fell to 0.5 mL/min, and his U_{osm} rose to 900 mOsmol/kg H_2O, after an infusion of hypertonic saline.

Questions and Discussion

Is this a water diuresis? Because the patient's urine volume was around 4 L/day and his U_{osm} was around 200 mOsmol/kg H_2O, the cause of his polyuria was a water diuresis (see Flow Chart 24.1). His osmole excretion rate was 800 mOsmol/day, which is within the usual rate of excretion of osmoles in a subject consuming a typical Western diet. In response to the administration of DDAVP, his urine flow rate decreased to 0.5 mL/min, and the U_{osm} rose to 900 mOsmol/kg H_2O. Hence, the diagnosis was central DI. Because his urine volume was only 4 L/day and not 10 to 15 L/day, he was thought to have partial central DI.

Central diabetes insipidus. The diagnosis of central DI was straightforward. Because he complained of thirst, his osmostat and his thirst center, as well as the fibers connecting them, appeared to be functionally intact (see Fig. 24.2). Interesting to note that the U_{osm} was greater than the P_{osm} in the first-voided morning urine (U_{osm} = 425 mOsmol/kg H_2O) when he stopped drinking water several hours before he went to sleep. This suggests that the vasopressin release center seems to function but only when there is a strong stimulus for the release of this hormone, presumably a higher P_{Na}. In keeping with this hypothesis is the fact that his urine flow rate fell to 0.5 mL/min and U_{osm} rose to 900 mOsmol/kg H_2O after an infusion of hypertonic saline. Therefore, a possible site for the lesion is destruction of some but not of all the fibers linking the osmostat to the vasopressin release center (Fig. 24.3).

Such a lesion might explain why polyuria was not present overnight if the patient stopped water intake several hours prior to going to sleep, because he might develop a negative water balance sufficient to cause his P_{Na} to rise to a level high enough to cause the release of vasopressin. This clinical case provides insights into the pathophysiology of partial central DI.[6]

Primary polydipsia. If the patient's P_{Na} was high enough early in the morning to stimulate the release of vasopressin, whereas during the daytime, when his P_{Na} was 137 mmol/L, his U_{osm} was consistently around 90 mOsmol/kg H_2O, this suggests that primary polydipsia was present while he was awake. Its basis probably was a learned behavior to avoid the uncomfortable feeling of thirst. This interpretation provides insights into understanding the pathophysiology of the polyuria in this patient and, importantly, to determine the options for therapy to decrease his urine volume.

What are the best options for therapy? The major point here is that a higher P_{Na} could stimulate the release of vasopressin in this patient. A rise in P_{Na} may be induced by a positive balance for Na^+ or a negative balance for water. The patient chose to use oral NaCl tablets to raise his P_{Na} to control his daytime polyuria. This therapy would avoid the risk of acute hyponatremia, which might occur if he were given DDAVP and drank an excessive quantity of water by habit. In contrast, he selected water deprivation starting several hours before going to bed to raise his P_{Na} overnight, which seemed to permit him to have undisturbed sleep.

CLINICAL CASE 2: IN A PATIENT WITH CENTRAL DIABETES INSIPIDUS, WHY DID POLYURIA PERSIST AFTER THE ADMINISTRATION OF DESMOPRESSIN?

A 16-year-old male (weight, 50 kg; total body water, 30 L) underwent craniopharyngioma resection. We are asked to see the patient because of polyuria and hypernatremia. His urine output was 3 L over 5 hours (urine flow rate = 10 mL/min), and his P_{Na} rose from 140 to 150 mmol/L. During this time period, he received 3 L of isotonic saline. His U_{osm} was 120 mOsmol/kg H_2O, and the urine $[Na^+ + K^+]$ concentration was 50 mmol/L. To confirm the diagnosis of central DI, he was given DDAVP, and the urine flow rate fell to 6 mL/min, the U_{osm} rose to 375 mOsmol/kg H_2O, and the urine $[Na^+ + K^+]$ concentration rose to 175 mmol/L.

Questions and Discussion

Does the drop in the patient's urine flow rate to 6 mL/min represent a partial response to DDAVP? When DDAVP acts, the urine flow rate is directly proportional to the osmole excretion rate and inversely proportional to the medullary interstitial osmolality. The expected urine flow rate in response to DDAVP can be calculated by considering several factors. First, the usual rate of excretion of osmoles in an adult subject consuming a typical Western diet is about 900 mOsmol/day; approximately half are urea osmoles and half are electrolyte osmoles. As will be detailed later, at its usual rate of excretion, urea is not an effective osmole in the lumen of the inner MCD. Therefore, around 450 effective mOsmol are excreted each day. Interstitial osmolality in the inner medulla is around 900 mOsmol/kg H_2O. If half of this is due to urea osmoles and half is due to electrolyte osmoles, the effective osmolality of the interstitium in the inner medulla is therefore around 450 mOsmol/kg H_2O. When DDAVP acts, the effective osmolality of the fluid exiting the inner medulla will be equal to the effective osmolality of the interstitium in the inner medulla—in other words, 450 mOsmol/kg H_2O. The 450 mOsmol of effective (electrolyte) osmoles will therefore bring 1 L of urine with them each day. This is a flow rate of 1000 mL/1440 min, or 0.7 mL/min. The osmole excretion rate in this patient before the administration of DDAVP was 1.2 mOsmol/min (U_{osm} = 120 mOsmol/kg H_2O × urine flow rate = 10 mL/min). This value is double the usual osmole excretion rate (900 mOsmol/1440 min = 0.6 mOsmol/min) in subjects consuming a typical Western diet. Another point merits emphasis with regard to the nature of the excreted osmoles. Prior to the administration of DDAVP, the concentration of $Na^+ + K^+$ in the urine was 50 mmol/L. Hence, the vast majority of the osmoles excreted in the urine (100 osmoles—50 × 2 to account for the accompanying anions—out of each 120 osmoles) were electrolyte osmoles, which are effective osmoles that obligate the excretion of H_2O when DDAVP acts. In this case, the likely source of this was the NaCl infusion that the patient was receiving concurrently.

It is also important to recognize that because of a prior water diuresis, there would be a degree of washout of the renal medulla. Hence, the maximum U_{osm} in response to the administration of DDAVP would be significantly lower than that observed in normal subjects. This may explain why this patient's U_{osm} rose to only 375 mOsmol/kg H_2O following the administration of DDAVP.

Therefore, the drop in the patient's urine flow rate to only about 6 mL/min does not represent a partial response to DDAVP but, rather, the expected response because of the high rate of excretion of effective osmoles (osmotic diuresis) and the low effective medullary interstitial osmolality (urinary concentrating defect due to medullary washout).

Why did the P_{Na} rise from 140 to 150 mmol/L during this large water diuresis? Although the tendency here is to assume that this patient's hypernatremia was due to a water deficit because he had a large water diuresis, the actual basis of the rise in his P_{Na} can be determined with a calculation of the tonicity balance.

Water balance. The patient received 3 L of isotonic saline, and hence had an input of 3 L of water. He excreted 3 L of urine, so there is a neutral balance of water.

$Na^+ + K^+$ balance. The patient received 450 mmol of Na^+ (3 L × 150 mmol Na^+/L) and excreted only 150 mmol of $Na^+ + K^+$ (3 L urine × 50 mmol $Na^+ + K^+$/L). Hence, he had a positive balance of 300 mmol of $Na^+ + K^+$. When one divides this surplus of $Na^+ + K^+$ by the total body water (60% of body weight of 50 kg = 30 L), the rise in P_{Na} of 10 mmol/L is largely due to a positive balance of Na^+ rather than a deficit of water. The proper treatment to restore body tonicity and the volume and composition of the ECF and ICF compartments in this patient was to induce a negative balance of 300 mmol of $Na^+ + K^+$.

OSMOTIC DIURESIS

Concept 4

When vasopressin acts, it causes the insertion of AQP2 into the luminal membrane of principal cells in the CCD and

MCD. Water is reabsorbed until the concentration of effective osmoles in the lumen of the CCD and MCD is nearly equal to their concentration in the surrounding cortical and medullary interstitial fluid, respectively. The volume of urine during an osmotic diuresis is directly proportional to the rate of excretion of effective osmoles and indirectly proportional to effective osmolality of the interstitial fluid in the inner medulla.

Because cells in the inner MCD have urea transporters in their luminal membranes when vasopressin acts, urea is usually an ineffective osmole—the concentration of urea is nearly equal in the interstitial fluid in the inner medulla and in the lumen of the inner MCD. Thus, urea does not obligate the excretion of water. The net result of excreting some extra urea is a higher U_{osm} but not a higher urine flow rate. Therefore, it is more correct to say that the urine flow rate is directly proportional to the number of nonurea or effective osmoles in the lumen of the inner MCD and is inversely proportional to the concentration of nonurea or effective osmoles in the interstitial fluid in the inner medulla.

Urea, however, may be an effective urine osmole when the rate of excretion of urea rises by a large amount because urea might not be absorbed fast enough to achieve equal concentrations in the lumen of the inner MCD and in the interstitial fluid in the inner medulla.

Concept 5

The medullary interstitial osmolality falls during an osmotic diuresis because of medullary washout. During an osmotic diuresis, a larger number of liters of fluid is delivered to and is reabsorbed in the MCD during an osmotic diuresis than during antidiuresis. Hence, medullary washout occurs, and medullary interstitial osmolality falls. The U_{osm} is usually close to 600 mOsmol/kg H_2O during an osmotic diuresis. Lower values of the U_{osm} that are even close to P_{osm} may be observed when there is a large rate of excretion of osmoles.

Tools for Evaluation of Osmotic Diuresis

Urine Osmolality. In a patient who has an osmotic diuresis, the U_{osm} should be higher than the P_{osm}.

Osmole Excretion Rate. In an adult during an osmotic diuresis, the rate of excretion of osmoles should be much greater than 1000 mOsmol/day (>0.7 mOsmol/min).

Nature of the Urine Osmoles. The nature of the urine osmoles should be determined by measuring the rate of excretion of the individual osmoles in the urine. One can deduce which solute is likely to be responsible for the osmotic diuresis by measuring the concentration in plasma (e.g., glucose, urea). A large amount of mannitol is not commonly given; hence, it is unlikely to be the sole cause of a large and sustained osmotic diuresis. A saline-induced osmotic diuresis may occur if the EABV was overly expanded with the infusion of a large amount of saline, or if the patient has cerebral or renal salt wasting. For diagnosis of a state of salt wasting, there must be an appreciable excretion of Na^+ when the EABV is definitely contracted.

Sources of the Urine Osmoles. In a patient with a glucose- or a urea-induced osmotic diuresis, it is important to determine whether these osmoles were derived from an exogenous source or from catabolism of endogenous proteins.

Source of Urea. Urea appearance rate. The rate of appearance of urea can be determined from the amount of urea that is retained in the body plus the amount that is excreted in the urine over a given period of time. The former can be calculated from the rise in the concentration of urea in plasma (P_{urea}) and by assuming a volume of distribution of urea that is equal to total body water (~60% of body weight).

One can use the following calculation to determine whether the source of urea was the breakdown of exogenous or endogenous proteins if the intake of proteins is known. Close to 16% of the weight of protein is nitrogen. Therefore if 100 g of protein were oxidized, 16 g of nitrogen would be formed. The molecular weight of nitrogen is 14, so about 1140 mmol of nitrogen would be produced. Because each molecule of urea contains two atoms of nitrogen, about 570 mmol of urea would be produced from the oxidation of 100 g of protein (or 5.7 mmol of urea/1 g protein). Because each kilogram of lean body mass has around 180 g of protein, the breakdown of 1 kg of lean body mass will produce about 1026 mmol of urea (5.7 mmol of urea/1 g protein × 180 g of protein).

Source of Glucose. The production of glucose from endogenous sources is relatively small. In more detail, only 60% of the weight of protein can be converted to glucose. Hence, to produce enough glucose from protein to induce 1 L of osmotic diuresis, which requires the excretion of around 300 mmol of glucose, one would need the catabolism of 90 g of protein (equivalent to the catabolism of about 0.5 kg of lean body mass). Therefore, if there is a large glucose-induced osmotic diuresis, the glucose must be from an exogenous source (e.g., the ingestion of large volumes of fruit juice or sugar-containing soft drinks in a patient who lacks insulin actions).

CLINICAL APPROACH TO THE PATIENT WITH AN OSMOTIC DIURESIS

The steps in the clinical approach to the patient with osmotic diuresis are illustrated in Flow Chart 24.3.

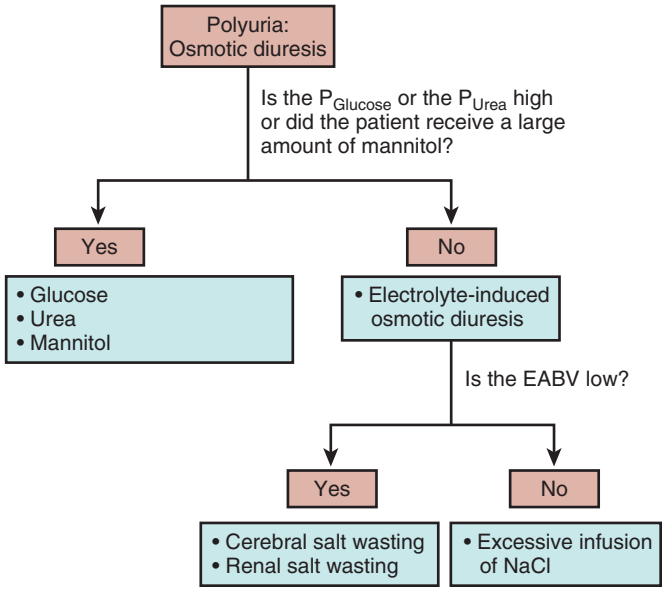

Flow Chart 24.3 *EABV,* Effective arterial blood volume. (From Kamel KS, Halperin ML. *Fluid, Electrolyte, and Acid-Base Physiology; A Problem-Based Approach.* ed 5. Philadelphia: Elsevier; 2017.)

Step 1: Calculate the Osmole Excretion Rate

If the U_{osm} is greater than the P_{osm}, and the osmole excretion rate significantly exceeds 1000 mOsmol/day (0.7 mOsmol/min), an osmotic diuresis is likely to be present.

Step 2: Define the Nature of the Excreted Osmoles

One can make a reasonable assessment of the likelihood that a solute will cause polyuria if its concentration in plasma is measured, the GFR is estimated, and the renal handling of that solute is known. One should also determine whether enough mannitol was administered to cause the observed degree of polyuria. Osmotic diuresis could be due to a saline diuresis if Na^+ and Cl^- are excreted at high rates and represent the majority of the urine osmoles.

Step 3: Identify the Source of the Osmoles in the Urine

In a patient with a glucose- or urea-induced osmotic diuresis, it is important to decide whether these osmoles were derived from an exogenous source or from catabolism of endogenous proteins. The clinician should also be aware of the possibility of a large amount of glucose in the lumen of the gastrointestinal tract because when it is absorbed it may contribute to the osmotic diuresis.

In a patient with a saline-induced osmotic diuresis, one must determine why so much NaCl is being excreted. Some potential causes are prior excessive saline administration (a common situation in hospitalized patients), administration of a loop diuretic in a patient with marked degree of peripheral edema, cerebral salt wasting, or renal salt wasting.

CLINICAL CASE 3: UNUSUALLY LARGE OSMOTIC DIURESIS IN A PATIENT WITH DIABETES MELLITUS

A 50-kg, 14-year-old female had a long history of type 1 diabetes mellitus, which was poorly controlled because she did not take insulin regularly. In the past 48 hours, she was thirsty, drank large volumes of fruit juice, and noted that her urine volume was very high. On physical examination, her EABV was not appreciably contracted. The urine flow rate was 10 mL/min over a 100-min period while she was in the emergency room. Other laboratory data included the following: pH = 7.33, plasma bicarbonate (HCO_3^-) concentration (P_{HCO_3}) = 24 mmol/L, plasma anion gap ($P_{anion\ gap}$) = 16 mEq/L, plasma K^+ concentration (P_K) = 4.8 mmol/L, plasma creatinine concentration (P_{Cr}) = was close to her usual values of 1.0 mg/dL (88 µmol/L), blood urea nitrogen (BUN) = 22 mg/dL (P_{urea} = 8 mmol/L), and hematocrit = 0.50. Of note, there was no decrease in her plasma glucose concentration (P_{Glu}) over that time period, despite the excretion of a large amount of glucose in her urine. The following results were also reported:

	Admission		*After 100 min*	
Parameter	***Plasma***	***Urine***	***Plasma***	***Urine***
Glucose, mg/dL (mmol/L)	1260 (70)	5400 (300)	1260 (70)	5400 (300)
Na^+, mmol/L	125	50	123	50
Osmolality, mOsmol/kg H_2O	320	450	316	450

Questions and Discussion

What is the basis of the polyuria?

U_{osm}. The U_{osm} of 450 mOsmol/kg H_2O indicates that this polyuria was due to an osmotic diuresis. The U_{osm} was lower than the expected value during an osmotic diuresis, probably reflecting the very high osmole excretion rate, which caused a larger fall in the patient's medullary interstitial osmolality due to medullary washout as a result of the reabsorption of a large volume of water in her MCD.

Osmole excretion rate. The product of her U_{osm} (450 mOsmol/L) and urine flow rate (10 mL/min) yielded an osmole excretion rate of 4.5 mOsmol/min, a value that is sevenfold higher than the usual value in an adult subject consuming a typical Western diet (≈0.6 mOsmol/min).

Nature of the urine osmoles. Because the patient's GFR was not low and her P_{Glu} was extremely high (1260 mg/dL, 70 mmol/L), the filtered load of glucose was markedly higher than the maximum tubular capacity for its reabsorption. Hence, this was a glucose-induced osmotic diuresis, confirmed by the finding of a U_{Glu} of about 300 mmol/L.

Sources of the urine osmoles. Of special emphasis, this patient's P_{Glu} did not decline despite such a high rate of excretion of glucose. In quantitative terms, the total content of glucose in her ECF compartment was 126 g—1260 mg/dL × 10 to convert to mg/L × 10 L ECFV ÷ 1000. During this 100-minute period, she excreted 54 g of glucose—5400 mg/dL × 10 to convert to mg/L × 1 L ÷ 1000. Therefore, although she excreted close to half of the content of glucose in her entire ECF compartment, there was no change in her P_{Glu}. Accordingly, to maintain this degree of hyperglycemia, she needed a large input of glucose over a short period of time. The only likely source of such a large amount of glucose was glucose that was retained in her stomach. As a reference, 1 L of apple juice contains about 135 g of glucose. Although the usual effect of hyperglycemia is to slow gastric emptying, this did not seem to be the case in this patient because she seemed to have had a rapid rate of exit of fluid from her stomach, with its subsequent absorption in her intestine.[7]

What dangers do you anticipate in this patient?

Cerebral edema. Brain cell swelling might occur if there were a significant fall in her effective P_{osm} (Eq. 24.2).[8] A fall in her effective P_{osm} may occur if the absorbed glucose and water from the gastrointestinal (GI) tract were retained in the body and glucose was subsequently metabolized; hence, there would be a gain of electrolyte-free water in the body.

$$\text{Effective } P_{osm} = 2(P_{Na} + P_{Glu})\ (\text{all values in mmol/L}) \qquad (24.2)$$

DECREASED EFFECTIVE ARTERIAL BLOOD VOLUME

Principles governing the regulation of EABV are briefly discussed here and in more detail in Chapter 14.

Concept 6

Water crosses cell membranes rapidly through AQP channels to achieve osmotic equilibrium. Hence, the numbers of effective osmoles in the ECF and ICF compartments determine their respective volumes. The effective osmoles in the ECF

compartment are primarily Na^+ and its attendant anions (Cl^- and HCO_3^-); their content in the ECF compartment determines its volume.

Concept 7

The hydrostatic pressure and the oncotic pressure across the capillary membrane are the major forces that determine the distribution of the ECF compartment volume between its intravascular and interstitial spaces.

The major driving force for outward movement of an ultrafiltrate of plasma across the capillary membrane is the hydrostatic pressure difference. The hydrostatic pressure at the venous end of the capillary is higher under conditions that lead to venous hypertension (e.g., venous obstruction, congestive heart failure).

The major driving force for inward fluid movement from the interstitial space to the intravascular space is the colloidal osmotic pressure difference. This is largely due to the higher concentration of albumin in the intravascular space (40 g/L) than in the interstitial space (10 g/L). Fluid accumulates in the interstitial space in patients with hypoalbuminemia (e.g., patients with nephrotic syndrome). Thus, the ECF volume (ECFV) in these patients may be increased but their EABV may be decreased.

Concept 8

Control mechanisms for Na^+ homeostasis are set to defend the EABV rather than the ECFV. EABV can be defined as the part of the ECFV that is located in the arterial blood system and that effectively perfuses tissues. Changes in the EABV are sensed by baroreceptors located in the large blood vessels (the carotid sinus and the aortic arch) and the afferent glomerular arterioles. These are stretch receptors that detect changes in the filling of these vessels.

TOOLS FOR EVALUATING DECREASED EFFECTIVE ARTERIAL BLOOD VOLUME

Quantitative Assessment of the Extracellular Fluid Volume

The physical examination, the plasma concentrations of HCO_3^-, creatinine, urea, and urate, as well as the fractional excretions of Na^+, Cl^-, urea, and urate are useful at times to suggest that the EABV is contracted. Nevertheless, they do not provide a quantitative estimate of the ECFV. A quantitative assessment of the ECFV can be obtained using the hematocrit (Table 24.2) or the concentration of total proteins in plasma, assuming that their values were normal to begin with.[9] The hematocrit is the ratio of red blood cells (RBCs) volume to blood volume, as given in the following formula:

$$\text{Hematocrit} = \text{RBC volume}/(\text{RBC volume} + \text{plasma volume}) \quad (24.3)$$

Blood volume in an adult subject is around 70 mL/kg body weight (i.e., around 5 L in a 70-kg subject). With a blood volume of 5 L and a hematocrit of 0.40, the RBC volume is 2 L and the plasma volume is 3 L (Eq. 24.3). When the hematocrit is 0.50, and assuming no change in the RBC volume (2 L), the blood volume is 4 L. Hence, the plasma volume is 2 L (i.e., reduced by one-third from its normal value of 3 L). If one ignores changes in Starling forces for simplicity, the ECFV should have declined by approximately one-third of its normal volume (see Table 24.2).

Table 24.2 Use of the Hematocrit to Estimate the Extracellular Fluid Volume[a]

Hematocrit	% Change ECFV
0.40	0
0.50	–33
0.60	–60

[a]The assumptions made when using this calculation are that the patient does not have anemia or erythrocytosis, that the red blood cell (RBC) volume is 2 L, and that the plasma volume is 3 L (blood volume 5 L). The formula is:
Hematocrit = RBC volume/(RBC volume + plasma volume)
Values between those listed can be deduced by interpolation.
ECFV, Extracellular fluid volume.

Table 24.3 Urine Electrolyte Values in a Patient With a Contracted Effective Arterial Blood Volume[a]

Condition	Urine Na^+	Urine Cl^-
Vomiting		
Recent	High	Low
Remote	Low	Low
Diuretics		
Recent	High	High
Remote	Low	Low
Diarrhea or laxative abuse	Low	High
Bartter syndrome or Gitelman syndrome	High	High

[a]Values of the urine electrolyte concentration must be adjusted when polyuria is present. Urine Cl^- is high in patients with diarrhea or laxative abuse if they have a high rate of excretion of NH_4^+. *High,* Urine concentration >15 mmol/L; *low,* urine concentration <15 mmol/L.

Urinary Tests for Low Effective Arterial Blood Volume

The expected response to a low EABV is to excrete as little Na^+ and Cl^- as possible in the urine. Because 24-hour urine collections to calculate rates of excretion of Na^+ and Cl^- are usually not practical in clinical circumstances in which a quick assessment is required, clinicians use the urinary concentrations of Na^+ (U_{Na}) and Cl^- (U_{Cl}) in a spot urine sample (Table 24.3) to assess the renal response to the presence of a low EABV. These, however, are concentration terms, which may not necessarily reflect low rates of excretion if the urine flow rate is high. To avoid this type of error, the U_{Na} and U_{Cl} should be related to the concentration of creatinine in the urine (U_{Cr}) because the rate of excretion of creatinine is relatively constant throughout the day; its 24-hour excretion rate can be estimated based on assessment of the patient's muscle mass. There are some caveats in using the urine Na^+ and Cl^- excretion rates to assess EABV.[10]

Low Rate of Excretion of Sodium and Chloride. A low rate of excretion of Na^+ and Cl^- in a patient with a decreased EABV suggests either a loss of NaCl via nonrenal routes (e.g., sweat, GI tract) or that there was a prior renal loss of Na^+ and Cl^- (e.g., remote use of diuretics). In the absence of a low EABV, a low rate of excretion of Na^+ and Cl^- may reflect a low intake of NaCl.

High Rate of Excretion of Sodium but Little Excretion of Chloride. In a patient with a low EABV, a high rate of excretion of Na^+ but not Cl^- suggests that there is an anion other than Cl^- being excreted with Na^+. If the anion is HCO_3^- (the urine pH is alkaline), suspect recent vomiting. The anion could also be one that was ingested or administered (e.g., penicillinate anion), in which case the urine pH would be close to 6.

High Rate of Excretion of Chloride but Little Excretion of Sodium. In a patient with a low EABV, a high rate of excretion of Cl^- but not Na^+ suggests that a cation other than Na^+ is being excreted with Cl^-. Most often the cation is NH_4^+, and the setting is diarrhea or laxative abuse, causing hyperchloremic metabolic acidosis.

Excretions of Sodium and Chloride Are Not Low. In a patient who has a low EABV, a high rate of excretion of both Na^+ and Cl^- suggests the absence of a stimulator of the reabsorption of Na^+ and Cl^- (e.g., aldosterone deficiency), the presence of an inhibitor of their reabsorption (e.g., a diuretic), or an intrinsic renal lesion that has effects similar to those of a diuretic (e.g., Bartter syndrome or Gitelman syndrome). The pattern of excretion of electrolytes in multiple spot urine samples throughout the day can provide a helpful clue to the cause of the loss of NaCl. For example, the use of diuretics is suspected if U_{Na} and U_{Cl} in spot urine samples are very low at times but high at others. By contrast, in a patient with Bartter syndrome or Gitelman syndrome, these rates of excretion are persistently high.

Fractional Excretion of Sodium or Chloride

Calculation of the fractional excretion of Na^+ (FE_{Na}) or Cl^- (FE_{Cl}) expresses the amount of Na^+ or Cl^- that is excreted in the urine as a percentage of the amount that is filtered. For example, adults consuming a typical Western diet excrete about 150 mmol/day each of Na^+ and Cl^-. Because a normal GFR is about 180 L/day, the kidney filters about 27,000 mmol of Na^+ and about 20,000 mmol of Cl^- per day (P_{Na} or $P_{Cl} \times$ GFR). Hence, FE_{Na} is about 0.5%, and FE_{Cl} is about 0.75%. (The formula for this calculation is shown in Eq. 24.4.)

$$FE_{Na} = 100 \times ([U_{Na}/P_{Na}]/[U_{Cr}/P_{Cr}]) \qquad (24.4)$$

Note that U_{Na} or U_{Cl} and P_{Na} or P_{Cl} must be in the same units (generally mmol/L), and U_{Cr} and P_{Cr} must be in the same units (e.g., either both in mg/dL or both in mmol/L).

One should bear in mind three practical points when using the FE_{Na} or FE_{Cl}:

1. The excretions of Na^+ and Cl^- are directly related to the dietary intake of NaCl.
   Hence, a low FE_{Na} or FE_{Cl} may represent a low intake of NaCl rather than a low EABV.
2. The numeric values for FE_{Na} and FE_{Cl} will be twice as high, at steady state, in a euvolemic subject who consumes 150 mmol of NaCl daily whose GFR is reduced by 50% as in another subject who consumes the same amount of NaCl and has a normal GFR.
   Hence, the numeric values of FE_{Na} and FE_{Cl} must be interpreted in the context of the GFR at the time the measurements are made.
3. As is the case with the use of U_{Na} or U_{Cl}, the FE_{Na} may be high in a patient with a low EABV when there is an unusually large excretion of another anion (e.g., HCO_3^-) in the urine, and the FE_{Cl} may be high in a patient with a low EABV when there is an unusually large excretion of another cation (e.g., NH_4^+) in the urine.
   Calculations of FE_{Na} and FE_{Cl} are commonly used in patients with acute kidney injury in the differential diagnosis of prerenal azotemia versus acute tubular necrosis (in the absence of diuretics).[11] The advantage of using fractional excretion in this setting over the urinary Na^+ and Cl^- concentrations is that the use of FE_{Na} and FE_{Cl} adjusts these concentration terms for water reabsorption in the nephron.

Determining the Nephron Site Where There Is a Defect in Reabsorption of Sodium

If another compound or an ion that should have been reabsorbed in a given nephron segment is being excreted, one has presumptive evidence for a defect in that nephron segment. For example, if the defect is in the PT, one might find glucosuria in the absence of hyperglycemia (e.g., Fanconi syndrome).

The presence of hypokalemia may suggest a defect in the TAL of the loop of Henle or in the DCT with enhanced rate of K^+ secretion in the aldosterone-sensitive distal nephron (ASDN, which includes the second portion of the DCT [DCT2], the connecting segment, and the CCD) due to both increased distal delivery of Na^+ and increased aldosterone levels because of decreased EABV. The presence of hypocalciuria would suggest that the site of the lesion is in the DCT (e.g., Gitelman syndrome, thiazide diuretics), whereas hypercalciuria suggests a lesion in the TAL (e.g., Bartter syndrome or use of loop diuretics). The presence of hyperkalemia suggests a lesion in the ASDN (e.g., Addison disease, use of potassium-sparing diuretics such as spironolactone).

CLINICAL CASE 4: ASSESSMENT OF THE EFFECTIVE ARTERIAL BLOOD VOLUME

A 25-year-old woman was assessed by her family physician because she was feeling weak. Although she admitted to being concerned about her body image, she denied vomiting and the intake of diuretics. Her blood pressure was 90/60 mm Hg, her pulse rate was 110 beats/min, and her jugular venous pressure was low. Measurements in a venous blood sample showed P_{HCO_3} = 24 mmol/L, $P_{anion\ gap}$ = 17 mEq/L, P_K = 2.9 mmol/L, hematocrit = 0.50, and plasma albumin concentration (P_{Alb}) = 5.0 g/dL (50 g/L). The urine electrolyte values were U_{Na} less than 5 mmol/L, U_{Cl} = 42 mmol/L, urinary K^+ concentration (U_K) = 10 mmol/L, and U_{Cr} = 7 mmol/L.

Questions and Discussion

How severe is the degree of this patient's ECFV contraction? The elevated value for the hematocrit (0.50) provides

quantitative information about her ECFV (see Table 24.2), as does the elevated P_{Alb}. Based on a hematocrit of 0.50, her ECFV was reduced by around 33%. If she had prior anemia, the degree of her ECFV contraction might be even greater.

What is the cause of her low EABV? The low U_{Na} implies that her EABV was low. The high U_{Cl} (42 mmol/L), which exceeded the sum of her $U_{Na} + U_K$, indicates that there was another cation in that urine, most likely NH_4^+.

Interpretation. Calculating the content of HCO_3^- in this patient's ECF compartment (P_{HCO_3} × her current ECFV) revealed that she had a deficit of $NaHCO_3$. Loss of NaCl plus $NaHCO_3$ via the GI tract was suspected as the cause of contracted EABV. The patient later admitted to the frequent use of a laxative. Hypokalemia could be explained by the loss of K^+ via the GI tract because her low U_K/U_{Cr} ratio suggests that the loss of K^+ was extrarenal (see section on potassium). Hypokalemia is associated with acidosis in PT cells, which stimulates ammoniagenesis. The increased rate of excretion of the cation NH_4^+ obligates the excretion of Cl^-, despite the presence of a low EABV.

HYPONATREMIA

Hyponatremia is defined as a P_{Na} less than 135 mmol/L.

Concept 9

Because water moves across cell membranes to achieve osmotic equilibrium, acute hyponatremia is associated with the swelling of brain cells. Brain cells adapt by exporting effective osmoles, mainly K^+ (and an anion from their ICF) and a number of organic solutes (e.g., taurine, myoinositol).

If hyponatremia is present for more than 48 hours, these adaptive changes have proceeded sufficiently to return brain cells back close to their normal volume. In this setting, a rapid increase in the P_{Na} shrinks cerebral vascular endothelial cells, leading to opening of the blood-brain barrier, allowing lymphocytes, complement, and cytokines to enter the brain, damage oligodendrocytes, and cause demyelination. Microglial activation also plays a role in this process. This has important implications for the management of patients with hyponatremia (see Chapter 15).

Concept 10

Chronic hyponatremia is usually due to a defect in the renal excretion of water. There are two causes for diminished renal excretion of water, low distal delivery of filtrate and the actions of vasopressin.

Hyponatremia is not a specific disease; rather, it is a diagnostic category with many different causes. The traditional approach to the pathophysiology of hyponatremia centers on a reduced electrolyte-free water excretion due to the actions of vasopressin. In some clinical settings, release of vasopressin is thought to be due to a diminished EABV. Nevertheless, at least in some patients with hyponatremia, the degree of decrease in EABV does not seem to be large enough to cause the release of vasopressin. We suggest that hyponatremia may develop in some patients in the absence of vasopressin actions. Two factors are important in this context, the volume of filtrate that is delivered to the distal nephron and the volume of water that is reabsorbed in the inner MCD through its RWP.[3]

The volume of distal delivery of filtrate is reduced if the GFR is decreased or the fractional reabsorption of NaCl in the PT is increased.

The fractional reabsorption of NaCl in the PT is increased in response to a decreased EABV. Decreased EABV can be due to a total body deficit of NaCl (e.g., diuretic use in a patient who consumes little salt, NaCl loss in diarrhea fluid or sweat) or to a disorder that causes a low cardiac output. Because there is an obligatory minimal loss of Na^+ in each liter of urine during a large water diuresis, a deficit of Na^+ can be created during the polyuria induced by a large intake of water in a subject who consumes little NaCl (e.g., a patient with beer potomania).

The driving force for water reabsorption via RWP is the osmotic pressure gradient generated by the difference in osmolality between the luminal fluid in the inner MCD and that in the medullary interstitium. As discussed previously, we estimate that somewhat more than 5 L of water is reabsorbed per day in the inner MCD by RWP during water diuresis.

In some patients, hyponatremia is caused by reduced electrolyte-free water excretion due to actions of vasopressin, but the release of vasopressin is not caused by a decreased EABV. This category is called the syndrome of the inappropriate secretion of antidiuretic hormone (SIADH). SIADH, however, is a diagnosis of exclusion; it cannot be made if the patient has a condition that may lead to a low distal delivery of filtrate. A rare cause of SIADH is a mutation in the gene encoding V2R, causing V2R to be constitutively active. This disorder is called "nephrogenic syndrome of inappropriate antidiuresis," and it is suspected in a patient with SIADH of undetermined cause in whom the vasopressin level is undetectable and who does not respond to the administration of a V2R antagonist (e.g., tolvaptan) with a water diuresis.

TOOLS FOR EVALUATING HYPONATREMIA

Measurement of Plasma Sodium Concentration

Pseudohyponatremia is present when the P_{Na} measured by the laboratory is lower than the actual ratio of Na^+ to plasma water in the patient. This occurs when the method used requires dilution of the plasma sample. This is because 7% of the plasma volume is a nonaqueous volume (i.e., lipids and proteins), which is not taken into account when adjusting for the volume of the diluent. Hence, although the concentration of Na^+ in plasma water is 150 mmol/L, the measured value by flame photometry is 140 mmol/L, and lower values will be obtained by this method if the nonaqueous volume in plasma is larger (e.g., in a patient with hypertriglyceridemia or hyperparaproteinemia) because the same volume of diluent is added to a smaller volume of plasma water. With the use of an ion-selective electrode, the activity of Na^+ in the aqueous plasma volume is measured; nevertheless, because of the use of automatic aspirators and dilutors to prepare the plasma samples, pesudohyponatremia remains an issue. This error in the measurement of P_{Na} is detected by the finding of a normal P_{osm} value in the absence of high concentration of other osmoles, such as urea, glucose, or alcohol.[12]

Hyponatremia Due to Hyperglycemia. In the absence of actions of insulin, glucose is an effective osmole for skeletal muscle and, if hyperglycemia is associated with a rise in plasma effective osmolality, there will be a shift of water out of skeletal

muscle. Although a number of formulas have been proposed to predict the fall in P_{Na} based on a given rise in P_{Glu}, these formulas are based on theoretic calculations with the addition of glucose without water to the ECF compartment. Different correction factors have been proposed based on assumptions made about ECFV and the volume of distribution of glucose in the absence of insulin actions. Moreover, because patients with hyperglycemia have variable fluid intake and variable loss of water and Na^+ in the urine, one cannot assume a fixed relationship between the rise in P_{Glu} and the fall in P_{Na}.

Detection of a Low Effective Arterial Blood Volume

A difficulty in making the diagnosis of SIADH is that patients may have a mild to modest degree of EABV contraction, causing a low distal delivery of filtrate that cannot always be detected by the physical examination. The following laboratory tests may provide helpful clues to detect the presence of EABV contraction. At times, however, EABV expansion with the infusion of saline may be required to rule out low distal delivery of filtrate as the cause of hyponatremia. Absence of water diuresis despite EABV expansion confirms the diagnosis of SIADH.

Concentrations of Sodium and Chloride in Urine. The assessment of U_{Na} and U_{Cl} are helpful to detect the presence of a low EABV, and they may also provide clues about its cause. In the absence of the caveats noted above, a U_{Na} and U_{Cl} higher than 30 mmol/L is thought to be in keeping with euvolemia and the diagnostic category of SIADH.

Concentrations of Urea and Urate in Plasma. Expansion of the EABV diminishes the rate of reabsorption of urea and urate in PT, resulting in higher rates of their fractional excretions and lower levels of their plasma concentrations. Because patients with SIADH are likely to have an expanded EABV, a P_{Urea} less than 3.6 mmol/L (BUN < 21.6 mg/dL), a plasma urate level less than 0.24 mmol/L (<4 mg/dL), a fractional excretion of urea greater than 55 %, and a fractional excretion of urate greater than 12% are thought to be more in keeping with the diagnostic category of SIADH. The fractional excretions of urea and urate, however, are not reliable markers in patients who are thought to have cerebral salt wasting and decreased EABV because the defect in Na^+ reabsorption in these patients seems to involve the PT. Therefore, these patients will have a high fractional excretion of urea and urate despite decreased EABV.

Because the reabsorption of urea in PT is strongly influenced by the EABV, the relative rise in P_{Urea} is usually larger than the rise in $P_{Creatinine}$ in patients with low EABV. A ratio of $P_{Urea}/P_{Creatinine}$ (where both are in mmol/L units) greater than 100, or $BUN/P_{Creatinine}$ (where both are in mg/dL units) greater than 20, suggests a low EABV. This, however, may not be the case if protein intake is low.

Other Tests. A rise in the P_{Cr} and a low or a high P_{HCO_3} level may suggest that the EABV is low.

The clinical approach to the diagnosis of the cause of chronic hyponatremia is illustrated in Flow Chart 24.4.

CLINICAL CASE 5: HYPONATREMIA WITH BROWN SPOTS

A 22-year-old woman had myasthenia gravis. In the previous 6 months, she noted a marked decline in her energy and weight loss (down from 50 to 47 kg). She often felt faint when standing up quickly. On physical examination, her blood pressure was 80/50 mm Hg, pulse rate was 126 beats/min, jugular venous pressure was below the level of the sternal angle, and there was no peripheral edema. Brown pigmented spots were evident in her buccal mucosa. The biochemistry data are as follows.

Findings	*Plasma*	*Urine*
Na^+, mmol/L	112	130
K^+, mmol/L	5.5	24
Urea	BUN: 28 mg/dL (10 mmol/L)	Urea: 130 mmol/L
Creatinine	1.7 mg/dL (150 µmol/L)	6.0 mmol/L
Osmolality, mOsmol/kg H_2O	240	438

Questions and Discussion

What is the most likely basis for the very low EABV? The very contracted EABV (manifested by the low blood pressure and tachycardia), the low P_{Na}, the high P_K of 5.5 mmol/L, and the renal salt wasting strongly suggest that the most likely diagnosis is adrenal insufficiency. This is likely due to autoimmune adrenalitis because the patient also had myasthenia gravis. The low EABV was due to renal salt wasting because of lack of aldosterone and was also caused in part by a lower degree of contraction of venous capacitance vessels because of glucocorticoid deficiency.

What dangers to the patient are present on presentation? Two potential emergencies dominate the initial management, a very contracted EABV and the lack of cortisol. To deal with the former and restore hemodynamic stability, the initial intravenous infusion can be given as 0.9% saline. Once the patient is hemodynamically stable, to expand her EABV further without changing her P_{Na}, the intravenous fluid should be changed to one that is isotonic to the patient. The second potential danger is related to the lack of cortisol and is dealt with by administering cortisol.

It did not seem that the patient had an acute component of hyponatremia requiring the induction of a rapid initial rise in her P_{Na} because she did not have significant symptoms that could be related to increased intracranial pressure and she also denied a recent large water intake.

What dangers should be anticipated during therapy, and how can they be avoided? Re-expansion of the patient's EABV could lead to an increased excretion of water due to an increased distal delivery of filtrate and suppression of the release of vasopressin. In addition, the administration of cortisol would improve her hemodynamic state and also inhibit the release of corticotropin-releasing hormone and, hence, of vasopressin. The net result of this therapy would be to cause water diuresis and thereby a dangerous rise in the P_{Na}. Because the patient had a small muscle mass (and therefore a small total body water volume), the excretion of a relatively small volume of electrolyte-free water could lead to too rapid a rise in P_{Na}. In addition, because of her poor nutritional state (which becomes even more evident if one interprets her weight loss in conjunction with a large gain of water in her cells, hence her loss of muscle mass was larger than revealed by her weight loss), she was at high risk for osmotic demyelination if her P_{Na} were to rise rapidly. The

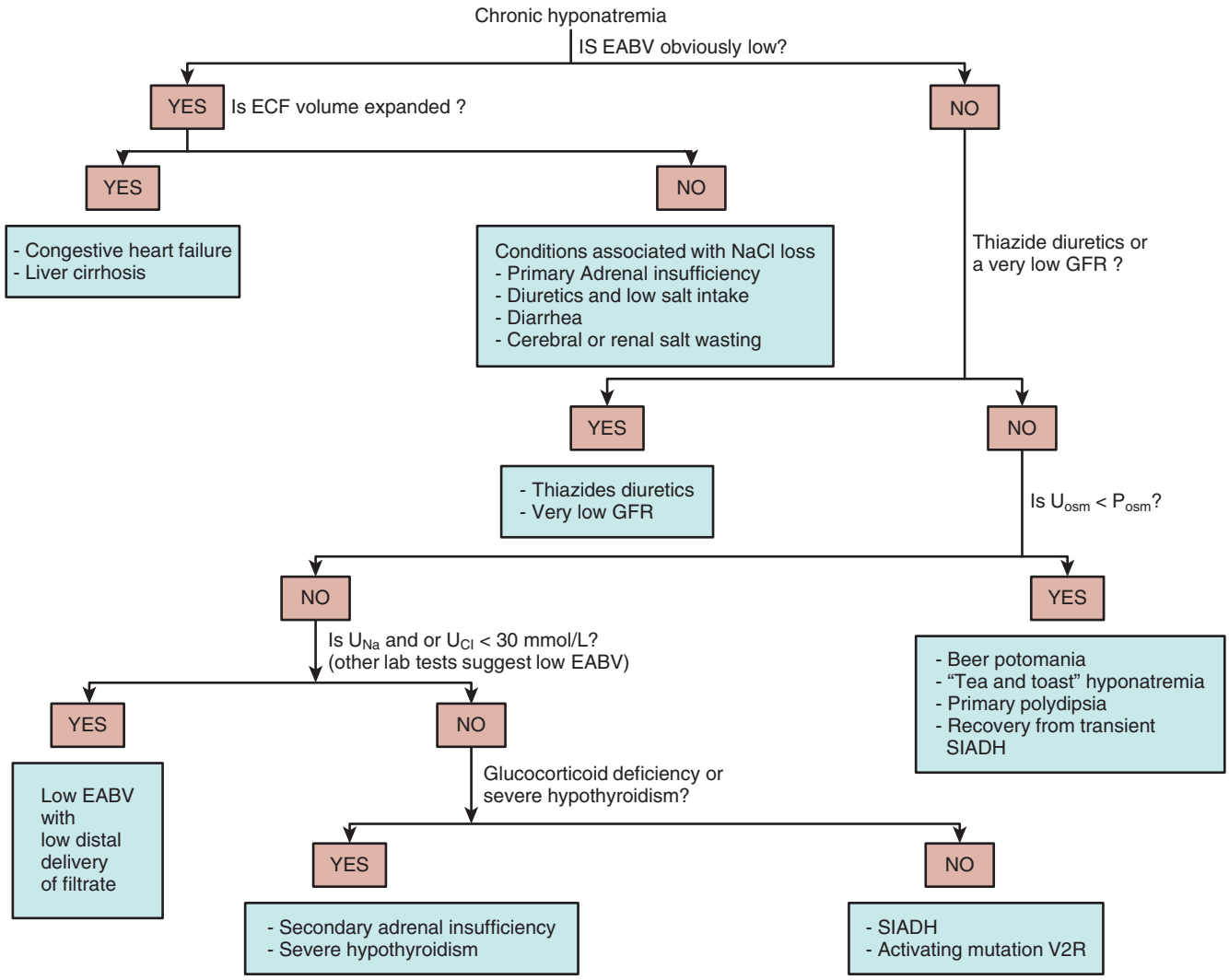

Flow Chart 24.4 *EABV,* Effective arterial blood volume; *ECF,* extracellular fluid; *GFR,* glomerular filtration rate; *SIADH,* syndrome of inappropriate diuretic hormone secretion. (From Kamel KS, Halperin ML. *Fluid, Electrolyte, and Acid-Base Physiology; A Problem-Based Approach.* ed 5. Philadelphia: Elsevier; 2017.)

rise in her P_{Na} should not exceed a maximum of 4 to 6 mmol/L/24 hours. Accordingly, we would administer DDAVP early in therapy to prevent water diuresis.

CLINICAL CASE 6: HYPONATREMIA IN A PATIENT ON THIAZIDE DIURETIC THERAPY

A 71-year-old woman was prescribed a thiazide diuretic for the treatment of hypertension. She had chronic kidney disease (CKD) due to ischemic nephropathy, with an estimated GFR of 28 mL/min/1.73 m^2 (around 40 L/day). She consumed a low-salt, low-protein diet and drank several large cups of water and tea a day following the advice to remain hydrated. A month later, she presented to her family doctor feeling unwell. Her blood pressure was 130/80 mm Hg, her heart rate was 80 beats/min, there were no postural changes in her blood pressure or heart rate, and her jugular venous pressure was about 1 cm below the level of the sternal angle. Her P_{Na} was 112 mmol/L. Other laboratory results are as follows.

Findings	*Plasma*	*Urine*
Na^+, mmol/L	112	22
K^+, mmol/L	3.6	10
HCO_3^-, mmol/L	28	0
Urea, mmol/L	8	241
Creatinine, µmol/L (mg/dL)	145 (1.3)	
Creatinine mmol/L (g/L)		6.1 (0.7)
Osmolality mOsmol/kg H_2O	240	325

Questions and Discussion

What is the most likely basis for the chronic hyponatremia in this patient? Although the patient was taking a thiazide diuretic, the degree of decrease in her EABV did not seem to be large enough to cause the release of vasopressin. The patient had a low baseline estimated GFR of 28 mL/min/1.73 m^2 (around 40 L/day). The use of diuretics and the low-salt diet led to a deficit of Na^+ and a mild reduction in the EABV. Even a relatively small decrease in EABV leads to increased release

of catecholamines, and activation of the renin angiotensin aldosterone system by β-adrenergic stimulation, both of which increase the reabsorption of sodium and water in the PT. If the patient were to reabsorb 90% of her GFR of 40 L/day (which may be even lower because of the mild reduction in her EABV) in the PT, instead of 83% (as discussed previously, this is the percentage of the filtrate that is usually reabsorbed in the PT in the absence of low EABV), less than 4 L/day of filtrate would be delivered distally. This is the maximum volume of urine she could excrete. This volume exceeds the usual daily intake of water, but hyponatremia might still develop in such a patient because there is water reabsorption by RWP along the inner MCD, even in the absence of vasopressin action.

The ability to generate electrolyte- free water is also diminished by the effect of thiazide diuretics to inhibit the reabsorption of NaCl (without water) in DCT. With regard to the volume of water that may be reabsorbed in her inner MCD, the driving force is the difference in osmolalality between the luminal fluid and the interstitial fluid in the inner MCD. Because of the low rate of excretion of osmoles, and because the volume of filtrate delivered to the inner MCD in the absence of vasopressin is larger than during antidiuresis, the osmolality of fluid in the lumen of the inner MCD will be low. If the osmole excretion rate in this patient is 300 mOsmol/day, and if 4 L are delivered to the inner MCD, the osmolality of the luminal fluid in the inner MCD would be 75 mOsmol/kg H_2O. Even if the medullary interstitial osmolality is substantially lower than normal—for example, 375 mOsmol/kg H_2O—there is still an enormous osmotic driving force for water reabsorption along the inner MCD because a difference of 1 mOsmol/kg H_2O generates a pressure of about 19.3 mm Hg.

A recent study suggested another mechanism for the decreased ability to excrete electrolyte-free water in patients with thiazide-induced hyponatremia, that is also independent of vasopressin. This study showed that nearly half the patients with thiazide-induced hyponatremia carry a single-nucleotide polymorphism in the prostaglandin transporter (PGT) encoded by *SLCO2A1*. Under normal conditions, the effect of vasopressin to cause the insertion of AQP2 into the luminal membrane of principal cells is counterbalanced by increased renal prostaglandin E2 (PGE2) production. PGE2 is directed to the basolateral side of the collecting duct by this prostaglandin transporter, where binding of PGE2 to its basolateral EP1 and EP3 receptors sends out signals for the retrieval of AQP2 from the apical membrane. Administration of a thiazide diuretic leads to increased PGE2 production, although the mechanism is not clear. In some patients with the SLCO2A1 variant, because of the decreased transport capacity of PGT, the concentration of PGE2 in the tubular lumen increases. Binding of PGE2 to its luminal EP4 receptors has the opposite effect and signals for the insertion of AQP2 into the apical membrane of principal cells. This results in increased water reabsorption, independently of vasopressin.[13]

What dangers should be anticipated during therapy, and how can they be avoided? Understanding this pathophysiology has clinical implications for the management of the patient with hyponatremia. Initially, this patient's hyponatremia was thought to be caused by stimulation of vasopressin release due to decreased EABV owing to her intake of a thiazide diuretic; hence, she was given isotonic saline to re-expand her EABV. Even a relatively small volume of saline (especially if it were given as a bolus) might be sufficient to reduce the fractional reabsorption of filtrate in the PT and increase its distal delivery. If the fractional reabsorption in PT were decreased to 83% of the GFR of 40 L/day, distal delivery of filtrate would increase to about 7 L/day. This may exceed the capacity for water reabsorption by RWP (or via the PGE2/EP4–mediated insertion of AQP2 into the luminal membrane of principal cells), so water diuresis would ensue. Because of the patient's small muscle mass, even a modest water diuresis might be large enough to cause a rapid rise in P_{Na} and increase the risk of osmotic demyelination syndrome, especially if she were malnourished or potassium-depleted.

POTASSIUM

Hypokalemia and hyperkalemia are common electrolyte disorders in clinical practice that may cause life-threatening cardiac arrhythmias. The analysis of the urine composition provides essential information to establish the underlying pathophysiology and plan therapy.

The regulation of K^+ homeostasis has two main aspects:

1. Control of the transcellular distribution of K^+, which is vital for survival because it limits acute changes in the P_K.
2. Regulation of K^+ excretion by the kidney, which maintains whole-body K^+ balance; this is, however, a much slower process.

TRANSCELLULAR DISTRIBUTION OF POTASSIUM

Concept 11

Three factors regulate the movement of K^+ across cell membranes—the concentration difference for K^+, the electrical voltage across cell membranes, and the presence of open K^+ channels in cell membranes.

Approximately 98% of K^+ in the body is in cells. Although the concentration difference would favor the movement of K^+ out of cells via K^+ channels in the cell membrane, K^+ ions are retained inside the cells by an electrical force because the cell interior has a negative voltage caused by the negatively charged intracellular organic phosphates. These chemical and electrical forces eventually come into balance, and the equilibrium potential for K^+ (E_K) is achieved. Because cell membranes have much higher permeability to K^+ ions than to Na^+ ions, the resting membrane potential (RMP) of cells is close to E_K.

The shift of K^+ into cells requires an increase in cell interior negative voltage. This can be achieved by increasing flux via the Na^+-K^+ adenosine triphosphatase pump (Na^+-K^+-ATPase). This is because Na^+-K^+-ATPase is an electrogenic pump that exports three Na^+ ions out of the cell while importing only two K^+ ions into the cell. Hence, activation of Na^+-K^+-ATPase leads to the net export of positive charges out of the cell. There are three ways to increase ion pumping acutely by the Na^+-K^+-ATPase:

1. A rise in the concentration of its limiting substrate—intracellular Na^+
2. An increase in the affinity (lower K_m [concentration for half-maximal activation]) for Na^+ and K^+ or an increase

in the V_{max} (maximal pump turnover rate) of the Na^+-K^+-ATPase units in cell membranes

3. An increase in the number of active Na^+-K^+-ATPase pump units in the cell membrane through the recruitment of new units

A long-term increase in Na^+-K^+-ATPase pump activity requires the synthesis of new pump units, as occurs with exercise training, excess thyroid hormones, or high dietary K^+ intake.

Insulin causes a shift of K^+ into cells as it promotes the translocation of Na^+-K^+-ATPase units from an intracellular pool to the cell membrane. Insulin causes the phosphorylation of FXYD1 (phospholemann) via atypical protein kinase C, which increases the V_{max} of Na^+-K^+-ATPase. Insulin also activates the Na^+-H^+ exchanger isoform 1 (NHE1) and hence increases the electroneutral entry of Na^+ into cells. β_2-Adrenergic agonists induce the phosphorylation of FXYD1 via cyclic adenosine monophosphate (cAMP)–mediated activation of protein kinase A. NHE1 is also activated by a rise in the intracellular H^+ concentration. Monocarboxylic acids (e.g., L-lactic acid, ketoacids) do not cause hyperkalemia. This is because they enter cells on the monocarboxylic acid cotransporter (MCT). An increase in intracellular H^+ concentration in the submembrane area where NHE1 is located may activate NHE1,which leads to an increase in the electroneutral entry of Na^+ into cells and, in the presence of insulin, a shift of K^+ into cells (Fig. 24.4).[14] A shift of K^+ out of cells may occur in patents with metabolic acidosis due to the gain of inorganic acids, which are not transported by the MCT (e.g., in patients with diarrhea causing the loss of $NaHCO_3$ [gain of HCl]).

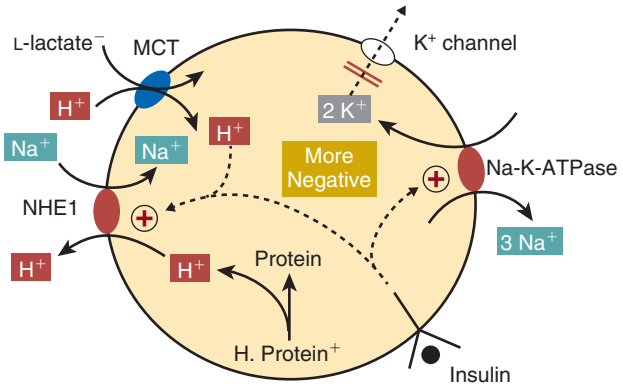

Fig. 24.4 Possible mechanism for how monocarboxylic acids may cause a shift of K^+ into cells. The *circle* represents a cell. The Na^+-H^+ exchanger isoform 1 *(NHE1)* in cell membranes is activated by insulin and by a high concentration of H^+ in the cell interior because H^+ binds to the modifier site of NHE1. The concentration of H^+ near NHE1 could rise when monocarboxylic acids (lactic acid in this example) enter cells on the monocarboxylic acid cotransporter *(MCT)* and their H^+ ions are released close to NHE1. In the presence of insulin, which activates the Na^+-K^+-ATPase and NHE1 in cell membranes, electroneutral entry of Na^+ into cells is increased. The subsequent transport of Na^+ out of cells via the electrogenic Na^+-K^+-ATPase increases the cell interior negative voltage and causes the retention of K^+ in cells. The source of bulk of H^+ ions transported out of the cell is H^+ ions that were bound to intracellular proteins (shown as H. Proteins$^+$) (From Kamel KS, Halperin ML. *Fluid, Electrolyte, and Acid-Base Physiology; A Problem-Based Approach.* ed 5. Philadelphia: Elsevier; 2017.)

RENAL EXCRETION OF POTASSIUM

Renal K^+ excretion. Control of K^+ secretion occurs primarily in the ASDN, which includes the DCT2, the connecting segment, and the CCD (see Chapter 6 for a detailed discussion). Two factors influence the rate of excretion of K^+—the net secretion of K^+ by principal cells in the ASDN, and the flow rate in the ASDN.

K^+ Secretion in the Aldosterone-Sensitive Distal Nephron

The process for secretion of K^+ by principal cells in the ASDN requires two elements.[15] First, a lumen-negative transepithelial voltage must be generated by the electrogenic reabsorption of Na^+ (i.e., reabsorption of Na^+ via the amiloride-sensitive sodium channel, ENaC, without an accompanying anion, which is usually Cl^-). Second, a sufficient number of open renal outer medullary K^+ (ROMK) channels in the luminal membranes of principal cells must be present.

Aldosterone actions lead to an increase in the number of open ENaC units in the luminal membranes of principal cells in the ASDN.

It was thought that the paracellular pathway plays an important role in the reabsorption of Cl^- in the ASDN, but the large peritubular-luminal concentration difference for Cl^- and the relatively small luminal-peritubular electrical driving force make this mechanism unlikely. An electroneutral, thiazide-sensitive, and amiloride-resistant NaCl transport process has been identified in the luminal membrane of β-intercalated cells of the CCD in mice. This seems to be mediated by the parallel activity of the Na^+-independent Cl^-/HCO_3^-exchanger (pendrin) and the Na^+-dependent Cl^-/HCO_3^- exchanger (NDCBE), resulting in electroneutral NaCl reabsorption.[16]

An increase in luminal fluid concentration of HCO_3^- and/or an alkaline luminal fluid pH seem to increase the amount of K^+ secreted in the ASDN.[17] It has been suggested that this effect might be due to a decrease in the paracellular permeability of Cl^-. A different mechanism for the effect of luminal HCO_3^- may be that because a gradient for HCO_3^- is needed to increase flux through the Cl^-/HCO_3^- exchanger; pendrin, an increase in luminal HCO_3^- concentration may inhibit flux through pendrin, and hence NDCBE, thereby decreasing the rate of electroneutral NaCl reabsorption, and in turn increasing the rate of electrogenic reabsorption of Na^+ and hence the secretion of K^+.

ROMK channels are the most important K^+ channels for the secretion of K^+ in the ASDN. Big K^+ conductance—BK or maxi-K^+—channels seem to play an important role in flow-dependent K^+ secretion, but their role in the physiologic regulation of renal excretion of K^+ and its disorders is not clear.[18]

A complex network of with-no-lysine (WNK) kinases, WNK4 and WNK1, via effects on the thiazide-sensitive NaCl cotransporter (NCC) in the DCT1 and ROMK in the ASDN, may function as a switch to change the aldosterone response of the kidney to conserve Na^+ or excrete K^+.[19] WNK4, and a full-length, kinase-active form of WNK1 (L-WNK1), can increase the activity of NCC, thereby diminishing the delivery of NaCl to the ASDN and hence the rate of electrogenic reabsorption of Na^+ and the ability to generate a large negative luminal voltage. Increasing delivery of Na^+ and hence the flow rate in the ASDN may also increase K^+ secretion via the

flow -activated BK channels. Both WNK4 and L-WNK1 also induce endocytosis of ROMK.[20] See Chapter 6 for a detailed discussion of this complex and rapidly evolving field.

Concept 12

When vasopressin acts, the flow rate in the ASDN is determined by the number of effective osmoles present in luminal fluid. Vasopressin causes the insertion of AQP2 channels into the luminal membranes of principal cells, the osmolality of fluid in the terminal CCD becomes equal to the P_{osm} and hence is relatively fixed. Therefore the number of osmoles present in the luminal fluid in the terminal CCD determines the number of liters of fluid that exit the terminal CCD. These osmoles are largely urea, Na^+, Cl^-, and K^+, with an accompanying anion. Owing to the process of intrarenal urea recycling, the largest fraction of the osmoles delivered to the ASDN is urea osmoles. In subjects eating a typical Western diet, the amount of urea that recycles would be approximately 600 mmol/day. This process of urea recycling adds an extra 2 L to the flow rate in the terminal CCD (600 mOsmol divided by a luminal fluid osmolality that is equal to plasma osmolality—that is, ≈300 mOsmol/kg H_2O).

In a quantitative analysis, Kamel and Halperin have illustrated that even in patients with a large defect in the ability to generate a lumen-negative voltage in the ASDN, a significant degree of hyperkalemia is not likely to develop with a usual K^+ intake unless there is decreased flow rate in the ASDN. Restricting protein intake may decrease the amount of urea that recycles and hence the rate of flow in the ASDN.[21]

Concept 13

There is no normal rate of K^+ excretion in the urine because normal subjects in a steady state excrete all the K^+ they eat and absorb from the GI tract. To assess the renal response to hypokalemia, we use the observed rate of excretion of K^+ in patients who developed hypokalemia due to a nonrenal cause. In subjects who became K^+-depleted because of low dietary K^+ intake, the rate of K^+ excretion fell to 10 to 15 mmol/day. In normal subjects given a large load of K^+ (>200 mmol/day) on a chronic basis, the rate of renal excretion of K^+ rose to match their intake, with only a modest rise in their P_K. Hence, the development of chronic hyperkalemia requires a defect in renal K^+ excretion.

TOOLS FOR EVALUATING A PATIENT WITH A DYSKALEMIA

Assess the Rate of Excretion of Potassium in the Urine

A 24-hour urine collection is not necessary to assess the daily rate of excretion of K^+. Taking advantage of the fact that creatinine is excreted at a near-constant rate throughout the day, we use the ratio of the concentration of K^+ in the urine (U_K) to the concentration of creatinine in the urine (U_{Cr})—U_K/U_{Cr}. This approach has the following advantages. The data can be available in a short time period, and more relevant information is gathered if one knows the stimulus, the P_K, that influences the rate of excretion of K^+ during that time frame. The limitation is that there is a diurnal variation in K^+ excretion, but this does not negate the advantages. The expected U_K/U_{Cr} in patients with hypokalemia due to an intracellular shift of K^+ and in those with chronic hypokalemia due to extrarenal loss of K^+ is less than 18 mmol K^+/g creatinine or less than 2 mmol K^+/mmol creatinine. The expected ratio in a patient with hyperkalemia and a normal renal response is more than 200 mmol K^+/g creatinine or more than 20 mmol K^+/mmol creatinine. To develop *chronic* hyperkalemia, however, one must have a defect in the renal excretion of K^+; hence, U_K/U_{Cr} does not provide clinically useful information in that situation. Because of diurnal variation in K^+ excretion, a 24-hour urine collection, rather than a random U_K/U_{Cr}, may be needed to assess the contribution of dietary K^+ intake to the degree of hyperkalemia.

Transtubular Potassium Concentration Gradient

The transtubular potassium concentration gradient (TTKG) was developed to provide a semiquantitative reflection of the driving force for K^+ secretion in the ASDN. The rationale behind this calculation was to adjust U_K for the amount of water that was reabsorbed in downstream nephron segments (i.e., the MCD) to estimate the concentration of K^+ in the luminal fluid in the terminal CCD (K_{CCD}) .To calculate the [K_{CCD}], we suggested dividing the U_K by the ratio of U_{osm} to the P_{osm} (U_{osm}/P_{osm}) because the osmolality in the luminal fluid in the terminal CCD should be equal to P_{osm} when vasopressin causes the insertion of AQP2 into the luminal membranes of principal cells in the CCD.

The assumption made with use of the U_{osm}/P_{osm} ratio is that most of the osmoles delivered to the MCD are not reabsorbed in this nephron segment, and therefore the rise in osmolality from its value in the terminal CCD and its value in the urine reflects water reabsorption in the MCD. Although the amount of electrolytes reabsorbed in the MCD should not pose a problem, this is not true for urea because of intrarenal urea recycling. We estimated that in subjects eating a typical Western diet, almost 600 mmol of urea is reabsorbed downstream from the CCD/day. It follows that the calculated K_{CCD} obtained from ($U_K \div [U_{osm}/P_{osm}]$) is likely to be appreciably higher than the actual value in vivo.[21] Therefore we no longer use the TTKG in the clinical assessment of patients with dyskalemia. Rather, we use the U_K/U_{Cr} ratio to provide the information needed to assess the renal response in these patients.

Establishing the Basis for the Abnormal Rate of Excretion of Potassium. In a patient with hypokalemia, a higher than expected rate of excretion of K^+ implies that there is a higher lumen-negative voltage in the ASDN, and that open ROMK channels are present in the luminal membranes of principal cells. The higher lumen-negative voltage is due to a higher rate of electrogenic Na^+ reabsorption in the ASDN. The converse is true in a patient with hyperkalemia, in whom there is a lower than expected rate of excretion of K^+.

The clinical indices that help in the differential diagnosis of the pathophysiology of the abnormal rate of electrogenic reabsorption of Na^+ in the ASDN are an assessment of the EABV and the presence or absence of hypertension. The measurement of the plasma renin concentration or activity (P_{Renin}) and the plasma aldosterone concentration (P_{Aldo}) are helpful in in this differential diagnosis (Table 24.4).

Table 24.4 Use of Plasma Renin and Plasma Aldosterone Values to Assess the Basis of Hypokalemia or Hyperkalemia

Parameter	Renin Value	Aldosterone Value
Lesions That Cause Hypokalemia		
Adrenal Gland		
• Primary hyperaldosteronism	Low	High
• Glucocorticoid-remediable hyperaldosteronism	Low	High
Kidney		
• Renal artery stenosis	High	High
• Malignant hypertension	High	High
• Renin-secreting tumor	High	High
• Liddle syndrome	Low	Low
• Disorders involving 11β-hydroxysteroid dehydrogenase-2	Low	Low
Lesions That Cause Hyperkalemia		
Adrenal Gland		
Addison disease	High	Low
Kidney		
Pseudohypoaldosteronism type 1	High	High
Hyporeninemic hypoaldosteronism	Low	Low

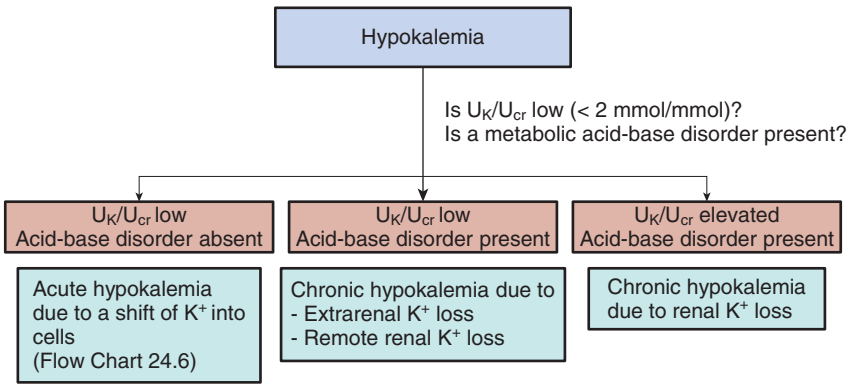

Flow Chart 24.5 (From Kamel KS, Halperin ML. *Fluid, Electrolyte, and Acid-Base Physiology; A Problem-Based Approach.* ed 5. Philadelphia: Elsevier; 2017.)

CLINICAL APPROACH TO THE PATIENT WITH HYPOKALEMIA

Step 1. Deal With Medical Emergencies That May Be Present on Presentation, and Anticipate and Prevent Risks That May Arise During Therapy

The major emergencies related to hypokalemia are cardiac arrhythmias and respiratory muscle weakness leading to respiratory failure. Patients with chronic hyponatremia and hypokalemia are also at a high risk for the development of osmotic demyelination, with a rapid rise in P_{Na}. Administration of KCl may lead to a rapid rise in P_{Na}[22] because K^+ ions enter and Na^+ ions leave muscle cells. This movement of Na^+ ions into the ECF compartment may also expand the EABV, leading to an increase in distal delivery of filtrate, resulting in water diuresis.

Step 2. Determine Whether the Basis for Hypokalemia Is an Acute Shift of Potassium Into Cells

A low rate of excretion of K^+ (U_K/U_{Cr} <18 mmol of K^+/g of creatinine or <2 mmol of K^+/mmol of creatinine) and the absence of a metabolic acid-base disorder suggest that the major basis of hypokalemia is an acute shift of K^+ into cells (Flow Chart 24.5).[23]

Having established that the major pathophysiology of the hypokalemia is an acute shift of K^+ into cells, the next step is to determine whether an adrenergic surge may have caused this shift of K^+ (Flow Chart 24.6). In these settings, tachycardia, a wide pulse pressure, and systolic hypertension are often present. It is very important to recognize patients with these features because the administration of nonspecific beta-blockers can lead to a very rapid recovery without the

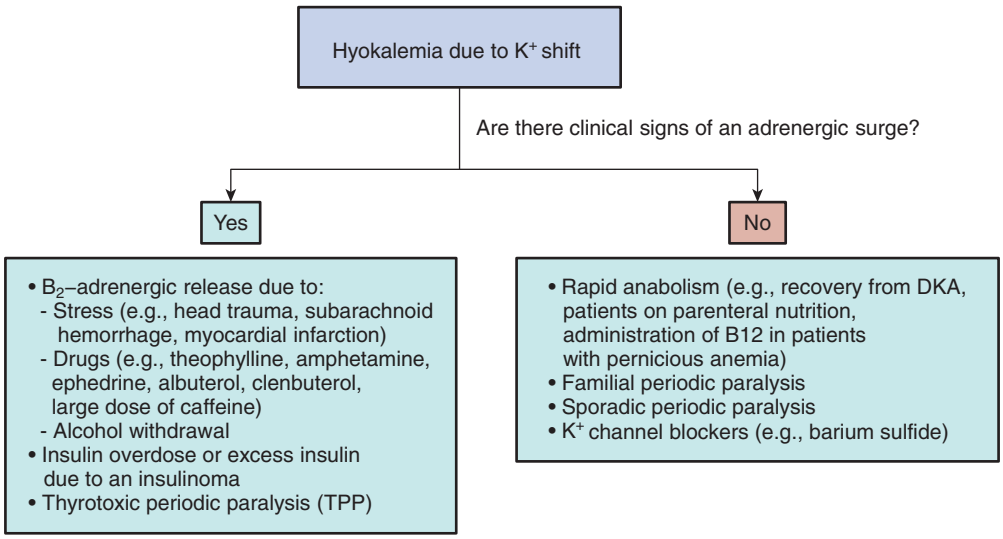

Flow Chart 24.6 *DKA,* Diabetic ketoacidosis. (From Kamel KS, Halperin ML. *Fluid, Electrolyte, and Acid-Base Physiology; A Problem-Based Approach.* ed 5. Philadelphia: Elsevier; 2017.)

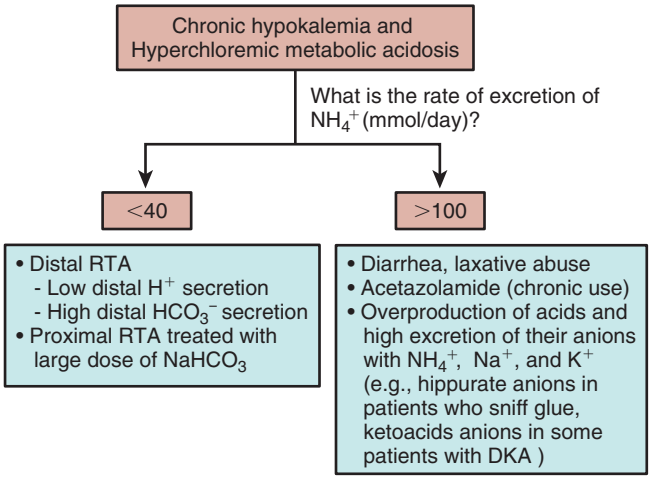

Flow Chart 24.7 *DKA,* Diabetic ketoacidosis; *RTA,* renal tubular acidosis. (From Kamel KS, Halperin ML. *Fluid, Electrolyte, and Acid-Base Physiology; A Problem-Based Approach.* ed 5. Philadelphia: Elsevier; 2017.)

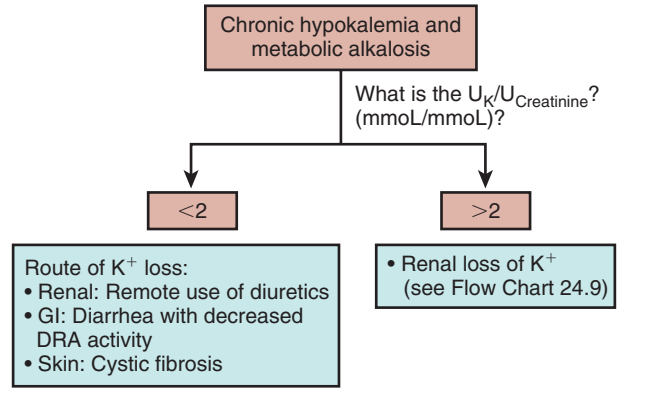

Flow Chart 24.8 *DRA,* Downregulated in adenoma Cl^-/HCO_3^- exchanger; *GI,* gastrointestinal. (From Kamel KS, Halperin ML. *Fluid, Electrolyte, and Acid-Base Physiology; A Problem-Based Approach.* ed 5. Philadelphia: Elsevier; 2017.)

administration of a large amount of KCl and hence avoid the risk of the development of rebound hyperkalemia when the stimulus for shift of K^+ ions abates.[24]

Step 3. Examine the Acid-Basis Status in the Patient With Chronic Hypokalemia

In the patient with chronic hypokalemia, the first step is to examine the acid-base status in plasma.

Subgroup With Metabolic Acidosis. The group of patients with metabolic acidosis (usually hyperchloremic metabolic acidosis) can be divided into two categories according to the rate of excretion of NH_4^+ in the urine (Flow Chart 24.7). The rate of excretion of NH_4^+ can be estimated with use of the urine osmolal gap (see discussion of metabolic acidosis).

Subgroup With Metabolic Alkalosis. The first step in the patient with metabolic alkalosis is to determine whether the site of loss of K^+ is renal or extrarenal on the basis of the assessment of the rate of renal excretion of K^+ using the U_K/U_{Cr} (Flow Chart 24.8). Patients with a low value for this ratio (i.e., <18 mmol of K^+/g of creatinine or <2 mmol of K^+/mmol of creatinine) have conditions with loss of K^+ via nonrenal routes, such as in sweat (e.g., patients with cystic fibrosis) or via the GI tract (e.g., patients with diarrhea associated with decreased activity of the colonic luminal Cl^-/HCO_3^- exchanger, DRA, such as congenital chloridorrhea, villous adenoma, and some patients with laxative abuse). On the other hand, patients in whom the U_K/U_{Cr} is higher than these values have a condition associated with a renal loss of K^+.[24a] The steps to take to determine the underlying pathophysiology in this latter group of patients are outlined in Flow Chart 24.9.

In essence, we are trying to determine the cause of a higher rate of electrogenic reabsorption of Na^+ in the ASDN. The

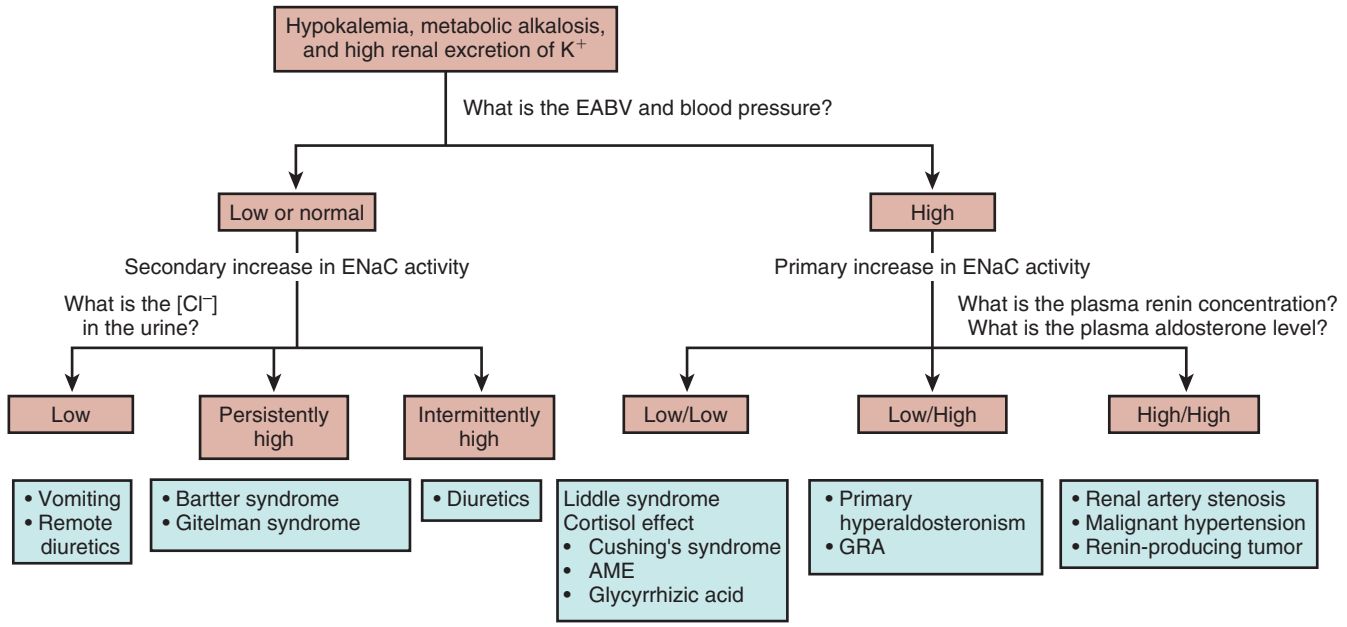

Flow Chart 24.9 *AME,* Apparent mineralocorticoid excess syndrome; *EABV,* effective arterial blood volume; *GRA,* glucocorticide remediable aldosteronism. (From Kamel KS, Halperin ML. *Fluid, Electrolyte, and Acid-Base Physiology; A Problem-Based Approach.* ed 5. Philadelphia: Elsevier; 2017.)

primary reason is an increased number of open ENaC units in the luminal membranes of principal cells in the ASDN. This increase could be due to two groups of disorders.

The first group involves a secondary increase in ENaC activity due to the release of aldosterone in response to a low EABV. Patients with these disorders are not likely to have high blood pressure. The most common causes are vomiting and the use of diuretic agents. In some patients, the diuretic effect may be due to an inherited disorder affecting NaCl reabsorption in the medullary TAL (i.e., Bartter syndrome) or in the DCT (i.e., Gitelman syndrome). Ligands that occupy the calcium-sensing receptor in the medullary TAL (e.g., ionized calcium in a patient with hypercalcemia), drugs (e.g., gentamicin, cisplatin), and possibly cationic proteins (e.g., cationic monoclonal immunoglobulins in a patient with multiple myeloma) could potentially mimic Bartter syndrome. The use of urine electrolyte values in the differential diagnosis of hypokalemia in a patient with a contracted EABV is summarized in Table 24.3. It is currently recommended that hypertensive patients who develop hypokalemia while taking diuretics be screened for primary hyperaldosteronism.

The second group of disorders involves conditions that are associated with a primary increase in ENaC activity (e.g., primary hyperreninemic hyperaldosteronism, primary hyperaldosteronism, disorders in which cortisol acts as a mineralocorticoid in the ASDN, or a constitutively active ENaC in the luminal membrane of principal cells in the ASDN). The EABV in these patients is not low, and the blood pressure is commonly high.

In some patients a decreased rate of electroneutral Na^+ reabsorption may contribute to the increased rate of electrogenic Na^+ reabsorption and enhanced kaliuresis. This may be the case when Na^+ is delivered to the ASDN with little Cl^- (e.g., delivery of Na^+ with HCO_3^- in a patient with recent vomiting or with an anion of a drug such as penicillin).

Magnesium (Mg^{2+}) deficiency is frequently associated with hypokalemia. This relationship is largely due to the underlying disorders that cause losses of both Mg^{2+} and K^+ (e.g., diarrhea, diuretic therapy, Gitelman syndrome). K^+ secretion in the ASDN is mediated by ROMK, a process that is inhibited by intracellular Mg^{2+}. A decrease in intracellular Mg^{2+}, caused by Mg^{2+} deficiency, releases the Mg^{2+}-mediated inhibition of ROMK. Mg^{2+} deficiency alone, however, does not necessarily cause hypokalemia, because an increase in the rate of electrogenic reabsorption of Na^+ is required to enhance the rate of secretion of K^+.

CLINICAL CASE 7: HYPOKALEMIA AND A LOW RATE OF POTASSIUM EXCRETION

A 28-year-old Asian woman presented with sudden onset of generalized muscle weakness and inability to ambulate on awakening one morning. She had lost 7 kg of body weight in the last 2 months but denied nausea, vomiting, diarrhea, or the use of diuretics, laxatives, exogenous thyroid hormone, herbal medications, or illicit drugs. The attack was not preceded by strenuous exercise or the consumption of a carbohydrate-rich meal. She had no family history of hypokalemia, periodic paralysis, or hyperthyroidism. On physical examination, she was alert and oriented; blood pressure was 150/70 mm Hg, heart rate was 116 beats/min, and respiratory rate was 18 breaths/min. The thyroid gland was not obviously enlarged, and there was no exophthalmos. Symmetric flaccid paralysis with areflexia was present in all four limbs. The remainder of the physical examination was unremarkable. The pH and P_{CO_2} values shown in the following table of laboratory findings were from an arterial blood sample,

whereas all other blood data were from a venous blood sample. The electrocardiogram (ECG) showed sinus tachycardia and prominent U waves.

Findings	*Blood*	*Urine*
K^+, mmol/L	1.8	12
Creatinine	0.7 mg/dL (62 µmol/L)	1.9 g/L (16.8 mmol/L)
Na^+, mmol/L	140	179
Cl^-, mmol/L	108	184
pH	7.41	—
P_{CO_2}, mm Hg	36	—
HCO_3^-, mmol/L	23	—
Glucose, mg/dL	112	0

Questions and Discussion

Is there a medical emergency? Because the ECG did not show changes due to hypokalemia other than U waves, and because respiratory muscle weakness causing hypoventilation was not present, as assessed from the arterial P_{CO_2}, there were no emergencies related to hypokalemia at this time.

What is the basis of the hypokalemia? A U_K/U_{Cr} ratio less than 1 (mmol/mmol) and the absence of a metabolic acid-base disorder on presentation suggest that the basis of the severe hypokalemia in this patient was an acute shift of K^+ into cells.

Possible reasons for potassium shift into cells: The presence of tachycardia, systolic hypertension, and wide pulse pressure suggest that an adrenergic surge was the cause of the acute shift of K^+ into cells. On further laboratory testing, she was found to have hyperthyroidism, so the diagnosis was thyrotoxic periodic paralysis (TPP). Patients with TPP often have only subtle signs and symptoms of thyrotoxicosis. In contrast to standard teaching, most patients with TPP do not have clear precipitating factors such as strenuous exercise or the consumption of a carbohydrate-rich meal. Increased Na^+-K^+-ATPase activity has traditionally been implicated in the pathogenesis of TPP. Studies have shown that susceptibility to TPP can be conferred by mutations in the skeletal muscle–specific, inward-rectifying K^+ (Kir) channel, Kir2.6.

What are the options for therapy? The patient received intravenous KCl at a rate of 10 mmol/hour by the administration of a solution of 0.9% saline with 40 mEq/L KCl at a rate of 250 mL/hour. In a patient with severe hypokalemia, one should not use a dextrose-containing solution because this may cause the release of insulin, which could induce a further shift of K^+ into cells and aggravate the severity of hypokalemia. Although she received only 80 mmol of KCl, rebound hyperkalemia (P_K, 5.7 mmol/L) developed; the P_K returned to normal 6 hours later. Studies have suggested that hypokalemia in patients with TPP can be rapidly corrected without the risk of rebound hyperkalemia by the administration of a nonselective beta-blocker and only a small dose of KCl.

CLINICAL CASE 8: HYPOKALEMIA AND HIGH RATE OF POTASSIUM EXCRETION

Progressive muscle weakness developed over the last 6 hours in a 76-year-old Asian man that became so severe that he was unable to move. He reported that he exercised that morning and ate a large carbohydrate meal for breakfast, which he usually does after he has a good exercise session. He had no other neurologic symptoms. He denied vomiting, or diarrhea, or the use of diuretics or laxatives. Hypokalemia (P_K, 3.3 mmol/L) and hypertension had been noted 1 year ago but had not been investigated further. On this admission, his blood pressure was 160/96 mm Hg and his heart rate was 70 beats/min. A neurologic examination revealed symmetric flaccid paralysis with areflexia but no other findings. The laboratory data prior to therapy are shown in the following table. The pH and P_{CO_2} values are from an arterial blood sample. Results of measurement of the P_{Renin} and P_{Aldo}, which became available later, showed that both levels were low. The plasma cortisol value was in the normal range.

Findings	*Blood*	*Urine*
K^+, mmol/L	1.8	26
Na^+, mmol/L	147	132
Cl^-, mmol/L	90	138
Creatinine	0.8 mg/dL (70 µmol/L)	0.6 g/L (5.3 mmol/L)
pH	7.55	
P_{CO_2}, mm Hg	40	—
HCO_3^-, mmol/L	45	0
Osmolality, mOsm/kg H_2O	302	482

Questions and Discussion

What is the cause of hypokalemia in this patient? In the presence of hypokalemia, the U_K/U_{Cr} was 5 (mmol/mmol), and metabolic alkalosis was also present. Hence, the hypokalemia was largely due to a disorder that caused excessive loss of K^+ in the urine. The acute presentation with extreme weakness was likely due to an acute shift of K^+ into cells in conjunction with a chronic disorder that caused the loss of K^+. This component, of an acute shift of K^+ into cells, was attributed to the predominant β_2-adrenergic effect during rest after vigorous exercise, and the release of insulin due to the large carbohydrate intake during breakfast prior to the onset of symptoms.

On clinical assessment, the patient's EABV volume was thought not to be contracted, and he had hypertension. Therefore, the increased electrogenic reabsorption of Na^+ in the ASDN was due to a primary increase in ENaC activity. The differential diagnosis was guided by measurements of the P_{Renin} and P_{Aldo} (see Table 24.4). Because both the P_{Aldo} and P_{Renin} were suppressed, the differential diagnosis was between disorders in which cortisol acts as mineralocorticoid and those with constitutively active ENaC in the luminal membranes of principal cells in the ASDN. Inherited disorders in which ENaC is constitutively active (Liddle syndrome) seemed unlikely, considering the patient's age. Plasma cortisol values were not elevated. Computed tomography of the chest did not show a lung mass. Although the patient denied consuming licorice or chewing tobacco, it turned out that he used an herbal preparation containing large amounts of glycyrrhizic acid (the active ingredient in licorice) to sweeten his tea. The patient was treated initially with intravenous KCl; the weakness improved when the P_K reached 2.5 mmol/L. Oral KCl supplementation was continued. Two weeks later, P_K and blood pressure values returned to normal levels, and his body weight had decreased from 78 to 74 kg as a result of natriuresis after stopping the glycyrrhizic acid–containing herbal preparation.

CLINICAL APPROACH TO THE PATIENT WITH HYPERKALEMIA

Step 1. Address Emergencies

Hyperkalemia constitutes a medical emergency, primarily because of its effect on the heart, which may lead to cardiac conduction abnormalities, arrhythmias and, ultimately, asystole.

Step 2. Determine Whether the Cause of the Hyperkalemia Is an Acute Shift of Potassium Out of Cells in vivo or Pseudohyperkalemia

Flow Chart 24.10 illustrates the initial approach for determining the cause of the hyperkalemia. If the time course for the development of hyperkalemia was short and/or the hyperkalemia developed while the intake of K^+ was low, then the following three categories should be considered.

Destruction of Cells in the Body. Cell destruction could be due, for example, to rhabdomyolysis or tumor lysis syndrome.

Shift of K^+ Out of Cells in the Body. Shift of K^+ out of cells in the body may occur in conditions in which there is a less negative voltage in cells. Such conditions include lack of a stimulus for Na^+-K^+-ATPase (e.g., lack of insulin in patients with diabetic ketoacidosis [DKA], β_2-adrenergic blockade), and conditions in which there is an α-adrenergic surge causing inhibition of the release of insulin or directly causing a shift of K^+ out of hepatic cells. Digoxin inhibits Na^+-K^+-ATPase, so digoxin overdose can result in hyperkalemia. A shift of K^+ may also occur in conditions with metabolic acidosis due to nonmonocarboxylic acids—that is, acids that cannot be transported on the MCT (e.g., metabolic acidosis due to a gain of HCl from loss of $NaHCO_3$ in a patient with diarrhea, ingestion of citric acid). Acute hyperkalemia may occur during exhaustive exercise or in patients with status epilepticus. Severe hyperkalemia has been described as a complication of the administration of mannitol for the treatment or prevention of cerebral edema. This is because a rise in effective osmolality in the interstitial fluid causes the movement of water out of cells via AQP channels in cell membranes, which raises the concentration of K^+ in the ICF and provides a chemical driving force for the movement of K^+ out of cells. Succinylcholine depolarizes muscle cells, resulting in the efflux of K^+ through acetylcholine receptors in conditions that may lead to the upregulation of acetylcholine receptors (e.g., burns, neuromuscular injury [upper or lower motor neuron], disuse atrophy, prolonged immobilization). Fluoride can open the Ca^{2+}-sensitive K^+ channels; as a result, fluoride intoxication can lead to fatal hyperkalemia. A positive family history for acute hyperkalemia suggests that there may be a molecular basis for this disorder (e.g., hyperkalemic periodic paralysis).

Pseudohyperkalemia May Be Present. The presence of changes in the ECG related to hyperkalemia rules out pseudohyperkalemia as the sole cause of the hyperkalemia. Pseudohyperkalemia is caused by the release of K^+ during or after venipuncture. Excessive fist clenching during blood sampling may increase K^+ release from local muscle and thus may raise the measured P_K by as much as 1 mmol/L. Pseudohyperkalemia can be present in cachectic patients in whom the normal T tubule architecture in skeletal muscle may be disturbed. Mechanical trauma to red blood cells

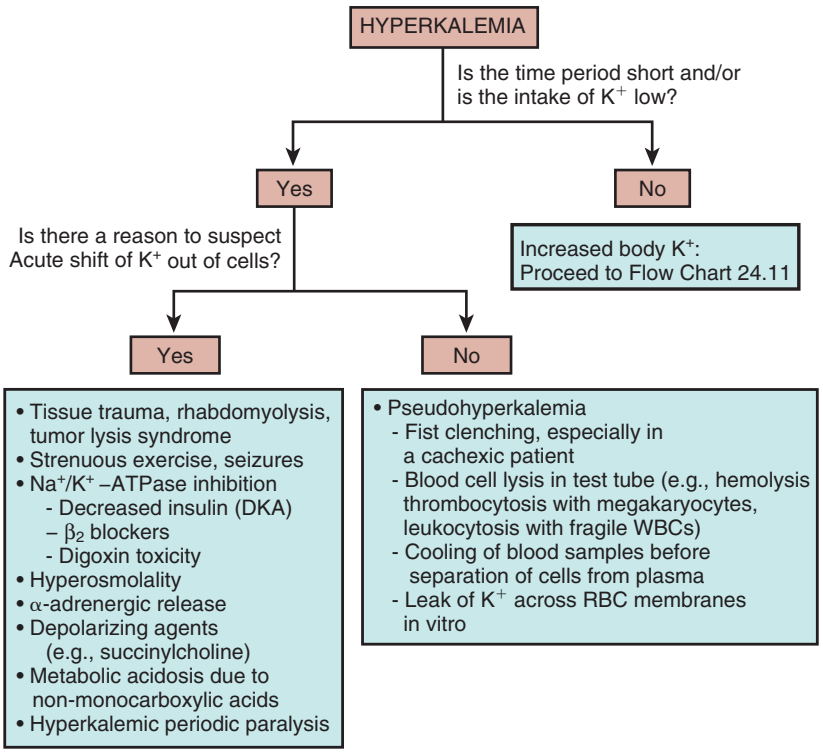

Flow Chart 24.10 *DKA,* Diabetic ketoacidosis; *RBC,* red blood cells; *WBC,* white blood cells. (From Kamel KS, Halperin ML. *Fluid, Electrolyte, and Acid-Base Physiology; A Problem-Based Approach.* ed 5. Philadelphia: Elsevier; 2017.)

during venipuncture, due for example to the use of a very small-gauge needle, can result in their hemolysis and the release of K^+ in the test tube. K^+ ions are normally released from platelets during blood clotting, so pseudohyperkalemia may be noted in patients with thrombocytosis (especially with megakaryocytosis). Pseudohyperkalemia may also be present in patients with severe leukocytosis, especially due to fragile leukemia cells, because of the breakdown of cells during venipuncture, when shaken by pneumatic transport, or during centrifugation. Cooling of blood prior to the separation of cells from plasma is another cause of pseudohyperkalemia. There are several hereditary subtypes of pseudohyperkalemia caused by an increase in passive K^+ permeability of erythrocytes. The P_K increases in blood samples from patients with this disorder when left at room temperature.

Step 3. What Is the Rate of Potassium Excretion?

In a patient with chronic hyperkalemia, pseudohyperkalemia should be ruled out first. In normal subjects, a K^+ load can augment the rate of excretion of K^+ to more than 200 mmol/day, with only a modest increase in P_K. Thus, patients with chronic hyperkalemia generally have some defect in renal K^+ excretion. In a steady state, they excrete what they eat (minus the amount of K^+ lost in stool), but at the expense of maintaining hyperkalemia. Therefore, the value of assessing the rate of K^+ excretion is primarily to determine the contribution of K^+ intake to the degree of hyperkalemia. A 24-hour urine collection is necessary for this purpose, rather than determination of U_K/U_{Cr} in a spot urine sample, because of the diurnal variation in K^+ excretion.

Step 4. What Is the Basis for the Defect in Renal Potassium Excretion?

The clinical approach to determine the basis for the renal defect in K^+ excretion is illustrated in Flow Chart 24.11. More than one cause may be present in a single patient (e.g., intake of a drug that blocks the renin-angiotensin-aldosterone system [RAAS] in a patient with chronic renal insufficiency).

Does the Patient Have Advanced Chronic Renal Failure? The estimated GFR is generally less than 15 ml/minute if this is the sole cause of hyperkalemia.

Is the patient taking drugs that interfere with the renal excretion of potassium? Drugs that may interfere with the renal excretion of K^+ include inhibitors of the RAAS axis, inhibitors of ENaC (including amiloride, trimethoprim, and

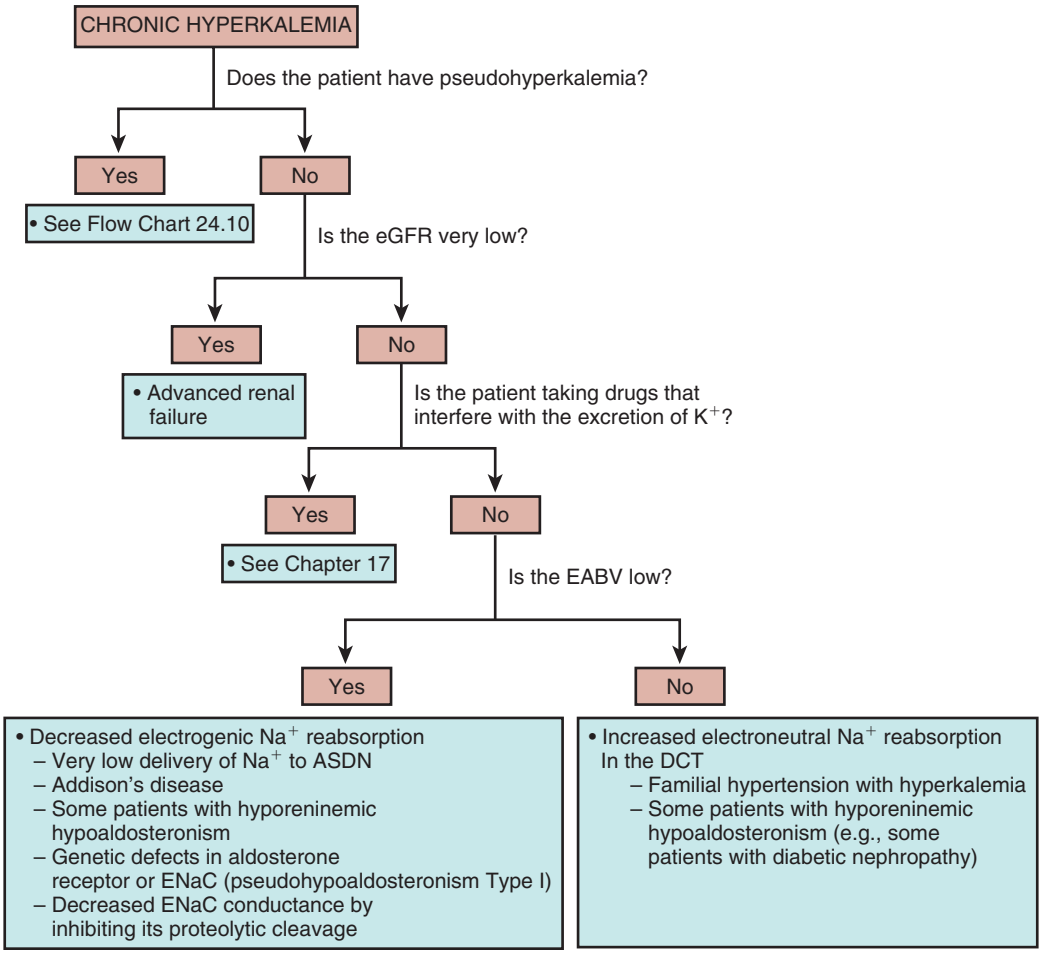

Flow Chart 24.11 *ASDN,* Aldosterone sensitive distal nephron; *DCT,* distal convoluted tubule; *EABV,* effective arterial blood volume; *eGFR,* estimated glomerular filtration rate; *ENaC,* epithelial sodium channel. (From Kamel KS, Halperin ML. *Fluid, Electrolyte, and Acid-Base Physiology; A Problem-Based Approach.* ed 5. Philadelphia: Elsevier; 2017.)

pentamidine), and serine protease inhibitors that interfere with activation of ENaC via proteolytic cleavage (nafamostat). See Chapter 17 for further discussion.

Does the Patient Have a Disorder That Leads to Diminished Reabsorption of Sodium via ENaC in the ASDN? One subgroup of patients may have a very low delivery of Na^+ to the ASDN due to marked decrease in the EABV. A second subgroup consists of patients who have lesions that lead to a diminished number of open ENaC units in the luminal membranes of principal cells in the ASDN. This includes patients who have hypoaldosteronism (e.g., adrenal insufficiency) and those with molecular defects that involve the aldosterone receptor or ENaC. Patients in this subgroup have a low EABV, higher than expected rates of excretion of Na^+ and Cl^- in a setting of low EABV and a high P_{Renin}. The P_{Aldo} is helpful to determine the reason for this diminished Na^+ reabsorption via ENaC in the ASDN.

A subset of patients with hypoaldosteronism has low P_{Renin} (hyporeninemic hypoaldosteronism) and a low EABV. Their lesions may be destruction of or a biosynthetic defect in the juxtaglomerular apparatus, leading to a low P_{Renin} and thereby a low P_{Aldo}. Patients with such disorders are expected to have a significant rise in U_K/U_{Cr} with the administration of exogenous mineralocorticoids for several days.

Does the Patient Have a Disorder That Increases Electroneutral Sodium Reabsorption in the Distal Convoluted Tubule? In this group of patients, the site of the lesion is the DCT1, where there is increased reabsorption of Na^+ and Cl^- via NCC, due to its activation by WNK4 or L-WNK1. Suppression of release of aldosterone by an expanded EABV leads to a diminished number of open ENaC units in the luminal membranes of principal cells in the ASDN. This, together with decreased delivery of Na^+ from the DCT lumen to the ASDN, and also a decreased flow rate, abrogates electrogenic Na^+ reabsorption and flow-induced K secretion (see Chapter 6). These kinases also cause endocytosis of ROMK from the luminal membranes of principal cells in the ASDN. Such patients tend to have an expanded EABV, hypertension, and suppressed P_{Renin} and P_{Aldo} (hyporeninemic hypoaldosteronism). Patients with this pathophysiology are expected to show a good response to the administration of thiazide diuretics in terms of lowering of blood pressure and correction of hyperkalemia.

The clinical picture in patients with the syndrome of familial hyperkalemia with hypertension (also known as pseudohypoaldosteronism type II or Gordon syndrome) resembles that of a gain-of-function in the thiazide-sensitive NCC. Major deletions in the gene encoding for WNK1 and missense mutations in the gene encoding for WNK4 have been reported in these patients.[25] A set of clinical findings similar to those in patients with familial hyperkalemia with hypertension may occur in other patients, most commonly those with diabetic nephropathy.[20] Support for the hypothesis that suppression of renin release in these patients is the result of EABV expansion are the findings that circulating atrial natriuretic peptide blood levels are elevated in these patients and many show response to NaCl restriction or furosemide therapy with an increased P_{Renin}. Another example of this pathophysiology is the hyperkalemia in patients treated with calcineurin inhibitors.[26]

Does the Patient Have a Disorder That Increases Electroneutral Reabsorption of Sodium in the Cortical Collecting Duct? We hypothesize that the pathophysiology of the hyperkalemia in some patients may be due to increased electroneutral Na^+ reabsorption in the CCD via parallel increases in the transport activity of pendrin and the NDCBE. This may be the pathophysiology for what used to be thought of as chloride shunt disorder.[27] These patients will also have an expanded EABV and suppressed P_{Renin} and P_{Aldo} (hyporeninemic hypoaldosteronism). Increasing the concentration of HCO_3^- in the luminal fluid in the CCD my diminish flux through pendrin and thereby NDCBE. Hence we speculate that this subset of patients may be more responsive, in terms of increasing K^+ excretion, to the induction of bicarbonaturia by the administration of the carbonic anhydrase inhibitor acetazolamide than to the administration of thiazide diuretics. This speculation, however, needs to be examined in a clinical study.

Step 5. Is a Low Flow Rate in the ASDN Contributing to Hyperkalemia?

Because of the process of intrarenal urea recycling, a large fraction of the osmoles delivered to the ASDN is urea osmoles. A low protein intake may decrease the amount of urea that recycles and hence the rate of flow in the ASDN. The usual rate of excretion of urea in subjects consuming a typical Western diet is about 400 mmol/day. If the rate of excretion of urea is appreciably lower than that, a low flow rate in the ASDN may be a contributing factor to the degree of hyperkalemia.

CLINICAL CASE 9: HYPERKALEMIA IN A PATIENT TAKING TRIMETHOPRIM

Pneumocystis jiroveci pneumonia (PJP) developed in a 35-year-old cachectic man with human immunodeficiency virus (HIV) infection. On admission, he was febrile, there were no physical findings indicating contraction of his EABV volume, and all plasma electrolyte values were in a normal range. He was treated with cotrimoxazole (sulfamethoxazole and trimethoprim). Three days later, he was noted to have low blood pressure, his EABV was low, and his P_K rose to 6.8 mmol/L. An ECG showed tall, peaked, narrow-based T waves. The urine volume was 0.8 L/day, and the U_{osm} value was 350 mOsmol/kg H_2O; other laboratory findings were as follows.

Findings	*Blood*	*Urine*
K^+, mmol/L	6.8	14
Na^+, mmol/L	130	60
Cl^-, mmol/L	105	43
Creatinine	0.9 mg/dL	0.8 g/L
pH	7.30	—
P_{CO_2}, mm Hg	30	—
HCO_3^-, mmol/L	15	0
Urea	BUN: 14 mg/dL	Urea concentration: 280 mmol/L

Questions and Discussion

What is the cause of hyperkalemia in this patient? The steps to follow are provided in Flow Charts 24.10 and 24.11. Although an element of pseudohyperkalemia could have been present because of repeated fist clenching during

venipuncture in this cachectic patient, the ECG changes indicated that he had true hyperkalemia.

Is the time course for the development of hyperkalemia short and/or did hyperkalemia develop while the intake of K^+ was low? The U_K was 14 mmol/L, and his rate of excretion of K^+ was extremely low in the presence of hyperkalemia (U_K/U_{Cr} of 17.5 [mmol K^+/g creatinine]), so one might conclude that the major basis for the hyperkalemia is the low rate of K^+ excretion. This severe degree of hyperkalemia developed over a relatively short period of time, and while the patient was consuming very little K^+. Therefore, a shift of K^+ from cells rather than a large positive external balance for K^+ is likely the major cause of hyperkalemia. The cause of this exit of K^+ from cells could be inhibition of the release of insulin by the α-adrenergic effect of adrenaline released in response to the low EABV. Nevertheless, he also had a large defect in renal K^+ excretion. Because the EABV was low and U_{Na} and U_{Cl} were inappropriately high in the presence of a contracted EABV, the low U_K/U_{Cr} was due to diminished reabsorption of Na^+ in the ASDN (see Flow Chart 24.11). The initial diagnosis was adrenal insufficiency due to an infection in a patient with HIV. However, plasma cortisol was measured and was appropriately high. In addition, there was no increase in U_K/U_{cr} in response to the administration of an exogenous mineralocorticoid. It was concluded that the diminished Na^+ reabsorption in the ASDN was due to inhibition of ENaC by the trimethoprim that was used to treat the PJP. Both the P_{Renin} and P_{Aldo} were high (results became available later), as expected in this setting (see Table 24.4).

Interpretation. Renal salt wasting due to blockade of ENaC by trimethoprim led to the development of a contracted EABV. The major cause of hyperkalemia was a shift of K^+ out of cells, probably because of inhibition of insulin release by the binding of catecholamines, released in response to the low EABV, to pancreatic islet cell α-adrenergic receptors. Blockade of ENaC by trimethoprim diminished the rate of electrogenic Na^+ reabsorption in the ASDN and the generation of lumen-negative voltage for K^+ secretion. Because of the low EABV and the low intake of proteins, there was a low rate of flow in the ASDN. This, in addition to diminishing the rate of K^+ excretion, caused the concentration of trimethoprim to be higher in the lumen of the ASDN; hence, trimethoprim became a more effective blocker of ENaC.

What are the implications of the pathophysiology of hyperkalemia for the choice of treatment in this patient? Because of the presence of changes in the ECG related to hyperkalemia, insulin (with glucose to prevent hypoglycemia) was given to induce a shift of K^+ into cells. The patient was given saline to expand his EABV, which would also suppress the release of catecholamines and remove the α-adrenergic inhibition of insulin release. Because the basis of hyperkalemia in this patient is a shift of K^+ out of cells, inducing a large loss of K^+ is not needed because there is no total body K^+ surplus. The question arose, thereafter, as to whether trimethoprim should be discontinued. Because the drug was needed to treat the PJP, a means to remove its renal ENaC-blocking effect was sought. The concentration of trimethoprim would fall in the lumen of the ASDN if the flow rate in the ASDN were to rise through an increase in the number of osmoles delivered to this nephron segment. To achieve this aim, one could increase the delivery of NaCl to the ASDN by inhibiting the reabsorption of Na^+ and Cl^- in the TAL of the loop of Henle using a loop diuretic, plus the infusion of enough NaCl to prevent EABV contraction. Because it is the cationic form of trimethoprim that blocks ENaC, increasing the delivery of HCO_3^- to the ASDN by inhibiting its reabsorption in the PT with administration of the carbonic anhydrase IV inhibitor acetazolamide could also be considered to lower the concentration of H^+ in the luminal fluid in the ASDN and thereby the concentration of the cationic form of the drug. Enough $NaHCO_3$ should be given to prevent the development of metabolic acidosis.

CLINICAL CASE 10: CHRONIC HYPERKALEMIA IN A PATIENT WITH TYPE 2 DIABETES MELLITUS

A 50-year-old man with a history of type 2 diabetes mellitus was referred for investigation of hyperkalemia; his P_K ranged from 5.5 to 6 mmol/L in a number of measurements that were done over the last several weeks. He was previously taking an angiotensin-converting enzyme (ACE) inhibitor for the treatment of hypertension, this medication was discontinued but hyperkalemia persisted. He is currently taking amlodipine, 10 mg, once a day. He was noted to have microalbuminuria but no other history of macrovascular or microvascular disease related to diabetes mellitus. On physical examination, his blood pressure was 160/90 mm Hg, his jugular venous pressure was about 2 cm above the level of the sternal angle, and he had pitting edema of the ankles bilaterally. Results of laboratory investigations were as follows:

Parameter	*Findings*
P_{Na}, mmol/L	140
P_K, mmol/L	5.7
P_{Cl}, mmol/L	108
P_{Renin}, ng/L	4.50 (range, 9.30–43.4)
P_{Ald}, pmol/L	321 (range 111–860)
P_{HCO_3}, mmol/L	19
P_{Alb}, g/L (mg/dL)	40 (4.0)
P_{Cr}, μmol/L (mg/dL)	100 (1.2)

Questions and Discussion

What is the cause of hyperkalemia in this patient? The first step is to rule out pseudohyperkalemia. The presence of hyperchloremic metabolic acidosis (HCMA) would suggest true hyperkalemia. Hyperkalemia is associated with an alkaline PT cell pH, which leads to the inhibition of ammoniagenesis. K^+ ions compete with NH_4^+ for transport on the Na^+-K^+-$2Cl^-$ cotransporter in the TAL of the loop of Henle, which leads to decreased medullary interstitial availability of NH_3. Studies have suggested that hyperkalemia is also associated with decreased expression of the ammonia transporter Rh type C glycoprotein in the collecting duct.[28]

The patient did not have advanced renal dysfunction and was not currently taking drugs that might interfere with renal excretion of K^+. The P_{Renin} was decreased and P_{Aldo} was suppressed compared with what is expected in a patient with hyperkalemia. He was then thought to have hyporeninemic hypoaldosteronism, commonly labeled as type IV renal tubular acidosis (RTA). This disorder is traditionally thought to be the result of destruction of, or a biosynthetic defect in, the juxtaglomerular apparatus (JGA), leading to low P_{Renin} and thereby to low P_{Aldo}. If this were the pathophysiology, one would expect the patient to have renal salt wasting with a decreased EABV and the absence of hypertension. These

features are not found in many patients with this disorder. Another hypothesis is that suppression of renin release in patients with this disorder is the result of EABV expansion because levels of atrial natriuretic peptide in the blood are elevated, and many cases respond to NaCl restriction or the administration of furosemide with an increased P_{Renin}. The basis of the disorder remains to be established. It is possible that the reabsorption of Na^+ and Cl^- may be augmented in the DCT as in patients with familial hyperkalemia with hypertension. Of interest in regard to patients with type 2 diabetes mellitus, who may have hyperinsulinemia and the metabolic syndrome, is the finding that long-term insulin infusion in rats is associated with the retention of NaCl owing to its enhanced reabsorption in different nephron segments, including the DCT.[20] Studies in hyperinsulinemic db/db mice have suggested that the phosphatidylinositol-3-kinase (PI3K)/Akt signaling pathway activates the WNK-NCC phosphorylation cascade.[29]

Differentiation between these two groups of patients with hyporeninemic hypoaldosteronism—those with a JGA defect or destruction and those with excessive Na^+ and Cl^- reabsorption in the DCT—has implications for therapy. The use of exogenous mineralocorticoids (e.g., 9α-fludrocortisone) is of benefit for the first group because it results in both a kaliuresis and re-expansion of the EABV. Diuretic therapy would pose a threat to these patients because it would cause a more severe degree of EABV contraction. In contrast, mineralocorticoids may aggravate the hypertension in patients with excessive reabsorption of Na^+ and Cl^- in the DCT. In this group, the administration of thiazide diuretics to inhibit NCC should lead to both kaliuresis and lowering of the blood pressure.

METABOLIC ALKALOSIS

Metabolic alkalosis is an electrolyte disorder that is accompanied by an elevated P_{HCO_3} and a high plasma pH. Most patients with metabolic alkalosis have a deficit of NaCl, KCl, and/or HCl, any of which may lead to a higher P_{HCO_3}.

Concept 14

The concentration of HCO_3^- in the ECF compartment (assessed by the measurement of the concentration of HCO_3^- in plasma), is the ratio of the content of HCO_3^- in the ECF compartment (numerator) and the ECFV (denominator), as shown in Eq. 24.5.

$$[HCO_3^-] \text{ in ECF} = \text{quantity of } HCO_3^- \text{ in ECF/ECFV} \quad (24.5)$$

A rise in the concentration of HCO_3^- in the ECF compartment might be due to an increase in its numerator (positive balance of HCO_3^-) and/or a decrease in its denominator (low ECFV) (Fig. 24.5; see Eq. 24.5). A quantitative assessment of the ECFV is critical to estimate the quantity of HCO_3^- in the ECF compartment and thereby to determine the basis of the metabolic alkalosis.

Concept 15

Electroneutrality must be present in every body compartment and in the urine. We do not use the term Cl^- depletion alkalosis because it does not provide an adequate description of the pathophysiology of metabolic alkalosis. The deficit of Cl^- must be defined as being due to a deficit of HCl, KCl, and/or NaCl to determine why the P_{HCO_3} level has gone up, what changes have occurred in the composition of the ECF and ICF compartments, and what is the appropriate therapy.[30] Although balance data are not available in clinical settings, with a quantitative assessment of the ECFV, tentative conclusions about the contribution of deficits of each of the different Cl^--containing compounds to the development of metabolic alkalosis can be deduced (Flow Chart 24.12; see also discussion of Clinical Case 11).

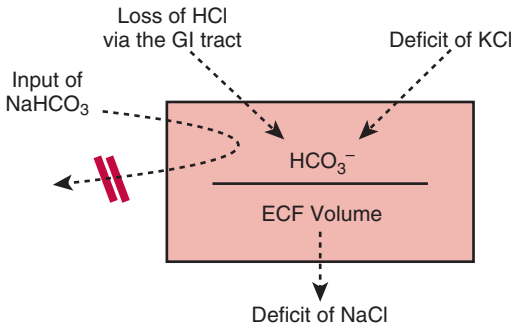

Fig. 24.5 Basis for a high concentration of HCO_3^- in the extracellular fluid *(ECF)* compartment. The *rectangle* represents the ECF compartment. The concentration of HCO_3^- is the ratio of the content of HCO_3^- in the ECF compartment (numerator) and the ECF volume (ECFV) (denominator). The major causes for a rise in the content of HCO_3^- in the ECF compartment are a deficit of HCl and a deficit of KCl (the latter leads increased excretion of NH_4Cl and diminished excretion of organic anions in the urine). The major cause for a fall in the ECFV is a deficit of NaCl. An intake of $NaHCO_3$ is not sufficient on its own to cause a sustained increase in the content of HCO_3^- in the ECF compartment unless there is also reduced renal output of $NaHCO_3$ (indicated by the double red lines on the arrow on the left side of the figure) due to marked reduction in the glomerular filtration rate or there is another lesion that leads to maintaining the stimuli for the reabsorption of $NaHCO_3$ in the proximal convoluted tubule. *Double red lines* on the arrow on the left portion of the figure indicate the reduced renal output of $NaHCO_3$. *GI,* Gastrointestinal. (From Kamel KS, Halperin ML. *Fluid, Electrolyte, and Acid-Base Physiology; A Problem-Based Approach.* ed 5. Philadelphia: Elsevier; 2017.)

Concept 16

There is no tubular maximum for renal HCO_3^- reabsorption. Central to understanding the pathophysiology of metabolic alkalosis is that contrary to the widely held view, there is no tubular maximum for the reabsorption of HCO_3^-. If there were a tubular maximum for the reabsorption of HCO_3^-, then if the filtered load of HCO_3^- were to exceed this maximum, the excess HCO_3^- would be spilled out in the urine. Therefore, maintaining a high concentration of HCO_3^- in the ECF compartments requires a marked reduction in the GFR or a derangement in the tubular handling of HCO_3^- that increases the reabsorption of HCO_3^- above this tubular maximum. The vast majority of HCO_3^- reabsorption occurs in the PT via H^+ secretion, mediated by the Na^+/H^+ exchanger 3 (NHE3). The usual circulating levels of angiotensin II (Ang II), the usual concentration of H^+ in PT cells, provide sufficient stimuli to NHE3 for the reabsorption of most of the filtered HCO_3^-. Experiments in which a tubular maximum for the reabsorption of HCO_3^- was demonstrated were carried out with the

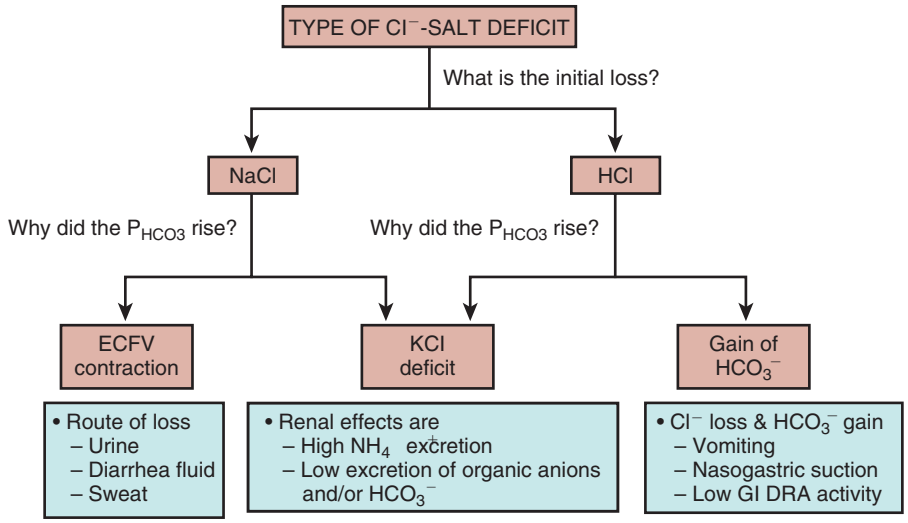

Flow Chart 24.12 *DRA,* Downregulated in adenoma Cl^-/HCO_3^- exchanger; *ECFV,* extracellular fluid volume; *GI,* gastrointestinal. (From Kamel KS, Halperin ML. *Fluid, Electrolyte, and Acid-Base Physiology; A Problem-Based Approach.* ed 5. Philadelphia: Elsevier; 2017.)

administration of a load of $NaHCO_3$. This, however, may have resulted in removal of the two stimuli for HCO_3^- reabsorption in PT because the Na^+ load expands the EABV, causing suppression of the release of Ang II, and the administered HCO_3^- load would increase the HCO_3^- concentration in the peritubular capillaries in the PT, causing inhibition of the reabsorption of HCO_3^-. In other experimental studies, in which a large increase in P_{HCO_3} was achieved without expanding the EABV, no bicarbonaturia was observed, in keeping with the notion that there is no tubular maximum for HCO_3^- reabsorption.[31,32] Filtered HCO_3^- ions are reabsorbed and retained in the ECF compartment as long as the above-mentioned stimuli for their reabsorption are maintained.

A deficit of NaCl or HCl may cause a higher P_{HCO_3} and may also lead to a secondary deficit of K^+ and hypokalemia. A deficit of K^+ may be associated with an acidified PT cell pH, which can then both initiate and sustain a high P_{HCO_3} as a result of new renal HCO_3^- generation (higher rate of excretion of NH_4^+) and enhanced reabsorption of HCO_3^- and organic anions (which are metabolized to produce HCO_3^-) in the PT (see Flow Chart 24.12).

TOOLS FOR ASSESSMENT OF METABOLIC ALKALOSIS

QUANTITATIVE ESTIMATE OF THE EXTRACELLULAR FLUID VOLUME

It is critical to have a quantitative estimate of the ECFV to determine its content of HCO_3^- and thereby why the P_{HCO_3} rose. As discussed earlier in this chapter, we use the hematocrit for this purpose, provided that anemia or polycythemia are not present (see Table 24.2).

BALANCE DATA FOR SODIUM, POTASSIUM, AND CHLORIDE

Balance data for Na^+, K^+, and Cl^- are rarely available in clinical medicine. Nevertheless, they can be deduced if one has a quantitative estimate of the ECFV and measurements of the P_{Na}, P_{Cl}, and P_{HCO_3}. One cannot know the balances for K^+ from these calculations, but its rough magnitude can be deduced by comparing the differences in the content of Na^+ versus that of Cl^- and HCO_3^- in the ECF compartment (see Clinical Case 11).

CLINICAL APPROACH TO THE PATIENT WITH METABOLIC AKALOSIS

Our clinical approach to a patient with metabolic alkalosis is outlined in Flow Chart 24.13. The first step is to rule out the common causes of metabolic alkalosis—namely, vomiting and the use of diuretics. Some patients may deny vomiting or the use of diuretics; measuring urine electrolyte levels may provide helpful clues if one of these diagnoses is suspected (see Table 24.3).

A very useful initial test to detect the cause of metabolic alkalosis is to examine the U_{Cl}. A very low U_{Cl} (<20 mmol/L) is expected when there is a deficit of HCl and/or NaCl. The U_{Cl} may not be low if there is recent intake of diuretics (see Table 24.3). If the U_{Cl} is not low, assessment of the EABV and blood pressure helps identify patients with disorders of primary high ENaC activity in the ASDN (see Flow Chart 24.9; the EABV is not low, hypertension is present) and distinguish them from patients with recent use of diuretics and those with Bartter syndrome or Gitelman syndrome (EABV is low, absence of hypertension). Measurements of U_{Cl} in multiple spot urine samples are helpful to separate patients with Bartter or Gitelman syndrome (persistent high U_{Cl}) from those with diuretic abuse (U_{Cl} is high only while the diuretic is acting).

CLINICAL CASE 11: METABOLIC ALKALOSIS WITHOUT VOMITING OR USE OF DIURETICS

After a forced 6-hour intense training exercise in the desert in the heat of the day, an elite corps soldier was the only one in his squad who collapsed. He perspired profusely during the training exercise and drank a large volume of water and sugar-containing fluids. He denied vomiting or the intake of any medications. Physical examination revealed a markedly contracted EABV. Initial laboratory data are shown in the

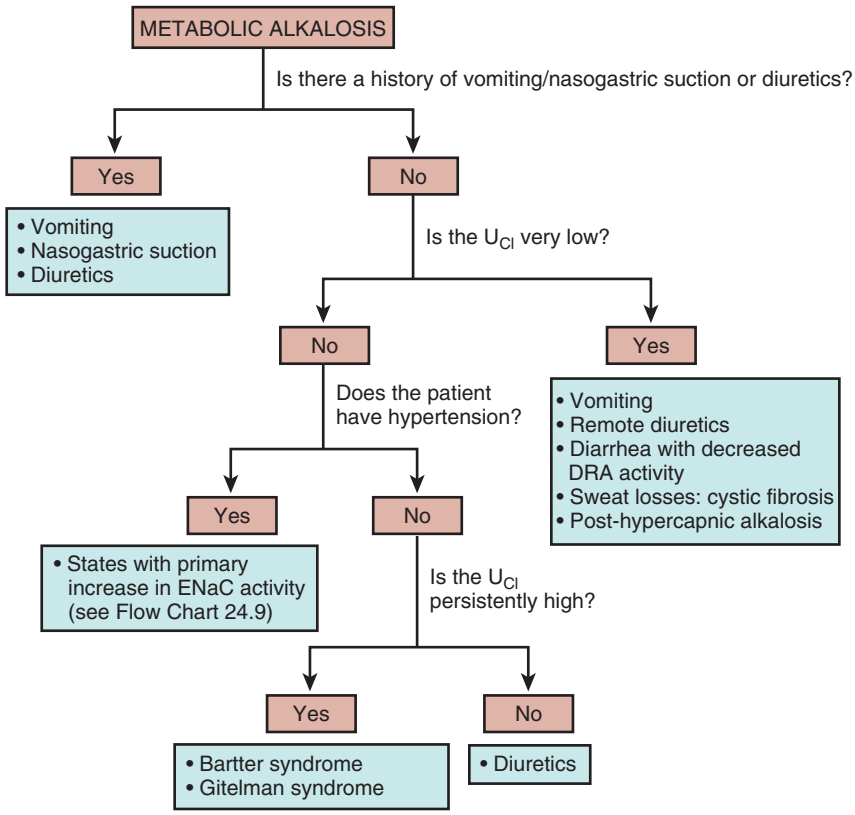

Flow Chart 24.13 *DRA,* Downregulated in adenoma Cl^-/HCO_3^- exchanger; *ENaC,* epithelial sodium channel. (From Kamel KS, Halperin ML. *Fluid, Electrolyte, and Acid-Base Physiology; A Problem-Based Approach.* ed 5. Philadelphia: Elsevier; 2017.)

table. The pH and P_{CO_2} values are from an arterial blood sample; all other findings are from a venous blood sample.

Parameter	*Findings*
P_{Na}, mmol/L	125
P_K, mmol/L	2.7
P_{Cl}, mmol/L	70
Hematocrit	0.50
pH	7.50
P_{HCO3}, mmol/L	38
P_{CO_2}, mm Hg	47

Questions and Discussion

What are the major threats to the patient, and how should they dictate therapy?

Acute hyponatremia. The danger is brain herniation due to increased intracranial pressure from swelling of brain cells.

Basis of hyponatremia. The patient weighed 80 kg and had a muscular build, so his initial total body water (TBW) was about 50 L (ECFV ≈ 15 L; ICF volume ≈ 35 L). Because he had hyponatremia, his ICF volume was expanded because of a water gain. The percentage expansion of ICF volume is close to the percentage fall in P_{Na} (i.e., ≈ 11%). Hence, he had a water gain in his ICF compartment of about 4 L. With a hematocrit of 0.50, his ECFV was decreased by one-third from its normal value of about 15 L to about 10 L; accordingly, he lost 5 L of ECFV. This represents the loss of 5 L of water and 700 mmol of Na^+ (5 L × P_{Na} 140 mmol/L). In addition, as the P_{Na} decreased from 140 to 125 mmol/L, each of the remaining 10 L of ECVF had a loss of 15 mmol of Na^+. Hence, his total Na^+ loss was 850 mmol. In total body balance terms, he had a loss of 850 mmol of Na^+ and 1 L of water—a loss of 5 L of water from the ECF compartment and a gain of 4 L of water in the ICF compartment. Therefore, the primary basis of his hyponatremia was Na^+ loss.

Hemodynamic instability. An infusion of isotonic saline was started in the field, and the patient was hemodynamically stable on arrival at the emergency department. After it was recognized that his P_{Na} was 125 mmol/L, intravenous therapy was changed from isotonic saline to 3% hypertonic saline. The goal of therapy was to raise the P_{Na} to 130 mmol/L. Because the hyponatremia was acute, there was little if any risk of osmotic demyelination from rapidly raising the P_{Na} to 130 mmol/L.

Hypokalemia. The hypokalemia did not represent an emergency because he did not have a cardiac arrhythmia or respiratory muscle weakness. An intravenous infusion of isotonic saline supplemented with 40 mmol/L of KCl was started. The P_K was followed closely.

What is the basis for metabolic alkalosis? To distinguish between HCl, KCl, and NaCl deficits, a quantitative analysis of the degree of contraction of the ECFV is needed. As mentioned previously, with a hematocrit of 0.50, this patient's

ECFV was decreased by one-third, from its normal value of 15 L to about 10 L, so he had lost 5 L of ECFV.

Deficit of HCl. There was no history of vomiting, so an HCl deficit is a very unlikely basis for the metabolic alkalosis.

Deficit of NaCl. The decrease in his ECFV was about 5 L. One can now calculate how much this degree of ECFV contraction would raise the P_{HCO_3} (divide the normal content of HCO_3^- in the ECF compartment (15 L × 25 mmol/L, or 375 mmol) by the new ECFV (10 L), and the result is 37.5 mmol/L. This value is remarkably close to the measured P_{HCO_3}, 38 mmol/L, suggesting that the major reason for the rise in the P_{HCO_3} is the fall in his ECFV.

Na^+ deficit. As calculated above, the deficit of Na^+ in the ECF compartment was about 850 mmol.

Cl^- deficit. Multiplying the P_{Cl} before the training exercise (103 mmol/L) by the normal ECFV (15 L) yields a Cl^- content of about 1545 mmol. After the training exercise, the P_{Cl} was 70 mmol/L, and the ECF volume was 10 L, so the ECF Cl^- content was 700 mmol. Accordingly, the deficit of Cl^- was about 840 mmol, a value close to the deficit of Na^+.

Deficit of KCl. There was little difference between the deficits of Na^+ and Cl^-, so there was no appreciable deficit of KCl to account for a drop in the P_K to 2.7 mmol/L. Especially in this muscular elite soldier, the loss of K^+ would have to be very large to account for this degree of hypokalemia. Accordingly, the major mechanism for the hypokalemia is likely to be a shift of K^+ into cells due to a β_2-adrenergic surge and possibly the alkalemia.

Routes for NaCl loss. The next issue is to examine possible routes for a large loss of NaCl in such a short time. Because diarrhea and polyuria were not present, the only route for a large NaCl loss was via sweat. To have a high electrolyte concentration in sweat and a large sweat volume, the likely underlying lesion would be cystic fibrosis. The diagnosis of cystic fibrosis was confirmed later by molecular studies.

What is the therapy for metabolic alkalosis in this patient? Because the basis for the metabolic alkalosis was largely an acute deficit of NaCl, the patient required a positive balance of about 850 mmol of NaCl to replace the deficit. He was initially given hypertonic saline to raise his P_{Na} to 130 mmol/L. If all of this deficit of NaCl were replaced with 3% hypertonic saline, which would also give him about 1.5 L of H_2O, his new total body Na^+ will be around 6975 mmol (initial TBW 49 L × initial P_{Na} 125 mmol/L = 6975 mmol; to that add 850 mmol = 7825 mmol), his new TBW will be around 50.5 L, and the P_{Na} would rise to about 138 mmol/L. He might, however, still have a large volume of water in the GI tract that could be absorbed later and cause the P_{Na} to drop. Hence, the P_{Na} should be followed closely. After the administration of only 40 mmol of KCl, the patient's P_K rose to 3.8 mmol/L, adding support to our conclusion that the major cause of the hypokalemia was an acute shift of K^+ into cells.

METABOLIC ACIDOSIS

Metabolic acidosis is a process that causes a drop in the P_{HCO_3} and a rise in the concentration of H^+ in plasma. Metabolic acidosis represents a diagnostic category with many different causes (see Chapter 16). The risks for the patient depend on the underlying disorder that caused the metabolic acidosis, the ill effects of the binding of H^+ to intracellular proteins in vital organs (e.g., the brain and the heart), and possible dangers associated with the anions that accompanied the H^+ load (e.g., chelation of ionized calcium by citrate in a patient with metabolic acidosis due to ingestion of citric acid).[33]

As previously articulated in Concept 14, the concentration of HCO_3^- in the ECF compartment is equal to the ratio of the content of HCO_3^- in the ECF compartment to the ECFV. It is important to distinguish between acidemia and acidosis. The term acidemia simply describes an elevation in the concentration of H^+ in plasma. Acidemia may not be present in a patient who has metabolic acidosis if there is, for example, a large decrease in the ECFV, which may sufficiently raise the P_{HCO_3}, even though there is a decreased content of HCO_3^- in the ECF compartment (e.g., in the patient with severe diarrhea[34] and in some patients with DKA). For a diagnosis of metabolic acidosis to be made in this setting, a quantitative estimate of the ECFV is needed to assess its content of HCO_3^- in the ECF compartment.

Concept 17

H^+ ions must be removed by the bicarbonate buffer system (BBS) to avoid their binding to intracellular proteins. Binding of H^+ to proteins could change their charge, shape, and possibly their functions. The bulk of BBS is in the ICF compartment and the interstitial spaces of skeletal muscles.[35]

TOOLS FOR ASSESSMENT OF METABOLIC ACIDOSIS

The tools for assessing metabolic acidosis are listed in Table 24.5.

QUANTITATIVE ASSESSMENT OF THE EXTRACELLULAR FLUID VOLUME

As discussed earlier in this chapter, we use the hematocrit to obtain a quantitative assessment of the ECFV, provided that anemia or polycythemia were not present (see Table 24.2).

Tools to Assess the Removal of Hydrogen by the Bicarbonate Buffer System

As shown in Eq. 24.6, the BBS is driven by pull—that is, by a lower P_{CO_2}. Effective buffering of H^+ by the BBS requires a low P_{CO_2} primarily in the interstitial space and ICF of skeletal muscles.

$$H^+ + HCO_3^- \leftrightarrow H_2CO_3 + CO_2 \qquad (24.6)$$

Acidemia stimulates the respiratory center, leading to a fall in arterial P_{CO_2}. Although the arterial P_{CO_2} sets the lower limit on the P_{CO_2} in capillaries, it does not guarantee that the capillary P_{CO_2} in skeletal muscles will be low enough to ensure effective buffering of H^+ by the BBS. Because the free-flowing brachial venous P_{CO_2} reflects the P_{CO_2} in capillary blood of skeletal muscles in its drainage pool, it should provide a means of assessing the effectiveness of the BBS in patients with metabolic acidosis. The capillary P_{CO_2} in skeletal muscles will be higher if the rate of blood flow to muscles is low—for example, as a result of a decreased EABV. If muscle oxygen consumption in this setting remains unchanged, more oxygen

Table 24.5 Laboratory Tests for Diagnosis of Metabolic Acidosis

Question	Parameter(s) Assessed	Tool(s) to Use
Is the total amount of HCO_3^- in the ECF compartment low?	ECFV	Hematocrit or total plasma proteins
Is metabolic acidosis due to overproduction of organic acids?	Appearance of new anions in the body or the urine	Plasma anion gap Urine anion gap
Is metabolic acidosis due to ingestion of alcohol?	Presence of alcohols as unmeasured osmoles	Plasma osmolal gap
Is effective bicarbonate buffering in skeletal muscle available?	Adequacy of tissue perfusion and CO_2 clearance from muscle, enabling buffering of H^+ by HCO_3^- in interstitial fluid and intracellular fluid compartments	Brachial venous P_{CO_2}
Is the renal response to chronic acidemia adequate?	Examine the rate of excretion of NH_4^+	Urine osmolal gap
If NH_4^+ excretion is high, which anion is excreted with NH_4^+?	Gastrointestinal loss of $NaHCO_3$ Acid added, but the anion is excreted in the urine	Urine Cl^- Urine anion gap
What is the basis for a low excretion of NH_4^+?	Low distal H^+ secretion Low NH_3 availability Both defects	Urine pH >7.0 Urine pH ≈ 5.0 Urine pH ≈ 6.0
Where is the defect in H^+ secretion?	Distal H^+ secretion Proximal H^+ secretion	P_{CO_2} in alkaline urine Fractional excretion of HCO_3, urine citrate excretion

ECF, Extracellular fluid; *ECFV,* extracellular fluid volume.
From Kamel KS, Halperin ML. Fluid, electrolytes and acid-base physiology. A problem-based approach, ed 5. Philadelphia: Elsevier; 2017.

will be extracted from, and more CO_2 will be added to, each liter of blood. The higher P_{CO_2} in muscle capillaries will diminish the effectiveness of the BBS to remove extra H^+. Hence, the circulating H^+ concentration rises, and a larger burden of H^+ will be titrated by intracellular proteins in muscle, as well as by other organs, including the brain. Notwithstanding this, because of autoregulation of cerebral blood flow, it is likely that the P_{CO_2} in brain capillary blood will change minimally unless there is a severe degree of contraction of the EABV and failure of autoregulation of cerebral blood flow. Hence, the BBS in the brain will continue to titrate much of this large H^+ load. Considering, however, the limited amount of HCO_3^- in the brain, and that the brain receives a relatively larger proportion of the cardiac output (and of the H^+ load), there is a risk of more H^+ binding to intracellular proteins in the brain, further compromising their function (Fig. 24.6).[36] At usual rates of blood flow and metabolic work at rest, the brachial venous P_{CO_2} is about 6 mm Hg greater than arterial P_{CO_2}. If the blood flow rate to muscles is low, their venous P_{CO_2} will be more than 6 mm Hg greater than the arterial P_{CO_2}. Enough saline should be administered to increase this blood flow rate to muscle to achieve a brachial venous P_{CO_2} that is no more than 6 mm Hg higher than the arterial P_{CO_2}.

CLINICAL APPROACH: INITIAL STEPS

The initial steps in the clinical approach to a patient with metabolic acidosis are summarized in Flow Chart 24.14.

1. Identify threats for that patient and anticipate and prevent dangers that may arise during therapy.
2. Determine if effective buffering of H^+ by the BBS in skeletal muscles is available.

METABOLIC ACIDOSIS DUE TO ADDED ACIDS

Concept 18

Addition of acids can by detected by the appearance of new anions. These new anions may remain in the body or may be excreted (e.g., in the urine or diarrhea fluid).

TOOLS FOR ASSESSING METABOLIC ACIDOSIS DUE TO ADDED ACIDS

Tools for assessment of metabolic acidosis due to added acids are summarized in Table 24.5.

Detect New Anions in Plasma

The accumulation of new anions in plasma can be detected from a calculation of the plasma anion gap ($P_{anion\ gap}$).[37,38] The major cation in plasma is Na^+, and the major anions are Cl^- and HCO_3^-. The difference between P_{Na} and (P_{Cl} + P_{HCO_3}) reflects the other negative charges in plasma, which are predominantly due to the negative charge on albumin. Although it is commonly said that the normal value of the $P_{anion\ gap}$ is 12 ± 2 mEq/L, the mean value of a normal $P_{anion\ gap}$ varies greatly among clinical laboratories because of different laboratory methods, and the range of normal values is wide. When using the calculation of the $P_{anion\ gap}$ to detect the presence of new anions in plasma, one must adjust the baseline value of the $P_{anion\ gap}$ for the P_{Alb}. As a rough estimate, the baseline value for the $P_{anion\ gap}$ falls (or rises) by 2.5 mEq/L for every 10-g/L or 1-g/dL fall (or rise) in the P_{Alb}.[39] Even with this adjustment, it seems that net negative valence on albumin is increased if there is an appreciable decrease in the EABV.[40]

Stewart has recommended another approach to detect new anions in plasma, the strong ion difference (SID).[41] This

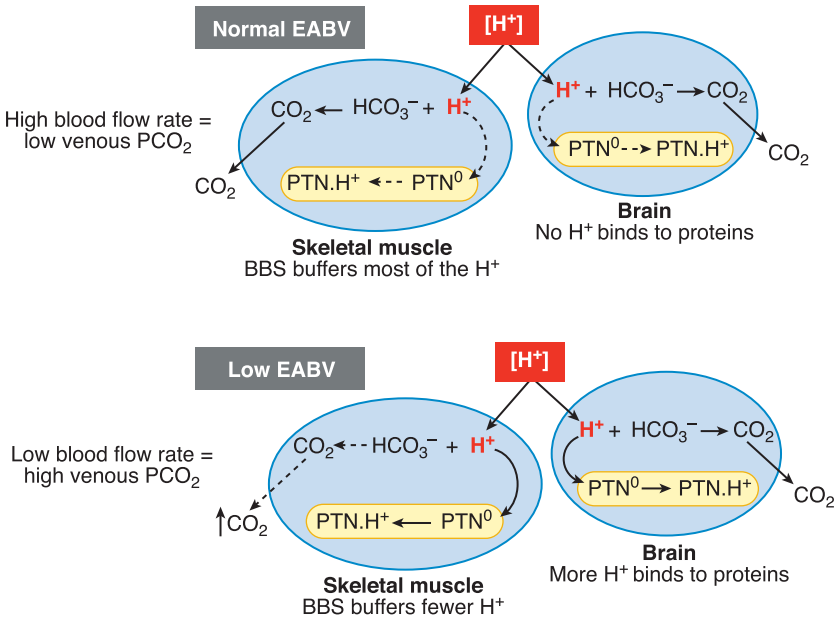

Fig. 24.6 Buffering of H^+ in the brain in a patient with metabolic acidemia and a contracted effective arterial blood volume (EABV). *Top,* Buffering of H^+ in a patient with a normal EABV and thereby a low muscle venous P_{CO_2}. The vast majority of H^+ removal occurs by the bicarbonate buffer system (BBS) in the interstitial space and in cells of skeletal muscles. *Bottom,* Buffering of an H^+ load in a patient with a contracted EABV and thereby a high muscle venous P_{CO_2} values. A high muscle venous P_{CO_2} prevents H^+ removal by muscle BBS. As a result, the degree of acidemia may become more pronounced, and more H^+ may bind to proteins (PTN·H^+) in other organs, including the brain. (From Kamel KS, Halperin ML. *Fluid, Electrolyte, and Acid-Base Physiology; A Problem-Based Approach.* ed 5. Philadelphia: Elsevier; 2017.)

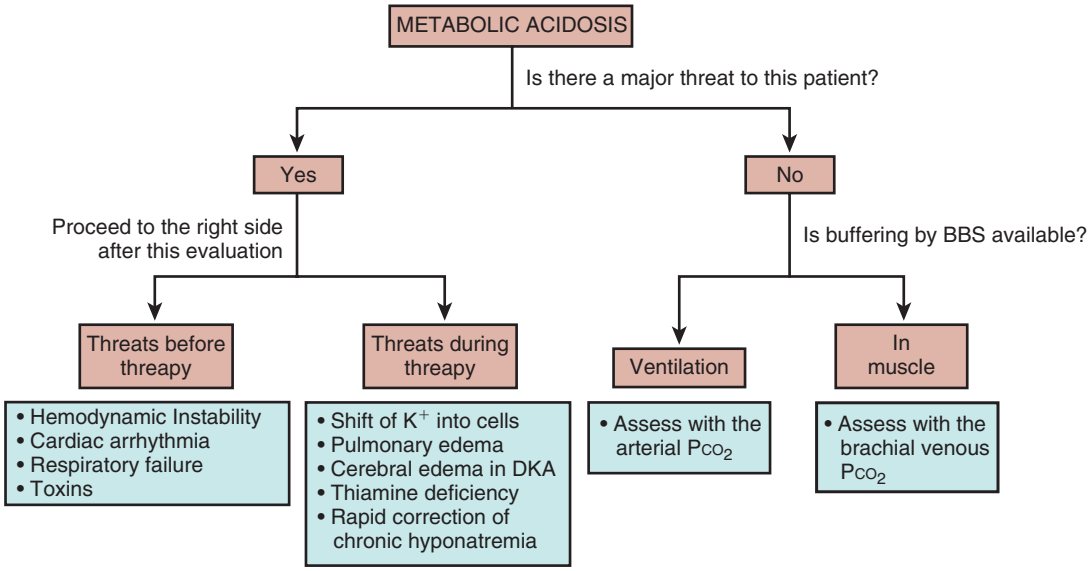

Flow Chart 24.14 *BBS,* Bicarbonate buffer system; *DKA,* diabetic ketoacidosis. (From Kamel KS, Halperin ML. *Fluid, Electrolyte, and Acid-Base Physiology; A Problem-Based Approach.* ed 5. Philadelphia: Elsevier; 2017.)

approach is rather complex and offers only a minor advantage over the $P_{anion\ gap}$ in that it includes a correction for the net negative charge on P_{Alb}.[42]

Use of the Delta Plasma Anion Gap/Delta Plasma HCO_3^-. The relationship between the rise in the $P_{anion\ gap}$ and the fall in the P_{HCO_3} (or the delta $P_{anion\ gap}$/delta P_{HCO_3}) is used to detect the presence of coexisting metabolic alkalosis (the rise in $P_{anion\ gap}$ is larger than the fall in P_{HCO_3}) or the presence of both an "acid overproduction" type and an "$NaHCO_3$ loss" type of metabolic acidosis (the rise in the $P_{anion\ gap}$ is smaller than the fall in the P_{HCO_3}).

There are several pitfalls in using this relationship. One is failure to adjust for changes in the ECFV.[43] Consider, for example, a patient with DKA who has a fall in P_{HCO_3} by 15 mmol/L, from 25 to 10 mmol/L, and the "expected" 1:1 ratio of a rise in $P_{anion\ gap}$ from a normal value of 12 mEq/L to 27 mEq/L. The patient had a normal ECFV of 10 L before

DKA developed but, as a result of the glucose-induced osmotic diuresis and natriuresis, the current ECFV is only 8 L. Although the fall in the P_{HCO_3} and the rise in the concentration of ketoacid anions (as judged from the rise in the $P_{anion\ gap}$) are equal, the deficit of HCO_3^- and the amount of ketoacids added to the ECF compartment are not. The sum of the content of HCO_3^- and ketoacid anions in the ECF compartment prior to the development of DKA is 250 mmol ([25 + 0 mmol/L] × 10 L). Their sum in the ECF compartment after DKA developed, however, is only 200 mmol ([10 + 15] mmol/L × 8 L). The deficit of HCO_3^- in this example is 170 mmol, but the quantity of new anions in the ECF is only 120 mmol. This is because there is another component of the loss of HCO_3^- that occurred when ketoacids were added that is not detected by an increase in the $P_{anion\ gap}$. Some of the ketoacid anions were excreted in the urine with Na^+ and/or K^+, an indirect form of $NaHCO_3$ loss. Hence the rise in the $P_{anion\ gap}$ underestimated the actual quantity of net production of ketoacids, and the fall in P_{HCO3} underestimated the actual magnitude of the deficit of HCO_3^-. When the ECFV is re-expanded with saline, the degree of deficit of HCO_3^- will become evident. In addition, the fall in the $P_{anion\ gap}$ will not be matched by a rise in the P_{HCO_3} because some ketoacid anions will be lost in urine when their filtered load is increased with the rise in GFR.

Another pitfall in the use of the delta $P_{anion\ gap}$/delta P_{HCO_3} is the failure to correct for the net negative valence attributable to P_{Alb}. When calculating the $P_{anion\ gap}$, one must adjust the base value for changes in the charge on the most abundant unmeasured anion in plasma, which is albumin. We emphasize that adjustments should be made for a decrease or an increase in P_{Alb}.

Detect New Anions in the Urine

New anions can be detected with the calculation of the urine anion gap ($U_{anion\ gap}$; Eq. 24.7).

$$U_{anion\ gap} = (U_{Na} + U_K + U_{NH4}) - U_{Cl} \qquad (24.7)$$

The concentration of NH_4^+ in the urine (U_{NH4}) is estimated from the urine osmolal gap ($U_{osm\ gap}$), as discussed in the next section. The nature of these new anions may sometimes be deduced by comparing their filtered load with their excretion rate. For example, when there is a very large quantity of the new anion in the urine in comparison with the rise in $P_{anion\ gap}$, one should suspect that this anion is secreted in the PT (e.g., hippurate anion from the metabolism of toluene) or is freely filtered and poorly reabsorbed by the PT (e.g., reabsorption of ketoacid anions may be inhibited by salicylate anions, D-lactate anions). On the other hand, a very low rate of excretion of new anions suggests that they are avidly reabsorbed in the PT (e.g., L-lactate anions).

Detect Toxic Alcohols

The presence of alcohols in plasma can be detected by calculating the plasma osmolal gap ($P_{osm\ gap;}$ Eq. 24.8). This occurs because alcohols are uncharged compounds, have a low molecular weight, and usually large quantities are ingested.

$$P_{osm\ gap} = \text{measured } P_{osm} - (2 \times P_{Na} + P_{Glu} + P_{Urea}) \qquad (24.8)$$

In Eq. 24.8, all terms are in mmol/L. If P_{Glu} is in mg/dL, divide by 180, and if P_{Urea} is expressed as mg/dL of urea nitrogen, divide by 2.8 to obtain units in mmol/L.

CLINICAL APPROACH TO THE PATIENT WITH METABOLIC ACIDOSIS DUE TO ADDED ACIDS

The steps in the clinical approach to the patient with metabolic acidosis due to added acids are shown in Flow Chart 24.15. If metabolic acidosis develops over a short period, the likely causes are overproduction of L-lactic acid (e.g., hypoxic L-lactic acidosis, ingestion of alcohol in a patient with thiamine deficiency) or ingestion of acids (e.g., metabolic acidosis due to ingestion of citric acid). Measurement of plasma levels of L-lactate and β-hydroxybutyrate confirms the diagnosis of L-lactic acidosis or ketoacidosis respectively. If suspected, measurements of blood levels levels of methanol, ethylene glycol, acetaminophen or acetylsalicylic acid should be obtained. Acetaminophen overdose may be associated with L-lactic acidosis or pyroglutamic acidosis. A detailed discussion of the various causes of metabolic acidosis due to added acids is provided in Chapter 16.

CLINICAL CASE 12: SEVERE METABOLIC ACIDOSIS IN A PATIENT WITH CHRONIC ALCOHOLISM

A 52-year-old man presented to the emergency department with abdominal pain, visual disturbances, and shortness of breath.[44] He had a history of drinking excessive amounts of alcohol on a regular basis. He admitted to drinking approximately 1 L of vodka the day before hospital admission but denied ingesting any other substances. During the 24 hours before admission, he had not eaten at all. In the 5 hours before his admission, he had had several bouts of vomiting and did not drink any alcohol. His dietary intake had been generally very poor over the last several months because he had diminished appetite.

On physical examination, he was fully conscious and oriented. His respiration rate was rapid (40 breaths/min). His pulse rate was also rapid (150 beats/min), and his blood pressure was 120/58 mm Hg. Neurologic examination was unremarkable.

The patient's urine tested strongly positive for ketones. His initial laboratory results on admission to the emergency department are shown in the following table. The pH and P_{CO_2} are from an arterial blood sample, whereas all other findings are from a venous blood sample.

Parameter	*Findings*
P_{Na}, mmol/L	132
P_K, mmol/L	5.4
P_{Cl}, mmol/L	85
P_{HCO3}, mmol/L	3.3
$P_{anion\ gap}$ mEq/L	44
P_{osm}, mOsmol/kg H_2O	325
Hematocrit	0.46
pH	6.78
P_{CO_2}, mm Hg	23
P_{Glu}, mmol/L	3.0
P_{Alb}, g/L	36
$P_{osm\ gap}$, mOsmol/kg H_2O	42

Questions and Discussion

What dangers may be present on admission or may arise during therapy?

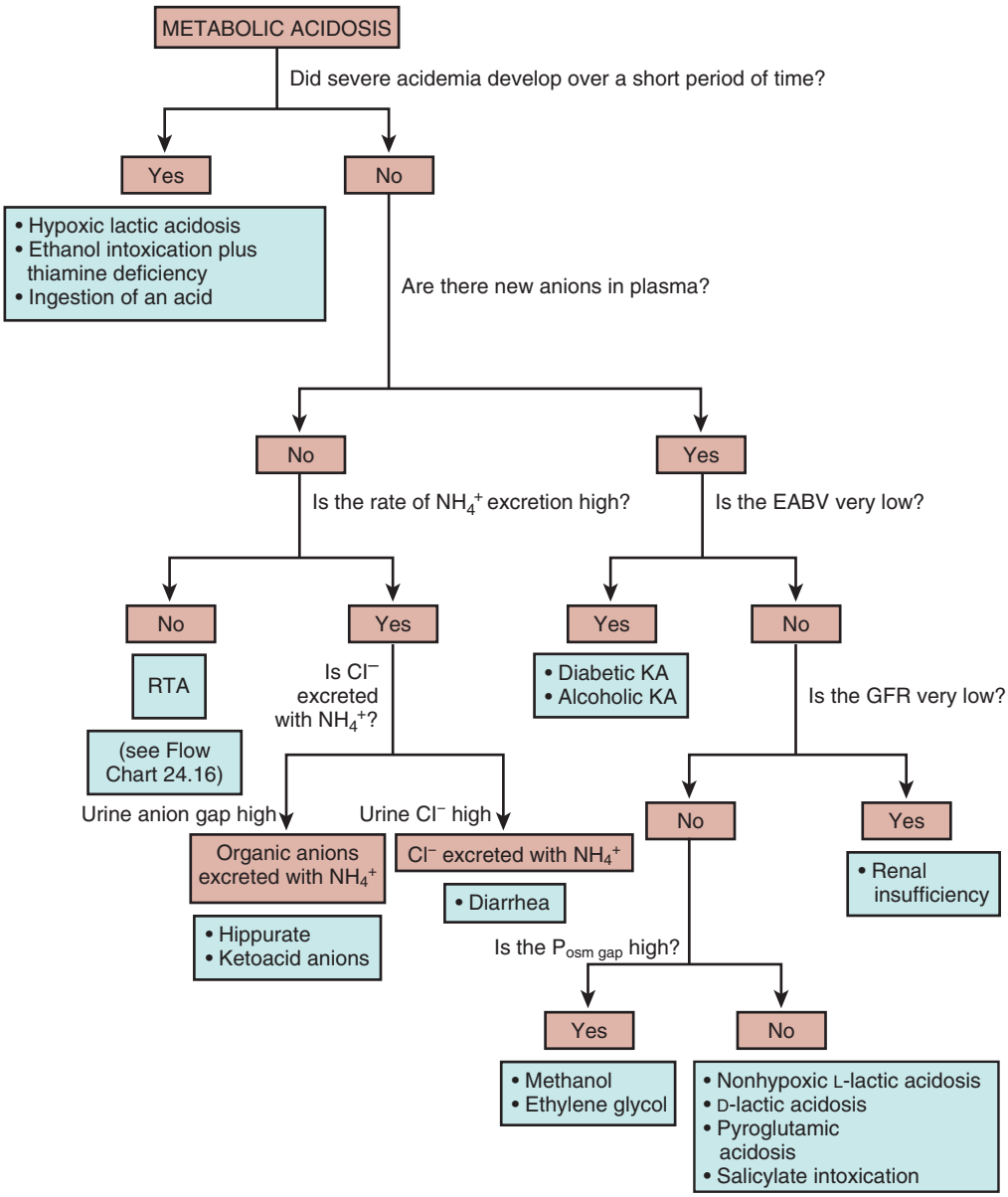

Flow Chart 24.15 *RTA,* Renal tubular acidosis; *KA,* ketoacidosis; *GFR,* glomerular filtration rate; *Posm gap,* plasma osmolal gap. (From Kamel KS, Halperin ML. Fluid, electrolytes, and acid-base physiology. A problem based approach, ed 5. Philadelphia: Elsevier, 2017.)

Severe acidemia. The patient had a severe degree of acidemia with a large increase in the $P_{anion\ gap}$, indicating overproduction of acids. For the time being, he is hemodynamically stable, but a quantitatively small additional H^+ load would produce a disproportionately large fall in the P_{HCO_3} and plasma pH. For example, halving the P_{HCO_3} would cause the arterial pH to drop by 0.30 unit if the arterial P_{CO_2} has not changed. By the same token, doubling of the P_{HCO_3} would raise the plasma pH by 0.30 unit. A large dose of $NaHCO_3$ would be needed to achieve this because the administered $NaHCO_3$ might lead to back titration of some of the large H^+ load that is bound to the patient's intracellular proteins and, in addition, he might still have ongoing production of acids.

Toxic alcohol ingestion. Because the patient had a severe degree of metabolic acidemia with a large $P_{osm\ gap}$, ingestion of methanol or ethylene glycol was suspected. Aldehydes produced from the metabolism of these alcohols by the enzyme alcohol dehydrogenase in the liver are the major cause of toxicity because they rapidly bind to tissue proteins. Although the patient ingested a large amount of ethanol, which could have caused the large $P_{osm\ gap}$, and his urine was strongly positive for ketones, such a severe degree of acidemia is not usual in patients with alcoholic ketoacidosis. Because of the strong clinical suspicion of toxic alcohol ingestion, the patient was started on fomepizole (an inhibitor of alcohol dehydrogenase) while waiting for the determination of the level of these toxic alcohols in his blood.

Thiamine deficiency. Malnourished patients who present with alcoholic ketoacidosis are at risk for the development of encephalopathy due to thiamine deficiency. Ketoacids,

when available, are the preferred brain fuel because they are derived from storage fat and, hence, proteins from lean body mass are spared as a source of glucose for the brain during prolonged starvation. After successful treatment of alcoholic ketoacidosis, ketoacids are no longer available as a brain fuel, so the brain must regenerate most of its ATP from the oxidation of glucose. Thiamine (vitamin B_1) is a key cofactor for pyruvate dehydrogenase (PDH). The activity of PDH is diminished by the lack of thiamine, so the rate of regeneration of ATP in brain cells will not be sufficient for their biologic work. Therefore, glycolysis will be stimulated in the brain to make ATP. As a result, there will be a sudden rise in the production of H^+ and L-lactate anions in areas of the brain where the metabolic rate is the most rapid and/or areas that have the lowest reserve of thiamine. Thiamine must be administered early in therapy in such patients.

More information. Two hours after presentation, additional laboratory results became available. The patient's plasma L-lactate level was 23 mmol/L, and the assays for methanol and ethylene glycol were negative.

What is the cause of the severe degree of L-lactic acidosis in this patient? A rise in the concentration of L-lactate anions and H^+ can be caused by an increased rate of production and/or a decreased rate of removal of L-lactic acid. The rapid development and severity of L-lactic acidosis in this patient suggest that the L-lactic acidosis is largely due to overproduction of L-lactic acid.

The degree of L-lactic acidosis in patients presenting with alcohol intoxication is usually mild (plasma L-lactate level is usually <5 mmol/L) because it is due to the increased nicotinamide adenine dinucleotide, reduced form ($NADH.H^+$)/nicotinamide adenine dinucleotide (NAD^+) ratio owing to the ongoing production of $NADH.H^+$ through ethanol metabolism, which is largely restricted to the liver where the enzymes alcohol dehydrogenase and aldehyde dehydrogenase are expressed. Other organs in the body are capable of oxidizing the L-lactate produced by the liver and, hence, the degree of L-lactic acidosis is usually mild.

$$\text{Pyruvate}^- + \text{NADH.H}^+ \leftrightarrow \text{L-lactate}^- + \text{NAD}^+ \quad (24.9)$$

However, a severe degree of L-lactic acidosis may develop rapidly if there is a large intake of alcohol in a patient who is thiamine-deficient. The site of L-lactic acid production is likely to be the liver because there will be both accumulation of pyruvate (owing to diminished activity of PDH) and a high $NADH.H^+/NAD^+$ ratio (due to metabolism of ethanol). There is also diminished removal of L-lactic acid by other organs due to diminished activity of PDH.

HYPERCHLOREMIC METABOLIC ACIDOSIS

Hyperchloremic metabolic acidosis is characterized by the absence of a rise in the $P_{\text{anion gap}}$; hence, it is often also called non–anion gap metabolic acidosis. There are two major groups of causes for this type of metabolic acidosis, the direct loss of $NaHCO_3$ and the indirect loss of $NaHCO_3$. The direct loss of $NaHCO_3$ may occur via the GI tract—for example, in patients with diarrhea or through the urine in patients at the early phase of a disease process that causes proximal renal tubular acidosis (pRTA). The indirect loss of $NaHCO_3$ may be due to a low rate of excretion of NH_4^+ that is insufficient to match the daily rate of production of sulfuric acid from the metabolism of sulfur-containing amino acids (e.g., in patients with chronic renal failure or patients with distal renal tubular acidosis [dRTA], or patients with pRTA in the steady state). Indirect loss of $NaHCO_3$ may also be due to an overproduction of an acid (e.g., hippuric acid formed during the metabolism of toluene, ketoacids), with the excretion of its conjugate base (e.g., hippurate anions, ketoacids anions) in the urine at a rate that exceeds the rate of excretion of NH_4^+.

Concept 19

The expected renal response to chronic metabolic acidosis is a high rate of excretion of NH_4^+. Based on findings in normal subjects given an acid load of ammonium chloride for several days, the expected normal renal response in a patient with chronic metabolic acidosis, is the excretion of close to 200 mmol of NH_4^+/day.[45] There is a lag period of a few days, however, before high rates of excretion of NH_4^+ can be achieved. Patients with a hyperchloremic metabolic acidosis that have an appropriately high rate of NH_4^+ excretion generally have diarrhea or an added organic acid the anion of which is excreted in the urine at a rapid rate. These two disorders can be differentiated by assessing the urine anion gap and urine chloride concentration (see Flow Chart 24.15).

Concept 20

A low rate of excretion of NH_4^+ in a patient with hyperchloremic metabolic acidosis could be due to a decreased medullary interstitial availability of NH_3 or a decreased net H^+ secretion in the distal nephron.[46]

A low rate of ammoniagenesis has several possible causes. One is intracellular alkalinization of PT cells due to hyperkalemia or a genetic or an acquired disorder that compromises proximal H^+ secretion or HCO_3^- exit from PT cells (also causing a reduced capacity to reabsorb HCO_3^- [i.e., pRTA]). The other involves a reduction in the GFR, which diminishes the filtered load of Na^+ because less work is performed in PT cells; thus, the availability of ADP is decreased and the rate of oxidation of glutamine in PT cells is reduced.

The other main cause of a low rate of excretion of NH_4^+ is a low net secretion of H^+ in the distal nephron. This could be due to an H^+-ATPase defect (e.g., autoimmune and hypergammaglobulinemic disorders, including Sjögren syndrome), backleak of H^+ (e.g., due to drugs such as amphotericin B), or a disorder associated with the distal secretion of HCO_3^- (e.g., in some patients with Southeast Asian ovalocytosis [SAO]). Patients with medullary interstitial disease (e.g., due to infections, drugs, infiltrations, precipitations, inflammatory disorders, sickle cell disease) may have a low rate of excretion of NH_4^+ because of both diminished accumulation of NH_4^+ in the medullary interstitium and a decreased rate of H^+ secretion in the MCD.

TOOLS FOR ASSESSING HYPERCHLOREMIC METABOLIC ACIDOSIS

Table 24.5 summarizes the steps for the assessment of patients with hyperchloremic metabolic acidosis.

Assess the Rate of Excretion of NH_4^+ in the Urine

Urine Osmolal Gap. A direct assay for urine NH_4^+ is not often available in clinical settings. In our opinion, calculation of the $U_{osm\ gap}$ provides the best indirect estimate of the U_{NH4} (Eq. 24.10) because it detects all NH_4^+ salts in the urine (Fig. 24.7).[47,48]

$$\begin{aligned} &U_{osm\ gap} = \text{measured } U_{osm} - \text{calculated } U_{osm} \\ &\text{Calculated } U_{osm} = 2\,(U_{Na} + U_K) + U_{Urea} + U_{Glu} \\ &\text{All values are in mmol/L.} \\ &\text{Urinary concentration of } NH_4 = U_{osm\ gap}/2 \end{aligned} \qquad (24.10)$$

We use the U_{NH4}/U_{Cr} ratio in a spot urine sample to assess the rate of excretion of NH_4^+. The rationale is that the rate of excretion of creatinine is relatively constant over a 24-hour period. In a patient with chronic metabolic acidosis, the expected normal renal response is a U_{NH4}/U_{Cr} ratio higher than 150 mmol NH_4^+/g creatinine (higher than 15 if creatinine is measured in mmol).

There are two issues in using the urine net charge (or urine anion gap) to assess the rate of excretion of NH_4^+ that, in our opinion, limit its utility. First, the calculation of the urine net charge detects high rates of excretion of NH_4^+ in the urine only when the anion excreted with NH_4^+ is Cl^-. Second, the equation that describes the relationship between U_{NH4} and the urine net charge, which was based on values obtained from 24 hour urine collection, is shown below (Eq. 24.11).

$$U_{NH4} = -0.8\ (\text{urine anion gap}) + 82 \qquad (24.11)$$

where 82 is the difference between the usual rates of excretion of other unmeasured anions and other unmeasured cations in the urine in subjects described as consuming normal diet.[48a] This value however may have large variations depending on dietary intake.

Determine Why the Rate of Excretion of NH_4^+ Is Low

Urine pH. The urine pH is not a reliable indicator for the rate of excretion of NH_4^+ (Fig. 24.8).[49] On the other hand, the basis for the low rate of excretion of NH_4^+ may be deduced from the urine pH. A urine pH about 5 suggests that the primary basis for a low rate of excretion of NH_4^+ is decreased availability of NH_3 in the medullary interstitial compartment due to a defect in NH_4^+ production or its transfer in the mTAL of the loop of Henle. A urine pH higher than 7.0 suggests that NH_4^+ excretion is low because there is a defect in net H^+ secretion in the distal nephron. Conversely, a urine pH about 6 would suggest a medullary interstitial disease that diminishes both accumulation of NH_4^+ in the medullary interstitium and H^+ secretion in the MCD.[50]

Assess Distal Hydrogen Secretion. H^+ secretion in the distal nephron can be evaluated using the measurement of the P_{CO_2} in an alkaline urine (U_{PCO_2}) during bicarbonate loading (Fig. 24.9).[51] The patient is given a load of $NaHCO_3$ to increase the filtered load of HCO_3^- and its delivery to the distal nephron; the urine must be freshly collected under mineral oil to minimize diffusion of CO_2 and must be analyzed immediately. A P_{CO_2} that is about 70 mm Hg in a second-voided alkaline urine implies that H^+ secretion in the distal nephron is likely to be normal, whereas much lower U_{PCO_2} values suggest that distal H^+ secretion is impaired. Some patients with low net distal H^+ secretion have a high U_{PCO_2}. This occurs if there is a lesion causing a backleak of H^+ from the lumen of the collecting ducts (e.g., due to the use of amphotericin B)[52] or distal secretion of HCO_3^- (as in some

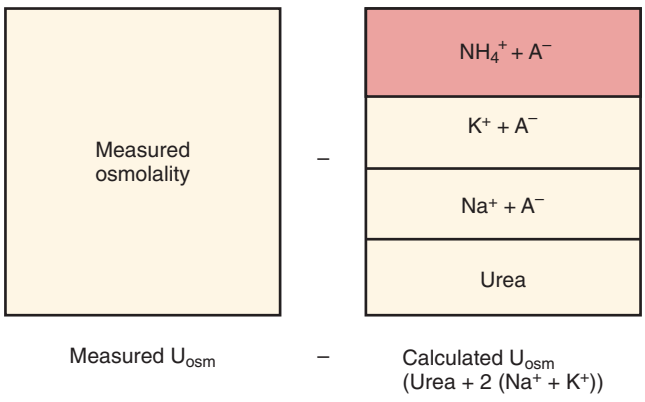

Fig. 24.7 Indirect assessment of the concentration of NH_4^+ in the urine using the urine osmolal gap. The essence of the test is that a high concentration of NH_4^+ (shown in the *red shaded region* on the *right*) is detected in the urine from its contribution to the urine osmolality. The urine osmolal gap is the difference between the measured urine osmolality and the urine osmolality calculated from the concentrations (in mmol/L) of the principal usual urine osmoles; urea, double the concentrations of $Na^+ + K^+$ (to account for the concentrations of the usual monovalent anions in the urine) and glucose in a patient with hyperglycemia. The concentration of NH_4^+ in the urine is the urine osmolal gap divided by 2. A^-, Anion. (From Kamel KS, Halperin ML. *Fluid, Electrolyte, and Acid-Base Physiology; A Problem-Based Approach.* ed 5. Philadelphia: Elsevier; 2017.)

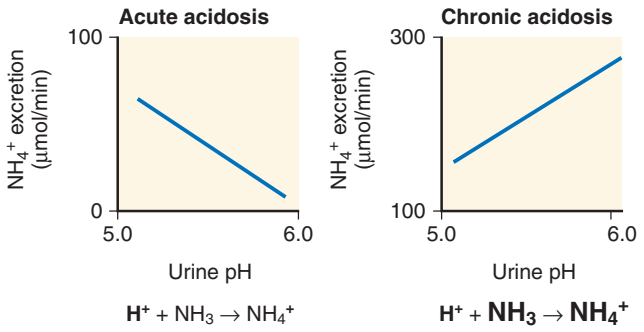

Fig. 24.8 The urine pH is not a reliable indicator for the rate of excretion of NH_4^+. *Left,* During acute metabolic acidosis, the rate of excretion of NH_4^+ is only modestly higher, and the urine pH is low. This is because distal H^+ secretion is enhanced, and there is a time lag before the rate of renal production of NH_4^+ and the availabilty of NH_3 in the medullary interstitial compartment are augmented. *Right,* In contrast, during chronic metabolic acidosis, the rate of renal production of NH_4^+ is so high that the availability of NH_3 in the medullary interstitial compartment provides more NH_3 in the lumen of the medullary collecting duct than H^+ secretion in this nephron segment. Note the much higher NH_4^+ excretion rate at a urine pH of 6. Note also the different scales on the *y*-axes. (From Kamel KS, Halperin ML. *Fluid, Electrolyte, and Acid-Base Physiology; A Problem-Based Approach.* ed 5. Philadelphia: Elsevier; 2017.)

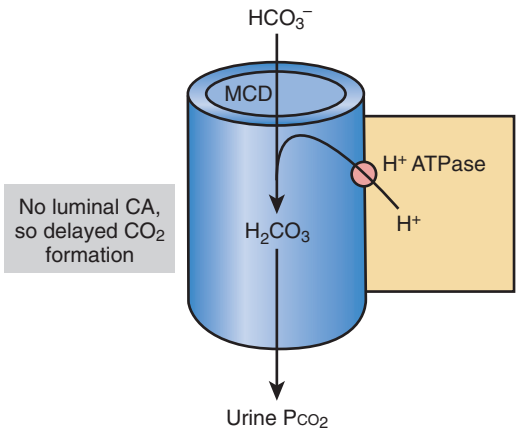

Fig. 24.9 Use of the P_{CO_2} in alkaline urine to assess the distal secretion of H^+. The cylinder represents the medullary collecting duct *(MCD)* and the rectangle on its right side represents an alpha-intercalated cell, which contains an H^+-ATPase pump. There are two requirements for using the urine P_{CO_2} in alkaline urine to reflect the capacity to secrete H^+. First, enough $NaHCO_3$ is administered to achieve a second voided-urine sample with a pH >7.0. Second, because the luminal membranes of the MCD lack carbonic anhydrase *(CA)*, the carbonic acid formed is delivered to the lower urinary tract, where it decomposes to CO_2 and H_2O and thereby elevates the urine P_{CO_2}. A high P_{CO_2} in alkaline urine (usually to ≈70 mm Hg) suggests that there is no major defect in H^+ secretory capacity in this nephron segment. (From Kamel KS, Halperin ML. *Fluid, Electrolyte, and Acid-Base Physiology; A Problem-Based Approach.* ed 5. Philadelphia: Elsevier; 2017.)

patients with SAO who have a mutation in the HCO_3^-/Cl^- anion exchanger that leads to its mistargeting to the luminal membranes of α-intercalated cells).[53]

Assessment of Proximal Cell pH

Fractional excretion of HCO_3^-. In patients suspected of having a disorder that leads to a reduced capacity for the reabsorption of HCO_3^- in the PT (pRTA), some clinicians would measure the fractional excretion of HCO_3^- after infusing $NaHCO_3$ to confirm this diagnosis. In our opinion, this evaluation is not needed. These disorders are recognized clinically by failure to correct the metabolic acidemia after the administration of large amounts of $NaHCO_3$. The defect in $NaHCO_3$ reabsorption in the PT may be an isolated defect or part of a generalized PT cell dysfunction (i.e., Fanconi syndrome), in which other Na^+-linked transport functions of PT are affected, leading to renal glucosuria, aminoaciduria, and increased rates of excretion of phosphate, urate, and citrate. The most common cause of Fanconi syndrome in the pediatric population is cystinosis, whereas common causes in the adult population are paraproteinemias and use of drugs such as tenofovir and ifosfamide.

Rate of citrate excretion. The rate of excretion of citrate is a marker of pH in cells of the PT.[54] The rate of excretion of citrate in children and adults consuming their usual diet is about 400 mg/day (≈2.1 mmol/day). The rate of excretion of citrate is very low during most forms of metabolic acidosis because of the effect of intracellular acidosis in PT cells to stimulate the reabsorption of citrate. The absence of hypocitraturia would suggest that the pathophysiology of the defect in proximal H^+ secretion is due to a disorder causing an alkaline PT cell pH, such as conditions associated with pRTA or carbonic anhydrase II deficiency (which also impairs distal H^+ secretion).

CLINICAL APPROACH TO THE PATIENT WITH HYPERCHLOREMIC METABOLIC ACIDOSIS

The steps in the clinical approach to the patient with hyperchloremic metabolic acidosis are shown in Flow Chart 24.15 and Flow Chart 24.16.

CLINICAL CASE 13: DOES THIS PATIENT HAVE DISTAL RTA?

A 28-year-old man had been intermittently sniffing glue for the last number of years. Over the past 3 days, he became profoundly weak and had a very unsteady gait. On physical examination, his blood pressure was 100/60 mm Hg and his pulse rate was 110 beats/min when he was lying flat. When he sat up, his blood pressure fell to 80/50 mm Hg and his pulse rate rose to 130 beats/min. Arterial blood pH was 7.20, arterial P_{CO_2} was 25 mm Hg, and P_{HCO_3} was 10 mmol/L. Venous blood and urine laboratory values were as follows.

Parameter	*Venous Blood*	*Urine*
pH	7.0	6.0
P_{CO_2}, mm Hg	60	—
HCO_3^-, mmol/L	12	—
Na^+, mmol/L	120	50
K^+, mmol/L	2.3	30
Cl^-, mmol/L	90	5
Creatinine	1.7 mg/dL (150 µmol/L)	3.0 mmol/L
Glucose	63 mg/dL (3.5 mmol/L)	0
Urea	BUN: 14 mg/dL (5.0 mmol/L)	150 mmol/L
Albumin	60 g/L: (6 g/dL)	—
Osmolality, mOsm/kg H_2O	260	400

Questions and Discussion

What dangers were present on admission?

Hemodynamic instability. The patient had a marked degree of EABV contraction.

Severe degree of hypokalemia. The dangers of a severe degree of hypokalemia are cardiac arrhythmias and respiratory muscle weakness. However, this patient's ECG demonstrated only prominent U waves. Analysis of arterial blood gases showed that the patient had an arterial P_{CO_2} of 25 mm Hg, which was appropriate for the fall in P_{HCO_3}; hence, there is no superimposed respiratory acidosis. Therefore, although he had a severe degree of hypokalemia that would require aggressive K^+ therapy, he did not have an emergency related to hypokalemia on admission.

Hyponatremia. Hyponatremia was likely chronic because there were no symptoms that would strongly suggest an appreciable acute component to the hyponatremia nor was there a history of a recent large water intake.

Binding of H^+ to proteins in cells. Because the brachial venous P_{CO_2} (60 mm Hg) was considerably higher than the arterial

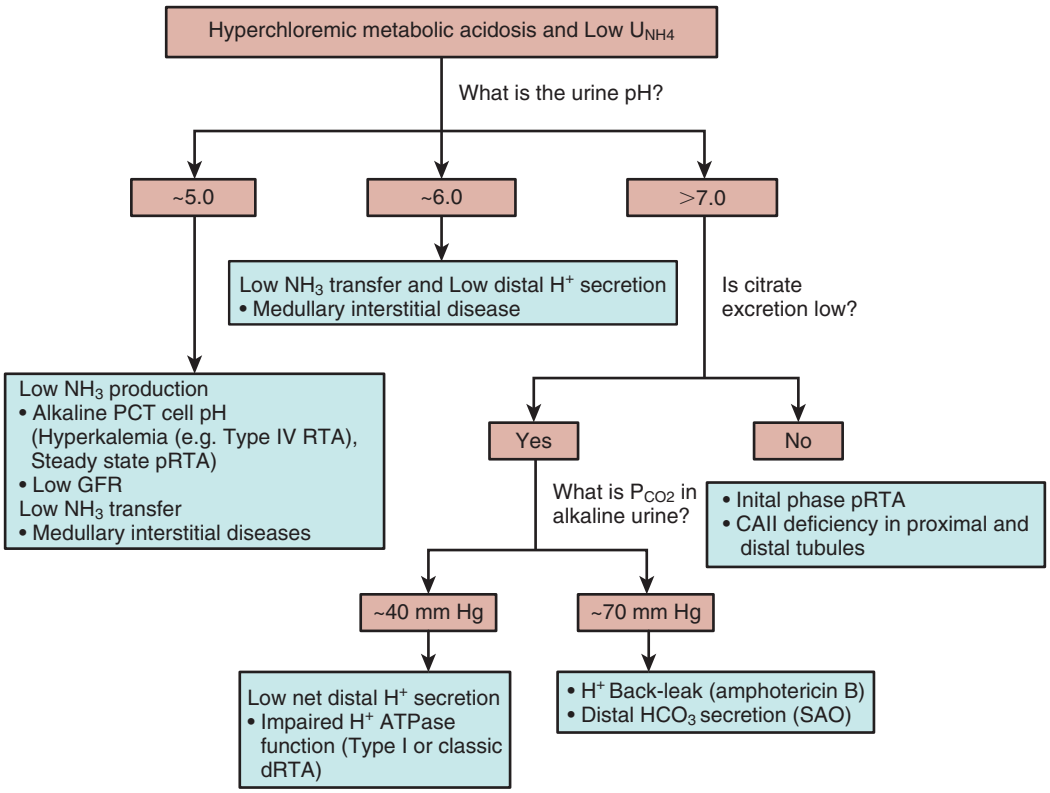

Flow Chart 24.16 *pRTA,* Proximal renal tubular acidosis; *GFR,* glomerular filtration rate; *CA II,* carbonic anhydrase type II; *dRTA,* distal RTA; *SAO,* South Asain ovalocytosis. (From Kamel KS, Halperin ML. Fluid, electrolytes and acid-base physiology. A problem based approach, ed 5. Philadelphia: Elsevier, 2017.)

P_{CO_2} (25 mm Hg), buffering of H^+ by the BBS in muscle was compromised, and there was a risk of more H^+ binding to proteins in cells of vital organs (e.g., the heart and brain; see Fig. 24.6).

What dangers should be anticipated during therapy?

A more severe degree of hypokalemia. Re-expansion of the EABV with the administration of saline can lead to decreased levels of catecholamines. This removes the inhibition of the release of insulin by the binding of catecholamines to pancreatic islet cells α-adrenergic receptors. The release of insluin could result in a shift of K^+ into cells, with worsening hypokalemia. Administration of $NaHCO_3$ to correct the metabolic acidemia may also cause a shift of K^+ into cells and a more severe degree of hypokalemia.

Rapid rise in P_{Na}. The P_{Na} may rise rapidly if water diuresis occurs with re-expansion of the EABV. As K^+ is administered, there will be a shift of K^+ into muscle cells in exchange for Na^+, which will also lead to a rise in P_{Na}. Patients who are malnourished and/or hypokalemic are at high risk of osmotic demyelination with a rapid rise in P_{Na}. It is our opinion that the maximum rise in P_{Na} in high-risk patients should not exceed 4 to 6 mmol/L in the first 24 hours.

Further fall in P_{HCO_3}. Expansion of the EABV with rapid administration of saline may also lead to a further fall in P_{HCO_3}. First, there is a dilution effect. Second, with improved blood flow to muscles and the fall in capillary P_{CO_2}, there will be titration of HCO_3^- by H^+ ions that are bound to intracellular proteins. The need to give $NaHCO_3$, however, must be balanced by the danger of creating more severe hypokalemia. We would not administer $NaHCO_3$ unless there is hemodynamic instability that is not responsive to the usual maneuvers to restore blood pressure and, with a central venous line in place, to give a sufficient amount of KCl rapidly if needed.

Plan for initial therapy. On arrival to the emergency department, the patient was given 1 L of intravenous isotonic saline. To correct the hypokalemia while also avoiding a rapid rise in P_{Na}, the intravenous solution was changed to 0.45% NaCl (77 mmol/L) to which KCl, 40 mmol/L, was added. The concentration of effective cation osmoles of this solution (77 + 40 = 117 mmol/L) is close to his P_{Na}, and thus should not itself lead to a rapid rise in P_{Na}. The danger of a rapid rise in P_{Na} due to enhanced delivery of filtrate to the distal nephron and/or due to eliminating decreased EABV-mediated release of vasopressin is still present. Therefore, the patient was given DDAVP to prevent a water diuresis, and water restriction was imposed. Hemodynamic status, P_K, P_{Na}, arterial pH, arterial P_{CO_2}, brachial venous P_{CO_2}, and P_{HCO_3} were monitored closely.

What is the basis for the metabolic acidosis? Because the $P_{anion\ gap}$ was not increased, despite the high value for the P_{Alb}, the metabolic acidosis was judged not to be due to a gain of acids. In fact, the initial diagnosis was type I or classic dRTA which was thought to explain the metabolic acidemia, urine pH of 6.0, and hypokalemia. Calculation of the $U_{osm\ gap}$ (90 mOsmol/kg H_2O), however, revealed a high

urinary concentration of NH_4^+ (45 mmol/L). Furthermore, the U_{NH4}/U_{Cr}, was about 15 (mmol/mmol) and the rate of excretion of creatinine in this patient was estimated to be 10 mmol/day (based on his body weight); hence, the rate of excretion of NH_4^+ was estimated to be around 150 mmol/day. Therefore, the basis for the patient's hyperchloremic metabolic acidosis was not dRTA.

The anion that was excreted with NH_4^+ was not Cl^-, so diarrhea was not the cause of the hyperchloremic metabolic acidosis. Hence, the patient had an acid gain–type of metabolic acidosis, with a high rate of excretion of its anion in the urine. Because the $P_{anion\ gap}$ was not elevated, these new anions were more likely to have entered the urine via secretion in the PT, akin to *p*-aminohippurate anions. The major chemical in glue is toluene; it is converted to benzoic acid by cytochrome P450 in the liver, and benzoic acid is in turn conjugated to the amino acid glycine to form hippuric acid.[55] H^+ titrate HCO_3^- resulting in metabolic acidosis, whereas the hippurate anions are actively secreted by PT, so their concentration is very low in plasma and very high in the urine. The rate of excretion of hippurate anions exceeds the rate of excretion of NH_4^+ in the urine because a limited amount of NH_4^+ can be made in the PT, so hippurate anions are excreted along with Na^+, resulting in the indirect loss of $NaHCO_3$ (HCO_3^- loss due to titration by added H^+; Na^+ loss due to excretion in the urine with hippurate anions) and contraction of the EABV. The low EABV, via activation of the RAAS, leads to high levels of aldosterone in plasma, causing electrogenic reabsorption of Na^+ in the ASDN and thereby a high rate of secretion of K^+, leading to hypokalemia.

CLINICAL CASE 14: DETERMINE THE CAUSE OF HYPERCHLOREMIC METABOLIC ACIDOSIS

A 23-year-old woman with SAO was referred for assessment of hypokalemia. Her physical examination was unremarkable. The laboratory results in plasma and a spot urine sample are summarized in the following table. The pH and P_{CO_2} are from an arterial blood sample, whereas all other blood findings are from a venous plasma sample. The urine was glucose-free.

Parameter	*Blood*	*Urine*
Arterial pH	7.35	6.8
Arterial P_{CO_2}, mm Hg	30	—
Na^+, mmol/L	140	75
K^+, mmol/L	3.1	35
Cl^-, mmol/L	113	95
HCO_3^-, mmol/L	15	10
Anion gap, mEq/L	12	5
Osmolality, mOsm/kg H_2O	290	450
Creatinine, mg/dL	0.7	6.0 mmol/L
Urea (mmol/L)		220
Citrate	—	Low

Questions and Discussion

What is the basis for the hyperchloremic metabolic acidosis?
The patient had a low U_{NH_4} because the measured U_{osm} (450 mOsmol/kg H_2O) was very similar to the calculated U_{osm}, 440 mOsmol/kg H_2O—that is, $2(U_{Na}$ [75 mmol/L] + U_K [35 mmol/L]) + U_{urea} (220 mmol/L) + U_{Glu} (0). The rate of excretion of NH_4^+ was low because the U_{NH_4}/U_{Cr} was very low. Hence, the diagnosis was RTA.

What is the cause of the low rate of excretion of NH_4^+?

Urine pH. Because the urine pH is 6.8, and urine citrate was low, the basis for the low rate of NH_4^+ excretion is a low net secretion of H^+ in the distal nephron (see Flow Chart 24.16).

Assessment of distal H^+ secretion. After hypokalemia was corrected, H^+ secretion in the distal nephron could be evaluated using U_{PCO_2} during bicarbonate loading. The U_{PCO_2} in alkaline urine was 70 mm Hg (see Flow Chart 24.16). Because the U_{PCO_2} was unexpectedly high and a backleak of an H^+-type of defect was unlikely, it was suggested that the defect may be one of increased distal HCO_3^- secretion. In some patients with SAO, another mutation in the Cl^-/HCO_3^- exchanger causes it to be targeted abnormally to the luminal membranes of α-intercalated cells. The U_{PCO_2} would be high with bicarbonate loading due to the distal secretion of HCO_3^- by alkaline intercalated cells, which increases the luminal fluid pH resulting in release of H^+ from monovalent phosphate ($H_2PO_4^-$) in the luminal fluid, the formation of H_2CO_3, which then dissociates to CO_2 and H_2O.

Complete reference list available at ExpertConsult.com.

KEY REFERENCES

1. Kamel KS, Halperin ML. *Fluid, Electrolyte, and Acid-Base Physiology; a Problem-Based Approach.* 5th ed. Philadelphia: Elsevier; 2017.
2. Zhai XY, Fenton RA, Andreasen A, et al. Aquaporin-1 is not expressed in descending thin limbs of short-loop nephrons. *J Am Soc Nephrol.* 2007;18:2937–2944.
3. Kamel KS, Halperin ML. The importance of distal delivery of filtrate and residual water permeability in the pathophysiology of hyponatremia. *Nephrol Dial Transplant.* 2012;27:872–875.
5. Carlotti AP, Bohn D, Mallie JP, et al. Tonicity balance, and not electrolyte-free water calculations, more accurately guides therapy for acute changes in natremia. *Intensive Care Med.* 2001;27:921–924.
9. Napolova O, Urbach S, Davids MR, et al. Assessing the degree of extracellular fluid volume contraction in a patient with a severe degree of hyperglycaemia. *Nephrol Dial Transplant.* 2003;18:2674–2677.
15. Kamel KS, Schrieber M, Halperin ML. Renal potassium physiology: integration of the renal response to dietary potassium depletion. *Kidney Int.* 2018;93:41–53.
21. Kamel KS, Halperin ML. Intrarenal urea recycling leads to a higher rate of renal excretion of potassium: an hypothesis with clinical implications. *Curr Opin Nephrol Hypertens.* 2011;20:547–554.
25. Wilson FH, Disse-Nicodeme S, Choate KA, et al. Human hypertension caused by mutations in WNK kinases. *Science.* 2001;293:1107–1112.
30. Halperin ML, Scheich A. Should we continue to recommend that a deficit of KCl be treated with NaCl? A fresh look at chloride-depletion metabolic alkalosis. *Nephron.* 1994;67:263–269.
35. Gowrishankar M, Kamel KS, Halperin ML. Buffering of a H^+ load; A "brain-protein-centered" view. *J Am Soc Nephrol.* 2007;18:2278–2280.
37. Kraut JA, Madias NE. Serum anion gap: its uses and limitations in clinical medicine. *Clin J Am Soc Nephrol.* 2007;2:162–174.
43. Kamel KS, Halperin ML. Acid-base problems in diabetic ketoacidosis. *N Engl J Med meant.* 2015;372:546–554.
47. Dyck R, Asthana S, Kalra J, et al. A modification of the urine osmolal gap: an improved method for estimating urine ammonium. *Am J Nephrol.* 1990;10:359–362.
48. Kamel KS, Halperin ML. An improved approach to the patient with metabolic acidosis: a need for four amendments. *J Nephrol.* 2006;65:S76–S85.
50. Kamel KS, Briceno LF, Santos MI, et al. A new classification for renal defects in net acid excretion. *Am J Kidney Dis.* 1997;29:136–146.

REFERENCES

1. Kamel KS, Halperin ML. *Fluid, Electrolyte, and Acid-Base Physiology; a Problem-Based Approach.* 5th ed. Philadelphia: Elsevier; 2017.
2. Zhai XY, Fenton RA, Andreasen A, et al. Aquaporin-1 is not expressed in descending thin limbs of short-loop nephrons. *J Am Soc Nephrol.* 2007;18:2937–2944.
3. Kamel KS, Halperin ML. The importance of distal delivery of filtrate and residual water permeability in the pathophysiology of hyponatremia. *Nephrol Dial Transplant.* 2012;27:872–875.
4. Halperin ML, Kamel KS, Oh MS. Mechanisms to concentrate the urine: an opinion. *Curr Opin Nephrol Hypert.* 2008;17:416–422.
5. Carlotti AP, Bohn D, Mallie JP, et al. Tonicity balance, and not electrolyte-free water calculations, more accurately guides therapy for acute changes in natremia. *Intensive Care Med.* 2001;27:921–924.
6. Kamel KS, Bichet DG, Halperin ML. Studies to clarify the pathophysiology of partial central diabetes insipidus. *Am J Nephrol.* 2001;37:1290–1293.
7. Carlotti ACP, St George-Hyslop C, Guerguerian AM, et al. Occult risk factor for the development of cerebral edema in children with diabetic ketoacidosis: possible role for stomach emptying. *Ped Diabetes.* 2009;10:522–533.
8. Hoorn EJ, Carlotti AP, Costa LA, et al. Preventing a drop in effective plasma osmolality to minimize the likelihood of cerebral edema during treatment of children with diabetic ketoacidosis. *J Pediatr.* 2007;150:467–473.
9. Napolova O, Urbach S, Davids MR, et al. Assessing the degree of extracellular fluid volume contraction in a patient with a severe degree of hyperglycaemia. *Nephrol Dial Transplant.* 2003;18:2674–2677.
10. Kamel KS, Magner PO, Ethier JH, et al. Urine electrolytes in the assessment of extracellular fluid volume contraction. *Am J Nephrol.* 1989;9:344–347.
11. Miller TR, Anderson RJ, Linas SL, et al. Urinary diagnostic indices in acute renal failure: a prospective study. *Ann Intern Med.* 1978;89:47–50.
12. Weisberg LS. Pseudohyponatremia: a reappraisal. *Am J Med.* 1989; 86:315–318.
13. Ware JS, Wain LV, Channavajjhala SK, et al. Phenotypic and pharmacogenetic evaluation of patients with thiazide-induced hyponatremia. *J Clin Invest.* 2017;127:3367–3374.
14. Cheema-Dhadli S, Chong CK, Kamel KS, et al. An acute infusion of lactic acid lowers the concentration of potassium in arterial plasma by inducing a shift of potassium into cells of the liver in fed rats. *Nephron Physiol.* 2012;120:p7–p15.
15. Kamel KS, Schrieber M, Halperin ML. Renal potassium physiology: integration of the renal response to dietary potassium depletion. *Kidney Int.* 2018;93:41–53.
16. Leviel F, Hubner CA, Houillier P, et al. The Na^+-dependent chloride-bicarbonate exchanger SLC4A8 mediates an electroneutral Na^+ reabsorption process in the renal cortical collecting ducts of mice. *J Clin Invest.* 2010;120:1627–1635.
17. Carlisle E, Donnelly S, Ethier J, et al. Modulation of the secretion of potassium by accompanying anions in humans. *Kidney Int.* 1991; 39:1206–1212.
18. Sansom SC, Welling PA. Two channels for one job. *Kidney Int.* 2007;72:529–530.
19. Welling PA, Chang YP, Delpire E, et al. Multigene kinase network, kidney transport, and salt in essential hypertension. *Kidney Int.* 2010;77:1063–1069.
20. Welling PA, Ho K. A comprehensive guide to the ROMK potassium channel: form and function in health and disease. *Am J Physiol Renal Physiol.* 2009;297:F849–F863.
21. Kamel KS, Halperin ML. Intrarenal urea recycling leads to a higher rate of renal excretion of potassium: an hypothesis with clinical implications. *Curr Opin Nephrol Hypertens.* 2011;20:547–554.
22. Berl T, Rastegar A. A patient with severe hyponatremia and hypokalemia: osmotic demyelination following potassium repletion. *Am J Kidney Dis.* 2010;55:742–748.
23. Lin SH, Lin YF, Halperin ML. Hypokalaemia and paralysis. *QJM.* 2001;94:133–139.
24. Lin SH, Lin YF. Propranolol rapidly reverses paralysis, hypokalemia and hypophosphatemia in thyrotoxic periodic paralysis. *Am J Kidney Dis.* 2001;37:620–624.

24a. Wu KL, Cheng CJ, Sung CC, et al. Identification of the causes for chronic hypokalemia: importance of urinary sodium and chloride excretion. *Am J Med.* 2017;130:846–855.

25. Wilson FH, Disse-Nicodeme S, Choate KA, et al. Human hypertension caused by mutations in WNK kinases. *Science.* 2001;293: 1107–1112.
26. Hoorn EJ, Walsh SB, McCormick JA, et al. The calcineurin inhibitor tacrolimus activates the renal sodium chloride cotransporter to cause hypertension. *Nat Med.* 2011;17:1304–1309.
27. Schambelan M, Sebastian A, Rector FC Jr. Mineralocorticoid-resistant renal hyperkalemia without salt wasting (type II pseudohypoaldosteronism): role of increased renal chloride reabsorption. *Kidney Int.* 1981;19:716–727.
28. Harris AN, Grimm PR, Lee HW, et al. Mechanism of hyperkalemia-induced metabolic acidosis. *J Am Soc Nephrol.* 2018;29(5): 1411–1425.
29. Nishida H, Sohara E, Nomura N, et al. Phosphatidylinositol 3-kinase/Akt signaling pathway activates the WNK-OSR1/SPAK-NCC phosphorylation cascade in hyperinsulinemic db/db mice. *Hypertension.* 2012;60:981–990.
30. Halperin ML, Scheich A. Should we continue to recommend that a deficit of KCl be treated with NaCl? A fresh look at chloride-depletion metabolic alkalosis. *Nephron.* 1994;67:263–269.
31. Scheich A, Donnelly S, Cheema-Dhadli S, et al. Does saline "correct" the abnormal mass balance in metabolic alkalosis associated with chloride depletion in the rat? *Clin Invest Med.* 1994;17: 448–460.
32. Rubin SI, Sonnenberg B, Zettle R, et al. Metabolic alkalosis mimicking the acute sequestration of HCl in rats: bucking the alkaline tide. *Clin Invest Med.* 1994;17:515–521.
33. DeMars C, Hollister K, Tomassoni A, et al. Citric acidosis: a life-threatening cause of metabolic acidosis. *Ann Emerg Med.* 2001;38: 588–591.
34. Zalunardo N, Lemaire M, Davids MR, et al. Acidosis in a patient with cholera: a need to redefine concepts. *QJM.* 2004;97: 681–696.
35. Gowrishankar M, Kamel KS, Halperin ML. Buffering of a H^+ load; A "brain-protein-centered" view. *J Am Soc Nephrol.* 2007;18: 2278–2280.
36. Halperin ML, Kamel KS. Some observations on the clinical approach to metabolic acidosis. *J Am Soc Nephrol.* 2010;21:894–897.
37. Kraut JA, Madias NE. Serum anion gap: its uses and limitations in clinical medicine. *Clin J Am Soc Nephrol.* 2007;2:162–174.
38. Emmett M. Anion-gap interpretation: the old and the new. *Nat Clin Pract Nephrol.* 2006;2:4–5.
39. Feldman M, Soni N, Dickson B. Influence of hypoalbuminemia or hyperalbuminemia on the serum anion gap. *J Lab Clin Med.* 2005;146:317–320.
40. Kamel KS, Cheema-Dhadli S, Halperin FA, et al. Anion gap: may the anions restricted to the intravascular space undergo modification in their valence? *Nephron.* 1996;73:382–389.
41. Stewart PA. Modern quantitative acid-base chemistry. *Can J Physiol Pharmacol.* 1983;61:1444–1461.
42. Rastegar A. Clinical utility of Stewart's method in diagnosis and management of acid-base disorders. *Clin J Am Soc Nephrol.* 2009;4: 1267–1274.
43. Kamel KS, Halperin ML. Acid-base problems in diabetic ketoacidosis. *N Engl J Med meant.* 2015;372:546–554.
44. Shull PD, Rapoport J. Life-threatening reversible acidosis caused by alcohol abuse. *Nat Rev Nephrol.* 2010;6:555–559.
45. Simpson DP. Control of hydrogen ion homeostasis and renal acidosis. *Medicine (Baltimore).* 1971;50:503–541.
46. Weiner ID, Verlander JW. Renal ammonia metabolism and transport. *Compr Physiol.* 2013;3:201–220.
47. Dyck R, Asthana S, Kalra J, et al. A modification of the urine osmolal gap: an improved method for estimating urine ammonium. *Am J Nephrol.* 1990;10:359–362.
48. Kamel KS, Halperin ML. An improved approach to the patient with metabolic acidosis: a need for four amendments. *J Nephrol.* 2006;65:S76–S85.

48a. Goldstein MB, Bear R, Richardson RMA, et al. The urine anion gap: a clinically useful index of ammonium excretion. *Am J Med Sci.* 1986;292:198–292.

49. Richardson RMA, Halperin ML. The urine pH: a potentially misleading diagnostic test in patients with hyperchloremic metabolic acidosis. *Am J Kidney Dis.* 1987;10:140–143.
50. Kamel KS, Briceno LF, Santos MI, et al. A new classification for renal defects in net acid excretion. *Am J Kidney Dis.* 1997;29:136–146.

51. Halperin ML, Goldstein MB, Haig A, et al. Studies on the pathogenesis of type I (distal) renal tubular acidosis as revealed by the urinary PCO2 tensions. *J Clin Invest.* 1974;53:669–677.
52. Roscoe JM, Goldstein MB, Halperin ML, et al. Effect of amphotericin B on urine acidification in rats: implications for the pathogenesis of distal renal tubular acidosis. *J Lab Clin Med.* 1977;89:463–470.
53. Kaitwatcharachai C, Vasuvattakul S, Yenchitsomanus P, et al. Distal renal tubular acidosis in a patient with Southeast Asian ovalocytosis: possible interpretations of a high urine PCO2. *Am J Kidney Dis.* 1999;33:1147–1152.
54. Simpson DP. Citrate excretion: a window on renal metabolism. *Am J Physiol.* 1983;244:F223–F234.
55. Carlisle EJF, Donnelly SM, Vasuvattakul S, et al. Glue-sniffing and distal renal tubular acidosis: sticking to the facts. *J Am Soc Nephrol.* 1991;1:1019–1027.

25 Diagnostic Kidney Imaging

Vinay A. Duddalwar | Hossein Jadvar | Suzanne L. Palmer

CHAPTER OUTLINE

KEY POINTS

- Imaging tests are tailored to answer specific clinical scenarios and are often modified to address specific clinical questions.
- Positron emission tomography with a number of different radiotracers may allow for imaging characterization of the underlying tumor biology in renal cell carcinoma.
- Contrast enhanced ultrasound is an additional imaging technique to consider using especially in the presence of abnormal renal function.
- The development of multiple radiation dose reduction techniques and the development of dual energy CT scans have made an impact in the imaging strategy of patients requiring follow-up imaging.
- Techniques such as dynamic contrast media-enhanced MR renography, diffusion-weighted imaging (DWI), and blood oxygen level-dependent (BOLD) MRI can help evaluate various aspects of renal function.

Medical imaging has made major strides over the past century since the discovery of x-rays by Wilhelm Roentgen. Imaging tools now include sophisticated systems that can noninvasively interrogate structure, function, and metabolism in health and disease states of all organ systems, including the urinary system. X-ray studies primarily provide anatomic information and include plain radiography, intravenous urography (IVU), antegrade and retrograde pyelography, and computed tomography (CT). Ultrasonography (US), which does not have ionizing radiation, involves the use of high-frequency sound waves. The development of additional techniques in US such as Doppler US, elastography, and contrast-enhanced US has led to an expansion of the role of US in the evaluation of the kidney. Magnetic resonance imaging (MRI) uses the phenomenon of nuclear magnetic resonance and yields primarily anatomic information but also can provide some functional information. Nuclear medicine studies, including planar and single-photon computed tomography (SPECT) techniques, contribute primarily functional information; positron emission tomography (PET) and integrated PET-CT and PET-MRI, in conjunction with a number of current and novel radiotracers, provide means for a quantitative assessment of a variety of physiologic parameters. In addition, there have been significant changes in image processing and visualization technology that have led to an increase in the imaging applications for the kidney. Understanding the diagnostic utility and limitation of each imaging modality facilitates the proper evaluation of patients in various specific clinical settings.

IMAGING TECHNIQUES

PLAIN RADIOGRAPH OF THE ABDOMEN

Historically, plain radiography of the abdomen was used as the starting point in the evaluation of the kidneys, as well as the rest of the abdomen. Relative to more advanced technology, radiography of the kidneys, ureters, and bladder (KUB) (Fig. 25.1) yields little significant information on its own and if used at all, should be the starting point for further evaluation of the kidneys, such as the scout film for IVU.

INTRAVENOUS UROGRAPHY

Previously IVU (also known as intravenous pyelography) was used as the primary means of evaluating the kidneys and urinary tract[1,2]; however, CT has supplanted IVU for routine imaging. An IVU is now seldom performed and usually only when specific clinical questions need to be answered.[3] A scout film (KUB) is performed before any contrast material is injected intravenously. Timed sequential images of the kidneys and the remainder of the genitourinary system are then obtained.[4,5] The nephrogram demonstrates the size and

Fig. 25.1 Plain radiograph of the abdomen: kidneys, ureters, and bladder. The kidneys lie posteriorly in the retroperitoneum in the upper abdomen. They are surrounded by fat. The ribs overlie the kidney, and bowel gas is visible in the right upper quadrant. The psoas muscles are also well visible because retroperitoneal fat abuts them.

Fig. 25.2 Intravenous urography: excretory phase. This image was obtained 10 minutes after the injection of the contrast material. The kidneys are well visualized; contrast material outlines the calyces, pelvis, ureters, and bladder.

shape of the kidney while anatomic depiction of the calyces, infundibula, and pelvis is best displayed on subsequent images by 5 to 10 minutes after injection. Imaging of the ureters is usually accomplished 10 to 15 minutes after injection[6] (Fig. 25.2).

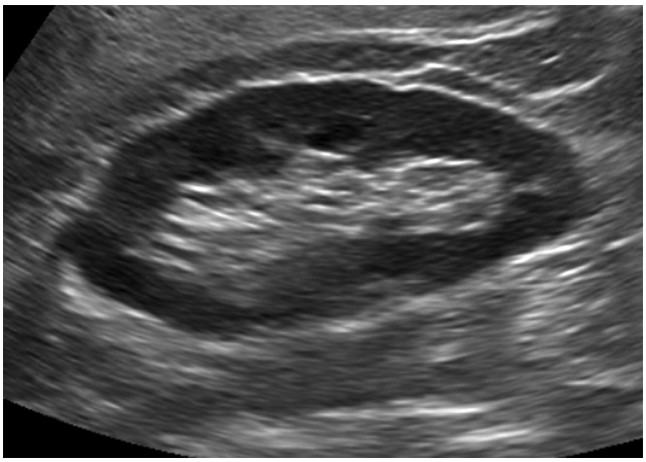

Fig. 25.3 Renal ultrasonography: normal kidney. The central echogenic structure represents the vascular elements, calyces, and renal sinus fat. The peripheral cortex is noted to be smooth and regular. Renal pyramids may be depicted as hypoechoic structures between the central echo complex and the cortex.

ULTRASONOGRAPHY

US is the most frequently used diagnostic examination for the evaluation of the kidneys and urinary tract.[7] It is noninvasive, uses no ionizing radiation, and requires minimal patient preparation. It is the first-line examination in azotemic patients to assess renal size and the presence or absence of hydronephrosis and obstruction. It is used to assess the vasculature of native and transplanted kidneys. US is also used to evaluate renal structure and to characterize renal masses. It is the primary modality of imaging for evaluation of a transplanted kidney. It is also the most commonly used modality for imaging guidance for a kidney biopsy.

Diagnostic US is an outgrowth of sound navigation and ranging (sonar) technology. In medical US, high-frequency sound waves are used to evaluate various organs. In the abdomen and, more particularly, the kidneys, 2.5- to 4.0-mHz sound waves are generally employed.

The US unit consists of a transducer, which sends and receives the sound waves; a microprocessor or computer, which obtains and processes the returning signal; and an image display system or monitor, which displays the processed images. The piezoelectric transducer converts electrical energy into high-frequency sound waves that are transmitted through the patient's body. It converts the returning reflected sound waves back into electrical energy that can be processed by a computer. Sound travels as a waveform through the tissues being imaged. The speed of the sound wave depends on the tissue through which it is traveling.

Different tissues and the interface between these tissues have different acoustic impedance. As the sound wave travels through different tissues, part of the wave is reflected back to the transducer. The depth of the tissue interface is measured by the time the sound wave takes to return to the transducer. A gray-scale image is produced by the measured reflected sound, in which the intensity of the pixels (picture elements) is proportional to the intensities of the reflected sound (Fig. 25.3). When the acoustic interfaces are quite large, strong echoes result. These are known as *specular reflectors* and are visible from the renal capsule and bladder wall.

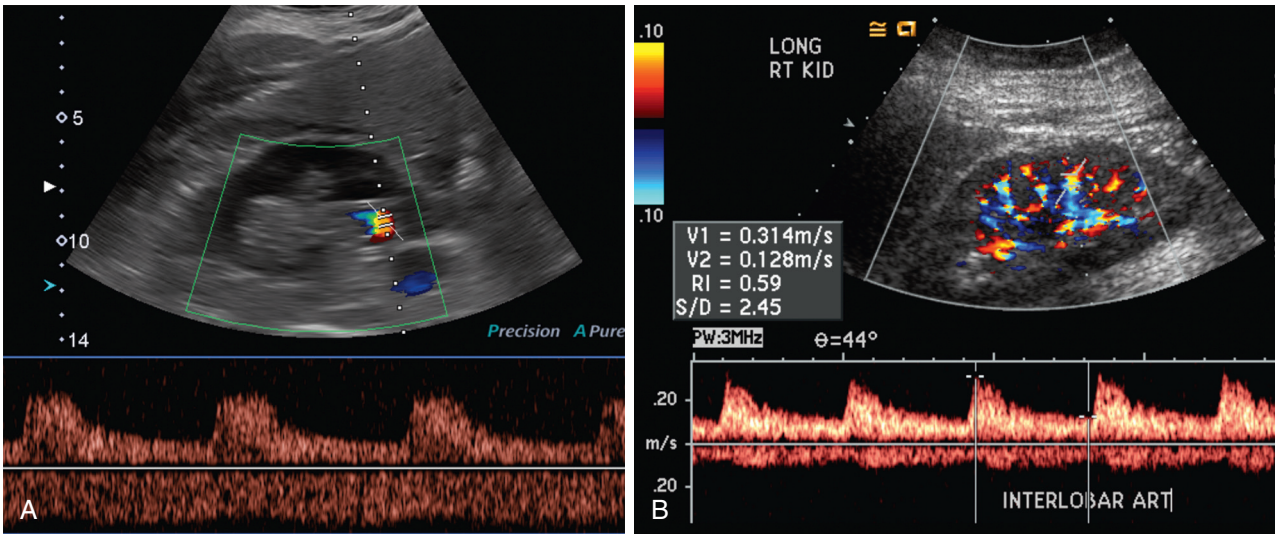

Fig. 25.4 Spectral Doppler ultrasound of the normal kidney. **A,** Normal waveform. **B,** Calculation of the resistive index (RI). *V1*, peak systolic velocity (S); *V2*, end diastolic velocity (D). RI = (S-D)/S.

Nonspecular reflectors generate echoes of lower amplitude and are visible in the renal parenchyma. Strong reflection of sound by bone and air results in little or no information from the tissues beneath; this appearance is known as *shadowing*. Lack of acoustic impedance as observed in fluid-filled structures, such as the urinary bladder and renal cysts, allows the sound waves to penetrate further, which results in a relative increase in intensity distal to the structures; this is known as *increased through transmission*. All of these features are used to help characterize various lesions. Real-time US, which provides sequential images at a rapid frame rate, allows the demonstration of motion of organs and pulsation of vessels.

Doppler US, based on the Doppler frequency shift of the sound wave caused by moving objects, can be used to assess venous and arterial blood flow.[8,9] The movement of blood cells in blood vessels is used to generate Doppler information, and this is used to derive diagnostic information. Spectral Doppler is a technique that displays the blood flow measurements graphically, displaying flow velocities over time. This can be in the form of a continuous wave (CW) Doppler or pulsed wave (PW) Doppler. CW Doppler permits measurement of flow along the line of evaluation whereas the PW technique allows evaluation of flow at a particular location. In clinical practice a combination of the two techniques is used together for evaluation. In a technique called pulsed wave Doppler US, quantification of this flow and assessment of the waveforms can be used in evaluating various organ systems (Fig. 25.4A). With Doppler color-flow US, the image is encoded with colors assigned to the pixels representing the direction and volume of flow within vessels (Fig. 25.5). In power Doppler US, the amplitude of the signal, without any directional information, is used to produce a color map of the intrarenal vasculature and flow within the kidneys (Fig. 25.6).

Resistive index is a measure of the resistance to blood flow caused by the microvascular bed distally. This serves as a nonspecific indicator of disease in both native and transplanted kidneys. In general, a normal resistive index is 0.70 or less (see Fig. 25.4B). An increased resistive index is a

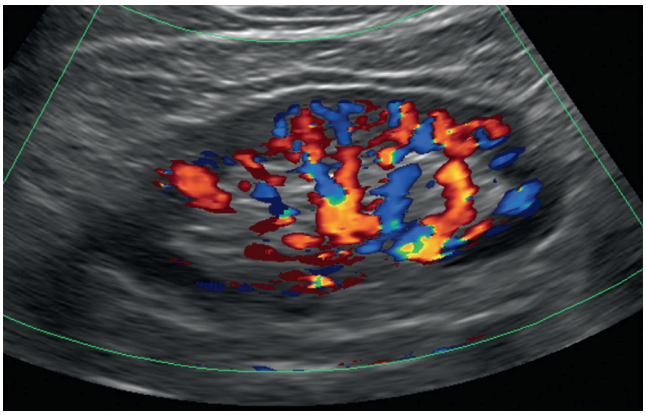

Fig. 25.5 Doppler color-flow ultrasonography: normal kidney. The red echogenic areas represent arterial flow (flow toward the transducer), and blue echogenic areas represent venous flow (flow away from the transducer).

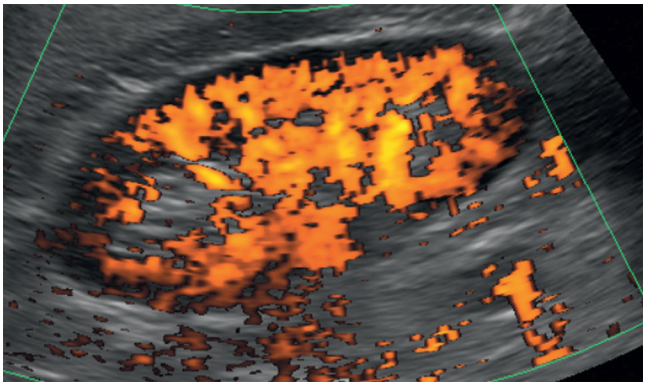

Fig. 25.6 Power Doppler ultrasonography: normal kidney. The color image represents a summation of all flow—arterial and venous—within the kidney.

nonspecific indicator of disease and a sign of increased peripheral vascular resistance.[8–10]

Elastography is another technique by which the mechanical properties of a target tissue are assessed. It is a measure of the stiffness in a tissue, and its role in the evaluation of chronic parenchymal disease is being evaluated. The change in the elasticity of a particular tissue is assessed by changes in the propagation velocity of ultrasound waves.[11] Elastography techniques are the focus of interest in evaluating both native kidneys in chronic kidney disease as well as evaluating transplant kidneys.

There has been an increase in the use of intravenous contrast agents with US for the evaluation of the kidneys and renal masses, a technique called contrast-enhanced ultrasound (CEUS).[12] The contrast agents are microbubbles of a high-molecular-weight gas such as perfluorocarbons that are stabilized by a thin capsule of lipid or protein. They are of the same size as blood cells and therefore are not filtered out in the lungs or the kidneys. The advantage of these agents is that they are excreted by pulmonary ventilation, and therefore they can be used in patients with very poor renal function. They remain in the vascular system (acting as blood pool agents) and can provide another method of providing information on organ perfusion and vascularity. These contrast agents have expanded the role of US and have given an additional option in the imaging of patients with compromised renal function. The development of these US-specific contrast agents enables the display of microvasculature and dynamic enhancement patterns which are not visible using other methodologies.

Imaging after injection of these contrast agents is performed using contrast-specific ultrasonographic modes using a low mechanical index technique. These are based on the cancellation of linear ultrasound signals from tissue and using a nonlinear response from microbubbles.

Uses for CEUS in the kidney include the following: (1) characterization of focal renal lesions: accurate characterization of complex renal cysts into different Bosniak groups, increase in diagnostic confidence in the evaluation of focal renal masses, permits differentiation of variant normal anatomy, including conditions such as a hypertrophied column of Bertin[13]; (2) evaluation of transplanted kidney: CEUS can help identify vascular complications such as arterial and venous thrombosis and ischemia; and (3) follow-up of renal trauma.[14] CEUS can also identify and characterize post-intervention complications.[15]

US is the most common imaging technique in guiding a renal biopsy. Its advantages include the lack of radiation and mobility, thus allowing bedside procedures. US guidance is also used for other interventional procedures such as percutaneous nephrostomy placement and renal mass ablations. In addition, US along with Doppler US is very commonly used for mapping and assessment of access sites in both arteriovenous (AV) shunts and fistulas in a patient undergoing dialysis.

ULTRASONOGRAPHY: NORMAL ANATOMY

US images of the kidneys are generally obtained in the longitudinal, transverse, and parasagittal planes.[16] The appearance of the perinephric fat varies from slightly less echogenic to highly echogenic in comparison with the renal cortex. The renal capsule is visible as an echogenic line surrounding the kidney. The centrally located renal sinus and hilum, containing renal sinus fat, vessels, and the collecting system, are usually echogenic because of the presence of fat (see Fig. 25.3). The amount of renal sinus fat generally increases with age. Tubular structures corresponding to vessels and the collecting system may be visible in the renal hilum. Doppler color-flow US may be used to differentiate the vessels from the collecting system.

The normal renal cortex is less echogenic (i.e., it appears darker) than the liver and spleen. The renal medullary pyramids are hypoechoic, and their triangular shape points to the renal hilum. The renal cortex lies peripherally, and its separation from the medulla is usually demarcated by an echogenic focus attributable to the arcuate arteries along the corticomedullary junction. Columns of Bertin have the same echogenicity as the renal cortex and separate the renal pyramids. On occasion, a large column of Bertin may simulate a mass. Even when a column of Bertin is large or prominent, its echogenicity is the same as the remainder of the cortex, and the vascular pattern observed on power Doppler images is also the same.

Renal size is accurately measured by US. Normal kidneys range from 8.5 to 13 cm, depending on the age, sex, and body habitus of the patient. The contours of the kidneys should be smooth; occasionally some slight nodularity is present as a result of developmental fetal lobulation. The renal arteries and veins may be visible extending from the renal hilum to the aorta and inferior vena cava (IVC). The veins lie anterior to the arteries. The renal arterial branching pattern within the kidneys may be visible on Doppler color-flow US (see Fig. 25.5).[17] The resistive indices of the main, intralobar, and arcuate vessels may be calculated (see Fig. 25.4B). With power Doppler US, the intrarenal vasculature may be assessed; it demonstrates an overall increased pattern in the cortex in relation to the medulla, which corresponds to the normal arterial flow to the kidney (see Fig. 25.6).[18,19] The renal calyces and collecting systems are not typically visible with US unless distension caused by diuresis or obstruction is present. When visible, the collecting systems are anechoic structures in the renal sinus fat, connecting together at the renal pelvis. The urinary bladder is visible in the pelvis as a fluid-filled anechoic structure. The entrance of the ureters into the bladder at the trigone may be visualized on Doppler color-flow US as ureteral jets (Fig. 25.7).

When a kidney is not identified in its normal location, the remainder of the abdomen and pelvis should be assessed. Ectopic kidneys may lie lower in the abdomen or within the pelvis and may also be located on the opposite side; the kidneys may even be fused (e.g., horseshoe kidneys). Horseshoe kidneys tend to lie lower in the retroperitoneum, and their axes may be different from those of normal kidneys.

COMPUTED TOMOGRAPHY

CT has become an essential imaging tool for diagnosis in all areas of the body. In the genitourinary tract, it has supplanted IVU, especially for the evaluation of flank pain, hematuria, renal masses, and trauma. Even in areas in which US is the first-line imaging modality, CT offers a complementary and sometimes superior means of imaging. CT is now the first examination to be performed in patients with renal colic, renal stone disease, renal trauma, renal infection and abscess, renal mass, hematuria, and urothelial abnormalities.

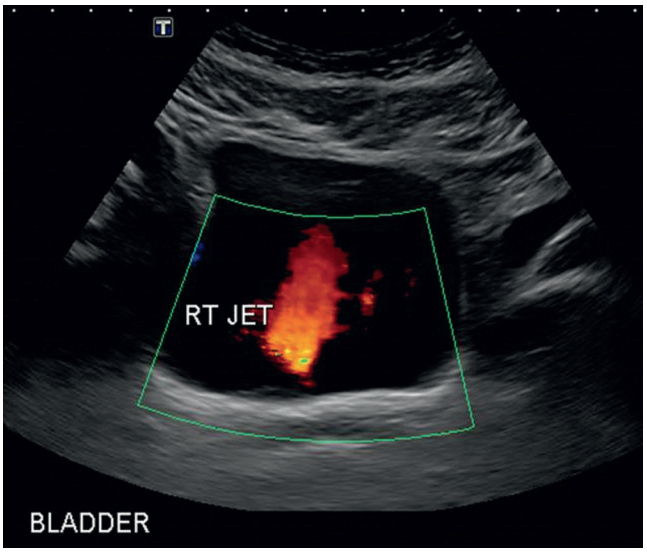

Fig. 25.7 Ureteral jet. Color-flow image of urine entering the bladder.

After CT was first developed in 1970, it evolved rapidly with new technical innovations, image processing, and visualization methods.[20] In addition, over the last decade, concerted efforts have resulted in the reduction of the radiation absorbed by patients during a CT scan.

CT is the computer reconstruction of a radiographically generated image that depicts a slice through the area being studied in the body. The x-ray tube produces a highly collimated fan beam and is mounted opposite an array of electronic detectors. This system rotates in tandem around the patient. The detector system collects hundreds of thousands of samples representing the attenuation of the x-ray along the line formed from the x-ray source to the detector as the rotation occurs. This data set is transferred to a computer, where the image is reconstructed. The CT image is made up of pixels (picture elements), each corresponding to a CT density number (Hounsfield unit [HU]) that represents the number of x-rays absorbed by the patient at a particular point in the cross-sectional image. These pixels represent a two-dimensional display of a three-dimensional object or volume element (voxel). The third dimension is the slice thickness or depth. Thus the HU is the average attenuation of x-rays of all the tissues within a specific voxel, which is then used to create the individual image. The images are then displayed on a computer monitor for reviewing and analysis.

The HU of water is 0. Tissues that attenuate more x-rays than water have positive HU, and those with less x-ray attenuation than water have negative HU. Different shades of gray on a scale of white to black are assigned to HU (the highest number is depicted as white, the lowest as black). The image of each slice is thus created on a display monitor, and this image may be manipulated on viewing monitors to accentuate the regions being imaged. The advantage of this digital image set is that by using various tools such as window levels and widths and different summation and reconstruction techniques, images can be optimized to evaluate a particular organ or region.

The initial CT scanners were relatively slow because the technology required a point-and-shoot process. This initial generation of body CT scanner led to a scan of the abdomen that took up to 2 to 4 minutes or more to complete. In 1990, helical/spiral technology was introduced in which the x-ray tube and detector system continuously rotated around the patient, and the patient moved continuously through the gantry. Scan time through the abdomen was significantly reduced. After helical/spiral CT, a two-detector system was introduced that produced two slices for every 360-degree rotation of the x-ray tube and detector system. Multidetector CT (MDCT) systems with 640 detectors are in use primarily for advanced applications, such as computed tomographic angiography (CTA) for the coronary arteries. Most commonly today, MDCT systems varying from 64 to 320 detectors are used in abdominal and pelvic scanning. With MDCT, each 360-degree rotation results in the number of slices equal to the number of detectors (i.e., a 64-detector system produces 64 slices in one 360-degree rotation). These technologic advances have led to a dramatic increase in the speed of scans (4–10 seconds), a routine use of thin slices or collimation (1–2 mm thick), and a marked improvement in spatial resolution (ability to display small objects clearly).[21]

As a result of the faster scanning times, the use of enhancement by intravenous contrast material has improved and become more widely used.[22] For example, the kidneys can be scanned in the arterial, corticomedullary, nephrographic, and delayed phases, which allows for a more complete assessment. Current, state-of-the-art MDCT acquires data as a volumetric study, and the slice thickness has been reduced to the point that sagittal, coronal, oblique, and off-axis images may be displayed with no loss of resolution. The data acquisition may also be displayed as a three-dimensional volumetric display with the regions of interest highlighted.[21] The kidneys are well suited for assessment with MDCT.[22–26]

More recent technical developments include dual-energy and spectral-energy scanners that offer the ability to image an organ at different energy strengths.[27] Tissues behave differently at different energies, and this fact is used in techniques such as characterization of calculi and obtaining virtual unenhanced images and iodine maps in different organs (Fig. 25.8).

COMPUTED TOMOGRAPHY TECHNIQUE, INCLUDING UROGRAPHY

Most clinical questions require the use of intravenous contrast and a tailored CT urography (CTU) is a way to provide a comprehensive examination of the genitourinary tract. CTU may be used to assess the kidney as a whole (anatomic), the vascular tree (function and perfusion), and the excretory (urothelial) patterns.[28] Noncontrast scans enable assessment of renal calculi, high-density cysts, and contour abnormalities.[29] Early-phase scans (12–15 seconds) enable arterial assessment, for example, the evaluation for renal artery stenosis (RAS). Scanning at 25 to 30 seconds (corticomedullary phase) results in clear corticomedullary differentiation, recommended for renal mass evaluation. At 90 to 100 seconds, true nephrographic-phase imaging of the kidneys is obtained.[22] Delayed imaging, typically at 5 to 10 minutes, enables the evaluation of the urothelium (calyces, renal pelvis, ureters, and bladder) in the excretory phase.[30] Axial images, multiplanar reconstructions, maximum-intensity projection images, and three-dimensional volumetric displays complement each other in CTU. CTU is superior to IVU.[31–34] Not all the phases are required for all clinical situations; therefore the examination should be tailored to a specific clinical question. Urothelial lesions can often be evaluated by combining the nephrographic and delayed phases into a single phase by

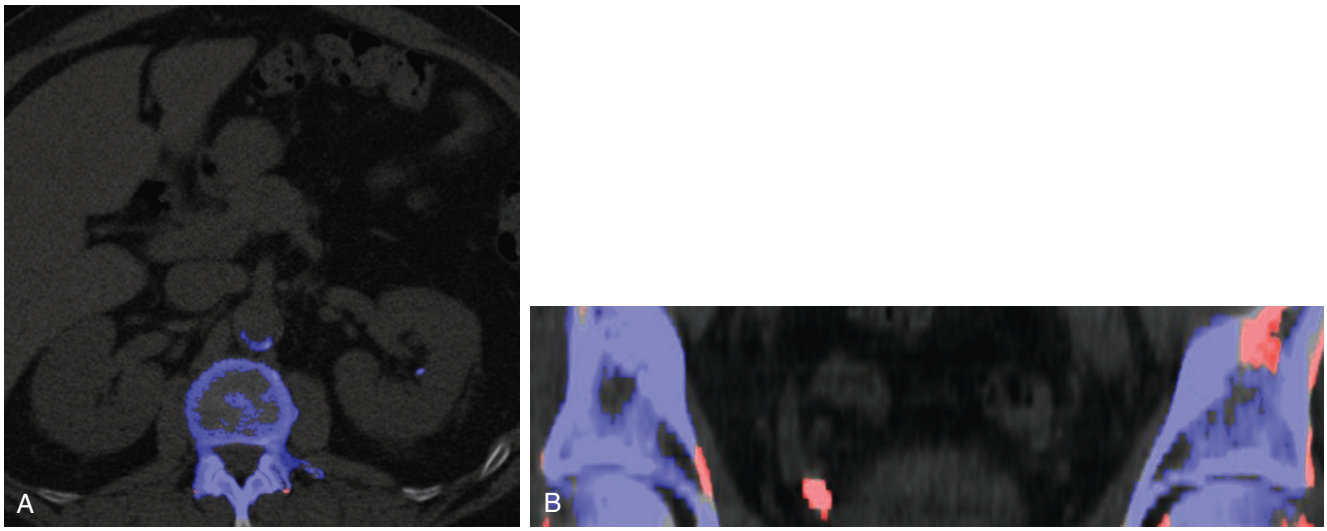

Fig. 25.8 Dual-energy computed tomography (CT) for stone characterization in two different patients. **A,** Postprocessed color-coded axial CT image in a 54-year-old patient obtained after dual-energy CT scanning shows a left renal calculus coded blue, indicating a nonuric acid stone. **B,** Postprocessed color-coded coronal CT image in a 66-year-old patient obtained after dual-energy CT scanning shows a right distal ureteric calculus color-coded red, indicating a uric acid stone. Technique: An initial routine stone protocol multidetector CT scan is performed for detection and localization of the calculi along the renal pelvicalyceal system. Subsequently, a focused dual-source CT scan is performed in the region of the stone. Dual-energy CT is performed on the dual-source CT scanner (Somatom Definition) with the following technique: 80 kV/350–380 mAs and 140 kV/80-98 mAs, 14 × 1.2 mm/64 × 0.6 mm. The postprocessing is performed using a three-material decomposition algorithm on the dual-energy software on the scanner console (Syngo.via). (Image courtesy Avinash Kambadakone, MD, Massachusetts General Hospital, Boston, MA.)

using a split–contrast bolus technique. This involves giving the iodinated contrast intravenously in two separate boluses but scanning only once.

Another technical innovation is the development of spectral CT or multienergy CT.[27] This involves the ability to scan a particular tissue with two or more different energies. Knowing how a target tissue attenuates at different energies can provide further details of the tissue composition. For example, spectral CT can help in differentiating types of renal calculi and characterizing renal masses. It also provides the ability to generate virtual unenhanced data sets, as well as increasing detection rates of iodine-containing tissues.

Work on reducing radiation exposure is also being aggressively pursued. Because of the development of new reconstruction algorithms such as iterative reconstruction and model-based reconstruction, there has been a significant (50%–70%) reduction in the resultant radiation dose without any change in the quality of the study. Further advances in technology will result in incremental reductions of dose.

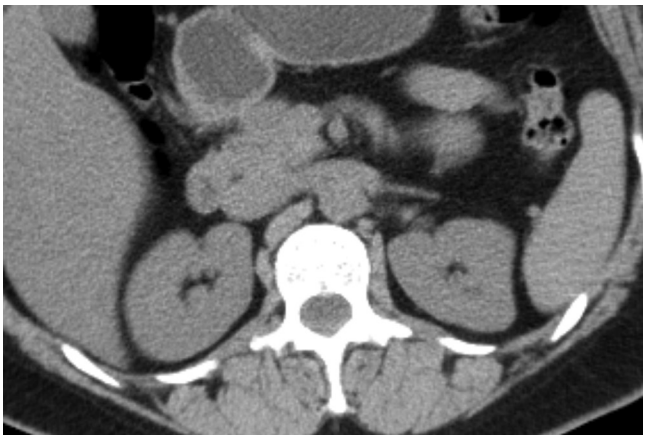

Fig. 25.9 Noncontrast computed tomographic scan through the midportion of normal kidneys. The kidneys lie in the retroperitoneum with the lumbar spine and psoas muscles more centrally. The liver is anterolateral to the right kidney, and the spleen anterolateral to the left kidney.

COMPUTED TOMOGRAPHY: NORMAL ANATOMY

The retroperitoneal anatomy is easily viewed with CT (Figs. 25.9 to 25.14). The kidneys lie in the retroperitoneum, surrounded by Gerota's fascia in the perinephric space. Perinephric fat surrounds the kidneys with the liver anterosuperior on the right, the spleen superior on the left, and the spine, aorta, and IVC central to each kidney. The abdominal intraperitoneal contents lie anteriorly. The renal arteries are easily seen on both arterial and venous phases, generally located posterior to the venous structures. The adrenal glands are found in a location superior to the upper poles of the kidneys. In corticomedullary phase imaging, it is easy to distinguish the renal cortex from the medulla. Cortical thickness and medullary appearance may be readily assessed. The nephrographic phase should demonstrate symmetric enhancement of each kidney.[22] At 7 to 10 minutes in the excretory phase, the calyces should be well depicted with sharp fornices, a cupped central section, and a narrow, smooth infundibulum leading to the renal pelvis.[30] Coronal images in slab maximum-intensity projection three-dimensional volumetric reformations help in displaying the anatomic details.[33] The excretory phase images delineate the ureters from the renal pelvis to the bladder. A curved reformatted series of images or three-dimensional display is needed to display the ureters in their entirety. Proper tailoring of the examination to the diagnostic problem provides guidance for the correct imaging acquisition.[23,25,34]

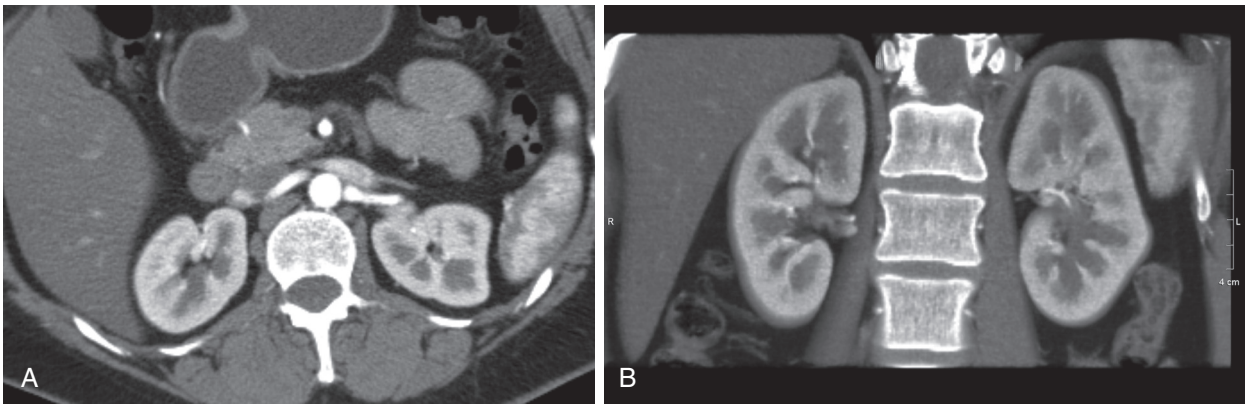

Fig. 25.10 Computed tomographic scan: normal corticomedullary phase. Axial slice **(A)** and coronal image **(B)** demonstrate the dense enhancement of the cortex in relation to the medulla containing the renal pyramids.

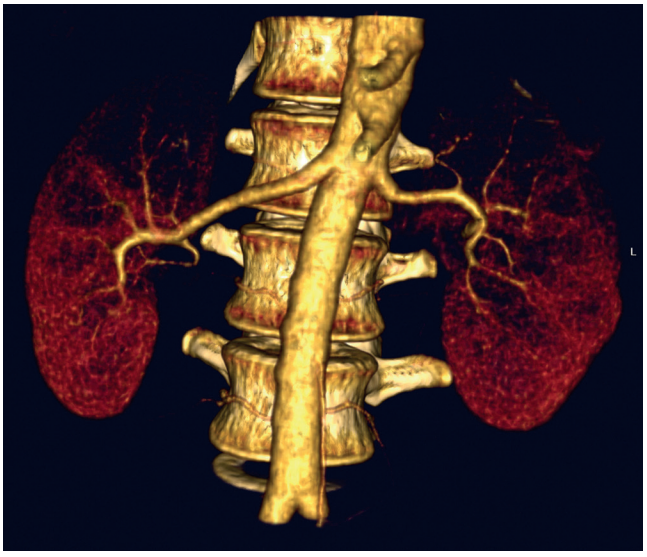

Fig. 25.11 Renal computed tomographic angiogram: normal findings. The aorta and the exiting renal arteries on the right and left are visible in this volume rendered reconstruction. The kidneys are visible peripherally with the branching renal arteries.

IODINATED CONTRAST MEDIA

Over the years, many different intravascular contrast media have been employed.[35] Since the mid-2000s, virtually all studies involving intravascular injection of contrast material have been performed with low osmolar (LOCM) or isoosmolar (IOCM) contrast media.

Contrast material has a plasma half-life of 1 to 2 hours in patients with normal renal function. Virtually all contrast material is excreted by the kidneys within 24 hours. In patients with renal failure, contrast media may be excreted via other routes, including the biliary system or gastrointestinal tract. All iodinated contrast agents are dialyzable.

Reactions to the injection of any of the contrast agents may occur; however, these reactions are not "allergic" responses in the sense of an antigen-antibody reaction and are referred to as idiosyncratic.[36] The exact causative mechanism is unclear but is likely as a result of complex effects on various vasoactive mediators such as histamine, complement and the kinin chain. Although the majority of these reactions are mild or minor, severe reactions and deaths do occur. With ionic high osmolar contrast media (HOCM) the reaction rate in the general population is 5% to 6%.[37] The rates of reactions to LOCM and IOCM agents are much lower, in the range of 1% to 2%.[38–40] Serious reactions are rare with a historical rate of 0.04%. Mild reactions consist of flushing, nausea, and vomiting, and treatment is not required. Mild dermal reactions, primarily urticaria, do occur and may or may not necessitate treatment. Moderate and severe reactions, which occur considerably less frequently, include bronchospasm, laryngeal edema, seizures, arrhythmias, syncope, shock, and cardiac arrest. All moderate and severe reactions necessitate treatment.

Because the reaction that occurs in patients after injection of contrast material is not antigen-antibody mediated, pretesting plays no role.[41] Neither the rate of injection nor the dose of contrast material has been clearly established as a determinant in the occurrence of contrast material–related reactions.[38,42] The only regimen that has proven to reduce the incidence of contrast-induced reactions is the modified Greenberger protocol[17]:

Clinical Relevance

The only regimens proven to reduce the incidence of contrast-induced reactions to include pretreatment with glucocorticoids and antihistamines.

Two frequently used regimens are as follows: (1) prednisone—50 mg orally at 13 hours, 7 hours, and 1 hour before contrast injection, plus diphenhydramine 50 mg intravenously, intramuscularly, or orally 1 hour before contrast medium.[42] (2) Methylprednisolone—32 mg orally 12 hours and 2 hours before contrast media injection.[43] An antihistamine (as in option 1) can also be added to this regimen. An alternative that may be used in specific clinical circumstances, although less desirable than the 13-hour protocol is a 5-hour protocol consisting of methyl prednisolone 40 mg intravenously or hydrocortisone 200 mg IV immediately and every 4 hours before contrast injection plus diphenhydramine 50 mg IV 1 hour before admission.[44]

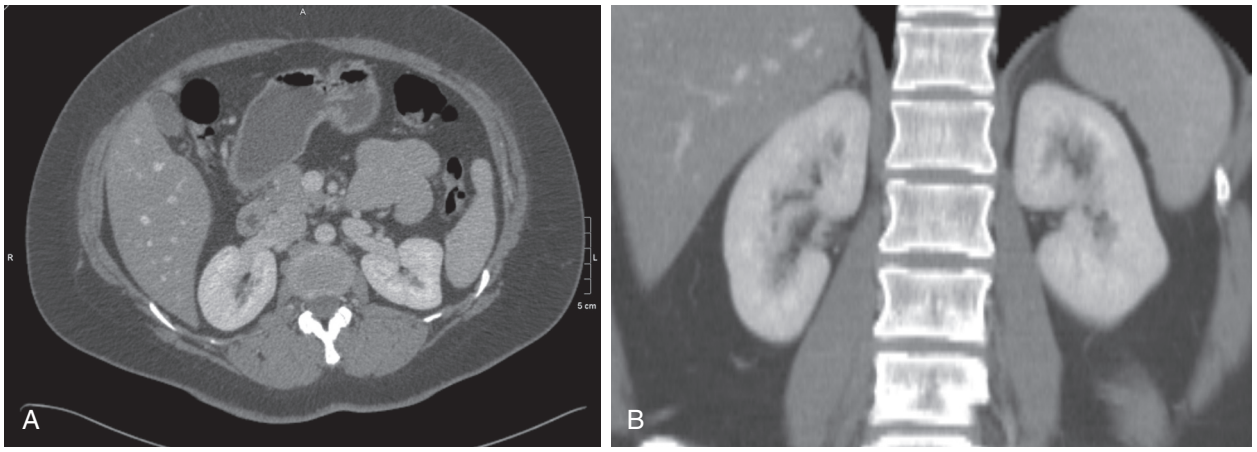

Fig. 25.12 Computed tomographic scan: normal nephrographic phase. The axial image **(A)** and the coronal image (**B**) demonstrate the homogeneous appearance of the kidneys, with the cortex and medulla no longer differentially enhanced. These images are typically obtained 80 to 120 seconds after the injection of contrast material.

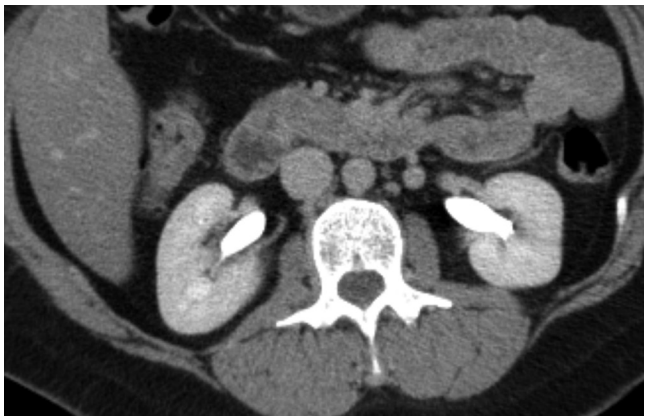

Fig. 25.13 Computed tomographic scan: normal excretory phase. The calyces and renal pelvis are now easily noted because they are opacified by the excreted contrast material. This scan is obtained 5 to 10 minutes after the injection of contrast material.

Currently, the success rate of this accelerated protocol is based on a large single trial which showed a noninferior result. The overall goal of the premedication strategy is to reduce the risk of contrast reactions through standardized protocols and recognizing that contrast reactions may still happen despite premedication (breakthrough reactions). Most experts believe that the likelihood of a reaction is reduced in patients who are premedicated.[45]

POSTCONTRAST ACUTE KIDNEY INJURY (PC-AKI) AND CONTRAST-INDUCED NEPHROPATHY (CIN)

There is an ongoing debate around occurrence, causes, screening strategies and management of PC-AKI. Please see Chapters 28 and 29 for a discussion of this topic in the context of the pathophysiology and management of AKI. For clarification, we describe the terms as in the American College of Radiology Manual on contrast media.[45] (v.10.3, https://www.acr.org/-/media/ACR/Files/Clinical-Resources/Contrast_Media.pdf)

PC-AKI.: a deterioration in renal function occurring within 48 hours following intravascular administration of iodinated contrast, regardless of the cause of the worsening of renal function. PC-AKI is a correlative diagnosis.

CIN: a subset of PC-AKI in which the intravascularly administered contrast is the cause of the deterioration of renal function. CIN is a causative diagnosis and is a subgroup of PC-AKI.

Contrast media–induced nephropathy (CIN) is most often qualitatively defined as acute kidney injury (AKI) occurring within 48 hours of exposure to intravascular radiographic contrast material that is not attributable to other causes. However, there is no universally accepted quantitative definition of CIN. The most commonly used definition is a 25% increase in serum creatinine from baseline value or an absolute increase of at least 0.5 mg/dL that appears within 48 hours after contrast administration and is maintained for 2 to 5 days.[46] Importantly, these definitions do not follow the Acute Kidney Injury Network (AKIN)[47] or Kidney Disease: Improving Global Outcomes (KDIGO)[48] definitions of AKI. Lack of uniformity in definition has contributed to significant variation in incidence of CIN reported in the literature. The American College of Radiology therefore proposed using AKIN/KDIGO criteria for a definition of AKI related to intravascular CIN:

The diagnosis of PC-AKI is made if any of the following occurs within 48 hours of contrast injection:

1. Absolute increase in serum creatinine level of 0.3 mg/dL or higher and more than 26.4 µmol/L
2. A percentage increase in serum creatinine level of 50% or higher (1.5-fold above baseline), or
3. Urine output reduced to 0.5 mL/kg/h or less for at least 6 hours

The concept that contrast agents pose serious risks has become a dogma with far-reaching consequences. Yet this belief stems from clinical studies with significant limitations. Inclusion of highly selected patient populations (e.g., those undergoing angiography), poor study design (i.e., uncontrolled case studies), larger volumes of contrast, especially hyperosmolar contrast and use of inconsistent definitions of CIN call into question to what extent the risk for CIN is applicable to the vast majority of people undergoing diagnostic

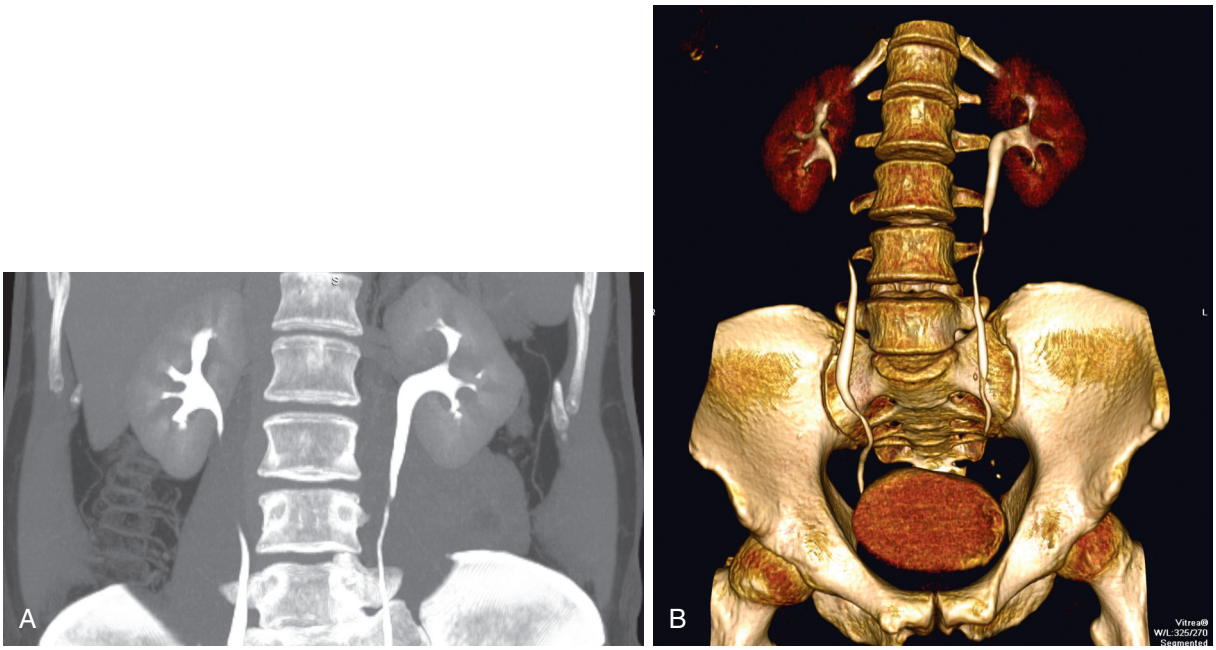

Fig. 25.14 Computed tomographic urogram: normal findings. The maximum-intensity projection (MIP) image **(A)** and the volume-rendered image **(B)** demonstrate the calyces, renal pelvis, ureters, and bladder. The MIP image is a slab, 15-mm thick, in the coronal plane. The volume-rendered image was taken as the extraneous tissues adjacent to the kidneys were removed, and it highlights the genitourinary tract.

radiology studies.[49] In addition, increased awareness in the last 15 years has led to optimized use of contrast in high-risk individuals. Another factor that has led to confounding data is that a lot of the studies may have referred to two distinct populations—those undergoing cardiac angiography and those undergoing contrast-enhanced CT. The patients undergoing angiography should be assessed separately as the contrast is administered differently. It is injected directly into the arterial system by a catheter which could potentially dislodge thromboemboli. In addition, the contrast bolus to the kidneys is more likely to be concentrated as well as abrupt compared with a peripheral intravenous injection of contrast.[50–52]

There is a relative paucity of controlled studies to evaluate the incidence and causality of CIN. Although these studies are a significant improvement over noncontrolled studies, bias in control group selection within the studies may also have introduced error. Two studies by Davenport et al, and McDonald et al, used prospective propensity matching to correct for potential bias introduced by assigning patients to contrast or noncontrast groups on the basis of factors such as age and the presence of a preexisting low eGFR, other than those which the experiment was designed to test.[53,54] Davenport et al, found that patients with a serum creatinine less than 1.5 mg/dL before CT scan were not at risk for nephropathy.[53] As creatinine levels increased, the risk for AKI after CT scan increased for both groups (contrast group and noncontrast group), but contrast medium administration remained an independent risk factor. In contrast, McDonald et al, concluded that intravenous contrast medium was not associated with increased risk for nephrotoxicity, even in those with preexisting chronic kidney disease (CKD).[54]

The clinical course of patients with PC-AKI and CIN depend on a number of factors including the baseline renal function, coexisting risk factors, medication, and hydration. The usual clinical course (which may be asymptomatic in PC-AKI) is of a transient elevation of serum creatinine within 24 hours of contrast administration, peaking within 96 hours and returning to baseline within 7 to 10 days.[55,56] Although in the vast majority of patients this is transient, many studies have reported that patients with PC-AKI have longer hospital stays, higher mortality and higher incidences of cardiac and neurologic events. However, these studies did not include control groups and some of the mortality and morbidity attributed to CIN in the past may be due to factors not associated with contrast administration.[45]

Because current data cannot definitely refute the existence of CIN, many professional society guidelines advise a conservative approach, and this fact in itself may have contributed to the reduction in observed incidence of CIN in recent years. The European Society of Urogenital Radiology guidelines identify an estimated glomerular filtration rate (eGFR) of 45 mL/min/1.73 m^2 as a threshold below which contrast medium poses a risk.[57,58] The Canadian Association of Radiologists suggests that nephropathy risk begins to increase at an eGFR of 45 mL/min/1.73 m^2 and increases significantly when the eGFR reaches 30 mL/min/1.73 m^2.[59]

The following section provides the protocols used at the University of Southern California Keck School of Medicine for administration of intravenous contrast in adults. These practices were developed based on consensus developed by a department clinical committee and based on review of multiple guidelines from national and international radiology organizations, practices at other academic institutions and advice from colleagues in nephrology and laboratory medicine.

Each patient referral should be considered on an individual basis within the context of this background information, and strict adherence to these guidelines in all cases is discouraged. Physician judgment is paramount.

SCREENING/EVALUATION OF RISK FACTORS

There have been a number of attempts to identify and isolate risk factors for CIN. These include patient age older than 60 years, history of renal disease (including dialysis, transplant, renal surgery), history of diabetes, hypertension and heart failure; however, volume depletion or renal hypoperfusion are the most significant risk factors.[59–61]

CONTRAST ADMINISTRATION IN PATIENTS WITH ELEVATED CREATININE LEVEL

The decision to proceed with contrast administration in patients with an eGFR below 45 mL/min/1.73 m^2 should always be a matter of clinical judgment. If contrast administration is considered essential, the following options should be considered:

HYDRATION or VOLUME EXPANSION is one of the most important methods for decreasing the incidence of CIN. Broad consensus exists that volume expansion reduces the risk for CIN. Adequate volume expansion improves renal blood flow, induces diuresis with dilution of contrast material within the tubules, reduces the activation of the renin angiotensin aldosterone system, suppresses the secretion of antidiuretic hormone, and minimizes reductions in the renal production of endogenous vasodilators such as nitric oxide and prostacyclin. The hydration protocol is not as important as the fact that some form of hydration is administered; however, controversy exists about the route of hydration and the composition. For example, intravenous hydration has not been proven superior to oral hydration and the use of intravenous sodium chloride versus sodium bicarbonate are also debated. In addition, the practicality of routine use of parenteral hydration protocols in an outpatient setting is questionable.

ORAL VERSUS INTRAVENOUS HYDRATION: Studies directly comparing intravenous with oral hydration are sparse because most of the hydration studies used intravenous hydration and included other forms of therapy for prevention of CIN. One study, Preparation for Angiography in Renal Dysfunction (PREPARED), showed no significant difference between outpatient oral hydration and inpatient intravenous hydration.[62] However, another study by Trivedi et al, favored intravenous hydration over oral hydration.[63] This study was limited by lack of an objective measurement of oral volume intake in the unrestricted oral hydration group. A study comparing oral fluids (1100 mL) versus intravenous fluids showed no difference in the incidence of CIN in patients with mild CKD.[64] KDIGO 2012 recommends volume expansion with intravenous fluids because there are currently not many studies showing oral volume expansion is as effective as intravenous volume expansion.[65] Because intravenous administration allows certainty of volume of hydration and may be achieved more rapidly, intravenous hydration is suggested when practical.[66]

SODIUM BICARBONATE VERSUS SALINE: The use of sodium bicarbonate instead of sodium chloride has been advocated as the resulting urinary alkalinization reduces the generation of harmful free radicals and may also increase urine flow. Several clinical trials and meta-analyses suggest that sodium bicarbonate provides equal or superior protection to isotonic saline.[67–70] However, these results have been subsequently challenged and the recently completed PRESERVE trial concluded that there was no benefit of using sodium bicarbonate in reducing PC-AKI. The 2018 American College of Radiology (ACR) guidelines do not recommend using sodium bicarbonate as a prophylactic measure to reduce the incidence of PC-AKI.[71]

VOLUME EXPANSION PROTOCOLS: The rationale of volume expansion before contrast administration is to reduce the possible risk of CIN, although the ideal route and volume of hydration is uncertain.[45] Studies have recommended that optimal hydration with intravenous normal saline is 1 to 1.5 mL/kg/h for at least 6 hours before and after contrast, in patients who are not at risk for volume overload. Although these protocols are impractical in the outpatient setting, they should be implemented for inpatients after discussion with the referring clinician, with particular attention to volume load and cardiac function. An alternative proposed intravenous volume expansion protocol (using either isotonic saline or sodium bicarbonate) is 3 mL/kg/h for 1 hour or 1 mL/kg/h for 6 hours before the procedure followed by 1 mL/kg/h for 6 hours after the procedure. Additional studies are required to assess whether a single bolus of sodium bicarbonate administered just before contrast medium administration is effective, as Tamura et al, suggested, because this protocol would be extremely useful in daily practice.[72] Due to the logistical complications of performing hydration protocols in an outpatient setting, the following regimen is suggested for outpatients with an eGFR of less than 45 mL/min/1.73 m^2: Oral hydration should be strongly encouraged in all such patients and if the patient can tolerate hydration, isotonic saline should be administered before and after the examination, adjusted according to cardiac status. In patients at risk of heart failure, but not in florid heart failure, a safer alternative to active hydration may be to withhold diuretics of the day prior to and/or the day of the contrast examination. If a patient is in overt heart failure it is preferable to delay contrast administration until heart failure is recompensated. Clinical judgment is always required.

USE OF LOW OSMOLAR CONTRAST MEDIA: Iopamidol (Isovue) and iohexol (Omnipaque) are LOCM. Most centers no longer use intravascular HOCM because of the higher incidence of various adverse effects associated with their use. Studies have failed, however, to show a clear advantage of the intravenous isoosmolar agent, iodixanol, over intravenous LOCM with regard to CIN.[71]

DECREASE TOTAL AMOUNT OF CONTRAST ADMINISTERED: It should be noted that robust data supporting a dose-toxicity relationship for intravenous iodinated contrast media administration are lacking. However, limiting volume of contrast injection and frequency in a short period of time is prudent clinical practice.[73]

INCREASE THE AMOUNT OF TIME BETWEEN CONTRAST-ENHANCED STUDIES: It takes approximately 24 hours for the entire administered dose of contrast media to be excreted by the kidneys (if the GFR is normal), so it has long been recommended to avoid intervals of less than 24 hours between studies except in urgent situations. For example, it has been recommended that patients should not receive more than 300 mL of contrast media within 24 hours unless the benefits clearly outweigh the risks.

Little solid data support this recommendation. A 2009 paper from Massachusetts General Hospital, although criticized by some authorities for methodologic issues, supports checking a repeat creatinine level before performing a second contrast media-enhanced CT (CE-CT) examination within 24 hours of a prior CE-CT scan.[68] The 2017 ACR guidelines, however, find there is insufficient evidence to justify this recommendation.[74]

Nephroprotective Strategies

N-ACETYLCYSTEINE: Multiple randomized controlled trials and meta-analyses have shown conflicting results regarding the utility of acetylcysteine to prevent CIN. It is controversial whether it is truly nephroprotective or simply lowers the serum creatinine level without preventing renal damage. Given the heterogeneity of data, it is difficult to support the administration of acetylcysteine as a proven and effective means by which to prevent CIN.[73,75] More recently, however, there is increasing literature on different pharmacologic measures including ascorbic acid, statins, fenoldopam, and others which require further study.[76]

DISCONTINUE CONCURRENT NEPHROTOXIC DRUGS, IF POSSIBLE

CORRECT ANY UNDERLYING CLINICAL CONDITIONS THAT MAY AFFECT RENAL PERFUSION

MAGNETIC RESONANCE IMAGING

Like CT, MRI is a computer-based, multiplanar imaging modality. Instead of ionizing radiation, however, electromagnetic radiation is used in MRI. MRI is an alternative to CE-CT, especially in patients with allergy to iodinated contrast material and in patients for whom reduction of radiation exposure is desired, such as pregnant women and children. MRI routinely allows detailed tissue characterization of the kidney and surrounding structures. The properties of physics underlying MRI are complex and are addressed only briefly.

Clinical MRI is based on the interaction of hydrogen ions (protons) and radiofrequency waves in the presence of a strong magnetic field.[77–79] The strong magnetic field, called the *external magnetic field*, is generated by a large-bore, high-field strength magnet. Most magnets in clinical use are superconducting magnets. The magnet strength is measured in teslas (T) and can range from 0.2 to 3 T for clinical imaging and up to 15 T for animal research. Renal imaging is performed best on high-field magnets (1.5–3 T) that allow for higher spatial resolution and faster imaging.

Images of the patient are obtained through a multistep process of energy transfer and signal transmission. When a patient is placed in the magnet, the mobile protons associated with fat and water molecules align longitudinal to the external magnetic field. No signal is obtained unless a resonant radiofrequency pulse is applied to the patient. The radiofrequency pulse causes the mobile protons within the patient to move from a lower, stable energy state to a higher, unstable energy state *(excitation)*. When the radiofrequency pulse is removed, the protons return to the lower-energy steady state while emitting frequency transmissions or signals *(relaxation)*. In radiologic terms, an external radiofrequency pulse "excites" the protons, causing them to "flip" to a higher energy state. When the radiofrequency pulse is removed, the protons "relax" with emission of a "radio signal." The signals produced during proton relaxation are separated from one another with applied magnetic field gradients. The emitted signals are captured by a receiving coil and reconstructed into images through a complex computerized algorithm: the Fourier transform.[77–79]

Different tissues have different relaxation rates that lead to different levels of signal production or signal intensity. The signal intensity of each tissue is determined by three characteristics:

1. *Proton density of the tissue.* The greater the number of mobile protons, the greater the signal produced by the tissue. For example, a volume of urine has more mobile protons than does the same volume of renal tissue; therefore, urine produces more signal than do the kidneys. Stones have far fewer mobile protons per unit volume and therefore produce little signal.
2. *T1 relaxation time.* The T1 time is how quickly a proton returns to the preexcitation energy state. The shortest T1 times (rapid relaxation) produce the strongest signal.
3. *T2 relaxation time.* The T2 time is how quickly the proton signal decays as a result of nonuniformity of the magnetic field. A nonuniform field accelerates signal decay and leads to signal loss.[77–79]

In MRI, multiple pulse sequences are obtained. A pulse sequence is a set of defined radiofrequency pulses and timing parameters used to obtain image data. These sequences include, but are not limited to, spin echo, gradient echo, inversion recovery, and steady-state free precession. The data are obtained in volumes (voxels), reconstructed as two-dimensional pixels, and displayed in relation to variations in tissue signal intensity (tissue contrast). Tissue contrast, like signal intensity, is determined by proton density and relaxation times. T1 weighting is related to the rate of T1 relaxation and the time allowed for relaxation, also known as the *pulse repetition time* (TR). T2 weighting is related to the rate of T2 relaxation and the time at which the "radio signal" is sampled by the receiver coil, also known as the *echo time* (TE). TR and TE are programmable parameters that can be altered to accentuate T1 and T2 weighting with contrast media.[77–79] For the general observer, T1-weighted sequences have short TR and TE and show simple fluid as black. T2-weighted sequences have long TR and TE and show simple fluid as white (Fig. 25.15).

Many programmable parameters other than TR and TE are used to optimize imaging. These include, but are not limited to, choice of pulse sequence, coil types and gradients, slice orientation and thickness, field of view and matrix, gating to reduce motion, and use of intravenous contrast material. Although many pulse sequences are used in clinical MRI, ultrafast sequences are preferred for renal imaging. These fast sequences can be obtained in less than 30 seconds while the patients hold their breath. The benefits of rapid acquisition include improvement in image quality, as a result of reduction of motion artifact, reduction of total scan time, and the ability to perform dynamic imaging.[80]

MRI is not possible for patients who have certain implanted medical devices, such as most pacemakers, ferromagnetic aneurysm clips, and ferromagnetic stapedial implants. Not all implants or devices cause problems, but knowledge of the type of device is crucial for determining whether the

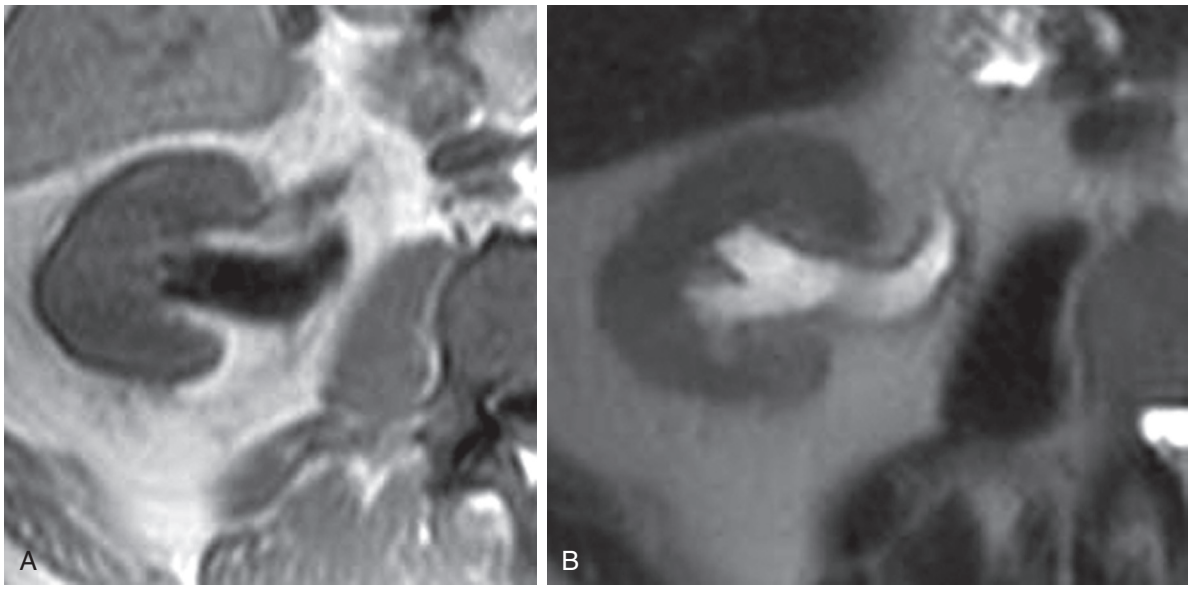

Fig. 25.15 Normal signal characteristics of simple fluids on magnetic resonance imaging. Urine appears dark on T1-weighted sequences **(A)** and bright on T2-weighted sequences **(B).**

patient can safely enter the magnet.[81] Regularly updated information regarding patient safety and the compatibility of a medical device in the MRI environment may be found at Shellock's MRIsafety.com.[82]

GADOLINIUM-BASED CONTRAST AGENTS (GBCA) AND NEPHROGENIC SYSTEMIC FIBROSIS

Intravenous contrast material is used routinely in renal imaging because it improves lesion detection and diagnostic accuracy. Gadolinium is a paramagnetic substance that shortens the T1 and T2 relaxation times, resulting in increased signal intensity on T1-weighted images and decreased signal intensity on T2-weighted sequences. The pharmacokinetics and enhancement patterns of intravenous gadolinium-based contrast agents (GBCA) used in renal imaging are similar to those of iodinated contrast agents used for IVU and CT examinations, with GBCA typically eliminated by the kidneys. There are a few agents with some amount of liver excretion. Unlike iodinated contrast agents, the dose response to GBCA is nonlinear; the signal intensity increases at low concentrations and then decreases at higher concentrations. Hence, the collecting systems, ureters, and bladder first brighten and then darken on T1-weighted sequences as the gadolinium concentration within the urine increases.

GBCA have been approved for parenteral use since the 1980s and are generally well tolerated with a good safety profile. Although most GBCA are clinically interchangeable, they can be differentiated on the basis of molecular stability, viscosity, and osmolality. GBCA can be divided into three categories based on molecular configuration: nonionic linear, ionic linear, and macrocyclic (Table 25.1). Macrocyclic agents have the greatest kinetic stability. Adverse reactions occur in approximately 0.07% to 2.4% of cases.[83] Minor reactions include coldness, warmth or pain at the injection site, nausea, vomiting, headache, paresthesia, dizziness, and itching. Rash, hives, or urticaria occurs in 0.004% to 0.07% of cases; and severe, life-threatening reactions occur in approximately 0.001% to 0.01%. Risk factors for adverse reactions include a history of prior reaction to GBCA, where rates are at an eightfold higher risk, and asthma, as well as other allergies, where rates are reported as high as 3.7%.[84] If a patient has had a prior adverse reaction to GBCA, premedication with antihistamines and corticosteroids is recommended (same premedication regimen as discussed for iodinated contrast media).

GBCA are considered to have no nephrotoxicity at the approved doses used for clinical MRI.[85–88] Because there have been some case reports of nephrotoxicity with high doses of intravenous GBCA in populations at high risk (moderate to severe kidney injury), the use of GBCA in conventional angiography is not recommended.[89,90] GBCA may interfere with serum calcium and magnesium measurements, especially in patients with renal insufficiency.[91] GBCA do not cause an

Table 25.1 Classification of Gadolinium-Based Contrast Agents Relative to Risk of Nephrogenic Systemic Fibrosis

Group I: associated with greatest number of nephrogenic systemic fibrosis (NSF) cases	Gadodiamide (Omniscan®) Gadopentetate dimeglumine (Magnevist®) Gadoversetamide (OptiMARK®)
Group II: associated with few/none unconfounded NSF cases	Gadobenate dimeglumine (MultiHance®) Gadoteridol (ProHance®) Gadobutrol (Gadavist®/ Gadovist) Gadoterate acid (Dotarem®)
Group III: data remain limited regarding NSF risk	Gadoxetic acid (Eovist®/ Primovis)

Modified from the ACR contrast manual 10.3, https://www.acr.org/Clinical-Resources/Contrast-Manual

actual reduction in serum calcium level; GBCA interfere with standard colorimetric methods of measuring serum calcium. As with iodinated contrast material, hemodialysis filters GBCA effectively, and dialysis is therefore recommended immediately after use of contrast material in patients already on hemodialysis.[92]

It is now widely accepted that there is an association between exposure to GBCA and nephrogenic systemic fibrosis (NSF), a rare, multiorgan, fibrosing condition that involves primarily the skin and subcutaneous tissues, including development of symmetric, dark red patches or papules on the skin, swelling of extremities, and thickening of skin that sometimes is described as "woody" and like an "orange peel"[93] (see also Chapter 58). Skin thickening can inhibit motion of joints, leading to contractures and immobility. Burning, itching, or severe pain in involved areas or "deep bone pain" in hips and ribs have been described. Other structures affected include the lungs, esophagus, skeletal muscles, and heart leading to restriction of function, and although NSF is not by itself a cause of death, the resulting restriction of function may contribute to death.[94] Symptoms may develop over a period of days to months; however, in approximately 5% of patients, the course may be rapidly progressive.[94] Diagnosis is confirmed by full-thickness skin biopsy, which reveals thickened collagen bundles, mucin deposition, and proliferation of fibroblasts and elastic fibers without signs of inflammation. There appears to be no predilection for gender or ethnicity. Although no treatment is known to be consistently successful, improving renal function appears to slow or stop the progression of NSF.[94]

NSF was first described in 1997. In 2006 several groups presented a possible causal relationship between the use of GBCA in patients with advanced renal disease and NSF.[95–97] This was quickly followed by published warnings and restrictive guidelines from the U.S. Food and Drug Administration (FDA), European Medicines Agency (EMA), and the ACR. These restrictive guidelines have resulted in a drastic reduction in the number of reported cases. Since 1988, more than 300 million patients have been exposed to GBCA; however, less than 600 cases of NSF have been reported in the literature. The patients at highest risk are those with severely impaired renal function, both acute and chronic. Based on data prior to the institution of restrictive use recommendations, the risk for developing NSF in patients with end-stage and severe chronic kidney disease was estimated to be from 1% to 7%, and higher with acute kidney injury.[74,98–100] The duration and underlying cause of the kidney disease appears to be irrelevant. The FDA, EMA, and ACR continue to update recommendations for the use of all classes of GBCA in high-risk patients as new information and products become available.[45,57,94,101,102]

Recently, residual gadolinium has been found in neural tissue of patients who have received multiple doses of GBCA over their lifetimes. To date, no known adverse clinical consequences have been found[103–107]; however, because the clinical significance and health implications of neural tissue deposition are unknown and relatively undefined, rigorous investigation has been initiated. Emerging data indicate that the amount of accumulated gadolinium varies with chelate stability, gadolinium deposition in the brain may be dose dependent, and gadolinium deposition has been found in patients with no evidence of kidney or liver disease.[105–109]

The most current 2018 recommendations for the use of GDCA are as follows[45,104]:

1. There are no absolute contraindications to the use of GBCA intravenously. Therefore there should be careful consideration of the clinical benefit of using GBCA for the diagnosis and treatment against the potential risks, known and unknown, especially if the patient may undergo multiple contrast-enhanced examinations over their lifetime or if the patient has acute kidney injury.
2. Screen for renal disease before the use of a GBCA. Patients who may be at high risk include those with a history of renal disease (prior dialysis, renal transplant, single kidney, kidney surgery, renal cancer), diabetes, and/or hypertension requiring medical therapy. If an outpatient is high risk for renal disease and has no prior eGFR, eGFR should be obtained. If the patient has eGFR obtained within 6 weeks of the exam, eGFR does not need to be repeated, unless the prior result was less than 45 mL/min/1.73m.[2] Outpatients with known eGFR values less than 45 mL/min/1.73 m^2 and inpatients should have eGFR obtained within two days of the MRI study. Estimated GFR is not helpful in patients on dialysis (any type) or in patients with acute kidney injury; therefore eGFR may not be necessary to obtain prior to the MRI study.
3. Severe renal impairment (eGFR ≤30 mL/min/1.73 m^2): There is a possibility that NSF may occur in this patient population; therefore contrast should be used in these patients only after careful consideration, including consideration of alternative imaging. If contrast is deemed necessary, Group II agents are recommended (see Table 25.1). Group I agents are contraindicated. Informed consent for contrast administration is not mandatory but may be obtained at the discretion of individual centers.
4. If a patient is on dialysis, determine whether the patient is a candidate for contrast-enhanced (CE) CT rather than GBCA-enhanced MRI. If MRI is to be performed, group II agents should be used because group I agents are contraindicated. Elective GBCA-enhanced MRI examinations should be performed as closely before hemodialysis as possible. Although GBCA are effectively removed with hemodialysis, no published report has proved that early dialysis prevents the development of NSF.[102] It is not recommended to start hemodialysis on patients not already on hemodialysis for the prevention of NSF. Peritoneal dialysis has not been adequately studied; however, switching to hemodialysis is not recommended after GBCA-enhanced MRI in these patients.
5. Patients with stable CKD 3 and patients with CDK 1 or 2 (stable eGFR >30 mL/min/1.73 m^2) do not require special precautions and may receive GBCA per routine protocol.
6. All contrast material should be avoided in patients with AKI due to increased risk for developing NSF. Group II GBCA should be administered only if absolutely necessary. Group 1 agents are contraindicated.

For further information regarding the different FDA-approved Gd-C agents, including their properties, how these properties may affect safety profiles, and updated recommendations to clinical practice, please refer to "ACR manual on contrast media, Version 10.3",[45] the "ACR Guidance Document for

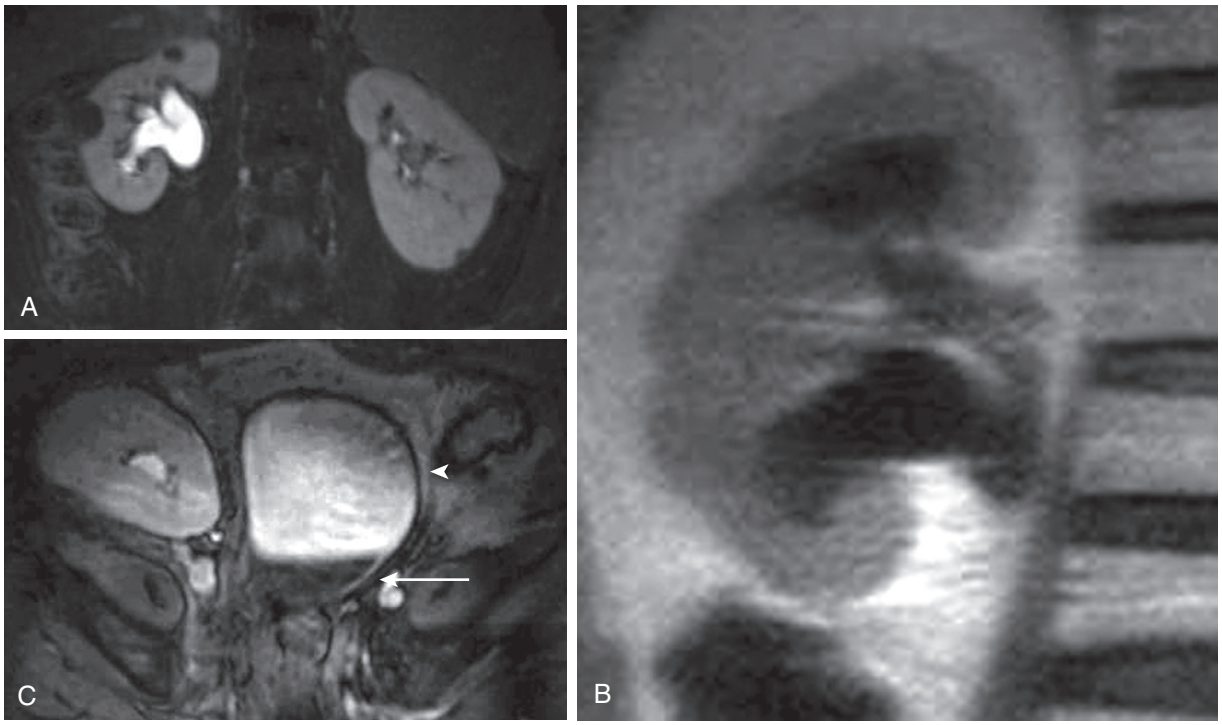

Fig. 25.16 Paramagnetic effects of gadolinium on urine. **A,** Coronal T1-weighted image from a magnetic resonance urogram (MRU) demonstrates enhancement of the urine in the collection system. **B,** Coronal T2-weighted image from an MRU demonstrates low signal intensity of urine in the collecting system secondary to effects of gadolinium. **C,** Axial T1-weighted, delayed image after contrast medium enhancement demonstrates layering of contrast material. The denser, more concentrated gadolinium is dark *(arrow).* The less concentrated gadolinium is brighter and layers above *(arrowhead).*

Safe MR Practices,"[101] and the FDA Drug Safety website (https://www.fda.gov/Drugs/DrugSafety).

DIAGNOSTIC MAGNETIC RESONANCE IMAGING TECHNIQUE

Routine MRI evaluation of the kidneys includes axial and coronal T1-weighted and T2-weighted sequences. Dynamic contrast media-enhanced T1-weighted sequences with fat suppression are also routinely obtained. Due to excellent tissue differentiation provided by MRI, the renal cortex and medullary pyramids are easily differentiated on sequences that are not enhanced by contrast media. On T1-weighted sequences the renal cortex has higher signal intensity than do the medullary pyramids. On T2-weighted sequences the renal cortex has lower signal intensity than do the medullary pyramids (Fig. 25.16). With kidney injury, this corticomedullary differentiation disappears.[45,110] Urine, like water, normally appears black on T1-weighted sequences and white on T2-weighted sequences (Fig. 25.15 and Fig. 25.17).

CE-MRI allows for dynamic evaluation of the kidneys and surrounding structures. Serial acquisitions are obtained after bolus injection of Gd-C (0.1–0.2 mmol per kilogram of body weight) at 2 mL/sec.[111,112] The injection should be administered by means of an automatic, MRI-compatible power injector to ensure accuracy of the timed bolus, including volume and rate of injection.[112,113] The corticomedullary-arterial phase (approximately 20 seconds after injection) is best for evaluating the arterial structures and corticomedullary differentiation. In the nephrographic phase (70–90 seconds after injection), tumor detection is maximized, and the renal veins and surrounding structures are best demonstrated (Fig. 25.18). Imaging can be performed in any plane, but the coronal plane is used most frequently for dynamic imaging because it allows imaging of the kidneys, ureters, vessels, and surrounding structures in the fewest number of images. The characteristics of parenchymal enhancement are similar to those observed on CE-CT.

The blood vessels can be variable in signal intensity on routine MRI that is not enhanced by contrast media, ranging from white to black. This is due to many factors, including, but not limited to, flow-related parameters, location and orientation of the imaged vessel, and choice of pulse sequence. By taking advantage of some of these factors, diagnostic angiography and venography may be performed without the use of intravenous contrast; these sequences are sometimes called "bright-blood" sequences. Although contrast media-enhanced magnetic resonance angiography (CE-MRA) remains the preferred method of vascular imaging, high-quality MRA that is not enhanced by contrast media has regained popularity because of the advancement in MR hardware and imaging sequences, as well as the risk of NSF in patients with poor renal function. MRA not enhanced by contrast media is particularly attractive for evaluating the renal arteries in patients with severe renal dysfunction or those with a relative contraindication for CE-CMA. The most robust sequences are based on inversion recovery, and balanced steady-state free precession techniques.[114,115] Older, less robust techniques include time-of-flight MRA, which is based on flow-related enhancement, and phase-contrast MRA, which is based on velocity and direction of flow. Phase-contrast

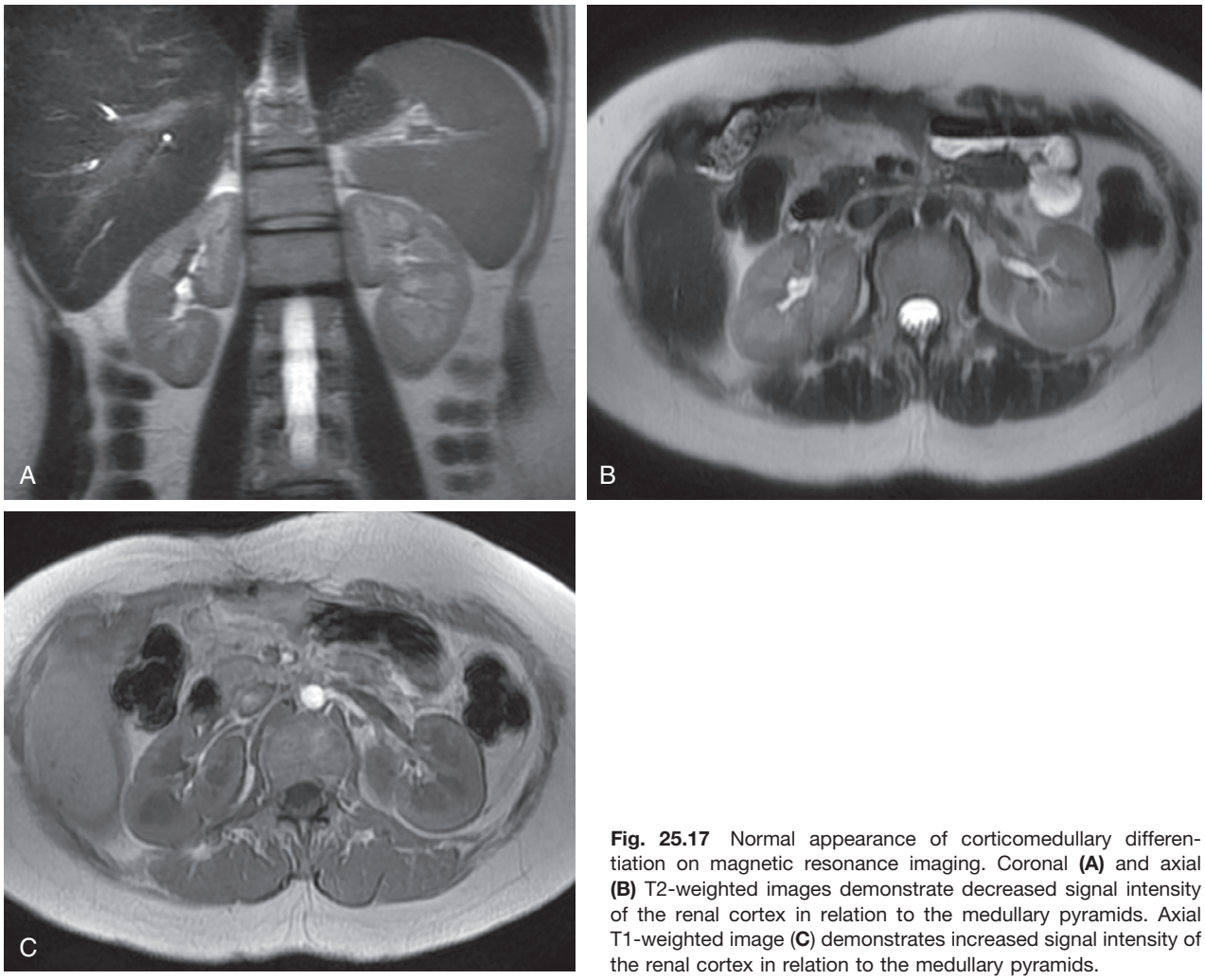

Fig. 25.17 Normal appearance of corticomedullary differentiation on magnetic resonance imaging. Coronal **(A)** and axial **(B)** T2-weighted images demonstrate decreased signal intensity of the renal cortex in relation to the medullary pyramids. Axial T1-weighted image (**C**) demonstrates increased signal intensity of the renal cortex in relation to the medullary pyramids.

MRA can be used in conjunction with CE-MRA to detect turbulent flow and high velocities associated with stenoses. Unlike MRA that is not enhanced by contrast media, CE-MRA minimizes flow-related enhancement and motion. The success of CE-MRA depends on the T1-shortening properties of gadolinium, which allow for faster imaging, increased coverage, and improved resolution.[77,116] Accurate timing of the bolus injection is critical in CE-MRA. The time at which the bolus arrives at the renal arteries may be determined with a bolus injection of 1 mL of Gd-C, followed by a saline flush. A three-dimensional T1-weighted gradient-echo MRI pulse sequence is then obtained in the coronal plane during the injection of approximately 15 to 20 mL of Gd-C at 2 mL/sec, timed to capture the arterial phase.[111,112] Sequential three-dimensional sequences are obtained to capture the venous phase (magnetic resonance venography). The data sets can be postprocessed into multiple formats, improving ease and accuracy of interpretation (Fig. 25.19).[117–119]

Magnetic resonance urography (MRU) consists of protocols tailored to the evaluation of the renal collecting system and the disease found there. MRU can be performed with heavily T2-weighted sequences, in which urine provides the intrinsic contrast, or with contrast media-enhanced T1-weighted sequences, which mimic conventional IVU and CTU. Heavily T2-weighted sequences are most useful in patients with dilated collecting systems, in whom all water-filled structures are bright (Fig. 25.20), and in patients with impaired renal excretion, in whom contrast media-enhanced urography is most limited. Unfortunately, without adequate distension of the collecting system, T2-weighted evaluation is limited. Although a good morphologic examination, T2-weighted urography is ultimately limited by a lack of functional information. For example, T2-weighted urography cannot reliably differentiate between an obstructed system and an ectatic collecting system (Fig. 25.21).[120] Contrast media-enhanced T1-weighted urography in the excretory phase is superior to T2-weighted urography because both structure and function can be evaluated.[120–122]

T2-weighted and contrast media-enhanced T1-weighted sequences are complementary and are frequently obtained together as part of a complete MRU examination. In patients with nondilated systems, both techniques require hydration and furosemide for adequate distension of the renal collecting system.[120,123] Typical MRU starts with a coronal, heavily T2-weighted sequence in which simple fluid (urine, cerebrospinal fluid, ascites) is bright and all other tissues are dark (see Fig. 25.20). This rapid breath-hold sequence takes less than 5 seconds to obtain and is presented as a urogram-like image. The T2-weighted sequence is used as an initial survey of fluid within the collecting system. Low-dose

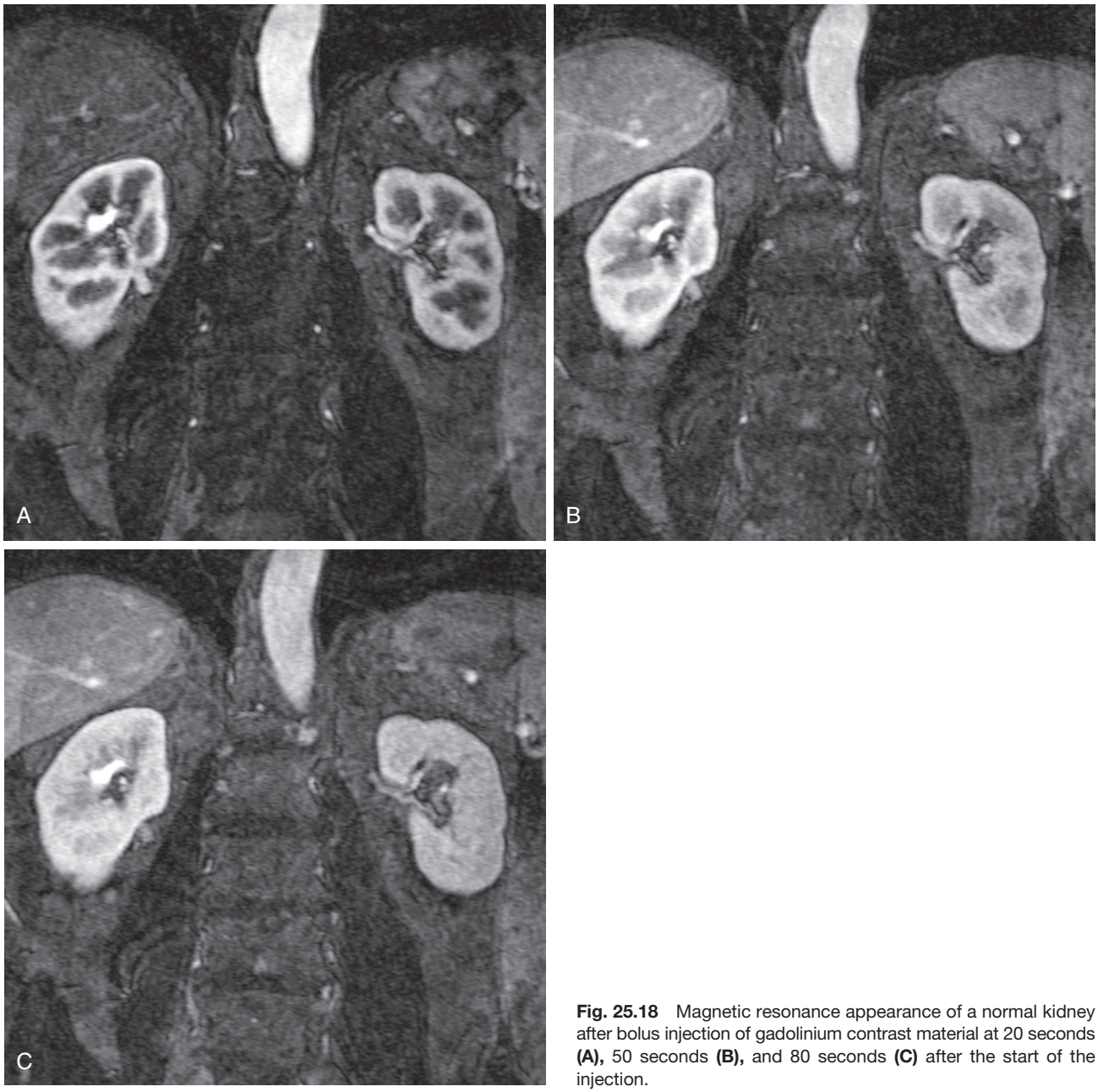

Fig. 25.18 Magnetic resonance appearance of a normal kidney after bolus injection of gadolinium contrast material at 20 seconds **(A),** 50 seconds **(B),** and 80 seconds **(C)** after the start of the injection.

furosemide (0.1 mg per kilogram of body weight; maximum dose, 10 mg) may be administered intravenously in selected cases, 30 to 60 seconds before the intravenous administration of Gd-C (0.1 mmol/kg).[121,122] Furosemide is given to increase urine volume and dilute the Gd-C within the collecting system.[121,123] Coronal, three-dimensional, contrast media-enhanced T1-weighted sequences are obtained with the same technique as in renal CE-MRA, in the corticomedullary-arterial phase, nephrographic phase, and excretory phase (see Fig. 25.20).[122] Additional sequences may be obtained in any plane to better evaluate suspected pathologic conditions.

By combining renal MRI and MRU, the clinician can obtain a comprehensive morphologic and functional evaluation of the urinary tract. MRU helps to accurately evaluate the upper urinary tract and is useful in the evaluation of anatomic anomalies, including duplications, ureteropelvic obstruction, anomalous crossing vessels, and ureteroceles[123,124] (Fig. 25.22). Obstructive disease is well evaluated regardless of whether the cause is intrinsic or extrinsic to the collecting system.

FUNCTIONAL MAGNETIC RESONANCE IMAGING OF THE KIDNEY

MRI is suited for measurement of various aspects of renal function, given the role of the kidney in fluid regulation. Techniques for the evaluation of renal function include dynamic contrast media-enhanced MR renography, diffusion-weighted imaging (DWI), and blood oxygen level-dependent (BOLD) MRI. Dynamic contrast media-enhanced MR renography is a contrast media-enhanced sequence in which dynamic images are obtained during the 7 to 10 minutes after administration of intravenous contrast material; tissue signal intensities are converted to tissue gadolinium concentrations, and these

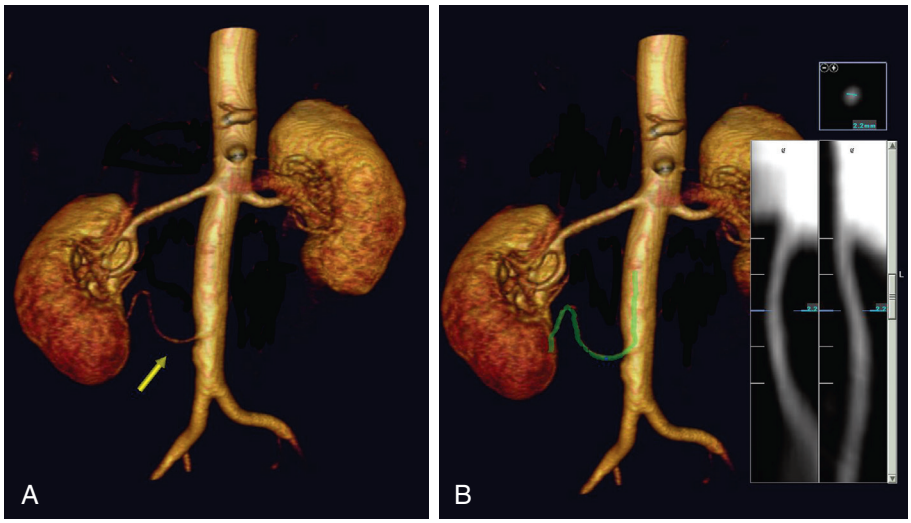

Fig. 25.19 Magnetic resonance angiogram reconstructed with three-dimensional software. **A,** Visualization of a small accessory right renal artery *(arrow)* is excellent. **B,** The accessory artery is depicted in a way to make more accurate luminal measurements.

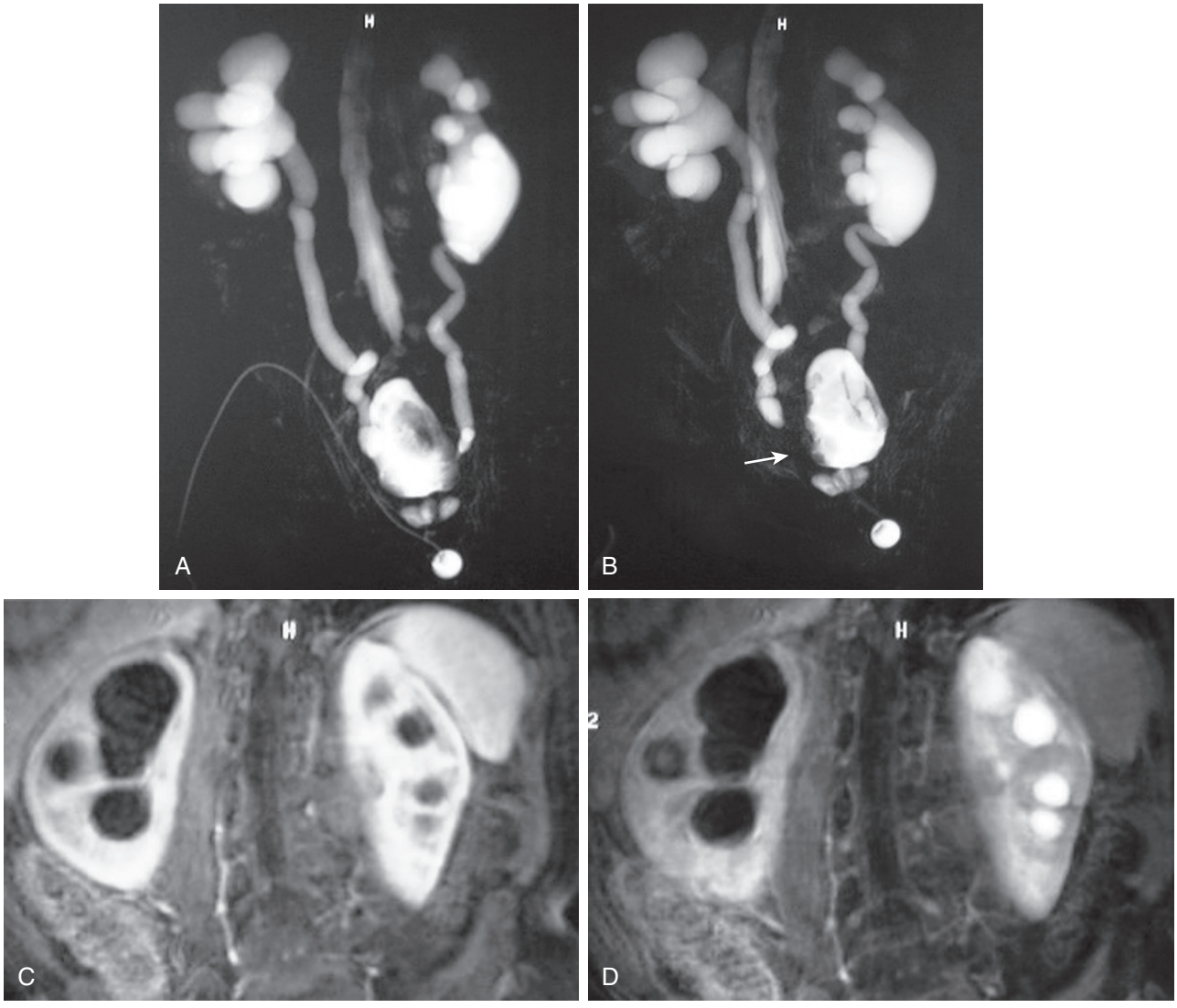

Fig. 25.20 Bilateral hydronephrosis secondary to bladder tumor. **A** and **B,** Heavily T2-weighted magnetic resonance urograms (MRUs) demonstrate bilateral hydronephrosis and hydroureter caused by bladder mass *(arrow).* **C,** Contrast medium-enhanced MRU in the nephrographic phase demonstrates asymmetric enhancement of the kidneys. **D,** MRU in the excretory phase demonstrates asymmetric excretion of gadolinium. There is no excretion on the right as demonstrated by unenhanced (dark) urine within the collecting system.

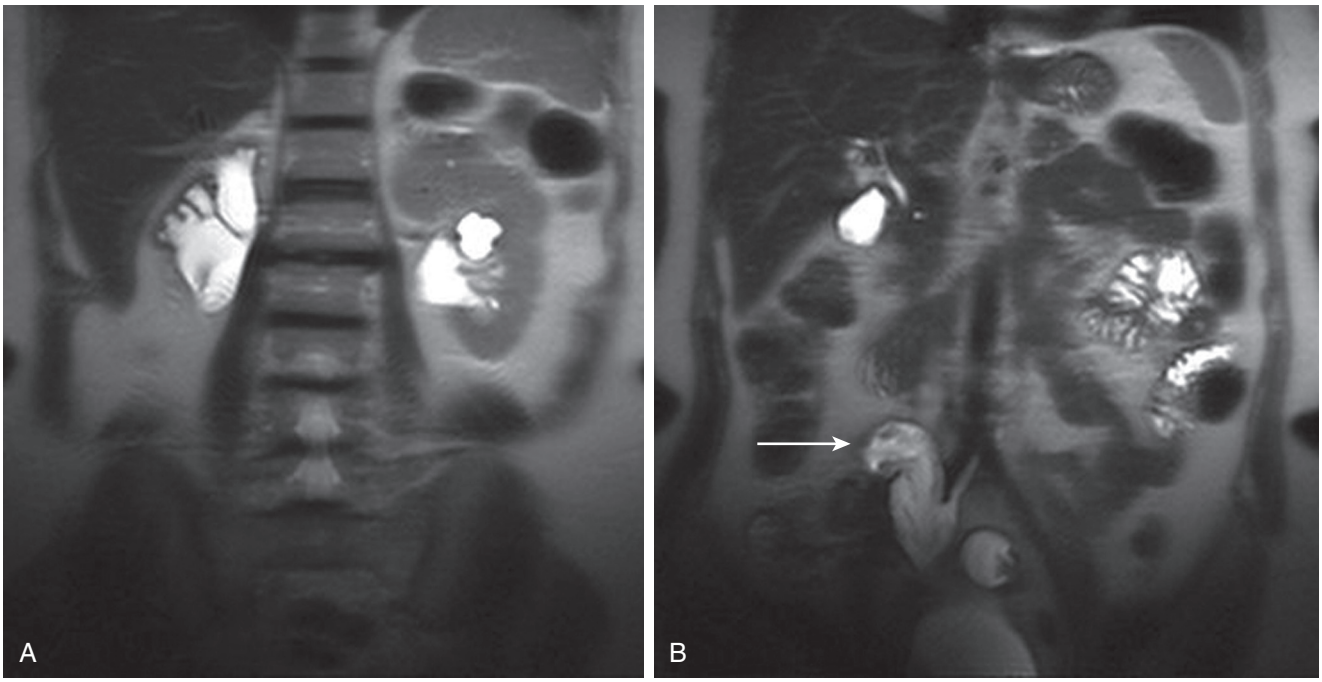

Fig. 25.21 **A** and **B,** Coronal T2-weighted images demonstrate right renal atrophy and dilation of the right collecting system in a patient who had undergone bladder resection and ilioconduit reconstruction *(arrow).* On these static images, it is difficult to differentiate between an obstructed system and a nonobstructed system. The patient had pelvocaliectasis without obstruction, demonstrated on the contrast medium-enhanced portion of the examination.

values are plotted against time. Current clinical applications include the evaluation of the renal artery stenosis, both with and without the use of angiotensin-converting enzyme (ACE) inhibitors, functional urinary obstruction, and the evaluation of early postoperative renal transplant dysfunction, to distinguish acute rejection from acute tubular necrosis. What prevents widespread clinical use, however, is the lack of consensus on optimal imaging technique and methods of data analysis.[125]

DWI is based on the Brownian motion of water molecules in tissue and is a noncontrast MRI technique that is used for both structural and functional imaging. Initial experience with DWI has yielded reproducible information on renal function, with the possibility of determining the degree of dysfunction.[126] No large studies have been performed, and further research is required before the usefulness of DWI is confirmed. Animal research is being performed with the hope of using noninvasive DWI as a tool for monitoring early renal graft rejection after transplantation.[127]

BOLD MRI is a noninvasive technique to estimate intrarenal oxygenation.[125] Various researchers use this technique to explore renal artery stenosis, renal transplant dysfunction, and diabetic nephropathy. Sadowski et al,[128] demonstrated the feasibility of using BOLD MRI to evaluate the oxygen status of renal transplants and to detect the presence of acute rejection. They concluded that BOLD MRI may differentiate acute rejection from normal function and acute tubular necrosis, but further research is required.

NUCLEAR MEDICINE

Scintigraphy offers imaging-based diagnostic information on renal structure and function.[129] Many single-photon radiotracers have long been in routine clinical use in renal scintigraphy; they are tailored to provide physiologic information complementing the primarily anatomic and structural-based imaging modalities, such as US, CT, and MRI. With the rapid expansion of PET and hybrid structural-functional imaging systems such as PET-CT, additional unprecedented opportunities have developed for quantitative imaging evaluation of renal diseases in clinical medicine and research.[127] Scintigraphy, including PET, makes a unique contribution to the imaging evaluation of renal structure and function. The common radiopharmaceuticals used in renal scintigraphy are described first.

RADIOPHARMACEUTICALS

Technetium 99M-Labeled Diethylenetriaminepentaacetic Acid

Technetium 99m-labeled diethylenetriaminepentaacetic acid (^{99m}Tc-DTPA) is a common agent for assessing GFR. The ideal agent for measuring GFR would be cleared only by glomerular filtration and would not be secreted or reabsorbed. ^{99m}Tc-DTPA satisfies the first requirement but has variable degrees of protein binding, which deviate its kinetics from an ideal agent such as inulin. For a 20-mCi (740-MBq) dose, the radiation exposures of the kidneys and the urinary bladder are 1.8 and 2.3 rad, respectively.[130]

Iodine 131-Labeled Ortho-Iodohippurate

The mechanisms underlying renal clearance of iodine 131-labeled ortho-iodohippurate (^{131}I-ortho-iodohippurate) are GFR (approximately 20%) and tubular secretion (approximately 80%). ^{131}I-ortho-iodohippurate is an acceptable alternative to *p*-aminohippuric acid (PAH) for determining

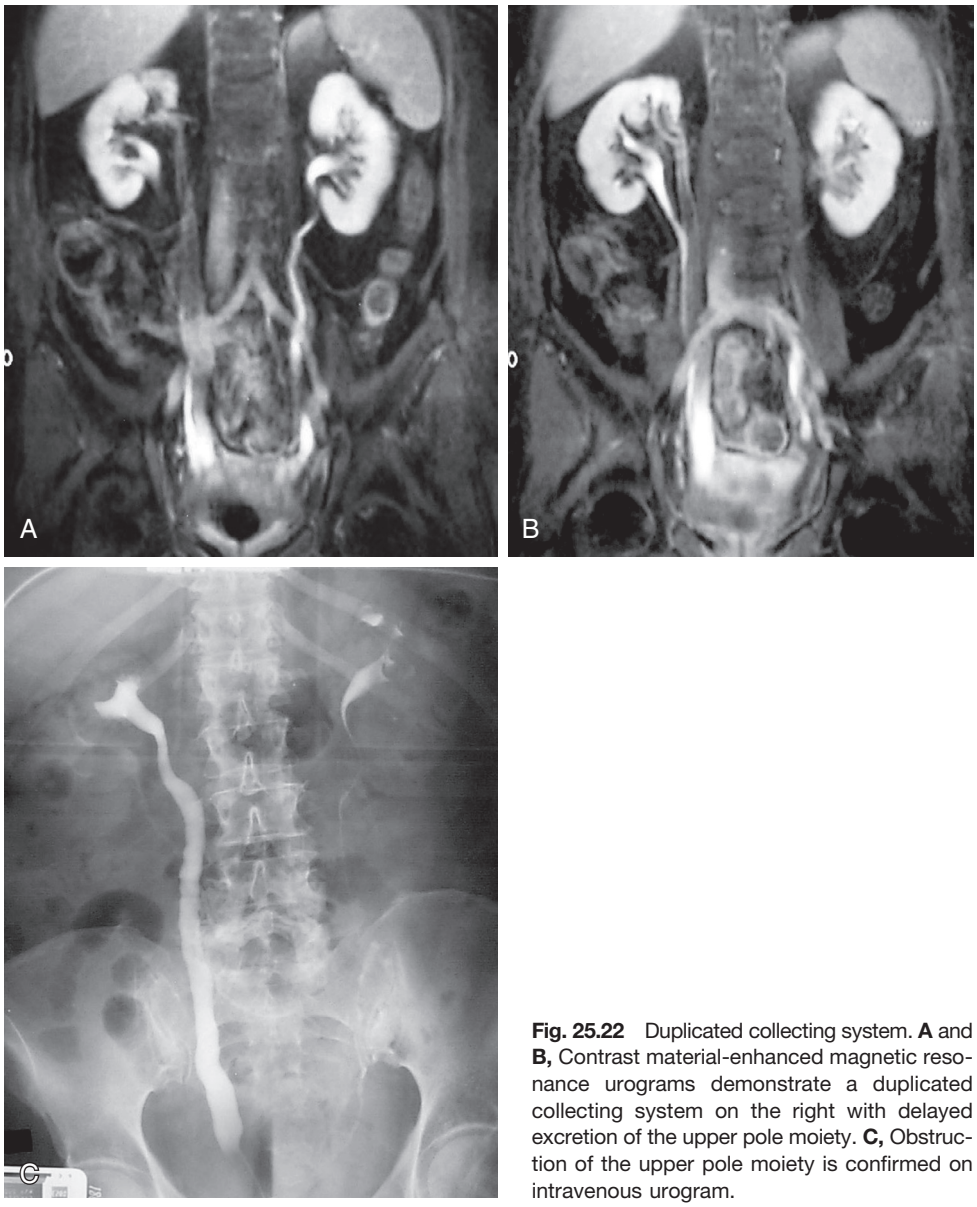

Fig. 25.22 Duplicated collecting system. **A** and **B,** Contrast material-enhanced magnetic resonance urograms demonstrate a duplicated collecting system on the right with delayed excretion of the upper pole moiety. **C,** Obstruction of the upper pole moiety is confirmed on intravenous urogram.

renal plasma flow (RPF), although the amount cleared is 15% lower than that of PAH. PAH is not entirely cleared by the kidneys; approximately 10% of arterial PAH remains in the renal venous blood. Therefore ^{131}I-ortho-iodohippurate helps measure effective RPF. The efficiency of tubular extraction of ^{131}I-ortho-iodohippurate is 90%, and there is no hepatobiliary excretion. Ortho-iodohippurate may also be labeled with iodine 123, which not only provides urinary kinetics equivalent to those provided by iodine 131 but also enables improved image quality because the administered dose is typically larger, in view of its more favorable profile of radiation exposure. For a 300-µCi (11.1-MBq) dose of ^{131}I-ortho-iodohippurate, the radiation exposures of the kidneys and the urinary bladder are 0.02 and 1.4 rad, respectively. A few drops of nonradioactive iodine (e.g., saturated solution of potassium iodide) administered orally help minimize the thyroid uptake of free iodine 131.[130]

Technetium 99M-Labeled Mercaptoacetyltriglycine

Technetium 99m-labeled mercaptoacetyltriglycine (^{99m}Tc-MAG3) has properties similar to those of ^{131}I-ortho-iodohippurate but has significant advantages of better image quality and less radiation exposure. The tubular extraction fraction of ^{99m}Tc-MAG3 is lower than that of ^{131}I-ortho-iodohippurate, at approximately 60% to 70%. Also, hepatobiliary excretion is approximately 3%, which increases with renal insufficiency. Despite these features, however, ^{99m}Tc-MAG3 is commonly used in scintigraphic evaluation of renal function. For a 10-mCi (370-MBq) dose, the radiation exposures of the kidneys and the urinary bladder are 0.15 and 4.4 rad, respectively.[130]

Technetium 99M-Labeled Dimercaptosuccinic Acid

Technetium 99m-labeled dimercaptosuccinic acid (^{99m}Tc-DMSA) localizes to the renal cortex at high concentration and has a slow urinary excretion rate. Approximately 50%

of the injected dose accumulates in the renal cortex in 1 hour. The tracer is bound to the renal proximal tubular cells. In view of the high retention of ^{99m}Tc-DMSA in the renal cortex, it has become useful for imaging of the renal parenchyma. For a 6-mCi (222-MBq) dose, the radiation exposures of the kidneys and the urinary bladder are 3.78 and 0.42 rad, respectively.[130]

Fluorine 18 2-Fluoro-2-Deoxy-D-Glucose

Fluorine 18 2-fluoro-2-deoxy-D-glucose (FDG) is the most common positron-labeled radiotracer in PET. FDG is a modified form of glucose in which the hydroxyl group in the 2′ position is replaced by the fluorine 18 positron emitter. FDG accumulates in cells in proportion to glucose metabolism. Cell membrane glucose transporters facilitate the transport of glucose and FDG across the cell membrane. Both glucose and FDG are phosphorylated in the 6′ position by the hexokinase. The conversion of glucose-6-phosphate or FDG-6-phosphate back to glucose or FDG, respectively, is affected by the enzyme phosphatase. In most tissues, including cancer cells, there is little phosphatase activity. FDG-6-phosphate cannot undergo further conversions and is therefore trapped in the cell.

FDG is excreted in the urine. The typical FDG dose is 0.144 mCi/kg (minimum, 1 mCi; maximum, 20 mCi). The urinary bladder wall receives the highest radiation dose from FDG.[128,131] The radiation dose depends on the excretion rate, the varying size of the bladder, the bladder volume at the time of FDG administration, and an activity curve of estimated bladder time. For a typical 15-mCi dose of FDG and voiding at 1 hour after tracer injection, the average estimated radiation dose absorbed by the adult bladder wall is 3.3 rad (0.22 rad/mCi).[132] The doses absorbed by other organs are between 0.75 and 1.28 rad (0.050–0.085 rad/mCi); the average dose absorbed is 1.0 rad.[133] Renal failure may alter the FDG biodistribution, which may necessitate reduction of dose or image acquisition time after tracer administration, or both.[134] Specifically, in patients with suspected renal failure (blood serum creatinine level in excess of 1.1 mg/dL), the FDG accumulation in the brain may decrease, whereas the blood pool activity is increased.[135]

IMAGING IN CLINICAL NEPHROLOGY

NORMAL RENAL FUNCTION

GFR and effective RPF may be assessed by means of dynamic quantitative nuclear imaging techniques. The GFR quantifies the amount of filtrate formed per minute (normal, 125 mL/min in adults). Only 20% of RPF is filtered through the semipermeable membrane of the glomerulus. The filtrate is protein free and almost completely reabsorbed in the tubules. Filtration is maintained over a range of arterial pressures with autoregulation. The ideal agent for the determination of GFR is inulin, which is only filtered but is neither secreted nor reabsorbed.[131,136]

In these studies, ^{99m}Tc-DTPA is often used to demonstrate renal perfusion and assess glomerular filtration, although 5% to 10% of injected ^{99m}Tc-DTPA is protein bound and 5% remains in the kidneys after 4 hours. A typical imaging protocol includes posterior 5-second flow images for 1 minute, followed by 1-minute-per-frame images for 20 minutes. The GFR may be obtained through the Gates method, in which images of renal uptake are obtained during the second and third minutes after ^{99m}Tc-DTPA administration. Regions of interest are drawn over the kidneys, and background activity correction is applied. A standard dose is counted by the gamma camera for normalization. Depth photon attenuation is corrected according to a formula relating body weight and height. A split GFR can be obtained for each kidney, which is not possible with the creatinine clearance method.[131,136]

The effective RPF (normal, 585 mL/min in adults) can be obtained with ^{131}I-ortho-iodohippurate and ^{99m}Tc-MAG3 imaging.[137] However, ^{131}I-ortho-iodohippurate has been largely replaced by ^{99}Tc-MAG3 because MAG3 has better imaging characteristics and dosimetry (when radiolabeled with ^{99m}Tc). Currently ^{99}Tc-MAG3 is the renal imaging agent of choice primarily because of the combined renal clearance of ^{99}Tc-MAG3 by both filtration and tubular extraction, which enables clinicians to obtain relatively high-quality images even in patients with impaired renal function. The imaging protocol includes posterior 1-second images for 60 seconds (flow study), followed by 1-minute images for 5 minutes and then 5-minute images for 30 minutes. The relative tubular function may be obtained by drawing renal regions of interest, corrected for background activity.[138,139] A renogram is constructed to depict the renal tracer uptake over time. The first portion of the renogram has a sharp upward slope occurring approximately 6 seconds after peak aortic activity (phase I); the upward slope represents perfusion. This is followed by extension to the peak value, which represents both renal perfusion and early renal clearance (phase II), which can be dependent on body position.[140] The next phase (phase III) is depicted by a downward slope, which represents excretion. Normal perfusion of the kidneys is symmetric (50% ± 5%). The peak of the renogram occurs at approximately 2 to 3 minutes (vs. 3–5 minutes with DTPA) in normal adults, and by 30 minutes, more than 70% of the tracer is cleared and present in the urinary bladder (Fig. 25.23).[120,126,131,136,141] Assessment of renal function is further discussed in Chapter 23.

Renal cortical structure can be imaged with ^{99m}Tc-DMSA; the appearance of these images is strongly correlated with differential GFR and differential renal blood flow. Imaging is started 90 to 120 minutes after administration of the tracer and can be obtained up to 4 hours later. Planar images are obtained in the anterior, posterior, left anterior oblique/right anterior oblique, and right posterior oblique/left posterior oblique projections. SPECT is also often performed. In a scan with normal results, renal cortical uptake is evenly distributed. Normal variations include dromedary hump (splenic impression on the left kidney), fetal lobulation, horseshoe kidney, crossed fused ectopy, and hypertrophied column of Bertin. The renal images also allow accurate assessment of the relative renal size, position, and axis.[131,136]

KIDNEY INJURY: ACUTE AND CHRONIC

When a patient presents with previously undiagnosed renal failure, the question is whether the kidney disease is acute or chronic. US is the most helpful initial imaging study for evaluating the patient with an elevated creatinine level of unknown duration. US can help separate chronic, end-stage kidney disease (ESKD) from potentially reversible AKI or

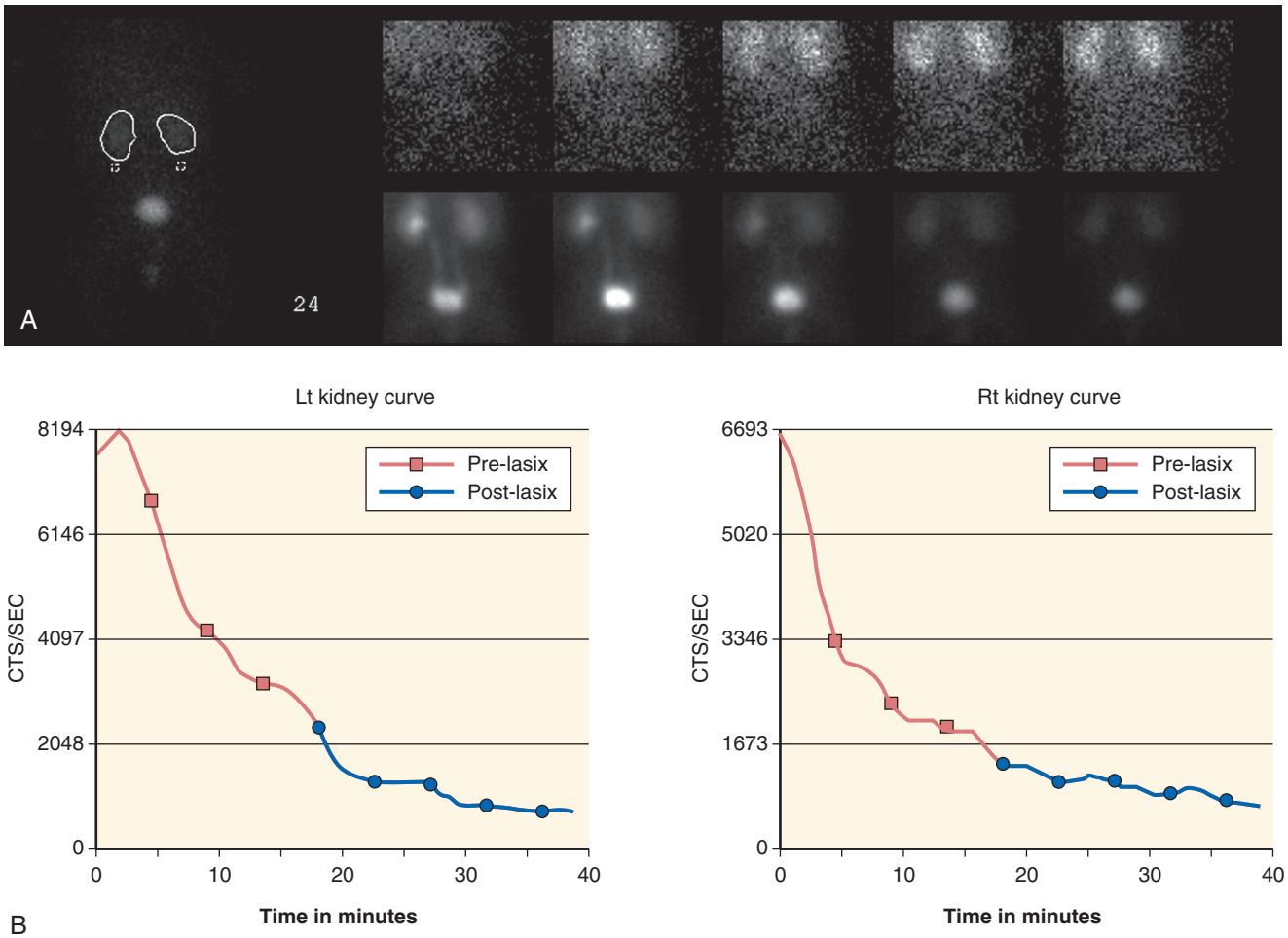

Fig. 25.23. Normal-appearing renogram with technetium 99m-labeled mercaptoacetyltriglycine (MAG3). **A**, Planar posterior images. *Left:* Static image with whole kidney regions of interest (ROI; *white outlines*), and background ROIs *(circular dashed lines)* inferiorly. *Right upper series:* Sequential flow images at 5-second intervals show prompt symmetric uptake of tracer in both kidneys. *Right lower series:* Sequential functional images at 1-minute intervals show normal excretion of tracer with visualization of the ureters and urinary bladder. **B,** Time-activity curves for each kidney, corrected for background, collected from the ROIs in A., showing the excretory phase. Less than 30% of peak activity is retained in each kidney after 20 minutes, which is normal. At 20 minutes, intravenous furosemide (Lasix) was given to demonstrate normal washout. *CTS/SEC*, Radioactivity counts per second.

CKD by defining renal size, echogenicity, and presence or absence of hydronephrosis and cystic disease. This is easily achieved using gray-scale US.[142] A thin rim of decreased echogenicity may surround the kidneys in patients experiencing kidney injury, also known as renal sweat.[143] Small, echogenic kidneys indicate preexisting CKD; however, acute reversible components must still be searched for. Acute, reversible components that can be diagnosed on imaging are few but include hydronephrosis and hypertension caused by renal artery stenosis. If no acute process is found on US, no further imaging workup is necessary (according to the ACR appropriateness criteria for elevated Cr of unknown duration).[144] Normal renal size, with or without increased echogenicity, typically requires more extensive evaluation for acute causes because gray-scale US may not be accurate in the minimally dilated obstructive situation.

Many causes of AKI are encountered in the hospital setting. Prerenal and renal causes include hypotension or dehydration resulting in hypoperfusion of the kidneys and nephrotoxic drugs[145] and account for more than 90% of all cases. Typically, prerenal and renal causes are diagnosed clinically, not with imaging. Although postrenal causes for AKI are less common, when they are identified and treated, the AKI is often rapidly reversible.

US is more than 95% accurate in detecting hydronephrosis (i.e., dilation of the collecting systems and renal pelvis)[144,146]; however, the cause of the hydronephrosis may not be seen. If US cannot determine the cause of obstruction, CT or MRI that is not enhanced by contrast media is the appropriate next imaging study.[147] The typical US findings of hydronephrosis are a dilated, anechoic, fluid-filled renal pelvis and calyces. Hydronephrosis is generally graded according to the extent of calyceal dilation and the degree of cortical thinning.[133,144,148] In mild (grade I) hydronephrosis the pelvicalyceal system is filled with fluid, which causes slight separation of the central renal sinus fat (Fig. 25.24). The calyces are not distorted, and the thickness of the renal cortex appears normal. In moderate (grade II) hydronephrosis the pelvicalyceal system appears more distended with greater separation of the central echo complex. The contour of the calyces is

rounded, but the cortical thickness is unaltered (Fig. 25.25). With moderate-to-severe (grade III) hydronephrosis the calyces are more distended, and cortical thinning is recognized. In severe (grade IV) hydronephrosis the calyceal system is markedly dilated (Fig. 25.26). The calyces appear as large, ballooned, fluid-filled structures with a dilated renal pelvis of variable size. Cortical loss is evident, with the dilated calyces approaching or reaching the renal capsule. In general, the length and overall size of a hydronephrotic kidney is increased. Long-standing obstruction may, however, result in renal parenchymal atrophy, and the kidney may be somewhat small, with marked cortical thinning. The degree of hydronephrosis is not always correlated with the amount of obstruction.

Although hydronephrosis is usually easily diagnosed with US, it must not be confused with renal cystic disease. In hydronephrosis the dilated calyces have a visibly direct communication with the renal pelvis, which is also dilated.[16] In cystic disease the round fluid-filled cysts have walls, and no direct communication is evident between each calyx and the renal pelvis. Cases of peripelvic cysts are frequently misdiagnosed as a dilated renal pelvis. Renal artery aneurysm may also be confused with a dilated renal pelvis but can be diagnosed correctly with added Doppler color-flow US.

The presence of hydronephrosis on US does not always indicate obstruction.[149,150] Grade I hydronephrosis and possibly more severe grades may be observed in patients in whom no obstructive cause is found. Nonobstructive causes of hydronephrosis include increased urine production and flow, acute and chronic infection, vesicoureteral reflux, papillary necrosis, congenital megacalyces, overdistended bladder, and postobstructive dilation.[151] In patients with repeated episodes of intermittent or partial obstruction, the calyces become quite distensible or compliant, which causes the appearance of hydronephrosis to vary, depending on the state of hydration and urine production. Patients with vesicoureteral reflux also demonstrate distensible pelvicalyceal systems. Doppler color-flow US has been suggested as an additive means of differentiating obstructive from nonobstructive hydronephrosis.[152,153] The measurement of resistive indices has been investigated as a means of diagnosing acute renal obstruction as well; the acutely obstructed kidney has an elevated resistive index, and the nonobstructed kidney has a normal resistive index of less than 0.70.[154,155] The results have been variable, and thus no consistent recommendation is available[155,156]

US is also used in patients with CKD. Cortical echogenicity may be increased in both acute and chronic renal parenchymal disease (Fig. 25.27).[157] The pattern should be bilateral in CKD, and the degree of cortical echogenicity is correlated with the severity of the interstitial fibrosis, global sclerosis, focal tubular atrophy, and number of hyaline casts per glomerulus.[10] Similar correlation is observed with decreasing renal size. These findings, however, are nonspecific, and kidney biopsy may be required for diagnosis. The normal corticomedullary differentiation is lost with increasing cortical echogenicity.[148] Cortical echogenicity may also be increased

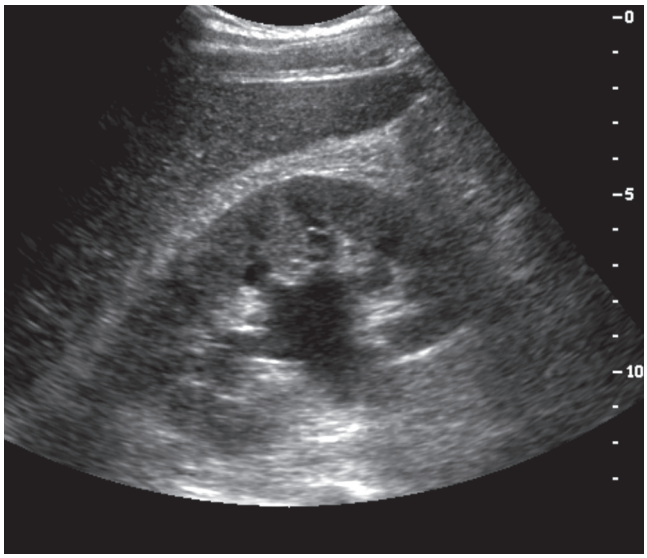

Fig. 25.24 Mild (grade I) hydronephrosis: ultrasonography. The central echo complex is separated by the mildly distended calyces and renal pelvis. Notice the connection between the calyces and the renal pelvis. The thickness of the cortex is preserved, and the renal border remains smooth.

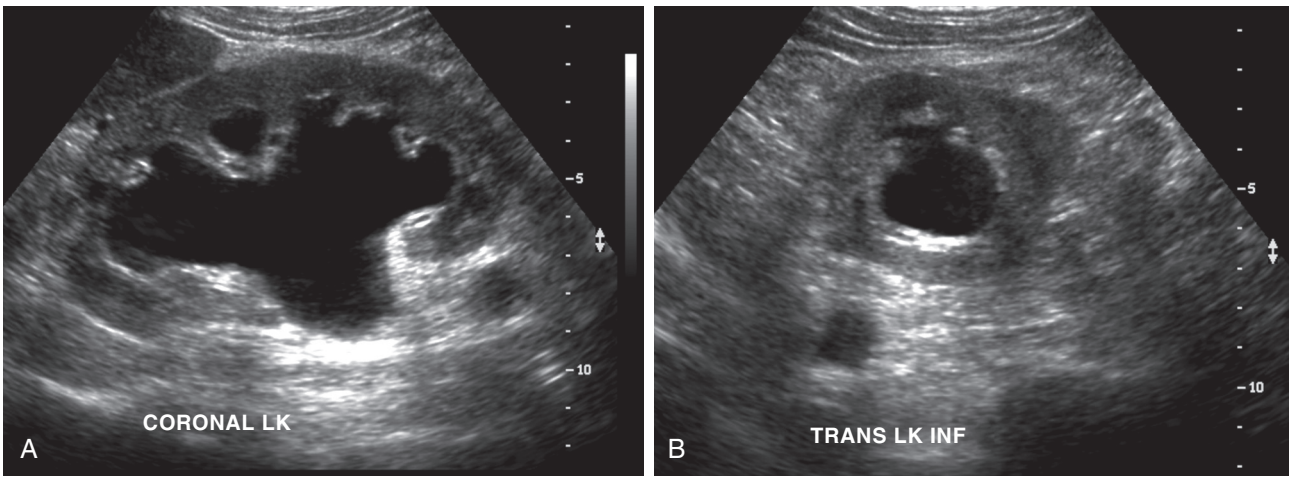

Fig. 25.25 Moderate (grade II) hydronephrosis: ultrasonography. Longitudinal image **(A)** and transverse image **(B)**. The dilated calyces are rounded and filled with urine. The renal pelvis is dilated as well. Again, note the connection between the calyces and the renal pelvis. The cortex remains relatively normal in thickness, and the renal border is smooth.

in some patients with AKI, as in glomerulonephritis and lupus nephritis. Sequential studies over time may be used to assess the progression of disease by monitoring the renal size and cortical echogenicity.

The key to the diagnosis of renal parenchymal disease is renal core biopsy and resulting histopathologic study.[157] US facilitates the performance of kidney biopsy by demonstrating the kidney and the proper location for biopsy. US may also be used to evaluate for complications associated with kidney biopsy, such as perirenal hematoma and arteriovenous fistula.

When US evaluation demonstrates hydronephrosis, but not the cause, it is usually followed by CT. Noncontrast CT will demonstrate the dilated pelvicalyceal systems in the kidney. The parenchymal thickness can be visualized in relation to the dilated collecting systems; the urine-filled calyces and pelvis are less dense than the surrounding parenchyma. The course of the dilated ureters may be followed distally to the bladder and prostate to establish the site of obstruction. The cause of obstruction is frequently visible and may include pelvic tumors, distal ureteral stones, and retroperitoneal adenopathy or mass. For patients in whom chronic long-standing obstruction is the cause of kidney injury, CT generally demonstrates large, fluid-containing kidneys with little or no cortex remaining.

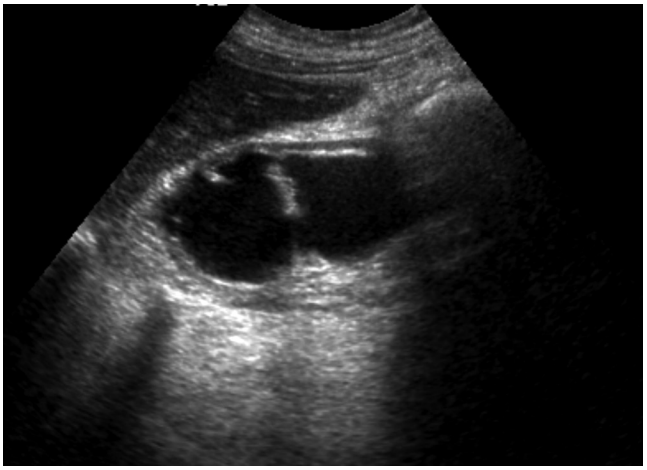

Fig. 25.26 Severe (grade IV) hydronephrosis: ultrasonography. Longitudinal image of the right kidney demonstrates a large fluid-filled sac; no normal elements of the kidney remain visible. The cortex is almost gone, but the outer border of the kidney remains smooth.

In CKD without obstruction, CT typically demonstrates small, contracted kidneys, which may also show evidence of adulthood-acquired polycystic disease if the patient is on dialysis (Fig. 25.28). In general, the overall size and thickness of the renal parenchyma appear to decrease with age.[158] Other causes for CKD may be demonstrated on imaging, including autosomal dominant polycystic kidney disease (Fig. 25.29); the kidneys are enlarged and contain innumerable cysts. Frequently some of the cyst walls may contain thin rims of calcification. The density of the internal contents of the cysts may also vary as a result of hemorrhage or proteinaceous debris. For patients undergoing regular dialysis, iodinated contrast may be given if necessary for CT scans because the material is dialyzable.

Like CT, MRI is accurate in demonstrating renal structure, as well as prerenal and postrenal causes of kidney injury. MRI is sensitive for the detection of renal parenchymal disease, but the renal parenchymal causes of injury have nonspecific features, and biopsy is generally required.[159] Noncontrast MRI routinely allows for detailed tissue characterization of the kidney and surrounding structures. Both iodinated contrast and Gd-C should be avoided if possible in patients with AKI and CKD stage 4 and 5. Newer MRI sequences, such as diffusion-weighted and bright blood techniques, provide a way to increase the detection of neoplastic and vascular causes of renal failure without the use of intravenous contrast agents.[102,160]

In kidney injury, glomerular and tubular dysfunctions are reflected by abnormal findings on renal scintigraphy and renography. Renal uptake of ^{99m}Tc-MAG3 is prolonged, with tubular tracer stasis and little or no excretion. In patients with AKI, if ^{99m}Tc-MAG3 has more renal activity than hepatic activity 1 to 3 minutes after injection, recovery is likely, whereas when renal uptake is less than the hepatic uptake, dialysis may be needed.[161] In CKD, renal perfusion, cortical tracer extraction, and tracer excretion are diminished. However, this imaging pattern is nonspecific and must be interpreted in the clinical context.[131]

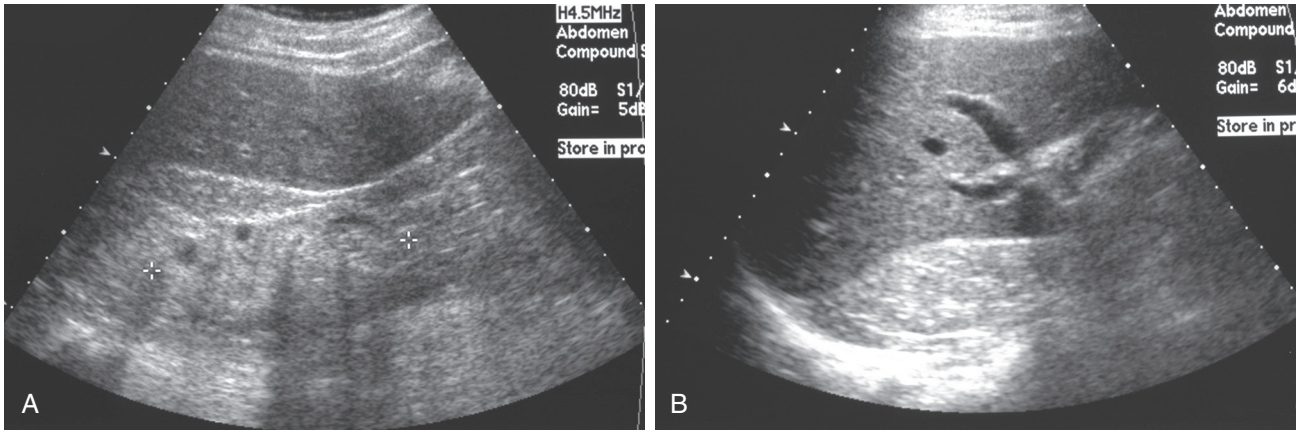

Fig. 25.27 End-stage kidney disease: ultrasonography. **A** and **B,** The kidneys are highly echogenic in relation to the adjacent liver. No normal renal structures are visible, but the kidneys remain smooth in overall contour. Note the two small hypoechoic renal cysts in the surface in **A.**

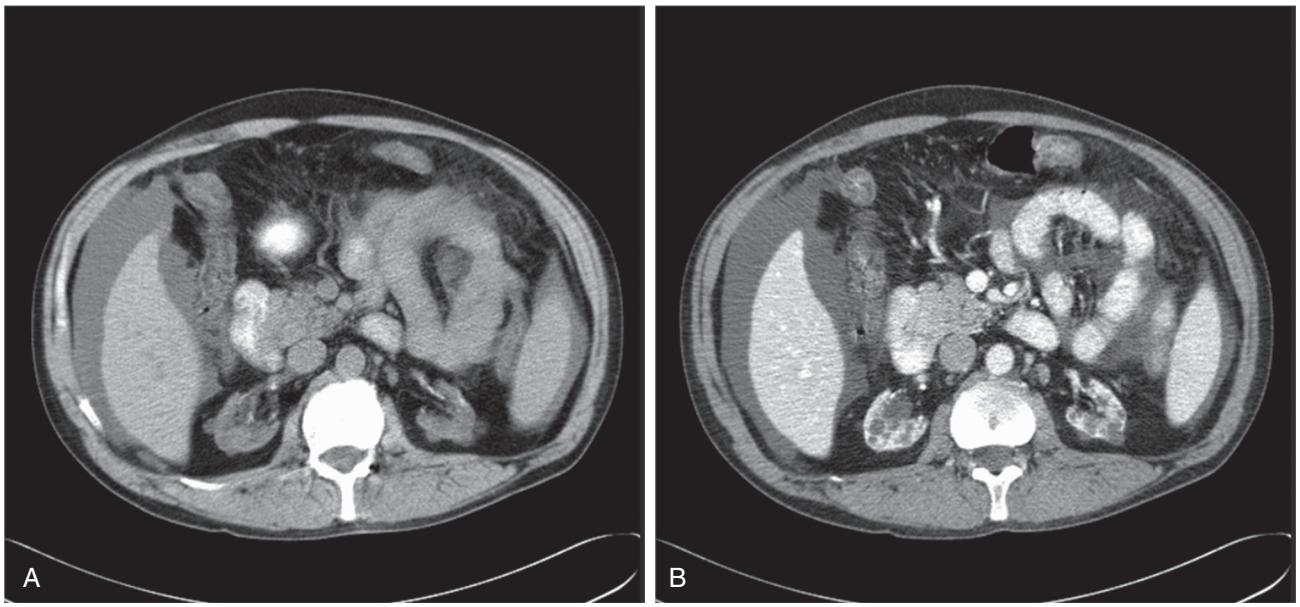

Fig. 25.28 Adulthood-acquired polycystic kidney disease: computed tomographic scan, axial image without contrast material **(A)** and axial image after administration of contrast material **(B).** The kidneys are small bilaterally with multiple 1-cm cysts primarily in the cortex.

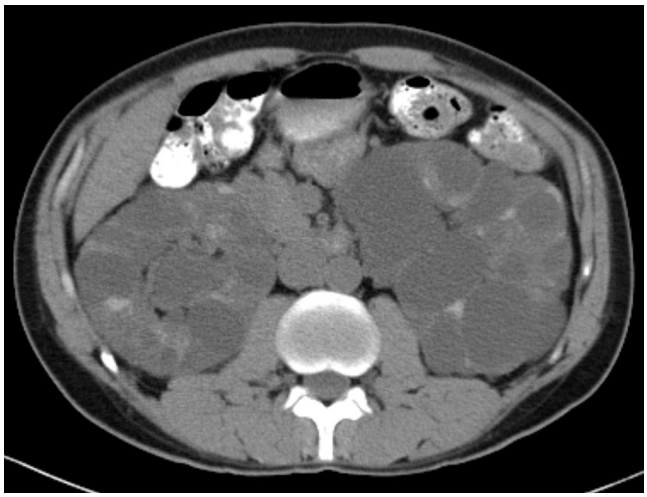

Fig. 25.29 Autosomal dominant polycystic kidney disease: computed tomographic (CT) scan without contrast material. This CT image demonstrates the markedly enlarged kidney bilaterally with multiple low-density cysts throughout both kidneys. The little remaining renal parenchyma is noted by the sparse, higher density material squeezed by the cysts.

UNILATERAL OBSTRUCTION

If US cannot determine the cause of obstruction, CT is the next imaging modality of choice due to rapid speed of acquisition and accuracy.[147] IVU and antegrade or retrograde pyelography may be used if CT is not available.[144] With IVU the site of obstruction may be visible, but the cause may be only inferred; this is also true with antegrade and retrograde pyelography.

CE-CT and, more specifically, CTU are most useful in assessing the patient with unilateral obstruction.[26] Small differences in the enhancement pattern of the kidneys are well demonstrated with CE-CT (Fig. 25.30). Differences in the excretion patterns by the kidneys are also sensitively depicted on CE-CT.[25,26] The urine-filled or contrast material-filled ureters point to the obstruction with demonstration of both intraureteral and extraureteral causes of the obstruction (Fig. 25.31). MRI demonstrates similar findings and may be used when CE-CT is contraindicated.

Nuclear medicine assessment by means of diuretic renography may also be used to evaluate for obstructive uropathy. Scintigraphy with ^{99m}Tc-MAG3 is often employed. Furosemide (Lasix) is administered intravenously (1 mg/kg; higher dose in cases of renal insufficiency) when the renal pelvis and ureter are maximally distended.[162] Regions of interest are drawn around each renal pelvis, with the background regions as crescent shapes lateral to each kidney. After furosemide administration, in cases of dilation without obstruction, the collecting system empties rapidly, with a subsequent steep decline in the renogram curve. Obstruction can be ruled out if the clearance half-time of the renal pelvic emptying is less than 10 minutes. A curve that reaches a plateau or continues to rise after administration of furosemide is indicative of obstruction, with a clearance half-time of more than 20 minutes (Fig. 25.32). A slow downward slope after furosemide administration may be indicative of partial obstruction. An apparent poor response to furosemide may also occur in patients with severe pelvic dilation (reservoir effect). Other pitfalls include poor injection technique of either the diuretic or the radiotracer, impaired renal function, and dehydration, in which delayed tracer transit and excretion may not be overcome by the effect of a diuretic. Kidneys in neonates (<1 month of age) may be too immature to respond to furosemide, and neonates are thus not suitable candidates for diuretic renal scintigraphy.[131,163]

Various protocols in relation to the timing of furosemide administration have also been reported. In the F0 method, furosemide is injected simultaneously with ^{99m}Tc-MAG3 administration. A 17-year clinical experience at one institution

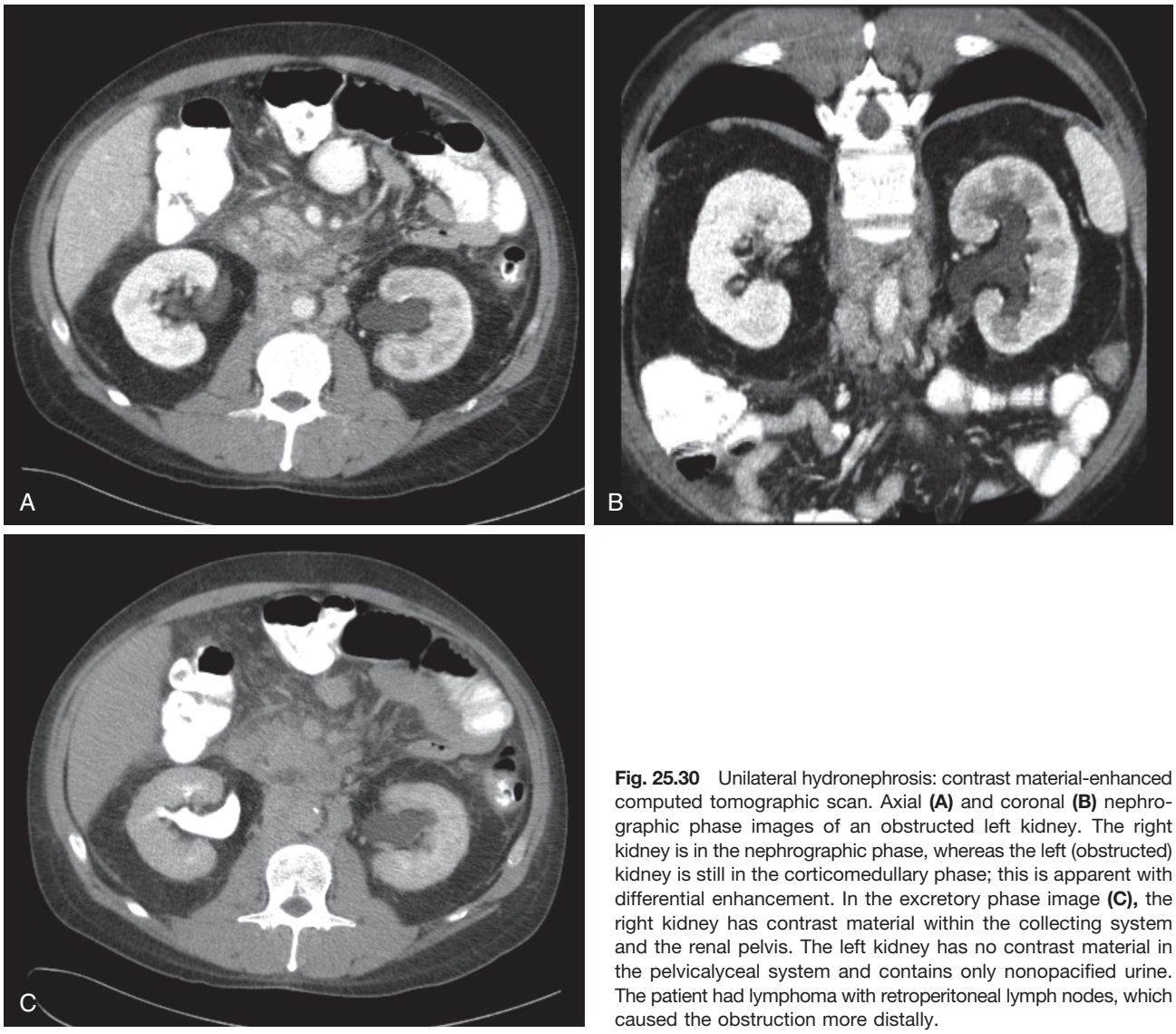

Fig. 25.30 Unilateral hydronephrosis: contrast material-enhanced computed tomographic scan. Axial **(A)** and coronal **(B)** nephrographic phase images of an obstructed left kidney. The right kidney is in the nephrographic phase, whereas the left (obstructed) kidney is still in the corticomedullary phase; this is apparent with differential enhancement. In the excretory phase image **(C),** the right kidney has contrast material within the collecting system and the renal pelvis. The left kidney has no contrast material in the pelvicalyceal system and contains only nonopacified urine. The patient had lymphoma with retroperitoneal lymph nodes, which caused the obstruction more distally.

proved that this protocol is useful for patients of all ages and for all indications.[164] Taghavi et al compared diuresis renographic protocols with injection of furosemide 15 minutes before (F–15) and 20 minutes after (F+20) administration of ^{99m}Tc-MAG3.[165] In this comparative study of 21 patients with dilation of the pelvicalyceal system, the F–15 protocol produced fewer equivocal results than did the F+20 method and therefore was considered the preferable protocol. Further experience is needed to determine the most optimal timing interval between furosemide and ^{99m}Tc-MAG3 injections in diuresis renography.

RENAL CALCIFICATIONS AND RENAL STONE DISEASE

Calcifications may occur in many regions of the kidney.[166] Nephrolithiasis or renal calculi are the most common and occur in the pelvicalyceal system. Nephrocalcinosis refers to diffuse or punctate renal parenchymal calcification occurring in either the medulla or cortex, usually bilaterally. Some patients with nephrocalcinosis may also develop nephrolithiasis. Calcifications also occur in vascular structures, particularly in patients with diabetes and advanced atherosclerotic disease. Rimlike calcifications may occur in simple renal cysts and polycystic disease. Patients with renal carcinomas may exhibit variable calcifications as well. All types of calcification are best demonstrated on noncontrast CT.

Cortical calcification is most often associated with cortical necrosis from any cause.[166] The calcifications are dystrophic and tend to resemble tram tracks and to be circumferential. Other entities in which cortical calcification are found include hyperoxaluria, Alport's syndrome, and, in rare cases, chronic glomerulonephritis. The stippled calcifications of hyperoxaluria may be found in both the cortex and the medulla, as well as in other organs, such as the heart. In Alport's syndrome, only cortical calcifications are found.

Calcifications in the medulla are much more common than cortical calcifications.[166] The most common cause of medullary nephrocalcinosis is primary hyperparathyroidism. The distribution appears to be within the renal pyramid and may be either focal or diffuse and either unilateral or bilateral. Nephrocalcinosis occurs in other diseases in which

Fig. 25.31 Unilateral obstruction: contrast material-enhanced computed tomographic scan. The coronal image demonstrates the difference in enhancement between the two kidneys, with the moderately dilated renal pelvis and calyces on the right. The large heterogeneous pelvis mass is the source of the obstruction: recurrent rectal carcinoma.

hypercalcemia or hypercalciuria occur, such as hyperthyroidism, sarcoidosis, hypervitaminosis D, immobilization, multiple myeloma, and metastatic neoplasms. These calcifications are nonspecific and punctate in appearance and are usually medullary in location.

In 70% to 75% of cases of renal tubular acidosis, there is evidence of nephrocalcinosis. The calcifications tend to be uniform and distributed throughout the renal pyramids bilaterally. With medullary sponge kidney and renal tubular ectasia, small calculi form in the distal collecting tubules, probably because of stasis. The appearance varies from involvement of only a single calyx to involvement of both kidneys throughout. The calcifications are small, round, and within the peak of the pyramid adjacent to the calyx. Medullary sponge kidney is also associated with nephrolithiasis, because the small calculi in the distal collecting tubules may pass into the collecting systems and ureters, resulting in renal colic.[165]

The calcifications that occur in renal tuberculosis are typically medullary in location and may mimic other forms of nephrocalcinosis.[169] Calcification occurs in the pyramids as part of the healing process. With overwhelming involvement of the kidney, the entire kidney may be destroyed; this results in diffuse, heavy calcification throughout the entire kidney, which becomes small and scarred. Medullary calcifications are also visible in patients with renal papillary necrosis. With necrosis of the papilla, the material is sloughed into the calyces. Retained tissue fragments may calcify and have the appearance of medullary nephrocalcinosis.

Nephrolithiasis is a common clinical entity. The lifetime risk for developing renal calculi is 12%, with males being two to three times more at risk than females.[167] Most urinary tract stones are composed of calcium salts of either oxalate or phosphate or a combination of the two.[168–171] This composition accounts for the dense appearance on imaging. Stasis contributes to the formation of stones in the urinary tract. Renal colic or flank pain is the most common presenting symptom. Most patients also have hematuria, although it may be absent if a ureter is completely obstructed by the stone. The pain that occurs with a passing renal stone is probably caused by the distension of the tubular system and renal capsule of the kidney and by the peristalsis associated with ureteral contractions as the stone moves distally.

Most urinary calculi that are 4 mm or smaller pass with conservative treatment.[172] The larger the stone, the more likely other measures will be necessary to treat the stone and associated obstruction.

Plain radiograph of the abdomen yields little significant information on its own and should not be used to diagnose stone disease.[173] The KUB is useful for following stone disease only when a stone is densely calcified and large enough to be visible (Fig. 25.33). For years, IVU was the method of choice for the assessment of patients with renal colic[174,175]; however, it has been supplanted by CT that is not enhanced by contrast media, which is a more rapid examination and more accurate than IVU.[173] In addition, a CT examination would also permit evaluation of nonurinary tract causes of pain.

Ultrasonographic assessment has also been used in the evaluation of renal colic.[176] This is a quick and usually easily performed examination. Unilateral hydronephrosis may be observed, although the examination results may be normal early in the passage of a renal stone. Renal stones may be visualized within the kidney as hyperechoic foci with distal acoustic shadowing or reverberation artifacts (Fig. 25.34).[176] Ureteral stones are rarely seen because of overlying bowel gas. Distal ureteral stones near the ureterovesical junction may be visualized through the urine-filled bladder transabdominally. US may demonstrate an absent ureteral jet in the bladder on the side in which a stone is being passed. Doppler US and assessment of the peripheral vasculature resistance may occasionally be helpful in pointing to the affected kidney, but the study results have been variable.[154]

Noncontrast CT scanning of the abdomen and pelvis has emerged as the standard evaluation in patients with renal colic.[177–181] The sensitivities for CT are 96% to 100%, the specificities are 95% to 100%, and the accuracy rates are 96% to 98%; for this reason, nonenhanced CT has supplanted plain radiography, IVU, and US.[178,182–184] In comparisons of nonenhanced CT and IVU, CT is much more useful, with 94% to 100% sensitivity and 92% to 100% specificity; IVU has 64% to 97% sensitivity and 92% to 94% specificity.[178] Also, when noncontrast CT was used as the reference standard in comparison with US, 24% sensitivity and 90% specificity were found for US.[185,186] An alternative diagnosis is made in patients with "renal colic" in 9% to 29% of cases in which noncontrast CT is used for evaluation.[187]

Nonenhanced CT is performed from the top of the kidneys to below the pubic symphysis. No preparation is needed. Intravenous contrast material is rarely needed. The studies are performed with 3-mm collimation or less, and the slices are reconstructed to be contiguous or slightly overlapping.[188–190] Virtually all renal stones are denser than the adjacent soft tissues (Fig. 25.35)[191]; exceptions are renal stones associated with indinavir (a protease inhibitor used in the management of acquired immunodeficiency syndrome (AIDS) and very

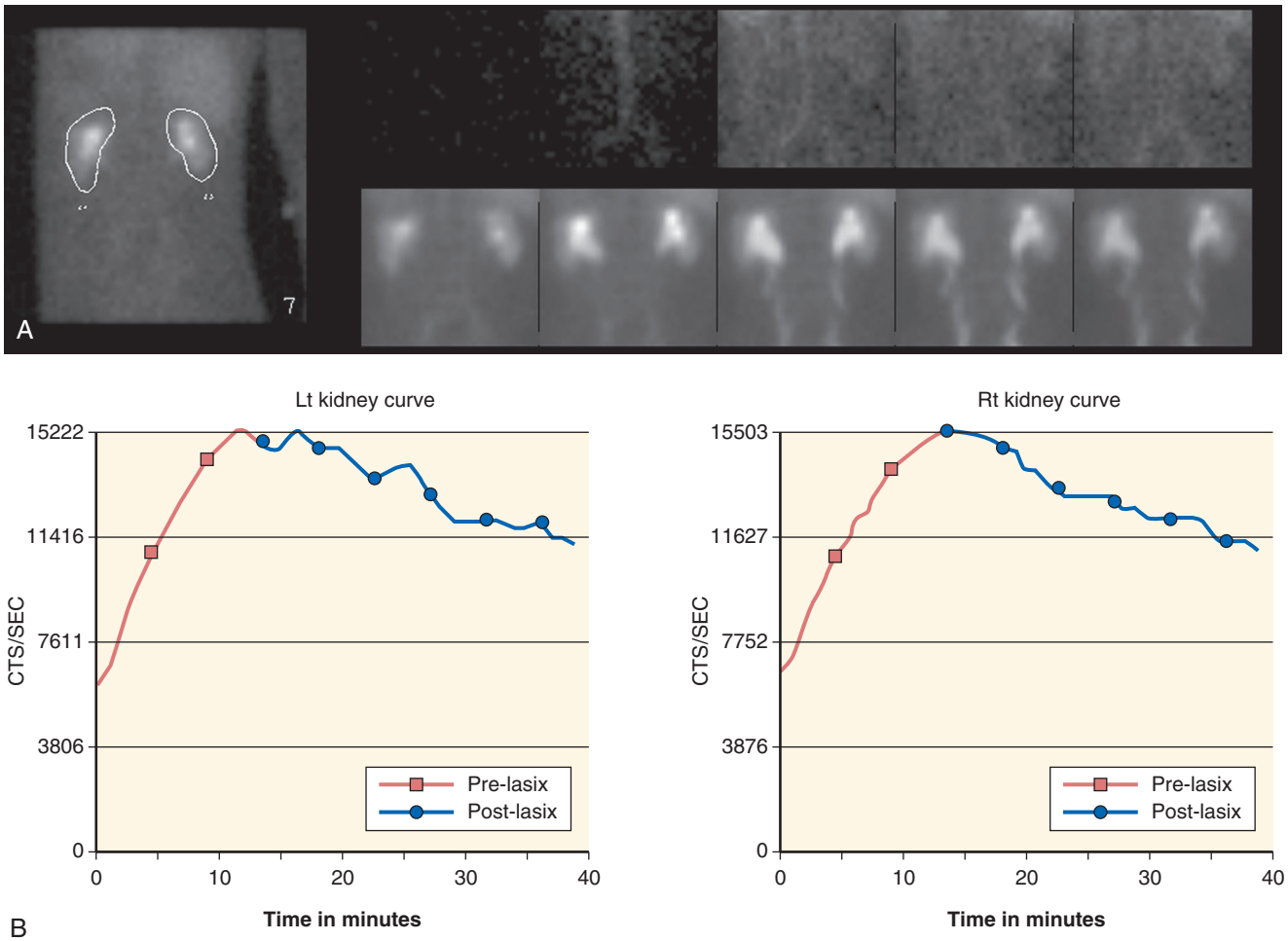

Fig. 25.32 Abnormal findings on renogram with technetium 99m-labeled mercaptoacetyltriglycine, demonstrating obstructive urinary kinetics with a poor response to furosemide. **A,** Static and timed images in the same format as in Fig. 25.23A. **B,** Individual time-activity curves for each kidney. Intravenous furosemide (Lasix) was given at 15 minutes. *CTS/SEC*, radioactivity counts per second.

Fig. 25.33 Renal stone: plain radiograph of the kidneys, ureters, and bladder. A large laminated stone is visible in the renal pelvis of the right kidney. The outline of the normal left kidney can be seen with no calcifications overlying it. The right kidney outline cannot be seen.

small uric acid stones (<1–2 mm in diameter).[192,193] As expected, calcium oxalate and calcium phosphate stones are the most dense.[168,169] Matrix stones, which are rare, may also be relatively low in density, but they usually contain calcium impurities that make them visible.[168,171]

For detecting stones, low-dose scanning has been shown to be as effective as CT with standard techniques.[194,195] The radiation dose is usually 20% to 25% of the standard dose. The development of iterative reconstruction techniques has also reduced radiation doses. Dual-energy imaging with CT has demonstrated the ability to distinguish different types of stones[187,196] (see Fig. 25.8).

Calculi may be visible in all parts of the collecting system and the urinary tract. Small punctate calcifications (≈1 mm) are occasionally observed just at the tip of the renal pyramid. These may represent the calcification noted in Randall plaques.[197] Obstruction occurs most commonly at the ureteropelvic junction, at the pelvic brim, where the ureters cross over the iliac vessels, and at the ureterovesical junction. The diagnosis is made on the noncontrast CT scan by demonstrating the calcified stone within the urine-filled ureters (Fig. 25.36).[188] Secondary signs may be present to assist in the diagnosis.[182] Hydronephrosis and hydroureter to the point of the stone may be visible. Asymmetric perinephric and periureteral stranding may also be related to forniceal rupture and urine leak (Fig. 25.37).[198] The involved

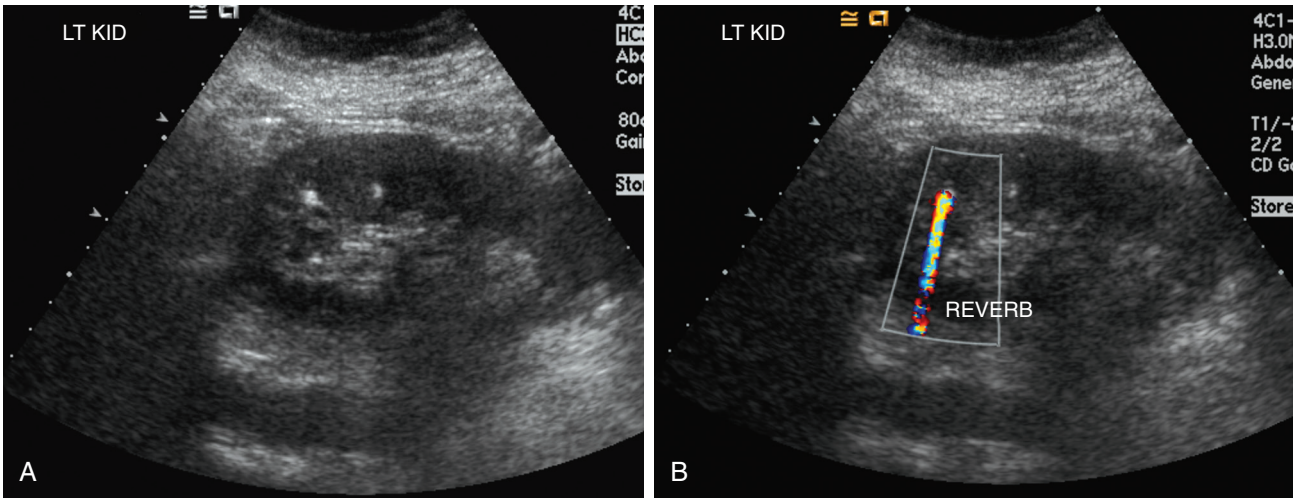

Fig. 25.34 Renal stone: ultrasonography. Longitudinal image **(A)** and Doppler color-flow image **(B)** demonstrate an echogenic focus at the corticomedullary junction. Not all stones show shadowing, but in this case, reverberation artifact (REVERB) is visible on the Doppler color-flow image, which helps establish the diagnosis.

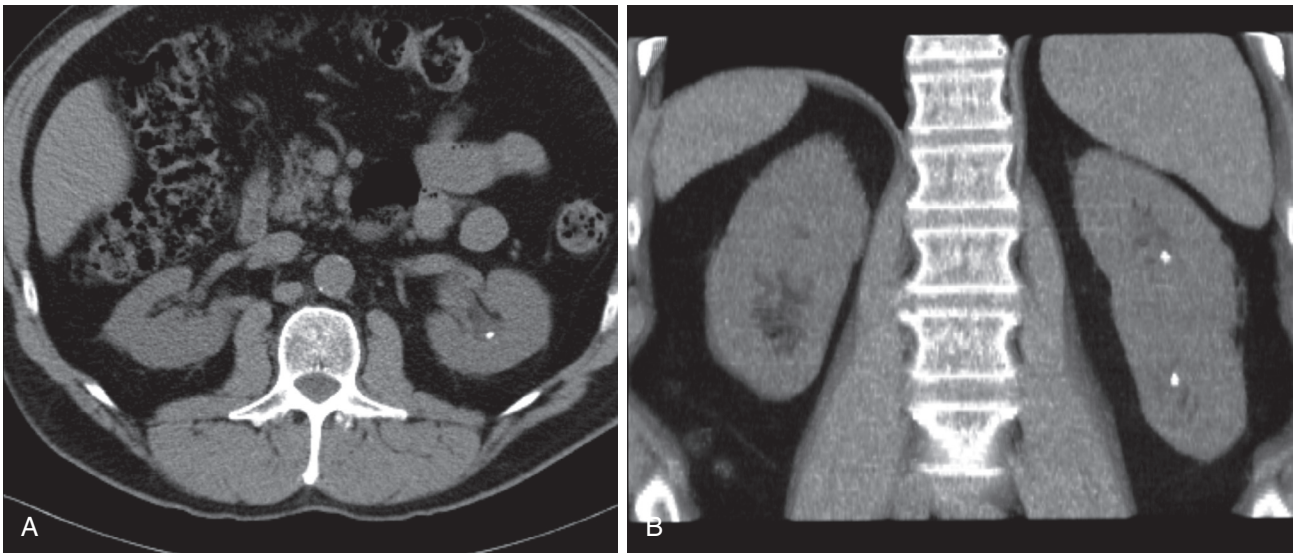

Fig. 25.35 Renal stones: noncontrast computed tomographic scan. Axial image **(A)** and coronal image **(B)** demonstrate 4- to 5-mm stones in the upper and lower poles of the left kidney. There are no signs of obstruction.

kidney may be less dense than the normal kidney because of increased interstitial fluid and edema.[199,200] The affected kidney may also be larger than the normal kidney. At the point of obstruction, the stone may be visible within the ureter, with soft tissue thickening of the ureteral wall at that level. This thickening is probably caused by edema and inflammation associated with the passage of the stone.

Noncontrast CT has the additional advantage of assessing the overall stone burden of the patient, not just the passing stone. Also, the size may be accurately measured, which enables clinicians to make treatment decisions.[173,201,202] Distal ureteral stones are occasionally confused with phleboliths, which are common in the pelvis (see Fig. 25.37). Images reconstructed in the coronal plane along the course of the ureters down to the level of the stone may be helpful.[203] Also, close inspection of phleboliths frequently reveals a small, soft tissue tag leading to the calcification: the "comet tail" sign.[204] Enhancement with contrast material is occasionally necessary in confusing or difficult cases. Also, CE-CT may be used in complicated cases in which the patient is febrile and pyelonephritis or pyohydronephrosis is suspected.[170]

In the evaluation of acute stone disease, MRI or MRU is not the examination of first choice, but it is a suitable alternative for selected patients, especially those in whom reduction of radiation exposure is desired (pediatric and pregnant patients).[205] Stones are difficult to identify in nondilated systems, even in retrospect. When stones are observed on MRI, they are visible as black foci on both T1- and T2-weighted sequences. Stones become more conspicuous in a dilated collecting system (Fig. 25.38); however, a nonenhanced filling defect is a nonspecific finding. Blood, air, or debris may have the same appearance. If stones or other calcifications are a concern, noncontrast CT is the examination of choice for improved conspicuity.

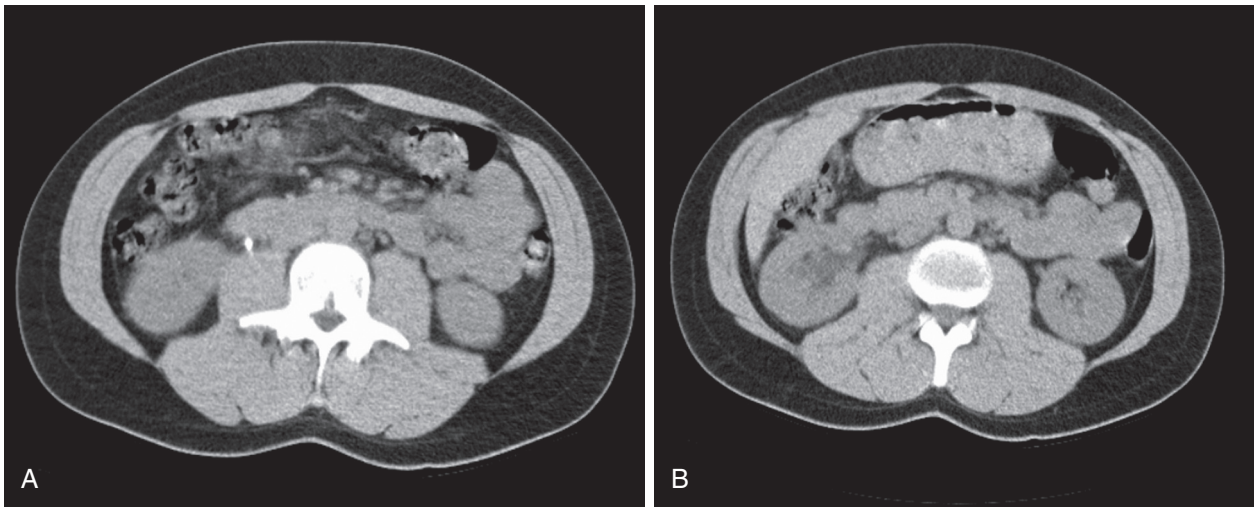

Fig. 25.36 Ureteral stone: noncontrast computed tomographic scan. **A,** A 5- to 6-mm stone is noted in the midportion of the right ureter. **B,** Axial image of the midportion of the kidneys reveals the urine-filled right renal pelvis and a right kidney that is slightly less dense than the left. These are signs of obstruction.

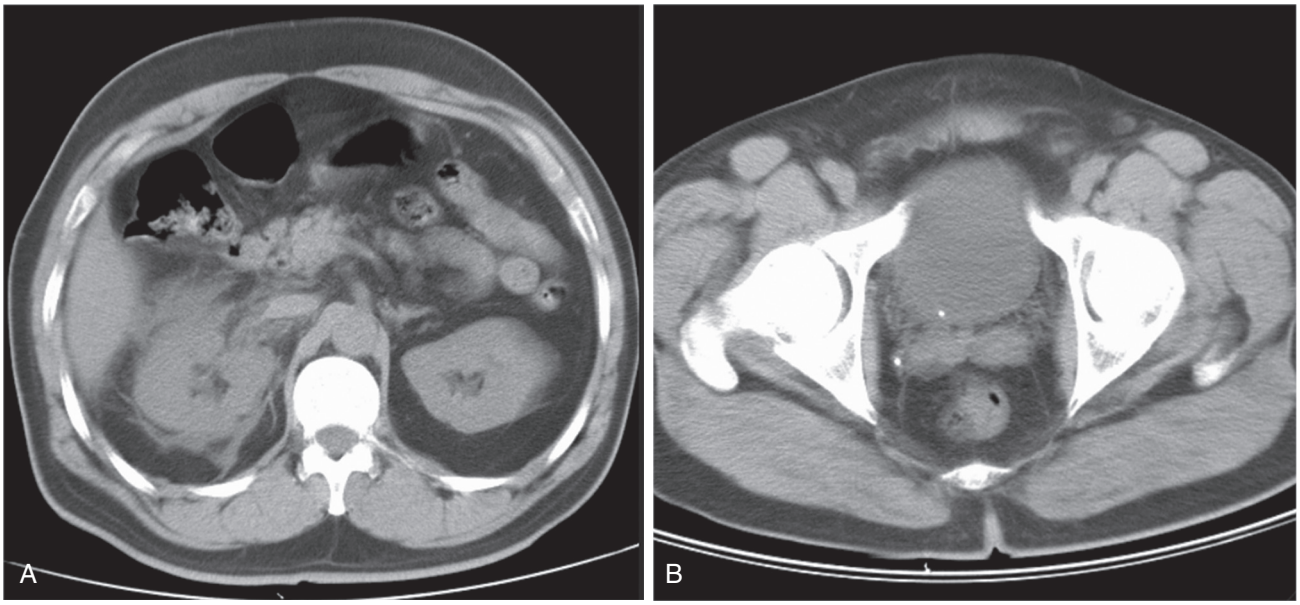

Fig. 25.37 Ureteral stone: noncontrast computed tomographic scan. Axial images of the kidneys show perinephric and peripelvic stranding and fluid on the right **(A)** caused by forniceal rupture and leakage of urine as a result of the distal obstructing stone at the right ureterovesical junction **(B)**. Note the phlebolith on the right posterior to the bladder and lateral to the seminal vesicle; phleboliths are commonly confused with distal ureteral stones.

When the use of iodinated contrast material is contraindicated, or when reduction of radiation exposure is desired, MRU can be used to determine the cause and location of an obstructing process (Fig. 25.39). MRU is highly accurate in demonstrating obstruction, regardless of whether the process is acute or chronic.[205] Acute obstruction may be associated with perinephric fluid, which is well demonstrated on T2-weighted sequences.[205,206] However, perinephric fluid is a nonspecific finding and can be found in association with other renal disease. MRI is useful in evaluating the patient who has recently undergone surgery for renal stone disease. MRI has been reported as being more accurate than CT in differentiating perirenal and intrarenal hematomas (Figs. 25.40 and 25.41).[207] CE-MRI can also demonstrate damage to the collecting system and areas of ischemia without the risk for nephrotoxicity. Stone disease is discussed further in Chapter 38.

RENAL INFECTION

Acute pyelonephritis is typically a diagnosis made clinically.[208] Most cases of acute pyelonephritis occur by the ascending

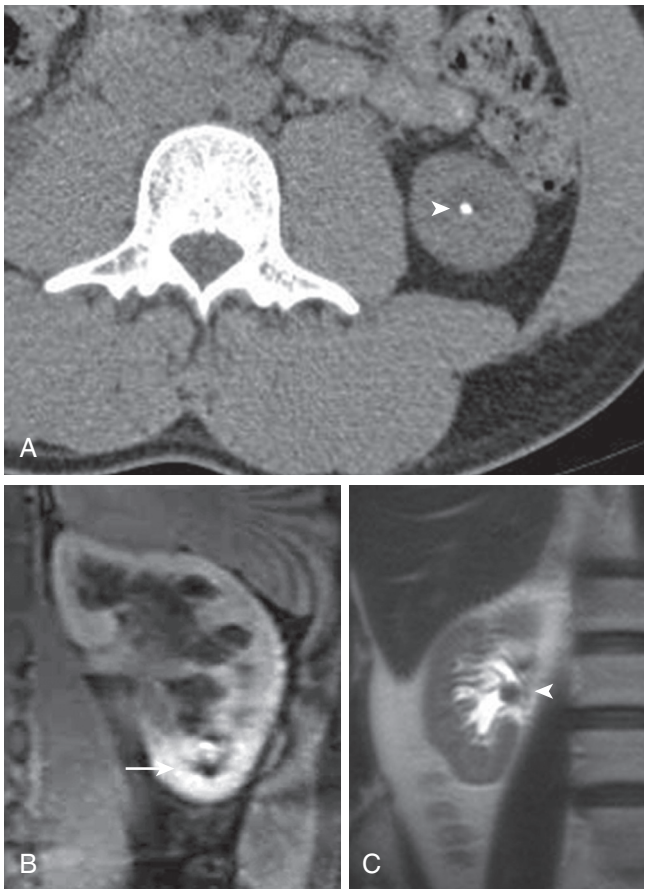

Fig. 25.38 Renal stones. Calcification *(arrowhead)* well viewed on computed tomography **(A)** is difficult to demonstrate on magnetic resonance imaging **(B)** *(arrow),* even in retrospect. **C,** A stone *(arrowhead)* is more conspicuous when it is located within a mildly dilated collection system.

route from the bladder and are caused by gram-negative bacteria.[209] Vesicoureteral reflux may contribute, although the ascent of the bacteria up the ureter also occurs in its absence. This is due to the presence of the adhesin P fimbriae and powerful endotoxins that appear to inhibit ureteral peristalsis creating a functional obstruction.[210] The bacteria are transported to the renal pelvis, where intrarenal reflux occurs and the bacteria traverse the calyceal system to the ducts and tubules within the renal pyramid. Enzyme release results in destruction of tubular cells with subsequent bacterial invasion of the interstitium. As the infection progresses, it spreads throughout the pyramid and to the adjacent parenchyma. The inflammatory response leads to focal or more diffuse swelling of the kidney. Without adequate treatment, necrosis of the involved regions and microabscess formation occur. These microabscesses may coalesce into larger macroabscesses, which tend to be surrounded by a rim of granulation tissue.[211] Perinephric abscess results from the rupture of an intrarenal abscess through the renal capsule or the leak from an infected and obstructed kidney (pyonephrosis). The overall distribution in the kidney is usually patchy or lobar, but sometimes it is diffuse.[209] Subsequent scarring of the kidney after treatment reflects the magnitude of the infection and tissue destruction that occurred.

Pyelonephritis may also occur by hematogenous spread of bacteria to the cortex of the kidney and eventual involvement of the medulla. The pattern of involvement is usually round, peripheral, and frequently multiple. Blood-borne infection is less common than ascending infection and is usually observed in intravenous drug abusers, immunocompromised patients, or patients with a source of infection outside the kidney, such as heart valves or teeth.

Imaging is rarely used or needed in uncomplicated pyelonephritis, and most patients respond to therapy within 72 hours. Imaging should be reserved for patients who are not responding to conventional antibiotic treatment, patients with an unclear diagnosis, patients with coexisting stone disease and possible obstruction, patients with diabetes and poor antibiotic response, and patients who are immunocompromised. Imaging is used to assess complications of acute pyelonephritis, including renal and perinephric abscess, emphysematous pyelonephritis, and xanthogranulomatous pyelonephritis.[212–214] All of these entities are imaged best with cross-sectional imaging techniques, specifically CT.

US results are normal in the majority of patients with acute pyelonephritis. When the examination results are abnormal, the findings are often nonspecific. US is performed to look for a cause for acute pyelonephritis, such as obstruction or renal calculi, and to search for complications. Altered parenchymal echogenicity is the most frequent finding with loss of the normal corticomedullary differentiation. The echogenicity is usually decreased or heterogeneous in the affected area (Fig. 25.42). There may be focal or generalized swelling of the kidney. Power Doppler imaging may improve sensitivity in demonstrating focal hypoperfusion, but this is nonspecific. Tissue harmonic US imaging may be more sensitive in demonstrating focal or segmental, patchy, hypoechoic areas extending from the medulla to the renal capsule.[215]

CE-CT is the most sensitive and specific imaging study in the patient with acute pyelonephritis.[216,217] The nephrographic phase of CT is best for imaging in patients with acute pyelonephritis (Fig. 25.43). Wedge-shaped areas of decreased density extending from the renal pyramid to the cortex are most characteristic.[216] The nephrogram may be streaky or striated in either a focal or global manner (Fig. 25.44).[218] There may be focal or diffuse swelling of the kidney.[219] The areas of involvement may appear almost mass-like (see Fig. 25.43). The changes in the nephrogram are related to decreased concentration of contrast media in the tubules with focal ischemia. Tubular destruction and obstruction with debris are also present. There is usually a sharp demarcation between diseased tissue and the normal parenchyma, which continues to enhance normally in the nephrographic phase. Soft tissue stranding and thickening of Gerota's fascia are caused by the adjacent inflammatory process (see Fig. 25.44).[211] The walls of the renal pelvis and proximal ureter may be thickened. The calyces and renal pelvis may be effaced. Mild dilation is also occasionally noted. With hematogenous-related pyelonephritis, the early findings tend to be multiple, round cortical regions of hypodensity that become more confluent and involve the medulla with time.[219] These findings may persist for weeks despite successful treatment with antibiotics.

MRI is comparable with CE-CT for the evaluation of pyelonephritis.[220] The enhancement characteristics of acute pyelonephritis on MRI are similar to those on CT. On

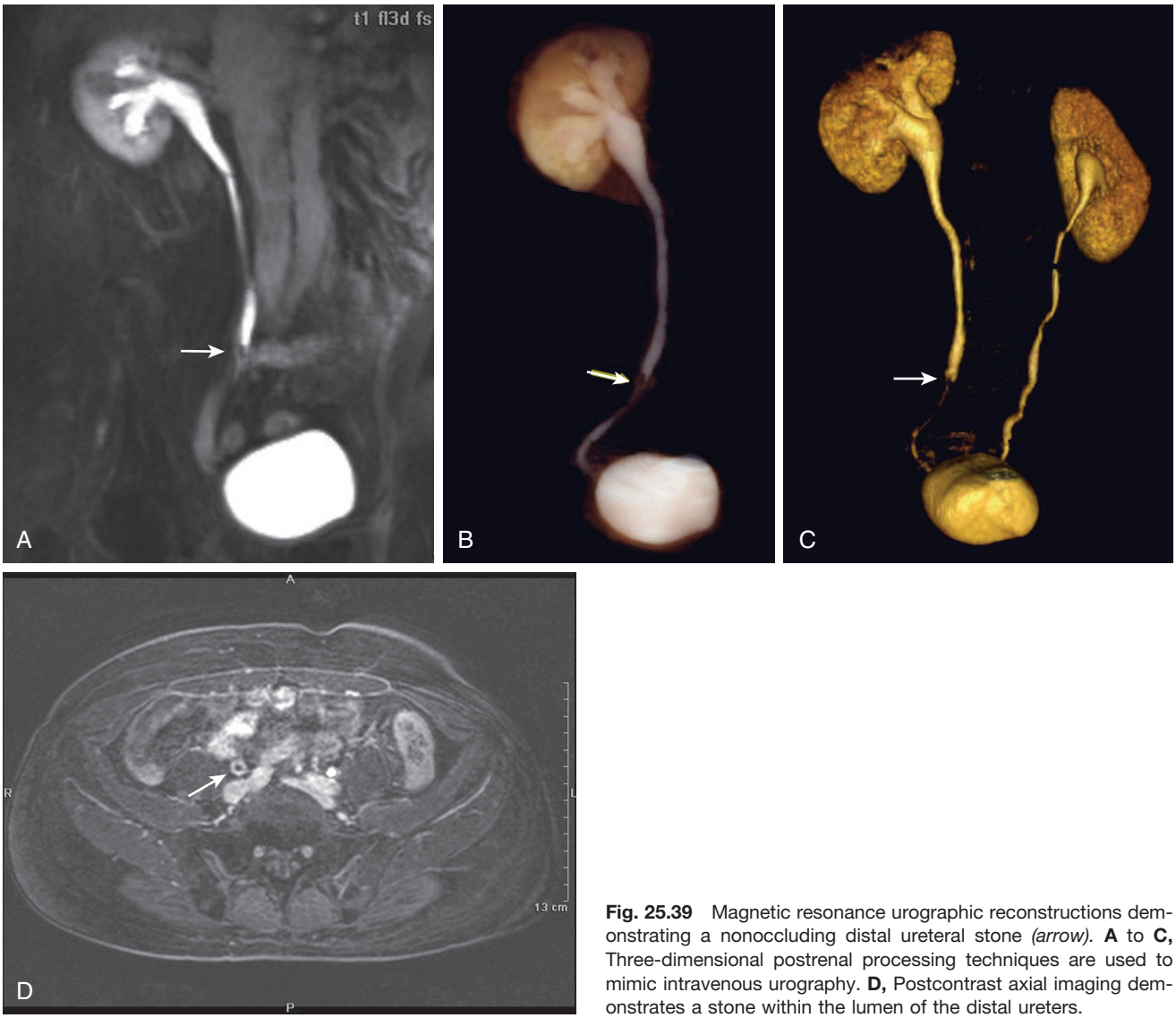

Fig. 25.39 Magnetic resonance urographic reconstructions demonstrating a nonoccluding distal ureteral stone *(arrow).* **A** to **C,** Three-dimensional postrenal processing techniques are used to mimic intravenous urography. **D,** Postcontrast axial imaging demonstrates a stone within the lumen of the distal ureters.

noncontrast sequences, the affected area has increased T2 signal intensity and decreased T1 signal intensity in relation to the normal renal parenchyma.

Other modalities do not have a significant role in evaluating acute pyelonephritis, unless CT is unavailable. IVU findings may appear normal in up to 75% of cases[211,216]; IVU has been shown to be noncontributory to clinical care in 90% of patients with pyelonephritis.[209,217] Radiolabeled leukocyte scans (e.g., indium 111-labeled white blood cells) and gallium 67 citrate scans can identify acute pyelonephritis. However, these methods have the drawbacks of extended imaging time (more than 24 hours) and higher radiation exposure. Cortical imaging with ^{99m}Tc-DMSA has been shown to be highly sensitive for detecting acute pyelonephritis in the appropriate clinical setting.[221,222] In acute pyelonephritis, segmental regions of decreased tracer uptake are demonstrated in oval, round, or wedge patterns. There may also be diffuse generalized decrease in renal uptake, which, in association with a normal or slightly enlarged kidney, is suggestive of an acute infectious process. The pathophysiologic basis for decline in ^{99m}Tc-DMSA cortical uptake in infection is related to diminished delivery of the tracer to the infected area and to direct infectious injury to the tubular cells, which compromises their function and tracer uptake. A wedge-shaped cortical defect with regional decrease in renal size is compatible with postinfectious scarring. Renal infarcts may also have similar appearance.[131,136] Attention to ^{99m}Tc-DMSA image processing and quality is paramount to achieving high interreader agreement.[223,224] There may also be a role for FDG PET-CT in the imaging evaluation of renal infection.[225]

Renal abscess results from severe pyelonephritis and occurs two to three times more frequently in patients with diabetes.[213] Abscesses are more common with hematogenous infection than with ascending infection.[208] CE-CT characteristics of renal abscess include a reasonably well-defined mass with a low-density central region and a thick, irregular wall or

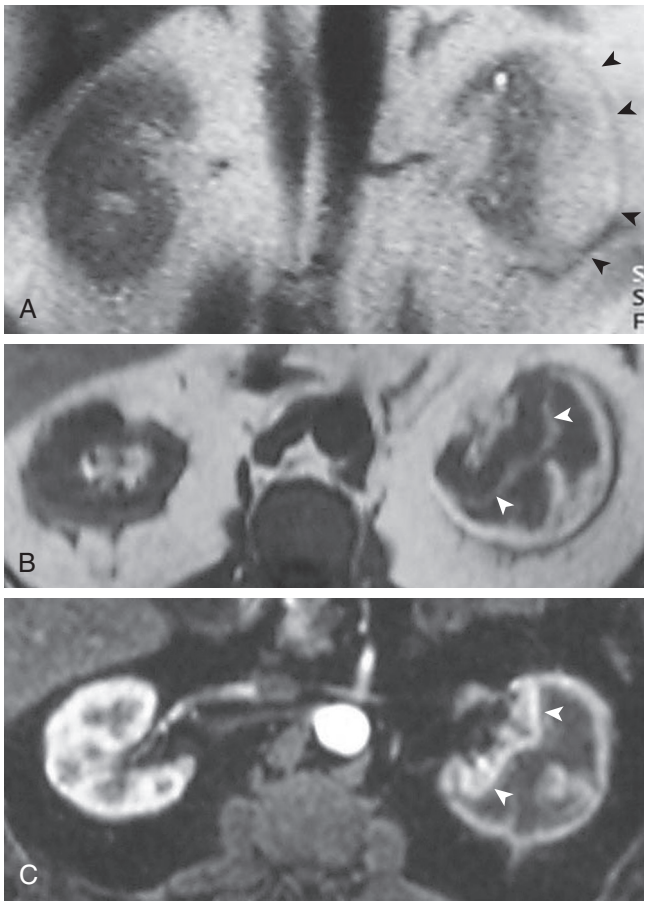

Fig. 25.40 Subcapsular hematoma after lithotripsy. Coronal T2-weighted sequence **(A)** demonstrates high-signal intensity blood contained by left renal capsule *(arrowheads).* Axial T1-weighted image **(B)** and gadolinium-enhanced T1-weighted image **(C)** show mass effect on left kidney *(arrowheads)* caused by a subcapsular hematoma. The signal intensity is consistent with the presence of intracellular methemoglobin.

pseudocapsule (Fig. 25.45).[216] Enhancement adjacent to the abscess is variable, depending on the amount of inflammation. Mature abscesses may demonstrate a more sharply demarcated border with peripheral rim enhancement. Gas may be visible within the abscess. MRI is comparable with CE-CT for the evaluation of renal abscess.[220] The central region of the abscess can have a variable appearance, but generally it is of decreased T1 and increased T2 signal intensity. The wall enhancement characteristics are also similar to those on CE-CT (Fig. 25.46).

Renal parenchymal infections can extend into the perinephric space with resulting abscess formation.[219] CT and MRI best reveal the involvement of the perinephric and paranephric spaces within the retroperitoneum. In general, inflammatory changes and heterogeneous fluid-density or signal intensity collections may be identified. Associated gas is best identified on CT.

In patients with preexisting cystic disease, suspected infection can be best evaluated using US, CT, or MRI. The presence of enhancement and documentation of changes compared with prior imaging is crucial.

Emphysematous pyelonephritis is a severe necrotizing infection of the renal parenchyma, usually caused by gram-negative bacteria (*Escherichia coli, Klebsiella pneumoniae, Proteus mirabilis*).[216] Of patients with emphysematous pyelonephritis, 90% have uncontrolled diabetes.[213] Emphysematous pyelonephritis is characterized by severe acute pyelonephritis, urosepsis, and hypotension. The gas found in the renal parenchyma is believed to form as a result of the high levels of glucose in the tissue by fermentation with the production of CO_2. The gas may also be observed in the pelvicalyceal system or perinephric space (or both). If the gas is extensive enough, it may be visible on plain radiographs or KUB images. The gas is usually mottled, bubbly, or streaky in appearance and may be observed in the areas over the kidneys. US may suggest the diagnosis of emphysematous pyelonephritis by demonstrating gas within the kidney.[226] With gas present, there is acoustic shadowing in the involved region. CT is the most specific and sensitive modality for the identification of renal gas.[227] The gas dissects through the parenchyma in a linear focal or global manner, radiating along the pyramid to the cortex. It may extend into the perinephric space. There is generally extensive parenchymal destruction with streaks or mottled collections of gas within the kidney (Fig. 25.47). Little or no fluid is seen. Emphysematous pyelitis represents gas within the pelvicalyceal system without parenchymal gas.[228] The distinction is important because emphysematous pyelitis carries a less grave prognosis.

Xanthogranulomatous pyelonephritis is an end-stage condition resulting from chronic obstruction with long-standing infection, usually with *Proteus* species or *E. coli.*[218] The renal parenchyma is destroyed and replaced by vast amounts of lipid-laden macrophages. The kidney is usually barely functional or nonfunctional. The destruction is typically global, but it may involve only a portion of the kidney. A staghorn calculus may be seen on KUB. On US the kidney appears enlarged with loss of identifiable landmarks. A large calculus or staghorn calculus usually fills the renal pelvis, with debris filling adjacent hypoechoic regions (Fig. 25.48). CT defines the extent and adjacent organ involvement best. The findings on CT include an enlarged but generally reniform mass filling the perinephric space.[214,229] Calcification is found in 75% of cases, excretion is absent or markedly decreased in 85% of cases, and the involved region appears as a mass in more than 85% of cases.[214] The process is focal in fewer than 15% of cases. There is frequent perinephric extension. Fistulas may occur in adjacent structures, with adenopathy noted in the retroperitoneum. MRI may show many similar findings when compared with CT, although calcifications are less conspicuous (Fig. 25.49).

Malacoplakia is a rare inflammatory condition that most commonly involves the bladder but may also involve the ureter and kidney. Typically, the kidney is affected by obstruction from the lower urinary tract. When the kidney is directly involved, it is a multifocal process that may appear similar to xanthogranulomatous pyelonephritis on imaging.

Renal tuberculosis occurs by hematogenous spread. The genitourinary tract is the second most common extrapulmonary site of involvement.[230] Evidence of previous pulmonary tuberculosis is found in fewer than 50% of patients with genitourinary tuberculosis.[231] Only 5% may have active tuberculosis. Renal involvement is bilateral; the findings are determined by the extent of the infection, the stage of the

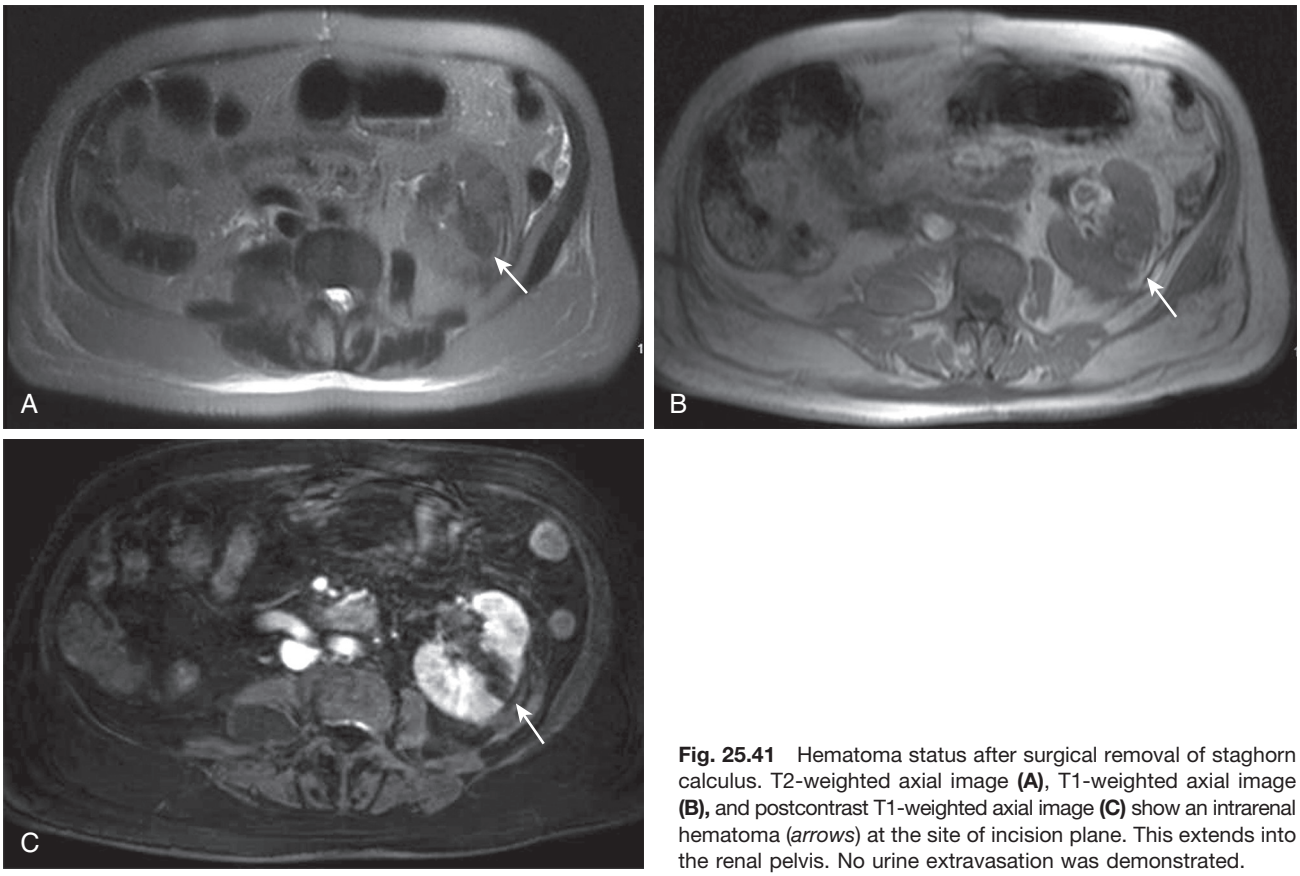

Fig. 25.41 Hematoma status after surgical removal of staghorn calculus. T2-weighted axial image **(A)**, T1-weighted axial image **(B),** and postcontrast T1-weighted axial image **(C)** show an intrarenal hematoma (*arrows*) at the site of incision plane. This extends into the renal pelvis. No urine extravasation was demonstrated.

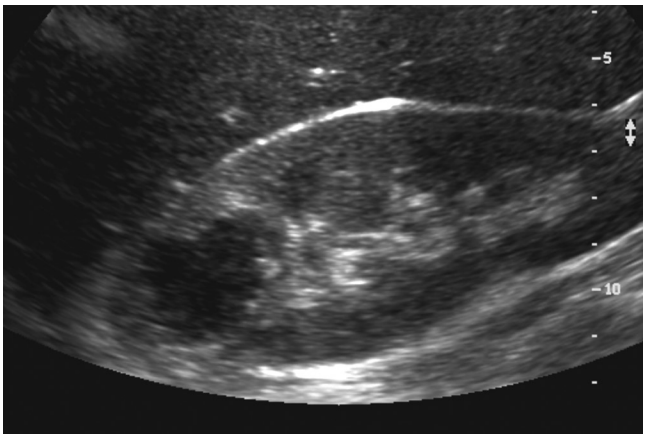

Fig. 25.42 Acute pyelonephritis: renal ultrasonography. The hypoechoic region in the upper pole represents an area affected by acute pyelonephritis. The surrounding parenchyma is somewhat distorted, with loss of the normal corticomedullary junction.

infection, and the host's response. Calcified granuloma may be found within the cortex or medulla, papillary necrosis may be visible (Fig. 25.50), and hydrocalyx with infundibular strictures may develop (Fig. 25.51). The kidney may become focally or globally scarred as the disease progresses. There may be areas of nonfunction with dystrophic calcifications. In the end stage, the kidney may be small and scarred with bizarre calcifications; this condition is the so-called autonephrectomy.[164,232]

Chronic pyelonephritis is usually associated with vesicoureteral reflux that occurs in childhood.[232] One or both kidneys may be involved. An affected kidney has focal scars that are associated with calyceal dilation. The scarring is often separated by normal regions of the kidney and normal-appearing calyces. When involvement is global, the kidney may be small. IVU demonstrates dilated or ballooned calyces that extend to the cortical surface, which is thinned. The outline of the affected kidney is distorted. With US the kidneys have irregular outlines with regions of cortical loss. Underlying dilated calyces may be visible. The regions of scarring may be echogenic in comparison with the adjacent normal kidney. CT and MRI demonstrate the abnormal architecture of the affected kidney.[219,220] Nephrographic phase images reveal the regions of cortical loss; the involved dilated calyces extend to the capsular surface. Dilation of the calyces is variable. Chronic pyelonephritis may be unilateral or bilateral. Excretory phase images best delineate the extent of involvement, especially in the coronal format.

In the patient with AIDS, urinary tract infections are quite common.[233,234] The infections are frequently hematogenous with unusual organisms such as *Pneumocystis jiroveci*, cytomegalovirus, and *Mycobacterium avium-intracellulare.* The infections may also be seen in other abdominal organs—liver, spleen, and adrenals.[235,236] In patients with AIDS, renal

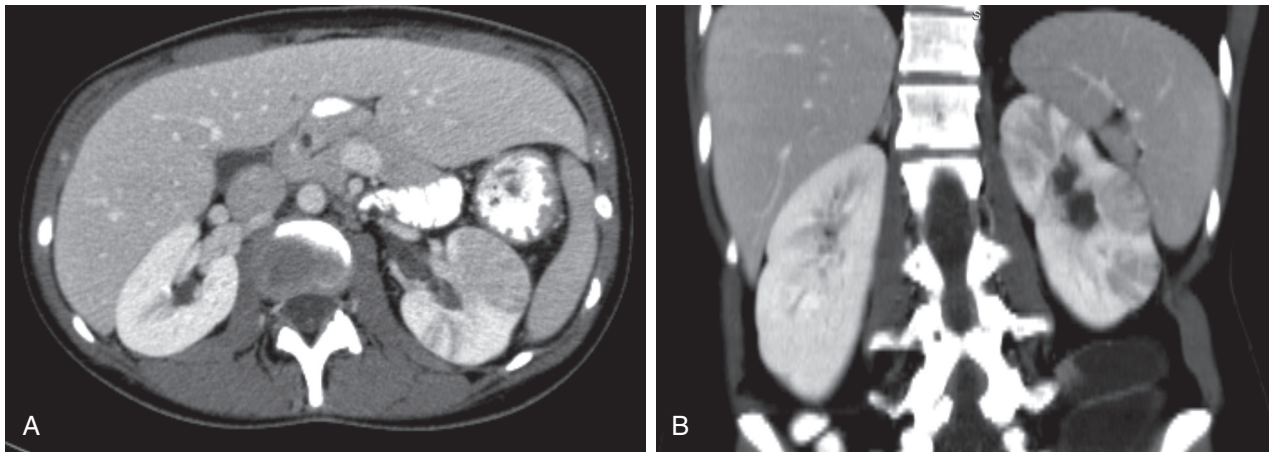

Fig. 25.43 Acute pyelonephritis: contrast material-enhanced computed tomographic scan, axial **(A)** and coronal **(B)** images. The left kidney shows multiple areas of involvement. The hypodense region in the midportion of the kidney appears almost mass-like (**A** and **B**). A nephrogram is striated in the region of involvement in the upper pole **(B)**.

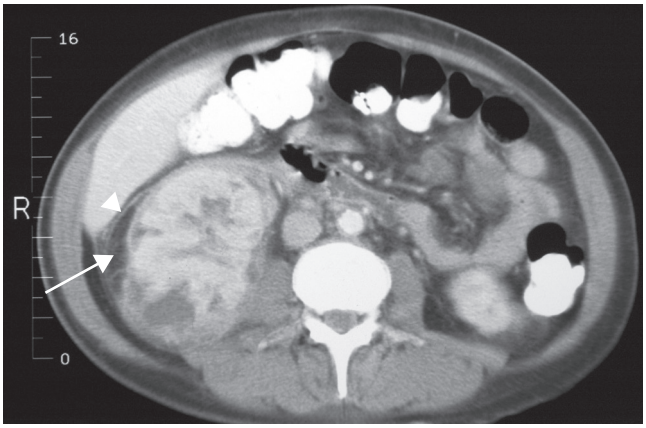

Fig. 25.44 Acute pyelonephritis: contrast material-enhanced computed tomographic (CT) scan. The heterogeneous CT nephrogram shows the diffuse involvement of the right kidney. Stranding and some fluid are visible in the perinephric space *(arrow)* with thickening of Gerota's fascia (*arrowhead*).

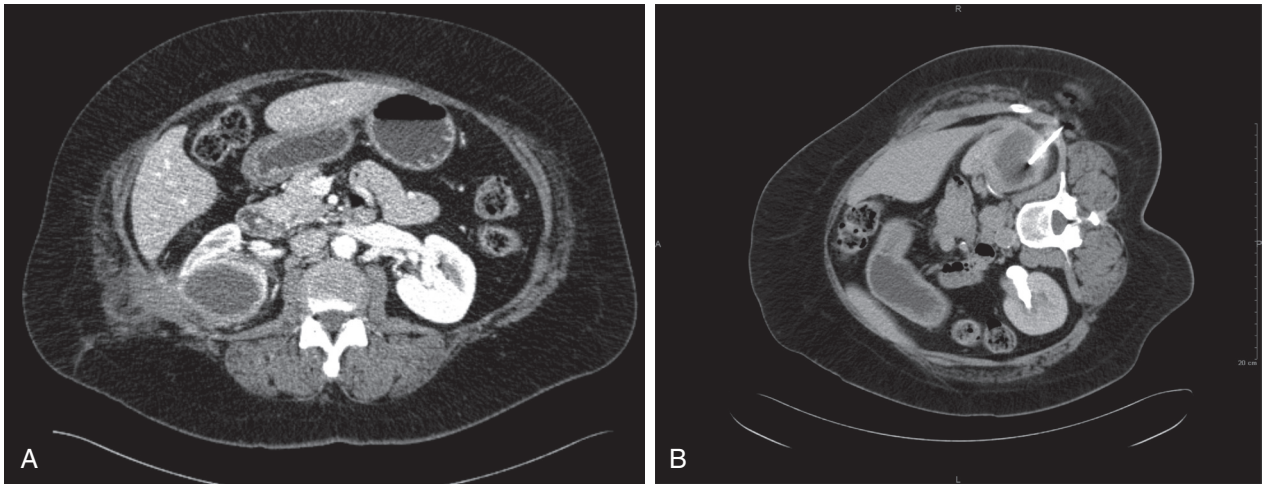

Fig. 25.45 Renal abscess: contrast material-enhanced computed tomographic scan. **A,** Axial image demonstrates the hypodense abscess in the right kidney with extension into the perinephric space and the right flank. **B,** Axial image with the patient in the decubitus position reveals the method of diagnosis: needle aspiration. A drainage catheter was subsequently placed for treatment.

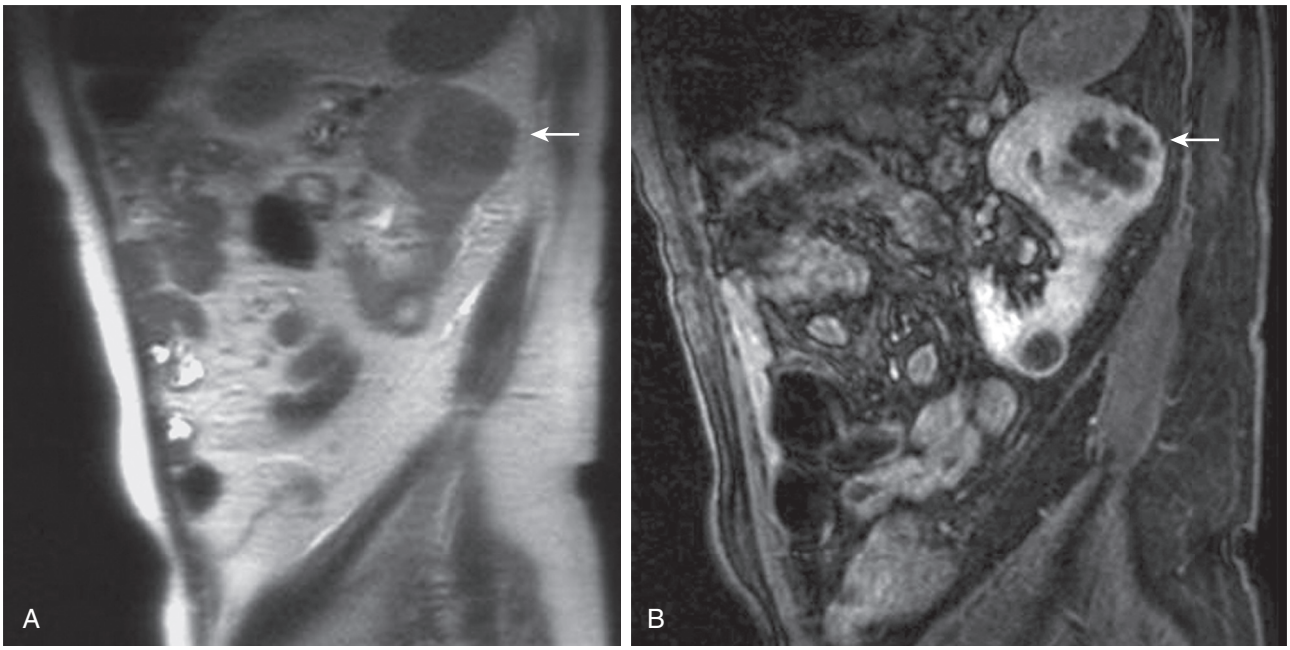

Fig. 25.46 Renal abscess. A mass in the upper pole of the left kidney demonstrates intermediate to low signal intensity *(arrow)* on the sagittal T2-weighted image **(A)** and heterogeneous but predominantly peripheral enhancement *(arrow)* on the sagittal postcontrast T1-weighted image **(B).** On biopsy, this mass was found to be *Aspergillus* infection.

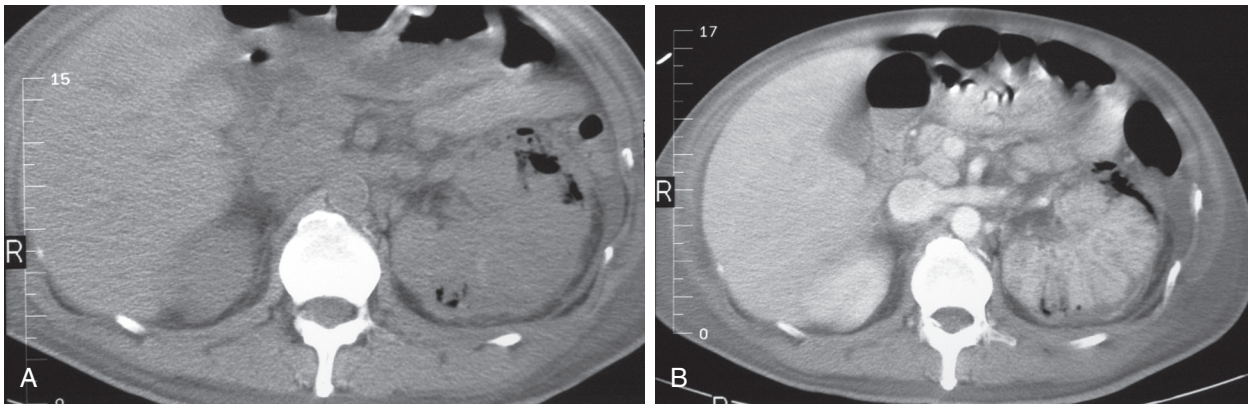

Fig. 25.47 Emphysematous pyelonephritis: contrast material-enhanced computed tomographic scan. A noncontrast image **(A)** and a contrast material-enhanced image **(B)** demonstrate gas in the left renal parenchyma with extension into the perinephric space. The nephrogram is striated throughout. Global involvement of the kidney is frequent.

Fig. 25.48 Xanthogranulomatous pyelonephritis: contrast material-enhanced computed tomographic scan. A large staghorn calculus fills the renal pelvis and collecting systems in the left kidney. Much of the remainder of the kidney is replaced by hypodense material—the xanthogranulomatous infection—within the calyces and parenchyma; some minimal enhancement of the cortex remains.

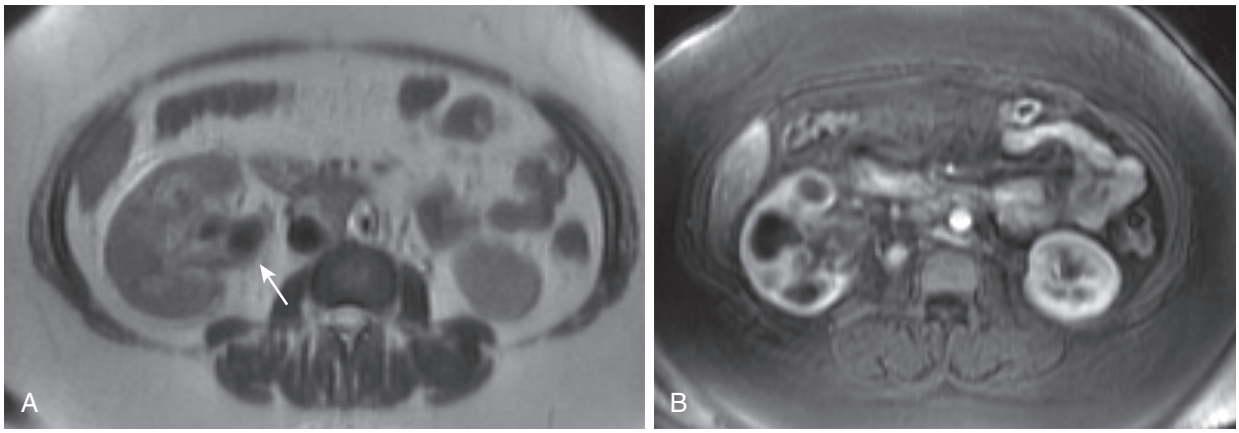

Fig. 25.49 Xanthogranulomatous pyelonephritis with staghorn calculus. **A,** Axial T2-weighted image demonstrates a stone of low signal intensity within the right renal pelvis *(arrow)* that is associated with increased renal size and replacement of the medullary pyramids and calyces with material of high signal intensity. **B,** Axial postcontrast T1-weighted image demonstrates asymmetric enhancement and hydronephrosis.

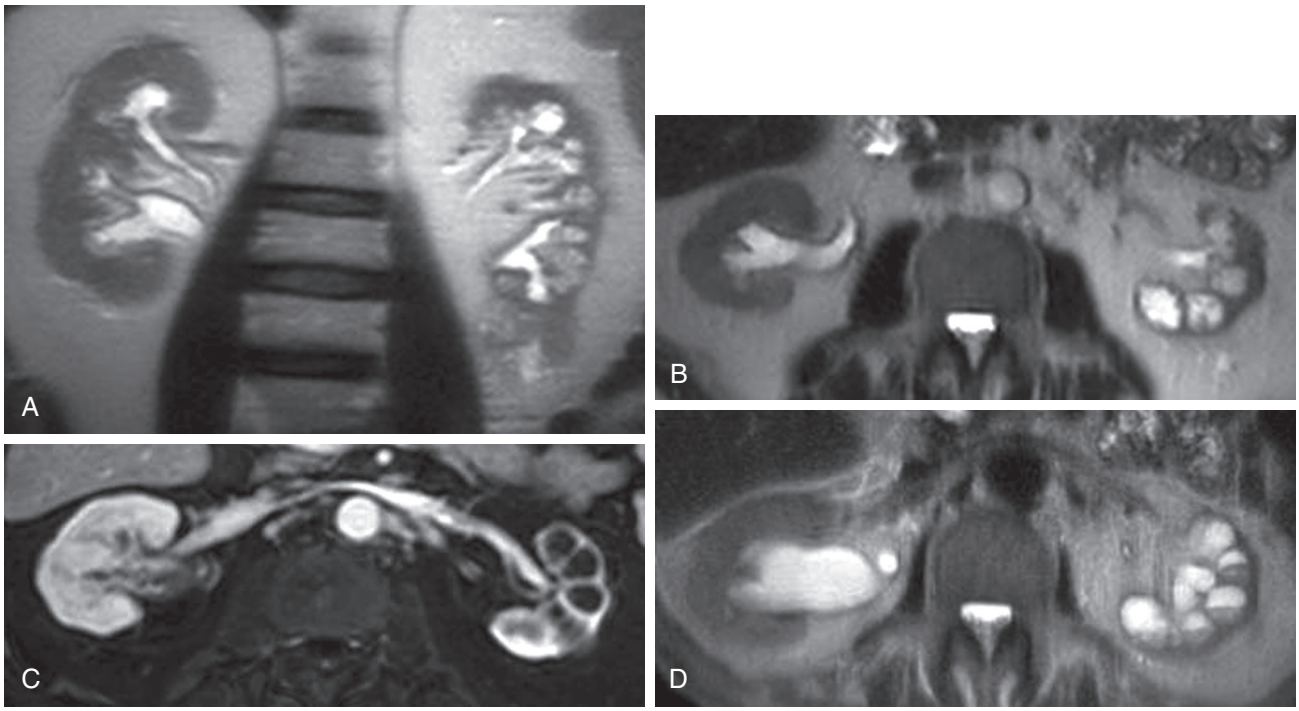

Fig. 25.50 Renal tuberculosis. **A** and **B,** T2-weighted images demonstrate asymmetric cortical thinning and focal areas of increased signal intensity in the distribution of the medullary pyramids. **C,** Postcontrast T1-weighted image shows absence of enhancement, which is consistent with the presence of granulomas with caseous necrosis. **D,** T2-weighted image after treatment shows distorted, dilated calyces containing debris. Right-sided hydronephrosis is present as a result of a distal ureteral stricture.

involvement may be detected in US demonstrating increased cortical echogenicity and loss of the corticomedullary differentiation (Fig. 25.52).[236] Renal size is also increased, and it is a bilateral process. Infections of the urinary tract are discussed further in Chapter 36.

RENAL MASS: CYSTS TO RENAL CELL CARCINOMA

Most renal masses are simple cysts, frequently found incidentally on US, CT, and MRI. They rarely occur in individuals younger than 25 years of age, but are found in more than 50% of patients older than 50 years of age. Typically, renal cysts are asymptomatic and cortical in location; they may be single or multiple. Their cause is unknown, although tubular obstruction has been postulated to be a necessary element.

Renal masses produce variable findings on imaging studies, depending on their location. For years IVU was the imaging modality of choice for detection of renal masses; however, the findings on IVU are frequently nonspecific, and further imaging is necessary to characterize most abnormalities found (Fig. 25.53). Studies have shown that IVU has low sensitivity

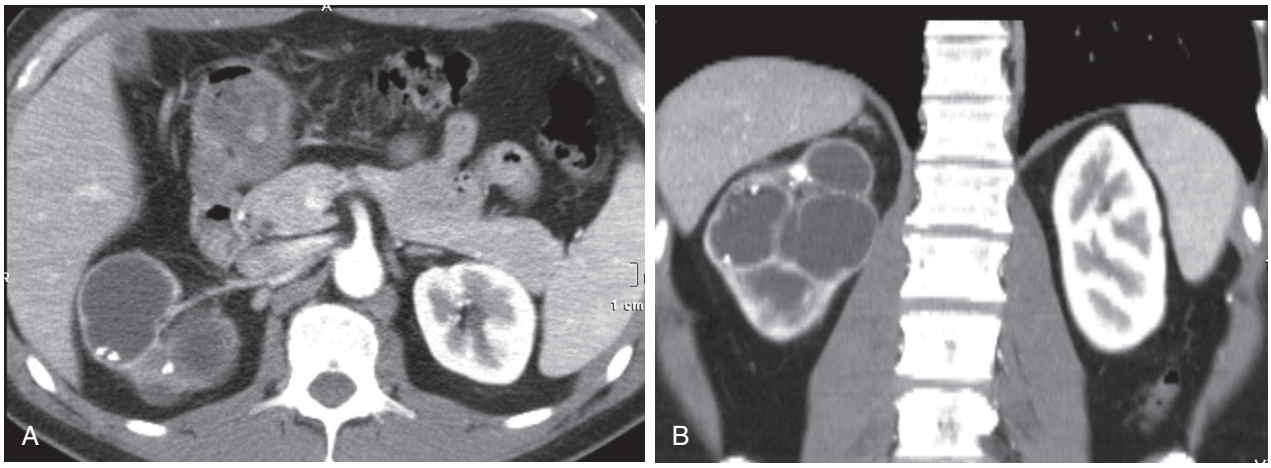

Fig. 25.51 Renal tuberculosis: contrast material-enhanced computed tomographic scan. Axial **(A)** and coronal **(B)** images show the destruction of the right kidney as a result of renal tuberculosis. Parenchymal calcifications are present with dilated calyces as a result of the attenuation and truncation of the renal pelvis and ureter.

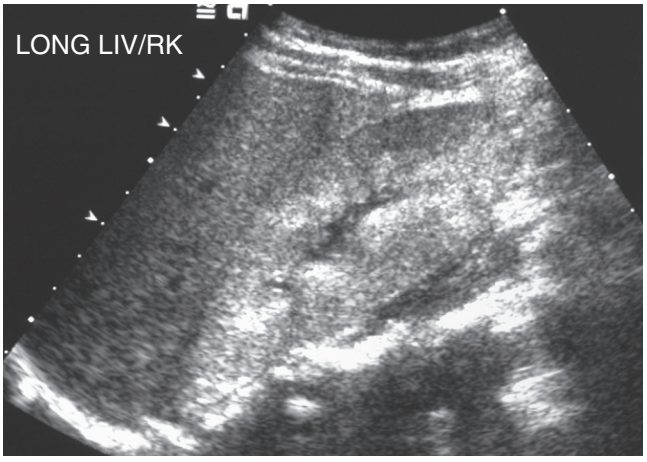

Fig. 25.52 Acquired immunodeficiency syndrome-related nephropathy: ultrasonography. Longitudinal image of the right kidney. The size of the kidney is normal to slightly increased. The corticomedullary distinction is lost with diffuse increased cortical echogenicity.

Fig. 25.53 Renal mass: nephrotomogram. A slightly hypodense mass projects off the lateral border of the left kidney (*arrow*). Subsequent imaging proved this to be a renal cyst.

for detection of renal masses, especially those smaller than 3 cm in diameter.[237] With CT as the gold standard, IVU detected 10% of masses smaller than 1 cm in diameter, 21% of masses 1 to 2 cm in diameter, 52% of masses 2 to 3 cm in diameter, and 85% of masses larger than 3 cm in diameter.[237] US fared better than IVU but detected only 26% of masses smaller than 1 cm, 60% of those 1 to 2 cm, 82% of those 2 to 3 cm, and 85% of those larger than 3 cm.[237]

The findings on IVU are nonspecific, and US, CT, and MRI are used to characterize the renal mass, differentiating solid from cystic.

US is an excellent means of diagnosing a simple renal cyst if all imaging criteria are met.[16] The lesion in the kidney must be round or oval and anechoic (Fig. 25.54); it must be well circumscribed with a smooth wall, and there must be enhanced through-transmission with a sharp interface between the wall and adjacent renal parenchyma. Thin septa may be visible within the cyst, but no nodules should be visible (Fig. 25.55). If all these criteria are met, the diagnosis of cyst is established. If there is any deviation from these criteria, further imaging with CT or MRI is necessary.

CE-CT is the method of choice for characterizing and differentiating renal masses.[238–240] A simple renal cyst appears as a well-circumscribed, round, water-density lesion with no measurable wall (Fig. 25.56). The contents should not enhance after the injection of contrast media. The contents may vary slightly from water density, but no more than 10 to 15 HU. The interface with the adjacent parenchyma is sharp. The margins are smooth with no perceptible nodules. Thin rim-like calcification may be visible. "High-density" cysts may be encountered with density ranging from 50 to 80 HU; these are cysts containing hemorrhagic or proteinaceous debris. Like simple cysts, they should demonstrate no wall nodularity

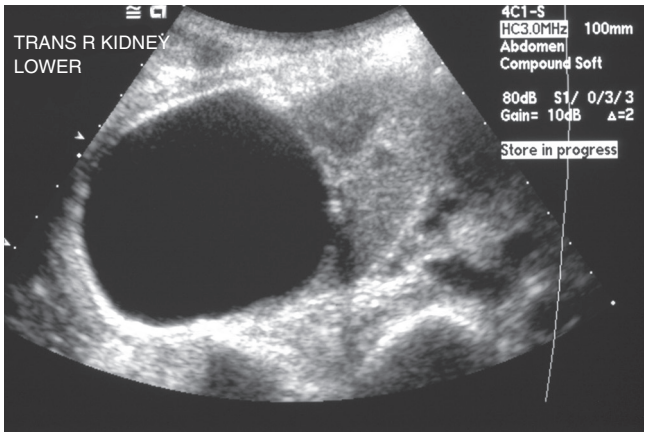

Fig. 25.54 Renal cyst: ultrasonography. A large, anechoic renal mass projects off the lateral border of the right kidney. The features of the cyst include a well-circumscribed lesion with a sharp back wall and increased through-transmission. There are no internal echoes or nodularity, and the wall is smooth. There is a clear interface with the kidney.

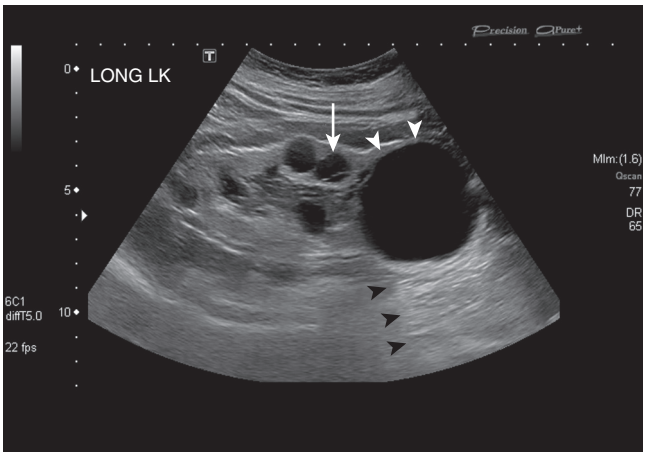

Fig. 25.55 Gray-scale ultrasonographic longitudinal image reveals a cyst *(white arrowheads)* that is completely anechoic, and there are no septations in it. The appearance of posterior acoustic enhancement *(black arrowheads)* further confirms that the lesion is a cyst. The small, more superficial lesion *(small white arrow)* has a single thin septation, thus representing a Bosniak category II cyst.

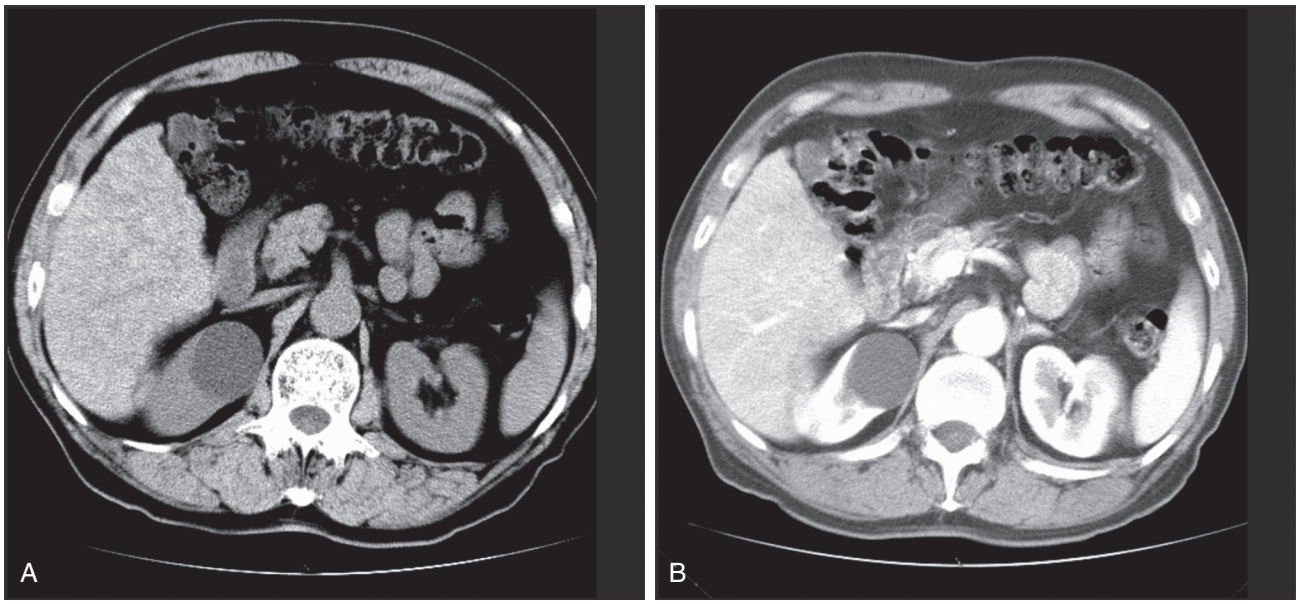

Fig. 25.56 Renal cyst: computed tomographic (CT) scan. Noncontrast **(A)** and postcontrast **(B)** axial images. The cyst is well circumscribed with no enhancement. It displays water density with CT numbers of 0 to 5. There is a sharp interface with the kidney and no perceptible wall. No nodules are visible, and the cyst is uniform throughout.

and have no significant enhancement after injection of contrast material. High-density cysts are common in polycystic or multicystic kidneys. Cysts are well demonstrated on MRI because of excellent soft tissue contrast. On MRI, simple cysts are well-circumscribed, thin-walled structures containing fluid that appears dark on T1-weighted sequences and bright on T2-weighted sequences (Fig. 25.57). Complex cysts contain proteinaceous or hemorrhagic fluid and may have septations and calcification. The T1 signal intensity of the fluid is higher than expected for simple fluid, ranging from isointense to hyperintense. T2 signal intensity is lower than expected for simple fluid and may be black, depending on the blood content. Cysts do not enhance. In comparison with CE-CT, CE-MRI has been found to have higher contrast material resolution, which allows for better visualization of septa.[241,242] MRI also better characterizes blood products and is more sensitive to subtle enhancement, especially when subtraction techniques are used. This makes MRI superior to CT in differentiating a complex cyst from a cystic neoplasm[241–243] (Figs. 25.58 and 25.59).

Polycystic renal disease is classified as infantile, adult, or acquired. The infantile form is inherited as an autosomal recessive disorder.[244] It has a variable manifestation: severe kidney injury is found in the neonatal period, and CHF and hepatic failure manifest in older children. Organomegaly is common, with bilateral symmetric renal enlargement. IVU yields poor visualization of the kidneys because of renal impairment, and the nephrogram is prolonged and mottled

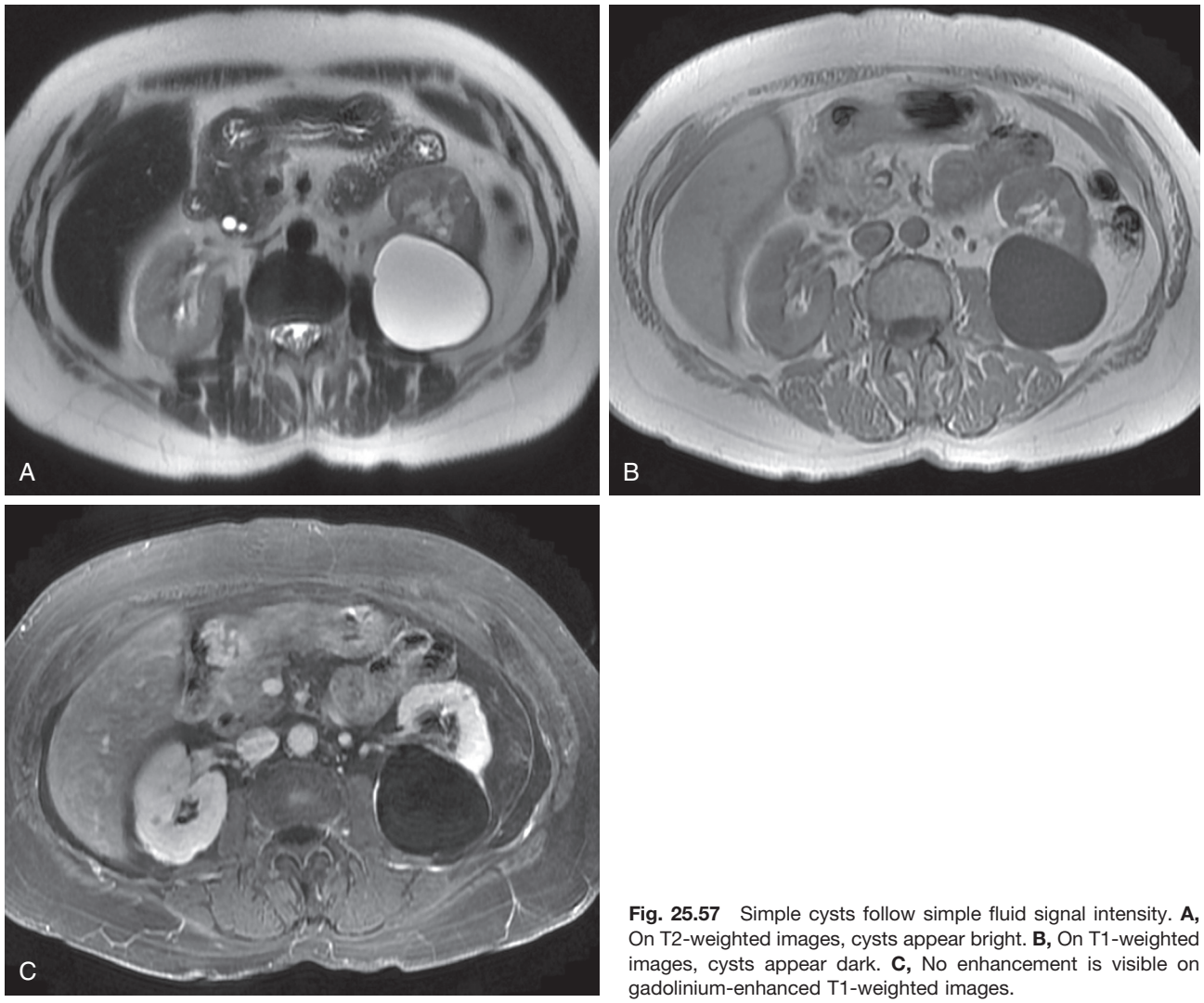

Fig. 25.57 Simple cysts follow simple fluid signal intensity. **A,** On T2-weighted images, cysts appear bright. **B,** On T1-weighted images, cysts appear dark. **C,** No enhancement is visible on gadolinium-enhanced T1-weighted images.

with a striated or streaky appearance. US reveals enlarged, diffusely hyperechoic kidneys as a result of dilated, ectatic collecting tubules.[245] There is loss of the corticomedullary differentiation as well. Because the diagnosis is made clinically with the associated US findings, CT and MRI are rarely used in this condition.

Autosomal dominant polycystic kidney disease (ADPKD) is the adult form.[246] There is no role for KUB or IVU in the evaluation for ADPKD. US reveals bilateral enlargement of the kidneys, which are markedly lobulated and contain multiple anechoic areas of varying size throughout.[247]

CT and MRI in ADPKD depict enlarged, lobulated kidneys with cysts of varying size throughout (Fig. 25.60). One kidney may be more involved than the other. The cysts may have calcifications with the wall. It is not uncommon to encounter cysts with varying density or signal intensity as a result of episodes of hemorrhage that occur within the cysts (Fig. 25.61). A fluid level may be visible as a result of the presence of debris or hemorrhage within some of the cysts. In the excretory phase, there is marked distortion of the calyces. The extent of renal involvement by ADPKD is better appreciated on CT and MRI than on US. Cysts may be found in the liver, spleen, and pancreas as well.

Adult-acquired polycystic kidney disease occurs in patients with kidney injury who are undergoing continuous peritoneal dialysis or hemodialysis[248] (Fig. 25.62). The longer the patient has undergone dialysis, the more likely the patient is to develop adult-acquired polycystic kidney disease.[249,250] The cysts are generally quite small (0.5–2 cm in most patients). Calcification may occur in the wall. Plain radiographs and IVU play no role in evaluation because renal function is impaired. US reveals small, shrunken kidneys with anechoic or hypoechoic regions that represent the cysts. The findings are usually bilateral. CT or MRI shows the small bilateral kidneys with cysts of size that varies, but usually in the range of 1 to 2 cm (Fig. 25.63; see Fig. 25.28).[251,252] These cysts must be closely evaluated for solid components because carcinomas and adenomas occur with increased frequency in these patients. Solid lesions smaller than 3 cm in diameter may represent either adenomas or renal cell carcinomas, whereas most lesions larger than 3 cm are renal cell carcinomas.[253,254] Screening for adult-acquired polycystic kidney disease is usually done with US every 6 months; CT or MRI is reserved for patients with questionable or solid lesions.[255]

Medullary sponge kidney, or renal tubular ectasia, is a nonhereditary developmental disorder with ectasia and cystic

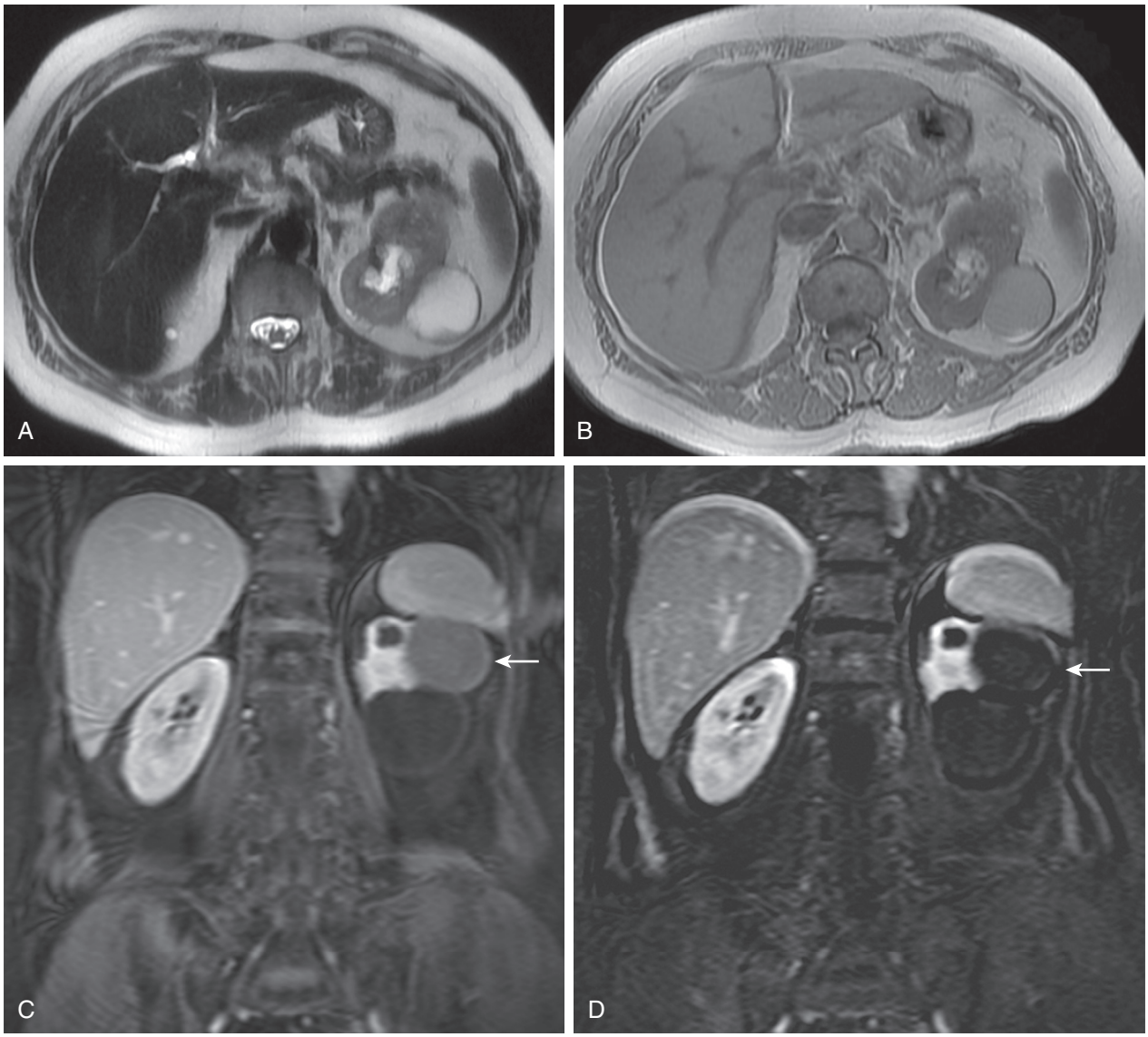

Fig. 25.58 Complex cyst confirmed by magnetic resonance imaging with image subtraction. **A,** T2-weighted axial image shows a bright left upper pole structure. **B,** T1-weighted axial image shows the same structure as intermediate in signal intensity. The cyst has internal debris that is visible on both sequences. Because the postcontrast T1-weighted coronal image **(C)** shows higher signal intensity than expected for a cyst *(arrow),* postcontrast subtraction images **(D)** are needed to confirm absence of enhancement *(arrow).*

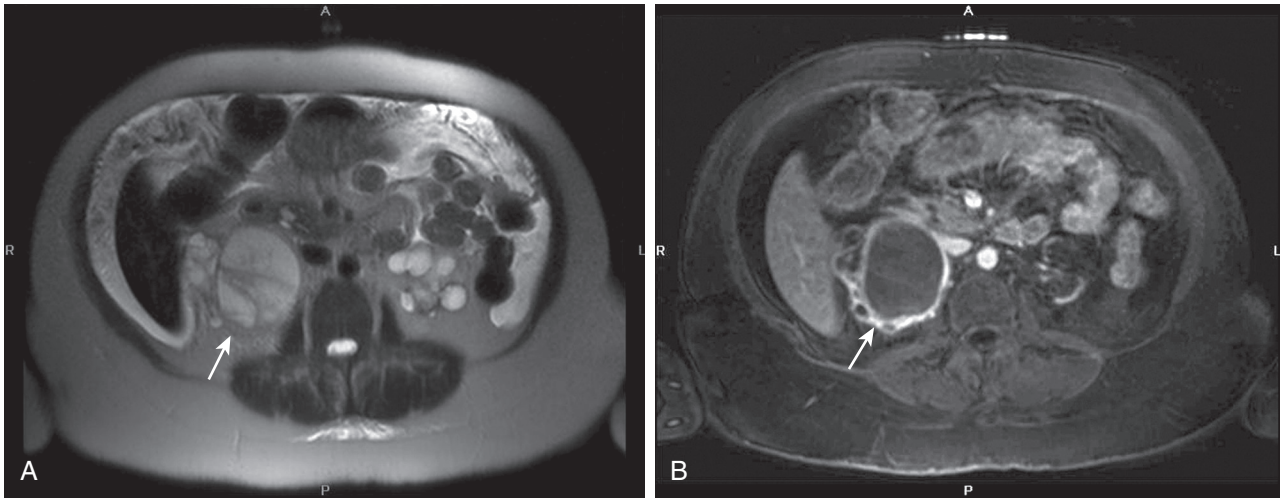

Fig. 25.59 Complex hemorrhagic cyst. **A,** T1-weighted axial images show a complex right renal structure, bright on both sequences and with internal septations *(arrow).* **B,** Gadolinium on T1-weighted images produced no enhancement *(arrow).* This structure was diagnosed on fine-needle aspiration as a hemorrhagic cyst.

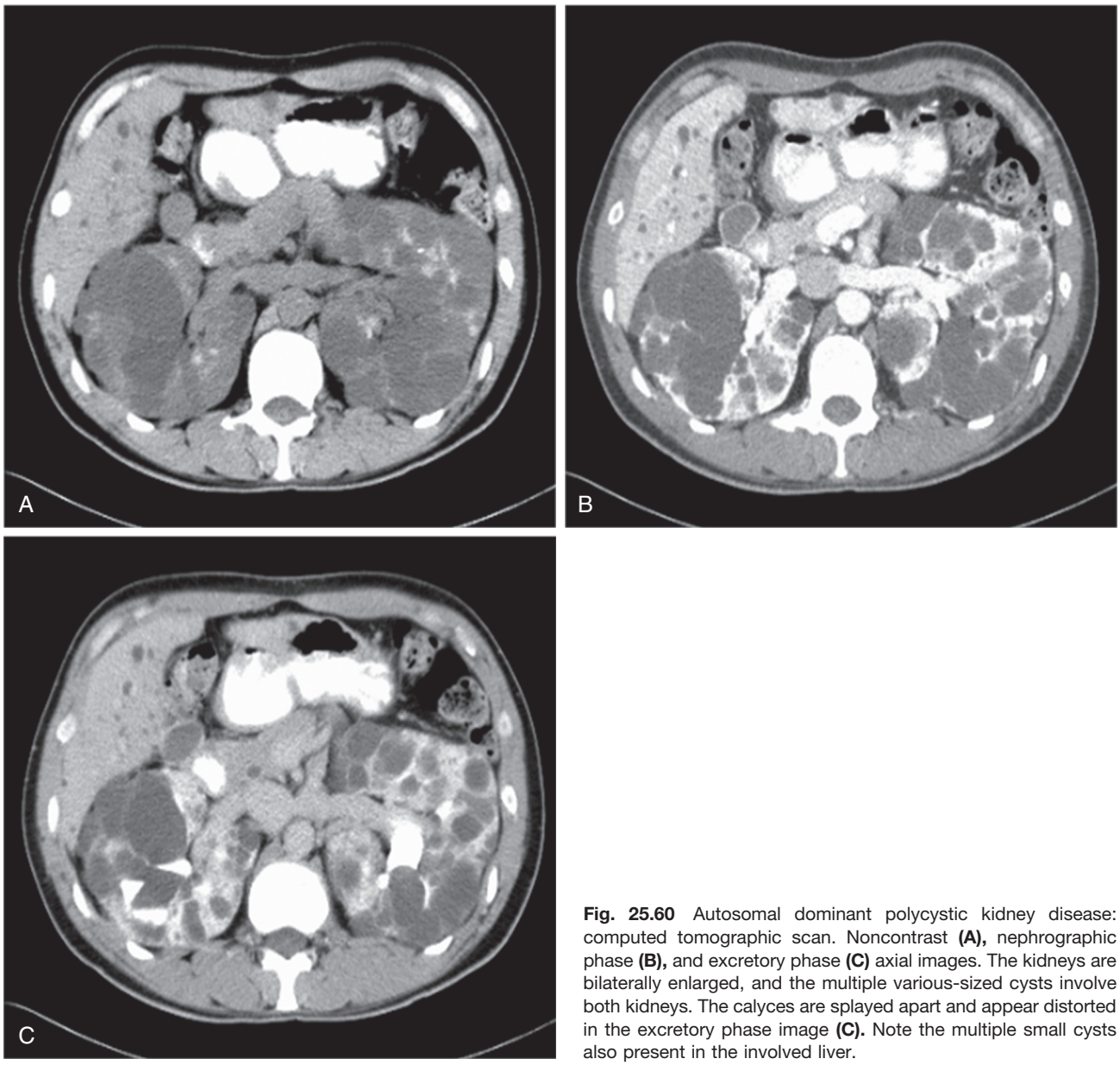

Fig. 25.60 Autosomal dominant polycystic kidney disease: computed tomographic scan. Noncontrast **(A),** nephrographic phase **(B),** and excretory phase **(C)** axial images. The kidneys are bilaterally enlarged, and the multiple various-sized cysts involve both kidneys. The calyces are splayed apart and appear distorted in the excretory phase image **(C).** Note the multiple small cysts also present in the involved liver.

dilation of the distal collecting tubules. The cystic spaces predispose to stasis, which leads to stone formation and potential infection. Involvement is usually bilateral, although not always symmetric, with as few as one calyx involved. The kidneys are typically normal sized with an appearance of medullary nephrocalcinosis when small stones are present.[165] IVU reveals linear or round collections of contrast material extending from the calyceal border, forming parallel brush-like striations. With more severe involvement, the cystic dilations may appear grape-like or bead-like. CT is an excellent method for demonstrating the calculi, although the striations or cystic dilation may be difficult to visualize even with thin-section excretory phase imaging.

Multicystic dysplastic kidney is an uncommon, congenital, nonhereditary condition. It is usually unilateral and affects the entire kidney. In rare cases only a portion of the kidney is involved. US reveals multiple anechoic cystic structures of varying size replacing the kidney, with no normal parenchyma. Calcification in the wall of the cystic spaces may be visible. CT demonstrates multiple fluid-filled structures filling the renal fossa. Septa and some rim-like calcifications may be visible. The density of the fluid is usually the same as or slightly higher than water. The kidney does not enhance after the injection of intravenous contrast material, and the renal artery on the affected side is not visible. It may be difficult to differentiate this condition from severe hydronephrosis if no cyst walls or septa are visible.

Small cortical cysts may occur in some hereditary syndromes (e.g., tuberous sclerosis) and in acquired conditions (e.g., lithium nephropathy; Fig. 25.63). These cysts are typically multiple and very small (millimeters). They are viewed best with MRI but may also be viewed on CT if the cysts are slightly larger.[256] Cortical cysts may be larger in hereditary disorders, such as von Hippel–Lindau disease (Fig. 25.64).[257] Pyelogenic cysts or calyceal diverticula are small cystic structures that connect with a portion of the pelvicalyceal system. On contrast

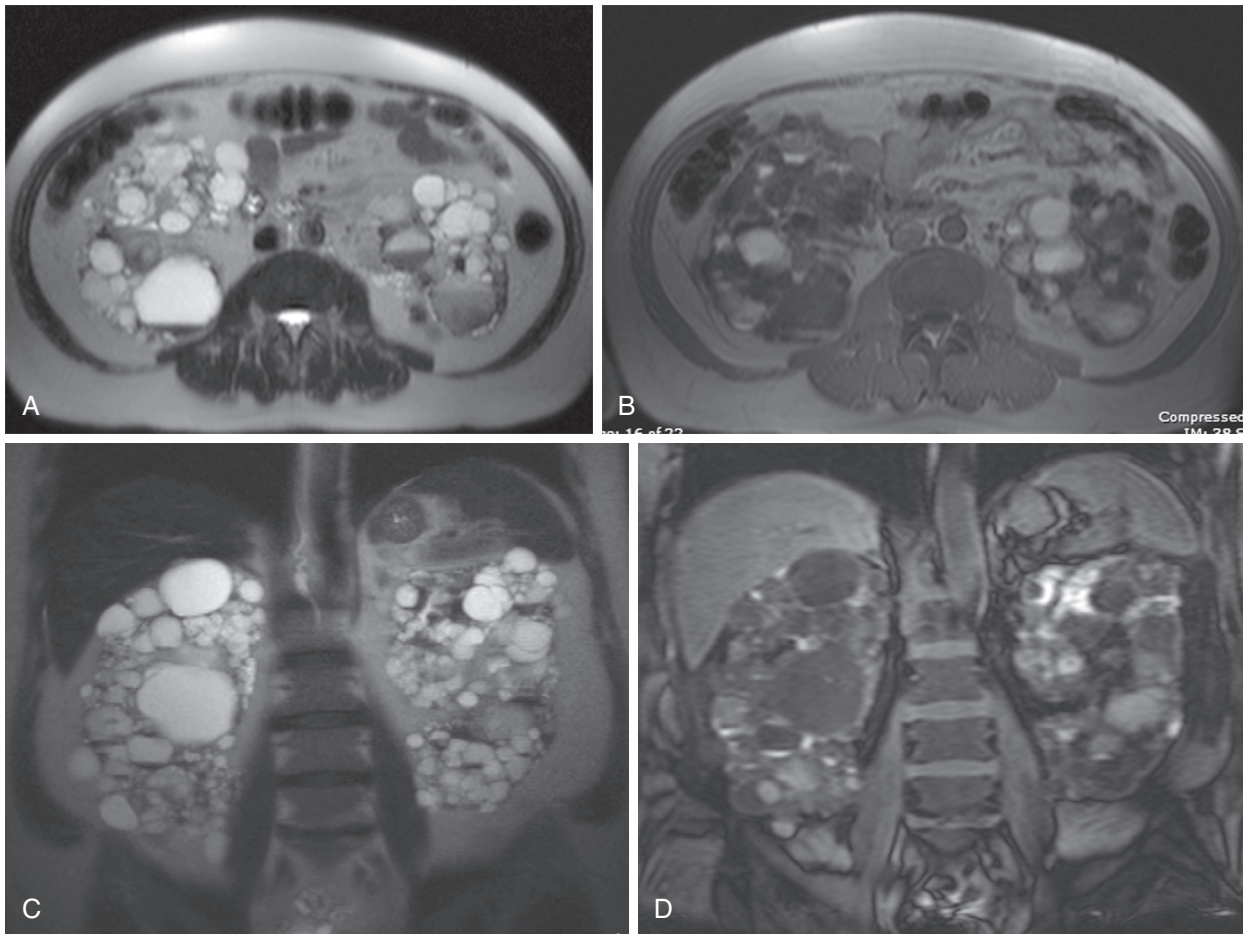

Fig. 25.61 Autosomal dominant polycystic kidney disease. Axial **(A)** and coronal **(C)** T2-weighted images show bilateral renal cortical atrophy and multiple cysts, most of which are bright. Axial T1-weighted image **(B)** shows multiple bright and dark structures that are not enhanced after gadolinium injection; this appearance was confirmed with subtraction image **(D)** and is therefore consistent with cysts.

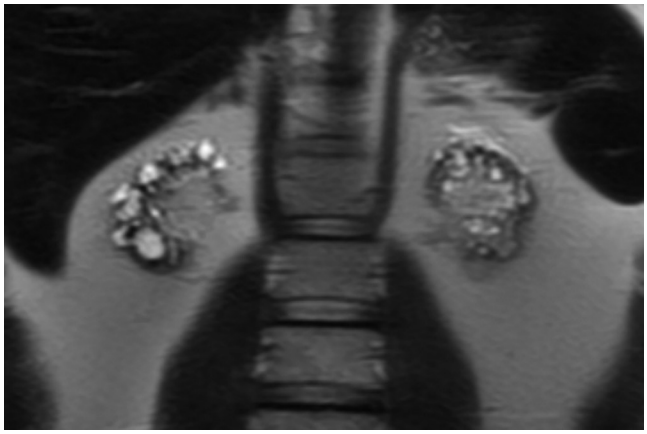

Fig. 25.62 End-stage kidney disease. T2-weighted coronal image shows diffuse atrophy and multiple acquired cysts in a patient on chronic dialysis.

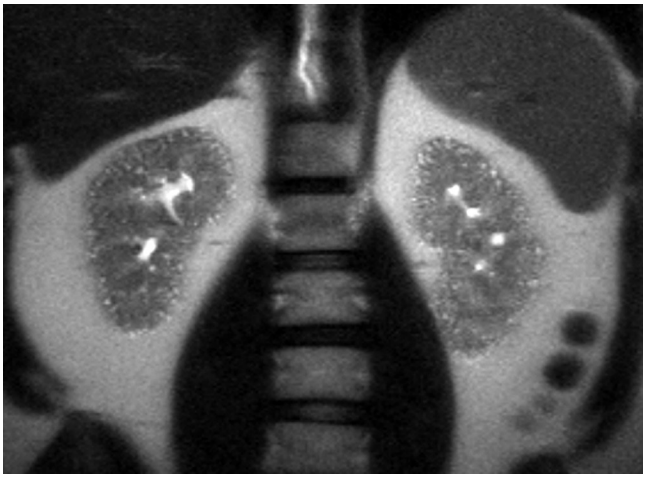

Fig. 25.63 Lithium toxicity. Coronal T2-weighted image demonstrates innumerable small renal cortical cysts, characteristic of lithium toxicity.

material-enhanced studies a calyceal diverticulum appears as a small round or oval collection of contrast material connected to the fornix of the calyx. As stasis occurs within the diverticulum, renal stone formation may occur.

Cystic renal masses present a diagnostic problem in that not all are benign.[258] In 1986, Bosniak developed a classification system based on CT imaging characteristics to help guide the clinical management of cystic renal masses.[256–263] Category I lesions are simple, benign cysts (see Fig. 25.56). Category II cysts are benign with thin septa, fine rim-like calcification, or they are uniform high-density cysts less than 3 cm in diameter that do not enhance (Fig. 25.65). Category IIF represents more

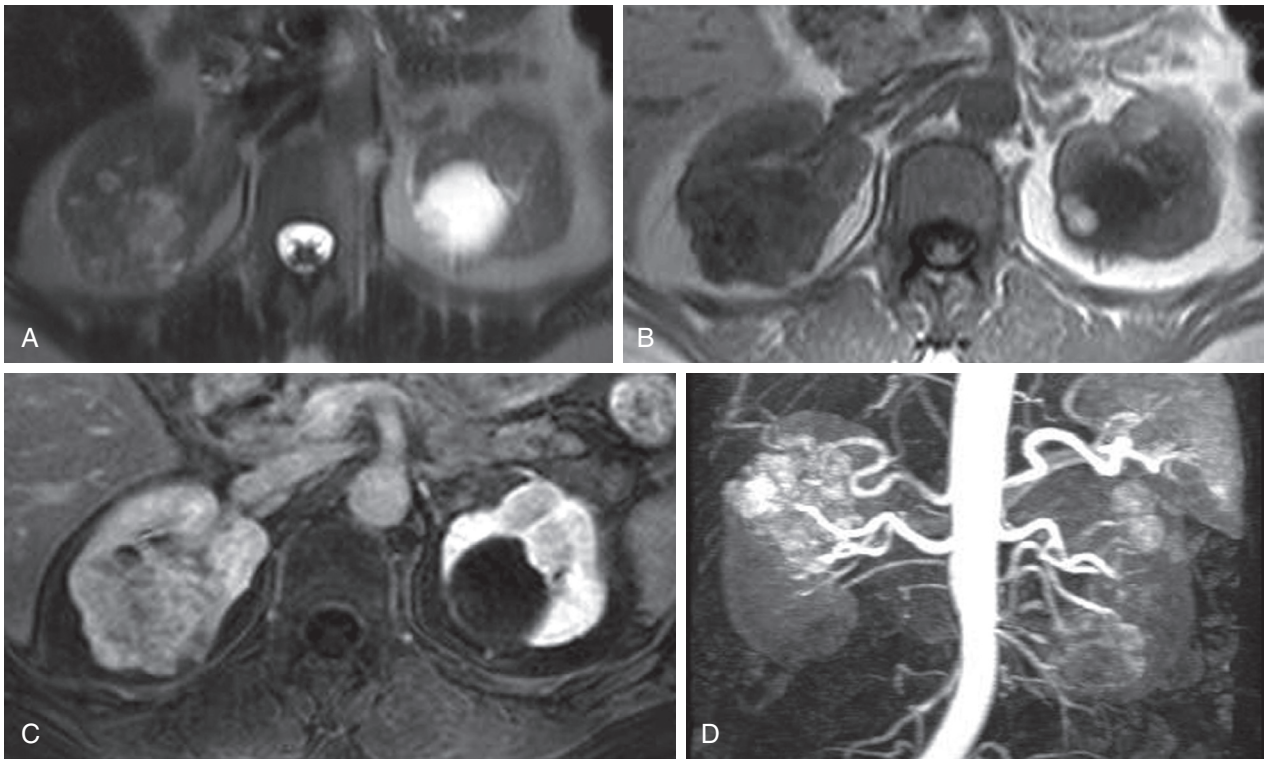

Fig. 25.64 Bilateral clear cell carcinoma in von Hippel-Lindau syndrome. Bilateral heterogeneous renal masses and left renal cyst are visible on T2-weighted image **(A)** and T1-weighted image **(B)**. **C,** The larger right renal mass demonstrates heterogeneous enhancement, and two smaller left renal masses demonstrate more homogeneous enhancement. **D,** Maximum-intensity projection depicts the multiple renal masses in angiographic format.

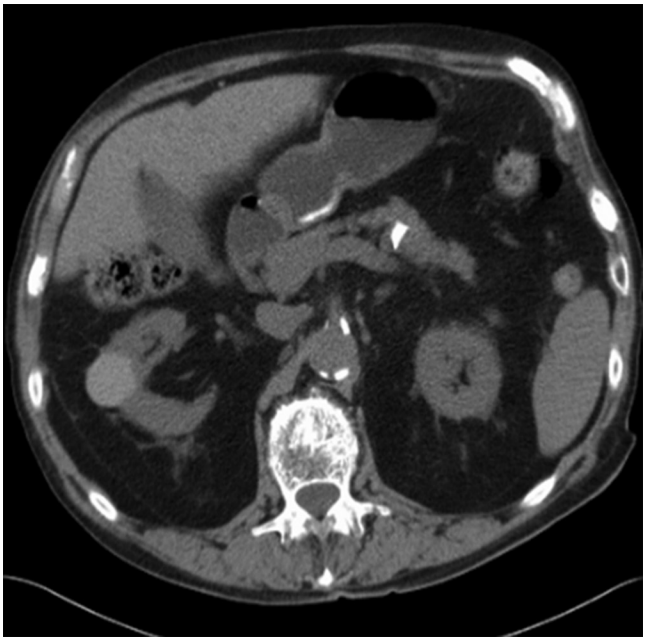

Fig. 25.65 Hyperdense renal cyst: computed tomographic scan, axial noncontrast image. A single well-circumscribed hyperdense mass is visible in the right kidney. This represents a Bosniak category II renal cyst. It is sharply defined and less than 3 cm in diameter, and it will demonstrate no enhancement on the contrast material-enhanced scan.

indeterminate category II lesions that necessitate follow-up, usually at 6 to 12 months, to prove benignity (Fig. 25.66).[262] These cystic lesions may have multiple septa, or an area of thick or nodular calcification, or they may be high-density cysts larger than 3 cm in diameter. Category III cystic lesions have thickened, irregular walls, which demonstrate some enhancement. Dense irregular calcification may also be visible. In these cases, clinical history may be helpful in determining whether they are renal abscesses or infected cysts. Although some of these lesions are benign, surgery may be necessary for diagnosis and treatment.[263] Biopsy has been advocated by some authorities.[264–267] Category IV cystic masses are clearly malignant and demonstrate distinct enhanced soft tissue masses or nodules within the cyst (Fig. 25.67).[268] Nephrectomy is required for these lesions, although if they are not larger than 5 to 6 cm and are in proper locations, a nephron-sparing procedure may be performed. Cystic diseases of the kidney are further discussed in Chapter 45.

CE-CT is the imaging modality of choice for the characterization of all solid masses, suspected solid masses, or masses that do not meet US criteria for a true renal cyst.[259,266,269] MRI has sensitivities and specificities similar to those of CT but is generally reserved for cases in which the patient has a contraindication to iodinated contrast medium or in which radiation dose must be limited. MRI may be helpful in cases of renal masses for which CT yielded indeterminate findings, in cases with venous involvement, and in distinguishing vessels from retroperitoneal lymph nodes. CEUS is now an additional technique that can be used especially in patients with compromised renal function (Fig. 25.68).

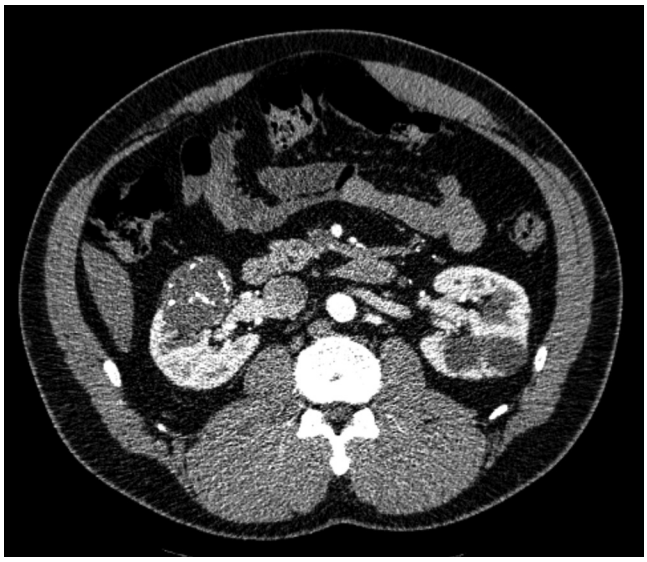

Fig. 25.66 Bosniak category IIF renal cyst: computed tomographic (CT) scan, axial nephrographic phase image. A cystic lesion in the right kidney also demonstrates large clumps of calcification on the outer wall and on internal septa. There was no change in the CT numbers between the noncontrast scan and the enhanced images. This cyst necessitates follow-up. Note the Bosniak category I cysts in the left kidney.

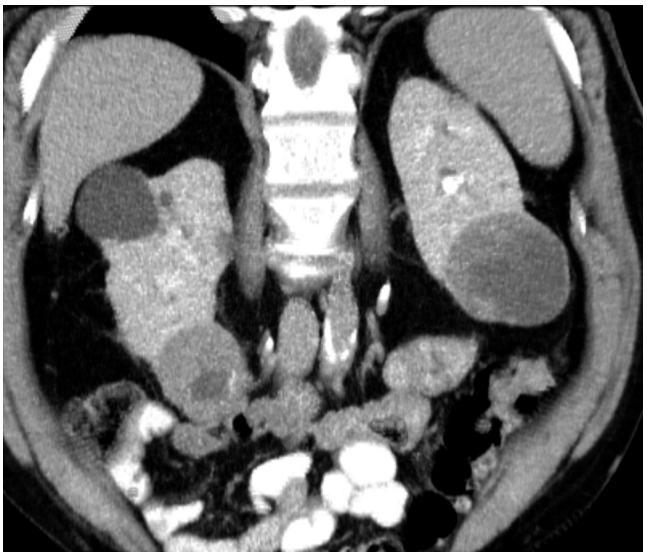

Fig. 25.67 Bosniak category IV left renal cyst: computed tomographic scan, coronal nephrographic phase image. A cystic mass is visible in the left kidney with an internal solid component in the lower pole. In the lower pole of the right kidney, there is a solid mass with central necrosis, which represents a renal cell carcinoma. Note the Bosniak category I cysts in the upper pole of the right kidney. A renal calculus is also present in the midportion of the left kidney. The left lower pole cystic lesion proved to be a renal cell carcinoma, papillary type.

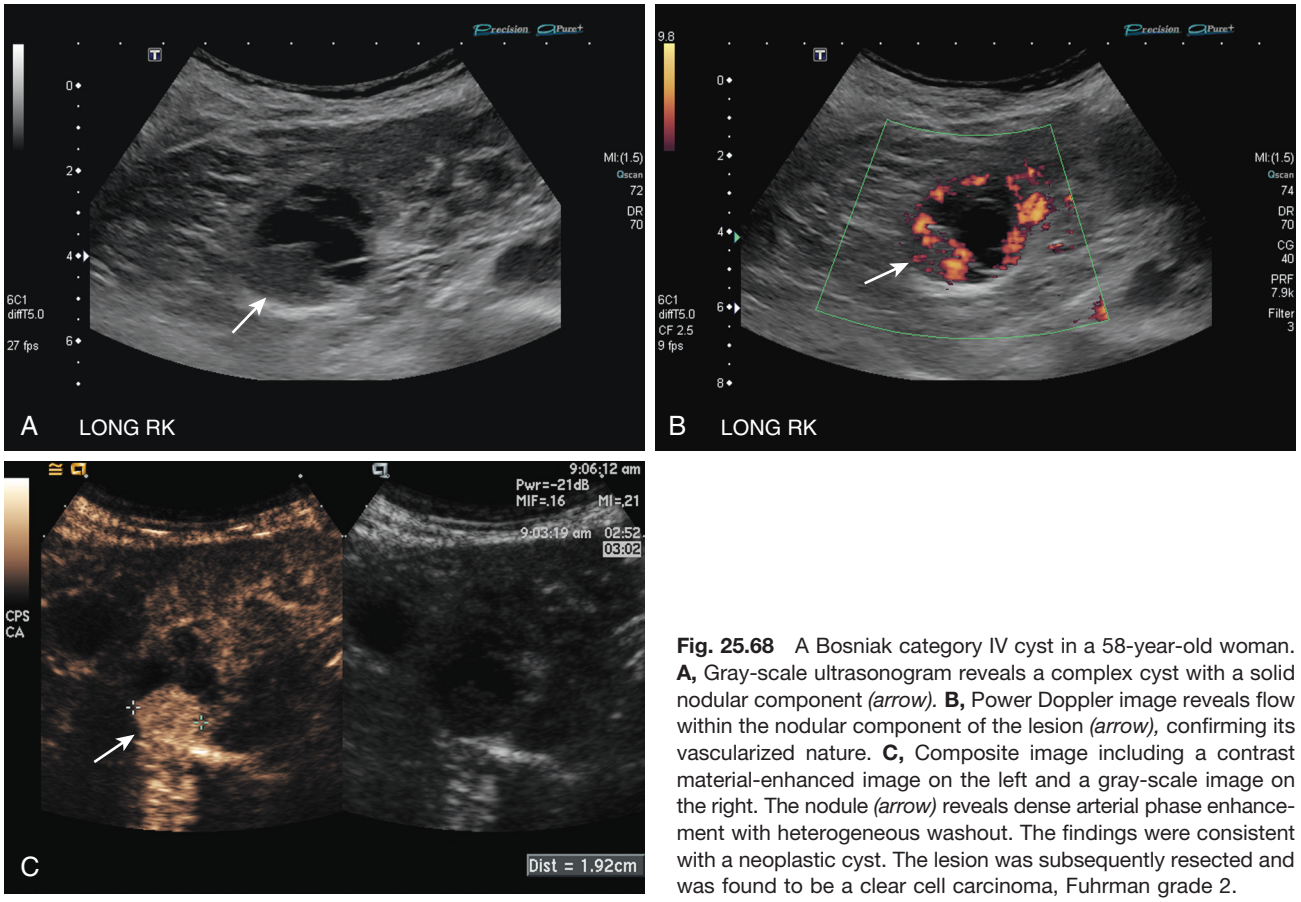

Fig. 25.68 A Bosniak category IV cyst in a 58-year-old woman. **A,** Gray-scale ultrasonogram reveals a complex cyst with a solid nodular component *(arrow).* **B,** Power Doppler image reveals flow within the nodular component of the lesion *(arrow),* confirming its vascularized nature. **C,** Composite image including a contrast material-enhanced image on the left and a gray-scale image on the right. The nodule *(arrow)* reveals dense arterial phase enhancement with heterogeneous washout. The findings were consistent with a neoplastic cyst. The lesion was subsequently resected and was found to be a clear cell carcinoma, Fuhrman grade 2.

Renal neoplasms may arise from either the renal parenchyma or the urothelium of the pelvicalyceal system. With the increased use of cross-sectional imaging techniques, more small neoplasms are discovered incidentally.[270,271] Renal adenoma is the most common benign neoplasm; it almost always is less than 2 to 3 cm in size and has no characteristic radiologic features to distinguish it from other solid tumors. Typically, renal adenomas are corticomedullary in location, appear solid on US, and demonstrate uniform enhancement on CE-CT.

Renal hamartomas, known as angiomyolipomas (AMLs), are benign renal tumors composed of different tissues, including fat, muscle, vascular elements, and even cartilage. It is the fat component that makes AML distinguishable radiologically (Fig. 25.69).[272,273] On US the mass is solid and hyperechoic due to the presence of fat.[274,275] On CT the diagnosis of AML can be made with ease, because most AML have a large amount of fat that exhibits low attenuation (<–10 HU). In uncommon cases, only a minimal amount of fat is present, and it must be searched for diligently.[276–279] MRI with fat-suppressed and opposed-phase chemical shift sequences can be used to make an accurate diagnosis.[280] Signal intensity of fat is high on both T1- and T2-weighted sequences. Macroscopic fat in AML has decreased signal intensity with fat-suppression sequences. Opposed-phase chemical shift sequences cause an "India ink" outline of the tumor at its interface with normal renal parenchyma. The enhancement pattern of AML may be variable, depending on the composition of the lesion. Fat should be searched for in all solid lesions in the kidney; if present, the diagnosis of AML is virtually ensured.[281–283] Most AMLs measuring 4 cm in diameter or smaller are monitored; surgery is reserved for larger ones, especially with hemorrhage.[284,285] Multiple, bilateral AMLs may be found in patients with tuberous sclerosis.

Oncocytoma is an uncommon benign tumor originating in the epithelium of the proximal collecting tubule. Radiologically, its features include a solid mass with homogeneous enhancement, a central stellate scar that may be visible on US, CE-CT, or MRI, and a spoked-wheel pattern on angiography.[286–288] These findings are nonspecific, however, and histologic confirmation is needed.[289,290] Oncocytic renal cell carcinomas also occur, and surgery is generally needed for the correct diagnosis.

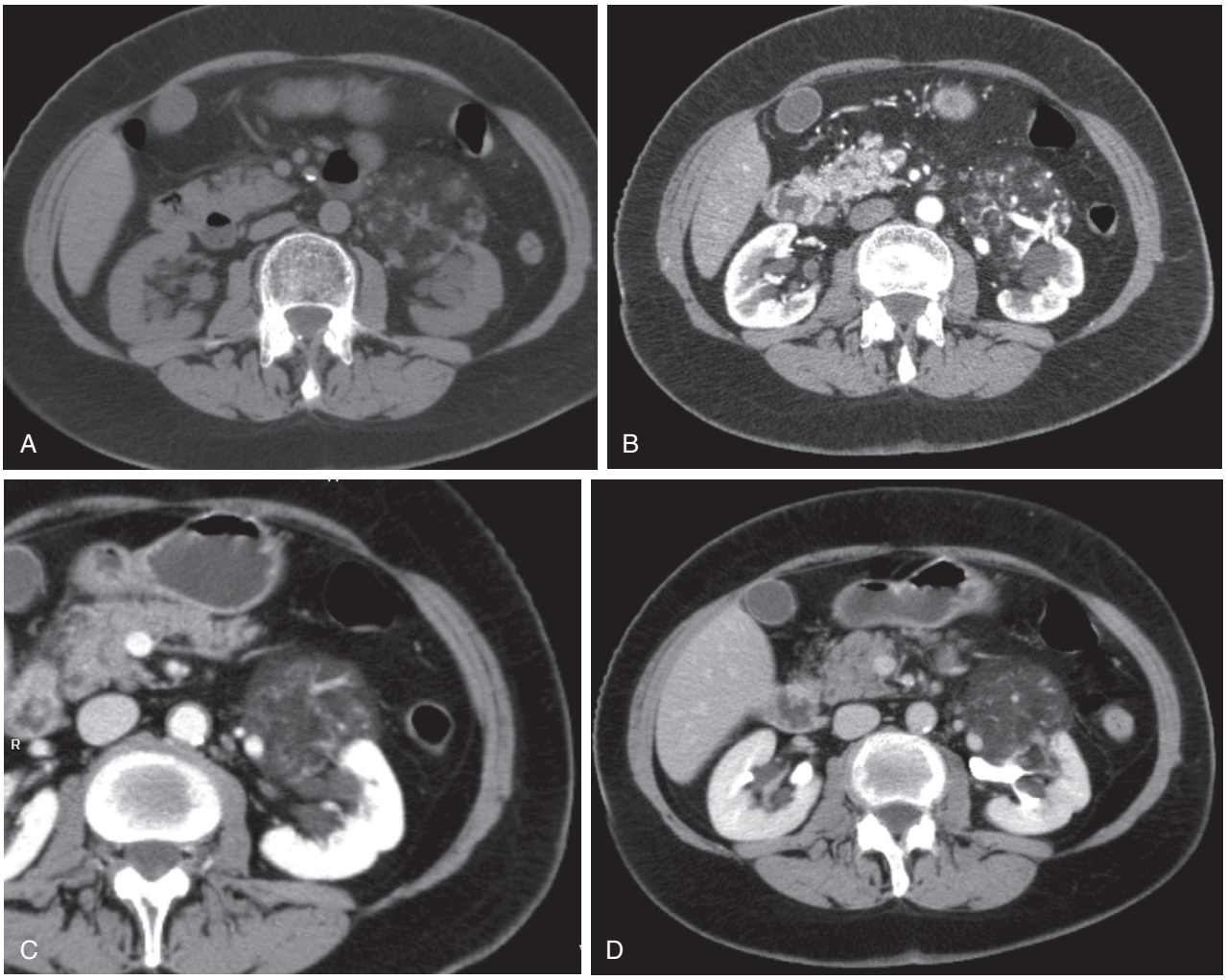

Fig. 25.69 Angiomyolipoma: computed tomographic scan, noncontrast **(A),** corticomedullary phase **(B),** nephrographic phase **(C),** and excretory phase **(D)** axial images. The fat-containing mass is visible projecting anteriorly from the left kidney. The internal structure in this very vascular benign tumor demonstrates enhancement.

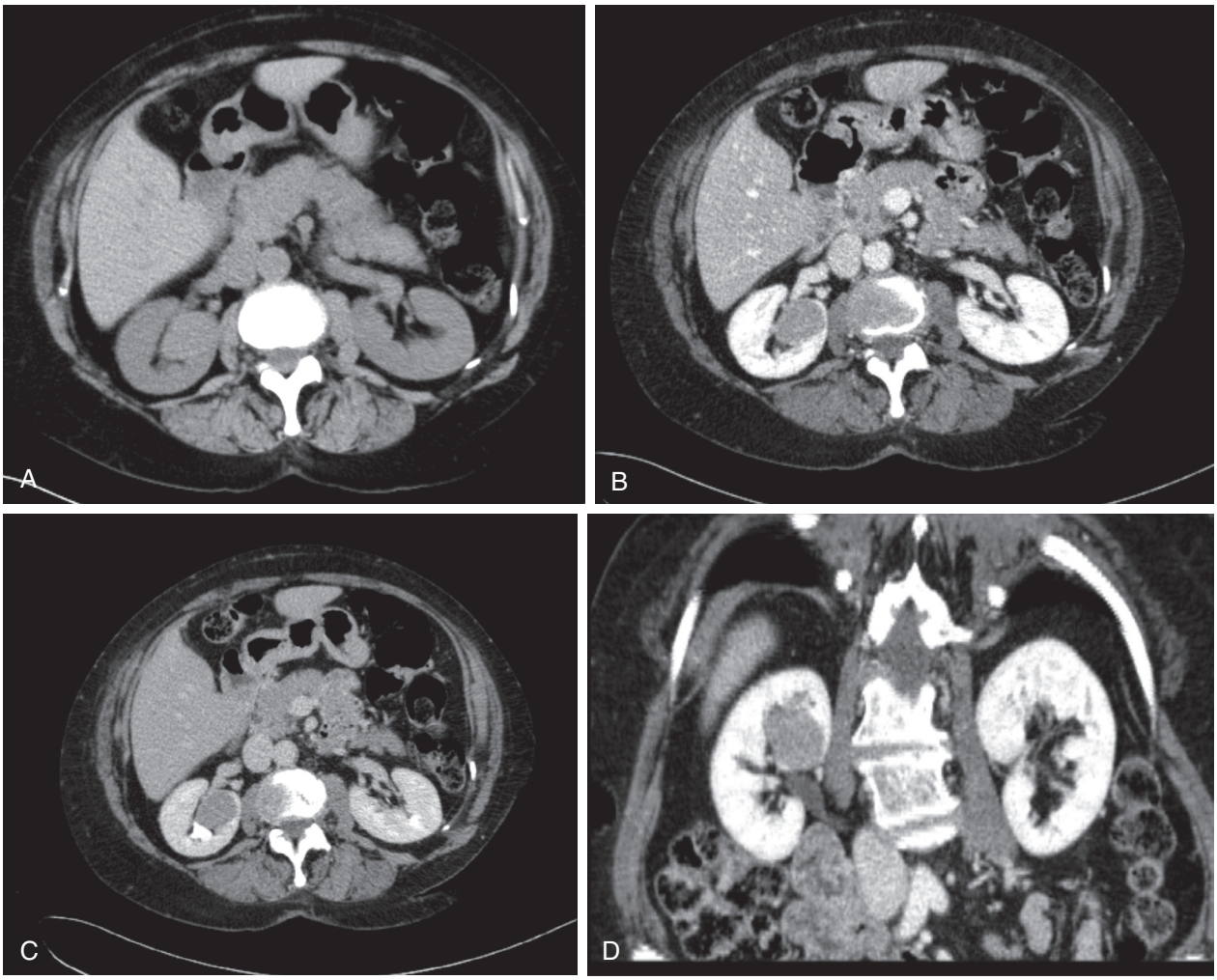

Fig. 25.70 Renal cell carcinoma: computed tomographic scan. Noncontrast **(A),** nephrographic phase **(B),** and excretory phase **(C)** axial images combined with a coronal nephrographic phase image **(D).** On the noncontrast scan **(A),** the right renal mass appears slightly hyperdense in relation to the rest of the kidney. Contrast material-enhanced scans (**B, C,** and **D**) show the enhanced structure surrounded by the normal renal parenchyma. This proved to be a renal cell carcinoma, chromophobe type.

Renal cell carcinoma is the third most common tumor of the genitourinary tract after carcinoma of the prostate and bladder. CE-CT is the modality of choice for imaging renal cell carcinoma because it has proved to be effective in detection, diagnosis, characterization, and staging, with accuracy exceeding 90%.[291,292] On noncontrast CT, renal cell carcinoma appears as an ill-defined area in the kidney with HU close to that of the renal parenchyma (Fig. 25.70). After the injection of intravenous contrast material, most renal cell carcinomas show enhancement. The best phase for depiction of the mass is the nephrographic phase (see Fig. 25.70).[293–295] The corticomedullary phase is most helpful for showing the relationship of the tumor to the vascular structures because there is maximal enhancement of the arteries and veins (Fig. 25.71).[296,297] The excretory phase is most helpful for showing the relationship of the tumor to the pelvicalyceal system and in preoperative planning for nephron-sparing partial nephrectomy (see Fig. 25.70).[298,299] Clear cell renal cell carcinoma tends to have greater and more heterogenous enhancement than the papillary types (see Figs. 25.64, 25.71, 25.72, and 25.73).[300,301] Chromophobe tumors typically have a homogeneous enhancement pattern

Fig. 25.71 Renal cell carcinoma: computed tomographic scan. Contrast material-enhanced axial image in the corticomedullary phase. Note the heterogeneously enhanced mass in the anterior aspect of the left kidney. This is a stage II renal cell carcinoma, inasmuch as it has extended through the renal capsule into Gerota's fascia. This proved to be a renal cell carcinoma, clear cell type.

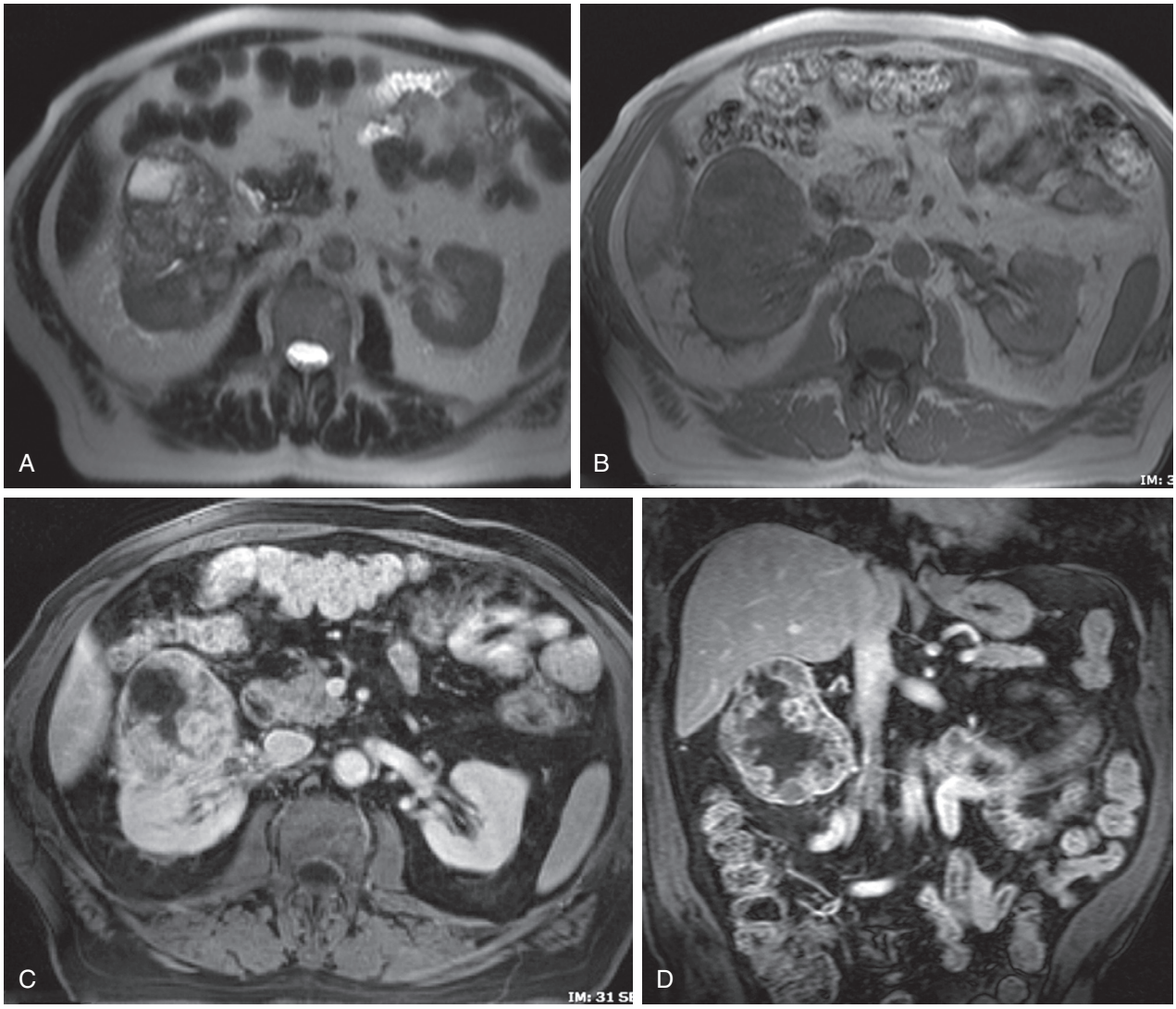

Fig. 25.72 Clear cell renal cell carcinoma, stage IIIA. **A,** Axial T2-weighted image shows a 7.5-cm right renal mass with areas of high signal intensity, consistent with necrosis and cystic degeneration. **B,** Axial T1-weighted image shows a heterogeneous, isointense mass with increased perinephric fat stranding. Axial **(C)** and coronal **(D)** gadolinium-enhanced images confirm central areas of necrosis. No venous invasion is visible. Focal microinvasion of the perinephric fat was found at surgery.

(see Fig. 25.70).[300] Chromophobe and papillary types more often contain calcification than does the clear cell type, and they demonstrate only mild enhancement of 25 to 30 HU.[302]

The appearance of renal cell carcinoma on MRI can vary with the histologic type. For example, the clear cell type tends to be larger and is associated more frequently with hemorrhage and necrosis (Figs. 25.72 and 25.73) than is the papillary type (Fig. 25.74) and chromophobe renal cell carcinoma. The feasibility of differentiating histologic types of renal cell carcinoma by means of advanced MRI techniques such as diffusion weighting is being evaluated, but further research is required.[303] Renal cell carcinoma is most commonly heterogeneously hyperintense on T2-weighted sequences and hypointense to isointense on T1-weighted sequences (Fig. 25.75). Renal cell carcinoma enhances less than normal renal cortex tissue. The heterogeneity increases with increasing size as a result of variable amounts of necrosis and intraluminal lipid. The intraluminal lipid may make areas of the mass drop in signal intensity on opposed-phase T1-weighted sequences.

The staging of renal cell carcinoma is important in predicting survival rates and planning the proper surgical approach to the mass. Both the World Health Organization and the Robson classifications are used in the staging of renal cell carcinoma.[291] In the Robson classification of renal cell carcinoma, a stage I tumor is confined to the renal parenchyma by the renal capsule (see Figs. 25.70, 25.74, and 25.75). In stage II renal cell carcinoma, the tumor extends through the renal capsule into the perinephric fat but is still within Gerota's fascia (see Fig. 25.71 and Fig. 25.64). Stage III lesions are subdivided: IIIA tumors extend into the renal vein or IVC (Fig. 25.73 and Fig. 25.76); IIIB tumors involve regional retroperitoneal lymph nodes; and IIIC tumors involve the veins and nodes. In stage IVA renal cell carcinoma, the tumor extends outside Gerota's fascia with involvement of adjacent organs or muscles other than the ipsilateral adrenal gland

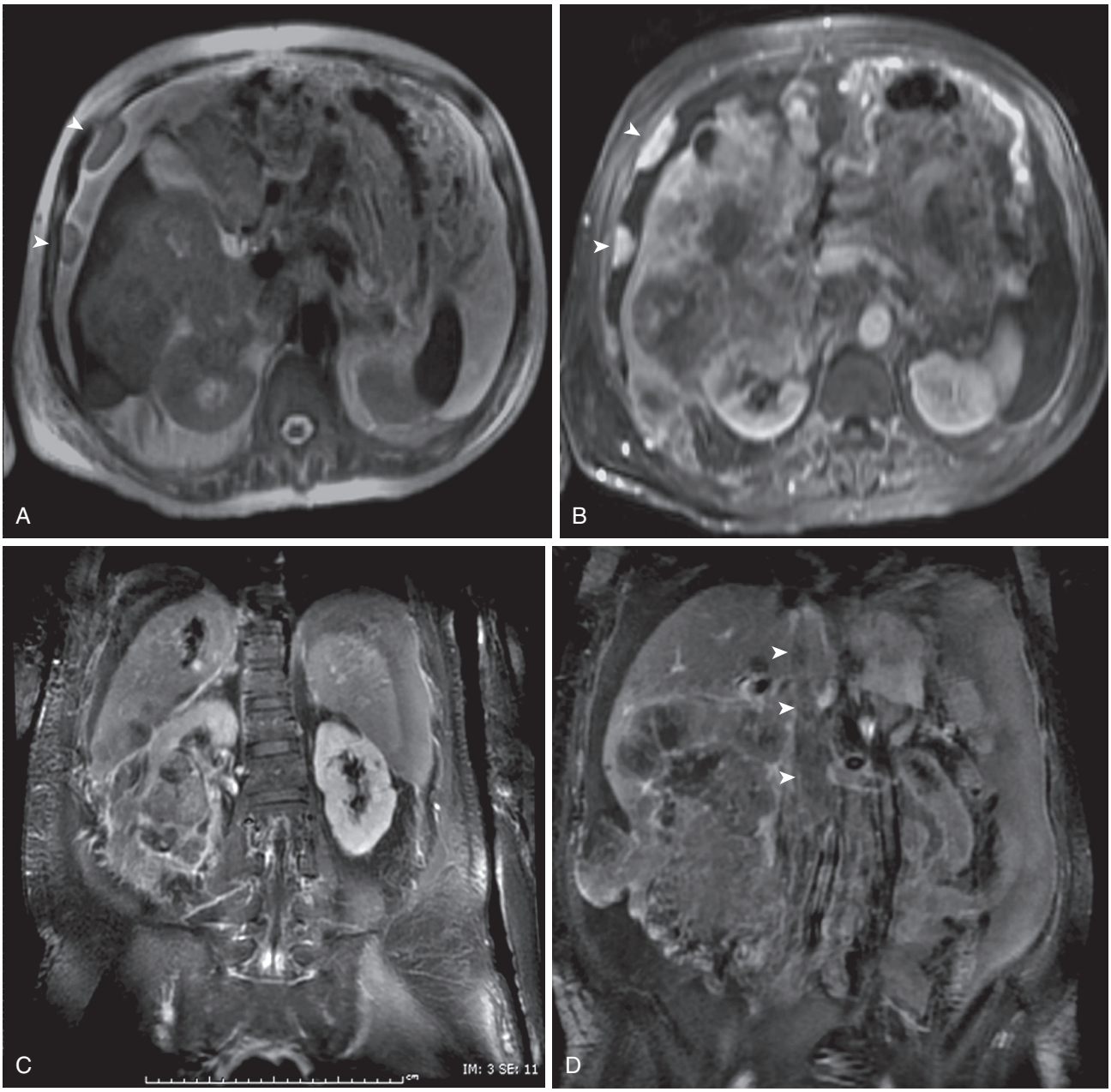

Fig. 25.73 Metastatic clear cell renal cell carcinoma, stage IV. T2-weighted **(A)** and gadolinium-enhanced T1-weighted **(B)** axial images show a large, heterogeneous mass with invasion of the adjacent liver and peritoneal metastases *(arrowheads).* **C** and **D,** Coronal gadolinium-enhanced T1-weighted images show the large mass extending inferiorly and medially, with invasion of the inferior vena cava to the level of the hepatic veins *(arrowheads).*

(see Fig. 25.77). Stage IVB renal cell carcinoma represents tumor with distant metastases, the most common sites being the lungs, mediastinum, liver, and bone. Kidney cancer is further discussed in Chapter 41.

MRI has been found to be highly accurate in staging renal cell carcinoma; however, as with CT, the areas of greatest challenge remain the evaluation for local invasion of the perinephric fat and direct invasion of adjacent organs, especially with large tumors.[304] The presence of an intact pseudocapsule aids in ruling out local invasion. A pseudocapsule is a hypointense rim around the tumor, viewed best on T2-weighted images (see Fig. 25.75A) and most frequently observed in association with small or slow-growing tumors. When the tumor extends beyond the confines of the kidney, the pseudocapsule is made of fibrous tissue; otherwise it is made up of compressed normal renal tissue.[305] If the pseudocapsule is intact, the perinephric fat is unlikely to have been invaded.[305]

Detecting and assessing vascular thrombosis in patients with renal cell carcinoma is highly accurate and reliable with MRI.[304,306] Coronal imaging in the venous and delayed phases demonstrates the presence or absence of venous invasion, determines the extent of venous invasion, if present, and differentiates enhancing intravascular tumor from nonenhanced bland thrombus (Fig. 25.77). Accurate determination of renal vein, IVC, and right atrial involvement is important for deciding the surgical approach.[307]

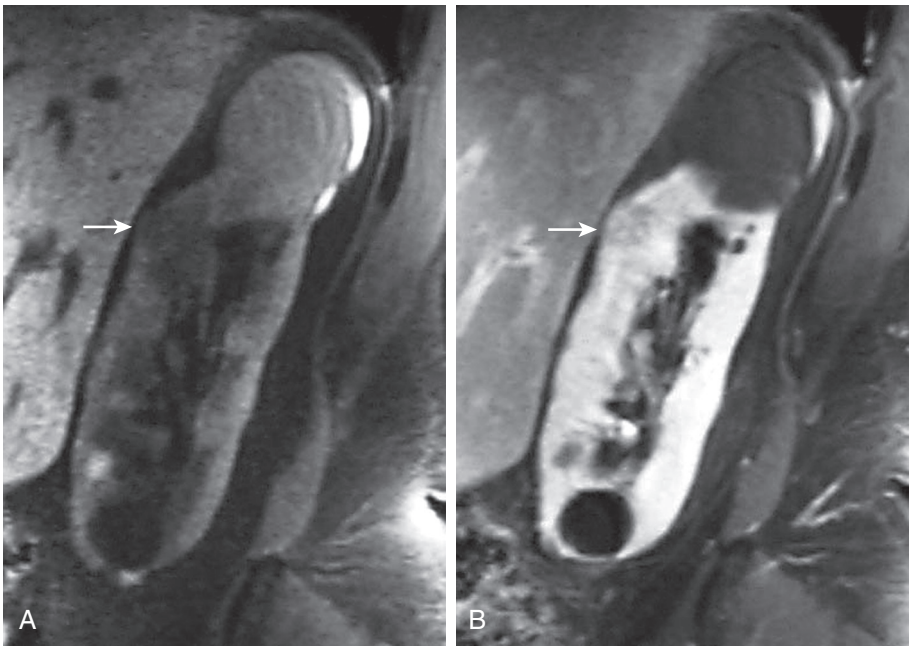

Fig. 25.74 Papillary renal cell carcinoma, stage I. Sagittal T1-weighted images before *(arrow)* **(A)** and after **(B)** the administration of gadolinium show a subtle mass *(arrow)* in the anterior cortex and multiple nonenhanced cysts. No perinephric invasion was found at surgery.

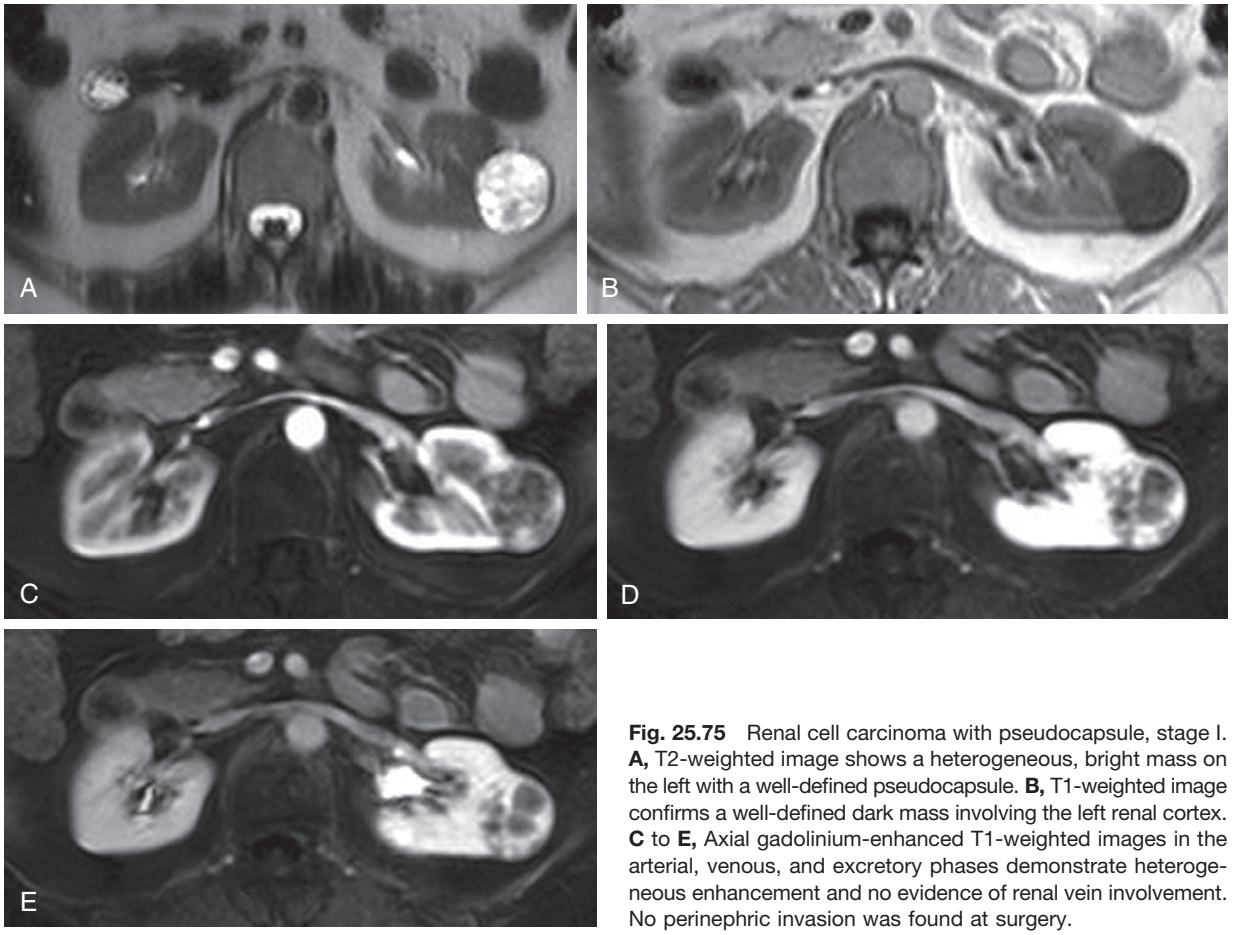

Fig. 25.75 Renal cell carcinoma with pseudocapsule, stage I. **A,** T2-weighted image shows a heterogeneous, bright mass on the left with a well-defined pseudocapsule. **B,** T1-weighted image confirms a well-defined dark mass involving the left renal cortex. **C** to **E,** Axial gadolinium-enhanced T1-weighted images in the arterial, venous, and excretory phases demonstrate heterogeneous enhancement and no evidence of renal vein involvement. No perinephric invasion was found at surgery.

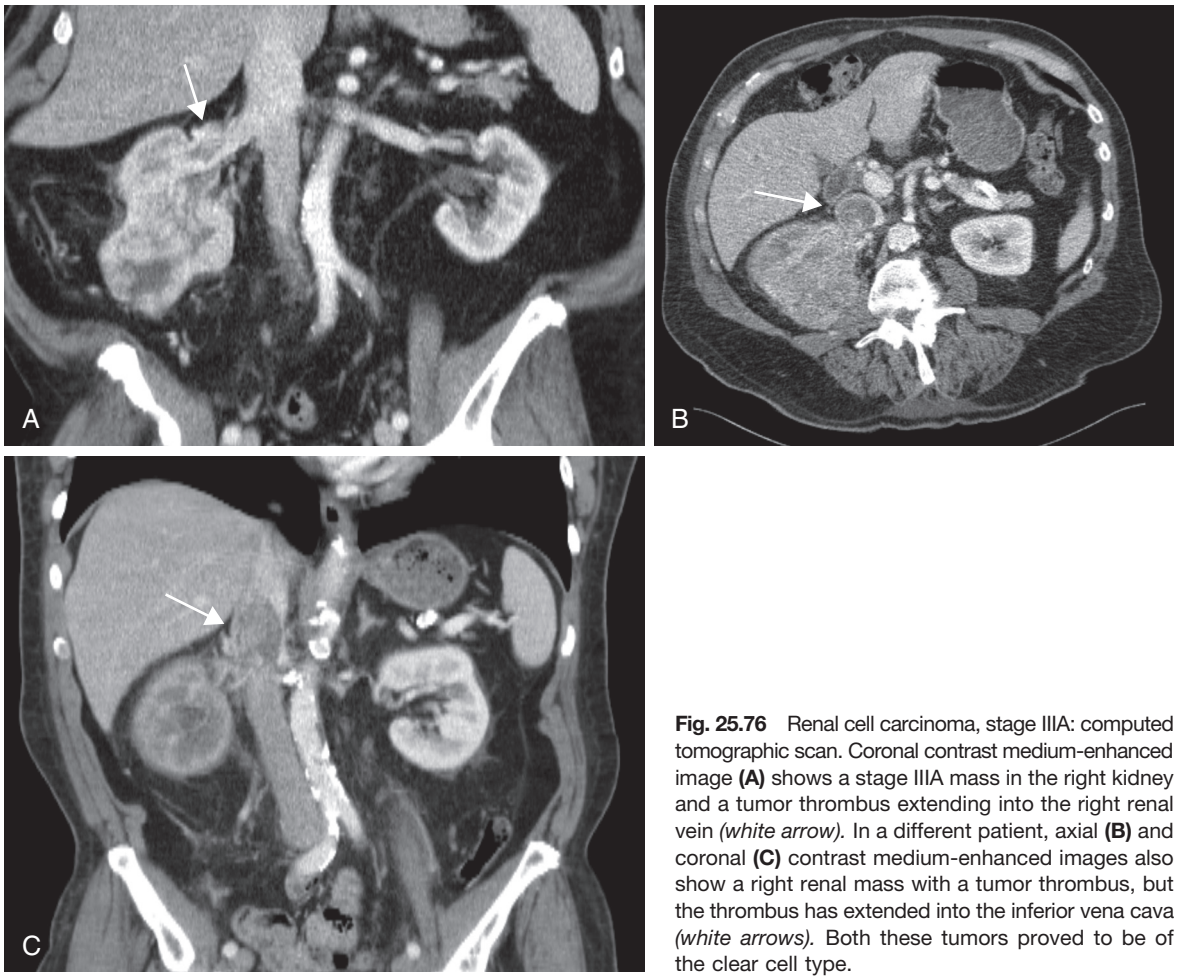

Fig. 25.76 Renal cell carcinoma, stage IIIA: computed tomographic scan. Coronal contrast medium-enhanced image **(A)** shows a stage IIIA mass in the right kidney and a tumor thrombus extending into the right renal vein *(white arrow).* In a different patient, axial **(B)** and coronal **(C)** contrast medium-enhanced images also show a right renal mass with a tumor thrombus, but the thrombus has extended into the inferior vena cava *(white arrows).* Both these tumors proved to be of the clear cell type.

Although renal cell carcinoma is the most common primary malignancy in the kidney, transitional cell carcinoma also occurs within the kidneys.[308] Most transitional cell carcinomas involve the urothelium and project into the lumen of the renal pelvis or ureter. As a result, IVU images show a filling defect within the renal pelvis or ureter that can be confused with a renal stone, blood clot, or debris (Fig. 25.78). Transitional cell carcinoma of the bladder is much more common than that of the kidney or ureter.[309] The neoplasm may extend into the renal parenchyma and, on imaging, appears as a mass within the kidney. The imaging findings are similar to those of renal cell carcinoma, except the lesions tend not to enhance as much on postcontrast imaging. Renal vein involvement is rare. CTU and MRU show similar findings; transitional cell carcinoma in the upper collecting system can be either a focal or irregular mass within the collecting system (Fig. 25.79) or an ill-defined mass infiltrating the renal parenchyma. When small, they may be difficult to identify on both CT and MRI. Evaluation of the entire collecting system is required because synchronous lesions may be present. Both CTU and MRU are valuable for complete evaluation of the collecting system; however, retrograde pyelography with ureteroscopy and biopsy will make the diagnosis.

Lymphoma may involve the kidney as part of multiorgan involvement or, in rare cases, as a primary neoplasm.[310] Lymphoma may be solitary or multifocal, within one or both kidneys. Perirenal extension may be visible as well. An infiltrative picture with lymphomatous replacement of the kidney may also be observed. This form is usually accompanied by adjacent retroperitoneal adenopathy. CE-CT is the imaging method of choice in these patients. MRI findings are similar to those on CE-CT. Lymphoma typically appears hypointense on T1-weighted sequences and heterogeneous to slightly hypointense on T2-weighted sequences. Enhancement is minimal on postcontrast sequences[311] (Fig. 25.80). Vessels are usually encased, not invaded, and necrosis is usually not observed. Treated lymphoma may vary in signal intensity, as a result of the effects of therapy.[311]

Metastatic disease may also involve the kidney. Metastases are most commonly hematogenous and usually result in multiple foci of involvement, although single lesions do occur (Fig. 25.81). They are observed most frequently with CE-CT, inasmuch as CT is used in the regular follow-up of most patients with cancer. Hypodense round masses, usually in the periphery, are the typical finding. When present as a single lesion, a metastasis cannot be differentiated from a primary renal neoplasm without biopsy.

RENAL CANCER: POSITRON EMISSION TOMOGRAPHY AND POSITRON EMISSION TOMOGRAPHY-COMPUTED TOMOGRAPHY

Preliminary studies of PET imaging of renal cell carcinoma have revealed a promising role in the evaluation of

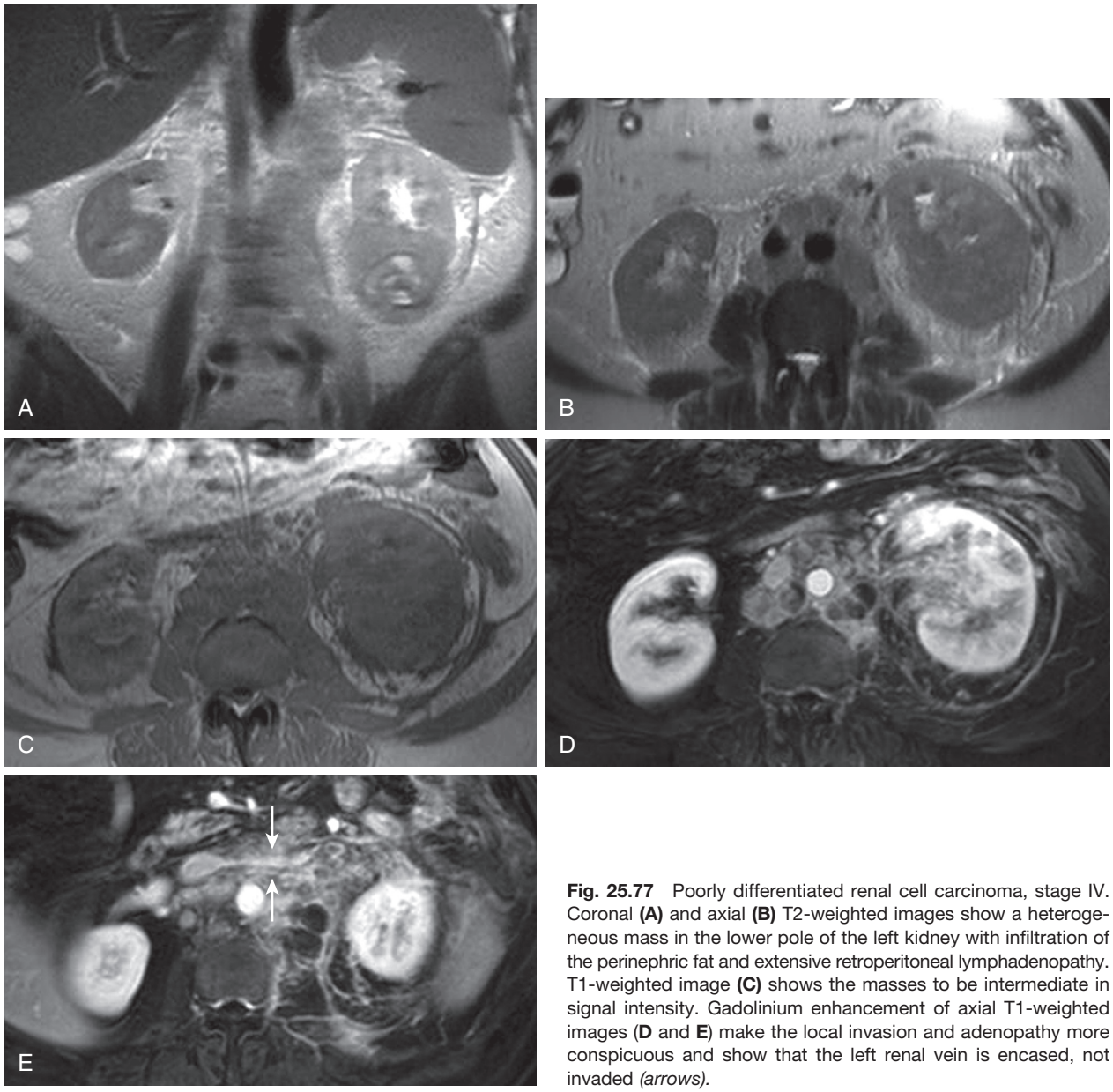

Fig. 25.77 Poorly differentiated renal cell carcinoma, stage IV. Coronal **(A)** and axial **(B)** T2-weighted images show a heterogeneous mass in the lower pole of the left kidney with infiltration of the perinephric fat and extensive retroperitoneal lymphadenopathy. T1-weighted image **(C)** shows the masses to be intermediate in signal intensity. Gadolinium enhancement of axial T1-weighted images (**D** and **E**) make the local invasion and adenopathy more conspicuous and show that the left renal vein is encased, not invaded *(arrows).*

indeterminate renal masses, preoperative staging and assessment of tumor burden, detection of osseous and nonosseous metastases (including vascular invasion), restaging after therapy, treatment evaluation, and the determination of effect of imaging findings on clinical management.[312–324] However, other PET studies have demonstrated less encouraging results and no advantage over standard imaging methods.[325–327]

A relatively high false-negative rate (23%) has been reported with FDG-PET in the preoperative staging of renal cell carcinoma in comparison with histologic analysis of surgical specimens.

Clinical Relevance
Sensitivity for PET scan for detection of renal cancer and metastases is lower than CT, as the lesions may be identified on CT before they can be seen as hypermetabolic foci on PET.

In one study, PET exhibited 60% sensitivity (vs. 91.7% for CT) and 100% specificity (vs. 100% for CT) for primary renal cell carcinoma tumors. For retroperitoneal lymph node metastases or renal bed recurrence, PET had 75.0% sensitivity (vs. 92.6% for CT) and 100% specificity (vs. 98.1% for CT). For metastases to the lung parenchyma, PET had 75% sensitivity (vs. 91.1% for chest CT) and 97.1% specificity (vs. 73.1% for chest CT). For bone metastases, PET had 77.3% sensitivity and 100% specificity (in comparison with 93.8% and 87.2% for combined CT and bone scan).[328] For restaging renal cell carcinoma, 87% sensitivity and 100% specificity have been reported.[329] A comparative investigation of bone scan and FDG-PET for detecting osseous metastases in renal cell carcinoma revealed that PET had 100% sensitivity (vs. 77.5% for bone scan) and 100% specificity (vs. 59.6% for bone scan).[317] Another report revealed a negative predictive value of 33% and a positive predictive value of 94% for restaging renal cell carcinoma.[313] Other studies have

Fig. 25.78 Transitional cell carcinoma: intravenous urogram. The irregular filling defect in the left renal pelvis represents a transitional cell carcinoma. Note that there is no significant obstruction of the left kidney, and the calyces appear normal.

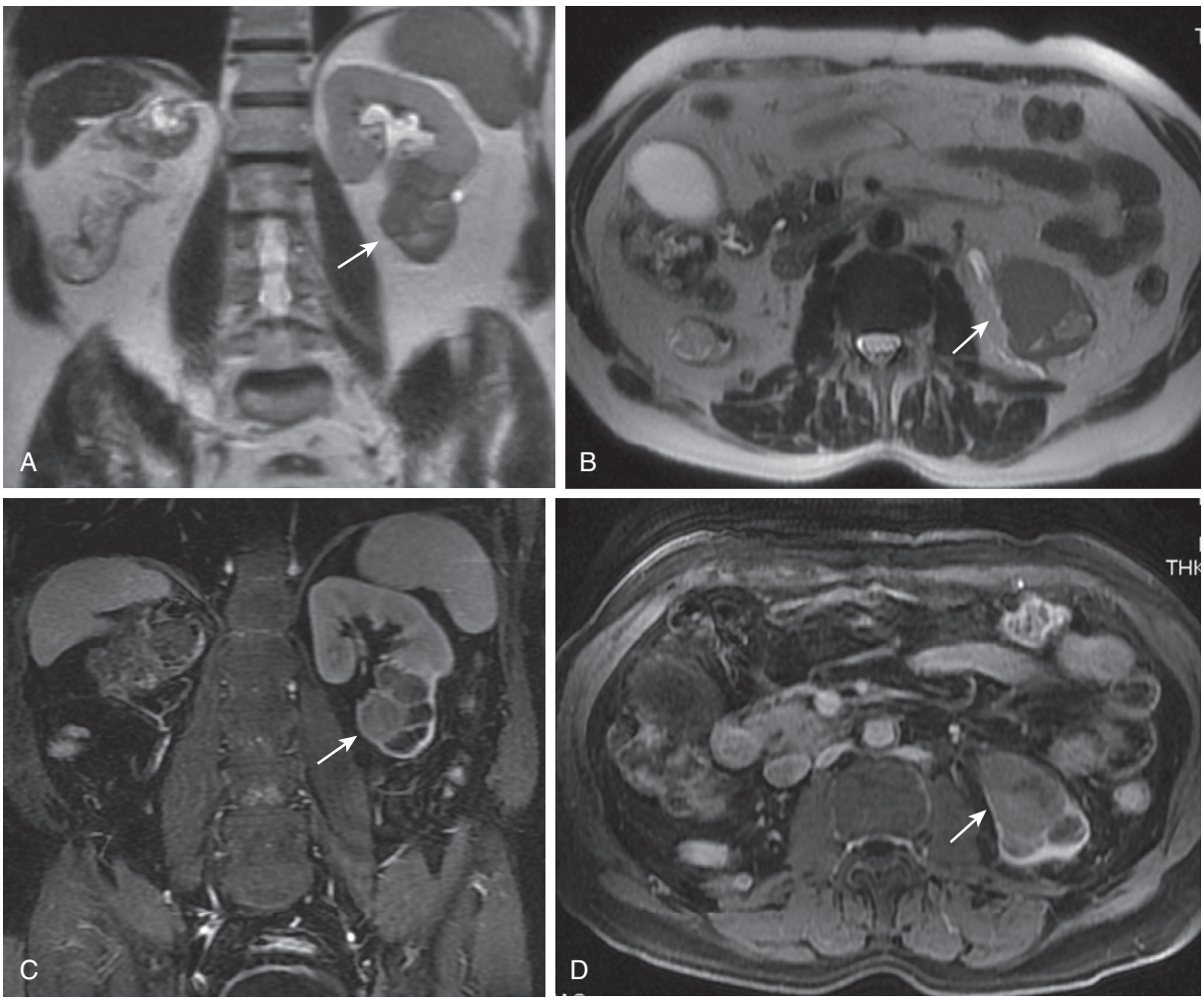

Fig. 25.79 Transitional cell carcinoma. Coronal **(A)** and axial **(B)** T2-weighted images show intermediate signal intensity and an infiltrating mass *(arrow)* within the atrophic lower pole moiety of a duplicated left kidney. Coronal **(C)** and axial **(D)** gadolinium-enhanced T1-weighted images show enhancing material within dilated calyces and pelvis of the lower pole moiety (*arrow*). The cortical atrophy is well demonstrated.

Fig. 25.80 Lymphoma. **A,** Coronal T2-weighted image shows a large, infiltrating left renal mass extending into the perirenal fat. **B,** Coronal gadolinium-enhanced T1-weighted image better differentiates the mass *(arrowhead)* from the renal cortex. **C,** Axial gadolinium-enhanced T1-weighted image shows encasement of the left renal vein *(arrows).*

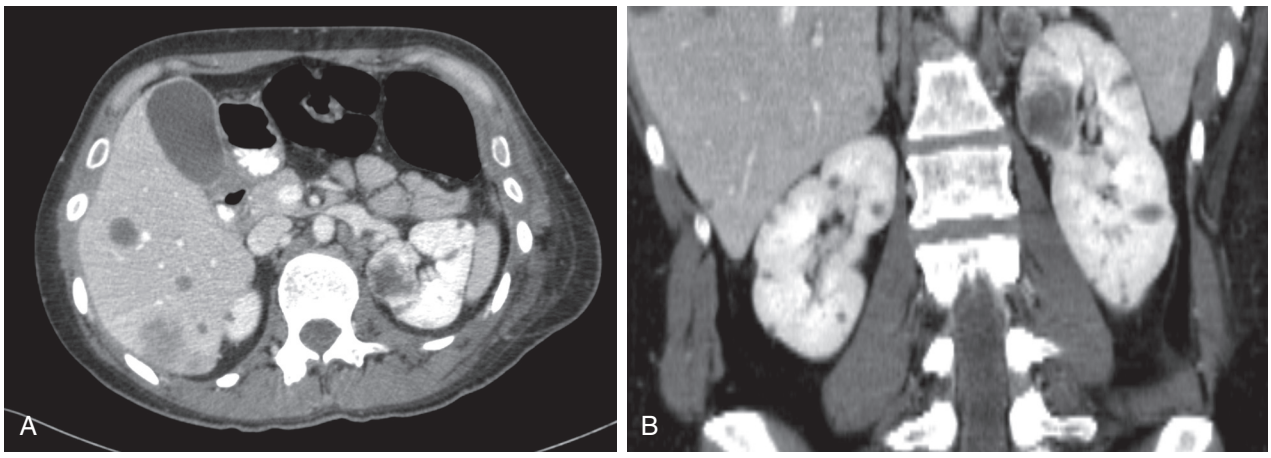

Fig. 25.81 Metastases to the kidney: computed tomographic scan. Axial **(A)** and coronal **(B)** contrast material-enhanced images in the nephrographic phase. Multiple heterogeneous but hypodense lesions are visible in the kidneys bilaterally; the largest is in the left upper pole. These appeared in a 2-month period in a patient with metastatic lung carcinoma. Note the metastases also present in the liver.

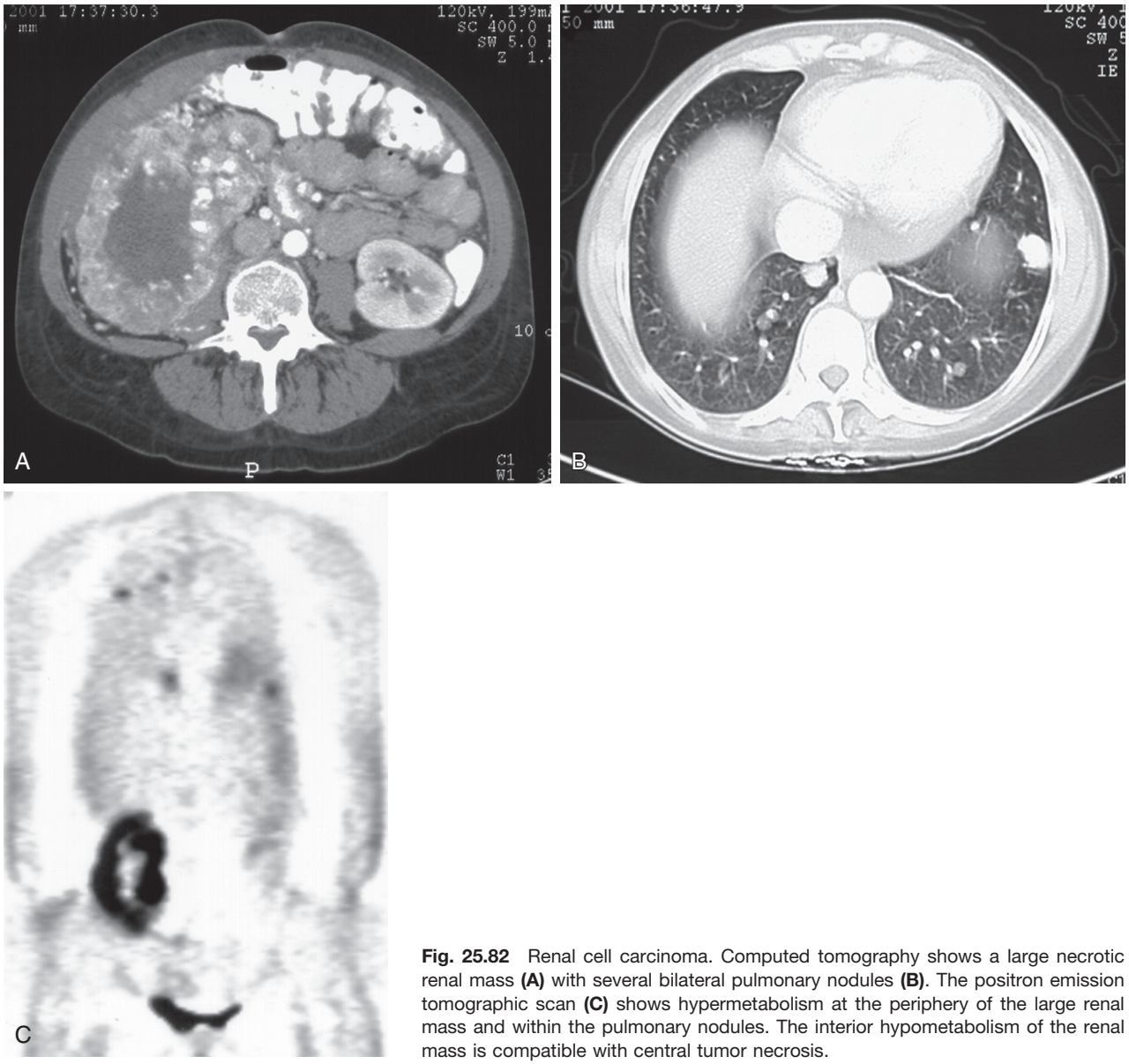

Fig. 25.82 Renal cell carcinoma. Computed tomography shows a large necrotic renal mass **(A)** with several bilateral pulmonary nodules **(B)**. The positron emission tomographic scan **(C)** shows hypermetabolism at the periphery of the large renal mass and within the pulmonary nodules. The interior hypometabolism of the renal mass is compatible with central tumor necrosis.

revealed high accuracy in characterizing indeterminate renal masses, with a mean tumor-to-kidney uptake ratio of 3.0 for malignancy.[312]

These mixed observations are probably related to the heterogeneous expression of glucose transporter 1 in renal cell carcinoma, which may not be correlated with the tumor grade or extent.[330,331] Negative study findings may not rule out disease, whereas a positive result is highly suspect for malignancy.[332] If the tumor binds FDG avidly, then PET can be a reasonable imaging modality for follow-up after treatment and for surveillance (Fig. 25.82). In fact, it has been shown that FDG-PET can alter clinical management in up to 40% of patients with suspected locally recurrent and metastatic renal cancer.[315] A meta-analysis of 14 published studies on the diagnostic utility of FDG-PET (FDG PET-CT) in renal cell carcinoma reported a pooled sensitivity of 62% and a pooled specificity of 88% for renal lesions.[333]

Because FDG is excreted in the urine, the intense urine activity may confound lesion detection in and near the renal bed. Intravenous administration of furosemide has been proposed to improve urine clearance from the renal collecting system, although the exact benefit of such intervention in improving lesion detection remains undefined.

Many investigators since have reported on the unique diagnostic synergism of the combined PET-CT imaging systems.[334] Studies have demonstrated that FDG PET-CT has a sensitivity of 46.6% and specificity of 66.6% for primary renal cell carcinoma in the imaging evaluation of indeterminate renal masses.[335] In a study by Park et al, in South Korea, 63 patients with renal cell carcinoma underwent both FDG PET-CT and conventional imaging evaluation during follow-up after surgical treatment.[336] FDG PET-CT demonstrated 89.5% sensitivity, 83.3% specificity, a positive predictive value of 77.3%, and a negative predictive value of 92.6% in detecting recurrent and metastatic disease; these values were not significantly different from the diagnostic performance of conventional imaging studies. Park et al, concluded that FDG PET-CT can replace multiple conventional imaging

studies without the need for contrast agents. The role of PET-CT in renal cancer imaging and its effect on both short- and long-term clinical management and decision making also must be investigated.

Studies have demonstrated that PET-CT might be potentially useful in treatment response evaluation and prognostication. One Japanese group of investigators reported on the use of FDG PET-CT in early assessment of therapy response to tyrosine kinase inhibitors in 35 patients with advanced renal cell carcinoma.[337] These authors found that improved progression-free survival and overall survival were both associated with favorable response to therapy (defined as decline in tumor maximum standardized uptake value by 20% or more from pretreatment scan to the scan obtained 1 month after completion of therapy). Similar findings have been reported by other investigators.[336,338–341] One study reported that although FDG PET-CT may be helpful in assessing treatment response to chemotherapy, it may not be useful in monitoring response to immunotherapy, such as with interferon alfa monotherapy or in combination with interleukin-2 and 5-fluorouracil.[342] Moreover, other studies have shown that the higher the FDG uptake in the renal cancer lesions, the higher the mortality.[343,344]

Other tracers used in PET (e.g., carbon 11–labeled acetate [^{11}C-acetate], ^{18}F labeled fluoromisonidazole [^{18}F-FMISO], ^{18}F–labeled sodium fluoride) have been investigated in the imaging evaluation of patients with renal cell carcinoma, but further studies are needed to establish the exact role of these and other non-FDG tracers in this clinical setting.[345–348] For example, one study revealed high accumulation of ^{11}C-acetate in 70% of renal cell carcinomas.[349] However, an earlier similar study had demonstrated that in most kidney tumors, accumulation of ^{11}C-acetate was not higher than in normal renal parenchyma.[350] Aside from renal cell carcinoma, ^{11}C-acetate has also been demonstrated to be useful in the imaging-based assessment of renal oxygen consumption and tubular sodium reabsorption.[351] Another investigation using a dual-tracer (^{11}C-acetate and FDG) method showed that AMLs are highly avid for ^{11}C-acetate but not at all for FDG. The uptake of ^{11}C-acetate in renal cell cancer was lower than that in AML. In fact, this study suggested that ^{11}C-acetate may be useful in differentiating "fat-poor angiomyolipoma" from renal cell cancer with a sensitivity of 93.8% and specificity of 98%.[352] ^{11}C-acetate has also been found to be potentially useful in early prediction of response to the tyrosine kinase inhibitor, sunitinib, in patients with metastatic renal cell carcinoma.[353]

Murakami et al used the hypoxia imaging probe ^{18}F-FMISO in preclinical models of renal cell carcinoma to show that ^{18}F-FMISO hypoxia imaging can confirm "tumor starvation" as the mechanistic explanation for tumor response to anti-angiogenic therapy.[354] A pilot clinical study with ^{18}F-FMISO also showed that patients with hypoxic metastatic tumors have shorter progression-free survival than those with non-hypoxic tumors.[355]

Other tracers that have been investigated include iodine 124 (^{124}I)– and zirconium 89–labeled anticarbonic anhydrase IX monoclonal antibody that is avid to clear cell renal cell carcinoma.[354] An early trial of the ^{124}I-labeled compound for detection of clear cell renal cell carcinoma (with histopathology as reference standard) showed an average sensitivity and specificity of 86.2% and 85.9%, respectively, for PET-CT, which were statistically higher than sensitivity and specificity of 75.5% and 46.8%, respectively, for CE-CT.[356]

Schuster et al reported on their initial experience with anti-1-amino-3-^{18}F-fluorocyclobutane-1-carboxylic acid, which is a nonmetabolized synthetic L-leucine analog with low urinary excretion, in the imaging evaluation of renal cell carcinoma.[357] Their preliminary results in six patients showed that the uptake of this amino acid-based radiotracer may be elevated in renal papillary cell carcinoma but not in clear cell carcinoma.

Other uses of PET in the imaging evaluation of renal perfusion, function, and metabolism have also been investigated.[358] In addition, there is some effort to evaluate the role of radiolabeled antibodies as therapeutic agents in the treatment of renal cell carcinoma.[357]

RENAL VASCULAR DISEASE

Diagnostic imaging for hypertension depends on the clinical index of suspicion for renovascular hypertension, which is found in less than 5% of the hypertensive population, but the percentage is higher in those with severe hypertension and ESKD.[359] The most common cause of renovascular hypertension is renal artery stenosis (RAS), with approximately 90% of cases due to atherosclerosis and approximately 10% due to fibromuscular dysplasia. Renovascular disease is discussed further in Chapter 47. The diagnosis of RAS at the time of screening has been problematic because the preintervention definition of significant RAS has varied. Significant RAS is best defined as a fall in blood pressure after intervention. According to the ACR, in patients with normal renal function in whom RAS is suspected, MRA or CTA is usually appropriate. Doppler US or ACE-inhibitor scintigraphy is appropriate if MRA is not desired or contraindicated, and conventional angiography is reserved for confirmation of RAS and definitive therapy. IVU has no role in the evaluation for RAS.[360]

Doppler US is a noninvasive screening test that can be used independent of the patient's renal function. In experienced hands, US has been reported to have high sensitivity and specificity; however, sensitivities have been reported as low as 0%. US screening can be technically challenging and therefore should be performed only in centers where US screening has been proven to be reliable and where there are dedicated technologists and physicians. In such centers 75% to 80% of scans are technically adequate.

Doppler US has been used with variable success to assess the main renal arteries for RAS and the intrarenal vasculature for secondary effects.[360,361] The success of Doppler US is highly operator dependent, and results may be inadequate or incomplete because of overlying bowel gas, body habitus, or aortic pulsatility.[361] A stable Doppler signal may be difficult to reproduce in some patients with renovascular hypertension. A complete examination has been possible in 50% to 90% of affected patients. Variant anatomy may also be a challenge; accessory renal arteries, which occur in 15% to 20% of affected patients, may not be imaged.[362]

The criteria used for evaluation of the main renal artery include an increase in the peak systolic velocity to more than 180 cm/sec, a renal/aortic ratio of peak systolic velocity of more than 3.0, and turbulent flow beyond the region of the stenosis.[363] Visualization of the main renal artery with no

detectable Doppler signal is suggestive of renal artery occlusion. Intrarenal vascular assessment with Doppler US has depicted the shape and character of the waveform. A dampened appearance of the waveform, with a slowed systolic upstroke and delay to peak velocity (tardus-parvus), has been shown in varying degrees in RAS.[364] Using resistive indices, a difference between the kidneys of more than 5% has also been suggestive of RAS. Sensitivity and specificity for the techniques have generally been in the range of 50% to 70%. CEUS has been suggested as a means of improving the accuracy of Doppler US.[364,365]

CTA performed with MDCT has sensitivity and specificity at or near 100% (Fig. 25.83).[366–368] CTA is an effective alternative to Doppler US and MRA. When compared with MRA, CTA has higher spatial resolution and shorter examination times. CTA evaluates calcified and noncalcified atherosclerotic plaques and may be used to assess stent grafts (Fig. 25.84).[369,370] A normal result should rule out RAS.[371] The main renal artery, as well as its segmental branches, can be viewed and evaluated (Figs. 25.85 and 25.86). Accessory renal arteries as small as 1 mm in diameter can be seen.[372] CTA and MRA are of equivalent quality in the detection of hemodynamically significant RAS.[373] Both CTA and MRA can demonstrate renal cortical volume and thickness as well as secondary signs of RAS, including poststenotic dilation, renal atrophy, and decreased cortical enhancement.

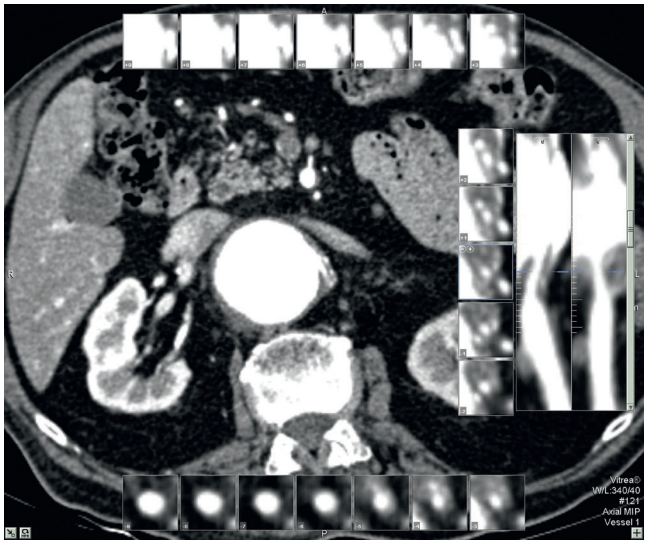

Fig. 25.83 Renal artery stenosis: computed tomographic angiogram, axial image with vessel analysis. The origin of the left renal artery is markedly narrowed by calcified and noncalcified atherosclerotic plaque. The vessel analysis demonstrates the renal artery in cross section for accurate calculation of the degree of stenosis, which in this case was greater than 70%.

Because CTA is sensitive, accurate, fast, and reproducible, MRA is reserved for patients for whom iodinated contrast material is contraindicated. Renal insufficiency is not uncommon in the population clinically at high risk for RAS. For this reason, MRA has been widely accepted as a reliable and accurate examination in the evaluation of RAS in this population.[107,118,373–375] CE-MRA is being used more selectively, given the risk for NSF in patients with CKD stage 4 and 5. Noncontrast MRA techniques are being used more frequently to reduce the amount of Gd-C needed. Like CTA, MRA is noninvasive and provides excellent visualization of the aortoiliac and renal arteries.[373]

CE-MRA is more than 95% sensitive in demonstrating the main renal arteries and has a high negative predictive value. A normal CE-MRA finding almost completely rules out a stenosis in the visualized vessels.[376] CE-MRA is a reliable examination but has been limited by incomplete visualization of segmental and small accessory vessels.[377] Whereas visualization of all accessory vessels is desired, Bude et al found isolated hemodynamically significant stenosis of an accessory artery in only 1 (1.5%) of their 68 patients.[378] Bude et al concluded that this limitation does not substantially reduce the rate of detection of renovascular hypertension by MRI. With the use of three-dimensional reconstruction, studies have demonstrated no significant difference between CE-MRA and CTA in the detection of hemodynamically significant RAS.[373] Volume rendering and multiplanar reformatting improve accuracy in depicting RAS.[117] Volume rendering increases the positive predictive value of CE-MRA by reducing the overestimation of stenosis yielded by earlier reconstruction

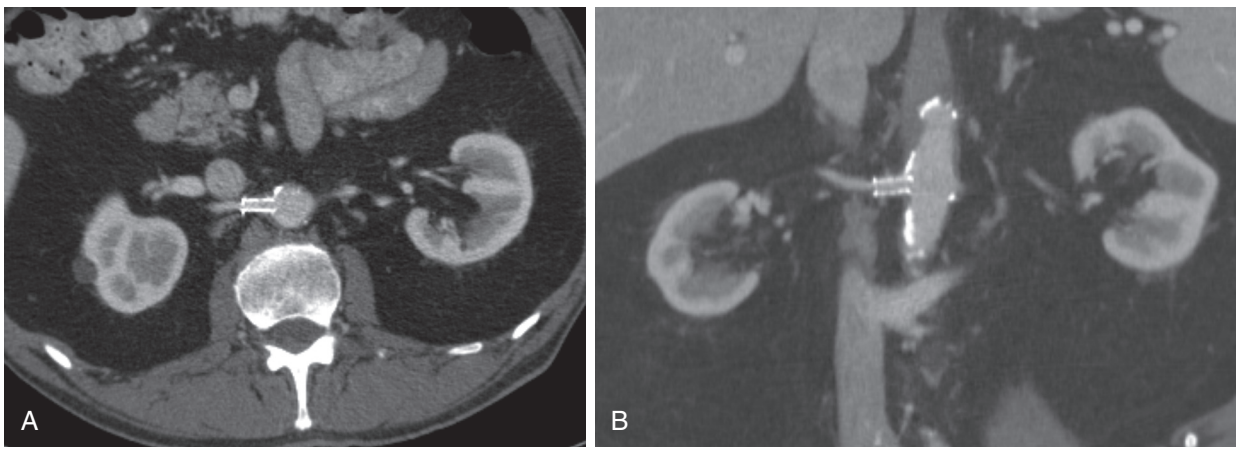

Fig. 25.84 Renal artery stent: computed tomographic scan. Axial **(A)** and coronal **(B)** images of a contrast material-enhanced scan in the corticomedullary phase. The metallic stent is visible at the origin of the right renal artery. It had been placed for treatment of renal artery stenosis that was caused by atherosclerosis. Good flow through the stent is observed as contrast material fills the lumen.

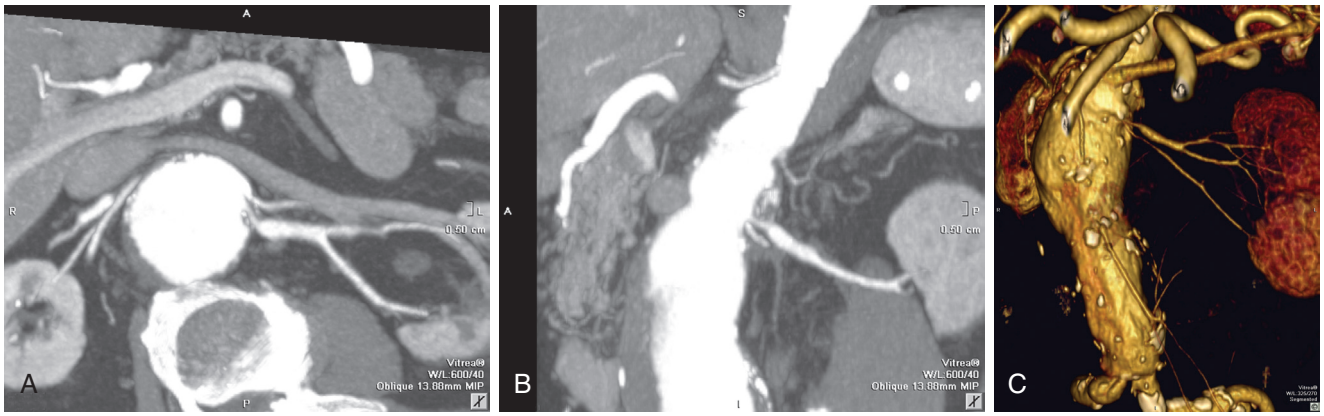

Fig. 25.85 Renal artery stenosis: computed tomographic angiography (CTA). Image processing was applied to the case depicted in Fig. 25.84. Axial **(A)** and coronal **(B)** slab maximum-intensity projection images demonstrate the atherosclerotic stenosis of the proximal renal artery. Note the accessory renal artery arising adjacent to the left main renal artery. Volume rendering of the CTA produced a three-dimensional display **(C),** which may be rotated for best viewing and analysis.

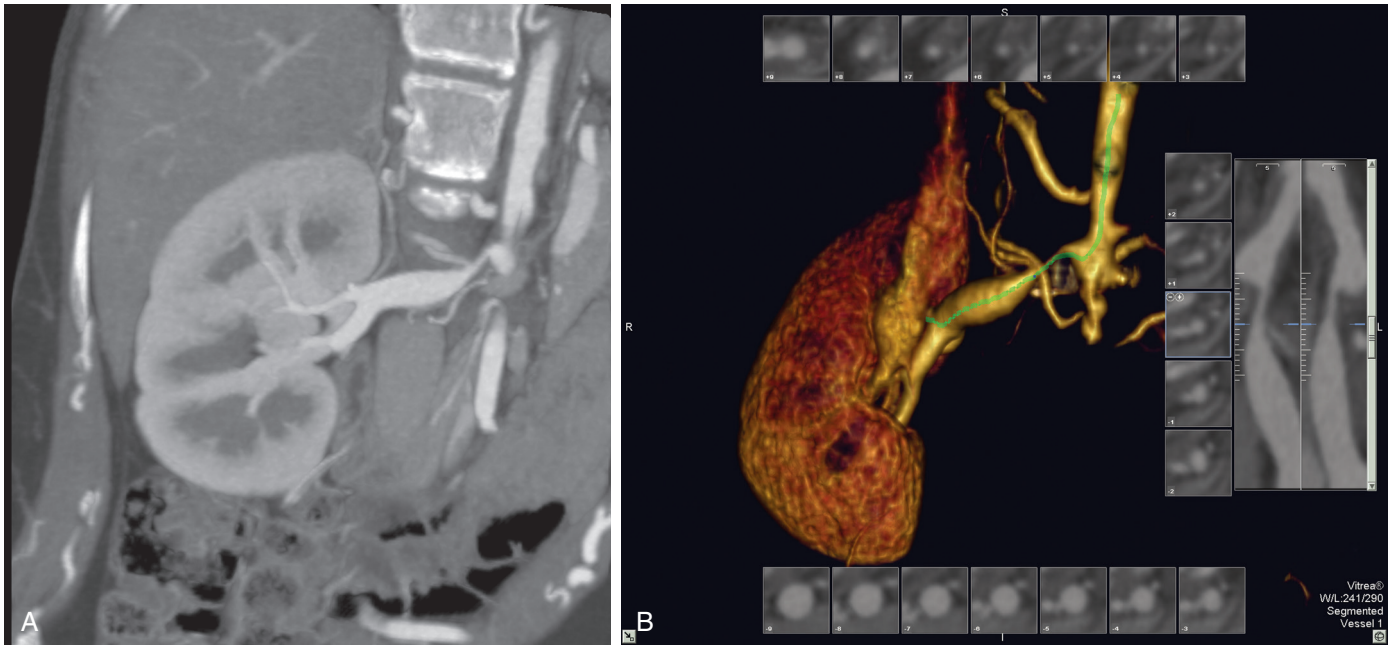

Fig. 25.86 Renal artery stenosis: abdominal computed tomographic angiography (CTA) with image processing. **A,** Coronal slab maximum-intensity projection demonstrates the smooth narrowing of the proximal right renal artery in a patient with Takayasu's arteritis. Note the markedly abnormal aorta with occlusion distal to the origin of the renal artery. **B,** Volume rendering of the CTA with vessel analysis reveals the 80% stenosis of the right renal artery. The left renal artery had been occluded previously, and the kidney was supplied by collateral vessels.

techniques (Fig. 25.87).[118,376] Volume rendering has better correlation with digital subtraction angiography and improves delineation of the renal arteries.[118]

The usefulness of MRA is restricted in part by limitations in spatial resolution and by motion artifacts.[378,379] Advancements in magnetic resonance gradient strengths and newer MRA techniques have improved image resolution and reduced motion artifacts, while reducing imaging times.[378] Higher magnetic field strength (3 T) can result in higher spatial and temporal resolution when compared with imaging at 1.5 T. This higher resolution was found to improve the evaluation of smaller structures.[380,381] As MRI hardware and software improve, so will noncontrast MRA. Noncontrast MRA may be performed independent of renal function, and small studies have shown good results for the diagnosis of RAS.

Phase-contrast MRA can be used to calculate blood flow through the renal artery.[382] Phase-contrast flow curves can be generated, and the severity of the hemodynamic abnormalities can be graded as normal, low-grade, moderate, and high-grade stenosis. This is similar to the Doppler US method. Grading can be used to evaluate the hemodynamic significance of a detected stenosis.[383] The significance of a stenosis on parenchymal function, however, is not currently evaluated by conventional MRA. Renal MRI perfusion studies are being performed to grade the effect of RAS on parenchymal perfusion; initial results show that MRI perfusion measurements

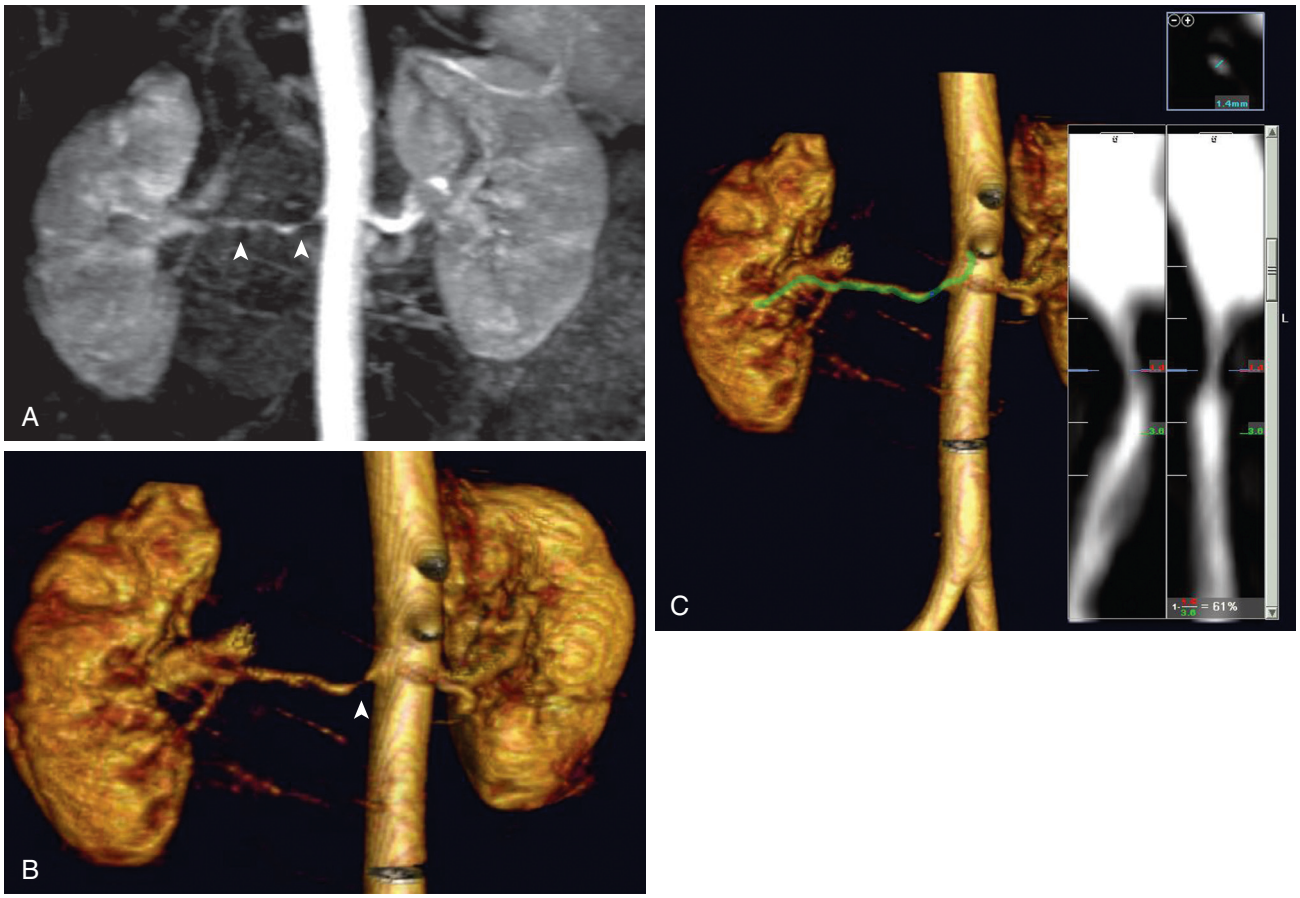

Fig. 25.87 Renal artery stenosis. Advancements in postprocessing allow for a more accurate evaluation of stenosis with magnetic resonance angiography. **A,** Maximum-intensity projection displays a high-grade stenosis near the origin of the renal artery *(arrowheads),* mimicking fibromuscular dysplasia. **B,** Volume rendering shows the proximal stenosis *(arrowhead),* but the midportion of the artery is more normal in appearance. **C,** A view of the artery in two dimensions allowed measurement of the proximal stenosis and demonstrated a normal midportion of the artery. This stenosis was confirmed with angiography.

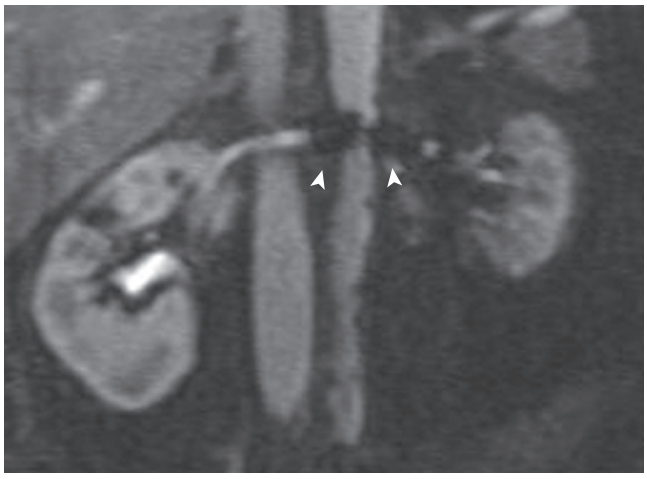

Fig. 25.88 Magnetic resonance angiography in a patient with bilateral renal artery stents *(arrowheads).* The metal in the stent causes artifact that obscures the vessel lumen. Contrast material is visible beyond the stent, which indicates that no complete occlusion is present.

with high spatial and temporal resolution reflect renal function as measured with serum creatinine level.[384] Volumetric analysis of functional renal cortical tissue may also yield clinically useful information in patients with RAS.[385] Further research is required before this will be known, however.

MRA is currently of limited value in the evaluation of restenosis in patients with renal artery stents. Although stent technology is rapidly changing, metal artifact still obscures the stent lumen to varying degrees as a result of susceptibility artifacts (Fig. 25.88). Phase-contrast MRA may be used to measure velocities proximal and distal to the stent, but this is an indirect approach to evaluating for stenosis. Work is being done to develop a metallic renal artery stent that will allow for lumen visualization on MRI; however, this is not currently available clinically.[386]

Fibromuscular dysplasia has a characteristic appearance of focal narrowing and dilation ("string of beads"; Fig. 25.89). Because fibromuscular dysplasia frequently involves the middle to distal portions of the renal artery and segmental branches, resolution limits MRA evaluation. For this reason, MRA is not as reliable for diagnosis of fibromuscular dysplasia as it is for atherosclerotic RAS. Renal infarctions are well demonstrated on MRA as wedge-shaped areas of decreased

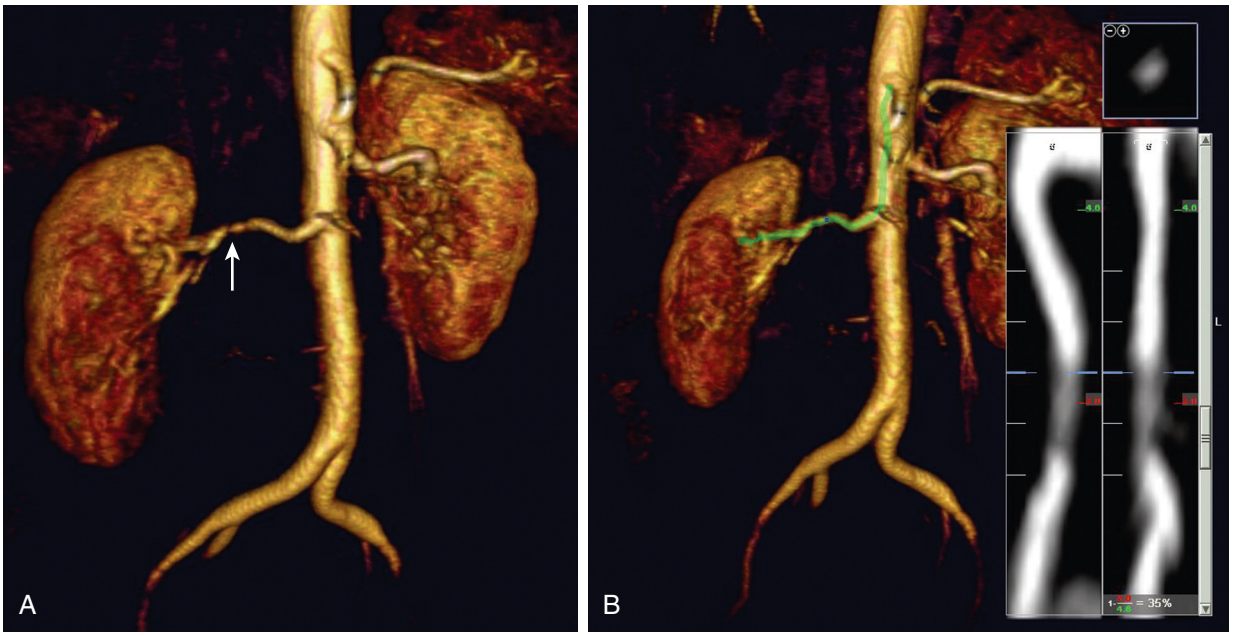

Fig. 25.89 **A** and **B,** Magnetic resonance angiography with volume reconstruction demonstrates a subtle irregularity in the midportion of the right renal artery *(arrow).* Fibromuscular dysplasia was confirmed with conventional angiography.

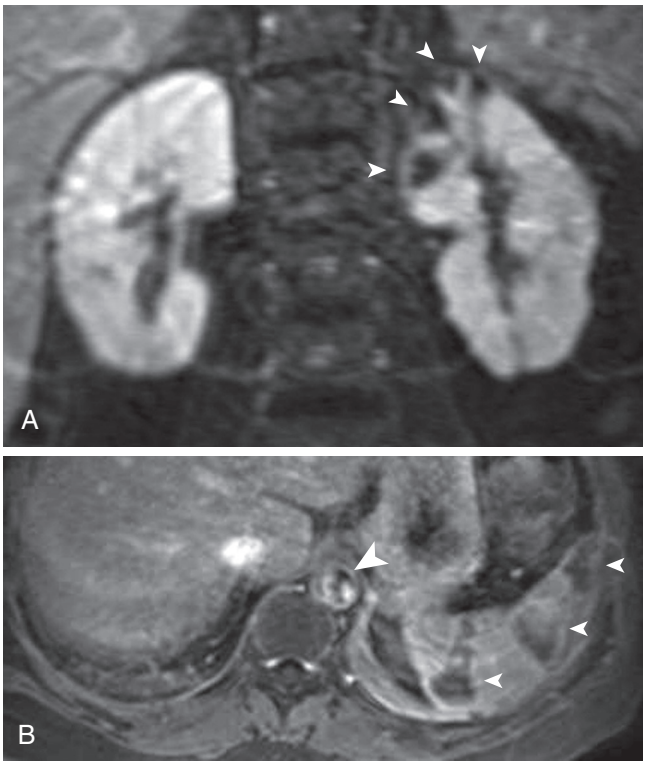

Fig. 25.90 Renal infarcts caused by embolic disease. **A,** Coronal gadolinium-enhanced T1-weighted image shows wedge-shaped cortical areas without enhancement *(arrowheads).* **B,** Axial gadolinium-enhanced T1-weighted image shows an irregular filling defect in the aorta *(large arrowhead),* which is consistent with thrombus, and three focal defects in the spleen *(small arrowheads),* which are consistent with splenic infarcts.

parenchymal enhancement. These areas are most conspicuous in the nephrographic phase. Evaluation of the arterial and venous structures may demonstrate the origin of the emboli or thrombosis (Fig. 25.90).

NUCLEAR IMAGING AND RENOVASCULAR DISEASE

ACE inhibition prevents conversion of angiotensin I to angiotensin II. In RAS, angiotensin II constricts the efferent arterioles as a compensatory mechanism to maintain GFR despite diminished afferent renal blood flow. Therefore ACE inhibition in RAS reduces GFR by interfering with the compensatory mechanism. Captopril-enhanced renography has been successful in evaluating patients with RAS.

Before the study the patient should be well hydrated, and ACE inhibitors should be discontinued (captopril for 2 days; enalapril or lisinopril for 4–5 days) because diagnostic sensitivity may otherwise be reduced. Diuretics should also be discontinued before the study, preferably for 1 week. Dehydration resulting from diuretics may potentiate the effect of captopril and contribute to hypotension. Captopril (25–50 mg) crushed and dissolved in 250 mL water is administered orally, followed by blood pressure monitoring every 15 minutes for 1 hour. Alternatively, enalaprilat (40 µg/kg with total dose not exceeding 2.5 mg) is administered intravenously over 3 to 5 minutes. A baseline scan can be performed before captopril-enhanced renography (1-day protocol) or the next day, only if captopril-enhanced study findings are abnormal (2-day protocol).

The affected kidney in renovascular hypertension often has a renogram curve with reduced initial slope, a delayed time to peak activity, prolonged cortical retention, and a slow downward slope after the peak (Fig. 25.91). These findings are caused by the slowing of renal tracer transit as

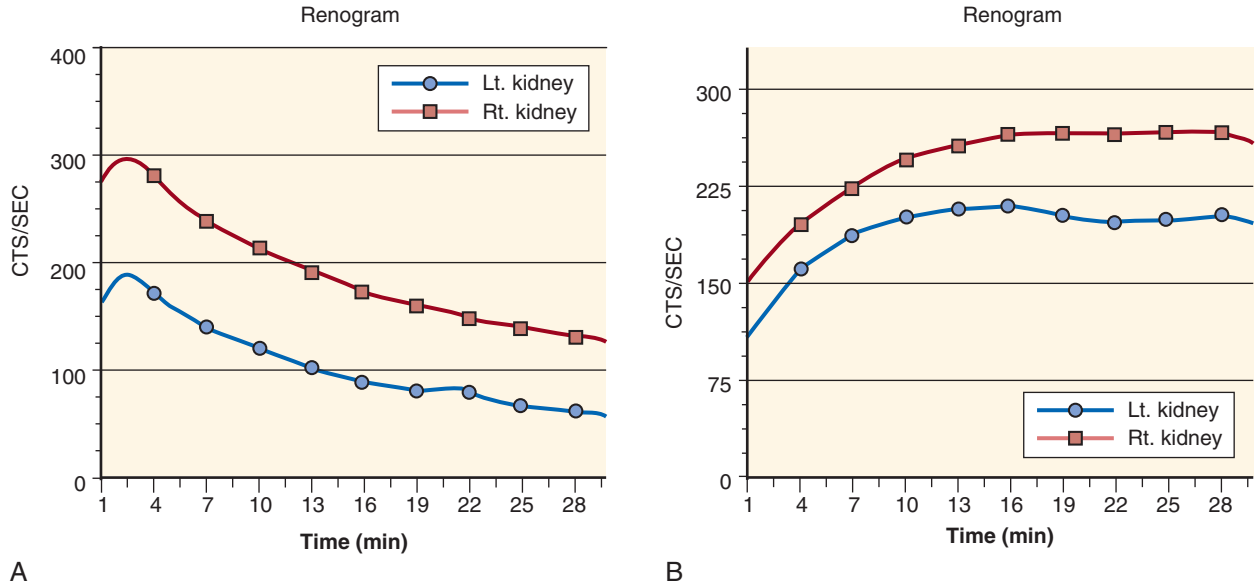

Fig. 25.91 Technetium 99m-labeled mercaptoacetyltriglycine renograms before **(A)** and after **(B)** angiotensin-converting enzyme (ACE) inhibition with captopril. Note the relatively normal renograms **(A)** and the reduced initial slope, delayed time to peak activity, and plateau compatible with captopril-induced cortical tracer retention **(B).** These findings suggest a high probability of hemodynamically significant bilateral renal artery stenosis that is more severe on the left side *(connected circles)* than the right side *(connected squares).* Bilateral renal artery stenosis was later confirmed with angiography. (Modified from Saremi F, Jadvar H, Siegel M. Pharmacologic interventions in nuclear radiology: indications, imaging protocols, and clinical results. *Radiographics*. 2002;22:447–490.)

a result of increased retention of solute and water in response to ACE inhibition. Reduced urine flow causes delayed and decreased washout of tracer into the collecting system in ^{99m}Tc-MAG3 and ^{131}I-ortho-iodohippurate studies. ^{99m}Tc-DTPA demonstrates reduced uptake on the affected side.[387]

Consensus reports regarding methods and interpretation of ACE-enhanced renograms elaborate on a scoring system of renographic curves.[388–390] It has been recommended that high (>90%), intermediate (10%–90%), and low (<10%) probability categories be applied to captopril-enhanced renography on the basis of the change of renographic curve score between baseline values and those after captopril-enhanced renograms. Among quantitative measurements, relative renal function, the time to peak activity, and the ratio of 20-minute renal activity to peak activity (20/peak) are used more commonly than other parameters. For ^{99m}Tc-MAG3 renal scintigraphy, a 10% change in relative renal function, peak activity increase of 2 minutes or more, and a parenchymal increase by 0.15 in 20/peak after captopril-enhanced study represent a high probability of renovascular hypertension.[391]

Captopril-enhanced renography has 80% to 95% sensitivity and 50% specificity for detecting impaired GFR; the detection of stenosis by captopril-enhanced renography may be more complicated.[394] With bilateral renovascular stenosis, it is more the exception than the rule for findings to be symmetric on captopril-enhanced renography. Studies in canine models with bilateral RAS demonstrated that captopril produced striking changes in the time-activity curve of each kidney, which are even more pronounced in the more severely stenotic kidney.[387] In practice, captopril-enhanced renography has largely been replaced by CTA or MRA for the investigation of renovascular disease.

RENAL VEIN THROMBOSIS

Renal vein thrombosis is usually clinically unsuspected. It is found in patients with a hypercoagulable state, underlying renal disease, or both.[387] The classic manifestation of acute renal vein thrombosis with gross hematuria, flank pain, and decreasing renal function is uncommon.[399] It may present clinically as nephrotic syndrome.[392] Other causes include collagen vascular diseases, diabetic nephropathy, trauma, and tumor thrombus. Renal vein thrombosis can be diagnosed by Doppler US, CT, and MRI.

IVU yields nonspecific findings in renal vein thrombosis and is no longer used for diagnosis. It may yield normal findings in more than 25% of cases. On gray-scale and Doppler US, the involved kidney appears enlarged and swollen with relative hypoechogenicity in comparison with the normal kidney.[393] The finding of a filling defect in the renal vein is both sensitive and specific for diagnosis and is the only convincing sign of renal vein thrombosis. The lack of flow on Doppler US, however, is a nonspecific finding and may be observed because of technical limitations of the study. Other findings include an absence or reversal of the diastolic waveform on Doppler US, but this may also be seen in other conditions.

CE-CT is needed to properly assess the patient with suspected renal vein thrombosis. If renal function is impaired, MRI can be used. Findings on CT include an enlarged renal vein with a low signal-attenuating filling defect that represents the clot within the renal vein.[394] Parenchymal enhancement may be abnormal, with prolonged corticomedullary differentiation and a delayed or persistent nephrogram. The kidney appears enlarged, with edema in the renal sinus leading to a striated nephrogram and attenuation of the pelvicalyceal

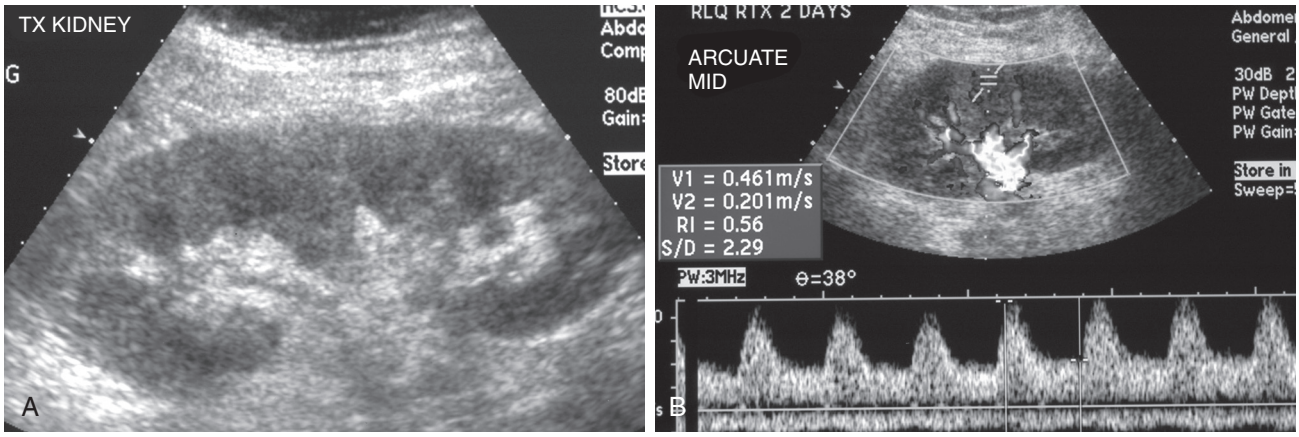

Fig. 25.92 Normal renal transplant: ultrasonography. Coronal image **(A)** of a recently transplanted kidney in the right lower quadrant. The central echo complex, medullary pyramids, and cortex are well depicted. The duplex Doppler image **(B)** demonstrates normal flow to the transplanted kidney with a normal resistive index of 0.56.

system, and in extreme cases the pelvicalyceal system is completely compressed. Stranding and thickening of Gerota's fascia may be observed. Within chronic renal vein thrombosis, the renal vein may be narrowed because of clot retraction, and pericapsular collateral veins may be noted. Affected patients have an increased risk for pulmonary emboli as well. With renal tumors and, in rare cases, adrenal tumors, thrombus may develop in the renal vein with extension to the IVC. Imaging appearances suggesting tumor thrombus rather than bland thrombus include arterial enhancement in the thrombus, significant expansion of the vein, and continuity of the thrombus with a mass.

The appearance of renal vein thrombosis on noncontrast MRI is variable. If the thrombosis is acute, the renal vein appears distended, no normal flow void is visible, and the affected kidney appears enlarged. Renal infarction may also be present. If the thrombosis is chronic, the renal vein is small and difficult to see. A nonenhanced filling defect in the vein is visible on contrast-enhanced magnetic resonance venography, which is consistent with thrombus.

ASSESSMENT FOR KIDNEY DONATION

The treatment of choice for patients with ESKD is renal transplantation. Although there have been significant improvements in continuous peritoneal dialysis and hemodialysis, patient survival is longer and overall quality of life is better after renal transplantation. Radiologic evaluation is performed on the potential renal transplant donor and in the postoperative assessment of the transplant recipient. Although IVU and angiography were used in the past, US, CT, MRI, and renal scintigraphy are the current methods used in evaluation of these patients (Fig. 25.92).[395–397]

A comprehensive radiologic assessment of the living renal transplant donor is crucial.[405] The anatomic information that is necessary is vascular, parenchymal, and pelvicalyceal. The renal artery must be visualized for number, length, location, and branching pattern. The parenchyma must be evaluated for scars, overall volume, renal masses, and calculi. The venous anatomy must be viewed, and the number of veins, anatomic variants, and significant systemic tributaries noted. The pelvicalyceal system must be scrutinized for anomalies such as duplication and papillary necrosis. The detailed anatomy and mapping techniques now possible have led to the increased use of laparoscopic techniques for donor kidney retrieval.[398–401]

With the development of MDCT, the complete evaluation of the living renal transplant donor is possible.[398,402,403] Noncontrast CT is performed with a low dose of radiation just to search for renal stones, locate the kidneys, and identify renal masses (see Fig. 25.9). Arterial phase scanning is generally performed at 15 to 25 seconds to demonstrate the main renal artery, branching pattern of the artery, and abnormalities such as atherosclerotic plaques or fibromuscular dysplasia (see Fig. 25.11); 25% to 40% of donors have accessory renal arteries, and 10% have early branching patterns in the main renal artery.[399,401] For transplantation the main renal artery should be free of branching for the first 15 to 20 mm. Because of the rapid transit of contrast material through the kidney, most renal veins are also well viewed in this phase (see Fig. 25.10). Venous variants occur in 15% to 28% of donors, with multiple renal veins being most common, especially on the right. On the left side, 8% to 15% have a circumaortic renal vein, and 1% to 3% have a retroaortic vein.[401,404] It is also important to visualize venous tributaries, including the gonadal, left adrenal, and lumbar veins. These are best viewed on the nephrographic phase.[399,400] Imaging in this phase is performed 80 to 120 seconds after injection of contrast material and is used to evaluate the cortex and medulla for scars and masses (see Fig. 25.12). Excretory phase imaging is performed with CT, CT digital radiography, or plain radiography to note anomalies or abnormalities in the pelvicalyceal system (see Fig. 25.13). CT has a demonstrated accuracy of 91% to 97% for arterial phase imaging, 93% to 100% for the venous phase, and 99% for the pelvicalyceal system.[403,405,406] Similar results have been noted for MRI; the biggest discrepancy is found in imaging accessory renal arteries.[407,408] Most centers today use CT in the evaluation of living renal transplant donors.

MRI, MRA, and MRU can be combined into one examination for the evaluation of the renal transplant donor.[409] MRI and CT are comparable for the evaluation of renal vasculature,

structure, and function. To avoid radiation exposure and nephrotoxicity, MRI may be preferred over CT for preoperative evaluation.

In healthy renal donors it is possible to quantify functional renal volume with MRA by determining only the cortical volume. The hypothesis supported by Van den Dool et al was that glomerular filtration is an important component of renal function, and because the majority of glomeruli are in the cortex, renal function should be well correlated with cortical volume.[410] Considerations in living donors are discussed further in Chapter 71.

ASSESSMENT OF TRANSPLANTED KIDNEYS

After surgically successful renal transplantation, radiologic evaluation is frequently necessary. Conventional US, Doppler US, CT, MRI, and renal scintigraphy are used in various settings. US assumes the primary role for assessing patients with changes in serum creatinine level, urine output, pain, or hematuria.[410] It is also used to direct kidney biopsy. Doppler US is used to evaluate renal perfusion, the patency of the renal artery and vein, and the integrity of the vascular anastomoses.[411] CT, MRI, and renal scintigraphy are adjunctive studies.

Conventional grayscale US is essential in assessing for transplant obstruction and fluid collections around the transplanted kidney.[397] Conventional US yields nonspecific findings in acute tubular necrosis and acute rejection, including obliteration of the corticomedullary junction, prominent swollen pyramids, and loss of the renal sinus echoes.[396,412] All these findings are indicative of edema of the transplanted kidney, which leads to increased peripheral vascular resistance, decreased diastolic perfusion, and elevation of the resistive index (>0.80) (Fig. 25.93).[407] Chronic rejection may lead to diffusely increased echogenicity throughout the kidney.

Doppler US adds valuable information pertaining to the integrity of the vascular elements. Despite early enthusiasm with the ability of Doppler US to differentiate acute transplant rejection from acute tubular necrosis, it is now known that the findings are nonspecific and cannot obviate the need for kidney biopsy in these cases.[413] Both acute tubular necrosis and acute rejection can cause an increase in peripheral vascular resistance.[413,414] A significant number of patients with acute rejection have a normal resistive index (<0.80).[399] It is now known that vascular rejection is no more likely to cause increases in peripheral vascular resistance than is cellular rejection.[415] Neither the timing nor clinical symptoms of the renal dysfunction can be used to differentiate acute rejection from acute tubular necrosis.[415] Doppler US is most helpful in detecting acute arterial thrombosis when signal in the artery is absent or renal vein thrombosis when the waveform is plateau-like and diastolic flow is retrograde. An abnormal Doppler waveform in the allograft indicates compromise of the transplanted kidney.[416] Sequential examinations may be used to show improvement or deterioration in the condition affecting the kidney and to note the progress of treatment.

MRI and CE-CT are useful in patients in whom the transplanted kidney is obscured by overlying bowel gas or in patients with large body habitus in whom US may be limited by the depth of the transplanted kidney. If any doubt exists after a thorough US evaluation, MRI or CT may be performed to clarify or confirm the US findings.

Fluid collections around a transplanted kidney are very common, occurring in up to 50% of cases.[418] These fluid collections may represent urinoma, hematoma, lymphocele, abscess, or seroma. The effects of the collection depend on the size and location. Urinomas and hematomas are found early, usually immediately after surgery. Lymphoceles generally are not found until 3 to 6 weeks after surgery. Abscesses are usually associated with transplant infection.

On US evaluation, extrarenal or subcapsular hematomas usually have a complex echogenic appearance, which becomes less echogenic with time (Fig. 25.94).[410] On CT they appear as high signal-attenuating fluid collections early. Such collections are usually too complex to be successfully drained percutaneously. Urine leaks and the associated urinomas are also found in the immediate postoperative period (Fig. 25.95).[410] On US these appear as anechoic fluid collection with no septations. They may rapidly increase in size. Drainage

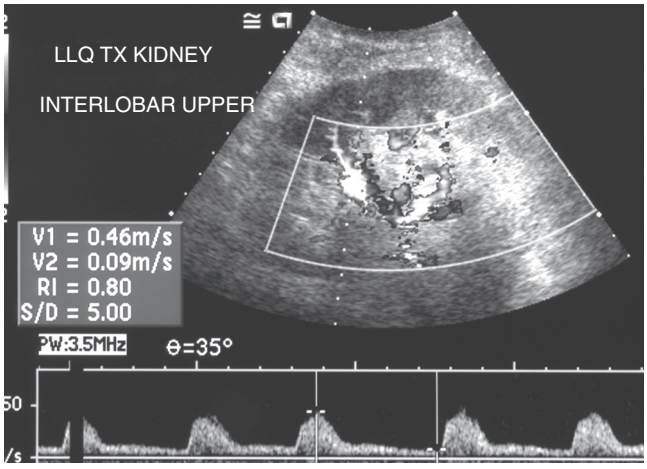

Fig. 25.93 Renal transplant with acute tubular necrosis: ultrasonography. Duplex Doppler image of the transplanted kidney shows normal size and normal appearance with a high resistive index of 0.80 in the interlobar artery. Calculation of the resistive index (RI): *V1*, peak systolic velocity (S); *V2*, end-diastolic velocity (D). RI = (S-D)/S. The patient recovered with return of normal renal function in 5 days.

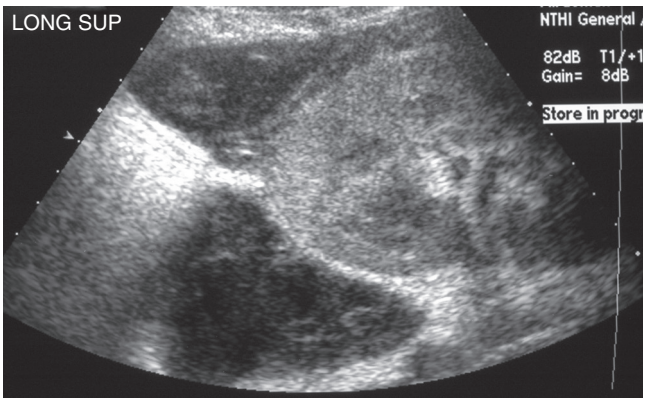

Fig. 25.94 Renal transplant with hematoma: ultrasonography. Longitudinal image of the upper aspect of the transplanted kidney reveals two hypoechoic collections adjacent to the kidney. The heterogeneous hypoechoic nature of the collections suggests that they are hematomas, as opposed to urinomas or lymphoceles, which in general are anechoic.

may be performed under guidance by either US or CT.[417] Antegrade pyelography via a percutaneous nephrostomy is needed to detect the site of leak, usually the ureteral anastomoses. Stent placement for treatment is necessary.

Lymphoceles are recognized weeks to years after transplantation and occur in up to 20% of cases.[410] They form from the leakage of lymph fluid from the interrupted lymphatic vessels at surgery. Lymphoceles appear on US as anechoic fluid collections with septations. The size and effect on the kidney determine the need for treatment. Because lymphoceles are frequently located medial and inferior to the kidney, they are a common cause of obstruction to the kidney. US or CT guidance for drainage may be used. In a minority of cases, sclerotherapy may be needed to treat the lymphocele.[417]

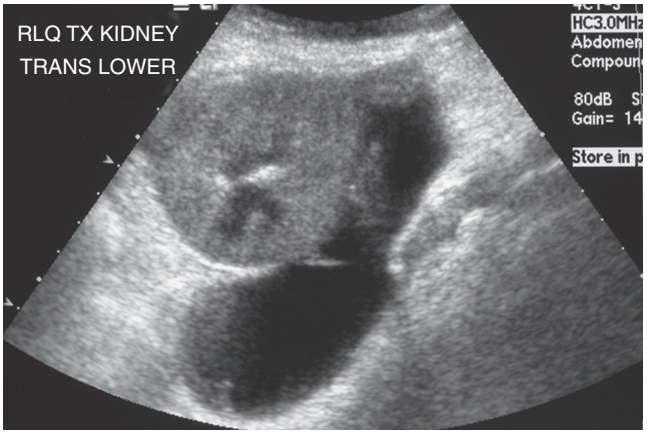

Fig. 25.95 Renal transplant with urinoma: ultrasonography. Transverse image through the lower aspect of the transplanted kidney reveals a normal appearance with a large anechoic fluid collection adjacent to the kidney. This fluid was aspirated under US guidance, and the findings led to the diagnosis of urinoma. The patient was treated with catheter placement and drainage, also performed with US guidance.

Abscess near the transplanted kidney usually develop in association with renal infection or the infection of other fluid collections in the immunocompromised patient. On US examination, abscess appears as a complex fluid collection, possibly containing gas.[410] Fluid aspiration is usually necessary for the accurate characterization of fluid within a collection. Because blood products have characteristic signal intensities on T1- and T2-weighted sequences, MRI can provide specific diagnostic information that may help avoid an unnecessary interventional procedure in cases of hematoma.

Renal obstruction or hydronephrosis may be observed in the transplanted kidney with renal dysfunction. US is the best means for assessment.[411] In the immediate posttransplantation period, mild caliectasis is common as a result of edema at the ureteral anastomosis site. Obstruction may also be caused by fluid collections around the transplanted kidney that may be visible also with US. Blood clots within the pelvicalyceal system may also lead to hydronephrosis. Later strictures may occur, primarily at the ureteral anastomosis site. Renal stones may also cause hydronephrosis during their passage to the bladder. A functional obstruction may be visible with an overdistended bladder. With bladder emptying, US demonstrates a resolution of the hydronephrosis.

Hypertension with or without renal dysfunction may be observed in many transplant recipients.[410] Vascular and nonvascular causes must be differentiated. Doppler US is the first step of evaluation. RAS may be found in up to 23% of patients.[418] The stenosis may occur before the anastomosis in the iliac artery, at the anastomosis site, or more distally. In more than one-half the cases, the stenosis is at the anastomotic site, and it is more common in end-to-end anastomosis. CT or MRA is used to determine the site and the degree of stenosis (Fig. 25.96). Angioplasty is successful in managing most cases.[418]

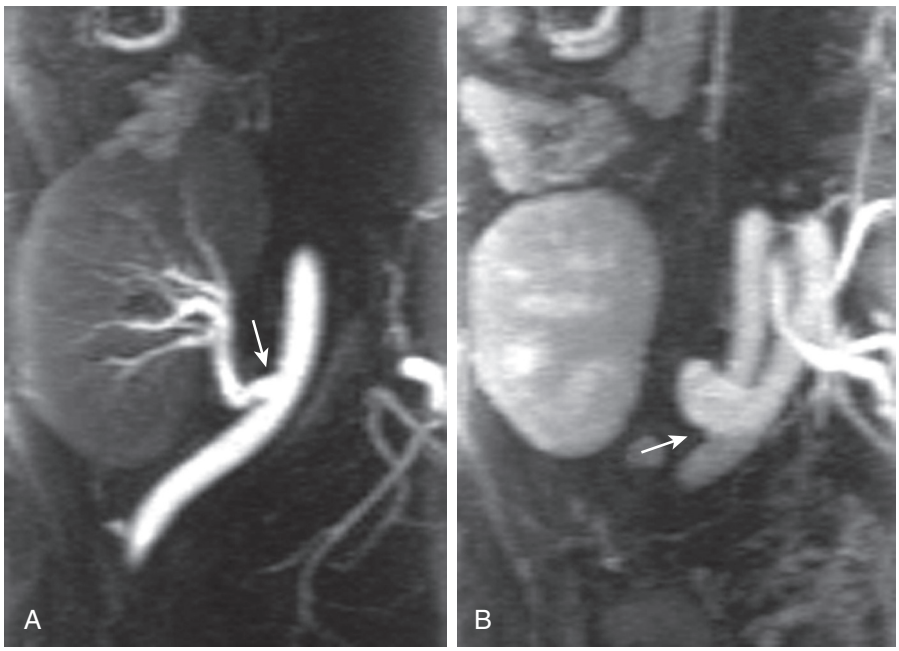

Fig. 25.96 Renal transplant magnetic resonance angiogram, showing normal arterial (**A**) and normal venous (**B**) anastomoses *(arrows).*

Arteriovenous fistulas may occur in transplant recipients after kidney biopsy. Most close spontaneously within 4 to 6 weeks. Grayscale images demonstrate only a simple- or complex-appearing cystic structure, whereas Doppler color-flow and duplex Doppler imaging demonstrate high-velocity and turbulent flow localized to a single segmental or interlobar artery and the adjacent vein. Arterialized flow is noted in the draining vein. If the structure is large and growing, embolization may become necessary.

Neoplasms occur in transplant recipients with increased frequency, up to 100 times more frequently than in the general population.[410] Neoplasms develop as a result of prolonged immunosuppression. The risk for renal cell carcinoma in the transplanted kidney may be increased.[419] Posttransplantation lymphoproliferative disorder may also occur in renal transplant recipients.[420] Although the transplanted kidney may be involved, the most frequent sites are the brain, liver, lungs, and gastrointestinal tract. The appearance is similar to that of conventional lymphomas with mass lesions in the organs, with or without associated adenopathy.

The MRI findings of renal transplant rejection are nonspecific (Fig. 25.97). Sadowski et al demonstrated the feasibility of using BOLD MRI to evaluate the renal transplant oxygen status and presence of acute rejection.[421] The authors concluded that MRI may differentiate acute rejection from normal function and acute tubular necrosis, but further research is required. Animal research is being performed with the hope of using noninvasive diffusion MRI techniques as a tool for monitoring early renal graft rejection after transplantation.[127]

Nuclear medicine procedures are also employed in the renal transplant recipient and play a role in the assessment of the complications associated with transplantation. These include vascular compromise (arterial or venous thrombosis), lymphocele formation, urine extravasation, acute tubular necrosis, drug toxicity, and organ rejection. Scintigraphy provides important imaging information about these potential complications, which can then guide corrective intervention.[422]

An early complication may be hyperacute rejection, which is often apparent immediately after transplantation and is caused by preformed cytotoxic antibodies. Other early complications include sudden decline in urine output and acute urinary obstruction. Scintigraphy with ^{99m}Tc-DTPA or ^{99m}Tc-MAG3 demonstrates absence of perfusion and function with complete thrombosis in the renal artery or renal vein. A sensitive but nonspecific sign of acute rejection is the finding of more than a 20% decline in the ratio of renal activity to the aortic activity.[423]

Renal scintigraphy performed a few days after the transplantation often reveals intact perfusion but delayed and decreased excretion of the tracer and some cortical retention of the tracer. These findings are typically caused by acute tubular necrosis and are more common with cadaveric grafts

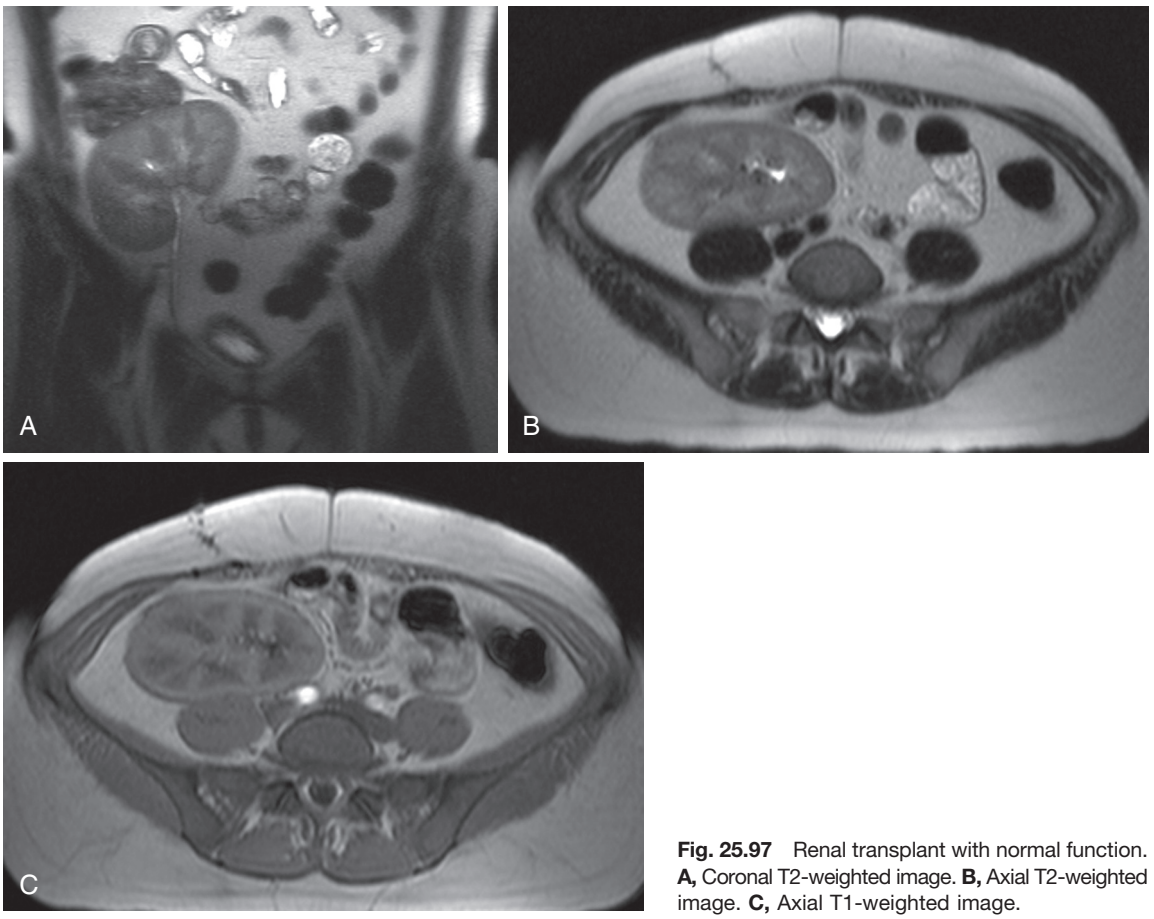

Fig. 25.97 Renal transplant with normal function. **A,** Coronal T2-weighted image. **B,** Axial T2-weighted image. **C,** Axial T1-weighted image.

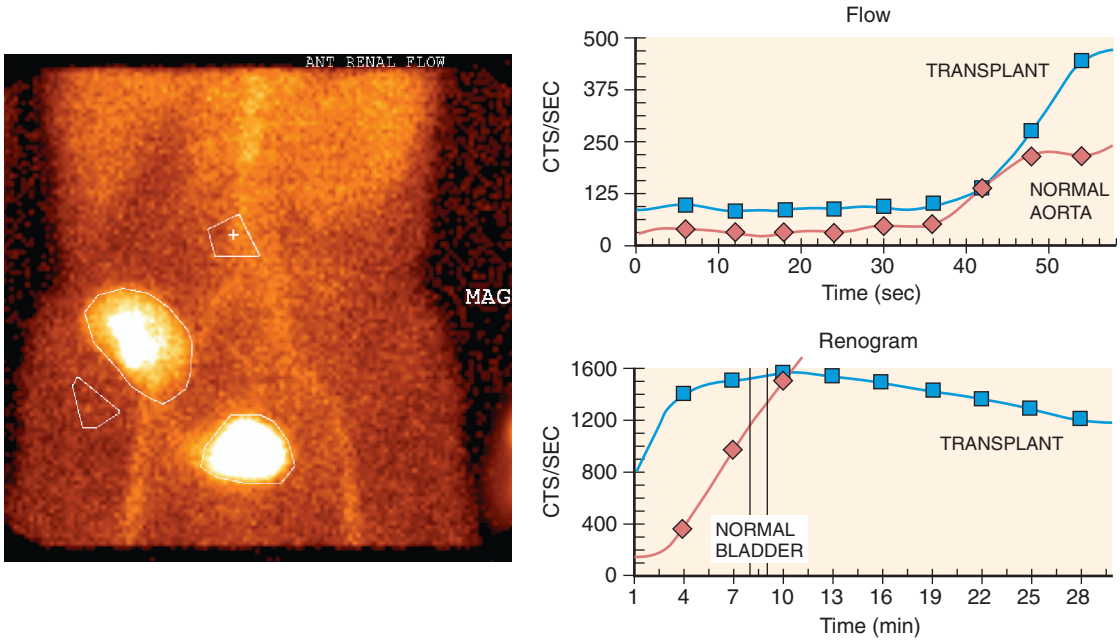

Fig. 25.98 Abnormal technetium 99m-labeled mercaptoacetyltriglycine renogram. The pattern involving the right pelvic renal transplant from a living related donor is compatible with acute tubular necrosis.

than with grafts from living related donors (Fig. 25.98). If both perfusion and function continue to decline, then the possibility of rejection should be considered. However, acute tubular necrosis, obstruction, drug (cyclosporine) toxicity, and rejection can produce relatively similar scintigraphic appearances. The differential diagnosis should be considered in the clinical context and with regard to the interval since transplantation, although two or more of these conditions may coexist. In one report, a nonascending second phase of ^{99m}Tc-MAG3 renogram curve was predictive of graft dysfunction. However, patients with acute tubular necrosis were not significantly more likely to have a nonascending curve than were those with acute rejection. An ascending curve was nonspecific and could be observed in both normally and poorly functioning grafts.[424]

Urine extravasation may be noted on the renal scans as collections of excreted radiotracers outside of the transplanted kidney and the urinary bladder. Because of small urine leaks and impaired renal transplant function, it may be difficult to identify a leak on scintigraphy. However, a cold-appearing defect that becomes warmer in appearance with time on the sequential images usually represents a urinoma or a urinary leak. If the activity declines with voiding, then the finding probably represents a urinoma. A chronic photopenic defect may represent a hematoma or a lymphocele (or both).[425] For assessing potential obstructive disease, scintigraphy with a diuretic may be considered, as previously discussed. Results of an animal-based study also suggested that FDG-PET may have a role in early detection of graft rejection by demonstrating significantly elevated graft tracer uptake induced by inflammatory infiltrates.[426]

ACKNOWLEDGMENTS

The authors would like to acknowledge Sona Devedjian for manuscript preparation and William Boswell for advice.

Complete reference list available at ExpertConsult.com.

KEY REFERENCES

3. ACR appropriateness criteria. *Hematuria.* Available at: https://acsearch.acr.org/docs/69490/Narrative/. Accessed July 26, 2018.
4. Dyer RB, Chen MYM, Zagoria RF. Intravenous urography: technique and interpretation. *Radiographics.* 2001;21:799–824.
25. Lang EK, Macchia RJ, Thomas R, et al. Improved detection of renal pathologic features on multiphasic helical CT compared with IVU in patients presenting with microscopic hematuria. *Urology.* 2003;61:528–532.
27. Coursey CA, Nelson RC, Boll DT, et al. Dual-energy multidetector CT: how does it work, what can it tell us, and when can we use it in abdominopelvic imaging? *Radiographics.* 2010;30:1037–1055.
45. American College of Radiology Committee on Drugs and Contrast Media: *ACR manual on contrast media, V 10.3*, 2017. Available at <https://www.acr.org/Clinical-Resources/Contrast-Manual>. Accessed January 11, 2018.
48. Kidney Disease: Improving Global Outcomes: *KDIGO clinical practice guideline for acute kidney injury.* Available at: <http://www.kdigo.org/clinical_practice_guidelines/AKI.php>. Accessed June 20, 2015.
53. Davenport MS, Khalatbari S, Dillman JR, et al. Contrast material-induced nephrotoxicity and intravenous low-osmolality iodinated contrast material. *Radiology.* 2013;267:94–105.
57. Thomsen HS. European Society of Urogenital Radiology guidelines on contrast media application. *Curr Opin Urol.* 2007;17:70–76.
79. Shellock FG, ed. *Reference Manual for Magnetic Resonance Safety, Implants and Devices.* ed 2014. Los Angeles: Biomedical Research Publishing Company; 2014.
80. Rofsky NM, Weinreb JC, Bosniak MA, et al. Renal lesion characterization with gadolinium-enhanced MR imaging: efficacy and safety in patients with renal insufficiency. *Radiology.* 1991;180:85–89.
127. Zhang JL, Rusinek H, Chandarana H, et al. Functional MRI of the kidneys. *J Magn Reson Imaging.* 2013;37:282–293.
130. He W, Fischman AJ. Nuclear imaging in the genitourinary tract: recent advances and future directions. *Radiol Clin North Am.* 2008;46:25–43.
143. Esteves FP, Taylor A, Manatunga A, et al. 99mTc-MAG3 renography: normal values for MAG3 clearance and curve parameters, excretory parameters, and residual urine volume. *AJR Am J Roentgenol.* 2006;187:W610–W617.

144. *ACR appropriateness criteria: renal failure*. Available at: <http://www.acr.org/Quality-Safety/Appropriateness-Criteria/Diagnostic/~/media/ACR/Documents/AppCriteria/Diagnostic/RenalFailure.pdf>. Accessed January 11, 2018.
164. Dyer RB, Chen MYM, Zagoria RJ. Abnormal calcifications in the urinary tract. *Radiographics*. 1998;18:1405–1424.
175. *ACR appropriateness criteria: acute onset flank pain*. Available at: <http://www.acr.org/Quality-Safety/Appropriateness-Criteria/Diagnostic/Urologic-Imaging>. Accessed January 11, 2018.
182. Cheng PM, Moin P, Dunn MD, et al. What the radiologist needs to know about urolithiasis: part I: pathogenesis, types, assessment, and variant anatomy. *AJR Am J Roentgenol*. 2012;198:W540–W547.
183. Cheng PM, Moin P, Dunn MD, et al. What the radiologist needs to know about urolithiasis: part II: CT findings, reporting, and treatment. *AJR Am J Roentgenol*. 2012;198:W548–W554, 165.
198. Boll DT, Patil NA, Paulson EK, et al. Renal stone assessment with dual-energy multidetector CT and advanced postprocessing techniques: improved characterization of renal stone composition—pilot study. *Radiology*. 2009;250:813–820.
204. Takahashi N, Kawashima A, Ernst RD, et al. Ureterolithiasis: can clinical outcome be predicted with unenhanced helical CT? *Radiology*. 1998;208:97–102.
209. Kawashima A, Sandler CM, Goldman SM, et al. CT of renal inflammatory disease. *Radiographics*. 1997;17:851–866.
219. *ACR appropriateness criteria: acute pyelonephritis*. Available at: <http://www.acr.org/Quality-Safety/Appropriateness-Criteria/Diagnostic/Urologic-Imaging>. Accessed January 11, 2018.
225. Ziessman HA, Majd M. Importance of methodology on (99m) technetium dimercapto-succinic acid scintigraphic image quality: imaging pilot study for RIVUR (Randomized Intervention for Children with Vesicoureteral Reflux) multicenter investigation. *J Urol*. 2009;182:272–279.
234. Kenney PJ. Imaging of chronic renal infections. *AJR Am J Roentgenol*. 1990;155:485–494.
240. Bosniak Morton A. The use of the Bosniak classification system for renal cysts and cystic tumors. *J Urol*. 1997;157:1852–1853.
243. Israel GM, Hindman N, Bosniak MA. Evaluation of cystic renal masses: comparison of CT and MR imaging by using the Bosniak classification system. *Radiology*. 2004;231:365–371.
245. Hecht EM, Israel GM, Krinsky GA, et al. Renal masses: quantitative analysis of enhancement with signal intensity measurements versus qualitative analysis of enhancement with image subtraction for diagnosing malignancy at MR imaging. *Radiology*. 2004;232:373–378.
260. Hartman DS, Choyke PL, Hartman MS. From the RSNA refresher courses: a practical approach to the cystic renal mass. *Radiographics*. 2004;24:S101–S115.
264. Israel GM, Bosniak MA. Follow-up CT of moderately complex cystic lesions of the kidney (Bosniak category IIF). *AJR Am J Roentgenol*. 2003;181:627–633.
272. Patard JJ. Incidental renal tumours. *Curr Opin Urol*. 2009;19:454–458.
273. Berland LL, Silverman SG, Gore RM, et al. Managing incidental findings on abdominal CT: white paper of the ACR incidental findings committee. *J Am Coll Radiol*. 2010;7:754–773.
285. Bosniak M, Megibow AJ, Hulnick DH, et al. CT diagnosis of renal angiomyolipoma: the importance of detecting small amounts of fat. *AJR Am J Roentgenol*. 1988;151:497–501.
294. Davidson AJ, Hartman DS, Choyke PL, et al. Radiologic assessment of renal masses: implications for patient care. *Radiology*. 1997;202:297–305.
297. Suh M, Coakley FV, Qayyum A, et al. Distinction of renal cell carcinomas from high-attenuation renal cysts at portal venous phase contrast–enhanced CT. *Radiology*. 2003;228:330–334.
304. Kim JK, Kim TK, Ahn HJ, et al. Differentiation of subtypes of renal cell carcinoma on helical CT scans. *AJR Am J Roentgenol*. 2002;178:1499–1506.
310. Browne RFJ, Meehan CP, Colville J, et al. Transitional cell carcinoma of the upper urinary tract: spectrum of imaging findings. *Radiographics*. 2005;25:1609–1627.
325. Zukotynski K, Lewis A, O'Regan K, et al. PET/CT and renal pathology: a blind spot for radiologists? Part 1: primary pathology. *AJR Am J Roentgenol*. 2012;199:W163–W167.
335. Wang HY, Ding HJ, Chen JH, et al. Meta-analysis of the diagnostic performance of [18F] FDG PET and PET/CT in renal cell carcinoma. *Cancer Imaging*. 2012;12:464–474.
341. Kayani I, Avril N, Bomanji J, et al. Sequential FDG-PET/CT as a biomarker of response to sunitinib in metastatic clear cell renal cancer. *Clin Cancer Res*. 2011;17:6021–6028.
360. *ACR appropriateness criteria: renovascular hypertension*. Available at: <https://acsearch.acr.org/docs/69374/Narrative/>. Accessed January 11, 2018.
377. Schoenberg SO, Knopp MV, Londy F, et al. Morphologic and functional magnetic resonance imaging of renal artery stenosis: a multireader tricenter study. *J Am Soc Nephrol*. 2002;13:158–169.
379. Soulez G, Oliva VL, Turpin S, et al. Imaging of renovascular hypertension: respective values of renal scintigraphy, renal Doppler US, and MR angiography. *Radiographics*. 2000;20:1355–1368.
390. Taylor A, Nally J, Aurell M, et al. Consensus report on ACE inhibitor renography for detecting renovascular hypertension. Radionuclides in Nephrourology Group. Consensus Group on ACEI Renography. *J Nucl Med*. 1996;37:1876–1882.
420. Patel NH, Jindal RM, Wilkin T, et al. Renal arterial stenosis in renal allografts: retrospective study of predisposing factors and outcome after percutaneous transluminal angioplasty. *Radiology*. 2001;219:663–667.
427. Canadian Association of Radiologists: *Consensus guidelines for the prevention of contrast induced nephropathy*. Available at: <http://www.car.ca/uploads/standards%20guidelines/20110617_en_prevention_cin.pdf>. Accessed June 20, 2015.

REFERENCES

1. Amis ES. Epitaph for the urogram. *Radiology*. 1999;213:639–640. [editorial].
2. Pollack HM, Banner MP. Current status of excretory urography: a premature epitaph? *Urol Clin North Am*. 1985;12:585–601.
3. ACR appropriateness criteria. *Hematuria* Available at: <https://acsearch.acr.org/docs/69490/Narrative/>. Accessed July 30, 2018.
4. Dyer RB, Chen MYM, Zagoria RF. Intravenous urography: technique and interpretation. *Radiographics*. 2001;21:799–824.
5. Hattery RR, Williamson B Jr, Hartman GW, et al. Intravenous urographic technique. *Radiology*. 1988;167:593–599.
6. Fry IK, Cattell WR. The nephrographic pattern during excretion urography. *Br Med Bull*. 1972;28:227–232.
7. Lasser EC, Berry CC, Talner LB, et al. Pre-treatment with corticosteroids to alleviate reactions to intravenous contrast material. *N Engl J Med*. 1987;317:845–849.
8. Amis ES, Hartman DS. Renal ultrasonography 1984: a practical overview. *Radiol Clin North Am*. 1984;22:315–332.
9. Chen P, Maklad N, Redwine M. Color and power Doppler imaging of the kidneys. *World J Urol*. 1998;16:41–45.
10. Jafri SZ, Madrazo BL, Miller JH. Color Doppler ultrasound of the genitourinary tract. *Curr Opin Radiol*. 1992;4:16–23.
11. Hricak H, Cruz C, Romanski R, et al. Renal parenchymal disease: sonographic-histologic correlation. *Radiology*. 1982;144:141–147.
12. Setola SV, Catalano O, Sandomenico F, et al. Contrast-enhanced sonography of the kidney. *Abdom Imaging*. 2007;32:21–28.
13. Gulati M, King K, Gill IS, et al. Contrast enhanced ultrasound (CEUS) of cystic and solid renal lesions: a review. *Abdom Imaging*. 2015;40(6):1982–1996. PubMed PMID: 25588715.
14. Catalano O, Aiani L, Barozzi L, et al. CEUS in abdominal trauma: multi-center study. *Abdom Imaging*. 2009;34:225–234.
15. Benozzi L, Cappelli G, Granito M, et al. Contrast-enhanced sonography in early kidney graft dysfunction. *Transplant Proc*. 2009;41:1214–1215.
16. Coleman BG. Ultrasonography of the upper genitourinary tract. *Urol Clin North Am*. 1985;12:633–644.
17. Wells PNT. Doppler ultrasound in medical diagnosis. *Br J Radiol*. 1989;62:399–420.
18. Tublin ME, Bude RO, Platt JF. Review—the resistive index in renal Doppler sonography: where do we stand? *AJR Am J Roentgenol*. 2003;180:885–892.
19. Keogan MT, Kliewer MA, Hertzberg BS, et al. Renal resistive indexes: variability in Doppler US measurements in a healthy population. *Radiology*. 1996;199:165–169.
20. Hounsfield GN. Computerized transverse axial scanning (tomography): part I: description of system. *Br J Radiol*. 1973;46:1016–1022.
21. Horton KM, Sheth S, Corl F, et al. Multidetector row CT: principles and clinical applications. *Crit Rev Comput Tomogr*. 2002;43:143–181.
22. Saunders HS, Dyer RB, Shifrin RY, et al. The CT nephrogram: implications for evaluation of urinary tract disease. *Radiographics*. 1995;15:1069–1085.
23. Perlman ES, Rosenfield AT, Wexler JS, et al. CT urography in the evaluation of urinary tract disease. *J Comput Assist Tomogr*. 1996;20:620–626.
24. Sudakoff GS, Dunn DP, Hellman RS, et al. Opacification of the genitourinary collecting system during MDCT urography with enhanced CT digital radiography: nonsaline versus saline bolus. *AJR Am J Roentgenol*. 2006;186:122–129.
25. Lang EK, Macchia RJ, Thomas R, et al. Improved detection of renal pathologic features on multiphasic helical CT compared with IVU in patients presenting with microscopic hematuria. *Urology*. 2003;61:528–532.
26. Kawashima A, Glockner JF, King BF. CT urography and MR urography. *Radiol Clin North Am*. 2003;41:945–961.
27. Coursey CA, Nelson RC, Boll DT, et al. Dual-energy multidetector CT: how does it work, what can it tell us, and when can we use it in abdominopelvic imaging? *Radiographics*. 2010;30:1037–1055.
28. McTavish JD, Jinzaki M, Zou KH, et al. Multi-detector row CT urography: comparison of strategies for depicting the normal urinary collecting system. *Radiology*. 2002;225:783–790.
29. Engelstad BL, McClennan BL, Levitt RG, et al. The role of precontrast images in computed tomography of the kidney. *Radiology*. 1980;136:153–155.
30. McNicholas MM, Raptopoulos VD, Schwartz RK, et al. Excretory phase CT urography for opacification of the urinary collecting system. *AJR Am J Roentgenol*. 1998;170:1261–1267.
31. Caoili EM. Imaging of the urinary tract using multidetector computed tomography urography. *Semin Urol Oncol*. 2002;20:174–179.
32. Kocakoc E, Bhatt S, Dogra VS. Renal multidetector row CT. *Radiol Clin North Am*. 2005;43:1021–1047.
33. Caoili EM, Cohan RH, Korobkin M, et al. Urinary tract abnormalities: initial experience with multi-detector row CT urography. *Radiology*. 2002;222:353–360.
34. Joffe SA, Servaes S, Okon S, et al. Multi-detector row CT urography in the evaluation of hematuria. *Radiographics*. 2003;23:1441–1455.
35. Katzberg RW. Urography into the 21st century: new contrast media, renal handling, imaging characteristics and nephrotoxicity. *Radiology*. 1997;204:297–312.
36. Lasser EC. Etiology of anaphylactorial responses: the promise of nonionics. *Invest Radiol*. 1985;20:579–583.
37. Shehadi WH. Contrast media adverse reactions: occurrence, recurrence, and distribution patterns. *Radiology*. 1982;143:11–17.
38. Katayama H, Yamaguchi K, Kozuka T, et al. Adverse reactions to ionic and nonionic contrast media: a report from the Japanese Committee on the Safety of Contrast Media. *Radiology*. 1990;175:621–628.
39. Jacobsson BF, Jorulf H, Kalantar MS, et al. Nonionic versus ionic contrast media in intravenous urography: clinical trial in 1000 consecutive patients. *Radiology*. 1988;167:601–605.
40. Callahan MJ, Poznauskis L, Zurakowski D, et al. Nonionic iodinated intravenous contrast material-related reactions: incidence in large urban children's hospital—retrospective analysis of data in 12,494 patients. *Radiology*. 2009;250:674–681.
41. Brasch RC. Allergic reactions to contrast media: accumulated evidence. *AJR Am J Roentgenol*. 1980;134:797–801.
42. Lasser EC. Basic mechanisms of contrast media reactions: theoretical and experimental considerations. *Radiology*. 1968;91:63–65.
43. Greenberger PA, Patterson R. The prevention of immediate generalized reactions to radiocontrast media in high-risk patients. *J Allergy Clin Immunol*. 1991;87(4):867–872. PMID: 2013681.
44. Mervak BM, Cohan RH, Ellis JH, et al. Intravenous corticosteroid premedication administered 5 hours before CT compared with a traditional 13-hour oral regimen. *Radiology*. 2017;285(2):425–433. doi:10.1148/radiol.2017170107. [Epub 2017 Jul 26]; PubMed PMID: 28745940.
45. American College of Radiology Committee on Drugs and Contrast Media: *ACR manual on contrast media, V 10.3*, 2018. Available at <https://www.acr.org/Clinical-Resources/Contrast-Manual> Accessed July 30, 2018.
46. Kolonko A, Wiecek A. Contrast-associated nephropathy: old clinical problem and new therapeutic perspectives. *Nephrol Dial Transplant*. 1998;13:803–806.
47. Mehta RL, Kellum JA, Shah SV, et al. Acute Kidney Injury Network: report of an initiative to improve outcomes in acute kidney injury. *Crit Care*. 2007;11:R31.
48. Kidney Disease: Improving Global Outcomes: *KDIGO clinical practice guideline for acute kidney injury*. Available at: <http://www.kdigo.org/clinical_practice_guidelines/pdf/KDIGO%20AKI%20Guideline.pdf> Accessed January 11, 2018.
49. Luk L, Steinman J, Newhouse JH. Intravenous contrast-induced nephropathy-the rise and fall of a threatening idea. *Adv Chronic Kidney Dis*. 2017;24(3):169–175. doi:10.1053/j.ackd.2017.03.001. PubMed PMID: 28501080. Review.
50. Davenport MS, Cohan RH, Khalatbari S, et al. The challenges in assessing contrast-induced nephropathy: where are we now? *AJR Am J Roentgenol*. 2014;202(4):784–789.
51. Karlsberg RP, Dohad SY, Sheng R. Contrast medium-induced acute kidney injury: comparison of intravenous and intraarterial administration of iodinated contrast medium. *J Vasc Interv Radiol*. 2011;22(8):1159–1165.
52. Nyman U, Almen T, Jacobsson B, et al. Are intravenous injections of contrast media really less nephrotoxic than intraarterial injections? *Eur Radiol*. 2012;22(6):1366–1371.
53. Davenport MS, Khalatbari S, Dillman JR, et al. Contrast material-induced nephrotoxicity and intravenous low-osmolality iodinated contrast material. *Radiology*. 2013;267:94–105.
54. McDonald RJ, McDonald JS, Bida JP, et al. Intravenous contrast material–induced nephropathy: causal or coincident phenomenon? *Radiology*. 2013;267:106–118.

55. Kim SM, Cha RH, Lee JP, et al. Incidence and outcomes of contrast-induced nephropathy after computed tomography in patients with CKD: a quality improvement report. *Am J Kidney Dis.* 2010;55(6):1018–1025.
56. Weisbord SD, Mor MK, Resnick AL, et al. Incidence and outcomes of contrast-induced AKI following computed tomography. *Clin J Am Soc Nephrol.* 2008;3(5):1274–1281.
57. Thomsen HS. European Society of Urogenital Radiology guidelines on contrast media application. *Curr Opin Urol.* 2007;17:70–76.
58. European Society of Urogenital Radiology: *ESUR guidelines on contrast media.* Available at: <http://www.esur.org/guidelines/>. Accessed June 27, 2015.
59. Wilhelm-Leen E, Montez-Rath ME, Chertow G. Estimating the risk of radiocontrast-associated nephropathy. *J Am Soc Nephrol.* 2017;28(2):653–659. doi:10.1681/ASN.2016010021. [Epub 2016 Sep 29]; PubMed PMID: 27688297. PubMed Central PMCID: PMC5280012.
60. Silver SA, Shah PM, Chertow GM, et al. Risk prediction models for contrast induced nephropathy: systematic review. *BMJ.* 2015;351:h4395. doi:10.1136/bmj.h4395. Review. Erratum in: *BMJ.* 2015;351:h5401.PubMed PMID: 26316642; PubMed Central PMCID: PMC4784870.
61. Su X, Xie X, Liu L, et al. Comparative effectiveness of 12 treatment strategies for preventing contrast-induced acute kidney injury: a systematic review and Bayesian network meta-analysis. *Am J Kidney Dis.* 2017;69(1):69–77. doi:10.1053/j.ajkd.2016.07.033. [Epub 2016 Oct 1]; PubMed PMID: 27707552. Review.
62. Taylor AJ, Hotchkiss D, Morse RM, et al. PREPARED: preparation for angiography in renal dysfunction: a randomized trial of inpatient vs outpatient hydration protocols for cardiac catheterization in mild-to-moderate renal dysfunction. *Chest.* 1998;114:1570–1574.
63. Trivedi HS, Moore H, Nasr S, et al. A randomized prospective trial to assess the role of saline hydration on the development of contrast nephrotoxicity. *Nephron Clin Pract.* 2003;93:C29–C34.
64. Cho R, Javed N, Traub D, et al. Oral hydration and alkalinization is noninferior to intravenous therapy for prevention of contrast-induced nephropathy in patients with chronic kidney disease. *J Interv Cardiol.* 2010;23:460–466.
65. *KDIGO clinical practice guideline for acute kidney injury.* Available at: <http://www.kdigo.org/clinical_practice_guidelines/pdf/KDIGO%20AKI%20Guideline.pdf> Accessed January 11, 2018.
66. Mao C, Chacko B. Contrast-associated nephropathy: does the route of administration matter? *Clin Nephrol.* 2018;doi:10.5414/CN109519. [Epub ahead of print]; PubMed PMID: 29932411.
67. Bader CD, Berger ED, Heede MB, et al. What is the best hydration regimen to prevent contrast media-induced nephrotoxicity? *Clin Nephrol.* 2004;62:1–7.
68. Merten GJ, Burgess WP, Gray LV, et al. Prevention of contrast-induced nephropathy with sodium bicarbonate: a randomized controlled trial. *JAMA.* 2004;291:2328–2334.
69. Brar SS, Hiremath S, Dangas G, et al. Sodium bicarbonate for the prevention of contrast induced acute kidney injury: a systematic review and meta-analysis. *Clin J Am Soc Nephrol.* 2009;4:1584–1592.
70. Trivedi H, Nadella R, Szabo A. Hydration with sodium bicarbonate for the prevention of contrast-induced nephropathy: a meta-analysis of randomized controlled trials. *Clin Nephrol.* 2010;74:288–296.
71. Heinrich MC, Haberle L, Muller V, et al. Nephrotoxicity of iso-osmolar iodixanol compared with nonionic low osmolar contrast media: meta-analysis of randomized controlled trials. *Radiology.* 2009;250(1):68–86.
72. Tamura A, Goto Y, Miyamoto K, et al. Efficacy of single-bolus administration of sodium bicarbonate to prevent contrast-induced nephropathy in patients with mild renal insufficiency undergoing an elective coronary procedure. *Am J Cardiol.* 2009;104:921–925.
73. Zagler A, Azadpour M, Mercado C, et al. *N*-acetylcysteine and contrast-induced nephropathy: a meta-analysis of 13 randomized trials. *Am Heart J.* 2006;151(1):140–145.
74. Prince MR, Zhang H, Morris M, et al. Incidence of nephrogenic systemic fibrosis at two large medical centers. *Radiology.* 2008;248:807–816.
75. Sun Z, Fu Q, Cao L, et al. Intravenous *N*-acetylcysteine for prevention of contrast-induced nephropathy: a meta-analysis of randomized, controlled trials. *PLoS ONE.* 2013;8:e55124.
76. Patschan D, Buschmann I, Ritter O. Contrast-induced nephropathy: update on the use of crystalloids and pharmacological measures. *Int J Nephrol.* 2018;2018:5727309. doi:10.1155/2018/5727309. PubMed PMID: 29854458. eCollection 2018. Review, PubMed Central PMCID: PMC5954945.
77. Schild HH. *MRI Made Easy.* Wayne, NJ: Berlex Laboratories; 1999.
78. Hashemi RH, Bradley WG, Lisanti CJ. *MRI: The Basics.* ed 2. Philadelphia: Lippincott Williams & Wilkins; 2004.
79. Shellock FG, ed. *Reference Manual for Magnetic Resonance Safety, Implants and Devices.* ed 2014. Los Angeles: Biomedical Research Publishing Company; 2014.
80. Rofsky NM, Weinreb JC, Bosniak MA, et al. Renal lesion characterization with gadolinium-enhanced MR imaging: efficacy and safety in patients with renal insufficiency. *Radiology.* 1991;180:85–89.
81. Mitchell DG, Cohen MS. *MRI Principles.* ed 2. Philadelphia: WB Saunders; 2004.
82. Keogan MT, Edelman RR. Technologic advances in abdominal MR imaging. *Radiology.* 2001;220:310–320.
83. Shellock FG, ed. *Reference Manual for Magnetic Resonance Safety, Implants and Devices.* ed 2014. Los Angeles: Biomedical Research Publishing Company; 2014.
84. Bansal GJ, Darby M. Measurement of change in estimated glomerular filtration rate in patients with renal insufficiency after contrast-enhanced computed tomography: a case-control study. *J Comput Assist Tomogr.* 2009;33:455–459.
85. <http://www.mrisafety.com>. Accessed January 11, 2018.
86. Prince MR, Zhang H, Zou Z, et al. Incidence of immediate gadolinium contrast media reactions. *AJR Am J Roentgenol.* 2011;196:W138–W143.
87. Prince MR, Arnoldus C, Frisoli JK. Nephrotoxicity of high-dose gadolinium compared with iodinated contrast. *J Magn Reson Imaging.* 1996;6:162–166.
88. Rofsky NM, Weinreb JC, Bosniak MA, et al. Renal lesion characterization with gadolinium-enhanced MR imaging: efficacy and safety in patients with renal insufficiency. *Radiology.* 1991;180:85–89.
89. Townsend RR, Cohen DL, Katholi R, et al. Safety of intravenous gadolinium (Gd-BOPTA) infusion in patients with renal insufficiency. *Am J Kidney Dis.* 2000;36:1207–1212.
90. Cohen MD. Safe use of imaging contrast agents in children. *J Am Coll Radiol.* 2009;6:576–581.
91. Sam AD, Morasch MD, Collins J, et al. Safety of gadolinium contrast angiography in patients with chronic renal insufficiency. *J Vasc Surg.* 2003;38:313–318.
92. Ergün I, Keven K, Uruc I, et al. The safety of gadolinium in patients with stage 3 and 4 renal failure. *Nephrol Dial Transplant.* 2006;21:697–700.
93. Nainani N, Panesar M. Nephrogenic systemic fibrosis. *Am J Nephro.* 2009;29:1–9.
94. *ACR Contrast manual—risk of nephrogenic systemic fibrosis.* Available at: <https://www.acr.org/-/media/ACR/Files/Clinical-Resources/Contrast_Media.pdf#page=88>. Accessed January 11, 2018.
95. Grobner T. Gadolinium: a specific trigger for the development of nephrogenic fibrosing dermopathy and nephrogenic systemic fibrosis? *Nephrol Dial Transplant.* 2006;21:1104–1108.
96. Marckmann P, Skov L, Rossen K, et al. Nephrogenic systemic fibrosis: suspected causative role of gadodiamide used for contrast-enhanced magnetic resonance imaging. *J Am Soc Nephrol.* 2006;17:2359–2362.
97. Maloo M, Abt P, Kashyap R, et al. Nephrogenic systemic fibrosis among liver transplant recipients: a single institution experience and topic update. *Am J Transplant.* 2006;6:2212–2217.
98. Sadowski EA, Bennett LK, Chan MR, et al. Nephrogenic systemic fibrosis: risk factors and incidence estimation. *Radiology.* 2007;243(1):148–157.
99. Wertman R, Altun E, Martin DR, et al. Risk of nephrogenic systemic fibrosis: evaluation of gadolinium chelate contrast agents at four American universities. *Radiology.* 2008;248(3):799–806.
100. Collidge TA, Thomson PC, Mark PB, et al. Gadolinium-enhanced MR imaging and nephrogenic systemic fibrosis: retrospective study of a renal replacement therapy cohort. *Radiology.* 2007;245(1):168–175.
101. Kanal E, Barkovich AJ, Bell C, et al. ACR guidance document for safe MR practices: 2013. *J Magn Reson Imaging.* 2013;37:501–530.
102. Cowper SE: *Nephrogenic systemic fibrosis.* Available at: <http://www.icnfdr.org>. Accessed January 11, 2018.
103. U.S. Food and Drug Administration: *FDA evaluating the risk of brain deposits with repeated use of gadolinium-based contrast agents for magnetic resonance imaging (MRI).* <https://www.fda.gov/downloads/drugs/drugsafety/ucm455390.pdf>. Accessed January 11, 2018.
104. FDA. <https://www.fda.gov/Drugs/DrugSafety/ucm559007.htm>.

105. Kanda T, Fukusato T, Matsuda M, et al. Gadolinium-based contrast agent accumulates in the brain even in subjects without severe renal dysfunction: evaluation of autopsy brain specimens with inductively coupled plasma mass spectroscopy. *Radiology*. 2015;276(1):228–232.
106. McDonald RJ, McDonald JS, Kallmes DF, et al. Intracranial gadolinium deposition after contrast-enhanced MR imaging. *Radiology*. 2015;275(3):772–782.
107. Hehra A, McDonald RJ, Bluhm AM, et al. Accumulation of gadolinium in human cerebrospinal fluid after gadobutrol-enhanced MRI imaging: a prospective observational cohort study. *Radilogy*. 2018;288:416–423.
108. Jost G, Frenzel T, Lohrke J, et al. Penetration and distribution of gadolinium-based contrast agents into the cerebrospinal fluid in healthy rats: a potential pathway of entry into the brain tissue. *Eur Radiol*. 2017;27(7):2877–2885.
109. Murata N, Gonzalez-Cuyar LF, Murata K, et al. Macrocyclic and other non-group 1 gadolinium contrast agents deposit low levels of gadolinium in brain and bone tissue: preliminary results from 9 patients with normal renal function. *Invest Radiol*. 2016;51(7):447–453.
110. Thomsen HS, Marckmann P, Logager VB. Update on nephrogenic systemic fibrosis. *Magn Reson Imaging Clin N Am*. 2008;16:551–560, vii.
111. Chung JJ, Semelka RC, Martin DR. Acute renal failure: common occurrence of preservation of corticomedullary differentiation on MR images. *Magn Reson Imaging*. 2001;19:789–793.
112. Semelka RC, Corrigan K, Ascher SM, et al. Renal corticomedullary differentiation: observation in patients with differing serum creatinine levels. *Radiology*. 1994;190:149–152.
113. Lee VS, Rofsky NM, Krinsky GA, et al. Single-dose breath-hold gadolinium-enhanced three-dimensional MR angiography of the renal arteries. *Radiology*. 1999;211:69–78.
114. Kopka L, Vosshenrich R, Rodenwaldt J, et al. Differences in injection rates on contrast-enhanced breath-hold three-dimensional MR angiography. *AJR Am J Roentgenol*. 1998;170:345–348.
115. Mitsuzaki K, Yamashita Y, Ogata I, et al. Optimal protocol for injection of contrast material at MR angiography: study of healthy volunteers. *Radiology*. 1999;213:913–918.
116. Wheaton AJ, Miyazik M. Non-contrast enhanced MR angiography: physical principles. *J Magn Reson Imaging*. 2012;36:286–304.
117. Worters PW, Saranathan M, Zu A, et al. Inversion-recovery-prepared Dixon bSSFP: initial clinical experience with a novel pulse sequence for renal MRA within a breathhold. *J Magn Reson Imaging*. 2012;35:875–881.
118. Alley MT, Shifrin RY, Pelc NJ, et al. Ultrafast contrast-enhanced three-dimensional MR angiography: state of the art. *Radiographics*. 1998;18:273–285.
119. Baskaran V, Pereles FS, Nemcek AA, et al. Gadolinium-enhanced 3D MR angiography of renal artery stenosis: a pilot comparison of maximum intensity projection, multiplanar reformatting, and 3D volume-rendering postprocessing algorithms. *Acad Radiol*. 2002;9:50–59.
120. Prince MR, Schoenberg SO, Ward JS, et al. Hemodynamically significant atherosclerotic renal artery stenosis: MR angiographic features. *Radiology*. 1997;205:128–136.
121. Willmann JK, Wildermuth S, Pfammatter T, et al. Aortoiliac and renal arteries: prospective intraindividual comparison of contrast-enhanced three-dimensional MR angiography and multi-detector row CT angiography. *Radiology*. 2003;226:798–811.
122. Jara H, Barish MA, Yucel EK, et al. MR hydrography: theory and practice of static fluid imaging. *AJR Am J Roentgenol*. 1998;170:873–882.
123. Nolte-Ernsting CCA, Bücker A, Adam GB, et al. Gadolinium-enhanced excretory MR urography after low-dose diuretic injection: comparison with conventional excretory urography. *Radiology*. 1998;209:147–157.
124. Sudah M, Vanninen RL, Partanen K, et al. Patients with acute flank pain: comparison of MR urography with unenhanced helical CT. *Radiology*. 2002;223:98–105.
125. Nolte-Ernsting CCA, Staatz G, Tacke J, et al. MR urography today. *Abdom Imaging*. 2003;28:191–209.
126. El-Diasty T, Mansour O, Farouk A. Diuretic contrast-enhanced magnetic resonance urography versus intravenous urography for depiction of nondilated urinary tracts. *Abdom Imaging*. 2003;28:135–145.
127. Zhang JL, Rusinek H, Chandarana H, et al. Functional MRI of the kidneys. *J Magn Reson Imaging*. 2013;37:282–293.
128. Perlman SB, Bushnell DL, Barnes WE. Genitourinary system. In: Wilson MA, ed. *Textbook of Nuclear Medicine*. Philadelphia: Lippincott-Raven; 1998:117–136.
129. Yang D, Ye Q, Williams DS, et al. Normal and transplanted rat kidneys: diffusion MR imaging at 7 T. *Radiology*. 2004;231:702–709.
130. He W, Fischman AJ. Nuclear imaging in the genitourinary tract: recent advances and future directions. *Radiol Clin North Am*. 2008;46:25–43.
131. Szabo Z, Xia J, Mathews WB. Radiopharmaceuticals for renal positron emission tomography imaging. *Semin Nucl Med*. 2008;38:20–31.
132. Mejia AA, Nakamura T, Masatoshi I, et al. Estimation of absorbed doses in humans due to intravenous administration of fluorine-18–fluorodeoxyglucose in PET studies. *J Nucl Med*. 1991;32:699–706.
133. Ellenbogen PH, Schieble FW, Talner LB, et al. Sensitivity of gray scale US in detecting urinary tract obstruction. *AJR Am J Roentgenol*. 1978;130:731–733.
134. Hays MT, Watson EE, Thomas SR, et al. MIRD dose estimate report no. 19: radiation absorbed dose estimates from ^{18}F-FDG. *J Nucl Med*. 2002;43:210–214.
135. Jones SC, Alavi A, Christman D, et al. The radiation dosimetry of 2[F-18]fluoro-2-deoxy-D-glucose in man. *J Nucl Med*. 1982;23:613–617.
136. Laffon E, Cazeau AL, Monet A, et al. The effect of renal failure on ^{18}F-FDG uptake: a theoretic assessment. *J Nucl Med Technol*. 2008;36:200–202.
137. Minamimoto R, Takahashi N, Inoue T. FDG PET of patients with suspected renal failure: standardized uptake values in normal tissues. *Ann Nucl Med*. 2007;21:217–222.
138. Kuni CC, duCret RP. Genitourinary system. In: *Manual of Nuclear Medicine Imaging*. New York: Thieme; 1997:106–128.
139. Bagni B, Portaluppi F, Montanari L, et al. ^{99m}Tc-MAG3 versus ^{131}I-orthoiodohippurate in the routine determination of effective renal plasma flow. *J Nucl Med Allied Sci*. 1990;34:67–70.
140. Caglar M, Gedik GK, Karabulut E. Differential renal function estimation by dynamic renal scintigraphy: influence of background definition and radiopharmaceutical. *Nucl Med Commun*. 2008;29:1002–1005.
141. Lezaic L, Hodolic M, Fettich J, et al. Reproducibility of ^{99m}Tc-mercaptoacetyltriglycine renography: population comparison. *Nucl Med Commun*. 2008;29:695–704.
142. Schwartz BF, Dykes TE, Rubenstein JN, et al. Effect of position on renal parenchyma perfusion as measured by nuclear scintigraphy. *Urology*. 2007;70:227–229.
143. Esteves FP, Taylor A, Manatunga A, et al. ^{99m}Tc-MAG3 renography: normal values for MAG3 clearance and curve parameters, excretory parameters, and residual urine volume. *AJR Am J Roentgenol*. 2006;187:W610–W617.
144. *ACR appropriateness criteria: renal failure*. Available at: <https://acsearch.acr.org/docs/69492/Narrative/2018> Accessed on July 26 2018.
145. Yassa NA, Peng M, Ralls PW. Perirenal lucency ("kidney sweat"): a new sign of renal failure. *AJR Am J Roentgenol*. 1999;173:1075–1077.
146. Taliercio CP, Vietstra RE, Fisher LD, et al. Risks of renal dysfunction with cardiac angiography. *Ann Intern Med*. 1986;104:501–504.
147. Ritchie WW, Vick CW, Glocheski SK, et al. Evaluation of azotemic patients: diagnostic yield of initial US examination. *Radiology*. 1988;167:245–247.
148. Platt JF. Looking for renal obstruction: the view from renal Doppler US. *Radiology*. 1994;193:610–612.
149. Platt JF. Advances in ultrasonography of urinary tract obstruction. *Abdom Imaging*. 1998;23:3–9.
150. Platt JF. Urinary obstruction. *Radiol Clin North Am*. 1996;34:1113–1129.
151. Kamholtz RG, Cronan JJ, Dorfman GS. Obstruction and the minimally dilated renal collecting system: US evaluation. *Radiology*. 1989;170:51–53.
152. Cronan JJ. Contemporary concepts in imaging urinary tract obstruction. *Radiol Clin North Am*. 1991;29:527–542.
153. Mallek R, Bankier AA, Etele-Hainz A, et al. Distinction between obstructive and nonobstructive hydronephrosis: value of diuresis duplex Doppler sonography. *AJR Am J Roentgenol*. 1996;166:113–117.
154. Scola FH, Cronan JJ, Schepps B. Grade I hydronephrosis: pulsed Doppler US evaluation. *Radiology*. 1989;171:519–520.
155. Platt JF, Rubin JM, Ellis JH, et al. Duplex Doppler US of the kidneys: differentiation of obstructive from nonobstructive dilatation. *Radiology*. 1989;171:515–517.
156. Cronan JJ, Tublin ME. Role of the resistive index in the evaluation of acute renal obstruction. *AJR Am J Roentgenol*. 1995;164:377–378.

157. Platt JF, Ellis JH, Rubin JM. Role of renal Doppler imaging in the evaluation of acute renal obstruction. *AJR Am J Roentgenol.* 1995;164:379–380.
158. Platt JF, Rubin JM, Bowerman RA, et al. The inability to detect kidney disease on the basis of echogenicity. *AJR Am J Roentgenol.* 1988;151:317–319.
159. Page JE, Morgan SH, Eastwood JB, et al. Ultrasound findings in renal parenchymal disease: comparison with histological appearances. *Clin Radiol.* 1994;49:867–870.
160. Gourtsoyiannis N, Prassopoulos P, Cavouras D, et al. The thickness of the renal parenchyma decreases with age: a CT study of 360 patients. *AJR Am J Roentgenol.* 1990;155:541–544.
161. Marotti M, Hricak H, Terrier F, et al. MR in renal disease: importance of cortical-medullary distinction. *Magn Reson Med.* 1987;5:160–172.
162. Kim S, Naik M, Sigmund E, et al. Diffusion-weighted MR imaging of the kidneys and the urinary tract. *Magn Reson Imaging Clin N Am.* 2008;16:585–596, vii–viii.
163. Lin EC, Gellens ME, Goodgold HM. Prognostic value of renal scintigraphy with Tc-99m MAG3 in patients with acute renal failure. *J Nucl Med.* 1995;36:232P–233P.
164. Dyer RB, Chen MYM, Zagoria RJ. Abnormal calcifications in the urinary tract. *Radiographics.* 1998;18:1405–1424.
165. Taghavi R, Ariana K, Arab D. Diuresis renography for differentiation of upper urinary tract dilatation from obstruction: F+20 and F−15 methods. *Urol J.* 2007;4:36–40.
166. Sfakianakis GN, Sfakianaki F, Georgiou M, et al. A renal protocol for all ages and all indications: mercapto-acetyl-triglycine (MAG3) with simultaneous injection of furosemide (MAG3-F0): a 17-year experience. *Semin Nucl Med.* 2009;39:156–173.
167. Ginalski JM, Portmann L, Jaeger PH. Does medullary sponge kidney cause nephrolithiasis? *AJR Am J Roentgenol.* 1990;155:299–302.
168. Gibson MS, Puckett ML, Shelly ME. Renal tuberculosis. *Radiographics.* 2004;24:251–256.
169. Clark JY, Thompson IM, Optenberg SA. Economic impact of urolithiasis in the United States. *J Urol.* 1995;154:2020–2042.
170. Tublin ME, Murphy ME, Delong DM, et al. Conspicuity of renal calculi at unenhanced CT: effects of calculus composition and size and CT technique. *Radiology.* 2002;225:91–96.
171. Newhouse JH, Prien EL, Amis ES, et al. Computed tomographic analysis of urinary calculi. *AJR Am J Roentgenol.* 1984;142:545–548.
172. Hillman BJ, Drach GW, Tracey P, et al. Computed tomographic analysis of renal calculi. *AJR Am J Roentgenol.* 1984;142:549–552.
173. Mostafavi MR, Ernst RD, Saltzman B. Accurate determination of chemical composition of urinary calculi by spiral computerized tomography. *J Urol.* 1998;159:673–675.
174. Coll DM, Varanelli MJ, Smith RC. Relationship of spontaneous passage of ureteral calculi to stone size and location as revealed by unenhanced helical CT. *AJR Am J Roentgenol.* 2002;178:101–103.
175. *ACR appropriateness criteria: acute onset flank pain.* Available at: <https://acsearch.acr.org/docs/69362/Narrative/>Accessed on July 26, 2018.
176. Smith RC, Rosenfield AT, Choe KA, et al. Acute flank pain: comparison of non–contrast-enhanced CT and intravenous urography. *Radiology.* 1995;194:789–794.
177. Haddad MC, Sharif HS, Abomelha MS, et al. Management of renal colic: redefining the role of the urogram. *Radiology.* 1992;184: 35–36.
178. Middleton WD, Dodds WJ, Lawson TL, et al. Renal calculi: sensitivity for detection with US. *Radiology.* 1988;167:239–244.
179. Gottlieb RH, La TC, Erturk EN, et al. CT in detecting urinary tract calculi: influence on patient imaging and clinical outcomes. *Radiology.* 2002;225:441–449.
180. Sourtzis S, Thibeau JF, Damry N, et al. Radiologic investigation of renal colic: unenhanced helical CT compared with excretory urography. *AJR Am J Roentgenol.* 1999;172:1491–1494.
181. Boulay I, Holtz P, Foley WD, et al. Ureteral calculi: diagnostic efficacy of helical CT and implications for treatment of patients. *AJR Am J Roentgenol.* 1999;172:1485–1490.
182. Cheng PM, Moin P, Dunn MD, et al. What the radiologist needs to know about urolithiasis: part I: pathogenesis, types, assessment, and variant anatomy. *AJR Am J Roentgenol.* 2012;198: W540–W547.
183. Cheng PM, Moin P, Dunn MD, et al. What the radiologist needs to know about urolithiasis: part II: CT findings, reporting, and treatment. *AJR Am J Roentgenol.* 2012;198:W548–W554.
184. Katz DS, Hines J, Rausch DR, et al. Unenhanced helical CT for suspected renal colic. *AJR Am J Roentgenol.* 1999;173:425–430.
185. Haddad MC, Sharif HS, Shahed MS, et al. Renal colic: diagnosis and outcome. *Radiology.* 1992;184:83–88.
186. Smith RC, Rosenfield AT, Choe KA, et al. Acute flank pain: comparison of non–contrast-enhanced CT and intravenous urography. *Radiology.* 1995;194:789–794.
187. Paulson EK, Weaver C, Ho LM, et al. Conventional and reduced radiation dose of 16-MDCT for detection of nephrolithiasis and ureterolithiasis. *AJR Am J Roentgenol.* 2008;190:151–157.
188. Catalano O, Nunziata A, Altei F, et al. Suspected ureteral colic: primary helical CT versus selective helical CT after unenhanced radiography and sonography. *AJR Am J Roentgenol.* 2002;178:379–387.
189. Rucker CM, Menias CO, Bhalla S. Mimics of renal colic: alternative diagnoses at unenhanced helical CT. *Radiographics.* 2004;24:S11–S33.
190. Tamm EP, Silverman PM, Shuman WP. Evaluation of the patient with flank pain and possible ureteral calculus. *Radiology.* 2003;228:319–329.
191. Diel J, Perlmutter S, Venkataramanan N, et al. Unenhanced helical CT using increased pitch for suspected renal colic: an effective technique for radiation dose reduction? *J Comput Assist Tomogr.* 2000;24:795–801.
192. Katz DS, Venkataramanan N, Napel S, et al. Can low-dose unenhanced multidetector CT be used for routine evaluation of suspected renal colic? *AJR Am J Roentgenol.* 2003;180:313–315.
193. Saw KC, McAteer JA, Monga AG, et al. Helical CT of urinary calculi: effect of stone composition, stone size, and scan collimation. *AJR Am J Roentgenol.* 2000;175:329–332.
194. Nadler RB, Rubenstein JN, Eggener SE, et al. The etiology of urolithiasis in HIV infected patients. *J Urol.* 2003;169:475–477.
195. Blake SP, McNicholas MMJ, Raptopoulos V. Nonopaque crystal deposition causing ureteric obstruction in patients with HIV undergoing indinavir therapy. *AJR Am J Roentgenol.* 1998;171:717–720.
196. Ciaschini MW, Remer EM, Baker ME, et al. Urinary calculi: radiation dose reduction of 50% and 75% at CT—effect on sensitivity. *Radiology.* 2009;251:105–111.
197. Grosjean R, Sauer B, Guerra RM, et al. Characterization of human renal stones with MDCT: advantage of dual energy and limitations due to respiratory motion. *AJR Am J Roentgenol.* 2008;190:720–728.
198. Boll DT, Patil NA, Paulson EK, et al. Renal stone assessment with dual-energy multidetector CT and advanced postprocessing techniques: improved characterization of renal stone composition—pilot study. *Radiology.* 2009;250:813–820.
199. Miller NL, Evan AP, Lingeman JE. Pathogenesis of renal calculi. *Urol Clin North Am.* 2007;34:295–313.
200. Boridy IC, Kawashima A, Goldman SM, et al. Acute uroterolithiasis: nonenhanced helical CT findings of perinephric edema for prediction of degree of ureteral obstruction. *Radiology.* 1999;213: 663–667.
201. Georgiades CS, Moore CJ, Smith DP. Differences of renal parenchymal attenuation for acutely obstructed and unobstructed kidneys on unenhanced helical CT: a useful secondary sign? *AJR Am J Roentgenol.* 2001;176:965–968.
202. Goldman SM, Faintuch S, Ajzen SA, et al. Diagnostic value of attenuation measurements of the kidney on unenhanced helical CT of obstructive ureterolithiasis. *AJR Am J Roentgenol.* 2004;182:1251–1254.
203. Narepalem N, Sundaram CP, Boridy IC, et al. Comparison of helical computerized tomography and plain radiography for estimating urinary stone size. *J Urol.* 2002;167:1235–1238.
204. Takahashi N, Kawashima A, Ernst RD, et al. Ureterolithiasis: can clinical outcome be predicted with unenhanced helical CT? *Radiology.* 1998;208:97–102.
205. Metser U, Ghai S, Ong YY, et al. Assessment of urinary tract calculi with 64-MDCT: the axial versus coronal plane. *AJR Am J Roentgenol.* 2009;192:1509–1513.
206. Dalrymple NC, Casford B, Raiken DP, et al. Pearls and pitfalls in the diagnosis of ureterolithiasis with unenhanced helical CT. *Radiographics.* 2000;20:439–447.
207. Sudah M, Vanninen RL, Partanen K, et al. Patients with acute flank pain: comparison of MR urography with unenhanced helical CT. *Radiology.* 2002;223:98–105.
208. Regan F, Bohlman ME, Khazan R, et al. MR urography using HASTE imaging in the assessment of ureteric obstruction. *AJR Am J Roentgenol.* 1996;167:1115–1120.
209. Kawashima A, Sandler CM, Goldman SM, et al. CT of renal inflammatory disease. *Radiographics.* 1997;17:851–866.
210. Ku JH, Jeon YS, Kim ME, et al. Is there a role for magnetic resonance imaging in renal trauma? *Int J Urol.* 2001;8:261–267.
211. Talner LB, Davidson AJ, Lebowitz RL, et al. Acute pyelonephritis: can we agree on terminology? *Radiology.* 1994;192:297–305.

212. Craig WD, Wagner BJ, Travis MD. Pyelonephritis: radiologic-pathologic review. *Radiographics.* 2008;28:255–277.
213. Papanicolaou N, Pfister RC. Acute renal infections. *Radiol Clin North Am.* 1996;34:965–995.
214. Grayson DE, Abbott RM, Levy AD, et al. Emphysematous infections of the abdomen and pelvis: a pictorial review. *Radiographics.* 2002;22:543–561.
215. Rodriguez-de-Velasquez A, Yoder IC, Velasquez PA, et al. Imaging the effects of diabetes on the genitourinary system. *Radiographics.* 1995;15:1051–1068.
216. Hayes WS, Hartman DS. Sesterbenn I. From the archives of the AFIP. Xanthogranulomatous pyelonephritis. *Radiographics.* 1991;11:485–498.
217. Kim B, Lim HK, Choi MH, et al. Detection of parenchymal abnormalities in acute pyelonephritis by pulse inversion harmonic imaging with or without microbubble ultrasonographic contrast agent: correlation with computed tomography. *J Ultrasound Med.* 2001;20:5–14.
218. Soulen MC, Fishman EK, Goldman SM, et al. Bacterial renal infection: role of CT. *Radiology.* 1989;171:703–707.
219. *ACR appropriateness criteria: acute pyelonephritis.* Available at <https://acsearch.acr.org/docs/69489/Narrative/> Accessed January 11, 2018.
220. Sheth S, Fishman EK. Multi-detector row CT of the kidneys and urinary tract: techniques and applications in the diagnosis of benign diseases. *Radiographics.* 2004;24:e20.
221. Majd M, Blask ARN, Markle BM, et al. Acute pyelonephritis: comparison of diagnosis with ^{99m}Tc-DMSA SPECT, spiral CT, MR imaging, and power Doppler US in an experimental pig model. *Radiology.* 2001;218:101–108.
222. Kanel KT, Kroboth FJ, Schwentker FN, et al. The intravenous pyelogram in acute pyelonephritis. *Arch Intern Med.* 1988;148:2144–2148.
223. Bjorgvinsson E, Majd M, Eggli KD. Diagnosis of acute pyelonephritis in children: comparison of sonography and ^{99m}Tc-DMSA scintigraphy. *AJR Am J Roentgenol.* 1991;157:539–543.
224. Rossleigh MA. Scintigraphic imaging in renal infections. *Q J Nucl Med Mol Imaging.* 2009;53:72–77.
225. Ziessman HA, Majd M. Importance of methodology on (99m) technetium dimercapto-succinic acid scintigraphic image quality: imaging pilot study for RIVUR (Randomized Intervention for Children with Vesicoureteral Reflux) multicenter investigation. *J Urol.* 2009;182:272–279.
226. Sheehy N, Tetrault TA, Zurakowski D, et al. Pediatric 99m-Tc-DMSA SPECT performed by using iterative reconstruction with isotropic resolution recovery: improved image quality and reduced radiopharmaceutical activity. *Radiology.* 2009;251:511–516.
227. Soussan M, Sberro R, Wartski M, et al. Diagnosis and localization of renal cyst infection by 18F-fluorodeoxyglucose PET/CT in polycystic kidney disease. *Ann Nucl Med.* 2008;22:529–531.
228. Gervais DA, Shitman GJ. Emphysematous pyelonephritis. *AJR Am J Roentgenol.* 1994;162:348.
229. Wan Y-L, Lee T-Y, Bullard MJ, et al. Acute gas-producing bacterial renal infection: correlation between imaging findings and clinical outcome. *Radiology.* 1996;198:433–438.
230. Wise GJ. Urinary tuberculosis: modern issues. *Curr Urol Rep.* 2009;10(4):313–318, Review. PubMed PMID: 19570494.
231. Merchant SA. Tuberculosis of the genitourinary system. *Indian J Radiol Imaging.* 1993;3:253–274.
232. Roy C, Pfleger DD, Tuchmann CM, et al. Emphysematous pyelitis: findings in five patients. *Radiology.* 2001;218:647–650.
233. Fan CM, Whitman GJ, Chew FS. Xanthogranulomatous pyelonephritis. *AJR Am J Roentgenol.* 1995;165:862.
234. Kenney PJ. Imaging of chronic renal infections. *AJR Am J Roentgenol.* 1990;155:485–494.
235. Hamper UM, Goldblum LE, Hutchins GM, et al. Renal involvement in AIDS: sonographic-pathologic correlation. *AJR Am J Roentgenol.* 1988;150:1321–1325.
236. Symeonidou C, Standish R, Sahdev A, et al. Imaging and histopathologic features of HIV-related renal disease. *Radiographics.* 2008;28:1339–1354.
237. Koh DM, Langroudi B, Padley SPG. Abdominal CT in patients with AIDS. *Imaging.* 2002;14:24–34.
238. Kay CJ. Renal diseases in patients with AIDS: sonographic findings. *AJR Am J Roentgenol.* 1992;159:551–554.
239. Warshauer DM, McCarthy SM, Street L, et al. Detection of renal masses: sensitivities and specificities of excretory urography/linear tomography, US, and CT. *Radiology.* 1988;169:363–365.
240. Bosniak Morton A. The use of the Bosniak classification system for renal cysts and cystic tumors. *J Urol.* 1997;157:1852–1853.
241. Jinzaki M, McTavish JD, Zou KH, et al. Evaluation of small (≤3 cm) renal masses with MDCT: benefits of thin overlapping reconstructions. *AJR Am J Roentgenol.* 2004;183:223–228.
242. Silverman SG, Lee BY, Seltzer SE, et al. Small (≤3 cm) renal masses: correlation of spiral CT features and pathologic findings. *AJR Am J Roentgenol.* 1994;163:597–605.
243. Israel GM, Hindman N, Bosniak MA. Evaluation of cystic renal masses: comparison of CT and MR imaging by using the Bosniak classification system. *Radiology.* 2004;231:365–371.
244. Semelka RC, Shoenut JP, Kroeker MA, et al. Renal lesions: controlled comparison between CT and 1.5-T MR imaging with nonenhanced and gadolinium-enhanced fat-suppressed spin-echo and breath-hold FLASH techniques. *Radiology.* 1992;182:425–430.
245. Hecht EM, Israel GM, Krinsky GA, et al. Renal masses: quantitative analysis of enhancement with signal intensity measurements versus qualitative analysis of enhancement with image subtraction for diagnosing malignancy at MR imaging. *Radiology.* 2004;232:373–378.
246. Hayden CK, Swischuk LE, Smith TH, et al. Renal cystic disease in childhood. *Radiographics.* 1986;6:97–116.
247. Lonergan GF, Rice RR, Suarez ES. Autosomal recessive polycystic kidney disease: radiologic-pathologic correlation. *Radiographics.* 2000;20:837–855.
248. Walker FC, Loney LC, Root ER, et al. Diagnostic evaluation of adult polycystic kidney disease in childhood. *AJR Am J Roentgenol.* 1984;142:1273–1277.
249. Nicolau C, Torra R, Badenas C, et al. Autosomal dominant polycystic kidney disease types 1 and 2: assessment of US sensitivity for diagnosis. *Radiology.* 1999;213:273–276.
250. Heinz-Peer G, Schoder M, Rand T, et al. Prevalence of acquired cystic kidney disease and tumors in native kidneys of renal transplant recipients: a prospective US study. *Radiology.* 1995;195:667–671.
251. Levine E. Acquired cystic kidney disease. *Radiol Clin North Am.* 1996;34:947–964.
252. Levine E, Slusher SL, Grantham JJ, et al. Natural history of acquired renal cystic disease in dialysis patients: a prospective longitudinal CT study. *AJR Am J Roentgenol.* 1991;156:501–506.
253. Takebayashi S, Hidai H, Chiba T, et al. Using helical CT to evaluate renal cell carcinoma in patients undergoing hemodialysis: value of early enhanced images. *AJR Am J Roentgenol.* 1999;172:429–433.
254. Taylor AJ, Cohen EP, Erickson SJ, et al. Renal imaging in long-term dialysis patients: a comparison of CT and sonography. *AJR Am J Roentgenol.* 1989;153:765–767.
255. Takase K, Takahashi S, Tazawa S, et al. Renal cell carcinoma associated with chronic renal failure: evaluation with sonographic angiography. *Radiology.* 1994;192:787–792.
256. Siegel SC, Sandler MA, Alpern MB, et al. CT of renal cell carcinoma in patients on chronic hemodialysis. *AJR Am J Roentgenol.* 1988;150:583–585.
257. Matson MA, Cohen EP. Acquired cystic kidney disease: occurrence, prevalence, and renal cancers. *Medicine (Baltimore).* 1990;69:217–226.
258. Farres MT, Ronco P, Saadoun D, et al. Chronic lithium nephropathy: MR imaging for diagnosis. *Radiology.* 2003;229:570–574.
259. Leung RS, Biswas SV, Duncan M, et al. Imaging features of von Hippel–Lindau disease. *Radiographics.* 2008;28:65–79.
260. Hartman DS, Choyke PL, Hartman MS. From the RSNA refresher courses: a practical approach to the cystic renal mass. *Radiographics.* 2004;24:S101–S115.
261. Bosniak MA. State of the art: the current radiological approach to renal cysts. *Radiology.* 1986;158:1–10.
262. Israel GM, Hindman N, Bosniak MA. Evaluation of cystic renal masses: comparison of CT and MR imaging by using the Bosniak classification system. *Radiology.* 2004;231:365–371.
263. Siegel CL, McFarland EG, Brink JA, et al. CT of cystic renal masses: analysis of diagnostic performance and interobserver variation. *AJR Am J Roentgenol.* 1997;169:813–818.
264. Israel GM, Bosniak MA. Follow-up CT of moderately complex cystic lesions of the kidney (Bosniak category IIF). *AJR Am J Roentgenol.* 2003;181:627–633.
265. Curry NS, Cochran ST, Bissada NK. Cystic renal masses: accurate Bosniak classification requires adequate renal CT. *AJR Am J Roentgenol.* 2000;175:339–342.
266. Harisinghani MG, Maher MM, Gervais DA, et al. Incidence of malignancy in complex cystic renal masses (Bosniak category III):

should imaging-guided biopsy precede surgery? *AJR Am J Roentgenol.* 2003;180:755–758.
267. Dechet CB, Sebo T, Farrow G, et al. Prospective analysis of intraoperative frozen needle biopsy of solid renal masses in adults. *J Urol.* 1999;162:1282–1285.
268. Wood BJ, Khan MA, McGovern F, et al. Imaging guided biopsy of renal masses: indications, accuracy and impact on clinical management. *J Urol.* 1999;161:1470–1474.
269. Freire M, Remer EM. Clinical and radiologic features of cystic renal masses. *AJR Am J Roentgenol.* 2009;192:1367–1372.
270. Choyke PL, Glenn GM, Walther MM, et al. Hereditary renal cancers. *Radiology.* 2003;226:33–46.
271. Zagoria RJ. Imaging of small renal masses: a medical success story. *AJR Am J Roentgenol.* 2000;175:945–955.
272. Patard JJ. Incidental renal tumours. *Curr Opin Urol.* 2009;19:454–458.
273. Berland LL, Silverman SG, Gore RM, et al. Managing incidental findings on abdominal CT: white paper of the ACR Incidental Findings Committee. *J Am Coll Radiol.* 2010;7:754–773.
274. Wagner BJ, Maj MC, Wong-You-Cheong JJ, et al. Adult renal hamartomas. *Radiographics.* 1997;17:155–169.
275. Bosniak MA, Megibow AJ, Hulnick DH, et al. CT diagnosis of renal angiomyolipoma: the importance of detecting small amounts of fat. *AJR Am J Roentgenol.* 1988;151:497–501.
276. Silverman SG, Pearson GDN, Seltzer SE, et al. Small (≤3 cm) hyperechoic renal masses: comparison of helical and conventional CT for diagnosing angiomyolipoma. *AJR Am J Roentgenol.* 1996;167:877–881.
277. Siegel CL, Middleton WD, Teefey SA, et al. Angiomyolipoma and renal cell carcinoma: US differentiation. *Radiology.* 1996;198:789–793.
278. Kim JK, Park SY, Shon JH, et al. Angiomyolipoma with minimal fat: differentiation from renal cell carcinoma at biphasic helical CT. *Radiology.* 2004;230:677–684.
279. Jinzaki M, Tanimoto A, Narimatsu Y, et al. Angiomyolipoma: imaging findings in lesions with minimal fat. *Radiology.* 1997;205:497–502.
280. Catalano OA, Samir AE, Sahani DV, et al. Pixel distribution analysis: can it be used to distinguish clear cell carcinomas from angiomyolipomas with minimal fat? *Radiology.* 2008;247:738–746.
281. Kim JY, Kim JK, Kim N, et al. CT histogram analysis: differentiation of angiomyolipoma without visible fat from renal cell carcinoma at CT imaging. *Radiology.* 2008;246:472–479.
282. Israel GM, Hindman N, Hecht E, et al. The use of opposed-phase chemical shift MRI in the diagnosis of renal angiomyolipomas. *AJR Am J Roentgenol.* 2005;184:1868–1872.
283. Lesavre A, Correas JM, Merran S, et al. CT of papillary renal cell carcinomas with cholesterol necrosis mimicking angiomyolipomas. *AJR Am J Roentgenol.* 2003;181:143–145.
284. Israel GM, Bosniak MA, Slywotzky CM, et al. CT differentiation of large exophytic renal angiomyolipomas and perirenal liposarcomas. *AJR Am J Roentgenol.* 2002;179:769–773.
285. Bosniak M, Megibow AJ, Hulnick DH, et al. CT diagnosis of renal angiomyolipoma: the importance of detecting small amounts of fat. *AJR Am J Roentgenol.* 1988;151:497–501.
286. Lemaitre L, Robert Y, Dubrulle F, et al. Renal angiomyolipoma: growth followed up with CT and/or US. *Radiology.* 1995;197: 598–602.
287. Yamakado K, Tanaka N, Nakagawa T, et al. Renal angiomyolipoma: relationships between tumor size, aneurysm formation, and rupture. *Radiology.* 2002;225:78–82.
288. Levine E, Huntrakoon M. Computed tomography of renal oncocytoma. *AJR Am J Roentgenol.* 1983;141:741–746.
289. Blake MA, McKernan M, Setty B, et al. Renal oncocytoma displaying intense activity on ^{18}F-FDG PET. *AJR Am J Roentgenol.* 2006;186:269–271.
290. Neisius D, Braedel HU, Schindler E, et al. Computed tomographic and angiographic findings in renal oncocytoma. *Br J Radiol.* 1988;61:1019–1025.
291. Davidson AJ, Hayes WS, Hartman DS, et al. Renal oncocytoma and carcinoma: failure of differentiation with CT. *Radiology.* 1993;186:693–696.
292. Curry NS, Schabel SI, Garvin AJ, et al. Case report. Intratumoral fat in a renal oncocytoma mimicking angiomyolipoma. *AJR Am J Roentgenol.* 1990;154:307–308.
293. Sheth S, Scatarige JC, Horton KM, et al. Current concepts in the diagnosis and management of renal cell carcinoma: role of multidetector CT and three-dimensional CT. *Radiographics.* 2001;21:S237–S254.
294. Davidson AJ, Hartman DS, Choyke PL, et al. Radiologic assessment of renal masses: implications for patient care. *Radiology.* 1997;202:297–305.
295. Yuh BI, Cohan RH. Different phases of renal enhancement: role in detecting and characterizing renal masses during helical CT. *AJR Am J Roentgenol.* 1999;173:747–755.
296. Cohan RH, Sherman LS, Korobkin M, et al. Renal masses: assessment of corticomedullary-phase and nephrographic-phase CT scans. *Radiology.* 1995;196:445–451.
297. Suh M, Coakley FV, Qayyum A, et al. Distinction of renal cell carcinomas from high-attenuation renal cysts at portal venous phase contrast–enhanced CT. *Radiology.* 2003;228:330–334.
298. Birnbaum BA, Jacobs JE, Ramchandani P. Multiphasic renal CT: comparison of renal mass enhancement during the corticomedullary and nephrographic phases. *Radiology.* 1996;200:753–758.
299. Kopka L, Fischer U, Zoeller G, et al. Dual-phase helical CT of the kidney: value of the corticomedullary and nephrographic phase for evaluation of renal lesions and preoperative staging of renal cell carcinoma. *AJR Am J Roentgenol.* 1997;169:1573–1578.
300. Macari M, Bosniak MA. Delayed CT to evaluate renal masses incidentally discovered at contrast-enhanced CT: demonstration of vascularity with deenhancement. *Radiology.* 1999;213:674–680.
301. Zeman RK, Zeiberg A, Hayes WS, et al. Helical CT of renal masses: the value of delayed scans. *AJR Am J Roentgenol.* 1996;167:771–776.
302. Benjaminov O, Atri M, O'Malley M, et al. Enhancing component on CT to predict malignancy in cystic renal masses and interobserver agreement of different CT features. *AJR Am J Roentgenol.* 2006;186:665–672.
303. Ruppert-Kohlmayr AJ, Uggowitzer M, Meissnitzer T, et al. Differentiation of renal clear cell carcinoma and renal papillary carcinoma using quantitative CT enhancement parameters. *AJR Am J Roentgenol.* 2004;183:1387–1391.
304. Kim JK, Kim TK, Ahn HJ, et al. Differentiation of subtypes of renal cell carcinoma on helical CT scans. *AJR Am J Roentgenol.* 2002;178:1499–1506.
305. Yoshimitsu K, Kakihara D, Irie H, et al. Papillary renal carcinoma: diagnostic approach by chemical shift gradient-echo and echo-planar MR imaging. *J Magn Reson Imaging.* 2006;23:339344.
306. Ergen FB, Hussain HK, Caoili EM, et al. MRI for preoperative staging of renal cell carcinoma using the 1997 TNM classification: comparison with surgical and pathologic staging. *AJR Am J Roentgenol.* 2004;182:217–225.
307. Roy C, El Ghali S, Buy X, et al. Significance of the pseudocapsule on MRI of renal neoplasms and its potential application for local staging: a retrospective study. *AJR Am J Roentgenol.* 2005;184:113–120.
308. Choyke PL, Walther MM, Wagner JR. Renal cancer: preoperative evaluation with dual-phase three-dimensional MR angiography. *Radiology.* 1997;205:767–771.
309. El-Galley R. Surgical management of renal tumors. *Radiol Clin North Am.* 2003;41:1053–1065.
310. Browne RFJ, Meehan CP, Colville J, et al. Transitional cell carcinoma of the upper urinary tract: spectrum of imaging findings. *Radiographics.* 2005;25:1609–1627.
311. Pickhardt PF, Lonergan GF, Davis CF, et al. From the archives of the AFIP. Infiltrative renal lesions: radiologic-pathologic correlation. *Radiographics.* 2000;20:215–243.
312. Urban BA, Fishman EK. Renal lymphoma: CT patterns with emphasis on helical CT. *Radiographics.* 2000;20:197–212.
313. Semelka RC, Kelekis NL, Burdeny DA, et al. Renal lymphoma: demonstration by MR imaging. *AJR Am J Roentgenol.* 1996;166:823–827.
314. Goldberg MA, Mayo-Smith WW, Papanicolaou N, et al. FDG PET characterization of renal masses: preliminary experience. *Clin Radiol.* 1997;52:510–515.
315. Jadvar H, Kherbache HM, Pinski JK, et al. Diagnostic role of [F-18]-FDG positron emission tomography in restaging renal cell carcinoma. *Clin Nephrol.* 2003;60:395–400.
316. Mankoff DA, Thompson JA, Gold P, et al. Identification of interleukin-2–induced complete response in metastatic renal cell carcinoma by FDG PET despite radiographic evidence suggesting persistent tumor. *AJR Am J Roentgenol.* 1997;169:1049–1050.
317. Ramdave S, Thomas GW, Berlangieri SU, et al. Clinical role of F-18 fluorodeoxyglucose positron emission tomography for detection and management of renal cell carcinoma. *J Urol.* 2001;166:825–830.
318. Wahl RL, Harney J, Hutchins G, et al. Imaging of renal cancer using positron emission tomography with 2-deoxy-2-(^{18}F)-fluoro-D-glucose: pilot animal and human studies. *J Urol.* 1991;146:1470–1474.

319. Wu HC, Yen RF, Shen YY, et al. Comparing whole body ^{18}F-2-deoxyglucose positron emission tomography and technetium-99m methylene diphosphate bone scan to detect bone metastases in patients with renal cell carcinomas—a preliminary report. *J Cancer Res Clin Oncol.* 2002;128:503–506.
320. Vercellino L, Bousquet G, Baillet G, et al. ^{18}F-FDG PET/CT imaging for an early assessment of response to sunitinib in metastatic renal carcinoma: preliminary study. *Cancer Biother Radiopharm.* 2009;24:137–144.
321. Snow D, Cohen D, Chapman WC, et al. Positron emission tomography enhancing tumor thrombus in patient with renal cell carcinoma. *Urology.* 2009;73:270–271.
322. Kumar R, Shandal V, Shamim SA, et al. Role of FDG PET/CT in recurrent renal cell carcioma. *Nucl Med Commun.* 2010;31:844–850.
323. Khandani AH, Rathmell WK. Positron emission tomography in renal cell carcinoma: an imaging biomarker in development. *Semin Nucl Med.* 2012;42:221–230.
324. Nakatani K, Nakamoto Y, Saga T, et al. The potential clinical value of FDG PET for recurrent renal cell carcinoma. *Eur J Radiol.* 2011;79:29–35.
325. Zukotynski K, Lewis A, O'Regan K, et al. PET/CT and renal pathology: a blind spot for radiologists? Part 1: primary pathology. *AJR Am J Roentgenol.* 2012;199:W163–W167.
326. Zukotynski K, Lewis A, O'Regan K, et al. PET/CT and renal pathology: a blind spot for radiologists? Part 2: lymphoma, leukemia, and metastatic disease. *AJR Am J Rontgenol.* 2012;199:W168–W174.
327. Majhail NS, Urbain JL, Albani JM, et al. F-18 fluorodeoxyglucose positron emission tomography in the evaluation of distant metastases from renal cell carcinoma. *J Clin Oncol.* 2003;21:3995–4000.
328. Seto E, Segall GM, Terris MK. Positron emission tomography detection of osseous metastases of renal cell carcinoma not identified on bone scan. *Urology.* 2000;55:286.
329. Zhuang H, Duarte PS, Pourdehand M, et al. Standardized uptake value as an unreliable index of renal disease on fluorodeoxyglucose PET imaging. *Clin Nucl Med.* 2000;25:358–360.
330. Kang DE, White RL Jr, Zuger JH, et al. Clinical use of fluorodeoxyglucose F 18 positron emission tomography for detection of renal cell carcinoma. *J Urol.* 2004;171:1806–1809.
331. Safaei A, Figlin R, Hoh CK, et al. The usefulness of F-18 deoxyglucose whole-body positron emission tomography (PET) for re-staging of renal cell cancer. *Clin Nephrol.* 2002;57:56–62.
332. Miyakita H, Tokunaga M, Onda H, et al. Significance of ^{18}F-fluorodeoxyglucose positron emission tomography (FDG-PET) for detection of renal cell carcinoma and immunohistochemical glucose transporter 1 (GLUT-1) expression in the cancer. *Int J Urol.* 2002;9:15–18.
333. Nagase Y, Takata K, Moriyama N, et al. Immunohistochemical localization of glucose transporters in human renal cell carcinoma. *J Urol.* 1995;153(3 Pt 1):798–801.
334. Dilhuydy MS, Durieux A, Pariente A, et al. PET scans for decision-making in metastatic renal cell carcinoma: a single institution evaluation. *Oncology.* 2006;70:339–344.
335. Wang HY, Ding HJ, Chen JH, et al. Meta-analysis of the diagnostic performance of [18F] FDG PET and PET/CT in renal cell carcinoma. *Cancer Imaging.* 2012;12:464–474.
336. Park JW, Jo MK, Lee HM. Significance of ^{18}F-fluorodeoxyglucose positron emission tomography/computed tomography for the postoperative surveillance of advanced renal cell carcinoma. *BJU Int.* 2009;103:615–619.
337. Ozulker T, Ozulker F, Ozbek E, et al. A prospective diagnostic accuracy study of F-18 fluorodeoxy glucose-positron emmission tomography/computed tomography in the evaluation of indeterminate renal masses. *Nucl Med Commun.* 2011;32:265–272.
338. Ueno D, Yao M, Tateishi U, et al. Early assessment by FDG-PET/CT of patients with advanced renal cell carcinoma with tyrosine kinase inhibitors is predictive of disease course. *BMC Cancer.* 2012;12:162.
339. Lyrdal D, Boijsen M, Suurkula M, et al. Evaluation of sorafenib treatment in metastatic renal cell carcinoma with 2-fluoro-2-deoxyglucose positron emission tomography and computed tomography. *Nucl Med Commun.* 2009;30:519–524.
340. Vercellino L, Bousquet G, Baillet G, et al. 18F-FDG PET/CT imaging for an early assessment of response to sunitinib in metastatic renal carcinoma: preliminary study. *Cancer Biother Radiopharm.* 2009;24:137–144.
341. Kayani I, Avril N, Bomanji J, et al. Sequential FDG-PET/CT as a biomarker of response to sunitinib in metastatic clear cell renal cancer. *Clin Cancer Res.* 2011;17:6021–6028.
342. Minamimoto R, Nakaigawa N, Tateishi U, et al. Evaluation of response to multikinase inhibitor in metastatic renal cell carcinoma by FDG PET/contrast-enhanced CT. *Clin Nucl Med.* 2010;35:918–923.
343. Revheim ME, Winge-Main AK, Hagen G, et al. Combined positron emission tomography/computed tomography in sunitinib therapy assessment of patients with metastatic renal cell carcinoma. *Clin Oncol (R Coll Radiol).* 2011;23:339–343.
344. Gilles R, de Geus-Oei LE, Mulders PF, et al. Immunotherapy response evaluation with (18F)F-FDG-PET in patients with advanced stage renal cell carcinoma. *World J Urol.* 2013;31:841–846.
345. Namura K, Minamimoto R, Yao M, et al. Impact of maximum standardized uptake value (SUVmax) evaluated by 18F-fluoro-2deoxy-D-glucose positron emission tomography/computed tomography (18F-FDG PET/CT) on survival for patients with advanced renal cell carcinoma: a preliminary report. *BMC Cancer.* 2010;10:667.
346. Ferda J, Ferdova E, Hora M, et al. 18F-FDG PET/CT in potentially advanced renal cell carcinoma: a role in treatment decisions and prognosis estimation. *Anticancer Res.* 2013;33:2665–2672.
347. Shreve P, Chiao PC, Humes HD, et al. Carbon-11–acetate PET imaging in renal disease. *J Nucl Med.* 1995;36:1595–1601.
348. Lawrentschuk N, Poon AM, Foo SS, et al. Assessing regional hypoxia in human renal tumors using 18F-fluoromisonidazole positron emission tomography. *BJU Int.* 2005;96:540–546.
349. Bhargava P, Hanif M, Nash C. Whole-body F-18 sodium fluoride PET-CT in a patient with renal cell carcinoma. *Clin Nucl Med.* 2008;33:894–895.
350. Perini R, Pryma D, Divgi C. Molecular imaging of renal cell carcinoma. *Urol Clin North Am.* 2008;35:605–611.
351. Oyama N, Okazawa H, Kusukawa N, et al. ^{11}C-Acetate PET imaging for renal cell carcinomas. *Eur J Nucl Med Mol Imaging.* 2009;36:422–427.
352. Kotzerke J, Linne C, Meinhardt M, et al. [1-(11)C] Acetate uptake is not increased in renal cell carcinoma. *Eur J Nucl Med Mol Imaging.* 2007;34:884–888.
353. Juillard L, Lemoine S, Janier MF, et al. Validation of renal oxidative metabolism measurement by positron emission tomography. *Hypertension.* 2007;50:242–247.
354. Murakami M, Zhao S, Zhao Y, et al. Evaluation of changes in the tumor microenvironment after sorafenib therapy by sequential histology and 18F-fluoromisonidazole hypoxia imaging in renal cell carcinoma. *Int J Oncol.* 2012;41:1593–1600.
355. Maleddu A, Pantaleo MA, Castellucci P, et al. 11C-Acetate PET for early prediction of sunitinib response in metastatic renal cell carcinoma. *Tumori.* 2009;95:382–384.
356. Hugonnet F, Fournier L, Medioni J, et al. Metastatic renal cell carcinoma: relationship between initial metastasis hypoxia, change after 1 month's sunitinib, and therapeutic response: an 18F-fluoromisonidazole PET/CT study. *J Nucl Med.* 2011;52:1048–1055.
357. Schuster DM, Nye JA, Nieh PT, et al. Initial experience with the radiotracer anti-1-amino-3-[18F]fluorocyclobutane-1-carboxylic acid (anti-[18F]FACBC) with PET in renal cell carcinoma. *Mol Imaging Biol.* 2009;11:434–438.
358. Divgi CR, Uzzo RG, Gatsonis C, et al. Positron emission tomography/computed tomography identification of clear cell renal cell carcinoma: results from the REDECT trial. *J Clin Oncol.* 2013;31:187–194.
359. Kudomi N, Koivuviita N, Liukko KE, et al. Parametric renal blood flow imaging using [^{15}O]H_2O and PET. *Eur J Nucl Med Mol Imaging.* 2009;36:683–691.
360. *ACR appropriateness criteria: renovascular hypertension.* Available at: https://acsearch.acr.org/docs/69374/Narrative/ Accessed July 30, 2018.
361. Hillman BJ. Imaging advances in the diagnosis of renovascular hypertension. *AJR Am J Roentgenol.* 1989;153:5–14.
362. Hamper UM, DeJong MR, Caskey CI, et al. Power Doppler imaging: clinical experience and correlation with color Doppler US and other imaging modalities. *Radiographics.* 1977;17:499–513.
363. Helenon O, El Rody F, Correas JM, et al. Color Doppler US of renovascular disease in native kidneys. *Radiographics.* 1995;15:833–854.
364. Halpern EJ, Needleman L, Nack TL, et al. Renal artery stenosis: should we study the main renal artery or segmental vessels? *Radiology.* 1995;195:799–804.

365. House MK, Dowling RJ, King P, et al. Using Doppler sonography to reveal renal artery stenosis: an evaluation of optimal imaging parameters. *AJR Am J Roentgenol.* 1999;173:761–765.
366. Melany ML, Grant EG, Duerinckx AJ, et al. Ability of a phase shift US contrast agent to improve imaging of the main renal arteries. *Radiology.* 1997;205:147–152.
367. Claudon M, Plouin PF, Baxter GM, et al. Renal arteries in patients at risk of renal arterial stenosis: multicenter evaluation of the echo-enhancer SH U 508A at color and spectral Doppler US. Levovist Renal Artery Stenosis Study Group. *Radiology.* 2000;214:739–746.
368. Urban BA, Ratner LE, Fishman EK. Three-dimensional volume-rendered CT angiography of the renal arteries and veins: normal anatomy, variants, and clinical applications. *Radiographics.* 2001;21:373–386.
369. Kaatee R, Beek FJA, DeLange EE, et al. Renal artery stenosis: detection and quantification with spiral CT angiography versus optimized digital subtraction angiography. *Radiology.* 1997;205:121–127.
370. Beregi JP, Elkohen M, Deklunder G, et al. Helical CT angiography compared with arteriography in the detection of renal artery stenosis. *AJR Am J Roentgenol.* 1996;167:495–501.
371. Mallouhi A, Rieger M, Czermak B, et al. Volume-rendered multidetector CT angiography: noninvasive follow-up of patients treated with renal artery stents. *AJR Am J Roentgenol.* 2003;180:233–239.
372. Behar JV, Nelson RC, Zidar JP, et al. Thin-section multidetector CT angiography of renal artery stents. *AJR Am J Roentgenol.* 2002;178:1155–1159.
373. Kawashima A, Sandler CM, Ernst RD, et al. CT evaluation of renovascular disease. *Radiographics.* 2000;20:1321–1340.
374. Bude RO, Forauer AR, Caoili EM, et al. Is it necessary to study accessory arteries when screening the renal arteries for renovascular hypertension? *Radiology.* 2003;226:411–416.
375. Willmann J, Wildermuth S, Pfammatter T, et al. Aortoiliac and renal arteries: prospective intraindividual comparison of contrast-enhanced three-dimensional MR angiography and multi-detector row CT angiography. *Radiology.* 2003;226:798–811.
376. Mallouhi A, Schocke M, Judmaier W, et al. 3D MR angiography of renal arteries: comparison of volume rendering and maximum intensity projection algorithms. *Radiology.* 2002;223:509–516.
377. Schoenberg SO, Knopp MV, Londy F, et al. Morphologic and functional magnetic resonance imaging of renal artery stenosis: a multireader tricenter study. *J Am Soc Nephrol.* 2002;13:158–169.
378. Bude RO, Forauer AR, Caoili EM, et al. Is it necessary to study accessory arteries when screening the renal arteries for renovascular hypertension? *Radiology.* 2003;226:411–416.
379. Soulez G, Oliva VL, Turpin S, et al. Imaging of renovascular hypertension: respective values of renal scintigraphy, renal Doppler US, and MR angiography. *Radiographics.* 2000;20:1355–1368.
380. Thornton MJ, Thornton F, O'Callaghan J, et al. Evaluation of dynamic gadolinium-enhanced breath-hold MR angiography in the diagnosis of renal artery stenosis. *AJR Am J Roentgenol.* 1999;173:1279–1283.
381. Wilson GJ, Hoogeveen RM, Willinek WA, et al. Parallel imaging in MR angiography. *Top Magn Reson Imaging.* 2004;15:169–185.
382. Gutberlet M, Noeske R, Schwinge K, et al. Comprehensive cardiac magnetic resonance imaging at 3.0 tesla: feasibility and implications for clinical applications. *Invest Radiol.* 2006;41:154–167.
383. Chen Q, Quijano CV, Mai VM, et al. On improving temporal and spatial resolution of 3D contrast-enhanced body MR angiography with parallel imaging. *Radiology.* 2004;231:893–899.
384. de Haan MW, van Engelshoven JMA, Houben AJHM, et al. Phase-contrast magnetic resonance flow quantification in renal arteries: comparison with ^{133}xenon washout measurements. *Hypertension.* 2003;41:114–118.
385. Schoenberg SO, Knopp MV, Londy F, et al. Morphologic and functional magnetic resonance imaging of renal artery stenosis: a multireader tricenter study. *J Am Soc Nephrol.* 2002;13:158–169.
386. Michaely HJ, Schoenberg SO, Oesingmann N, et al. Renal artery stenosis: functional assessment with dynamic MR perfusion measurements—feasibility study. *Radiology.* 2006;238:586–596.
387. van den Dool SW, Wasser MN, de Fijter JW, et al. Functional renal volume: quantitative analysis at gadolinium-enhanced MR angiography—feasibility study in healthy potential kidney donors. *Radiology.* 2005;236:189–195.
388. Spuentrup E, Ruebben A, Stuber M, et al. Metallic renal artery MR imaging stent: artifact-free lumen visualization with projection and standard renal MR angiography. *Radiology.* 2003;227:897–902.
389. Nally JV Jr, Black HR. State-of-the-art review: captopril renography—pathophysiological considerations and clinical observations. *Semin Nucl Med.* 1992;22:85–97.
390. Taylor A, Nally J, Aurell M, et al. Consensus report on ACE inhibitor renography for detecting renovascular hypertension. Radionuclides in Nephrourology Group. Consensus Group on ACEI Renography. *J Nucl Med.* 1996;37:1876–1882.
391. Taylor AT Jr, Fletcher JW, Nally JV Jr, et al. Procedure guideline for diagnosis of renovascular hypertension. Society of Nuclear Medicine. *J Nucl Med.* 1998;39:1297–1302.
392. Fine EJ. Interventions in renal scintigraphy. *Semin Nucl Med.* 1999;29:128–145.
393. Llach F, Papper S, Massey SG. The clinical spectrum of renal vein thrombosis: acute and chronic. *Am J Med.* 1980;69:819–827.
394. Llach F, Koffler A, Finck E, et al. On the incidence of renal vein thrombosis in the nephrotic syndrome. *Arch Intern Med.* 1977;137:333–336, 381.
395. Witz M, Kantarovsky A, Baruch M, et al. Renal vein occlusion: a review. *J Urol.* 1996;155:1173–1179.
396. Gatewood OMB, Fishman EK, Burrow CR, et al. Renal vein thrombosis in patients with nephrotic syndrome: CT diagnosis. *Radiology.* 1986;159:117–122.
397. Sebastia C, Quiroga S, Boye R, et al. Helical CT in renal transplantation: normal findings and early and late complications. *Radiographics.* 2001;21:1103–1117.
398. Letourneau JG, Day DL, Ascher NL, et al. Perspective: imaging of renal transplants. *AJR Am J Roentgenol.* 1988;150:833–838.
399. Kelcz F, Pazniak MA, Pirsch JD, et al. Pyramidal appearance and resistive index: insensitive and nonspecific sonographic indicators of renal transplant rejection. *AJR Am J Roentgenol.* 1990;155:531–535. PubMed PMID: 2117350.
400. Smith PA, Ratner LE, Lynch FC, et al. Role of CT angiography in the preoperative evaluation for laparoscopic nephrectomy. *Radiographics.* 1998;18:589–601.
401. Holden A, Smith A, Dukes P, et al. Assessment of 100 live potential renal donors for laparoscopic nephrectomy with multi-detector row helical CT. *Radiology.* 2005;237:973–980.
402. Rydberg J, Kopecky KK, Tann M, et al. Evaluation of prospective living renal donors for laparoscopic nephrectomy with multisection CT: the marriage of minimally invasive imaging with minimally invasive surgery. *Radiographics.* 2001;21:S223–S236.
403. Kawamoto S, Montgomery R, Lawler LP, et al. Multi-detector row CT evaluation of living renal donors prior to laparoscopic nephrectomy. *Radiographics.* 2003;24:1513–1514.
404. Hofmann LV, Smith PA, Kuszyk BS, et al. Original report. Three-dimensional helical CT angiography in renal transplant recipients: a new problem-solving tool. *AJR Am J Roentgenol.* 1999;173:1085–1089.
405. Pozniak MA, Balison DJ, Lee FT, et al. CT angiography of potential renal transplant donors. *Radiographics.* 1998;18:565–587.
406. Kawamoto S, Lawler LP, Fishman EK. Evaluation of the renal venous system on late arterial and venous phase images with MDCT angiography in potential living laparoscopic renal donors. *AJR Am J Roentgenol.* 2005;184:539–545.
407. Sahani DV, Rastogi N, Greenfield AC, et al. Multi-detector row CT in evaluation of 94 living renal donors by readers with varied experience. *Radiology.* 2005;235:905–910.
408. Rubin GD. Invited commentary. Helical CT of potential living renal donors: toward a greater understanding. *Radiographics.* 1998;18:601–604.
409. Hohenwalter MD, Skowlund CJ, Erickson SJ, et al. Renal transplant evaluation with MR angiography and MR imaging. *Radiographics.* 2001;21:1505–1517.
410. Van den Dool SW, Wasser MN, de Fijter JW, et al. Functional renal volume: quantitative analysis at gadolinium-enhanced MR angiography—feasibility study in healthy potential kidney donors. *Radiology.* 2005;236:189–195.
411. Akbar SA, Jafri ZH, Amendola MA, et al. Complications of renal transplantation. *Radiographics.* 2005;25:1335–1356.
412. Brown ED, Chen MYM, Wolfman NT, et al. Complications of renal transplantation: evaluation with US and radionuclide imaging. *Radiographics.* 2000;20:607–622.
413. Grant EG, Perrella RR. Commentary. Wishing won't make it so: duplex Doppler sonography in the evaluation of renal transplant dysfunction. *AJR Am J Roentgenol.* 1990;155:538–539.

414. Reuther G, Wanjura D, Bauer H. Acute renal vein thrombosis in renal allografts: detection with duplex Doppler US. *Radiology.* 1989;170:557–558.
415. Allen KS, Jorkasky DK, Arger PH, et al. Renal allografts: prospective analysis of Doppler sonography. *Radiology.* 1998;169:371–376.
416. Buckley AR, Cooperberg PL, Reeve CE, et al. The distinction between acute renal transplant rejection and cyclosporine nephrotoxicity: value of duplex sonography. *AJR Am J Roentgenol.* 1987;149:521–525.
417. Kaveggia LP, Perrella RR, Grant EG, et al. Duplex Doppler sonography in renal allografts: the significance of reversed flow in diastole. *AJR Am J Roentgenol.* 1990;155:295–298.
418. Voegeli DR, Crummy AB, McDermott JC, et al. Percutaneous management of the urological complications of renal transplantation. *Radiographics.* 1986;6:1007–1022.
419. Frascà GM, Sandrini S, Cosmai L, et al. Renal cancer in kidney transplanted patients. *J Nephrol.* 2015;28(6):659–668. doi:10.1007/s40620-015-0219-8. [Epub 2015 Jul 23]; PubMed PMID: 26202137. Review.
420. Patel NH, Jindal RM, Wilkin T, et al. Renal arterial stenosis in renal allografts: retrospective study of predisposing factors and outcome after percutaneous transluminal angioplasty. *Radiology.* 2001;219:663–667.
421. Sadowski EA, Fain SB, Alford SK, et al. Assessment of acute renal transplant rejection with blood oxygen level–dependent MR imaging: initial experience. *Radiology.* 2005;236:911–919.
422. Vrachliotis TG, Vaswani KK, Davies EA, et al. Pictorial essay. CT findings in posttransplantation lymphoproliferative disorder of renal transplants. *AJR Am J Roentgenol.* 2000;175:183–188.
423. Dubovsky EV, Russell CD, Erbas B. Radionuclide evaluation of renal transplants. *Semin Nucl Med.* 1995;25:49–59.
424. Dunagin P, Alijani M, Atkins F, et al. Application of the kidney to aortic blood flow index to renal transplants. *Clin Nucl Med.* 1983;8:360–364.
425. Lin E, Alavi A. Significance of early tubular extraction in the first minute of Tc-99m MAG3 renal transplant scintigraphy. *Clin Nucl Med.* 1998;23:217–222.
426. Berlyne N, Berlyne GM. Acute renal failure following intravenous pyelography with hypaque. *Acta Med Scand.* 1962;171:39–41.

BOARD REVIEW QUESTIONS

1. A patient with an eGFR of 30 mL/min/1.73 m^2 needs an imaging study with contrast to evaluate and characterize the presence of an indeterminate renal mass. The following are all acceptable as the initial investigation except:
   a. CT scan with iodinated contrast
   b. MRI with contrast
   c. Ultrasound of the retroperitoneum along with contrast enhancement
   d. FDG PET-CT study
   e. Tc-99m DTPA scan

   Answer: e

   Rationale: Although many of these evaluations would be appropriate, perhaps the best test would be the contrast enhanced ultrasound in the presence of abnormal renal function. (https://acsearch.acr.org/docs/69367/Narrative/). The Tc-99 DTPA scan has no role in characterizing a renal mass.

2. A patient is referred for evaluation of unilateral renal colic. The most appropriate first radiologic examination would be:
   a. Intravenous pyelogram
   b. Noncontrast-enhanced CT scan
   c. MRI scan without contrast
   d. PET
   e. Cystoscopy

   Answer: b

   Rationale: The correct answer would be a noncontrast-enhanced CT scan. The American College of Radiology appropriateness criteria for evaluation of renal colic (https://acsearch.acr.org/docs/69362/Narrative/) rate a noncontrast-enhanced CT scan as the most accurate and appropriate test in this emergent clinical situation. Even when performed with appropriate radiation dose reduction techniques, it is highly accurate in diagnosing both the cause and level of obstruction. In addition, it may also be accurate in identifying a nonurologic cause of the patient's symptoms.

3. A 46-year-old patient who had a renal transplant 5 months ago comes in with symptoms and signs of a failing transplant with an abnormal renal function profile. What would be the most appropriate first imaging investigation in this scenario?
   a. Tc-99m DTPA scan
   b. US duplex Doppler of the kidney transplant
   c. MRI of the abdomen and pelvis with and without contrast
   d. Selective angiogram of the renal transplant
   e. CT scan of the abdomen and pelvis with contrast

   Answer: b

   Rationale: The correct answer be a duplex ultrasound scan of the transplant. (https://acsearch.acr.org/docs/71096/Narrative/). This is an ideal first imaging study and can determine the next investigation or intervention as the case may be. It could differentiate between obstruction, presence of fluid collections, and assess vascularity without the use of potentially nephrotoxic contrast agents.

4. Which statement below is a true regarding use of PET/CT in RCC?
   a. All RCC subtypes are markedly avid for FDG.
   b. Lack of FDG uptake in an indeterminate renal mass excludes RCC.
   c. Restaging with FDG PET/CT is a reasonable imaging strategy in the setting of an FDG-avid primary tumor.
   d. Non-FDG radiotracers are categorically not useful in imaging evaluation of RCC.

   Answer: c

   Rationale: A meta-analysis of 14 published studies on the diagnostic utility of FDG-PET(FDG PET-CT) in renal cell carcinoma reported a pooled sensitivity of 62% and a pooled specificity of 88% for renal lesions.[324] These mixed observations are probably related to the heterogeneous expression of glucose transporter 1 in renal cell carcinoma, which may not be correlated with the tumor grade or extent.[321,322] Negative study findings may not rule out disease, whereas a positive result is highly suspect for malignancy.[323] If the tumor binds FDG avidly, then PET can be a reasonable imaging modality for follow-up after treatment and for surveillance.

5. All of the following regarding gadolinium chelate agents (GBCA) are true, except:
   a. The use of GBCA in patients with an eGFR of less than 30 mL/min/1.73 m^2 should be avoided except when absolutely necessary.
   b. The risk of nephrogenic systemic fibrosis is increased when GBCA is administered to patients who have had a liver transplant.
   c. Dialysis should be scheduled soon after GBCA administration, only in patients already on hemodialysis.
   d. Nonionic linear agents (gadodiamide, gadoversetamide) and gadopentetate dimeglumine are contraindicated in patients with an eGFR of less than 30 mL/min/1.73 m^2 due to higher incidence of nephrogenic systemic fibrosis.
   e. There are fewer allergic-like reactions associated with the use of GBCA when compared with iodine contrast agents.

   Answer: b

   Rationale: An eGFR of less than 30 mL/min/1.73 m^2 is a relative contraindication to the use of GBCA. The use of Gd-C should be at the discretion and judgment of the referring physician. If possible, alternative imaging should be considered. The patients at highest risk are those with severely impaired renal function, both acute and chronic, for whom the risk for developing NSF is 1% to 7%. Liver transplant is no longer thought to be an independent variable. Gd-C agents are effectively removed with hemodialysis; however, no published report has proved that early dialysis prevents the development of NSF.